

**GEOLOGY AND GEOCHEMISTRY OF MAFIC ROCKS FROM  
OPHIOLITES OF EAST NELSON, NEW ZEALAND**

**CENTRE FOR NEWFOUNDLAND STUDIES**

**TOTAL OF 10 PAGES ONLY  
MAY BE XEROXED**

**(Without Author's Permission)**

**PAUL J. MOORE. B.Sc.**







National Library  
of Canada

Bibliothèque nationale  
du Canada

Canadian Theses Service

Service des thèses canadiennes

Ottawa, Canada  
K1A 0N4

## NOTICE

The quality of this microform is heavily dependent upon the quality of the original thesis submitted for microfilming. Every effort has been made to ensure the highest quality of reproduction possible.

If pages are missing, contact the university which granted the degree.

Some pages may have indistinct print especially if the original pages were typed with a poor typewriter ribbon or if the university sent us an inferior photocopy.

Reproduction in full or in part of this microform is governed by the Canadian Copyright Act, R.S.C. 1970, c. C-30, and subsequent amendments.

## AVIS

La qualité de cette microforme dépend grandement de la qualité de la thèse soumise au microfilmage. Nous avons tout fait pour assurer une qualité supérieure de reproduction.

S'il manque des pages, veuillez communiquer avec l'université qui a conféré le grade.

La qualité d'impression de certaines pages peut laisser à désirer, surtout si les pages originales ont été dactylographiées à l'aide d'un ruban usé ou si l'université nous a fait parvenir une photocopie de qualité inférieure.

La reproduction, même partielle, de cette microforme est soumise à la Loi canadienne sur le droit d'auteur, SRC 1970, c. C-30, et ses amendements subséquents.

GEOLOGY AND GEOCHEMISTRY OF MAFIC ROCKS FROM  
OPHIOLITES OF  
EAST NELSON, NEW ZEALAND

By

© PAUL J. MOORE, B.Sc.

A thesis submitted to the school of Graduate  
Studies in partial fulfillment of the  
requirements for the degree of  
Master of Science

Department of Earth Sciences  
Memorial University of Newfoundland

January 1991

St. John's

Newfoundland





National Library  
of Canada

Bibliothèque nationale  
du Canada

Canadian Theses Service    Service des thèses canadiennes

Ottawa, Canada  
K1A 0N4

The author has granted an irrevocable non-exclusive licence allowing the National Library of Canada to reproduce, loan, distribute or sell copies of his/her thesis by any means and in any form or format, making this thesis available to interested persons.

The author retains ownership of the copyright in his/her thesis. Neither the thesis nor substantial extracts from it may be printed or otherwise reproduced without his/her permission.

L'auteur a accordé une licence irrévocable et non exclusive permettant à la Bibliothèque nationale du Canada de reproduire, prêter, distribuer ou vendre des copies de sa thèse de quelque manière et sous quelque forme que ce soit pour mettre des exemplaires de cette thèse à la disposition des personnes intéressées.

L'auteur conserve la propriété du droit d'auteur qui protège sa thèse. Ni la thèse ni des extraits substantiels de celle-ci ne doivent être imprimés ou autrement reproduits sans son autorisation.

ISBN 0-315-65341-8

## ABSTRACT

In the East Nelson area, ophiolitic rocks of the Dun Mountain Ophiolite Belt (East Nelson ophiolites) have been described by past workers as representing either a single disrupted ophiolite suite or a number of distinct ophiolite suites.

Through geochemical evaluation of mafic rocks of the East Nelson ophiolites, it has been determined that potentially three separate ophiolite suites exist; the Dun Mountain Ophiolite, the Patuki mélange and the Croisilles mélange.

The Dun Mountain Ophiolite represents a semi-complete ophiolite suite. Geochemical evidence indicates that mafic rocks of this ophiolite are of island-arc tholeiite composition and have been produced by partial melting of depleted mantle above a subduction zone. The disrupted and relatively incomplete nature of the ophiolite is considered to be the result of tectonic activity associated with obduction and later orogenesis.

Unconformably overlying the Dun Mountain Ophiolite are local accumulations of conglomeratic material, known as the Upukerora Formation. Clasts within this formation closely resemble lithologies observed within the Dun Mountain Ophiolite and pyroxenes analyzed from clasts are found to be compositionally similar to those observed within the ophiolite.

Rocks of the Patuki and Croisilles mélanges lie in fault contact with, and underlie the Dun Mountain Ophiolite. Blocks within the mélanges consist

of sedimentary, mafic to ultramafic volcanic and plutonic rocks suspended in matrices dominated by sheared serpentinite. Although these rocks are highly disrupted, they are considered to represent vestiges of true ophiolitic assemblages, as representative lithologies of an ophiolite are observed within the blocks. These rocks likely represent fragments of oceanic crust subducted beneath the Dun Mountain Ophiolite.

Basaltic rocks of the Fatuki and Croisilles mélanges are divided into two petrographically and geochemically defined suites; a mid-ocean ridge suite and an alkaline within-plate suite. Geochemical evidence suggests mid-ocean ridge basalts of the mélanges are indistinguishable and therefore it is suggested that the mélanges may represent dislocated portions of the same oceanic basement.

A fore-arc environment of formation is favoured for the origin of the Dun Mountain Ophiolite. By this model the Patuki and Croisilles mélanges are considered fragments of normal ocean crusts sheared off the subducted slab during subduction.



## ACKNOWLEDGEMENTS

The preparation of this thesis was made possible with tremendous assistance from the faculty and staff of the Universities of Otago, Auckland University, and the Department of Science and Industrial Research (Nelson); in particular: Dr. D. S Coombs, Dr. Patricia Black and Dr. Mike Johnston. Others in New Zealand I would like to thank include: Don and Isabelle Muirhead and Peter and Barbara James of the Richmond Motel for their kind and overwhelming hospitality, as well as the many "happy campers" that wandered through that summer, particularly Mr. Mike "Mic" Brown and Mr. Paul Butler (thanks for the potatoes!).

Many thanks to the faculty and staff of the Department of Earth Sciences at Memorial University for making my stay at Memorial both enjoyable and productive. Thanks to G. Andrews for providing major element geochemical analyses, D. Clark and G. Vienott for assistance with trace element and microprobe analyses, Dr. H Longrich, P. King, B. Gosse, S. Jackson, and D. Healy for ICP analyses. Thanks also to R. Sober, F. Thornhill, L. Warford for preparing my thin sections. A special note of thanks to Mr. Pat Browne, Bill Collins and Nancy Fagan for not losing patience with me and for always being helpful.

I am also indebted to my colleagues at Memorial particularly Steve Edwards, Terry Brace, Sandy Sears and Nick Sargeant with whom, along with Dave Molloy, many pleasant hours of discussion and relaxation were spent while at Memorial.

I am especially indebted to Dr. John G. Malpas for his patience, encouragement and advice throughout this study and for adding a twenty-fifth hour to many days to read my chapters. His performance as my supervisor and friend were exemplary and will always be remembered.

Special thanks to my family and friends for their undying support and to Carolyn for her patience and faith in me during this undertaking.

## TABLE OF CONTENTS

ABSTRACT .....	ii
ACKNOWLEDGEMENTS .....	iv
TABLE OF CONTENTS .....	vi
LIST OF TABLES .....	x
LIST OF FIGURES .....	xi
LIST OF PLATES .....	xvi

### CHAPTER 1

#### INTRODUCTION

1.1 Preface .....	1
1.2 Location .....	6
1.3 Physiography .....	7
1.4 Climate .....	9
1.5 Previous Work .....	10
1.6 Method and Scope .....	15

### CHAPTER 2

#### REGIONAL GEOLOGY

2.1 Geological History .....	16
2.1.1 Cenozoic to Recent .....	16
2.1.2 The Pre-Cenozoic .....	19
2.2 Regional Geology .....	23
2.3 Geological Outline of the Eastern Province .....	28
2.3.1 Torlesse Terrane .....	28
2.3.2 Caples-Pelorus Terrane .....	30
2.3.3 Croisilles and Greenstone Ophiolitic Mélanges .....	33
2.3.4 Patuki Mélange .....	35
2.3.5 Dun Mountain-Maitai Terrane .....	37
2.3.6 Murihiku Terrane .....	40
2.3.7 Brook Street Terrane .....	41



## CHAPTER 3

## GEOLOGY OF THE EAST NELSON OPHIOLITES

3.1 Introduction . . . . .	43
3.2 Field Relationships . . . . .	46
3.2.1 Introduction . . . . .	46
3.2.2 Red Hills Western Margin . . . . .	46
3.2.3 Lee River . . . . .	67
3.2.4 Serpentine River . . . . .	76
3.2.5 Roding River . . . . .	80
3.2.5.1 Champion Creek . . . . .	80
3.2.5.2 United Creek . . . . .	84
3.2.5.3 Dun Mountain Track . . . . .	91
3.2.6 Tinline River . . . . .	92
3.2.7 Croisilles Harbour . . . . .	100
3.2.8 Taipare Bay . . . . .	106
3.3 Summary . . . . .	110
3.3.1 Field Relationships . . . . .	110
3.3.2 Structure and Metamorphism . . . . .	112

## CHAPTER 4

## PETROGRAPHY OF THE EAST NELSON OPHIOLITE

4.1 Introduction . . . . .	115
4.2 Upukerora Formation . . . . .	115
4.3 Dun Mountain Ophiolite . . . . .	121
4.3.1 Lee River Group Volcanic Rocks . . . . .	121
4.3.1.1 Dun Mountain Track . . . . .	122
4.3.1.2 Taipare Bay . . . . .	124
4.3.2 Lee River Group Subvolcanic Rocks . . . . .	129
4.3.3 Sheared Serpentinite Complex . . . . .	144
4.3.3.1 Lee River Group Diabase and Gabbro Inclusions . . . . .	145
4.3.3.2 Layered Series Gabbro Inclusions . . . . .	148
4.3.4 Dun Mountain Ultramafics Group . . . . .	150
4.4. Patuki Mélange . . . . .	154
4.4.1 Patuki Volcanics . . . . .	154
4.4.2 Patuki Subvolcanics . . . . .	161
4.5 Croisilles Mélange . . . . .	162
4.5.1 Croisilles Volcanics . . . . .	164
4.5.2 Croisilles Subvolcanics . . . . .	166
4.5.3 Croisilles Ultramafics . . . . .	169

4.6 Summary .....	169
-------------------	-----

## CHAPTER 5

### GEOCHEMISTRY OF VOLCANIC AND SUBVOLCANIC ROCKS OF THE EAST NELSON OPHIOLITES

5.1 Introduction .....	175
5.2 Presentation of Data .....	176
5.2.1 Effects of Alteration .....	177
5.2.1.1 Major Elements .....	178
5.2.1.2 Trace Elements .....	193
5.3 Basalt Geochemistry .....	194
5.3.1 Introduction .....	194
5.3.2 Trace Elements .....	195
5.3.3 Rare Earth Elements .....	202
5.3.4 Pyroxene Chemistry .....	209
5.3.5 Geochemical Discrimination Diagrams .....	233
5.3.6 MORB Normalized Trace Element Diagrams .....	254
5.4 Summary .....	264

## CHAPTER 6

### PETROGENESIS OF THE BASALTIC ROCKS OF THE EAST NELSON OPHIOLITES

6.1 Introduction .....	267
6.2 Petrogenetic Modelling .....	270
6.2.1 Introduction .....	270
6.2.2 Source Variations .....	271
6.2.3 Partial Melting and Fractional Crystallization .....	285
6.3 Summary .....	293

## CHAPTER 7

### TECTONIC MODELS

7.1 Introduction .....	295
7.2 Previous Tectonic Models .....	295
7.2.1 Age Dates .....	297
7.2.2 Field Relationships .....	298

7.2.3 Petrological and Geochemical Data . . . . .	300
7.2.4 Regional Setting . . . . .	301
7.3 Tectonic Models . . . . .	302
7.4 Discussion . . . . .	308

## CHAPTER 8

### SUMMARY AND CONCLUSIONS

SUMMARY AND CONCLUSIONS . . . . .	312
REFERENCES . . . . .	317

### APPENDIX A. ANALYTICAL METHODS

A.1 Sampling Procedure . . . . .	333
A.2 Sample Preparation . . . . .	333

### APPENDIX B ANALYTICAL METHODS

B.1 Major Elements . . . . .	334
B.2 Trace Elements (XRF) . . . . .	335
B.3 Trace and Rare Earth Elements (ICP) . . . . .	335
B.4 Mineral Analysis . . . . .	337

### APPENDIX C GEOCHEMICAL ANALYSES

C.1 Major and Trace Element Analyses . . . . .	340
C.1a Basaltic Rocks . . . . .	341
C.1b Gabbroic Rocks . . . . .	354
C.2 Mineral Analyses . . . . .	360



**LIST OF TABLES**

<b>Table No.</b>	<b>Page</b>
2.1 Provisional terranes of the Eastern Province of New Zealand. . .	27
5.1 Averaged rare earth element abundances for basaltic suites of the East Nelson ophiolites . . . . .	203
5.2 Average clinopyroxene analyses from basaltic rocks of the East Nelson ophiolites . . . . .	210
B.1 Precision and accuracy estimates for trace element analyses by XRF. . . . .	336
B.2 Precision and accuracy estimates for trace element analyses by ICP. . . . .	338

## LIST OF FIGURES

Figure No.	Page
1.1 Location map of New Zealand . . . . .	2
1.2 Geology sketch map of the East Nelson ophiolites . . . . .	7
1.3 Geological sketch map of South Island, New Zealand . . . . .	5
2.1 Sketch map of the New Zealand Region . . . . .	17
2.2 Sketch map of the pre-Carboniferous geological terranes of the Western Province . . . . .	18
3.2.1 Geology map of the Red Hills area . . . . .	back pocket
3.2.2 Geology map of the Lee River area . . . . .	back pocket
3.2.3 Geology map of the Serpentine River area . . . . .	back pocket
3.2.4 Geology map of the Roding River area . . . . .	back pocket
3.2.5 Geology map of the Tinline River area . . . . .	back pocket
3.2.6 Geology map of the Croisilles Harbour area . . . . .	back pocket
5.1a Modified Hughes (1972) igneous spectrum diagram after Stauffer et al. (1975); basaltic rocks . . . . .	180
5.1b Modified Hughes (1972) igneous spectrum diagram after Stauffer et al. (1975); gabbroic rocks . . . . .	180
5.2a Igneous spectrum diagram after Stephens (1982); basaltic rocks of the East Nelson ophiolites . . . . .	183
5.2b Igneous spectrum diagram after Stephens (1982); gabbroic rocks of the East Nelson ophiolites . . . . .	183
5.3 Histogram of SiO <sub>2</sub> contents within basaltic rocks of the Dun Mountain Ophiolite Belt . . . . .	186
5.4a Variation diagrams of selected trace, rare earth and major elements plotted against Mg#. Samples plotted are basalts . . . . .	189
5.4b Variation diagrams of selected trace, rare earth and major elements plotted against Mg#. Samples plotted are basalts . . . . .	191

5.4c Variation diagrams of selected trace, rare earth and major elements plotted against Mg#. Samples plotted are basalts . . . . .	192
5.5 Cr versus Ni (ppm) plot for basaltic rocks of the Dun Mountain Ophiolite Belt . . . . .	197
5.6a Immobile trace element variation diagrams for basaltic rocks of the East Nelson ophiolites . . . . .	200
5.6b Immobile trace element variation diagrams for basaltic rocks of the East Nelson ophiolites . . . . .	200
5.6c Immobile trace element variation diagrams for basaltic rocks of the East Nelson ophiolites . . . . .	201
5.7a Chondrite normalized rare earth element patterns for average basaltic suite compositions of the East Nelson ophiolites . .	205
5.7b Chondrite normalized rare earth element patterns for altered basaltic rocks . . . . .	205
5.8 Pyroxene quadrilateral diagram of averaged clinopyroxene analysis from basaltic rocks of the East Nelson ophiolites .	214
5.9a SiO <sub>2</sub> versus FeO*/MgO plot of pyroxenes from basaltic rocks of the East Nelson ophiolites . . . . .	217
5.9b TiO <sub>2</sub> versus FeO*/MgO plot of pyroxenes from basaltic rocks of the East Nelson ophiolites . . . . .	217
5.10a MgO versus Al <sub>2</sub> O <sub>3</sub> plot for pyroxenes of the various basaltic rocks of the East Nelson ophiolites . . . . .	220
5.10b TiO <sub>2</sub> versus Al <sub>2</sub> O <sub>3</sub> plot for pyroxenes of the various basaltic rocks of the East Nelson ophiolites . . . . .	220
5.11a SiO <sub>2</sub> versus Al <sub>2</sub> O <sub>3</sub> plot for pyroxenes of the various basaltic rocks of the East Nelson ophiolites . . . . .	223
5.11b Al <sub>2</sub> versus TiO <sub>2</sub> plot for pyroxenes from basaltic suites of the East Nelson ophiolites . . . . .	223
5.12a Pyroxene discrimination diagram of Leterrier et al. (1982) . . . . .	226
5.12b Pyroxene discrimination diagram of Leterrier et al. (1982) . . . . .	226



5.12c Pyroxene discrimination diagram of Leterrier et al. (1982) . . . . .	227
5.13 Pyroxene discrimination diagram of Beccaluva et al. (1989) . . . . .	229
5.14a Pyroxene discrimination diagram of Beccaluva et al. (1989) . . . . .	231
5.14b Pyroxene discrimination diagram of Beccaluva et al. (1989) . . . . .	231
5.14c Pyroxene discrimination diagram of Beccaluva et al. (1989) . . . . .	232
5.14d Pyroxene discrimination diagram of Beccaluva et al. (1989) . . . . .	232
5.15 Tectonic discrimination diagram of Pearce and Nisbet (1977) . . . . .	234
5.16a Plot of $\text{TiO}_2$ versus $\text{FeO}^*/\text{MgO}$ for basaltic rocks of the Dun Mountain Ophiolite Belt . . . . .	237
5.16b Plot of $\text{FeO}^*$ versus $\text{FeO}^*/\text{MgO}$ for basaltic rocks of the Dun Mountain Ophiolite Belt . . . . .	237
5.17 Basaltic discrimination diagram after Jensen (1976) . . . . .	239
5.18 AFM plot of basaltic rocks of the East Nelson ophiolites . . .	239
5.19 Zr/ $\text{TiO}_2$ versus Log Nb/Y discrimination diagram of Winchester and Floyd (1977) . . . . .	242
5.20 Basalt tectonic discrimination diagram of Pearce and Cann (1973) . . . . .	242
5.21 Basalt tectonic discrimination diagram of Pearce and Norry (1979) . . . . .	245
5.22 Th/Yb versus Ta/Yb covariation diagram of Pearce et al. (1981) . . . . .	245
5.23 Cr versus Y variation diagram of Pearce (1980), Pearce et al. (1981) and Pearce et al. (1984) . . . . .	249
5.24 Th-Hf-Ta basalt tectonic discrimination diagram of Wood (1980) . . . . .	249

5.25 V versus Ti tectonic discrimination diagram of Shervais (1982) . . . . .	253
5.26a MORB normalized geochemical patterns for basalts of the East Nelson ophiolites . . . . .	256
5.26b MORB normalized geochemical patterns for basalts of the East Nelson ophiolites . . . . .	256
5.26c MORB normalized geochemical patterns for basalts of the East Nelson ophiolites . . . . .	257
5.26d MORB normalized geochemical patterns for basalts of the East Nelson ophiolites . . . . .	257
5.26e MORB normalized geochemical patterns for basalts of the East Nelson ophiolites . . . . .	258
5.26f MORB normalized geochemical patterns for basalts of the East Nelson ophiolites . . . . .	258
5.27 MORB normalized average basaltic suite geochemical patterns for basaltic suites of the East Nelson ophiolites . . . . .	261
5.28a MORB normalized geochemical patterns for basalts of known, non arc related tectonic settings . . . . .	263
5.28b MORB normalized geochemical patterns for basalts of known, arc related tectonic settings . . . . .	263
6.1a Th/Yb versus Ta/Yb covariation diagram showing vectors of within-plate enrichment and depletion as well as supra-subduction zone enrichment . . . . .	275
6.1b Th/Yb versus Ta/Yb covariation diagram of Pearce et al. (1984) . . . . .	275
6.2a Petrogenetic pathways on a Th-Hf-Ta diagram for ophiolites of different tectonic affinities . . . . .	278
6.2b Th-Hf-Ta basalt tectonic discrimination diagram of Wood (1980) . . . . .	278
6.3a Basalt discrimination diagram of Pearce and Norry (1979) . .	281
6.3b Petrogenetic pathways for basaltic rocks from some typical volcanic suites plotted on a Zr/Y versus Zr diagram after Pearce and Norry (1979) . . . . .	281

6.3c Estimated petrogenetic pathways for basaltic suites of the Dun Mountain Ophiolite Belt plotted on a Zr/Y versus Zr diagram . . . . .	282
6.4a Cr versus Y variation diagram of Pearce (1980), Pearce et al. (1981) and Pearce et al. (1984) . . . . .	287
6.4b Petrogenetic pathways for ophiolites of different tectonic affinities plotted on a Cr versus Y diagram after Pearce et al. (1984) . . . . .	287
6.4c Estimated petrogenetic trends for basaltic rocks of the Dun Mountain Ophiolite plotted on a Cr versus Y diagram . . . . .	289
6.4d Estimated petrogenetic trends for "olivine-poor" suite basaltic rocks of the Patuki and Croisilles mélanges plotted on a Cr versus Y diagram . . . . .	289
7.1 Tectonic model for the genesis of the East Nelson ophiolites . . . . .	305

## LIST OF PLATES

Plate No.	Page
3.1 Wooded Peak limestones of the Maitai Group (Red Hills, R-916) . . . . .	48
3.2a Upukerora conglomerates of the Maitai Group . . . . .	49
3.2b Angular clasts suspended in a hematite-stained muddy matrix, Upukerora Formation . . . . .	49
3.3 Diabase dyke intruding medium-grained Lee River Group gabbro	51
3.4 Wooded Peak limestone intercalated with sandstone . . . . .	51
3.5a Microphotograph of sandstone containing abundant crystal fragments and altered clasts . . . . .	52
3.5b Microphotograph of fine-grained sandstone containing abundant fragments of sponge spicules . . . . .	52
3.5c Microphotograph of sandstone containing abundant fragments of sponge spicules . . . . .	53
3.6a Forty metre wide sheared serpentinite shear zone in Sheared Serpentinite Complex Zone . . . . .	55
3.6b Close up of sheared serpentinite shear zone in Sheared Serpentinite Complex Zone . . . . .	55
3.7 Competent blocks of gabbroic material suspended in sheared serpentinite . . . . .	56
3.8 Competent blocks of amphibolitized and foliated medium-grained gabbro suspended in sheared serpentinite . . . . .	57
3.9a Rodingite dyke in sheared serpentinite . . . . .	58
3.9b Close up of rodingite dyke in sheared serpentinite truncated by a block of amphibolitized and strongly foliated medium-grained gabbro . . . . .	58
3.9c Close up of amphibolitized and strongly foliated medium-grained gabbro . . . . .	59
3.10 Disrupted rodingite dykes in sheared serpentinite . . . . .	59

3.11a	Knocker of foliated and amphibolitized melanocratic gabbro suspended in sheared serpentinite of the Sheared Serpentine Complex Zone . . . . .	61
3.11b	Close up of foliation within amphibolitized, medium-grained melanocratic gabbro knocker . . . . .	61
3.12	Boulder of transition series banded rock . . . . .	62
3.13	Outcrop of vertically banded transition series rocks . . . . .	63
3.14	Boulder of transition series rock . . . . .	64
3.15	Boulder of transition series gabbro cut by a 5 centimetre wide dyke of amphibolitized gabbroic material . . . . .	64
3.16a	Outcrop of foliated transition series rocks . . . . .	65
3.16b	Close up of transition series rock . . . . .	65
3.17	Outcrop of banded Harzburgite within the Red Hills Ultramafic massif (Dun Mountain Ultramafics Group) . . . . .	66
3.18	Fine-grained Maitai Group clastic sediments with cleavage developed along bedding surfaces . . . . .	66
3.19	Large block of pillowed basalts . . . . .	70
3.20	Close up of inclusion of rodingitized material within sheared serpentine . . . . .	70
3.21	Patuki pillow basalts . . . . .	72
3.22a	Nonconformable contact between Patuki pillow basalts (right) and argillaceous sediments . . . . .	73
3.22b	Close up of argillaceous sediments above nonconformable contact . . . . .	74
3.23	Close up of highly foliated gabbro . . . . .	77
3.24	Medium-grained Lee River Group gabbro intruded by a diabase dyke . . . . .	82
3.25	Lee River Group (g) gabbro intruded by a diabase dyke . . . . .	82
3.26	Outcrop of Lee River Group gabbro . . . . .	83

3.27 Boulder of strongly foliated to flazered, medium- to coarse-grained Lee River Group gabbro . . . . .	83
3.28 Looking southwest across Champion Creek to derelict shafts of the abandoned Champion Creek mine . . . . .	85
3.29 Abandoned shaft, east bank of Champion Creek, Champion Creek mine . . . . .	86
3.30 Boulder of Upukerora conglomerate in Champion Creek . . . . .	87
3.31 Outcrop of vertically dipping, sheeted Lee River Group diabase dykes . . . . .	87
3.32 Outcrop of Lee River Group gabbro intruded by a diabase dyke	88
3.33 Outcrop of Lee River Group gabbro with xenoliths of lighter coloured gabbro . . . . .	88
3.34 Outcrop of Lee River Group gabbro intruded by diabase dykes .	89
3.35 Faulted contact between foliated Lee River Group gabbro and sheared serpentinite of the Dun Mountain Ultramafics Group .	89
3.36 Block of rodingitized material suspended in sheared serpentinite . . . . .	90
3.37 Boulder of diabase breccia . . . . .	94
3.38 Highly fractured outcrop of Lee River Group gabbro in contact with diabase dykes . . . . .	94
3.39 Outcrop of quartz vein gossan zone . . . . .	95
3.40 Outcrop of Lee River Group sheeted dykes with well preserved chilled margins and flow foliation . . . . .	95
3.41 Outcrop of foliated Lee River Group gabbro cut by two generations of diabase dykes . . . . .	96
3.42 Outcrop of flazered medium to coarse-grained Lee River Group gabbro . . . . .	96
3.43 Outcrop of foliated and amphibolitized gabbro containing an inclusion of coarse-grained amphibolite . . . . .	98
3.44 Boulder of plagioclase porphyritic gabbro . . . . .	99

3.45 Microphotograph of plagioclase porphyritic diabase from United Creek . . . . .	99
3.46 Looking southeast down Tinline River section from stop TI-781 . . . . .	101
3.47 Outcrop of partially rodingitized, sheared ultramafic material in contact with sheared sediments . . . . .	101
3.48a Hummocky topography of Croisilles mélange . . . . .	103
3.48b Croisilles mélange with blocks of serpentized ultramafic and gabbroic rocks suspended in a sheared serpentinite matrix . . .	103
3.48c Close up of Croisilles mélange with blocks of serpentized ultramafic and gabbroic rocks suspended in a sheared serpentinite matrix . . . . .	104
3.49a Outcrop of Croisilles pillowed basalts . . . . .	105
3.49b Close up of Croisilles pillowed basalts . . . . .	105
3.50 View looking northwest towards Taipare Bay . . . . .	107
3.51 Outcrop of weathered pillowed basalts of the Lee River Group .	107
3.52 Outcrop of pillowed mafic flows, Taipare Bay . . . . .	108
3.53 Outcrop of basalt breccia with sandy matrix material, Taipare Bay . . . . .	108
3.54 Outcrop of basalt breccia, Taipare Bay . . . . .	109
3.55 Outcrop of basaltic breccia with abundant volcanoclastic sand matrix . . . . .	109
4.1 Close up of Upukerora conglomerate with angular to subrounded clasts of gabbro, basalt and siltstone . . . . .	117
4.2 Microphotograph of gabbro clasts within Upukerora conglomerate	117
4.3 Microphotograph of gabbro clast within Upukerora conglomerate .	118
4.4 Microphotograph of trachytic textured basalt clast within Upukerora conglomerate . . . . .	118
4.5 Microphotograph of quenched glassy basalt clast from the Upukerora conglomerate . . . . .	120

4.6 Microphotograph of a flow banded, glassy basalt clast within Upukerora conglomerate . . . . .	120
4.7 Plagioclase and olivine porphyritic Lee River Group basalt . . . . .	123
4.8 Microphotograph of weakly altered intergranular Lee River Group basalt . . . . .	123
4.9 Microphotograph of porphyritic Lee River Group basalt . . . . .	125
4.10 Microphotograph of amygdaloidal, chloritized basalt with patches of preserved basaltic texture . . . . .	125
4.11a Microphotograph of intergranular basalt with epidote and quartz filled vesicles . . . . .	127
4.11b Microphotograph of intergranular basalt with epidote and quartz filled vesicles . . . . .	127
4.12 Microphotograph of weakly chloritized intergranular basalt . . . . .	128
4.13 Microphotograph of fine-grained diabase with intergranular texture . . . . .	128
4.14a Microphotograph of medium-grained Lee River Group gabbro . . . . .	131
4.14b Microphotograph of medium-grained Lee River Group gabbro . . . . .	131
4.15 Microphotograph of intergranular Lee River Group diabase . . . . .	132
4.16 Microphotograph of intergranular Lee River Group diabase with chlorite replaced olivine microphenocryst . . . . .	132
4.17 Microphotograph of intergranular, medium-grained Lee River Group gabbro . . . . .	133
4.18 Microphotograph of amphibolitized medium-grained, Lee River Group gabbro . . . . .	133
4.19a Microphotograph of amphibolitized and foliated medium-grained, Lee River Group diabase cut by veinlets of prehnite and albite . . . . .	135
4.19b Microphotograph of amphibolitized and foliated medium-grained, Lee River Group diabase . . . . .	135
4.20 Microphotograph of foliated and amphibolitized Lee River Group gabbro cut perpendicular to the foliation . . . . .	136



4.21 Microphotograph of amphibolitized gabbro with brown pleochroic hornblende (an inclusion within a sheared serpentinite fault zone) . . . . .	136
4.22 Microphotograph of rodingitized Lee River Group gabbro . . . . .	138
4.23 Microphotograph of altered plagioclase porphyritic gabbro . . . . .	138
4.24a Microphotograph of Lee River Group gabbro . . . . .	140
4.24b Microphotograph of medium-grained Lee River Group gabbro . . . . .	140
4.25a Microphotograph of weakly altered Lee River Group diabase . . . . .	141
4.25b Microphotograph of weakly altered Lee River Group diabase . . . . .	141
4.26a Microphotograph of weakly altered, intergranular to subophitic Lee River Group gabbro . . . . .	142
4.26b Microphotograph of weakly altered, intergranular to subophitic Lee River Group gabbro . . . . .	142
4.27 Microphotograph of weakly altered, intergranular Lee River Group diabase . . . . .	143
4.28 Microphotograph of a medium-grained gabbro inclusion (a block within the Sheared Serpentinite Complex Zone, Red Hills) . . . . .	143
4.29 Rodingitized fine-grained diabase (block within the Sheared Serpentinite Complex Zone, Red Hills) . . . . .	146
4.30 Microphotograph of foliated, brown hornblende amphibolitized, medium-grained gabbro (a block within the Sheared Serpentinite Complex Zone, Red Hills) . . . . .	146
4.31 Orthopyroxene and plagioclase rich band within a band of transition series rock (inclusion in the Sheared Serpentinite Complex Zone, Red Hills) . . . . .	149
4.32 Olivine rich layer in transition series rock (inclusion in the Sheared Serpentinite Complex Zone) . . . . .	149
4.33 Microphotograph of strained and granulated texture within an orthopyroxenite band within the Red Hills massif . . . . .	152
4.34 Microphotograph of partially serpentitized harzburgite from the Red Hills ultramafic massif . . . . .	152

4.35 Microphotograph of brown-coloured spinel in orthopyroxenite band of the Red hills ultramafic massif . . . . .	153
4.36 Partially serpentinized harzburgite of the Dun Mountain Ultramafics Group . . . . .	153
4.37 Microphotograph of altered olivine microphenocryst in quenched textured variolitic Patuki basalt . . . . .	156
4.38 Microphotograph of fresh intergranular, fine-grained Patuki basalt . . . . .	156
4.39 Microphotograph of plagioclase phenocrysts in Patuki basalt . . .	157
4.40 Quenched textured variolitic Patuki basalt . . . . .	157
4.41 Microphotograph of olivine microphenocrysts within quenched, vesicular Patuki Basalt . . . . .	158
4.42 Microphotograph of quenched texture, olivine porphyritic Patuki basalt . . . . .	158
4.43 Microphotograph of fine-grained, quenched Patuki basalt cut by veinlets of pumpellyite and prehnite . . . . .	159
4.44 Microphotograph of Patuki basaltic breccia . . . . .	159
4.45 Microphotograph of Patuki diabase with partially amphibolitized clinopyroxene phenocrysts . . . . .	160
4.46 Microphotograph of partially amphibolitized, medium-grained Patuki gabbro . . . . .	160
4.47 Microphotograph of partially amphibolitized Patuki gabbro . . . . .	163
4.48 Microphotograph of rodingitized orthopyroxene-bearing, Patuki gabbro . . . . .	163
4.49 Microphotograph of hyalopilitic, glassy Croisilles basalt . . . . .	165
4.50 Microphotograph of variolitic to subophitic Croisilles basalt . . . .	165
4.51a Microphotograph of nonfoliated, medium-grained Croisilles gabbro . . . . .	167
4.51b Microphotograph of nonfoliated, medium-grained Croisilles gabbro . . . . .	167

4.52 Microphotograph of intensely foliated and amphibolitized Croisilles gabbro . . . . .	168
4.53 Microphotograph of partially resorbed spinel crystals in serpentinized dunite of the Croisilles mélange . . . . .	168

## CHAPTER 1

### INTRODUCTION

#### 1.1 Preface

New Zealand, or Ateora (land of the long white cloud), is situated in the Southwest Pacific more than 1,600 kilometres southeast of its nearest neighbour, Australia (Figure 1.1). The country has a total land area of approximately 260,000 square kilometres, of which a third is mountainous. It consists of two major islands (North Island and South Island) and a number of small islands, of which some lie hundreds of kilometres from the main group.

Despite its size, New Zealand is as geologically complex as any continent, having been formed by processes characteristic of both continental and oceanic crusts. To a large degree, much of this complexity can be attributed to New Zealand's past and present plate tectonic mobility.

The geology of New Zealand provides a dynamic example of accretionary and consuming plate boundary processes as it represents a fragment of the continental margin of its parent super-continent, Gondwana and is today, situated within a tectonically active boundary zone between the Indian-Australian and Pacific plates (Figure 1.1 inset).

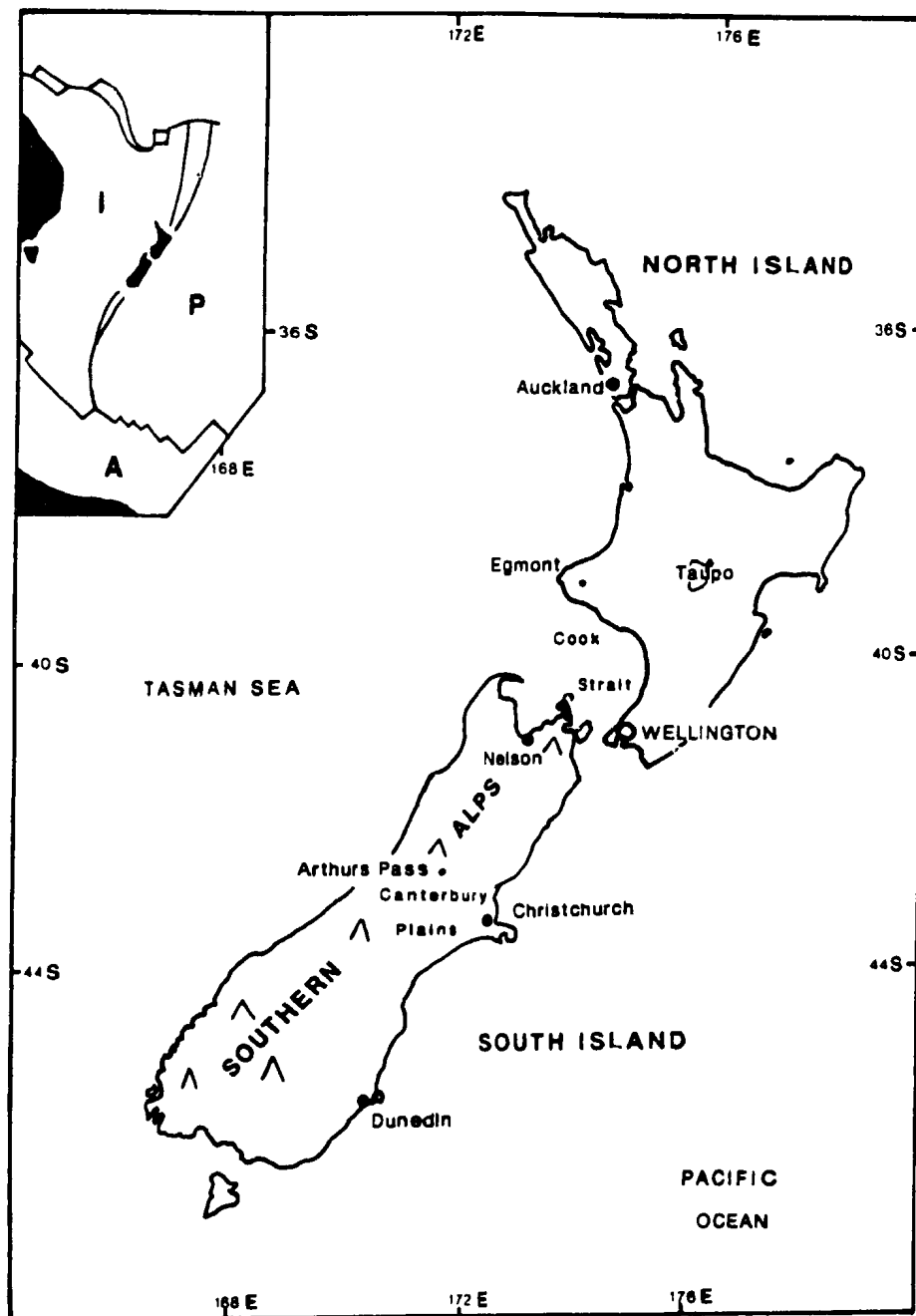


Figure 1.1 Location map of New Zealand with inset map showing plate boundaries between the Indian-Australian Plate (plate I), the Pacific Plate (plate P) and the Antarctic Plate (plate A).

Of particular interest to this study is a belt of Late Palaeozoic mafic and ultramafic rocks exposed in the mountain ranges to the east of Nelson (Richmond and Bryant Ranges) at the north end of South Island (Figure 1.2). This belt contains three distinct ophiolitic assemblages: the Dun Mountain Ophiolite (as defined by Johnston, 1981), a relatively undeformed and incomplete ophiolite sequence comprised of mafic volcanic and plutonic rocks of the Lee River group and the underlying ultramafic rocks of the Dun Mountain Ultramafics; and the Patuki and Croisilles ophiolitic mélanges which consist of large blocks of sedimentary, mafic to ultramafic volcanic and plutonic rocks suspended in a matrix of sheared serpentinite (eg. Johnston, 1981).

These three ophiolite assemblages are collectively referred to as the Dun Mountain Ophiolite Belt (Figure 1.3). The belt stretches the length of the South Island and is divisible into two structural segments, dextrally offset by the Alpine Fault. These segments are known as the Nelson segment in the north and the Otago segment in the south (Figure 1.3).

The ophiolites of the Dun Mountain Ophiolite Belt are components of the geological terranes which make up the Eastern Geological Province of South Island. Within this province rocks of the Dun Mountain Ophiolite are considered part of the Dun Mountain-Maitai terrane while rocks of the Croisilles and Patuki mélanges are considered discrete terranes which may represent components of the Caples-Pelorus terrane (Figure 1.3).

Over the past three decades ophiolitic assemblages of the Dun Mountain Ophiolite Belt have received considerable attention from numerous

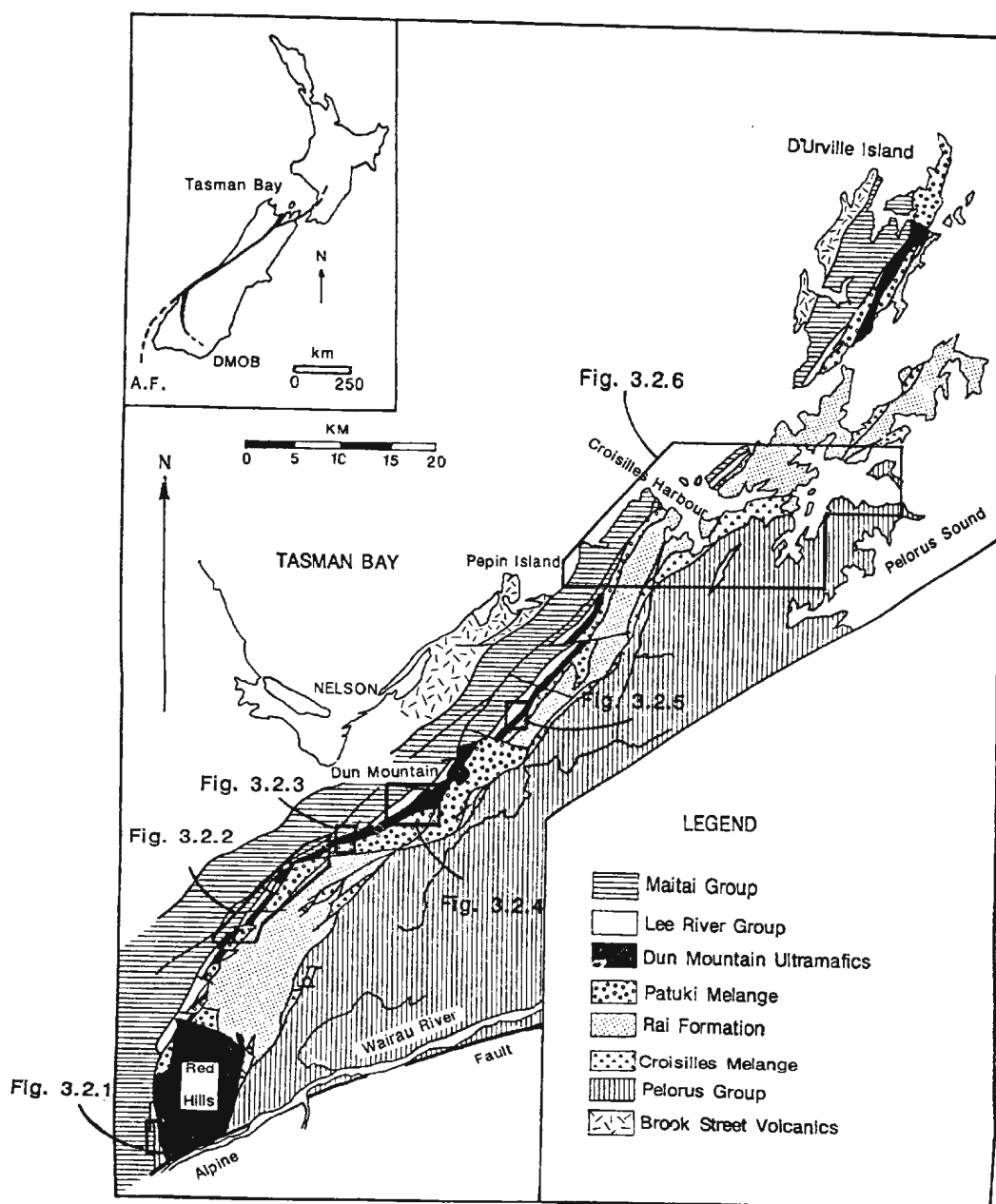


Figure 1.2 Geology sketch map of the East Nelson ophiolites (Nelson segment of the Dun Mountain Ophiolite Belt (DMOB)) modified after Davis et al. (1980), Landis and Blake (1987) and Sivell, 1988. Inset map shows the location of the Dun Mountain Ophiolite Belt's Nelson and Otago segments (DMOB) as well as the Alpine Fault (A.F.). Study areas and respective figure numbers are outlined (Figures 3.2.1 to 3.2.6).

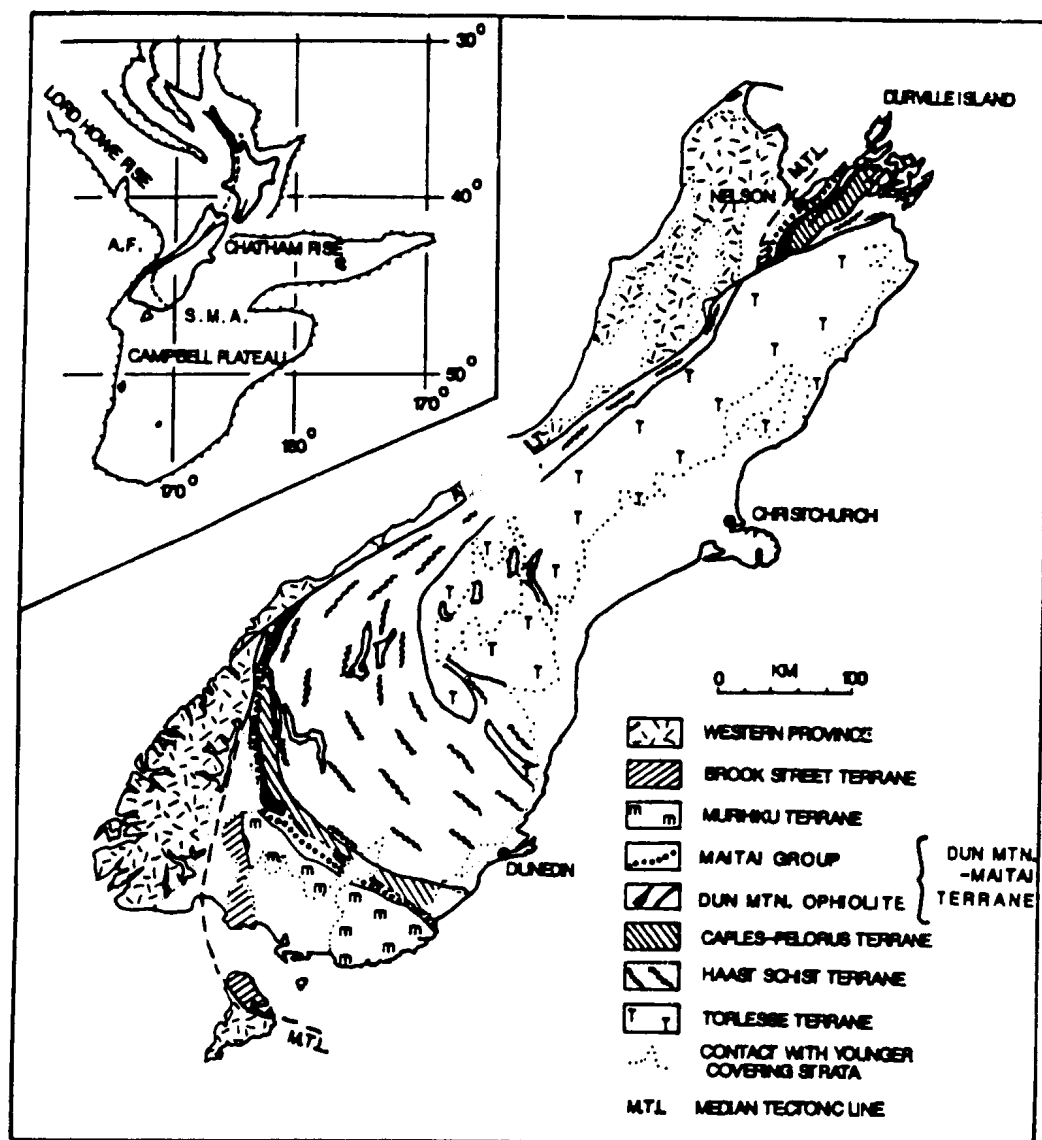


Figure 1.3: Geological sketch map of South Island, New Zealand. Geologic terranes have been modified after Coombs et al. (1976), Bishop et al. (1985) and Landis and Blake, (1987). Inset shows location with respect to Southwest Pacific bathymetric features (2000 metre isobath; see Landis and Blake, 1987) and structural trends as defined by the Alpine Fault (A.F.) and Stokes magnetic anomaly (S.M.A.). The highly indented coastline in the area southeast of D'Urville Island is referred to as the Marlborough Sounds.



workers particularly since the development of plate tectonic and ophiolite theory (e.g., Blake and Landis, 1973; Coombs et al., 1973; Coombs et al., 1976; Davis et al., 1980; Sivell et al., 1982; Sivell, 1988). To date it has been suggested that these rocks represent ocean crust of probably mid-ocean ridge (MORB) affinity (eg., Davis et al., 1980; Sinton, 1980; Sivell et al., 1982; Sivell et al., 1984; Dickins et al., 1986; Landis and Blake, 1987; Sivell, 1988), but that they may possess compositions which were influenced by a nearby subduction zone (Sinton, 1980; Davis et al., 1980; Sivell, 1988).

The aim of this thesis is to describe and interpret the mafic volcanic and plutonic rocks of the northern segment of the Dun Mountain Ophiolite Belt (ie. the Dun Mountain Ophiolite and the Croisilles and Patuki ophiolitic mélanges) and to make inferences about the ophiolites' environment(s) of formation. It is hoped that this work will provide constraints on the modelling of the ophiolites' generation and emplacement history.

## 1.2 Location

The Nelson province of New Zealand consists of the northwestern corner of South Island and centred around the city of Nelson and its neighbouring boroughs of Richmond and Hope situated at the head of Tasman Bay (Figure 1.2). To the east of Nelson lies the northern extension of the Southern Alps, a 500 kilometre long chain of fold mountains which runs the length of South Island. It is within these mountains that rocks of the Dun Mountain Ophiolite Belt of East Nelson are found. To avoid confusion in distinguishing the Dun Mountain Ophiolite from the Dun Mountain Ophiolite

Belt, the ophiolites of the Dun Mountain Ophiolite Belt of East Nelson are referred to here as the East Nelson ophiolites. In the East Nelson area the ophiolites outcrop as three semi-continuous, subvertical, northeast trending belts stretching from the Red Hills in the southwest to D'Urville Island in the northeast.

Study of the East Nelson ophiolites concentrated on six separate areas where representative sections through the ophiolites were both reasonably well exposed and accessible (Figure 1.2). These areas include: (i) the southwestern margin of the Red Hills, (ii) an area between the left branch of the Wairoa River and United Creek, (iii) the Dun Mountain railway, (iv) the Tinline River, (v) Croisilles Harbour and (vi) Taipare Bay. Within these areas, representative rocks of the East Nelson ophiolites previously delineated by other workers (e.g., Waterhouse, 1959, 1964; Johnston, 1981, 1982), were reinterpreted. As part of this study some of the areas were mapped in detail (1:10,000) and maps appear in the pocket at the back of this thesis (Figures 3.2.1 to 3.2.6).

### 1.3 Physiography

New Zealand is bisected longitudinally by mountains on South Island and ranges of hills on North Island. The physiography of New Zealand is largely the result of the latest mountain building episode, the Kaikoura Orogeny (mid-Cretaceous to present), which continues to the present day. This orogeny generated the mountains of the Southern Alps along with numerous faults which divide the landscape into large fault-bounded blocks.

The main structural lineament of this system is the strike-slip Alpine Fault of South Island (Figure 1.3). This feature represents the present day plate boundary between the Indian-Australian and Pacific plates. The erosion and continued movement of these blocks, together with the active volcanism of the North Island, define to a large extent, New Zealand's landscape.

On the South Island, mountains of the Southern Alps are flanked by extensive alluvial plains to the east while to the west, a narrow coastal strip flanked by steep slopes dominates the landscape. The eastern plains are known as the Canterbury Plains (Figure 1.1) and are used to a great extent for the production of grain and livestock. Glaciers are fairly common in the central mountains of southern South Island, but are rare on North Island (eg. Mount Ruapehu). The Southern Alps of South Island form a continuous chain of mountains stretching from the island's southwest corner to the northeast coast. Northwest of Arthur's Pass the Alps fan out into a number of steep, subparallel ridges to terminate in a series of sounds to the northeast (the Marlborough Sounds) and a coastline flanked by the Cook Strait to the east (between North and South Islands). Many northwesterly striking ridges have mineral deposits (chrome and copper) outcropping on their western slopes, particularly those directly south of Nelson. In southern areas of South Island the Alps break up into a rugged, disjunct landscape of difficult access and spectacular scenery.

The North Island is much less rugged than South Island. Its central region consists of a volcanic plateau which rises abruptly from the southern shores of Lake Taupo (Figure 1.1), New Zealand's largest natural lake (Taupo

itself, represents the ruins of an Quaternary volcanic crater). To the east of the central plateau, ranges are superseded by more rolling country, while to the southwest, the ranges end at the shores of the Cook Strait. West of the plateau, the mountains give way to the low undulating farmlands of Taranaki and extend to the slopes of Mount Egmont, a solitary volcano which has been active 0.018 Ma. to recent time (Stipp, 1968). North of Taupo the landscape is dominated by volcanic landforms consisting of low rolling hills, broad terraced valleys, and scattered dacite volcanoes and rhyolite domes.

#### 1.4 Climate

New Zealand's climate is dictated by its latitude, isolation, and physiography. Temperatures are generally buffered by the vast surrounding oceans while the mountains induce climatic differences between eastern and western areas. Western areas tend to receive more rainfall from the prevailing westerly and northwesterly winds, while eastern areas lie in a rain shadow. Annual rainfalls range from 330 millimetres in central Otago to as much as 8,000 millimetres in the Southern Alps. Most areas receive between 635 and 1,500 millimetres per year.

Mean temperatures at sea-level range from 15 °C in the far north to 9 °C in the far south. New Zealand is a sunny country, with many areas receiving up to 2,000 hours of sunshine a year, much of it in winter. In general, New Zealand's climate ranges from semi-temperate in the extreme south to sub-tropical in the extreme north.

The indigenous flora and fauna of New Zealand consists mainly of mixed evergreen forests, two species of lizards, some primitive frogs, and two species of bat. Since settlement by Europeans in the early 1800's many foreign species of plants and animals have been introduced with varying degrees of success. Today, much of the country has been claimed for pastoral and agricultural use with sheep farming representing the cornerstone of the economy.

### 1.5 Previous Work

The East Nelson ophiolites (Dun Mountain Ophiolite Belt), previously known as the Dun Mountain Mineral Belt and other names (see Challis, 1969), has not always been recognized as highly disrupted ophiolitic material. Since the 1850's, the various components of the belt have inspired numerous interpretations. These components can be summarized into a general but somewhat inconsistent sequence, consisting, from west to east of:

- (i) Late Permian Maitai Group sediments (sandstones, siltstones, mudstones, and limestones) which unconformably overlie;
- (ii) mafic plutonic and volcanic rocks of the Dun Mountain Ophiolite known as the Lee River Group (spilites, spilitic breccias, sheeted diabase dykes, and isotropic gabbros). Rocks of the Lee River Group are likely directly related to and are in fault contact with underlying;
- (iii) ultramafic rocks of the Dun Mountain Ultramafics Group of the Dun Mountain Ophiolite (mostly harzburgite and lesser proportions of dunite and pyroxenite). These rocks likely represent residual mantle material produced

during the evolution of Lee River Group magmas and basalts. Beneath the Dun Mountain Ultramafics lies another fault separating the ultramafics from rocks of;

(iv) the Patuki and Croisilles mélanges; a mixture of sedimentary, mafic volcanic, and mafic to ultramafic plutonic rocks suspended as blocks in a matrix dominated by sheared serpentinite. These mélanges generally separate rocks of the Dun Mountain Ultramafics from the Late Permian;

(v) Pelorus Group sediments; these are generally well bedded, graded sandstones with minor units of limestone, siltstone, mudstone and lenses of pebble conglomerate.

It should be pointed out here however, that neither the Maitai nor the Pelorus Group sediments are formally considered part of either of the belt's ophiolite assemblages and are discussed above only because they share contacts with ophiolitic rocks of the East Nelson ophiolites.

The earliest interpretations of the origin of the East Nelson ophiolites focuses on the Dun Mountain Ophiolite and its ultramafic rocks (Dun Mountain Ultramafics Group). In 1859, Hochstetter (Fleming, 1959) visited Dun Mountain and collected the rock he named "dunite". Hochstetter noted an overall concordancy of the ultramafic and adjacent rocks and suggested a sill-like intrusive origin for the ultramafites. MacKay (1879) observed concordancy of the overlying Maitai Group and postulated that the basaltic and ultramafic rocks formed on the sea floor. Later workers (eg., Park, 1887, 1921, and Benson, 1926), envisaged the ultramafic rocks as intrusions, probably in a semisolid state, emplaced along major Mesozoic thrust faults

into Maitai Group sediments. Other workers (eg., Turner, 1930; Macpherson, 1946; Kingma, 1959) favoured Mesozoic intrusion along a large scale thrust zone as a means of emplacement.

In 1958, Grindley suggested a coetaneous relationship between the ultramafic rocks, and the Lower Permian spilites, dolerites, and associated sediments. Grindley proposed that the ultramafites (including serpentinites) were submarine lava flows. Waterhouse (1959) also favoured an Early Permian volcanic origin for the ultramafites.

During the 1960's, with the development of the "Alpine-type" theory for ultramafic rocks in mountain belts (eg., Ross et al., 1954; Thayer, 1963), many detailed studies of ultramafic massifs of the Nelson segment of the Dun Mountain Ophiolite were undertaken. Lauder, (1965a,b) and Challis and Lauder (1966) suggested that the ultramafic rocks of the Dun Mountain massif were products of crystal accumulation in a Cretaceous magma chamber or volcanic pipe.

Studies at Red Hills, another ultramafic massif 45 kilometres southwest of Dun Mountain (Figure 1.2), resulted in additional interpretations. Challis (1965a,b) and Walcott (1969) preferred its formation as a high-temperature Permian intrusion, citing the existence of an unfaulted contact between cumulate ultramafite and a metamorphic aureole of pyroxene hornfels-facies as the essential evidence. Challis (1965a,b) suggested that the peridotitic rocks of the Red Hills massif and other massifs of the Dun Mountain Ophiolite were subvolcanic differentiates produced beneath a belt of Permian volcanoes. Walcott (1969) also interpreted the Red Hills massif as a

high-temperature Permian intrusion. Challis and Lauder (1966) and Challis (1968, 1969) went further to suggest that the ultramafic rocks were formed by crystal accumulation beneath a Permian volcanic arc.

In the mid-1960's, Coleman (1962, 1966) suggested a means of emplacement other than that of igneous intrusion for ultramafic rocks of the Dun Mountain massif. He observed low-temperature, high-pressure mineral assemblages at ultramafic rock contacts which lead him to suggest the massif was emplaced as a cold tectonic protrusion.

Blake and Landis (1973) concluded that the East Nelson ophiolites represent oceanic crust and upper mantle upon which Upper Permian Maitai Group sediments were deposited. They suggested the belt had been extensively disrupted to form ophiolitic *mélanges* after deposition of the overlying Maitai sediments. Coombs et al. (1976), Hunt (1978), and Davis et al. (1980) also concluded that the Dun Mountain Ophiolite represents a highly disrupted ophiolite in which ultramafic rocks of the Dun Mountain Ophiolite represent portions of uplifted oceanic mantle. On a more regional scale, it is generally accepted that the Maitai Group and other specific lithologic groups can be correlated across the Alpine Fault, to both the Nelson and Otago segments of the ophiolite belt (eg., Wellman, 1956; Landis, 1980). Landis (1980) further concluded that units within the Maitai Group were derived from an earlier Permian basaltic-andesitic volcanic arc that existed to the west of the Maitai basin. These source rocks were probably similar to the arc volcanic rocks of the Brook Street terrane to the northwest. This argument appears invalid in light of more recent data.



Recent workers have concentrated on the geochemical signature of the ophiolites. Sivell and Rankin (1982) investigated metabasalts of the Patuki mélange at D'Urville Island (Figure 1.2), the northernmost terrestrial extension of the Dun Mountain Ophiolite belt. They defined two distinct suites of lavas with one suite being large-ion lithophile element enriched, the other depleted. They suggested that the lavas were formed during early-stage spreading of a poorly evolved Middle Permian sea. Sivell and Waterhouse (1984a) went on to suggest that the Patuki intrusive suite formed by closed system fractionation beneath a slow spreading oceanic ridge. As evidence, they cited the anomalously small thickness of the intrusive sequence, the non-sheeted nature of the dyke suite and the chemical characteristics of the lavas which comprise the extrusive components of the ophiolite. It was at this time that the present study commenced but since that time Sivell (1988) has delineated three stages of sea-floor magmatism within the ophiolitic rocks of the Patuki and Croisilles mélanges. These rocks include compositions characteristic of within-plate ocean islands and N-type mid-ocean ridge basalts, and a later stage of subduction-related magmas derived from a second stage melting of depleted upper mantle in a supra-subduction zone environment. Also, Korsch and Wellman (1988) have suggested that the ophiolitic mélanges (Patuki and Croisilles mélanges) are actually components of the Caples-Pelorus terrane (to the east). They propose that these ophiolitic rocks represent pieces of oceanic crust sheared off the subducted slab (ie. the basement material beneath the Caples and Pelorus sediments) during subduction. These fragments were then accreted against the inner trench wall of a westward

dipping subduction zone (represented by the base of the Dun Mountain Ultramafics).

### 1.6 Method and Scope

The aims of this present work are to investigate and describe the geology of the mafic plutonic and volcanic rocks of the East Nelson ophiolites. The study includes:

(i) a geochemical investigation of the mafic volcanic rocks of the three ophiolitic assemblages, the Dun Mountain Ophiolite and the Patuki and Croisilles ophiolitic mélanges;

(ii) an investigation of the field relationships displayed by the ophiolitic rocks; presented here as geological maps of traverses across the East Nelson ophiolites; and

(iii) a model for the evolution and emplacement of the East Nelson ophiolites.

In this study six specific areas were studied where representative rocks of the belt were both accessible and well exposed (Figure 1.2). This investigation includes detailed mapping within these areas with geochemical and petrological samples being taken in each area. Selected samples were analyzed for bulk rock major and trace element compositions as well as mineral chemistry while a lesser number were also analyzed for rare earth element abundances.

## CHAPTER 2

### REGIONAL GEOLOGY

#### 2.1 Geological History

##### 2.1.1 Cenozoic to Recent

Regionally, New Zealand occupies only a small area compared to that of the plates immediately bordering it (the Indian, Pacific and Antarctic plates). It is the interaction and relative movements of these plates which have dictated the recent geological evolution of the New Zealand region (Figure 1.1). Many of the major tectonic boundaries of New Zealand can be traced into the sea-floor well beyond the country's coastline (Figure 2.1). Tectonic movements along these boundaries produced the complex geology of New Zealand in the Cenozoic, particularly the Late Cenozoic (Korsch and Wellman, 1988). According to the relative movements along these tectonic boundaries, most of the oceanic crust surrounding New Zealand was created in the Cenozoic. A pre-Cenozoic reconstruction produced by removing the Cenozoic crust and rejoining the older elements (Figure 2.2) shows that relative displacements along the Alpine Fault match relative movements inferred from the unbending and unfauling of the New Zealand landmass for the Cenozoic (Korsch and Wellman, 1988).

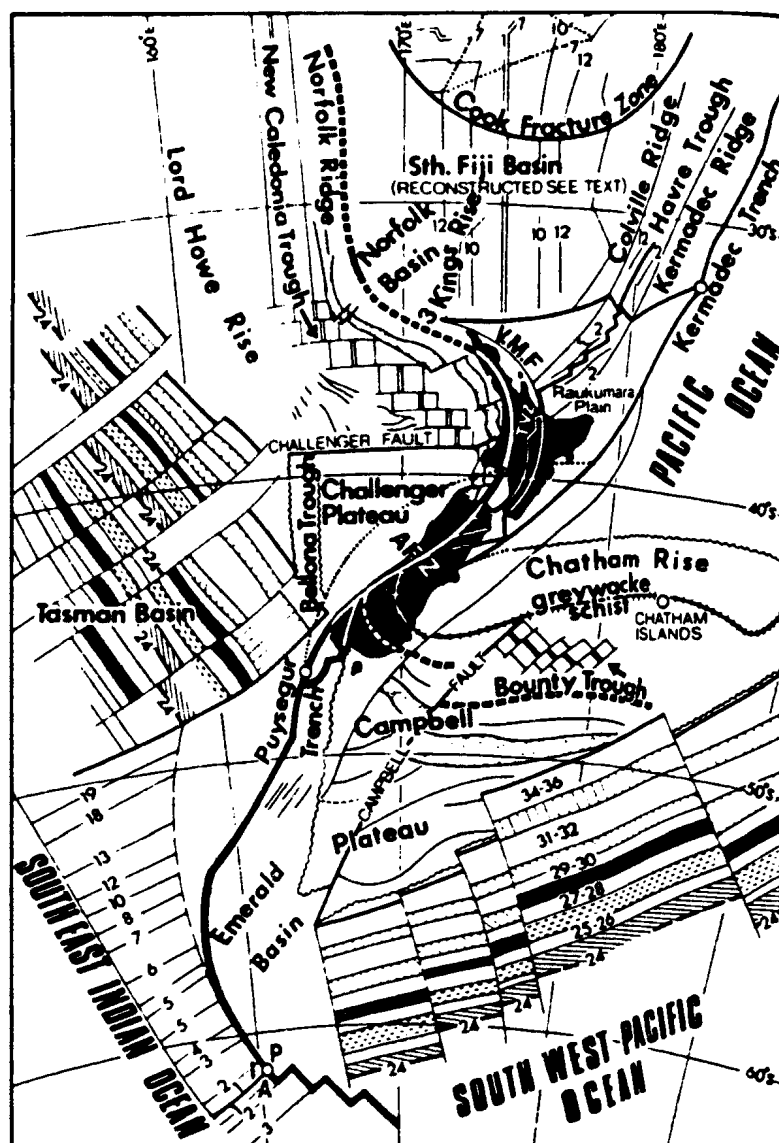


Figure 2.1 Sketch map of the New Zealand Region showing oceanic and continental magnetic lineations (from Korsch and Wellman, 1988). The map is on conical projection with standard parallels at 30°S and 50°S. V.M.F, Vening Meinesz Fault; AFZ, Alpine Fault Zone; IPA, Indian-Pacific-Antarctic Triple Junction. Triangle of dotted lines (above Cook Fracture Zone) represents the three vectors for the South Fiji Basin triple opening junction. The Stokes Magnetic Lineation (associated with the Dun Mountain Ophiolite) is shown by a heavy dashed line. Movement of the Endeavour and "3" Three Kings slides has been taken out (see Korsch and Wellman, 1988).

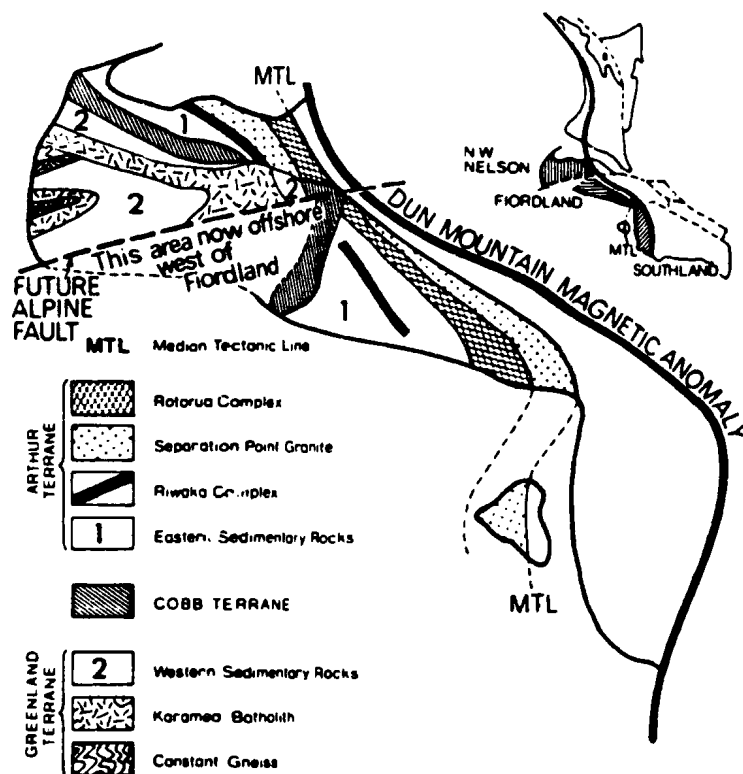


Figure 2.2 Sketch map of the pre-Carboniferous distribution of geological terranes of the Western Province (from Korsch and Wellman, 1988). The reconstruction was produced by removing Cenozoic crust and rejoining older elements of the Western Province. This suggests that relative displacements along the Alpine Fault match relative movements inferred from the unbending and unfauling of the New Zealand landmass for the Cenozoic (Korsch and Wellman, 1988). Terrane and unit names are from Korsch and Wellman (1988).

### 2.1.2 The Pre-Cenozoic

New Zealand's pre-Cenozoic geological history can be divided into three main phases of evolution after Suggate et al. (1978), related to the landmass's attachment and separation from its parent super-continent of Gondwana. These phases involved the creation and interaction of New Zealand's two geological provinces, the Western and Eastern Provinces (Figure 1.3).

In mid-Cretaceous times, the New Zealand segment of Gondwana split away and drifted towards its present position; the Western Province represents a sliver of the Gondwana craton and the Eastern Province represents a variety of terranes derived from, or accreted to the Gondwana continental margin (Molnar et al., 1975). Since this time, movement along the Alpine Fault and probable oroclinal bending have imposed an arcuate shape to rocks of the Eastern Province (eg. MacKinnon, 1983).

The first phase (the Early Geosynclinal Cycle), includes the Precambrian to Carboniferous evolution of New Zealand while it was still part of Gondwana. This phase involves older rocks of the Western Province (ie. those rocks to the west of the Alpine Fault and the Median Tectonic Line of Landis and Coombs (1967) (Figure 1.3)).

The Second phase (the Era of the New Zealand Geosyncline), Carboniferous to mid-Cretaceous, deals with subduction on Gondwana's Pacific coast and the source and accretion of the huge mass of greywacke and coesaneous rocks of the Eastern Province.

The third and last phase (the Late Mobile Phase), mid-Cretaceous to present, deals with the pre-Cenozoic separation of New Zealand from Gondwana as well as the more recent, complex tectonic activity of the Cenozoic.

These phases are discussed below in more detail. The names of the phases as given by Suggate et al. (1978) are still used here as they have been commonly used by past workers (e.g., Coombs et al., 1976), although they imply theories which are now considered inadequate in terms of modern-day plate tectonic theory. For a more complete and detailed review of New Zealand's evolution the reader is referred to descriptions by Suggate et al. (1978) and Korsch and Wellman (1988).

The first phase or the "Early Geosynclinal Cycle" includes rocks of three distinct terranes of the Western Province ranging from Precambrian to Devonian in age. These terranes consist mainly of sedimentary rocks and some crystalline rocks of both igneous and metamorphic affinity. Included in this group of rocks are the oldest known rocks of New Zealand, the Late Precambrian Constant Gneiss of northwest Nelson which have a Rb-Sr isochron age of  $680 \pm 21$  Ma (Adams, 1975). Rocks of this phase are considered vestiges of the continental forelands of Australia and Antarctica (then the supercontinent Gondwana), (eg., Campbell, 1975; Grikurov and Lopatin, 1975; Mildenhall, 1976; Carter et al., 1978; Adams et al., 1979; Crook and Feary, 1982; Korsch and Wellman, 1988). Sedimentation during this period appears to have ended during Devonian time due to uplift associated with the advancement of the Tuhua Orogeny which extended into

the Mesozoic and the second phase of New Zealand's evolution.

The second phase, the "Era of the New Zealand Geosyncline", includes Carboniferous to mid-Cretaceous rocks of the Eastern Province. During this phase, active subduction and uplift during the Tuhua Orogeny induced deformation of Gondwana's continental margin (rocks of the "Early Geosynclinal Cycle") to form the new continental forelands of Gondwana (the "New Zealand Geanticline"). Along this active continental margin arc-related plutonism may have occurred with a string of andesitic volcanoes being created above the subduction zone. Erosion of these continental forelands and volcanic arcs may have supplied a western source of abundant sedimentary material to the new Pacific continental margin of Gondwana, the "New Zealand Geosyncline" and the adjacent trench (eg., Coombs et al., 1976; MacKinnon, 1983; Korsch and Wellman, 1988). Local facies changes along this margin were common during this period as subduction-related tectonism and volcanism strongly affected the margin's topography and stability. During subduction, sedimentary material deposited within the trench was accreted against rocks of the western dipping subduction zone's inner trench wall (eg., Coombs et al., 1976; Carter et al., 1978; Sporti, 1978; Davis et al., 1980; MacKinnon, 1983). Sedimentation along the margin ceased as a result of uplift during the Mesozoic Rangitata Orogeny, although in local areas not affected by early orogenic uplift events, sedimentation persisted well into the Cretaceous (Suggate et al., 1978).

Of particular interest to this study are the volcanic and plutonic rocks of the second phase which include rocks of the East Nelson ophiolites. Until



recently, the rocks of this belt were considered by many workers (eg., Coombs et al., 1976; Davis et al., 1980; MacKinnon, 1983) to represent crust from the fore-arc basin of the western volcanic arc (ie. a fore-arc basin to the east of the Brook Street volcanics) and postulated that the Patuki and Croisilles ophiolitic mélanges represent material eroded off the fore-arc basin or outer-arc ridge (e.g. Davis et al., 1980), and deposited adjacent to the inner trench wall of the subduction zone. It has recently been suggested; however, that the ophiolitic mélanges are composed of ophiolitic rocks of different composition than those of the Dun Mountain Ophiolite (eg. Sivell and Rankin, 1984). Korsch and Wellman (1988) have further suggested that the mélanges were derived from oceanic basement material scraped off the subducted plate. In addition, Landis et al. (1987), Landis (1987) and Haston et al. (1989) have suggested that rocks of the Brook Street terrane are allochthonous to the continental margin of Gondwana and have no clearly demonstrable link with the East Nelson ophiolites.

During mid-Cretaceous time a major environmental change occurred with the climax of the Rangitata Orogeny, causing a hiatus in sedimentation over much of New Zealand. This erosional period lasted over variable lengths of time in different areas, finally ending in the Oligocene. The beginning of the third period of sedimentation, the "Late Mobile Phase", is represented by a major angular unconformity. The first sediments to be deposited above this unconformity were typically non-marine in character and coal seams are common. These rocks were in most places deposited on top of deeply weathered material and in many areas, typical basal sequences of

the Late Mobile Phase are underlain by large thicknesses of sediment suggesting differential tectonism or local changes in relief. The general sequence of sediments to be laid down during the Late Mobile Phase started with non-marine facies followed by marine sandstones, siltstones and limestones overlain by Quaternary conglomerate or gravel, suggesting marine transgression followed by regression. This was the result of either a eustatic change in sea-level or the isostatic rebound of the New Zealand landmass (Suggate et al., 1978).

The latest activity of the Late Mobile Phase began early in the Miocene and continues to the present day, as the Kaikoura Orogeny. This orogenic activity has largely resulted from Late Cenozoic movements and interactions of New Zealand's bordering oceanic plates. It involves down-warping as well as uplift and is associated with abundant volcanic activity, particularly on the North Island.

## 2.2 Regional Geology

The depositional, igneous and deformational events described above resulted in two geologically distinct provinces on South Island, the Eastern and Western Provinces (eg. Landis and Coombs, 1967). The older rocks of the Western Province are Late Precambrian to Ordovician in age, while rocks of the Eastern Province are Upper Carboniferous to Middle Cretaceous in age (eg. Korsch and Wellman, 1988). The provinces are separated by tectonically complex zones marked by faulting and intrusions referred to as the Median Tectonic Line (Landis and Coombs, 1967), and the younger, still active Alpine

Fault (Figure 1.3). The Median Tectonic Line is considered to mark the change from continental to oceanic basement (Landis and Coombs, 1967).

The Western Province consists of Palaeozoic sediments and a wide variety of crystalline rocks of Late Precambrian to Cretaceous age covering a basement of unknown, possibly sialic, composition (Landis and Coombs, 1967). Late Precambrian to Middle Devonian sediments of the Western Province are composed mainly of detritus derived from the ancient continental forelands of Gondwana. These rocks are considered to have undergone extensive high-temperature-low-pressure metamorphism and are also considered to have formed part of the Gondwana continental foreland by the mid-Palaeozoic (Cooper, 1976).

As this thesis is concerned with the East Nelson ophiolites of the Eastern Province, the geology of the Western Province is not considered further.

The Eastern Province of South Island is composed mainly of quartzofeldspathic and volcanogenic sediments of the Rangitata Orogen; the basement of which has not been recognized (Landis and Coombs, 1967). These sediments are dominated by greywackes and siltstones and contain lesser amounts of highly aluminous and quartz-rich clastic sediments than those of the Western Province. The Eastern Province contains relatively abundant mafic and ultramafic volcanic and plutonic rocks of Permian age while lacking any significant volumes of granitic intrusive rocks, other than along its western margin. This suggests that rocks of the New Zealand Geosyncline may have formed on a thin, somewhat incompetent continental

margin or possibly on oceanic crust (Landis and Coombs, 1967).

The stratigraphic nomenclature for older rocks of the Eastern Province is somewhat complicated. Coombs et al. (1976) stated, "Lithostratigraphic and tectonic nomenclature for the older rocks of New Zealand is confusing" and suggested that in many cases the problem was compounded by the different names given to similar units outcropping on opposite sides of the Alpine Fault. Recent workers have attempted to unravel much of the confusion with some success (eg., Carter et al., 1974; Coombs et al., 1976; Carter et al., 1978; Landis, 1980; MacKinnon, 1983).

In this thesis a limited number of units are recognized based on nomenclature similar to that of Coombs et al. (1976). By this scheme, the various rocks of South Island's Eastern Province are informally grouped together into lithologic units referred to as "terrane", "ophiolite belts" and "mélanges". Although more formal classifications have been proposed for the terranes of New Zealand's Eastern Province, Coomb's informal terrane classification is adopted here with modifications being made to bring the scheme in line with more recent classifications (eg., Bishop et al., 1985; Landis and Blake., 1987). From the Pacific (eastern) side inward, these terranes are the:

- (i) Torlesse terrane;
- (ii) Caples-Pelorus terrane;
- (iii) Greenstone and Croisilles ophiolitic mélanges;
- (iv) Patuki ophiolitic mélange;
- (v) Dun Mountain-Maitai terrane;

(vi) Murihiku terrane; and,

(vii) Brook Street terrane (Figure 1.3).

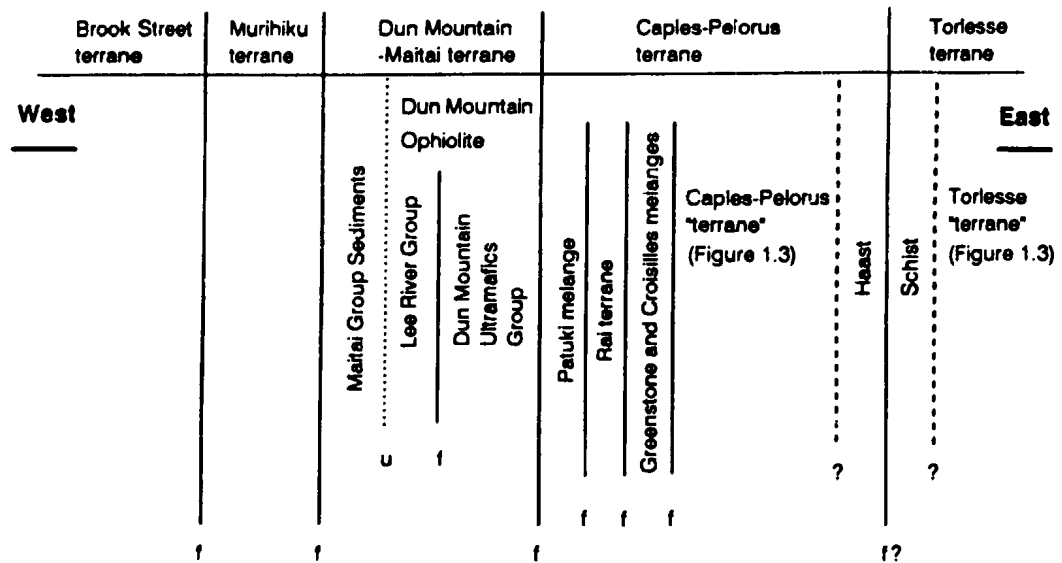
Each terrane is fault bounded and regional in its extent and is defined by differences in lithology, structure, and metamorphism. An outline of these terranes is presented in Table 2.1.

The main deviation from the classification of Coombs et al. (1976) is the omission of the Haast Schist as a separate terrane. This omission is in line with that of Bishop et al. (1985) who pointed out that the Haast schists represented a zone of increased metamorphic grade which straddles the contact between the two terranes and therefore represents metamorphosed equivalents of the adjacent Torlesse and Caples-Pelorus terranes. Bishop et al. (1985) considered the boundary between these terranes to exist as a cryptic suture within the Haast schists.

Another modification made here to the classification scheme of Coombs et al. (1976) is the grouping together of the Dun Mountain Ophiolite and the Maitai terranes. This reclassification was initially made by Bishop et al. (1985) to conform with modern terrane theory (eg. Jones et al., 1982) as the Maitai Group sediments are known to locally share stratigraphic contacts with rocks of the underlying Dun Mountain Ophiolite.

Other, in depth descriptions of the Eastern Province has been given by Blake et al. (1974), Coombs et al. (1976), Carter et al. (1978), Korsch and Wellman (1988) and Bradshaw, (1989).

## PROVISIONAL TERRANES OF THE EASTERN PROVINCE OF NEW ZEALAND



f = fault  
u = unconformity

Table 2.1 Classification of provisional terranes used in this study. The table indicates the various terranes of the Eastern Province of South Island, New Zealand (from west to east). Lines noted by "f" indicate a faulted contact; "u" indicates an unconformity. Question marks indicate debated contact relationships (particularly between the Haast Schist and the bordering terranes. Within this study (as indicated by the table) the Patuki melange, Rai terrane and Croisilles terrane have been classified as a sub-terrane of the Caples-Pelorus terrane. It should be noted; however, that this classification scheme is strictly informal and not to be confused with formal tectonostratigraphic schemes such as that of Bishop et al. (1985).

## 2.3 Geological Outline of the Eastern Province

### 2.3.1 Torlesse Terrane

The Torlesse terrane (Figure 1.3) makes up the eastern side of the Eastern Province and is composed predominantly of quartzo-feldspathic sandstones, greywacke-argillite assemblages (eg., Dickinson, 1971, 1982; Beggs, 1980; MacKinnon, 1983) with minor occurrences of metabasalt, chert, red and green argillite, conglomerate, and limestone. The sediments of this terrane are considered to have been derived from a complex source as they are composed of a mixture of plutonic, sedimentary, and volcanic detritus, probably representing convergent Andean-type margin deposits (Coombs et al., 1976). These rocks are structurally complex in character occurring within steeply plunging, overturned folds (Lillie and Gun, 1964), local tectonic slides (Bradshaw, 1972) and *mélange* zones (Bradshaw, 1973).

Basaltic units of the Torlesse terrane are widespread and spilitic in character, occurring with subordinate hyaloclastites, and are commonly accompanied by rare occurrences of radiolarian cherts, red to pale-green argillites, and rarer shelly limestones (eg., Reed, 1957; Bradshaw, 1972, 1973; Pringle, 1980; Grapes and Palmer, 1984). Flows are in places pillowed and usually occur in packages less than 50 metres thick extending over distances of a few hundred metres to several kilometres along strike. The largest occurrence is about 750 metres thick and can be traced approximately 25 kilometres along strike (Bishop et al., 1976; Pringle, 1980). Some of the basaltic rocks occur within sedimentary *mélange* zones devoid of gabbroic and ultramafic rocks (Bradshaw, 1973). These basalts are considered by

Grapes and Palmer (1984) to have been tectonically intruded among the sediments (Torlesse terrane) and have tholeiitic compositions similar to those erupted at mid-ocean ridge and intra-plate (ocean island) settings. Coombs et al. (1976) and MacKinnon (1983), on the other hand, consider these basaltic rocks to be representative of interbedded submarine flows.

The majority of sediments within the unmetamorphosed Torlesse terrane are thought to represent material deposited in major, deep marine fans occurring along a continental margin (Carter et al., 1978).

Along the western margins of the Torlesse terrane, sedimentary and metasedimentary rocks grade laterally into rocks of dominantly greenschist grade metamorphism, known as the Haast schists. These schists are generally more volcanogenic in composition than unmetamorphosed Torlesse sediments and are associated with metacherts considered to have been derived from pelagic sediments similar to those associated with the Torlesse and Caples-Pelorus submarine volcanics (Coombs et al., 1976). Because of the high content of volcanogenic material and the schistose character of these rocks, it has been suggested by Norris and Henley (in Coombs et al., 1976), that this zone represents an imbricated suture between the largely volcanogenic Caples-Pelorus terrane (described below) and the more quartzofeldspathic sandstones of the Torlesse terrane. MacKinnon (1983) went further to suggest that the Haast schists represent Torlesse and Caples-Pelorus terrane rocks metamorphosed during collision with a volcanic arc system along an oblique transform fault during Late Triassic to Early Jurassic time.



Included in the Haast schists are rare pods of serpentinite (Cooper, 1976) which form the Pounamu ultramafics of central Westland (the western side of South Island) (Coombs et al., 1976).

The source area for the Torlesse terrane is somewhat equivocal. Some models suggest an eastern source area where oceanic crust now prevails (eg., Bradshaw and Andrews, 1973; Blake et al., 1974, Coombs et al., 1976; Carter et al., 1978) while others agree with earlier models in which the sediments were derived from the western forelands of Gondwana (eg., MacKinnon, 1983; Korsch and Wellman, 1988).

Continental drift models have suggested that during mid-Cretaceous time, the Campbell Plateau-New Zealand landmass separated from the Marie Byrd Land region of West Antarctica (Molnar et al., 1975). One point worth noting here however, is that it is generally accepted that rocks of the East Nelson ophiolites were juxtaposed against rocks of the older Caples-Pelorus terrane prior to the deposition of the younger sediments of the younger Torlesse terrane (eg., Coombs et al., 1976; Carter et al., 1978). This suggests that older terranes had already been juxtaposed (accreted) within a subduction zone prior to the deposition of younger Torlesse sediments.

### 2.3.2 Caples-Pelorus Terrane

Separating the Torlesse terrane from rocks of the Dun Mountain Ophiolite to the west, is the Caples-Pelorus terrane (Figure 1.3). Within the terrane classification used here, the Caples-Pelorus terrane is considered to include a number of smaller terranes which may represent disrupted slivers of

basement and sedimentary material of the Caples-Pelorus terrane or exotic material, particularly the Patuki mélange, Rai terrane and the Croisilles mélange (Table 2.1). As the nature of these smaller terranes is a topic of debate, they have been included within the Caples-Pelorus terrane as a matter of convenience. It should be emphasized however, that this classification does not represent a formal tectonostratigraphic classification of the terranes of the Eastern Province.

Rocks of the Caples-Pelorus terrane are dominated by relatively unmetamorphosed, largely unfossiliferous greywackes and argillites which are associated with minor spilitic volcanic, limestone, and cherty horizons (eg. Coombs et al., 1976). These rocks grade towards the east into progressively more strongly metamorphosed rocks of the Haast Schists.

Sedimentary rocks of the Caples-Pelorus terrane were initially given separate names in the Otago and Nelson areas; as a result these rocks include the Caples Group of Western Otago, the Pelorus Group of East Nelson. Also included within the terrane are rocks of the Waipapa Group of North Island (not discussed here).

Excluding rocks of the Haast Schists, rocks of the Caples-Pelorus terrane are generally complexly deformed (e.g. Turnbull, 1980) and weakly metamorphosed, and locally are divided longitudinally by sheared ophiolitic rocks of the Croisilles mélange (Nelson Segment) and Greenstone mélange (Otago segment).

In the Nelson area (Figure 1.2), Caples-Pelorus terrane rocks occur to the east of the Dun Mountain Ophiolite and Patuki mélange and west of the

Marlborough schists of the Torlesse terrane. In this area the rocks are here known as Pelorus Group sediments (Coombs et al., 1976). Rocks of the Pelorus Group are dominated by semi-schistose to less deformed volcanogenic sandstones and argillites considered to have been derived from an andesitic source composition (Vitaliano, 1968).

As previously mentioned, rocks of the Caples-Pelorus terrane can be further subdivided into a number of smaller tectonic terranes (eg. Landis and Blake, 1987). Included within these are the Rai terrane, Croisilles ophiolitic mélange and the Patuki ophiolitic mélange. The Rai terrane is composed of sandstone dominated sediments which occur west of, and possibly on top of (Dickins et al., 1986) rocks of the Croisilles mélange (Figure 1.2). These sediments are somewhat similar to those of the Caples-Pelorus which outcrop east of the Croisilles mélange. As this is the case, rocks of the Rai are informally grouped together here with those of the Caples-Pelorus terrane (eg., Davis et al., 1980; Johnston, 1981).

Until recently, the sediments were considered to represent more distal relatives of sedimentary rocks of the Murihiku and Dun Mountain-Maitai terranes described below (eg., Blake et al., 1974; Coombs et al., 1976; Carter et al., 1978; Davis et al., 1980; and MacKinnon, 1983). Landis and Blake (1987) however, suggest on the basis of sedimentological and petrochemical data that these rocks may be distinct from the Maitai and Brook Street rocks and therefore may not be regarded as shallow-, intermediate- and deep-water portions of one contemporaneous sedimentary system. They proposed that the sediments of the Caples-Pelorus terrane may have been derived from an

arc terrane since removed by tectonic processes, rather than the Brook Street terrane. The origin of these sediments therefore still remains a subject of debate.

### 2.3.3 Croisilles and Greenstone Ophiolitic Mélanges

As previously mentioned, rocks of the Rai terrane are separated from other sediments of the Caples-Pelorus terrane by a narrow belt of sheared, discontinuous ophiolitic rocks known as the Croisilles mélange (Waterhouse, 1964). Rocks of this mélange (Figure 1.2) are also similar to those of the nearby Patuki mélange 3 to 5 km to the west. Locally, the Croisilles mélange reaches a maximum width of 3 km; however, it generally pinches out along strike as discontinuous slivers between rocks of the Rai terrane to the west and other sedimentary rocks of the Caples-Pelorus terrane to the east. Rocks of the mélange are exposed as a mixture of discrete tectonic blocks set in a matrix of sheared serpentinite and occasionally sheared argillite (Davis et al., 1980). Blocks are composed of a variety of lithologies including: spilitic basalt, gabbro, diabase, amphibolite, serpentized peridotite, rare plagiogranite, argillite, volcanic sandstone, chert, volcanic breccia, and exogenous conglomerate (Coombs et al., 1976). Many of the blocks are strongly altered containing albite, tremolite, stilpnomelane and hydrogrossular (rodingitized), and are resistant to erosion. As a result, the typical topography developed within the mélange is relatively low and hummocky with knockers of more resistant material jutting out above the more easily eroded sheared serpentinite-argillite matrix.

Blocks of volcanic breccia from the *mélange* have yielded a restricted assemblage of fossils, particularly the Early Permian gastropod, Mourlonia impressa (Waterhouse, 1966) and the allegedly younger, Mourlonia (strzeleckiana) (Dickins et al., 1986). Sandstones of the adjacent Rai terrane to the west; however, have yielded poorly preserved plant remains (McQueen, 1954), worm borings and atomodesmatinid fragments (Dickins et al., 1986).

Although little has been published on the nature of the Croisilles *mélange* (eg., Waterhouse, 1966; Coombs et al., 1976), some workers (eg., Dickins et al., 1986; Landis and Blake, 1987) have suggested that rocks of the Croisilles and Patuki *mélanges* were developed from the same Lower Permian sea-floor sequence as the Dun Mountain Ophiolite. More recently Sivell (1988) has postulated on the basis of geochemical data, that basalts of the Croisilles and Patuki *mélanges* are chemically different from those recognized within the Dun Mountain Ophiolite.

Rocks of the Greenstone *mélange* of west Otago are similar to those of the Patuki and Croisilles *mélanges* containing packages of ophiolitic rocks smeared out along discontinuous belts east of the Otago portion of the Dun Mountain Ophiolite (eg., Kawachi, 1974 and Coombs, 1976). Blocks in the *mélange* are in places up to 1 km across and include: metagabbro, amphibolite, pillow lavas, mafic, psammitic and pelitic schists as well as other rodingitized and metasomatized rocks (Coombs et al., 1976).

Some noticeable differences between the Dun Mountain Ophiolite and the Greenstone and Croisilles *mélanges* are the lack of a strong aeromagnetic signature for the *mélanges*, and the fact that the *mélanges* do not appear to

represent zones of major dislocation as they are sometimes flanked on both sides by rocks of the Caples-Pelorus terrane without any obvious, significant dislocation (Bishop et al., 1976). As a consequence, the relationship between the ophiolitic mélanges and the Dun Mountain Ophiolite is not clear.

#### 2.3.4 Patuki Mélange

Directly to the east of the Dun Mountain Ophiolite lies a belt of sheared ophiolitic and sedimentary blocks in a matrix dominated by sheared serpentinite. This semi-continuous belt is known as the Patuki mélange (Figure 1.2). The belt possesses a hummocky topography and is up to 4.5 km wide with blocks of more resistant material standing up to 20 m high or more. Sizes of individual blocks range from a few metres to a few kilometres and include such features as Little Twin and Maungatapu mountains (Davis et al., 1980). For the most part, the lithologies are similar to those observed within the Croisilles mélange but appear to be less deformed and faulted.

The origin of the Patuki mélange is equivocal and a number of theories have been proposed. In the past it was generally thought that the ultramafic and mafic rocks of Patuki mélange represented portions of the Dun Mountain Ophiolite that had been highly disrupted to form a tectonic mélange (eg. Blake and Landis, 1973) with similar origins being proposed by Coombs et al. (1973); Hunt (1974); and Coombs et al. (1976). Davis et al. (1980); however, proposed an olistostromal origin for these rocks suggesting they were composed of material eroded off the Brook Street volcanics and Dun Mountain Ophiolite to the west. They proposed that this eroded material had

been transported eastwards and deposited within an active trench.

Sivell and Rankin (1982) and Sivell and Waterhouse (1984a,b), on the other hand, consider that volcanic and plutonic sequences of the Patuki mélange from D'Urville Island formed by closed system fractionation during slow spreading of poorly evolved Mid-Permian sea-floor. Later, Sivell and Waterhouse (1986) suggested that these lavas as well as lavas of the Croisilles mélange were not genetically related to the ultramafic rocks of the adjacent Dun Mountain Ophiolite. They concluded that the Patuki and Croisilles mélanges were not derived from the Dun Mountain Ophiolite and suggested that the lavas of the mélanges predate it as they are intruded by serpentinized ultramafic rocks of the Dun Mountain Ophiolite as sill-like bodies occupying slightly different levels along strike within the Patuki mélange.

More recently, Sivell (1988) has shown that the Patuki lavas were produced during three distinct magmatic episodes whereby initial generation of the Croisilles and Patuki magmas (stage 1 and 2 magmas) occurred within a small ocean basin (most likely in a "leaky" transform fault setting), followed by generation of lavas (stage 3) produced in a fore-arc environment above a subduction zone. He also suggests that both the Patuki and Croisilles mélanges comprise identical lava suites not recognized within volcanic rocks of the Lee River Group of the Dun Mountain Ophiolite. Therefore, he concludes that volcanic rocks of the Patuki and Croisilles mélanges do not represent mélange material derived from the adjacent ophiolite.

### 2.3.5 Dun Mountain-Maitai Terrane

In fault contact with the Patuki and Croisilles mélanges to the east and rocks of the sedimentary Murihiku terrane to the west, lies the Dun Mountain-Maitai terrane. This terrane is described here in two parts, the Dun Mountain Ophiolite to the east, and the overlying Upper Permian, Maitai Group sediments to the west (Figure 1.2). These units had previously been informally classified as two separate terranes (eg. Coombs et al., 1976) but may now be considered as one (Bishop et al., 1985).

The fault contact between rocks of the Dun Mountain Ophiolite to the west and the Patuki mélange to the east is generally considered to be a zone of major tectonic discontinuity and likely represents the contact between rocks of the overriding plate and the subducted slab in a westward dipping subduction zone (e.g., Coombs et al., 1973; Coombs et al., 1976; Davis et al., 1980).

Johnston (1981) described the ophiolite as two distinct lithological components, (or groups); a distinctive suite of ultramafic rocks (the Dun Mountain Ultramafics Group), and a suite of mafic volcanic and plutonic rocks (the Lee River Group). Together, these rocks make up the basal and upper components of the Dun Mountain Ophiolite respectively. Rocks of the Dun Mountain Ultramafics Group vary in composition from basal, protoclastic harzburgites up through tectonized dunite and harzburgite, layered peridotites and pyroxenites, to serpentinite with gabbro dykes at the upper contact (Davis et al., 1980). Rodingite dykes are also widespread in the upper part of the sequence. In fault contact above these ultramafic rocks lie mafic plutonic and



volcanic rocks of the Lee River Group. This sequence ranges upwards through gabbros and sheeted mafic dykes, to poorly developed sequences of mafic, spilitized volcanic rocks (including pillowed flows and breccias).

Contacts between individual lithologies of the Lee River Group are generally steeply dipping and stratigraphically higher units outcrop along the western margin of the belt. The upper contact is unconformable with Maitai Group sediments. Coombs et al. (1976) suggested that the Dun Mountain Ophiolite represented pieces of oceanic crust formed by sea-floor spreading east of a volcanic arc (the Brook Street terrane, described below) and west of a possibly westward dipping subduction zone. By this model, the adjacent Caples-Pelorus and Torlesse terranes were rafted into the subduction zone to flank the Dun Mountain-Maitai and Murihiku terranes described below.

The Red Mountain Ophiolite Complex, an Otago segment exposure of the Dun Mountain Ophiolite, was described by Sinton (1980) as an almost complete ophiolite. He also proposed that the ophiolite was formed by sea-floor spreading in a marginal basin environment. Davis et al. (1980) considered the Dun Mountain Ophiolite of the Nelson segment to have evolved in a similar environment, where the volcanic rocks were formed as either a mid-ocean ridge tholeiite or low-K tholeiite at an island-arc. A Lower Permian mid-ocean spreading ridge was favoured however, in which basaltic melts were produced by melting of a depleted mantle source. In their model, the Dun Mountain Ophiolite formed a fore-arc basin to the east of the Brook Street volcanic arc, adjacent to the continental margin of Gondwana. This fore-arc basin was positioned on the leading edge of the obducting plate

while oceanic crust was subducted westward below the ophiolite. During this period Maitai Group sediments, mostly derived from the Brook Street volcanic arc were deposited in the fore-arc basin on top of the ophiolite.

Thus the ophiolite has been interpreted to have formed in two possible environments, either at a mid-ocean ridge (eg., Davis et al., 1980; Sinton, 1980) or in close proximity of a subduction zone (eg., Sinton, 1980; Davis et al., 1980).

Rocks of the Maitai Group are found associated with both the Nelson and Otago segments of the ophiolite, being known as the Bryneira Group in western Otago (Waterhouse, 1964). The contact between these sediments and the ophiolite is commonly tectonic in character although unfaulted, unconformable contacts are exhibited locally (eg. Waterhouse, 1964). The base of the Maitai Group is sometimes difficult to define as splitic breccias commonly occur at the top of the ophiolite sequence. These breccias are close in character to the basal formation of the Maitai Group, the Upukerora Formation (described below) (Landis, 1974a; Coombs et al., 1976).

The basal formation of the Maitai sequence is generally considered to be the Upukerora Formation and its correlatives (eg., Landis, 1974a; Coombs et al., 1976). This formation is composed of red and green volcanic conglomerates and breccias. Although its origin is somewhat speculative, most workers consider it to have been derived from the uppermost volcanics of the Dun Mountain Ophiolite. This formation is succeeded by discontinuous units of fossiliferous limestones (eg. Davis et al., 1980) of the Wooded Peak Limestone (Waterhouse, 1964). Overlying these limestones are sequences of

deep water sandstones, the youngest of which indicate a return to shallower conditions (eg., Coombs et al., 1976; Davis et al., 1980). The Maitai Group is folded about the north-northeast to northeast and east-northeast striking axis of the broad, near isoclinal, Nelson Regional Syncline (eg., Coombs et al., 1976; Davis et al., 1980).

Coombs et al. (1976) and others (eg., Carter et al., 1978; Landis, 1980; MacKinnon, 1983; Cawood, 1984; Landis and Blake, 1987) consider the Maitai Group to be composed of material derived from the erosion of a largely inactive volcanic arc to the west, while Davis et al. (1980) suggest the sequence also contains material eroded off an outer-arc ridge. Although the Brook Street terrane has previously been considered a likely source of Maitai Group sedimentary material, recent work suggests this to be unlikely (eg., Landis et al., 1987; Haston et al., 1989, Frost and Coombs, 1987).

#### 2.3.6 Murihiku Terrane

In fault contact with sediments of the Maitai Group to the northwest (Nelson segment) and southwest (Otago segment) lies the largely sedimentary Murihiku terrane (Figure 1.3) (Landis et al., 1987, Landis, 1987). This terrane consists of a sequence of folded, highly volcanogenic, mostly marine, Triassic and Jurassic sediments. The sequence has a maximum preserved thickness of 10 km and was previously known as the Murihiku Supergroup (Campbell and Coombs, 1966). As the Murihiku sediments lack volcanic flow material and are richer in ash material than sediments of the Maitai terrane they are considered to have been derived from a more mature volcanic arc source

than that which supplied the underlying Maitai Group (Coombs et al., 1976).

The source for the Murihiku sediments is considered to have changed a number of times during its evolution (Boles, 1974) and is considered to have an arc or continental origin (eg. Frost and Coombs, 1987). In the Middle Triassic the composition of the sediments changed from being dominantly andesitic to dominantly acidic in composition. Later, in Late Triassic times, the source was again of andesitic composition (Boles, 1974). These changes most likely reflect a compositional change in the volcanism and associated plutonism of the source to the west.

In the past, many workers considered these sediments to have been derived from a western source, likely the Brook Street terrane (eg., Coombs et al., 1976; Stevens and Speden, 1978; MacKinnon, 1983); but recent work (eg., Landis et al., 1987; Haston et al., 1989, Frost and Coombs, 1987) has shown that these terranes are likely spatially and genetically unrelated.

#### 2.3.7 Brook Street Terrane

Outcropping on the western margin of the Eastern Province are metabasaltic pillow lavas, porphyritic andesites, volcanic breccias, volcanogenic sediments, and associated intrusives of Early to Middle Permian age (eg., Wellman, 1952; Bruce, 1962; Waterhouse, 1964; Mossman and Force, 1969). These rocks are variously known as the Brook Street Volcanics (Figures 1.2 and 1.3), Eglinton Volcanics, Takitimu Group, Greenhills Group and the Brook Street terrane. Although it has been interpreted to unconformably underlie sediments of the Murihiku terrane recent

workers suggest the contact to be faulted (Landis et al., 1987; Landis, 1987). Rocks of the Brook Street terrane have been intruded by complexes of varying compositions from dunite-wehrlite-eucrite (Mossman, 1973) to gabbroic and granitic intrusions (Grindley, 1958). This terrane is generally considered to represent a volcanic arc (eg. Wellman, 1956) which was active during Permian to possibly Upper Jurassic time (Stephens and Speden, 1978; MacKinnon, 1983).

The Brook Street terrane has generally been considered to have evolved to the east of the Gondwana continental margin as a volcanic arc (Wellman, 1956) and has previously been credited with having provided sedimentary material to the marginal basin and arc-trench system of the Dun Mountain Ophiolite (e.g., Coombs et al., 1976, Davis et al., 1980, MacKinnon, 1983). Recent palaeomagnetic investigations; however, suggest that the Brook Street terrane is allochthonous to the margin of Gondwana (Haston et al., 1989) and therefore shares no clearly demonstratable links with other terranes of the Eastern Province prior to Cretaceous time (see Haston et al., 1989).

## CHAPTER 3

### GEOLOGY OF THE EAST NELSON OPHIOLITES

#### 3.1 Introduction

The ophiolites of East Nelson occur as three separate, mappable occurrences: the Dun Mountain Ophiolite, the Patuki ophiolitic mélange and the Croisilles ophiolitic mélange. All three occur in close proximity to one another (generally within 8 kilometres) as three parallel belts (Figure 1.2). This close proximity in conjunction with the general similarity of the lithologies observed within the belts, had in the past, promoted their grouping together into a single unit or belt (see Challis, 1969). It is now generally accepted that such a grouping is an oversimplification and many workers now describe the ophiolites of East Nelson as three separate entities; although, many suggest that they were derived from the same oceanic crust (eg., Coombs et al., 1976; Johnston, 1981; Davis et al., 1980; Blake and Landis, 1987). In this section the three ophiolites are described individually in an attempt to determine if and how they are related.

The Dun Mountain Ophiolite of the Dun Mountain-Maitai terrane is the best preserved and studied of the ophiolites of East Nelson (eg., Challis, 1965a,b; Challis and Lauder, 1966; Walcott, 1969; Hunt, 1978; Davis et al., 1980; Johnston, 1981; Sivell et al., 1986). This ophiolite outcrops as a semi-

continuous belt which stretches a distance of approximately 150 kilometres along strike and extends from the southwest margin of the Red Hills to the northeast coast of D'Urville Island (Figure 1.2). Locally the belt reaches an exposed width of 8 kilometres (Red Hills) but generally is no more than 2 kilometres wide.

The Dun Mountain Ophiolite is made up of at least two distinct lithologic groups, the Lee River Group and the underlying Dun Mountain Ultramafics Group (after Johnston, 1981). The Lee River Group makes up the upper portion of the ophiolite and consists of basaltic flows, a poorly developed sheeted dyke complex, and a thin sequence of gabbroic rocks. Lying structurally beneath and in fault contact with rocks of the Lee River Group to the east are rocks of the Dun Mountain Ultramafics Group (Figure 1.2). The rocks of this group are predominantly composed of harzburgite, pyroxene peridotites, and dunite; and possess foliations considered to have been produced during primary mantle deformation (Davis et al., 1980).

Some sections through the ophiolite are incomplete and lack rocks of either the Lee River Group or the Dun Mountain Ultramafics Group. Many of these local absences have been attributed to faulting within the Dun Mountain Ophiolite as the East Nelson ophiolites are traversed by major faults striking between north-northeast and northeast (eg., Davis et al., 1980). These faults branch off the Alpine Fault to the southwest and in places display recent traces. Many are considered to have significant vertical and dextral transcurrent components (Davis et al., 1980). Associated with this system is a second set of subordinate faults which strikes approximately perpendicular

to the major faults. These are commonly truncated by the major northeast striking system and movements along the subordinate faults are generally almost entirely vertical (Davis et al., 1980).

In the East Nelson area the Patuki *mélange* (Figure 1.2) forms a semi-continuous belt which strikes parallel to the Dun Mountain Ophiolite and stretches from the western margin of the Red Hills to the northern tip of D'Urville Island. Locally the *mélange* reaches an exposed width of 6 kilometres (near Dun Mountain) but is typically no more than a kilometre wide. Although the *mélange* is not subdivided into formations here, a crude basalt stratigraphy has been identified locally on north D'Urville Island (Sivell and Rankin, 1982). Rocks of the Patuki *mélange* are also cut by the same network of faults that disrupt rocks of the Dun Mountain Ophiolite (Johnston, 1981).

The Croisilles *mélange* (Figure 1.2) is similar in character to the Patuki *mélange* in the East Nelson region but is often significantly more disrupted. It consists of a disconnected trail of isolated ophiolitic *mélange* segments and extends from the eastern margin of the Red Hills to the Trio Islands (Beck, 1964) of Admiralty Bay (ie. a small group of tiny islands approximately 1.5 kilometres due east of D'Urville Island). Locally, the Croisilles *mélange* reaches a width of approximately 2.25 kilometres (Dickins et al., 1986) but often is no more than 0.5 kilometres wide. This *mélange* has not been subdivided into formations here and no internal stratigraphy has previously been identified (eg. Landis and Blake, 1987). Rocks of the Croisilles *mélange* are also disrupted by the same system of faults that dissect the other East



**Nelson ophiolites (Johnston, 1981).**

To date the most comprehensive maps of the East Nelson ophiolites are the 1:50,000 scale maps of Johnston (1981, 1982). In addition to these, local areas have recently been mapped in greater detail particularly in the vicinity of Croisilles Harbour (e.g., Dickins et al., 1986; Blake and Landis, 1987) and D'Urville Island (Sivell, 1986).

### **3.2 Field Relationships**

#### **3.2.1 Introduction**

In this section the geology of each of the East Nelson ophiolites is discussed with reference to seven areas studied as part of this thesis (Figures 3.2.1 to 3.2.6). The rocks are described using the classification scheme of Johnston (1981) with some minor modifications being made so that the ophiolites are described in terms of lithologies rather than formations. Thus, under the classification scheme used here the Lee River Group of the Dun Mountain Ophiolite is not subdivided into the Glennie and Tinline Formations (Johnston, 1981), but rather into basalt, sheeted dyke, and gabbro complexes according to the stratigraphy of an ophiolite as defined by participants of the Penrose Ophiolite Conference (1972).

#### **3.2.2 Red Hills Western Margin (Figure 3.2.1)**

In this area rocks of the Dun Mountain-Maitai terrane were mapped and interpreted. These rocks include from west to east: Maitai Group clastic sediments; limestones of the Wooded Peak Formation; representative

lithologies of the Upukerora Formation; isotropic gabbros and diabase dykes of the Lee River Group; a complex of sheared serpentinite and tectonic inclusions; and, deformed ultramafic rocks of the Dun Mountain Ultramafics Group.

The Maitai Group clastic sediments consist of grey-blue, finely bedded siltstones and sandstones which generally strike northeast and dip steeply towards the southeast (unit mt, Figure 3.2.1). These rocks are interpreted to lie in fault contact to the east with a package of rocks consisting of lower formations of the Maitai Group and gabbro and diabase dykes of the Lee River Group. This package of rocks appears to be an unfaulted sequence.

Stratigraphically, the highest rocks of this unfaulted sequence are grey, finely bedded, fine-grained limestones of the Wooded Peak Formation (Plate 3.1) (unit wp, Figure 3.2.1). These limestones generally strike in a northeasterly direction, are in places steeply tilted, and locally are overturned in the northern half of the map area. Rocks of the Wooded Peak Formation lie unconformably above conglomerates of the Upukerora Formation and locally, where the Upukerora Formation is absent, on top of gabbro of the Lee River Group (north side of the map area).

Within this sequence the Upukerora Formation (unit up, Figure 3.2.1) consists of a conglomerate composed of angular to sub-rounded clasts of basalt and gabbro supported in a red, hematite-stained, mud and sand matrix (Plates 3.2a and b). The clasts range in size from less than a centimetre to 20 centimetres in diameter.



**Plate 3.1** Fine-grained, grey-blue weathering Wooded Peak limestones of the Maitai Group (Red Hills, R-916). Hammer for scale.





**Plate 3.2a Hematite-stained Upukerora conglomerates of the Maitai Group (Red Hills, R-931).**



**Plate 3.2b Angular clasts suspended in a hematite-stained muddy matrix, Upukerora Formation (Red Hills, R-931).**

Unconformably underlying the Upukerora conglomerates are isotropic gabbros of the Lee River Group (Plate 3.3) (unit Ir, Figure 3.2.1). These gabbros are almost entirely composed of clinopyroxene (altered to green amphibole) and altered plagioclase, and are in places cut by numerous fine-grained diabase dykes. These dykes are generally steeply dipping and strike in a northeast-southwest direction. Although the Lee River Group gabbros are isotropic in character with little, if any, compositional or textural changes being observed from outcrop to outcrop, a weak foliation is locally observed. The grain size of the gabbros typically ranges between 1 and 3 millimetres.

Locally (in the north half of the map area), limestones of the Wooded Peak Formation overly gabbro of the Lee River Group along, what is interpreted to be, an angular unconformity. Associated with limestone beds directly above this contact are intercalated beds (2 to 10 centimetres thick) of green, fine-grained sandstone (Plate 3.4). These fine-grained sandstone beds contain abundant crystal fragments (dominantly plagioclase) and altered rock fragments, in an altered, fine clay-like matrix (Plate 3.5a). Other clasts observed in the sandstones include sponge spicules of unknown origin (Plates 3.5b and c). Similar sandstone units up to 30 m wide are also observed at other levels in the Wooded Peak limestone in the map area and are considered to be tuffaceous in origin (Figure 3.2). In this map area Lee River Group gabbros are therefore considered to represent basement material upon which Maitai Group sediments were deposited.

The above sequence is bounded to the east by a wide fault zone consisting of metamorphosed inclusions of both the Lee River Group and the



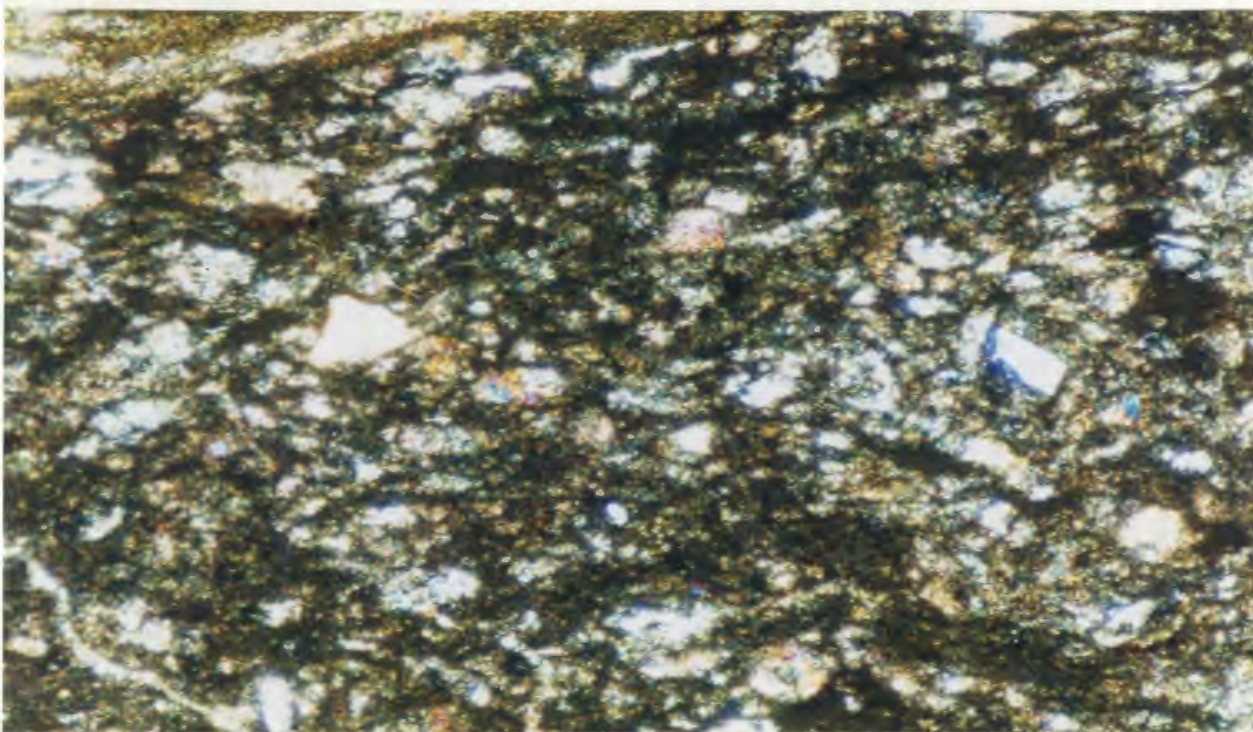


**Plate 3.3** Diabase dyke intruding medium-grained Lee River Group gabbro (Red Hills, R-907).

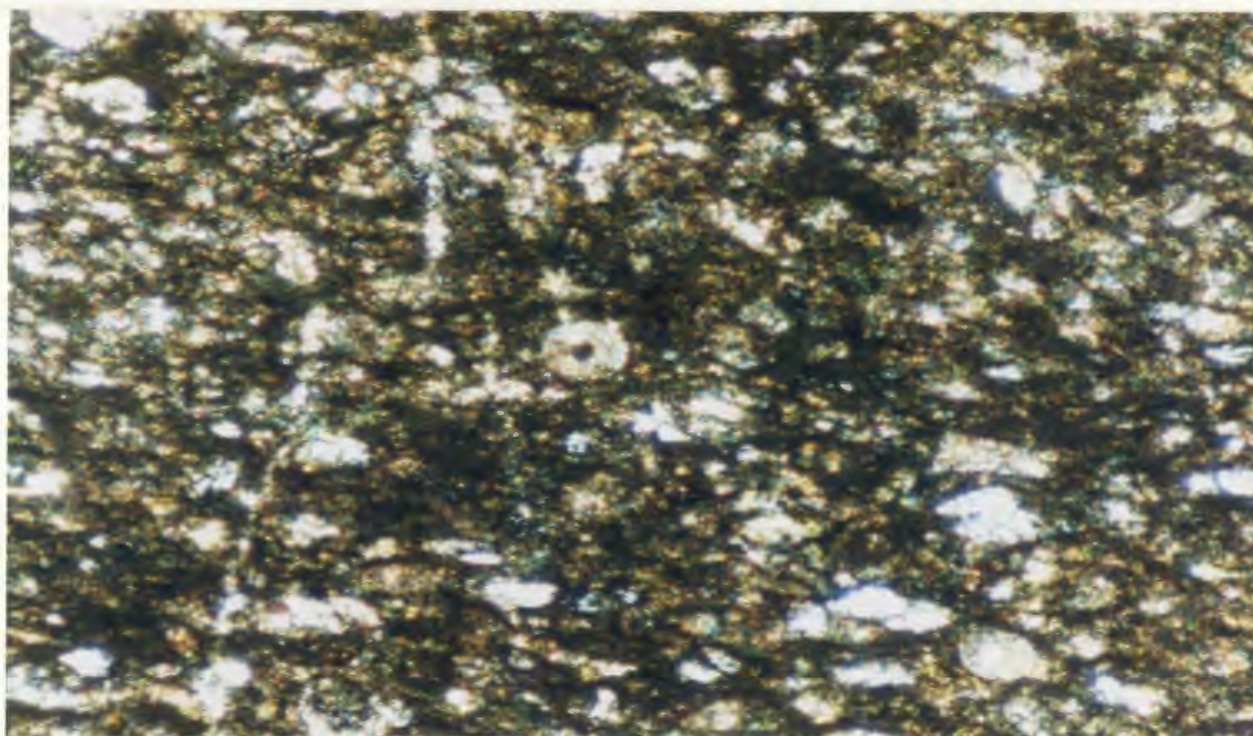


**Plate 3.4** Wooded Peak limestone intercalated with beds of green, fine-grained sandstone (Red Hills, R-921). Sandstone beds are between 2 and 10 centimetres thick and are partially overgrown by moss in the bottom left of the picture.



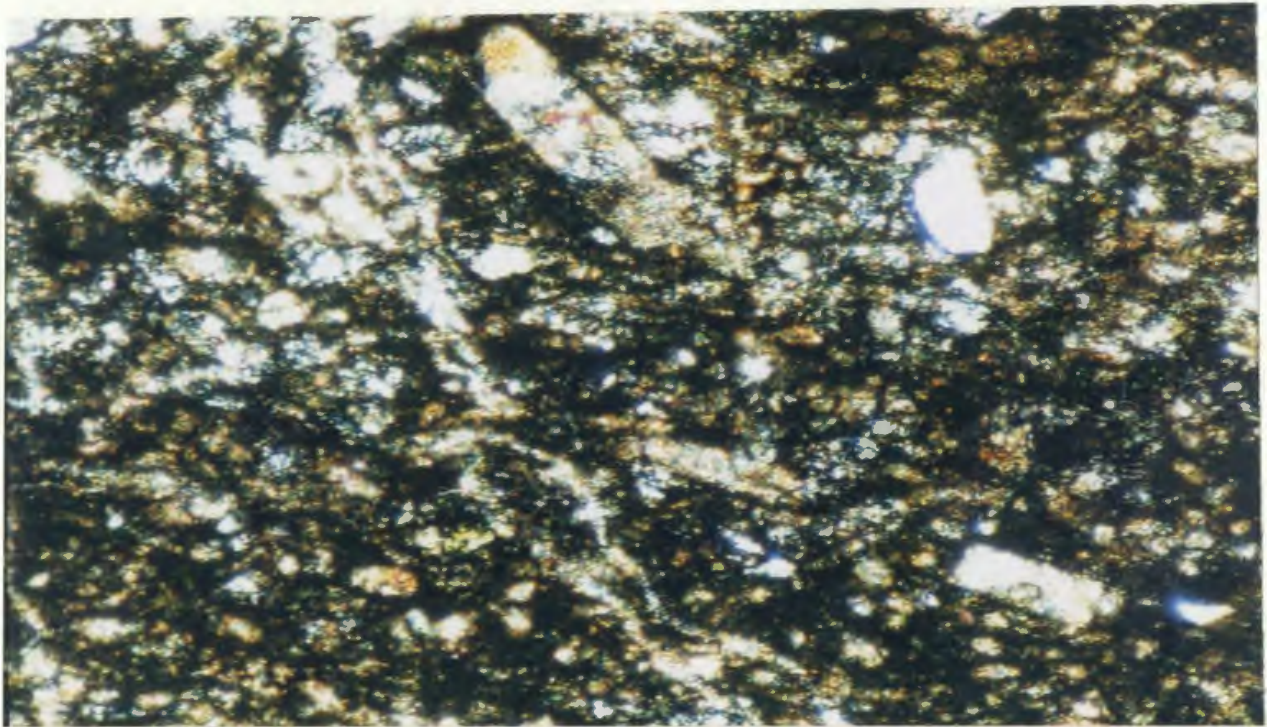


**Plate 3.5a** Microphotograph of fine-grained sandstone containing abundant crystal fragments (dominantly plagioclase) and altered clasts of what were likely rock fragments, in an altered, fine clay-like matrix (Red Hills, R-919). Crossed nicols, x100.



**Plate 3.5b** Microphotograph of fine-grained sandstone containing abundant fragments of sponge spicules (cross sections) (Red Hills, R-919). Crossed nicols, x100.





**Plate 3.5c** Microphotograph of fine-grained sandstone containing abundant fragments of sponge spicules (longitudinal sections) (Red Hills, R-919). Crossed nicols, x100.



Dun Mountain Ultramafics Group suspended in a matrix of sheared serpentinite (unit Ir/dm, Figure 3.2.1). These inclusions are considered to represent material incorporated into serpentinite (Sheared Serpentinite Complex) by shearing along the contact between the lower Maitai-Lee River Group package of rocks to the west and ultramafic rocks of the Dun Mountain Ultramafics Group to the east. The complex strikes roughly north-south and is generally between 200 and 400 metres wide. Within the complex, shearing is defined by vertical to sub-vertical schistosity planes in serpentinite which strike parallel to the zone's margins (Plates 3.6a and b). Schistosities are often highly irregular in orientation, and are often observed wrapping around blocks (inclusions) of more competent material such as gabbro and rodingite (Plates 3.7 and 3.8). Inclusions are generally less than a metre in diameter but are observed up to tens of metres in diameter. Rodingitized mafic dykes are also common as boudinaged lenses in sheared serpentinite (Plates 3.9a,b,c and 3.10).

Inclusions within this zone (unit Ir/dm, Figure 3.2.1) include blocks of: rodingitized and amphibolitized foliated gabbro; rodingitized banded gabbroic cumulates ("critical zone" rocks); ultramafic rocks; and rodingitized mafic dykes. Of particular interest here are the gabbroic cumulates, as they were likely derived from levels within the Dun Mountain Ophiolite not preserved in other areas investigated in this study. Similar "critical zone" or layered series rocks have been described from other ophiolites and are considered to represent the transition between the ultramafic and mafic plutonic rocks of an ophiolite (Smith, 1958; Maipas, 1977). These rocks are therefore considered



**Plate 3.6a** 40 metre wide sheared serpentinite shear zone in Sheared Serpentinite Complex Zone (Red Hills, R-900). Schistosity planes dip steeply towards the left of the picture (west). Knapsack for scale.



**Plate 3.6b** Close up of sheared serpentinite shear zone in Sheared Serpentinite Complex Zone (Red Hills, R-900). Note blocks of sheared and serpentinized ultramafic rocks in left half of picture.





**Plate 3.7** Competent blocks of gabbroic material suspended in sheared serpentinite (Red Hills, R-926).



**Plate 3.8** Competent blocks of amphibolitized and foliated medium-grained gabbro suspended in sheared serpentinite (Red Hills, R-950b).





**Plate 3.9a** Rodingite dyke in sheared serpentinite truncated by a block of amphibolitized and strongly foliated medium-grained gabbro (Red Hills, R-902). Note: Rodingite dyke has been disrupted by shearing within the serpentinite matrix. Hammer for scale (in foreground).



**Plate 3.9b** Close up of rodingite dyke in sheared serpentinite truncated by a block of amphibolitized and strongly foliated medium-grained gabbro (Red Hills, R-902).





**Plate 3.9c** Close up of amphibolitized and strongly foliated medium-grained gabbro block (Red Hills, R-902). Foliation is sub-horizontal and dip towards the left side of the photo. Note numerous veinlets of prehnite intruding along joints and foliation planes.



**Plate 3.10** Disrupted rodingite dykes in sheared serpentinite (Red Hills, R-925). Hammer for scale.

to represent basal cumulate sequences of the Lee River Group gabbroic complex (unit t, Figure 3.2.1).

Within the map area, rocks of this type are preserved as distinctively banded, partially serpentized and rodingitized gabbroic inclusions suspended in sheared serpentinite (Plates 3.11a,b to 3.16a,b).

To the east of the serpentinite fault zone (unit lr/dm, Figure 3.2.1) lie ultramafic rocks of the Red Hills ultramafic massif (unit dm, Figure 3.2.1). Within the map area this massif consists of harzburgite with minor pods and lenses of dunite, wehrlite, and orthopyroxenite. These rocks are generally "dun coloured" on weathered surfaces with dunite having a smooth weathered surface while harzburgites possess rough "hob nail" weathered surfaces due to the presence of erosion resistant orthopyroxene crystals (Plate 3.17).

Within these ultramafic rocks occur numerous bands or dykes of pyroxenite and pyroxene peridotite. These appear to have been produced in many generations with most now being aligned parallel to foliations developed within the harzburgite, while later dykes cut the harzburgite at various angles to the foliation. This suggests that deformation took place while the massif was still magmatically evolving beneath the ocean floor. In places, these dykes are observed as tightly closed folds in which the limbs are aligned parallel to the foliation (Plate 3.17). For the most part they are 10 to 30 centimetres thick and are generally more abundant in harzburgites than dunites.

Dunite pods and lenses within the ultramafic rocks are typically 0.5 to 50 metres wide and generally share sharp contacts with the more plentiful





**Plate 3.11a** Knocker of foliated and amphibolitized melanocratic gabbro suspended in sheared serpentinite of the Sheared Serpentine Complex Zone (Red Hills, R-904). Hammer for scale.



**Plate 3.11b** Close up of foliation within amphibolitized, medium-grained melanocratic gabbro knocker (Red Hills, R-904).





**Plate 3.12** Boulder of transition series banded rock (Red Hills, R-911). Dark bands are predominantly composed of serpentized dunite while lighter coloured bands are composed of hydrogrossular and diopside from the alteration of plagioclase and clinopyroxene (gabbro).



**Plate 3.13** Outcrop of vertically banded transition series rocks (Red Hills, R-926).





**Plate 3.14** Boulder of transition series rock (Red Hill, R-926). Note black bands of serpentinized dunitic material.



**Plate 3.15** Boulder of transition series gabbro cut by a 5 centimetre wide dyke of amphibolitized gabbroic material (Red Hills, R-926).





**Plate 3.16a** Outcrop of foliated transition series rocks (Red Hills, R-926).



**Plate 3.16b** Close up of transition series rock (Red Hills, R-926). White grains are composed of hydrogrossular replacing plagioclase.





**Plate 3.17** Outcrop of banded Harzburgite within the Red Hills Ultramafic massif (Dun Mountain Ultramafics Group). The outcrop contains numerous pyroxenite bands aligned parallel to the foliation. The head of the hammer rests on the hinge area of a folded band (Red Hills, R-956a).



**Plate 3.18** Fine-grained Maitai Group clastic sediments with cleavage developed along bedding surfaces (Lee River area, T-565). Hammer and note book for scale.

harzburgites.

### 3.2.3 Lee River (Figure 3.2.2)

In the Lee River map area rocks of the Dun Mountain-Maitai terrane, Patuki mélange, and Pelorus terrane were mapped and interpreted (Figure 3.2.2). These rocks include from west to east: Maitai Group sediments; Lee River Group gabbros and diabase dykes; ultramafic rocks of the Dun Mountain Ultramafics Group; clastic sediments and mafic volcanic, plutonic, and ultramafic rocks of the Patuki mélange; and clastic sedimentary rocks of the Pelorus Group.

The Maitai Group rocks are predominantly composed of clastic sediments (Plate 3.18) with only local minor amounts of Wooded Peak limestone and Upukerora conglomerate outcropping along the Group's eastern (basal) contact. For the most part, the contact between the Maitai Group sediments and the Dun Mountain Ophiolite to the east is faulted; however, Maitai Group sediments (Upukerora Formation conglomerates) are locally observed unconformably overlying gabbro and diabase dykes of the Lee River Group near Little Ben.

East of the Maitai Group sediments, rocks of the Dun Mountain Ophiolite are observed as an incomplete ophiolite sequence in which mafic gabbroic rocks of the Lee River Group overlie and are in fault contact with ultramafic rocks of the Dun Mountain Ultramafics Group to the east.

The Lee River Group gabbroic rocks are generally isotropic in character and are locally intruded by small numbers of sub-vertical, east-west striking

diabase dykes, particularly along the top (western contact) of the gabbro sequence. These dykes are typically between 0.5 and 1 metre wide and in places display well preserved chilled margins. The gabbroic rocks are mostly composed of fine to medium-grained (1 to 3 millimetres) gabbro made up of altered clinopyroxene (green pleochroic amphibole) and saussuritized plagioclase. Diabase dykes are typically more fine-grained (less than 1 millimetre) than the gabbros but are of similar composition.

For the most part, gabbroic rocks are undeformed although a few intensely foliated blocks are observed as inclusions within serpentinite shear zones between the Lee River Group gabbros and ultramafic rocks of the Dun Mountain Ultramafics Group. These inclusions commonly have a flasered appearance indicating that the rocks were deformed at high temperatures. It is suggested here that many of these highly foliated inclusions were likely brought in contact with the higher level, nondeformed, Lee River Group gabbros along deep-rooted fault zones.

Ultramafic rocks of the Dun Mountain Ultramafics Group lie in fault contact to the southeast with gabbroic rocks of the Lee River Group and are considered to have formerly underlain them. These ultramafic rocks are for the most part, strongly serpentinitized and are predominantly composed of harzburgite with minor bands and lenses of serpentinitized dunite and pyroxene peridotite.

In outcrop, rocks of the Dun Mountain Ultramafics occur as large fault bounded blocks which range from approximately 0.25 to 2 kilometres in diameter (as defined on Figure 3.2.3). These larger blocks are internally cut

by innumerable serpentinite shear zones into numerous smaller blocks 1 to 10 metres in diameter.

Within some sections through the ophiolite sequence, rocks of the Lee River Group are absent where ultramafic rocks of the Dun Mountain Ultramafics Group lie in fault contact with Maitai group sediments to the west. In these areas it is assumed that the Lee River Group has been removed by faulting as there is no evidence of sedimentary contacts between the rocks of the Dun Mountain Ultramafics Group and Maitai Group sediments. In addition, tectonic inclusions of gabbro (Lee River Group) are commonly observed suspended within serpentinite shear zones which run along contacts between rocks of the Dun Mountain Ultramafics Group and Rocks of the Lee River and Maitai Groups.

In the map area the ophiolite has been disrupted by a series of faults (as previously described) which crosscut it in approximately north-south and east-west directions. These faults commonly contain inclusions of material derived from adjacent rocks; however, some inclusions are considered to have been tectonically transported considerable distances as they are composed of material different from that observed immediately adjacent to the shear zones (Plates 3.19 and 3.20). It appears that some of these faults follow previous zones of displacement produced prior to, or during the initial emplacement of the ophiolite (ie. on the sea floor) particularly along: (i) the contact between the Lee River Group gabbros and rocks of the Dun Mountain Ultramafics Group; and (ii) the western contact of the Patuki mélange (Dun Mountain Ultramafics-Patuki mélange contact).





**Plate 3.19** Large block of pillowed basalts (Patuki Basalts, Lee River area, T-257). Outcrop is a large block suspended in a serpentinite shear zone.



**Plate 3.20** Close up of inclusion of rodingitized material within sheared serpentinite (Lee River area, T-560). Note the margins of the inclusion are partially replaced by serpentinite.

Lying to the east of, and in faulted contact with rocks of the Dun Mountain Ophiolite are clastic sediments and mafic volcanic, plutonic, and ultramafic rocks of the Patuki mélange. In the Lee River area, these rocks are exposed as a highly disrupted belt of weakly to highly deformed blocks separated by, and sometimes suspended in, serpentinite shear zones. The blocks range in size from less than a metre to hundreds of metres in diameter and display a high degree of internal deformation as individual blocks are commonly cut and disrupted by innumerable serpentinite fault zones.

Within the mélange three types of blocks are observed including: (i) blocks of associated clastic sedimentary and basaltic rocks; (ii) blocks composed of medium-grained gabbros and fine-grained diabase dykes; and (iii) rare blocks of serpentinitized ultramafic rock.

Most blocks are composed of pillowed to massive, mafic flows and volcanic breccias locally overlain by thin sequences of very fine-grained clastic sediments (Plates 3.21 and 3.22a,b). These sediments are predominantly grey to green argillites and fine sandstones; however, red hematized mudstone is also locally observed in contact with underlying basaltic flows and breccias.

Basaltic rocks within the Patuki mélange are generally observed in outcrop as red (hematite-stained) to green weathering pillows or massive flows. Pillowed outcrops commonly contain very little, if any, interstitial material and individual pillows are typically less than 0.5 metres in diameter (Plates 3.21 and 3.22a,b).





**Plate 3.21 Patuki pillow basalts (Lee River area, B-131).**



**Plate 3.22a** Nonconformable contact between Patuki pillow basalts (right) and green, fine-grained argillaceous sediments (left) (Lee River area, B-132).





**Plate 3.22b** Close up of fine-grained argillaceous sediments above nonconformable contact (Lee River area, B-132).

In outcrop, gabbroic rocks of the Patuki mélange appear to be similar in composition to those of the Lee River Group as both are commonly isotropic in character and of similar grain size. One visible difference between these rocks is however, their degree of deformation, as Patuki gabbros are commonly foliated while gabbros of the Lee River Group are typically less deformed. Diabase dykes also intrude gabbros of the Patuki mélange but are less common.

In the Lee River area ultramafic rocks of the Patuki mélange are generally strongly serpentinized and sheared, usually being observed as slivers or blocks (generally 5 to 200 metres in diameter) in serpentinite fault zones between larger blocks (generally hundreds of metres in diameter) of the Patuki mélange to the west and clastic sediments of the Pelorus terrane to the east. These packages or blocks of ultramafic rock make up only a small fraction of the total volume of the Patuki mélange in the Lee River area and may represent, in some instances, material squeezed up along deep-rooted serpentinite shear zones.

For the most part, Patuki ultramafic rocks are composed of strongly serpentinized harzburgite and lesser amounts of serpentinized dunite and pyroxene peridotite. In outcrop these rocks are commonly broken up along serpentinite shear zones which have obliterated original textures and structures. Less sheared ultramafic rocks generally weather an orange-brown colour in which olivine has been almost entirely altered to serpentine and less altered relict orthopyroxene and spinel crystals stand out on weathered surfaces.

Locally, Patuki ultramafic rocks are observed in fault contact with Patuki gabbros. In places along these contacts gabbroic rocks are strongly foliated and have a flasered or banded appearance (Plate 3.23). The strongly foliated gabbroic rocks of these zones are considered similar to those previously mentioned within the Red Hills area (amphibolitized foliated gabbroic blocks suspended within the Sheared Serpentinite Complex) and likely represent foliated basal gabbros of the Lee River Group.

East of, and in fault contact with rocks of the Patuki mélange, lie clastic sedimentary rocks of the Pelorus terrane. These sediments are generally dark grey to blue, fine-grained, well-bedded siltstones, sandstones, and mudstones. Within the Lee River area they were mapped along their western contact where they outcrop as subvertical to horizontal beds, locally folded or buckled around northeast-southwest striking axes. Although sedimentary rocks of the Pelorus terrane were mapped during this study, a detailed investigation of these rocks was not conducted.

#### 3.2.4 Serpentine River (Figure 3.2.3)

In the Serpentine River map area rocks of the Dun Mountain-Maitai Terrane and Patuki mélange were mapped and interpreted along a section of the Serpentine River. These rocks include from north to south: Maitai Group sediments, diabase dykes and gabbros of the Lee River Group, ultramafic rocks of the Dun Mountain Ultramafics Group, and clastic sediments and mafic volcanic rocks of the Patuki mélange.



**Plate 3.23** Close up of medium to coarse-grained, highly foliated gabbro (Patuki gabbro, Lee River area, B-181).



Maitai Group sedimentary rocks outcrop over the northern portion of the map area and are dominated by thinly bedded, fine-grained siltstones and sandstones. These sediments are, for the most part, unfaulted and make up a sequence of vertical beds which strike roughly parallel to the group's eastern faulted contact. Along this eastern contact outcrops a fault bounded sequence (approximately 30 metres wide) of thinly bedded, grey to purplish-grey limestones and siltstones of the Wooded Peak Formation. In fault contact with these limestones to the south are gabbro and diabase dykes of the Lee River Group (Dun Mountain Ophiolite).

Here the Lee River Group is composed predominantly of isotropic, medium-grained (1 to 2 millimetres), unfoliated gabbros. These gabbros are intruded by rare diabase dykes (0.5 to 1 metre wide) and closely resemble those gabbros of the Lee River map area (near Little Ben) which lie in unconformable contact with conglomerates of the Upukerora Formation (Figure 3.2.2).

In fault contact with the gabbros to the south are strongly serpentinized and sheared ultramafic rocks of the Dun Mountain Ultramafics Group. Along this contact dykes of rodingitized mafic material are common as blocks (less than 0.5 metres wide) in sheared serpentinite.

The ultramafic rocks of the Dun Mountain Ultramafics Group are predominantly composed of sheared serpentinite and contain numerous blocks (less than 1 metre to tens of metres in diameter) of serpentinized harzburgite. These rocks are typically highly disrupted by innumerable serpentinite shear zones.

In fault contact with rocks of the Dun Mountain Ultramafics to the south are fine-grained clastic sediments and pillowed to massive basaltic flows of the Patuki mélange.

In the Serpentine River area, rocks of the Patuki mélange occur as two large semi-continuous blocks (500 metres or more wide) separated by a serpentinite shear zone (approximately 25 metre wide). This shear zone dips vertically and strikes roughly northeast-southwest.

Both blocks of the Patuki mélange are disrupted by numerous narrow (less than 0.5 metres wide) shear zones (of which some are lined with sheared serpentinite) that crosscut the blocks as vertical to subvertical, northeast-southwest striking faults.

The northern block of the mélange is predominantly composed of red coloured, hematite-stained basalts which outcrop as pillowed to massive flows and breccias overlain by thin sequences of poorly bedded, grey to dark grey mudstones, siltstones and sandstones.

The adjacent block to the south is predominantly composed of fine-grained clastic sediments. Basaltic rocks were not observed in outcrop; however, a complete section through the southern block was not mapped. The clastic sediments of this block are dominated by poorly bedded, fine-grained, dark grey-blue sandstones and siltstones. Bedding within these rocks is best defined by rare beds of light grey coarse sand (less than 1 centimetre thick) which generally strike northeast-southwest and dip vertically.

### 3.2.5 Roding River (Figure 3.2.4)

In the Roding River area three separate sections through rocks of the Lee River Group were mapped and reinterpreted. From west to east these sections include: (i) Champion Creek, (ii) United Creek, and (iii) the Dun Mountain track. Each of these sections are unconformably overlain by steeply dipping, northeast-southwest striking limestones of the Wooded Peak Formation (Maitai Group) and lie in fault contact to the east with ultramafic rocks of the Dun Mountain Ultramafics Group.

Within these sections the composition of Lee River Group rocks ranges from gabbros and diabase dykes along the Champion and United Creek sections to massive basaltic flows and possibly sills along the Dun Mountain track section.

#### 3.2.5.1 Champion Creek

The Champion Creek section consists of a 700 metre wide section through Lee River Group diabase dykes and gabbros which are unconformably overlain by Wooded Peak limestones to the northwest.

Diabase dykes dominate the upper portion of this section and become less plentiful at lower levels (towards the eastern contact) where screens of medium-grained gabbro increase in number. The diabase dykes intrude the gabbros as subvertical, northeast striking, 0.5 to 1.5 metre wide dykes and in many places display well preserved chilled margins.

Rocks of the top 200 metres of the section are almost entirely composed of fine-grained diabase dykes and a small number of medium-

grained gabbro screens (5 to 15 percent). Throughout this part of the section gabbro screens range in width from 0.5 to 3 metres and are generally weakly to moderately foliated. Diabase dykes on the other hand, are both unfoliated and foliated suggesting that they were intruded in multiple events and that deformation took place while the rocks were forming on the sea floor.

The remainder of the section (the lower 500 metres) is for the most part, composed of roughly equal proportions of foliated, medium-grained gabbro screens and fine-grained diabase dykes (Plates 3.24 to 3.26). The dykes of this part of the section are often foliated although a large number of undeformed diabase dykes are also observed. The lower 50 metres of the section is dominated by weakly to strongly foliated gabbros (Plate 3.27) and a small number of foliated diabase dykes. The foliation is particularly well developed over the bottom 10 to 15 metres where it is aligned roughly parallel to the section's basal sheared contact and imparts a flasered appearance to the gabbros.

The basal sheared contact between rocks of the Lee River Group and ultramafic rocks of the Dun Mountain Ultramafics Group strikes in a northeast-southwesterly direction and dips roughly vertical. Along the fault zone a small number of blocks composed of partially rodingitized, foliated gabbro and diabase dykes (up to 3 metres in diameter) outcrop in a matrix of sheared serpentinite. In the Roding River area this shear zone extends across all three sections and varies in width from approximately 3 to 10 metres. It is also associated with a small number of small massive sulphide deposits some of which were mined at the turn of the century for their copper content. One



**Plate 3.24** Medium-grained Lee River Group gabbro intruded by a fine-grained diabase dyke, (d) (Champion Creek, Roding River area, H-758).



**Plate 3.25** Medium-grained Lee River Group (g) gabbro intruded by a fine-grained diabase dyke (d), (Champion Creek, Roding River area, H-758).





**Plate 3.26** Outcrop of medium-grained Lee River Group gabbro (Champion Creek, Roding River area, H-755).



**Plate 3.27** Boulder of strongly foliated to flasered, medium- to coarse-grained Lee River Group gabbro (Champion Creek, Roding River area, H-754). Note foliated diabase dyke to right of hammer.

such deposit is located within the fault zone between rocks of the Lee River Group and the Dun Mountain Ultramafics Group near Champion Creek (Plates 3.28 and 3.29) and another near United Creek (Figure 3.2.3). It is worth noting here that numerous boulders of varied lithologies were observed in Champion Creek including a small number of conglomerate boulders, 1.5 to 2 metres in diameter (Plate 30). This conglomerate is similar in character to outcrops of Upukerora conglomerate in the Red Hills and Lee River areas and was likely eroded from a nearby contact between the Maitai Group and the Lee River Group.

#### 3.2.5.2 United Creek

For the most part the United Creek section is similar to that of Champion Creek and consists of a 700 metre wide section through rocks of the Lee River Group.

The top 300 metres are dominated by diabase dykes with 5 to 10 percent screens of foliated medium-grained gabbro (Plate 3.31), while further down in the section the number of diabase dykes dwindles from 50 to 15 percent as the proportion of gabbro screens increase (Plates 3.32 to 3.34). In terms of field relationships and the lithologies observed, the United Creek section appears to be an extension of rocks observed within the Champion Creek section. Within the United Creek section the faulted contact between rocks of the Lee River Group and the Dun Mountain Ultramafics Group is particularly well exposed and blocks of rodingitized material are commonly observed in a matrix of sheared serpentinite (Plates 3.35 and 3.36).





**Plate 3.28** Looking southwest across Champion Creek to derelict shafts of the abandoned Champion Creek mine (H-753). Knapsack for scale (in foreground, left).





**Plate 3.29** Abandoned shaft, east bank of Champion Creek, Champion Creek Mine (H-752). Wooden two-by-four beams mark shaft's entrance.





Plate 3.30 Boulder of Upukerora conglomerate in Champion Creek (Roding River area, H-754).



Plate 3.31 Outcrop of vertically dipping, sheeted Lee River Group diabase dykes (United Creek, Roding River area, H-770). Hammer for scale.





**Plate 3.32** Outcrop of medium-grained Lee River Group gabbro intruded by a diabase dyke (United Creek, Roding River area, H-765).



**Plate 3.33** Outcrop of medium-grained Lee River Group gabbro with xenoliths of lighter coloured gabbro (United Creek, Roding River area, H-763).





**Plate 3.34** Outcrop of medium-grained Lee River Group gabbro intruded by fine-grained diabase dykes (United Creek, Roding River, H-761).



**Plate 3.35** Faulted contact between foliated, medium-grained, Lee River Group gabbro and sheared serpentinite of the Dun Mountain Ultramafics Group (United Creek, Roding River area, H-760). Hammer for scale.





**Plate 3.36** Block of rodingitized material suspended in sheared serpentinite (United Creek, Roding River area, H-760). Hammer for scale.

Also observed in this area are boulders of various lithologies including a small number composed of plagioclase porphyritic gabbro. The latter are predominantly altered medium-grained intergranular gabbro and contain between 10 and 30 percent altered plagioclase phenocrysts (less than 0.5 centimetres in diameter). Similar porphyritic rocks are also observed in outcrops of the Tinline River map area (approximately 17 kilometres northeast of United Creek) and are described in detail later in this chapter.

#### 3.2.5.3 Dun Mountain Track

In this section Lee River Group rocks were mapped and sampled along a 600 metre stretch of the Dun Mountain track southwest of Wooded Peak (Figure 3.2.4). Here, rocks of the Lee River Group are unconformably overlain by limestones of the Wooded Peak Formation (Maitai Group) to the northwest and lie in fault contact with ultramafic rocks of the Dun Mountain Ultramafics Group to the southeast.

The Lee River Group rocks of this section are composed of red-coloured (hematite-stained), massive basalt flows and minor thicknesses of basaltic breccia. The breccia units are generally less than 3 metres thick and are composed of basaltic clasts (less than 0.5 metres in diameter) in a hematite-stained mud matrix. These breccia units are not considered representative of Upukerora conglomerates as gabbroic clasts are absent and no sand component of the matrix is observed.

In a few outcrops, the basaltic rocks appear to have an almost sheeted character in which chilled margins are rarely visible between individual sheets.

These outcrops may represent basaltic sills, or dykes; however, outcrops were too limited to make conclusive observations about their identity, orientations, or thicknesses.

It is the author's opinion that this sequence of nonpillowed basaltic rocks may represent lower levels of an eroded basaltic pile in which massive basaltic flows, sills, and dykes dominate the stratigraphy. Similar sequences have been described from other ophiolites including the Troodos ophiolite of Cyprus. In Cyprus, pillow lavas dominate the basalt sequence but sills, dykes, massive flows, thin sheet-flows, flow breccias, and hyaloclastites are often observed, particularly within the Lower Pillow Lavas and Basal Group.

#### 3.2.6 Tinline River (Figure 3.2.5)

In the Tinline River map area an incomplete section through rocks of the Lee River Group was mapped and interpreted along a tributary of the Tinline River. Within this section rocks of the Lee River Group include fine-grained diabase dykes and screens of medium-grained gabbro. The northwestern contact of these rocks was not mapped in this study; however, the southeastern contact was mapped and is faulted against fine-grained clastic sediments of the Patuki mélange.

Diabase dykes dominate the northwestern (upper) part of the section and gradually become less plentiful at lower levels where screens of medium-grained gabbro increase in abundance. In Figure 3.2.5 the Lee River Group rocks of this section have been separated into three segments according to the relative proportions of diabase dykes and gabbro.

The northwestern (upper) segment of the section consists of a sheeted dyke complex in which medium-grained, weakly to unfoliated gabbro screens make up approximately 10 percent of the outcrop. The diabase dykes of this segment are typically between 0.5 to 1.5 metres wide and outcrops and boulders of diabase dyke-breccia are common (Plate 3.37). Gabbro screens observed within this segment are generally less than 3 metres wide and tend to weather a paler green colour than adjacent diabase dykes (Plate 3.38).

Also observed within the northwestern segment are two northeast striking gossan zones (Plate 3.39). These gossans appear to be associated with east-west striking, brittle fault zones which crosscut the section. The gossans are less than 4 metres wide and are predominantly composed of quartz with minor concentrations of pyrite and chalcopyrite and secondary occurrences of malachite and chrysocolla (see Johnston (1981) for a more detailed description).

Within the section's middle segment gabbro screens gradually increase in abundance to represent approximately 50 percent of the outcrop. The diabase dykes of this segment are typically well preserved and chilled margins are easily recognised in outcrop (Plate 3.40), while the gabbros are generally weakly to moderately foliated and medium-grained.

The section's southwestern (lower) segment is dominated by moderately to strongly foliated, medium-grained gabbro which has been intruded by approximately 10 percent diabase dykes (Plate 3.41). Within this segment the rocks range from medium- to coarse-grained gabbro and become progressively more deformed (foliated) and coarser grained towards the





**Plate 3.37** Boulder of diabase breccia (Lee River Group, Tinline River area, TL-781). Angular clasts of diabase suspended in a net-veined matrix of prehnite and carbonate.



**Plate 3.38** Highly fractured outcrop of light green coloured, medium-grained, Lee River Group gabbro screen in contact with dark coloured diabase dykes (Tinline River area, TL-781). Hammer on log for scale.





**Plate 3.39** Outcrop of quartz vein gossan zone (Tinline River area, TL-781).  
Note concentration of pyrite immediately above head of hammer.



**Plate 3.40** Outcrop of Lee River Group sheeted dykes with well preserved chilled margins and flow foliation (Tinline River area, TL-532).





**Plate 3.41** Outcrop of medium-grained, foliated, Lee River Group gabbro cut by two generations of diabase dykes (Tinline River area, TL-523). Note horizontal trending dark blue dyke (left of hammer) is cut by steeply dipping dykes to the right of the hammer.



**Plate 3.42** Outcrop of flasered medium to coarse-grained Lee River Group gabbro (Tinline River area, TL-789).

southeastern (lower) fault contact of the Lee River Group. Along this contact gabbroic rocks are intensely foliated to flasered in appearance (Plate 3.42) and contain several bands and boudinaged blocks of fine-grained diabasic rocks as well as a small number of bands composed of coarser grained amphibolitic material (Plate 3.43). The amphibolite bands are almost entirely composed of coarse-grained, weakly pleochroic green amphibole while the diabase blocks are composed of altered fine-grained material. Within lower levels of this segment foliated gabbros and diabase dykes have been intruded by a small number of undeformed diabase dykes and gabbro stocks suggesting that much of the deformation of the section took place while the rocks were forming on the sea floor.

Three distinct suites of subvolcanic rocks were observed within rocks of the Tinline section. These include: a suite of weakly to strongly amphibolitized aphyric, intergranular, medium-grained gabbros; a suite of undeformed, fine-grained, nonamphibolitized aphyric diabase dykes; and a suite of plagioclase porphyritic gabbro screens and diabase dykes (Plate 3.44).

Rocks of the porphyritic suite are relatively rare but are easily recognised in outcrop as they contain between 10 and 30 percent, cloudy white plagioclase phenocrysts which range from 1 centimetre in diameter in the gabbros to less than 0.5 centimetres in diameter in the diabase dykes. Rocks of this suite are not considered to represent an isolated and unique occurrence present only in the Tinline River area as boulders of similar porphyritic rocks have also been observed in United Creek (Roding River map



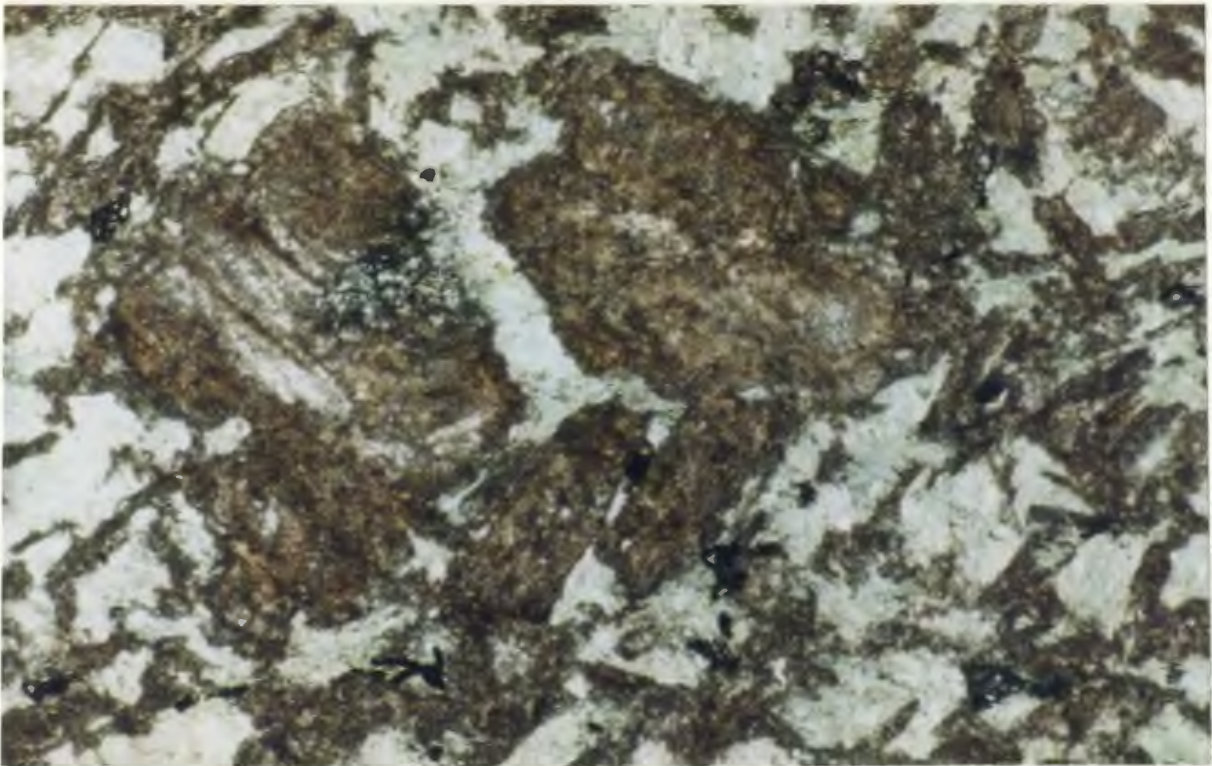


**Plate 3.43** Outcrop of foliated and amphibolitized gabbro with an inclusion of coarse-grained amphibolite (Lee River Group, Tinline River area, TL-787).





**Plate 3.44** Boulder of plagioclase porphyritic gabbro (Lee River Group, Tinline River area, TL-787).



**Plate 3.45** Microphotograph of plagioclase porphyritic diabase (Lee River Group) from United Creek (Roding River area, H-823). Note plagioclase is altered a brown colour suspended within intergranular green pleochroic amphibole. Plane-polarized light, x50.



area) approximately 17 kilometres southwest of the Tinline River section (Plate 3.45).

As the Tinline River section is exposed on a steep hillside (roughly 45 degrees), relative ages and orientations of the rocks were difficult to interpret as most outcrops are poorly exposed and covered by scree material (Plate 3.46). Despite the limited availability of comprehensive outcrop it is estimated that diabase typically intrudes the gabbros as steeply north dipping, northeast to east striking dykes. These dykes are generally 0.5 to 1.5 metres wide and in places display well preserved chilled margins.

### 3.2.7 Croisilles Harbour (Croisilles Mélange) (Figure 3.2.6)

In the Croisilles Harbour area ophiolitic rocks of the Croisilles mélange were examined and sampled along a segment of the mélange stretching from Ronga Saddle to Elaine Bay. Due to time constraints these rocks were not mapped in detail; however, sample locations were plotted on a recent detailed map of the area after Landis and Blake (1987).

In the map area the Croisilles mélange is composed of a wide variety of rock types including fine-grained clastic sediments, spilitic pillow basalts, altered gabbros, and serpentinized ultramafic rocks. These rocks are exposed as highly disrupted tectonic blocks or "knockers" suspended in matrices of sheared serpentinite and/or sheared clastic sediments. The blocks are often rimmed by rodingite, particularly those composed of sedimentary or mafic igneous material (Plate 3.47) and typically range in size from tens of metres to less than 10 centimetres in diameter; however, Landis



**Plate 3.46** Looking southeast down Tinline River section from stop TI-781. Knapsack for scale.



**Plate 3.47** Outcrop of partially rodingitized, sheared ultramafic material in contact with sheared sediments (Croisilles Harbour area, C-703). Hammer for scale.

and Blake (1987) have observed blocks up to 2 kilometres in length in the map area. Within the *mélange* no internal stratigraphic order is observed and the *mélange*'s highly disrupted nature is reflected in its characteristic hummocky topography (Plates 3.48a,b and c).

Basaltic rocks in the *mélange* generally occur as blocks of altered, pillowed flows and breccias in which individual pillows are typically less than 0.5 metres in diameter (Plates 3.49a and b). In outcrop these basalts are often hematite-stained and massive in appearance; however, weathered outcrops typically display well developed pillows, particularly in outcrops exposed to coastal weathering.

Gabbroic blocks generally occur as medium-grained aphyric gabbros and range in composition from massive undeformed gabbro to strongly foliated amphibolitized gabbro.

For the most part, ultramafic rocks of the *mélange* occur as blocks of rusty weathering, highly serpentized material in which original textures and compositions have been obliterated by serpentization. In some outcrops however, relict pyroxenes are visible on weathered surfaces together with minor amounts of fine-grained disseminated chromite and magnetite.

In general, the Croisilles *mélange* bears a close resemblance to the Patuki *mélange* although rocks of the Croisilles *mélange* appear to be more intensely deformed and disrupted. It should be noted; however, that this observation may only apply locally.





**Plate 3.48a** Hummocky topography of Croisilles melange looking towards Mount McLaren from stop C-720 (Croisilles Harbour area).



**Plate 3.48b** Croisilles melange with blocks of serpentinitized ultramafic and gabbroic rocks suspended in a sheared serpentinite matrix (Croisilles Harbour area, C-721).





**Plate 3.48c** Close up of Croisilles melange with blocks of serpentinitized ultramafic and gabbroic rocks suspended in a sheared serpentinite matrix (Croisilles Harbour area, C-721).





**Plate 3.49a** Outcrop of Croisilles pillowed basalts on the beach of Samson Bay, Croisilles Harbour (C-718). Knapsack for scale (front, left).



**Plate 3.49b** Close up of Croisilles pillowed basalts on the beach of Samson Bay, Croisilles Harbour (C-718).



### 3.2.8 Taipare Bay (Lee River Group) (Inset A, Figure 3.2.6)

Within the Croisilles Harbour area a wedge of basaltic volcanic rocks of the Lee River Group outcrop as a small subvertical, northwest dipping sequence of pillowed mafic flows on the western shore of Taipare Bay (Plate 3.50). These basalts lie to the east of limestones of the Wooded Peak Formation (possibly along an unconformable contact) and lie in fault contact to the east with ophiolitic rocks of the Patuki tectonic mélange (Figure 3.2.6 inset A).

The rocks of this sequence are predominantly composed of fine-grained pillowed mafic flows and minor thicknesses of pillow breccia. The flows are typically 2 to 10 metres thick and are generally separated by lenses of pillow breccia 2 to 4 metres thick. Within these flows, individual pillows generally range from 20 centimetres to 0.75 metres in diameter and are composed of aphyric, epidote and/or carbonate amygdaloidal basalt (Plates 3.51 and 3.52). Most of these flows weather green to grey in colour and contain minor amounts of chert (and or jasper), carbonate, epidote, and hematite-stained muddy interpillow material.

Pillow breccias are generally composed of angular basalt clasts and contain matrices of fine, hematite-stained mud or grey to green volcanoclastic sand (Plates 3.53 to 3.55). These units commonly contain between 20 and 30 percent matrix material. Contacts between pillowed flows and pillow breccia are typically gradational over thicknesses of 1 metre or less, although in places are defined well enough to reveal reliable strike and dip (Plate 3.54).



**Plate 3.50** View looking northwest towards Taipare Bay. Grey-coloured cliffs at point of peninsula are composed of Wooded Peak limestones.



**Plate 3.51** Outcrop of weathered pillowed basalts (Lee River Group, Taipare Bay, SD-804).





**Plate 3.52** Outcrop of pillowed mafic flows, Taipare Bay (Lee River Group, SD-806).



**Plate 3.53** Outcrop of basalt breccia with sandy matrix material, Taipare Bay (Lee River Group, SD-808).





**Plate 3.54** Outcrop of basalt breccia, Taipare Bay (Lee River Group, SD-808). Note breccia units dip steeply towards the right (northwest). Author for scale.



**Plate 3.55** Outcrop of basaltic breccia with abundant volcanoclastic sand matrix, Taipare Bay (SD-801).

The intensity of alteration within the sequence varies greatly from unit to unit although all basaltic rocks have been affected by greenschist facies metamorphism and some units (flows and breccias) have been intensely chloritized.

### 3.3 Summary

#### 3.3.1 Field Relationships

Within the East Nelson region field relationships displayed between rocks of the three ophiolites of the East Nelson ophiolites (Dun Mountain Ophiolite, Patuki mélange, and Croisilles mélange) do not provide conclusive evidence by which each of the ophiolites can be individually distinguished; however, some relationships do consistently infer their individuality. These relationships are as follows:

(i) Although rocks of the Dun Mountain Ophiolite are often observed in fault contact with sediments of the Maitai Group, Lee River Group rocks are in places unconformably overlain by sediments of the Maitai Group;

(ii) Deposition of Maitai Group sediments occurred after extensive erosion of Dun Mountain Ophiolite and locally directly overlie gabbros of the Lee River Group. Associated with many of these unconformable contacts are basaltic conglomerates of the Upukerora Formation (Maitai Group). These conglomerates are predominantly composed of subangular clasts of basaltic and gabbroic material suspended in matrices of red (hematite-stained) mud and fine sand. Clasts closely resemble lithologies observed within high levels of the Dun Mountain Ophiolite and are considered to represent material



eroded off the ophiolite. It is suggested here that these conglomerates were deposited as submarine slumps or slurries as they are unsorted and individual clasts often display injection textures whereby mud and sand material was injected along fractures under high hydraulic pressure. These injection textures are best observed in thin section and are described fully in the following chapter.

(iii) Initiation of Wooded Peak limestone deposition likely took place sometime after deposition of conglomerates of the Upukerora Formation as clasts of Wooded Peak limestone are not observed within the Upukerora conglomerates.

(iv) Although only poorly developed sheeted dyke complexes were observed within sections through the Dun Mountain Ophiolite, diabase dykes are generally orientated subparallel to the Maitai-Lee River Group contact. Since these dykes were initially formed with vertical orientations this suggests that listric faulting and block rotation may have commonly occurred prior to deposition of Maitai Group sediments;

(v) Rocks of the Patuki mélange are always separated from rocks of the Lee River Group (Dun Mountain Ophiolite) to the west by rocks of the Dun Mountain Ultramafics Group (Dun Mountain Ophiolite). The contact between these ophiolites is always faulted and it appears that rocks of the Patuki mélange structurally underlie those of the Dun Mountain Ultramafics Group.

(vi) Both the Patuki and Croisilles ophiolites are, in fact, tectonic ophiolitic mélanges in which blocks of ophiolitic material are suspended in

matrices of sheared serpentinite (and locally sheared sediments); while the Dun Mountain Ophiolite is less disrupted and generally outcrops as a less deformed, semi-complete ophiolite sequence. In most places within the ophiolitic mélanges no internal order could be consistently established as blocks of various lithologies are randomly distributed throughout the mélanges; however, at some localities (Lee River area) the Patuki mélange appears to be semi-ordered as sedimentary and volcanic rocks outcrop along the mélange's western contact while blocks of ultramafic material outcrop along the eastern contact.

(vii) Ophiolitic rocks of the Croisilles mélange consistently outcrop to the east of the Patuki mélange separated by the sedimentary rocks of the Pelorus terrane<sup>1</sup> (Rai Sandstones, (Johnston, 1981, 1982).

### 3.3.2 Structure and Metamorphism

Within the East Nelson ophiolites two discrete, major episodes of deformation and metamorphism are identified. The first episode is credited with metamorphism and deformation of the ophiolites on the ocean floor while the second major episode is attributed to regional tectonism and metamorphism of the ophiolites produced during and after emplacement.

Features produced while the ophiolites formed on the ocean floor include lower greenschist to amphibolite facies metamorphism of the rocks

---

<sup>1</sup>The origin of those sedimentary rock situated between rocks of the Patuki and Croisilles mélange is unclear and therefore classification of these rocks with those of the Pelorus terrane remains a subject of debate (eg., Dickins et al., 1986; Landis and Blake, 1987).

whereby higher level rocks were altered to lower greenschist grade while lower level rocks such as the gabbros approached amphibolite facies metamorphism. Most of the more highly metamorphosed rocks (upper greenschist and amphibolite grade gabbros) are foliated and flazered in appearance and are locally intruded by undeformed and unmetamorphosed diabase dykes. This relationship provides evidence that upper greenschist and amphibolite grade rocks were metamorphosed and deformed while the rocks formed on the ocean floor (pre-Late Permian).

Features attributed to regional tectonism and metamorphism of the ophiolites include the disruption of the ophiolites along brittle shear zones lined with sheared serpentinite and sub-greenschist facies metamorphism. These faults are considered to be related to movements along the Alpine fault during the Rangitata Orogeny (Jurassic to Early Cretaceous; Johnston, 1981) and the on going Kaikoura Orogeny (after Johnston, 1981). Sub-greenschist facies metamorphism is considered to have taken place during the Rangitata Orogeny (eg. Landis and Blake, 1987) and is preserved as secondary veinlets and alteration phases composed of prehnite-pumpellyite facies assemblages which occur in all lithologies of each of the three ophiolites.

Serpentinization within the ophiolites appears to occur in two ways: (1) along shear zones in the Dun Mountain Ophiolite and within sheared matrices of the ophiolitic mélanges; and (2) within blocks of ultramafic massif (of the Dun Mountain Ophiolite and the Patuki and Croisilles ophiolitic mélanges). Most of the serpentinization within these rocks is likely attributable to the interaction of seawater with ultramafic material exposed

during the emplacement of the ophiolites (Hangitata Orogeny); however, serpentinization of some of these rocks may have taken place while the ophiolites were evolving on the ocean floor.

Serpentinization on the ocean floor may have taken place when seawater was introduced to great depths along active faults that operated during sea-floor spreading (due to the tectonic readjustment at the spreading ridge). Although these processes may have taken place, there is no conclusive evidence to confirm that serpentinization took place in this way. On the other hand, deep submarine erosion of the Lee River Group (Dun Mountain ophiolite) and the relative orientations displayed between dykes of the Lee River Group and Maitai Group sediments (often subparallel) suggest tectonic movements of significant magnitude may have taken place (ie. major faults were active on the sea floor and may have acted as seawater passage ways).



## CHAPTER 4

### PETROGRAPHY OF THE EAST NELSON OPHIOLITE

#### 4.1 Introduction

In this chapter, the petrography of each of the East Nelson ophiolites is described with each of their respective components (ie. volcanics, subvolcanics, and ultramafics) being discussed individually. The petrography of the various lithologic components is described with reference to the seven study areas outlined in the previous chapter (Figures 3.2.1 to 3.2.6). In addition to the Dun Mountain, Patuki, and Croisilles ophiolites, the Upukerora Formation of the Maitai Group is also discussed as it contains abundant ophiolitic material as clasts in conglomeratic units unconformably overlying the Dun Mountain Ophiolite.

As part of this study approximately 275 hand samples were taken of the respective lithologies, of which approximately 160 were studied in thin section.

#### 4.2 Upukerora Formation

Representative outcrops of the Upukerora Formation were encountered in two of the study areas of East Nelson: (i) along the Red Hills western margin (Figure 3.2.1, Plates 3.2a and b); and (ii) in the Lee River area near Little Ben (Figure 3.2.2, Plate 4.1). In addition to these outcrops, boulders of

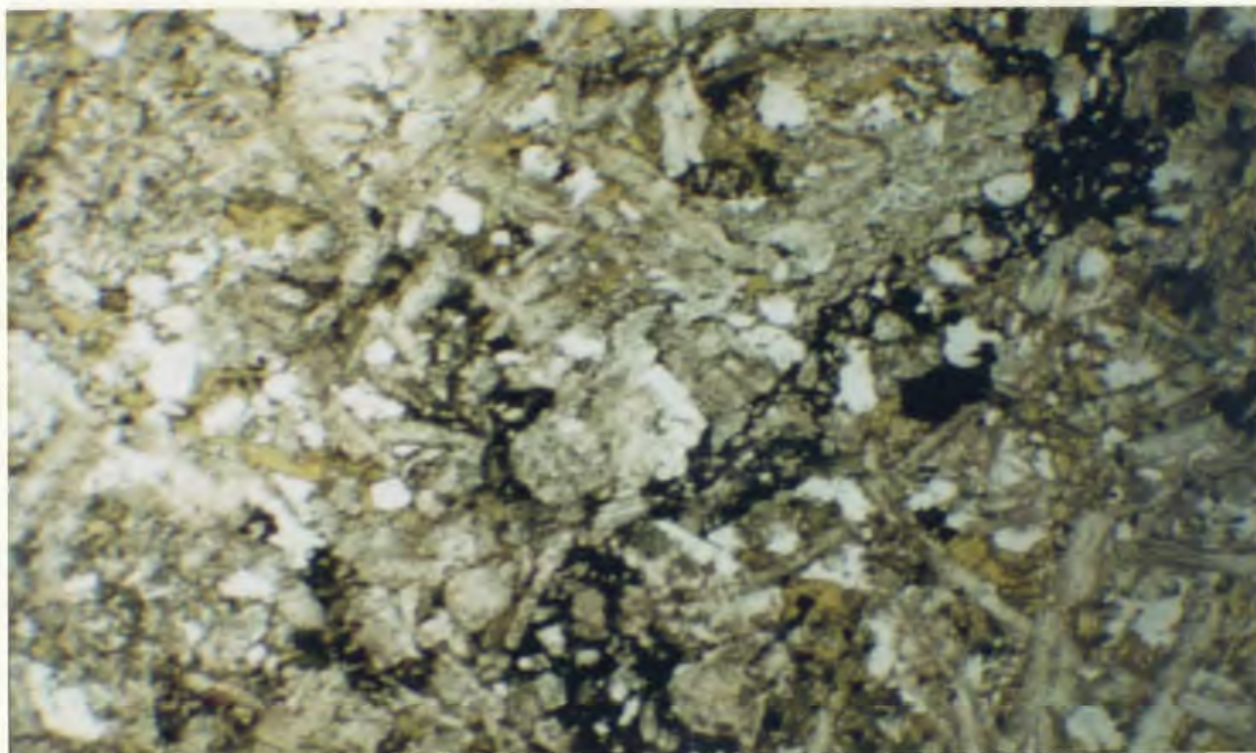
Upukerora conglomerate were also observed in Champion Creek (Roding River area, Figure 3.2.4, Plate 3.30). Where observed, conglomerates of the Upukerora Formation are found to be largely composed of clasts of basalt and gabbro supported in a red-coloured (hematite-stained) mud and sand matrix; however, in the Lee River area gabbro clasts dominate. Clasts are generally angular to sub-angular in shape and vary in size from 1 to 25 centimetres in diameter. Their compositions range from devitrified glass to fine-grained intergranular basalt and medium-grained intergranular gabbro (Plate 4.2). In thin section, large clasts appear broken into smaller clasts of identical composition separated by injections of mud (opaque) and sand material (Plate 4.3). These injection textures suggest that the conglomerates were deposited under high hydraulic pressure whereby clasts were fractured and injected with mud and sand during transport and deposition.

In outcrop the conglomerates are unsorted and bedding is not observed (Plates 3.2a and b) and it is proposed that they represent material eroded off the underlying Lee River Group (Dun Mountain Ophiolite) and deposited as submarine slurries or slides. As no limestone blocks or clasts are observed within this Formation, overlying limestones of the Wooded Peak Formation must have been deposited after a depositional hiatus which followed deposition of the Upukerora Formation.

Although basalt clasts occur with a wide range of textures and compositions, the majority are fine-grained, intersertal to intergranular basalts in which the primary phases are plagioclase, clinopyroxene and magnetite. Other clasts include: trachytic basalts composed of fluxioned plagioclase



**Plate 4.1** Close up of Upukerora conglomerate with angular to subrounded clasts of gabbro, basalt (red, below hammer) and siltstone.

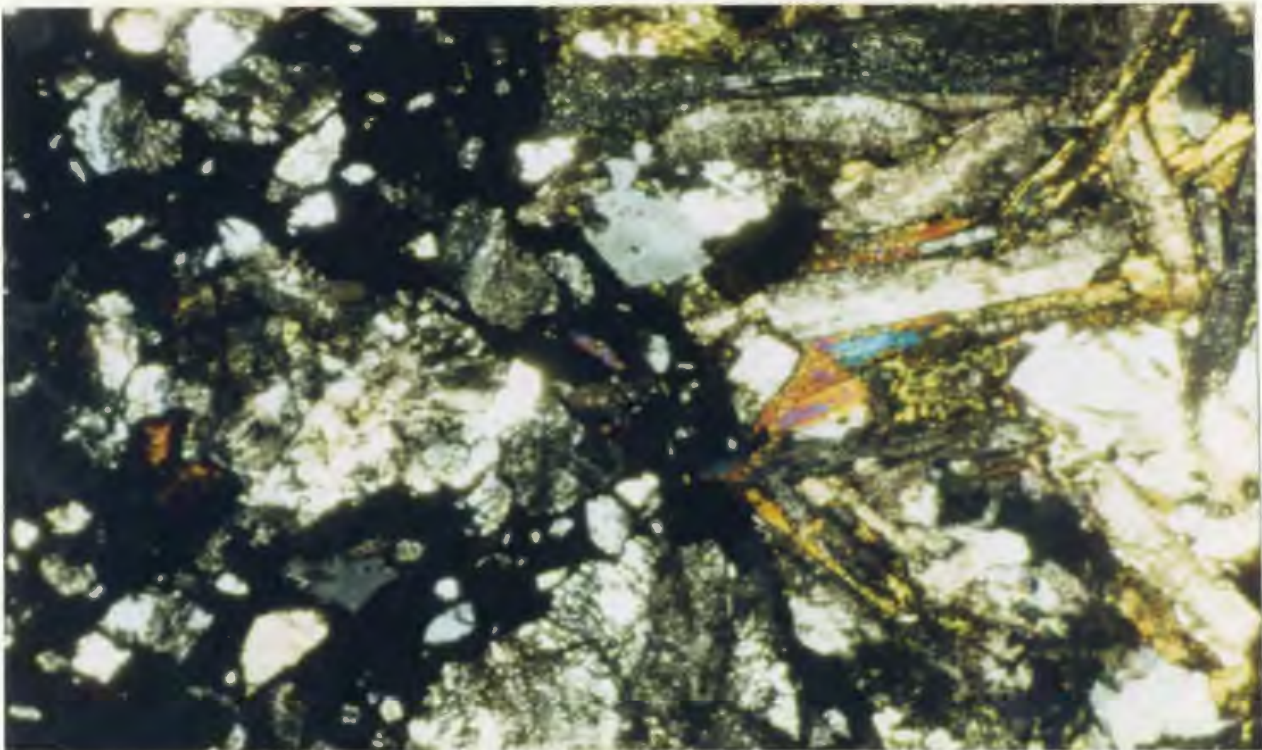


**Plate 4.2** Microphotograph of gabbro clasts within Upukerora conglomerate (red Hills, R-930). Note hematite-stained mud matrix separates clasts of identical composition. Crossed nicols, x25.





**Plate 4.3** Microphotograph of gabbro clast within Upukerora conglomerate (Lee River area, T-291a). Crossed nicols, x50.



**Plate 4.4** Microphotograph of trachytic textured basalt clast within Upukerora conglomerate (Red Hills). Crossed nicols, x100.



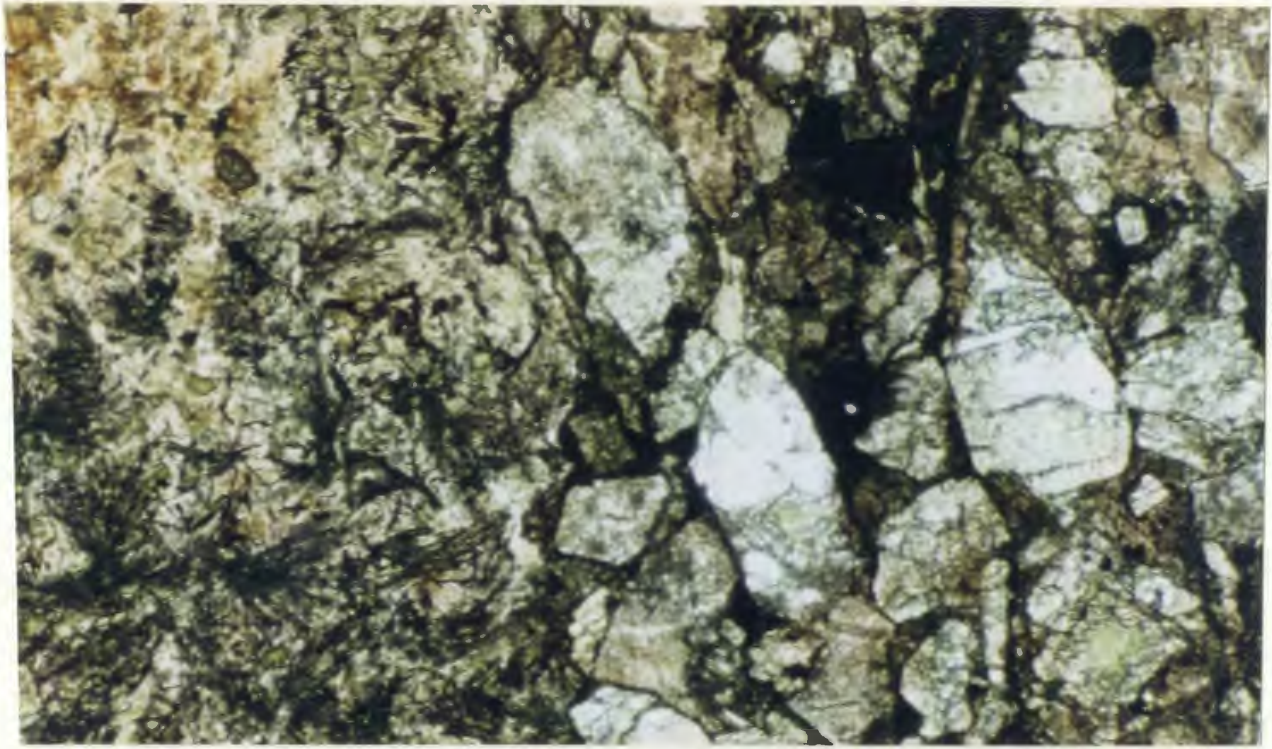
microlites and chloritized intersertal glass (Plate 4.4); intersertal to intergranular basalts composed of numerous, equant, subhedral to euhedral clinopyroxene phenocrysts suspended within a matrix of plagioclase microlites and chloritized intersertal glass; glassy variolitic basalts composed of radiating growths of quenched plagioclase suspended within a weakly chloritized glass matrix (Plate 4.5); and flow-banded, devitrified basaltic glass (Plate 4.6).

Clinopyroxene is generally unaltered in basalt clasts while plagioclase is typically weakly saussuritized with some larger crystals displaying relict albite and Carlsbad twinning.

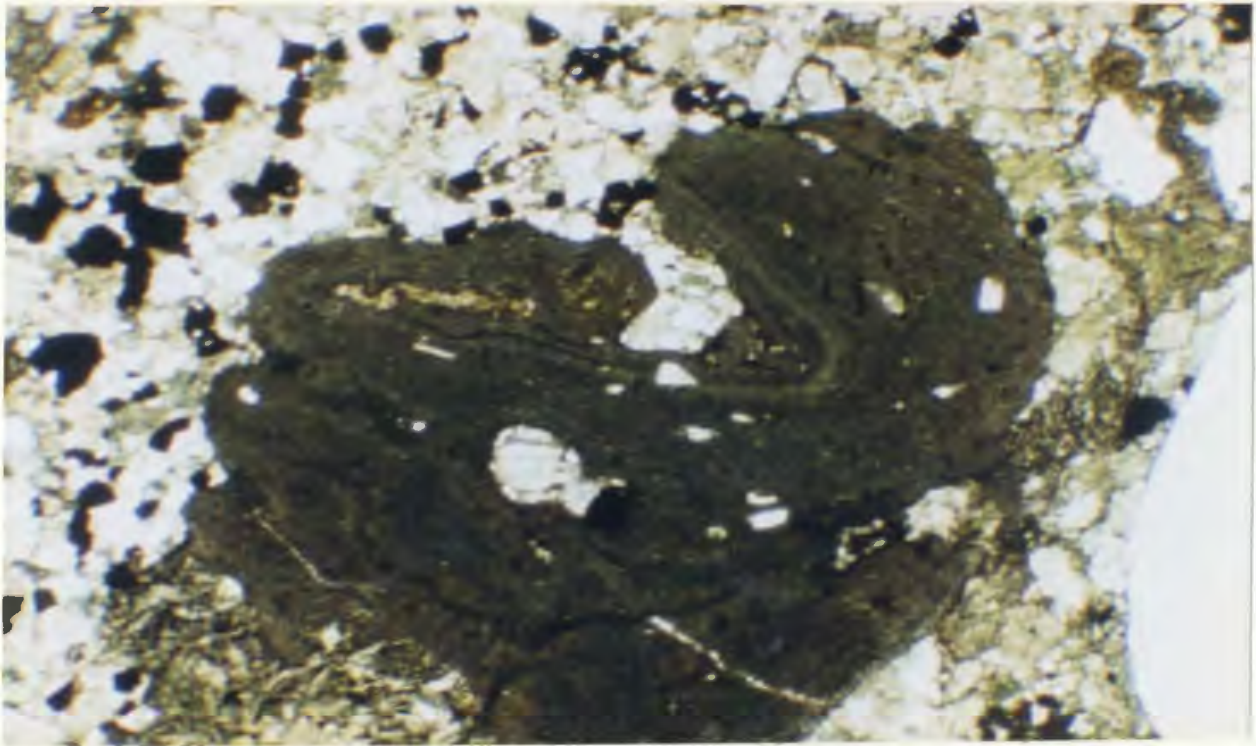
Gabbroic and microgabbroic clasts of the Upukerora conglomerate are typically undeformed, fine- to medium-grained intergranular gabbros 0.5 to 2 millimetres in grain size (Plate 4.2). Primary phases observed in these rocks include plagioclase, clinopyroxene, and iron-titanium oxides. Some dioritic gabbro clasts also contain small percentages of intersertal glass and interstitial granophyric intergrowths of quartz and sodic feldspar.

In the gabbro clasts plagioclase occurs as weakly to moderately saussuritized subhedral crystals that generally display poorly preserved Carlsbad and albite twinning while clinopyroxene generally occurs as intergranular crystals which have been partially amphibolitized to a pale-green pleochroic amphibole. Other minerals observed in gabbro clasts include trace amounts of sphene and secondary carbonate.

The matrix material of the Upukerora Formation is dominated by fine hematite-stained mud and local concentrations of poorly sorted sandy material. The sand component of the matrix is mainly crystal fragments of:



**Plate 4.5** Microphotograph of quenched glassy basalt clast with radiating patterns of opaque and plagioclase microlites from the Upukerora conglomerate (Red Hills, R-912a). Note sandy matrix adjacent to the basalt clast. Plane-polarized light, x50.



**Plate 4.6** Microphotograph of a flow banded, glassy basalt clast within Upukerora conglomerate (Red Hills, R-912a). Plane-polarized light, x25.

clinopyroxene (sometimes partially altered to green pleochroic amphibole); green pleochroic amphibole; weakly to strongly saussuritized plagioclase; and minor amounts of detrital albite, quartz, epidote, sphene, and chloritized glass. Also observed within this sandy matrix are rare detrital grains of quartz and sodic feldspar in granophyric intergrowths. These granophyric grains are considered to have been derived from eroded dioritic gabbros or possibly plagiogranite.

Secondary minerals observed within these rocks include calcite, quartz, chlorite, and pumpellyite in vugs as well as calcite in rare veins.

#### 4.3 Dun Mountain Ophiolite

##### 4.3.1 Lee River Group Volcanic Rocks

Volcanic rocks of the Dun Mountain Ophiolite were encountered in two of the study areas of East Nelson: (i) along the Dun Mountain Track section of the Roding River map area (Figure 3.2.4); and (ii) north of Croisilles Harbour along the western shore of Taipare Bay (inset A, Figure 3.2.6).

The volcanic rocks of the Dun Mountain Ophiolite (Lee River Group) include glassy to fine-grained, pillowed to massive, basaltic flows and breccias. These rocks are dominated by clinopyroxene-phyric intergranular to intersertal basalts with minor occurrences of more glass-rich plagioclase porphyritic basalt. Within these rocks the proportions of clinopyroxene phenocrysts range from less than 1 percent in the glass-rich basalts to 25 percent in the intergranular basalts.

Within the intergranular basalts clinopyroxene phenocrysts are generally equant in shape, commonly zoned, and are typically less than 0.25 centimetres in diameter. Other primary mineral phases include abundant intergranular plagioclase and rare phenocrysts of olivine (pseudomorphed by pale-green pleochroic, cryptocrystalline chlorite). These rocks also contain variable amounts of iron-titanium oxides which are commonly altered to disseminated iron oxides (usually hematite).

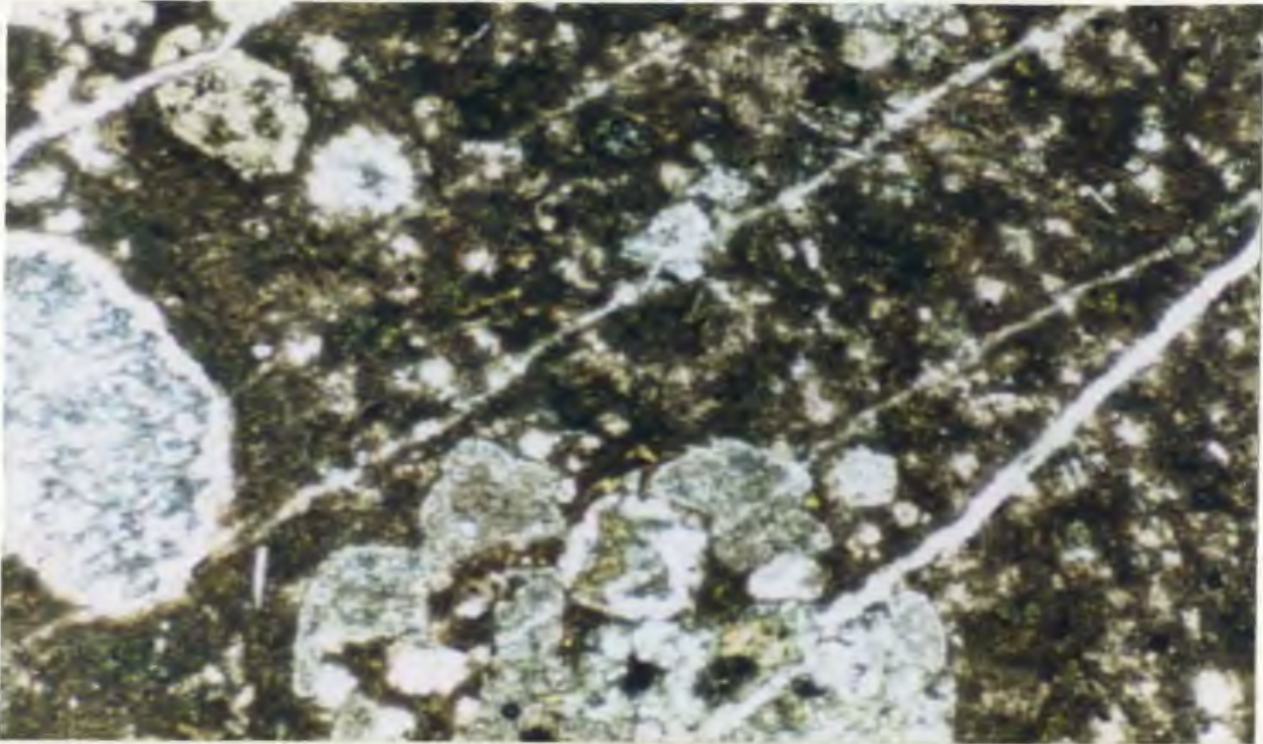
In the Roding River and Tinline River areas (Figures 3.2.4 & 3.2.5) clinopyroxene-phyric dykes of similar composition and texture intruded Lee River Group gabbros and likely served as conduits for Lee River Group basalts.

#### 4.3.1.1 Dun Mountain Track (Figure 3.2.4)

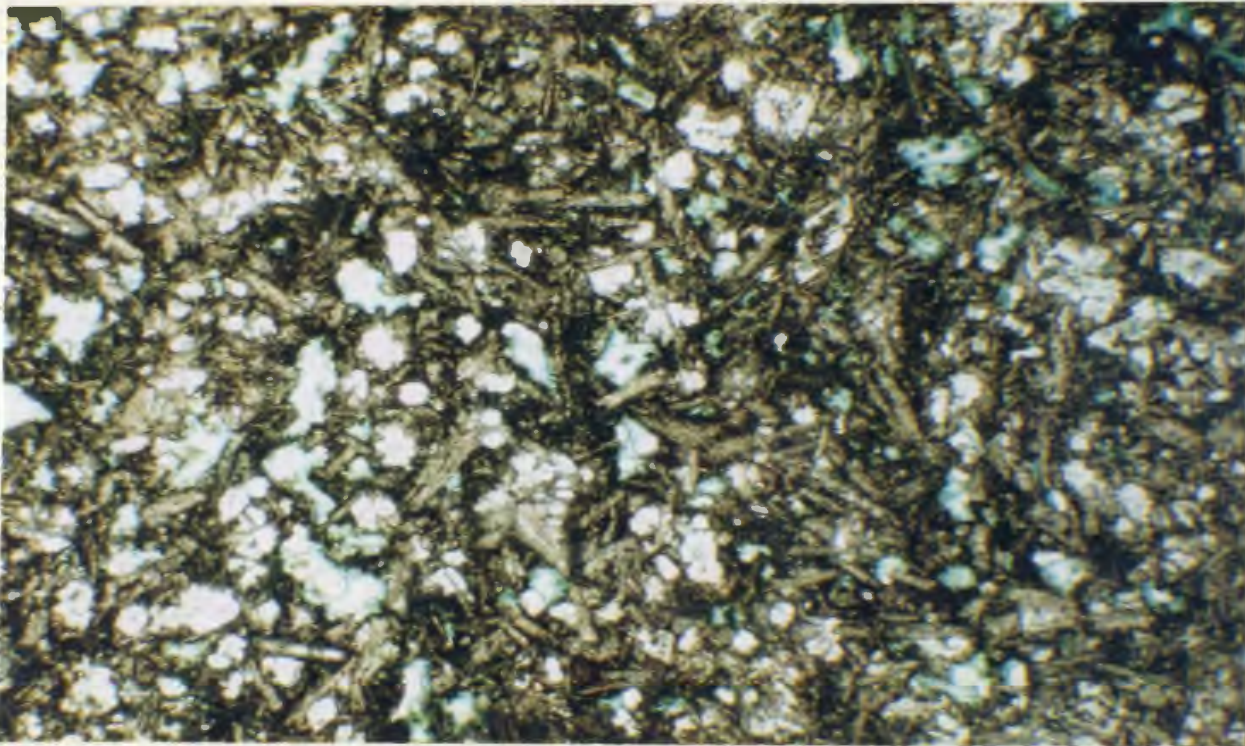
In the Dun Mountain Track section basaltic volcanic rocks of the Lee River Group are predominantly composed of massive, locally vesicular, hematite-stained basaltic flows and breccias. These rocks are relatively undeformed and range in composition from glassy plagioclase and clinopyroxene-phyric basalts, to fine-grained, intergranular, clinopyroxene-phyric flows.

Within the lower half of the Dun Mountain Track section (eastern half) basaltic rocks range in composition from glassy plagioclase- and clinopyroxene-phyric quenched basalts (Plate 4.7) to intersertal and intergranular, clinopyroxene-phyric basalts which contain up to 5 percent intersertal glass (Plate 4.8). Higher up in the section; however, basalts





**Plate 4.7** Plagioclase and olivine porphyritic Lee River Group basalt (Dun Mountain track, Roding River area, D-1003). Plagioclase is strongly saussuritized and olivine has been pseudomorphed by pale-green pleochroic chlorite. Plane-polarized light, x50.



**Plate 4.8** Microphotograph of weakly altered intergranular Lee River Group basalt with numerous equant intergranular crystals of fresh clinopyroxene (Dun Mountain Track, D-1000). Note green pleochroic pumpellyite and chlorite replacing glass. Plane-polarized light, x25.

gradually become coarser grained and comprise intergranular, clinopyroxene-phyric flows and breccias (Plate 4.9).

Within glassy flows, plagioclase, clinopyroxene and rare olivine phenocrysts (olivine phenocrysts are generally less than 1 millimetre in diameter) are observed within a matrix of quenched glassy to variolitic material (Plate 4.8), while fine- to medium-grained flows are composed of clinopyroxene-phyric basalts which contain numerous equant, subhedral clinopyroxene phenocrysts in an intergranular matrix of subhedral to euhedral plagioclase laths (Plate 4.9).

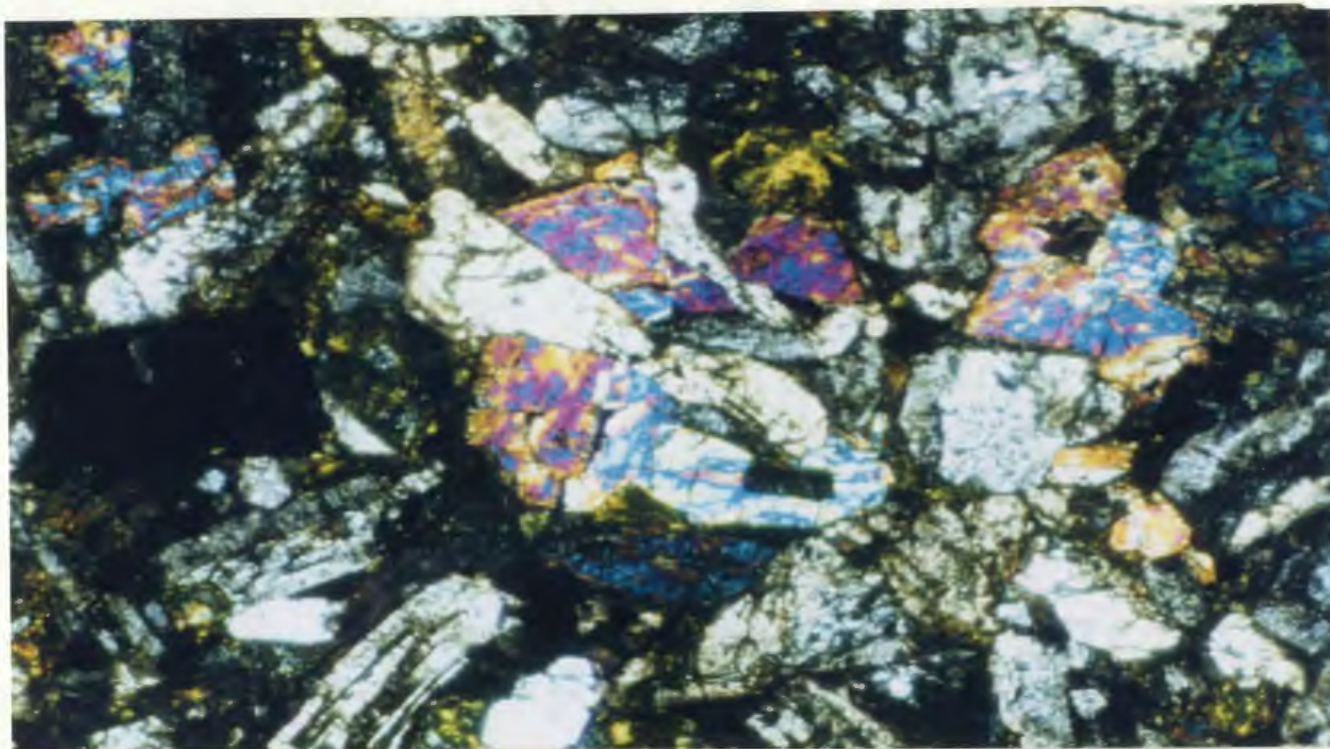
For the most part, basalts of the Dun Mountain track section have undergone lower greenschist and sub-greenschist facies metamorphism. Evidence of lower greenschist metamorphism includes the pseudomorphic replacement of olivine micro-phenocrysts by pale-green pleochroic, cryptocrystalline chlorite (Plate 4.7) and the saussuritization and albitization of plagioclase. Chlorite and albite are also observed in these rocks infilling vesicles and vuggy cavities.

Secondary metamorphic minerals related to later sub-greenschist facies metamorphism include: pumpellyite, carbonate, and quartz (trace amounts) which commonly occur in veinlets and infilling vesicles and vuggy cavities.

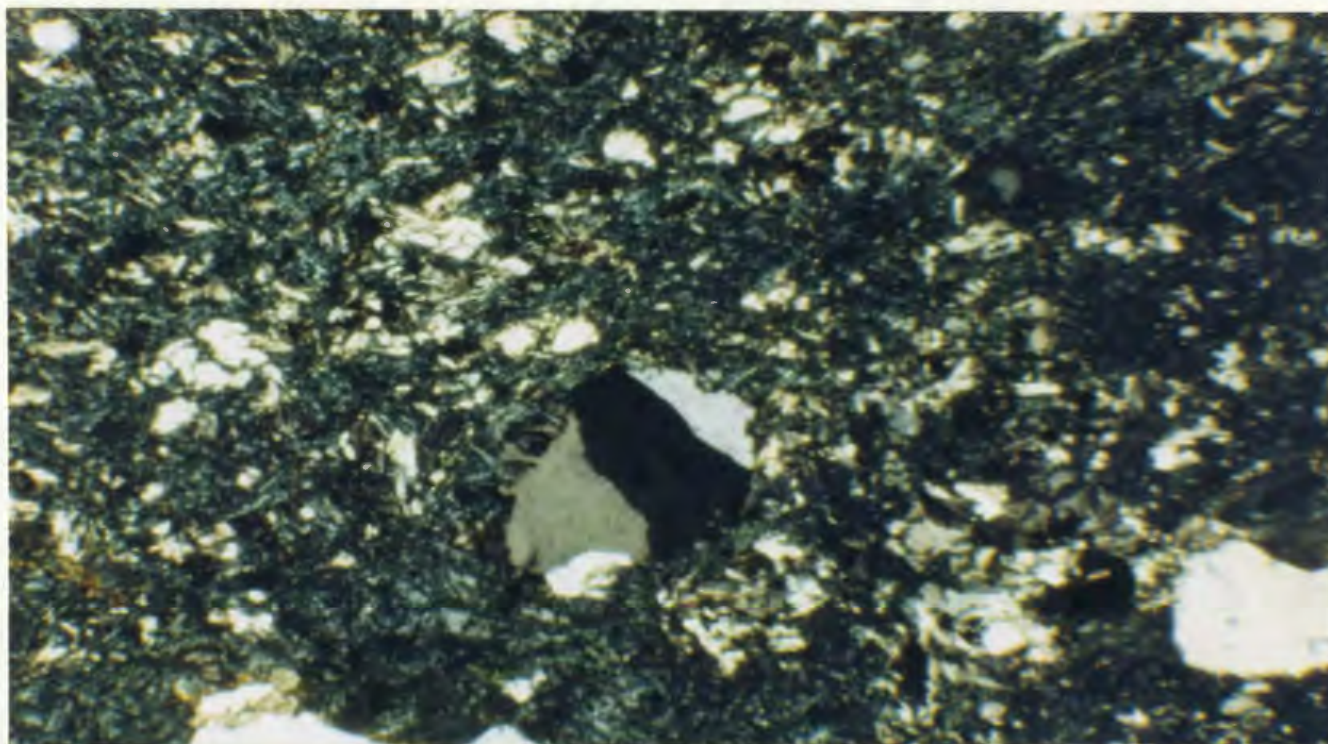
#### 4.3.1.2 Taipare Bay (Inset A, Figure 3.2.6)

Lee River Group basalts of Taipare Bay are compositionally quite similar to those of the Dun Mountain Track sequence being predominantly composed of clinopyroxene-phyric intergranular basalts with minor occurrences





**Plate 4.9** Microphotograph of porphyritic Lee River Group basalt (Dun Mountain Track, Roding River area, D-1007). Crossed nicols, x50.



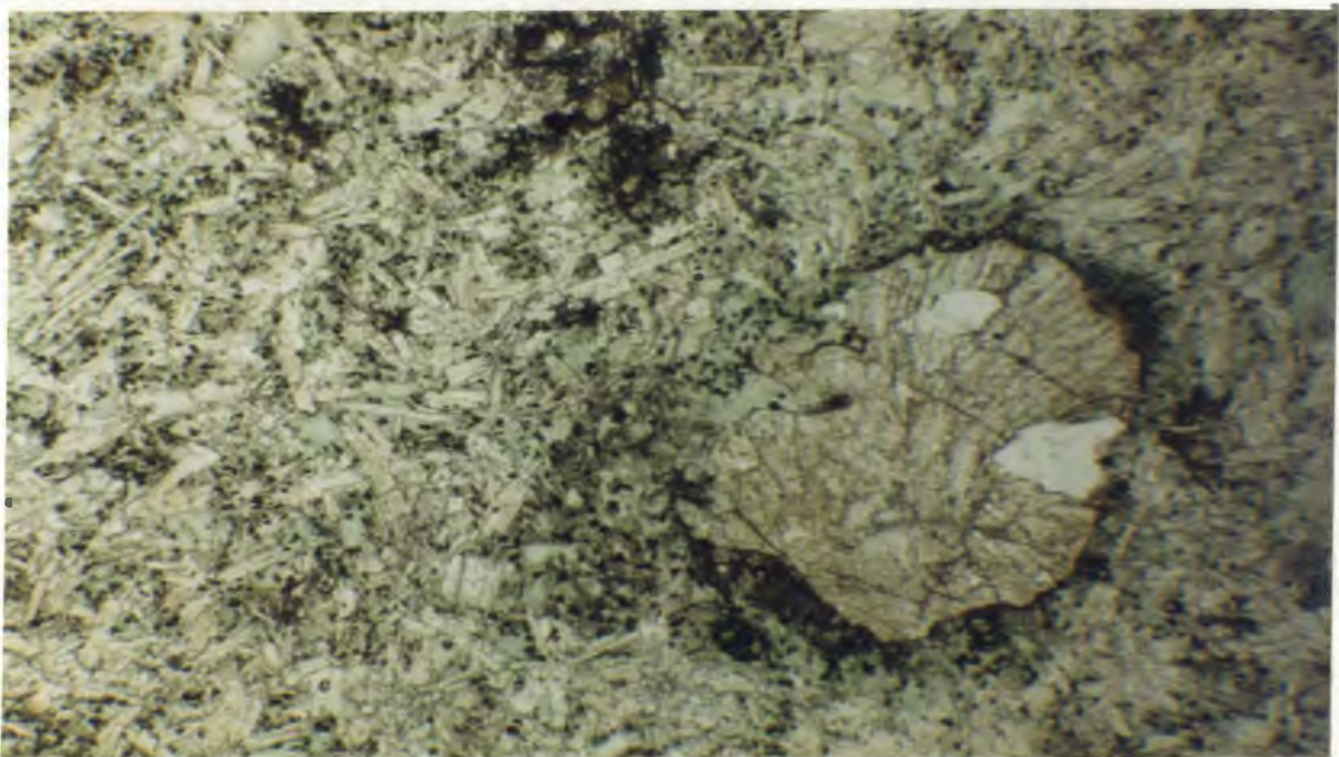
**Plate 4.10** Microphotograph of amygdaloidal, chloritized basalt with patches of preserved basaltic texture (Lee River Group, Taipare Bay, SD-810). Vesicles are filled with quartz. Crossed nicols, x25.

of finer grained to glassy basalt; however, basalts of Taipare Bay are pillowed and are generally more intensely vesiculated. Another notable difference between these two basalt sequences is the degree of alteration as Taipare Bay basalts are in places intensely chloritized (Plate 4.10). These rocks also contain a large variety of secondary minerals including amygdaloidal chlorite, epidote, carbonate, and quartz. Minor amounts of later pumpellyite are also observed infilling vuggy cavities suggesting that these rocks also underwent some degree of sub-greenschist facies metamorphism in addition to earlier greenschist metamorphism.

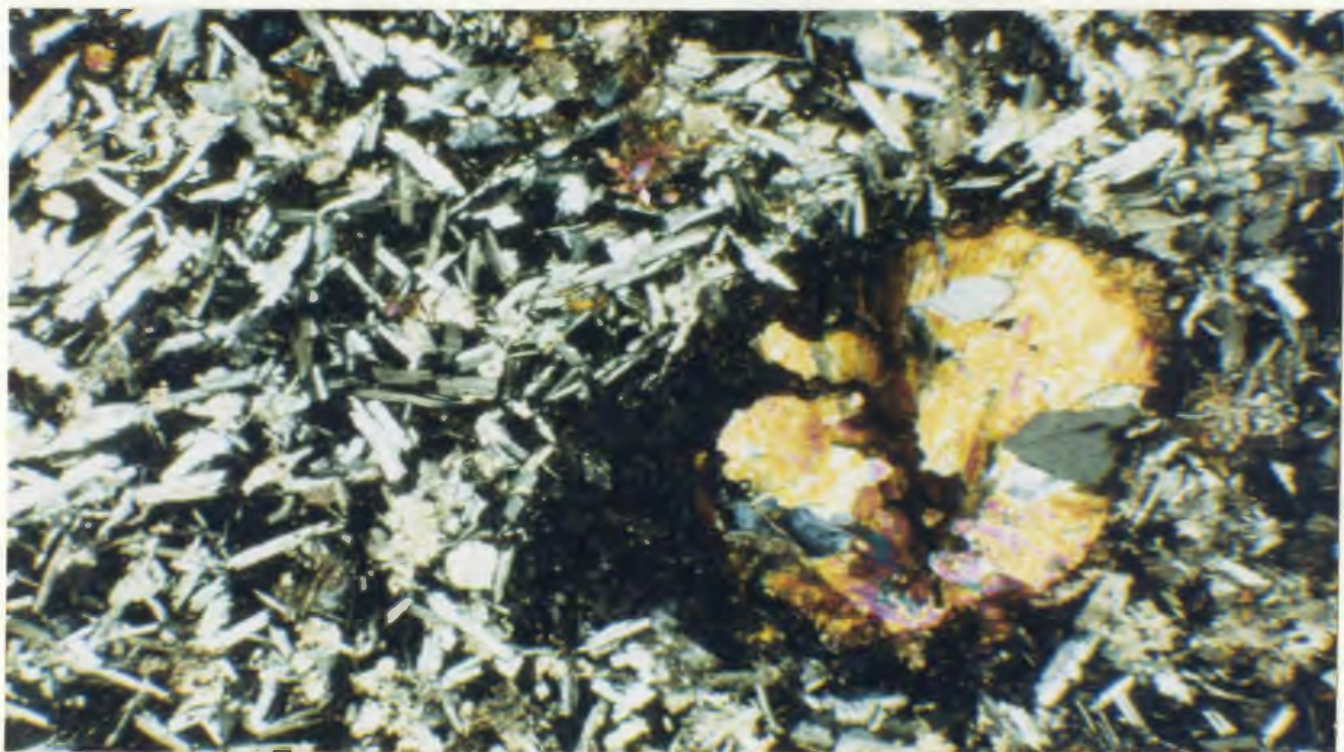
The basalts of Taipare Bay range in composition from glassy and fine-grained hyalopilitic basalts to fine- and medium-grained intergranular, clinopyroxene-phyric basalts. Glassy basalts are generally made up of subhedral laths of plagioclase set in a matrix of intersertal chloritized glass (Plate 4.10). Fine-grained basalts; however, range from plagioclase rich, hyalopilitic basalts (Plates 4.11a and b) to coarser grained, intergranular, clinopyroxene-phyric basalts which may contain up to 20 percent equant, clinopyroxene phenocrysts (Plate 4.12). Iron-titanium oxides are also present within the basalts as small grains along larger crystal grain boundaries or as fine disseminations within chloritized glass (Plate 4.11a).

Within Taipare Bay basalts, alteration has mainly affected plagioclase and iron-titanium oxides while clinopyroxene is relatively unaltered. Plagioclase is typically moderately to strongly saussuritized and occasionally is replaced by chlorite and quartz; particularly in zones of more intense chloritization. Iron-titanium oxides are commonly altered to fine wispy



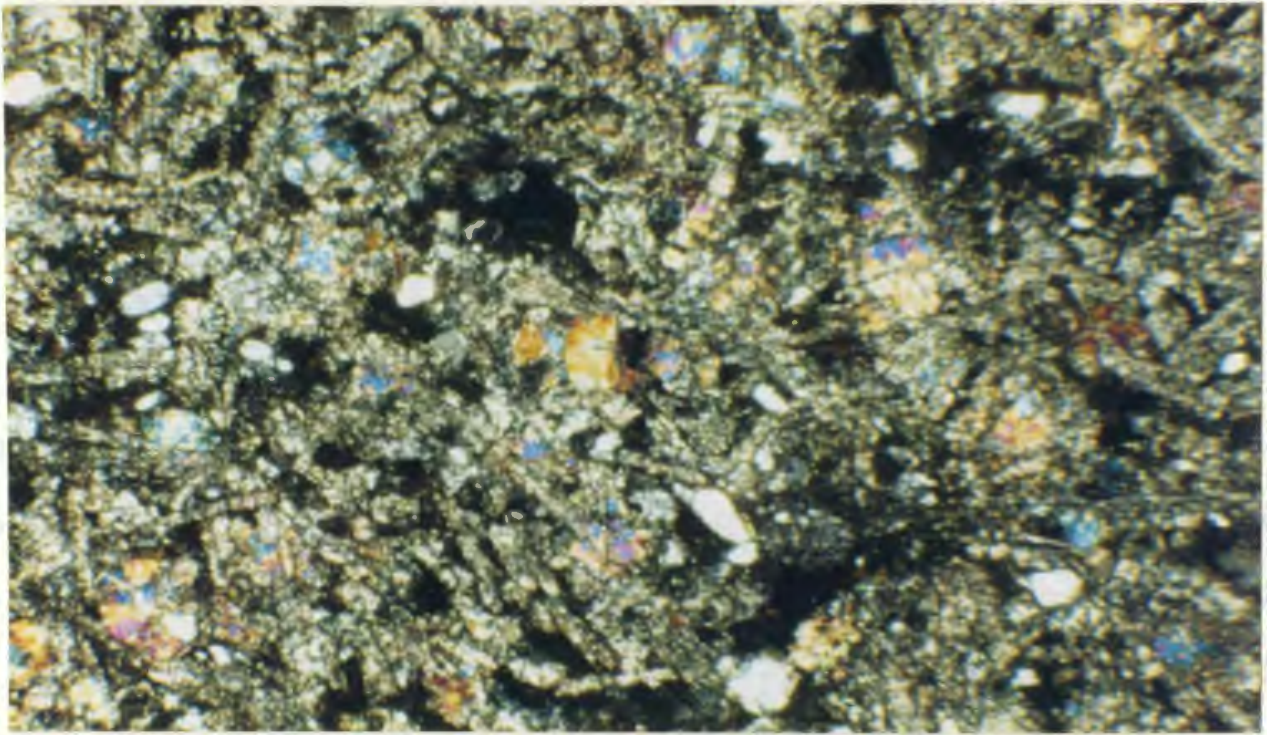


**Plate 4.11a** Microphotograph of intergranular basalt with epidote and quartz filled vesicles (Lee River Group, Taipare Bay, Sd-805). Crossed nicols, x25.



**Plate 4.11b** Microphotograph of intergranular basalt with epidote and quartz filled vesicles (Lee River Group, Taipare Bay, Sd-805). Crossed nicols, x25.





**Plate 4.12** Microphotograph of weakly chloritized intergranular basalt (Lee River Group, Taipare Bay, SD-809). Note abundant clinopyroxene as intergranular equidimensional crystals suspended within a matrix of intersertal to intergranular basalt. Crossed nicols, x25.



**Plate 4.13** Microphotograph of fine-grained diabase (Lee River Group) with well preserved intergranular texture (Red Hills, R-907). Note prehnite veinlet (second order birefringence). Crossed nicols, x25.

disseminations of hematite while intersertal glass is typically altered to pale-green pleochroic chlorite.

#### 4.3.2 Lee River Group Subvolcanic Rocks

Subvolcanic rocks of the Lee River Group are dominated by medium-grained isotropic gabbros cut by small numbers of fine- to medium-grained diabase dykes. Throughout the East Nelson region the relative amounts of these components vary with location and stratigraphic level within the Lee River Group as do their compositions and metamorphic character. Within the areas investigated, three distinct suites of Lee River Group subvolcanic rocks (gabbros and diabase dykes) were observed: (i) an aphyric suite of fine- to medium-grained, amphibolitized gabbros and diabase dykes; (ii) a suite of medium-grained, amphibolitized, plagioclase porphyritic diabase dykes and gabbros; and (iii) a suite of fine- to medium-grained, nonamphibolitized, clinopyroxene-phyric, diabase dykes and gabbros similar in composition and mineralogy to the clinopyroxene-phyric Lee River Group volcanics.

The most abundant and oldest of these suites is the aphyric suite which hosts rocks of the other two suites. In the areas studied, gabbros and dykes of this suite represent more than 90 percent of the Lee River Group's (Dun Mountain Ophiolite) subvolcanic sequence and vary from weakly amphibolitized and unfoliated to strongly amphibolitized and strongly foliated (flazered) dykes and gabbros. The majority of the rocks belonging to this suite were observed within the semicontinuous sequence of subvolcanic rocks of the Lee River Group; however, blocks and tectonic inclusions of these

subvolcanic rocks were also observed in sheared serpentinite fault zones separating the Lee River Group from the Dun Mountain Ultramafics.

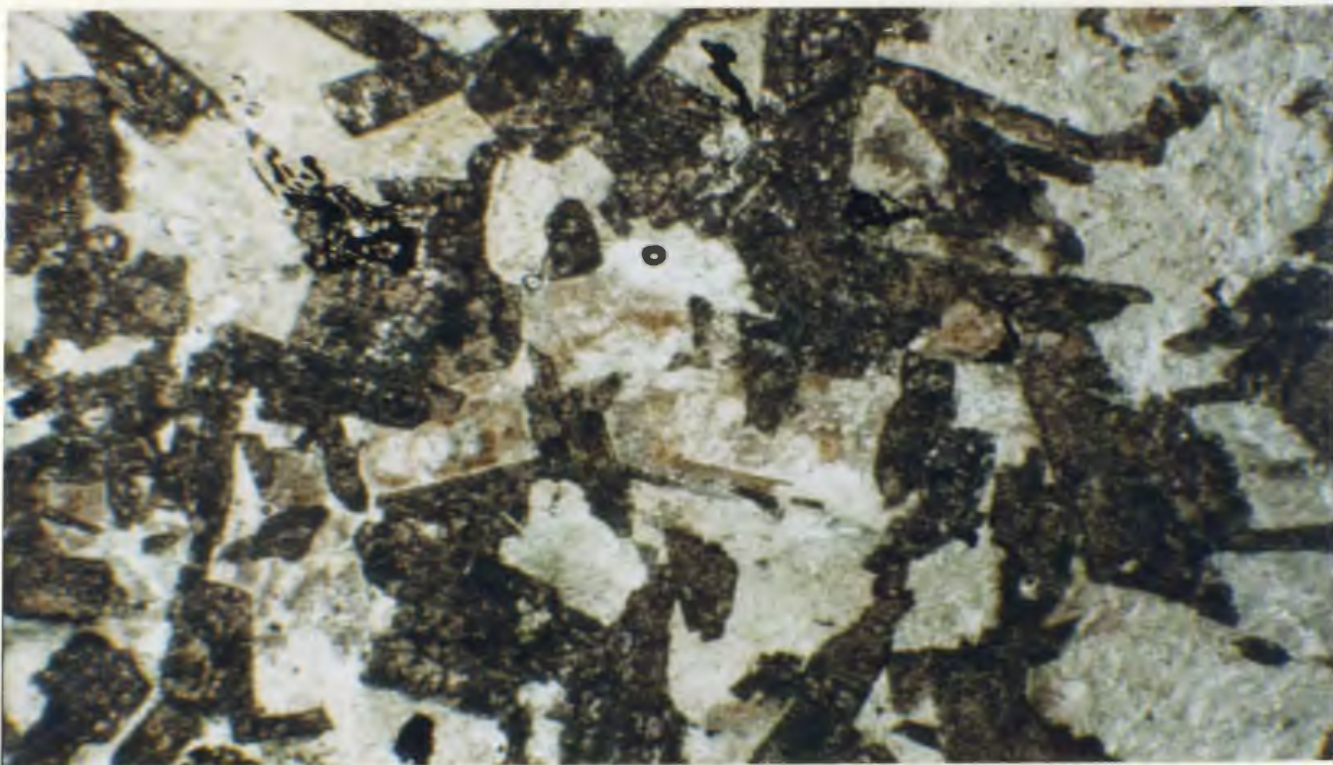
Rocks of the aphyric suite are predominantly composed of: intergranular, altered clinopyroxene (partially to completely amphibolitized to green or brown pleochroic amphibole); weakly to strongly saussuritized plagioclase; minor amounts of iron-titanium oxides; chloritized intersertal glass; sphene; and very rare olivine phenocrysts (pseudomorphed by chlorite) in some of the diabase dykes (Plates 4.13 and 4.18).

Within these rocks, original crystal boundaries are generally obscured by the alteration of clinopyroxene to amphibole (eg., Plates 4.14a and b); however, in less metamorphosed samples primary intergranular textures survive. In the more strongly metamorphosed (amphibolitized) gabbros and dykes, primary intergranular textures are often still identifiable where relict, primary plagioclase crystal boundaries are preserved (eg., Plate 4.14a and b).

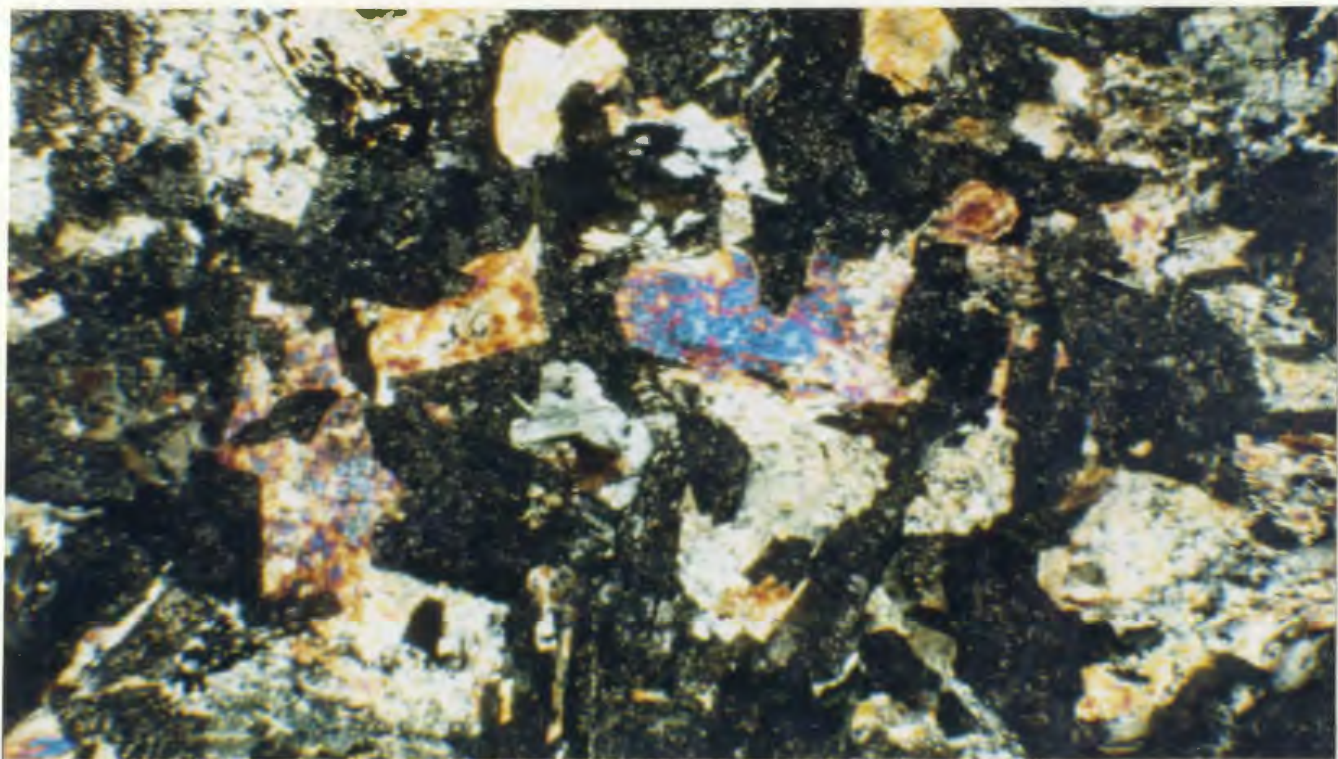
Plagioclase is generally observed in rocks of the aphyric suite as weakly to strongly saussuritized, rectangular crystals in which relict albite and Carlsbad twinning is preserved in less altered crystals. At some localities, particularly where rocks are strongly amphibolitized and in close proximity to the Lee River Group-Dun Mountain Ultramafics fault contact, plagioclase is partially replaced by prehnite and hydrogrossular.

Clinopyroxene is rarely preserved within aphyric suite rocks and is typically altered to a pale-green pleochroic amphibole within high levels of the subvolcanic sequence. At these levels gabbros and dykes are generally undeformed; however, at lower levels (along the sequence's eastern contacts)



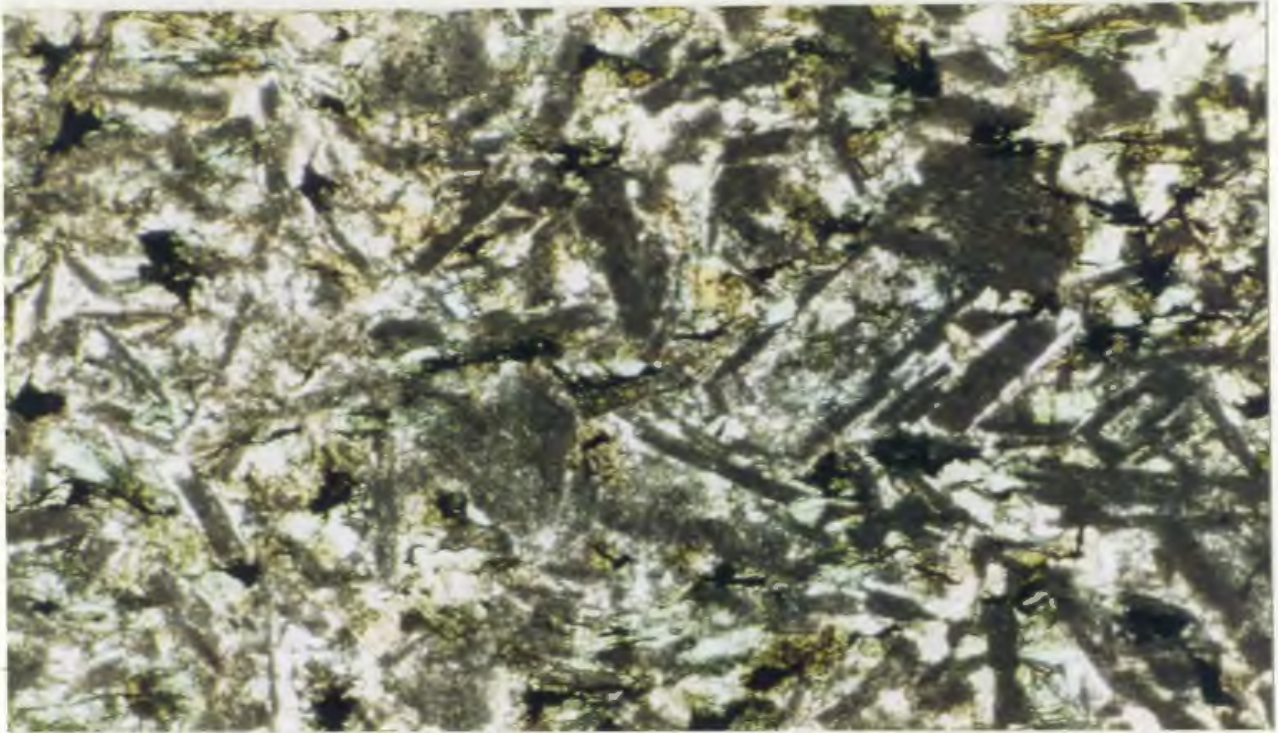


**Plate 4.14a** Microphotograph of medium-grained Lee River Group gabbro (Serpentine River area, S-7). Plane-polarized light, x25.

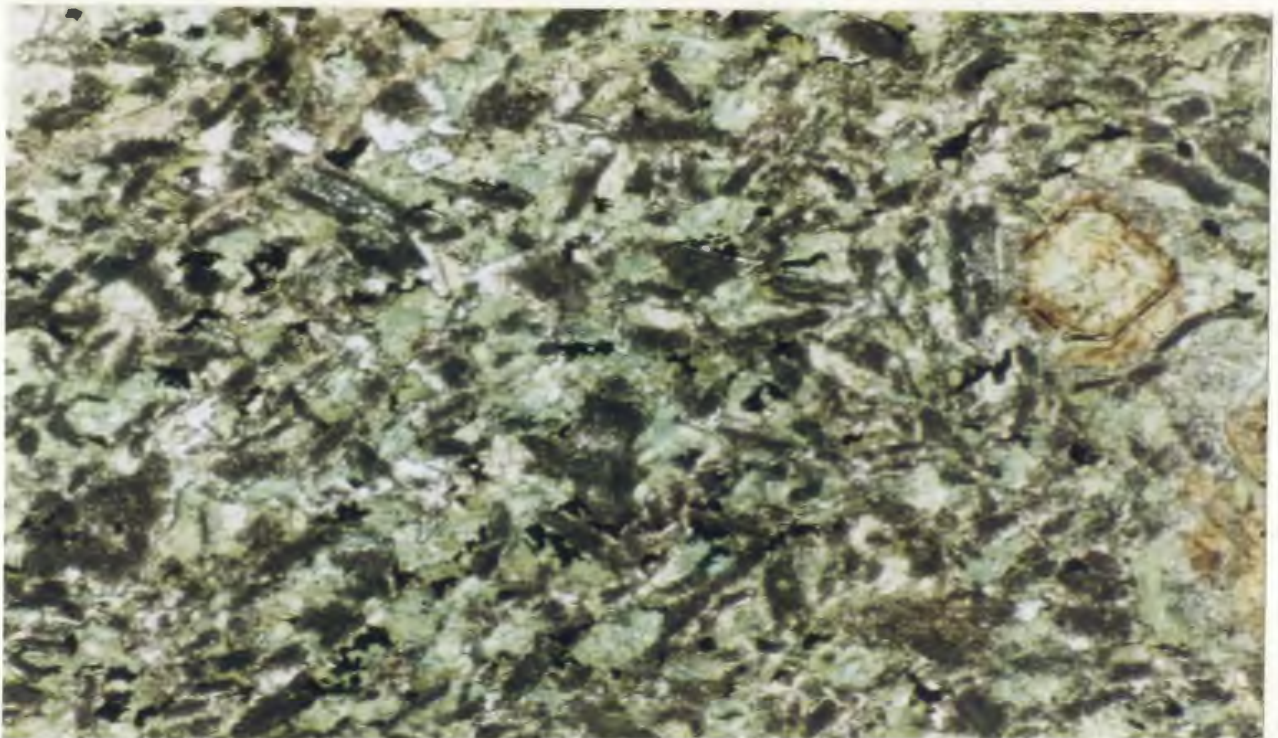


**Plate 4.14b** Microphotograph of medium-grained Lee River Group gabbro (Serpentine River area, S-7). Crossed nicols, x25.



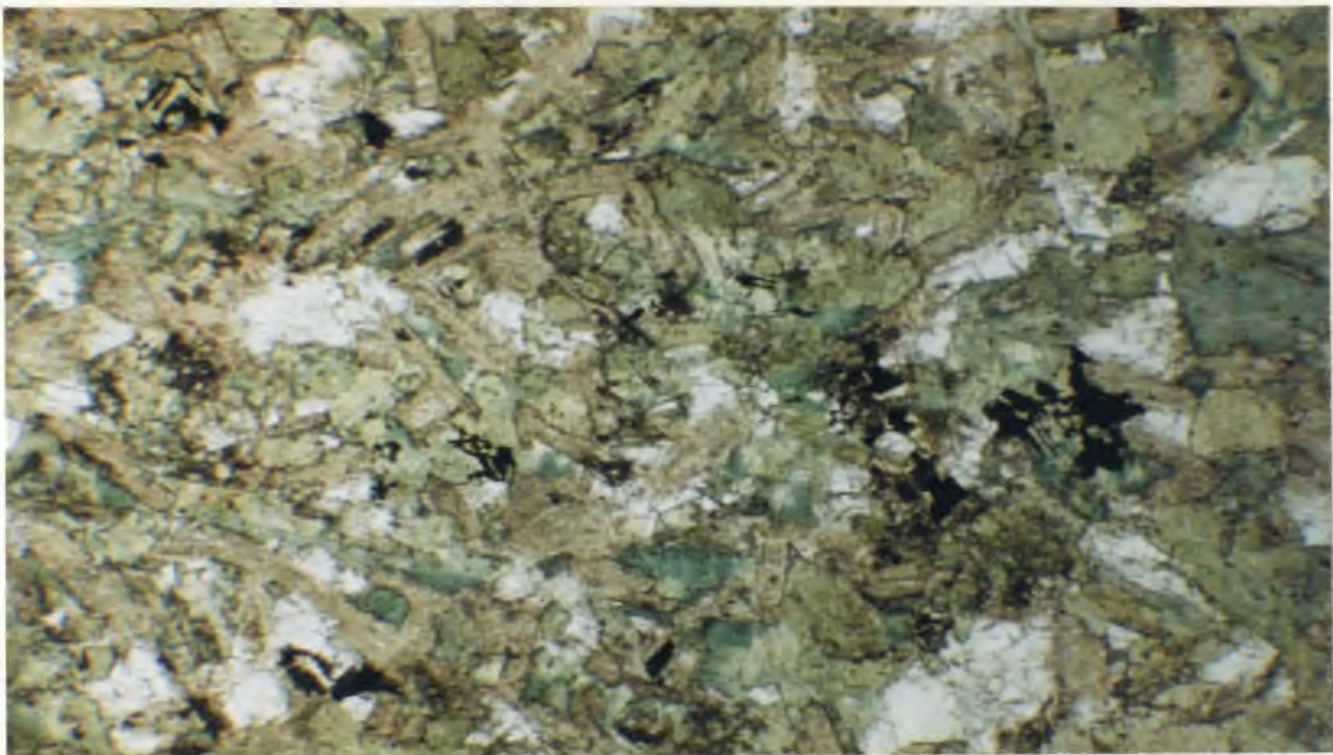


**Plate 4.15** Microphotograph of intergranular Lee River Group diabase (United Creek, Roding River area, H-761b). Plane-polarized light, x50.



**Plate 4.16** Microphotograph of fine-grained, intergranular Lee River Group diabase with chlorite replaced olivine microphenocryst (Tinline River area, TL-525b). Plane-polarized light, x50.





**Plate 4.17** Microphotograph of intergranular, medium-grained Lee River Group gabbro (Tinline River area, TL-530a). Clinopyroxene is altered to green pleochroic amphibole. Plane-polarized light, x25.



**Plate 4.18** Microphotograph of amphibolitized (brown hornblende), medium-grained, Lee River Group gabbro (Champion Creek, Roding River area H-756). Plane-polarized light, x50.

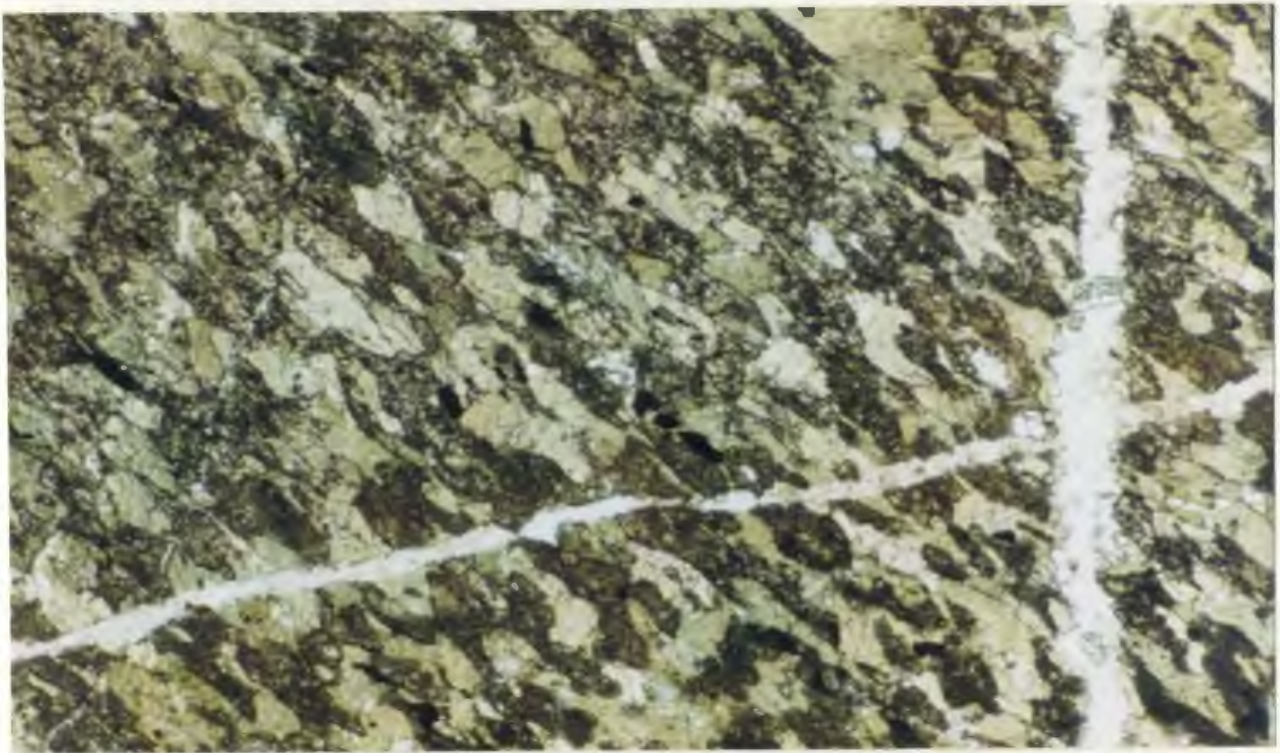
the rocks are commonly strongly amphibolitized and foliated, whereby clinopyroxene is completely metamorphosed to a pale-brown pleochroic amphibole (Plates 4.18 to 4.20).

Olivine is also rarely observed in this suite as scarce microphenocrysts (less than 1 millimetre in diameter) in fine-grained diabase dykes (Plate 4.16) but olivine is always pseudomorphed by pale-green pleochroic, cryptocrystalline chlorite containing fine disseminations of opaque oxides.

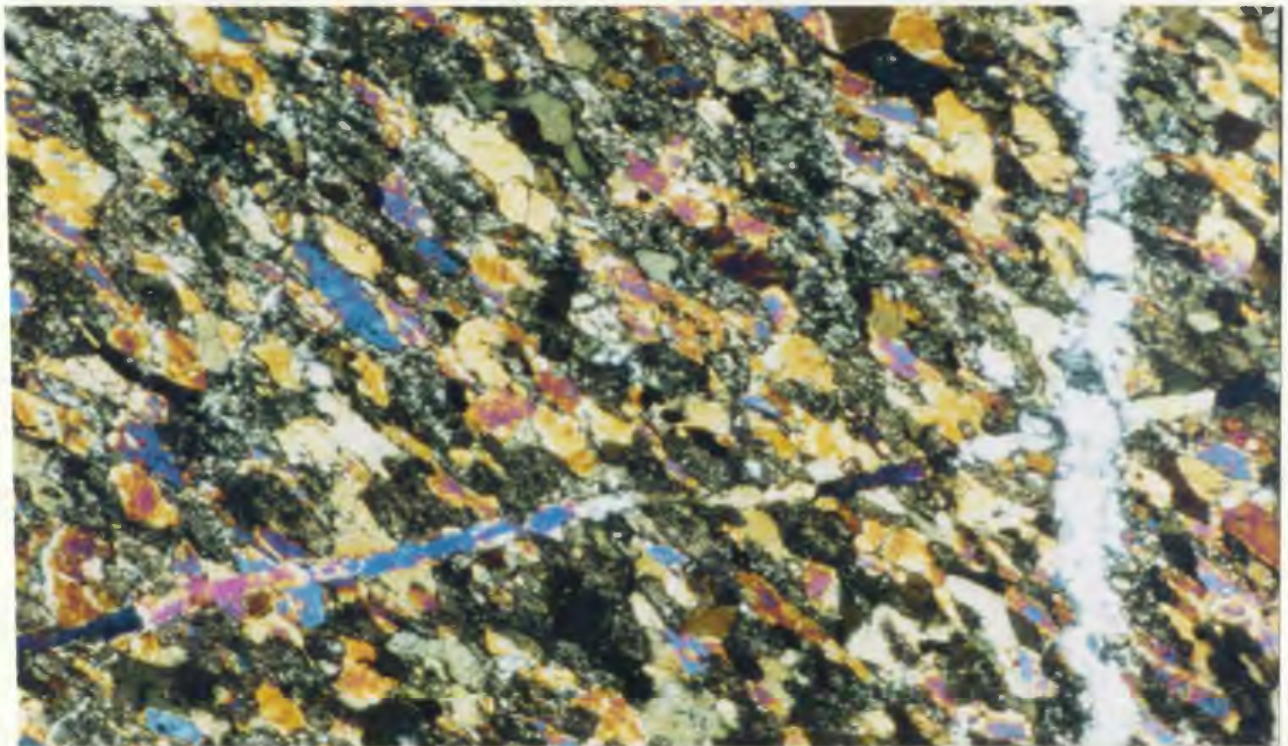
Deformation of this suite of rocks appears to increase in intensity towards the southeastern fault contact with the Dun Mountain Ultramafics Group. Near this contact, gabbros and dykes of the aphyric suite are strongly amphibolitized and foliated (flazered) whereby original igneous intergranular textures have been obliterated through recrystallization and deformation (Plates 4.18 to 4.20). Within these strongly amphibolitized rocks clinopyroxene is recrystallized to equant, interlocking crystals of pale-brown pleochroic, foliated, amphibole.

Aphyric suite subvolcanic rocks of the Lee River Group are also observed in some places as tectonic inclusions in serpentinite shear zones separating ultramafic rocks of the Dun Mountain Ultramafics Group from subvolcanic and sedimentary rocks of the Lee River and Maitai groups. These inclusions are generally composed of amphibolitized, strongly foliated medium-grained gabbro and fine-grained diabase. Within these rocks (Plate 4.21) clinopyroxene is altered to a brown pleochroic hornblende and plagioclase to later prehnite. The presence of brown amphibole suggests they were metamorphosed at greater depths and pressures than higher level



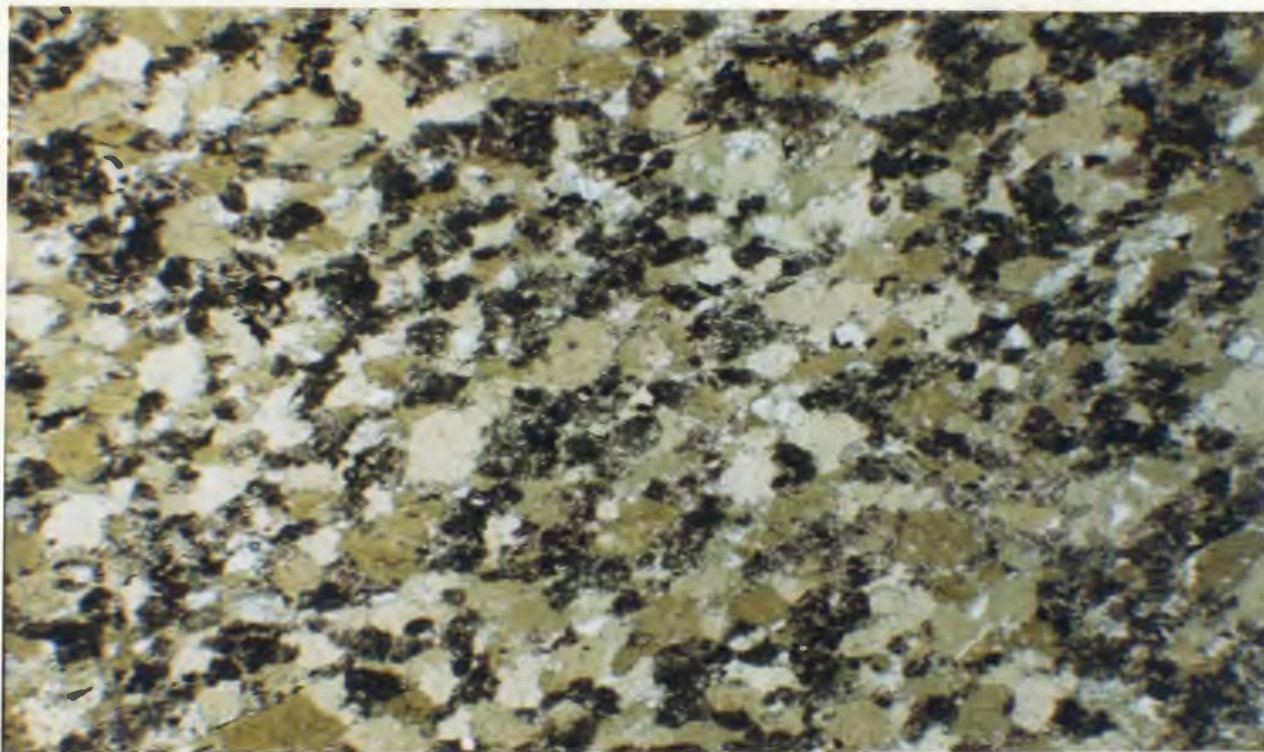


**Plate 4.19a** Microphotograph of amphibolitized (brown pleochroic hornblende) and foliated medium-grained, Lee River Group diabase cut by veinlets of prehnite and albite (Champion Creek, Roding River area, H-758a). Plane-polarized light, x50.

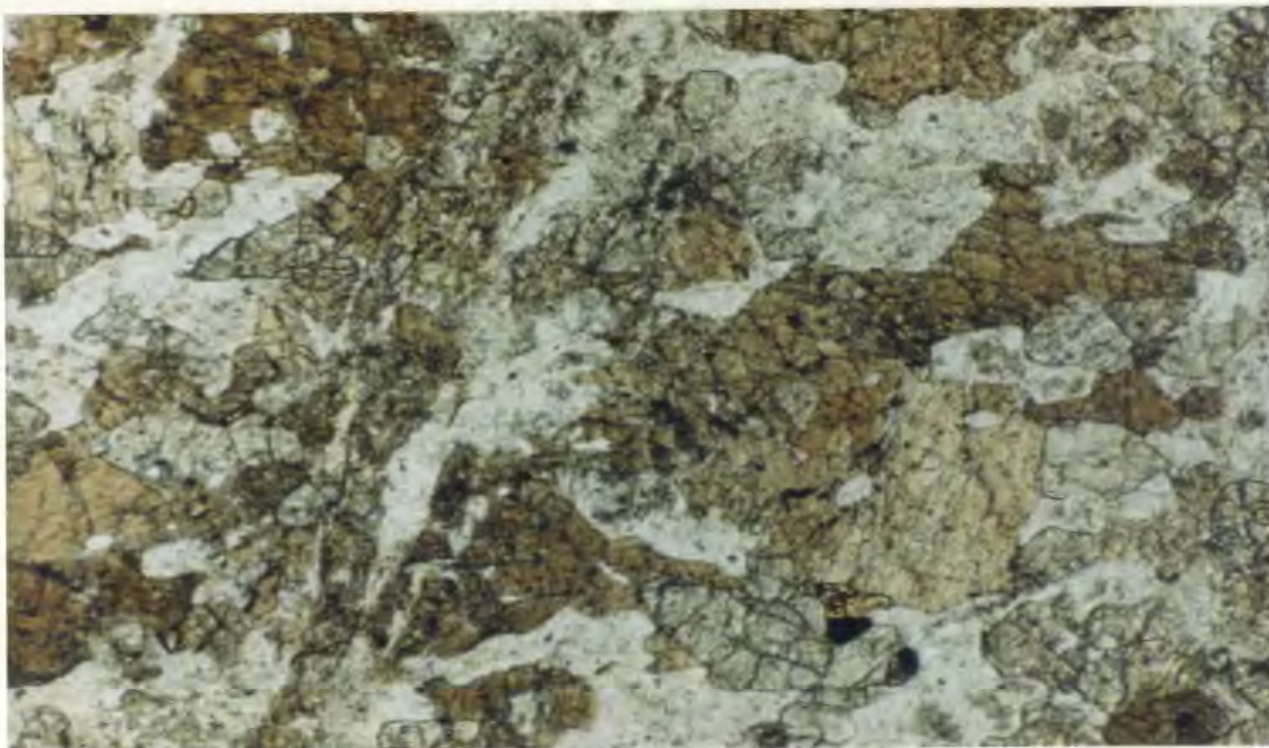


**Plate 4.19b** Microphotograph of amphibolitized and foliated medium-grained, Lee River Group diabase cut by veinlets of prehnite (second order birefringence) and albite (Champion Creek, Roding River area, H-758a). Crossed nicols, x50.





**Plate 4.20** Microphotograph of foliated and amphibolitized (brown hornblende) Lee River Group gabbro cut perpendicular to the foliation (Tinline River area, TL-524). Plane-polarized light, x25.



**Plate 4.21** Microphotograph of amphibolitized gabbro with brown pleochroic hornblende (an inclusion within a sheared serpentinite fault zone, Lee River area, T-288). Plane-polarized light, x50.

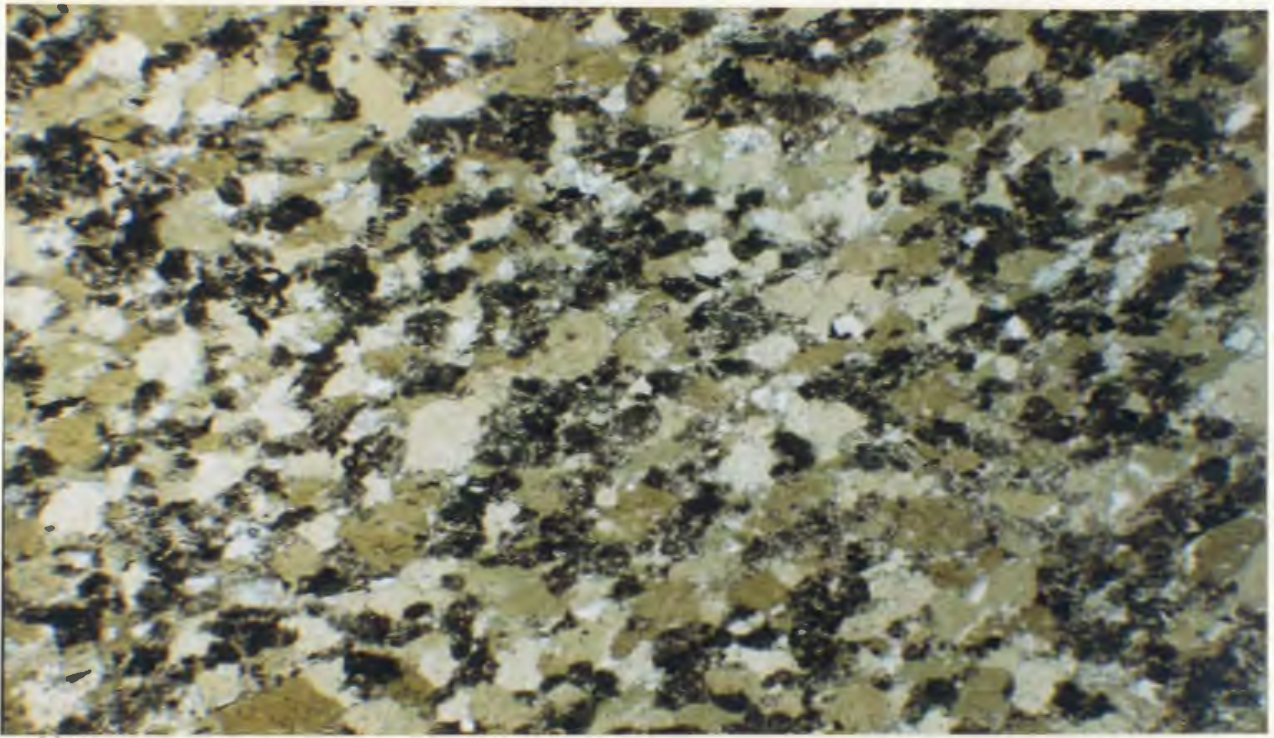
gabbros (containing pale-green pleochroic amphibole) as found in unconformable contact with Maitai Group sediments near Little Ben, and are therefore considered to represent deeper level rocks of the Lee River Group brought into contact with higher level rocks by faulting.

These tectonic inclusions may be in part rodingitized (Plate 4.22) and tremolitic amphibole (non-pleochroic) is in places observed partially replacing actinolitic amphibole (pale-green pleochroic) while plagioclase is strongly saussuritized. Rodingitization of these rocks was likely the result of low-temperature reactions between mafic subvolcanic rocks and fluids produced during serpentinization of the adjacent ultramafic rocks of the Dun Mountain Ultramafics Group. This suggests serpentinization of Dun Mountain Ultramafics Group rocks occurred after low-grade (greenschist) metamorphism of the Lee River Group gabbros in which clinopyroxene altered to actinolitic amphibole, and subsequently to tremolitic amphibole during rodingitization.

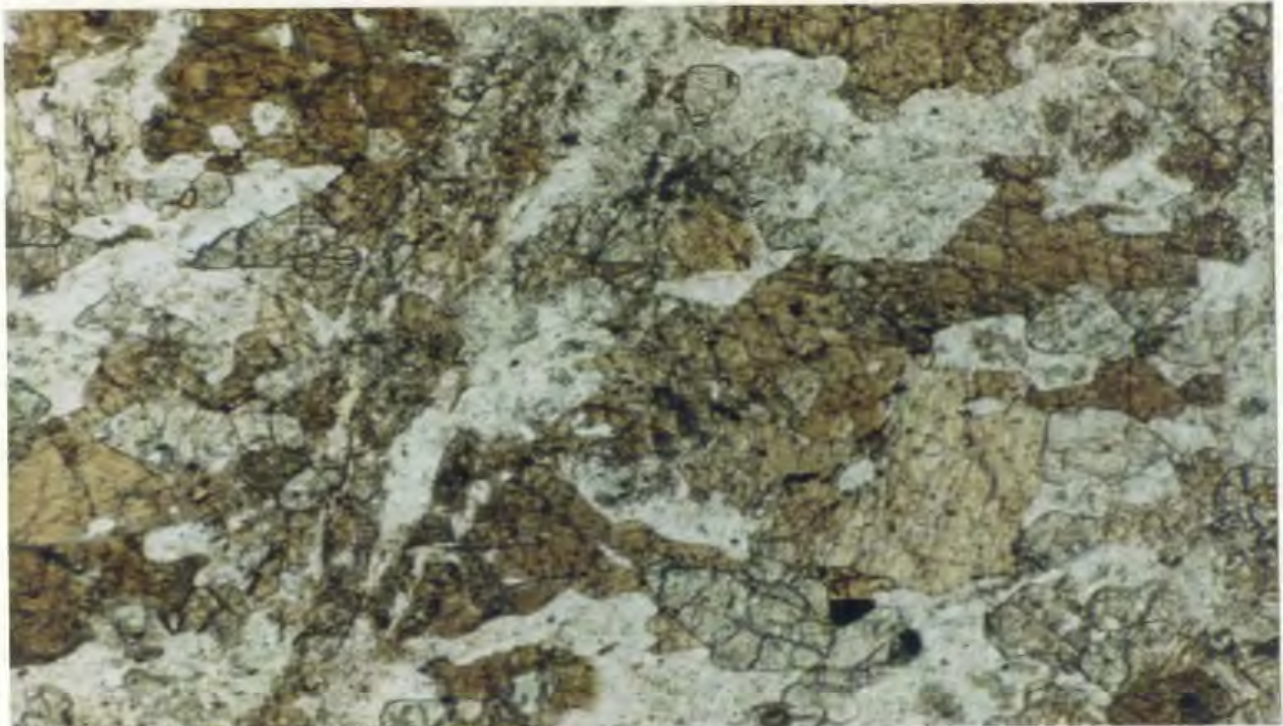
The second suite of Lee River Group subvolcanic rocks is composed of weakly to non-foliated, weakly to moderately amphibolitized, plagioclase porphyritic diabase dykes and gabbros. These rocks comprise medium- to fine-grained intergranular diabase dykes and gabbros similar to those of the aphyric suite but contain between 10 and 30 percent, rectangular-shaped plagioclase phenocrysts (0.25 to 1 centimetre in length; Plate 4.23).

Plagioclase crystals (including phenocrysts) are typically strongly saussuritized and partially altered to prehnite, while clinopyroxene is generally completely altered to a pale-green pleochroic amphibole. For the most part plagioclase phenocrysts are fractured and possess sharply defined, euhedral





**Plate 4.20** Microphotograph of foliated and amphibolitized (brown hornblende) Lee River Group gabbro cut perpendicular to the foliation (Tinline River area, TL-524). Plane-polarized light, x25.



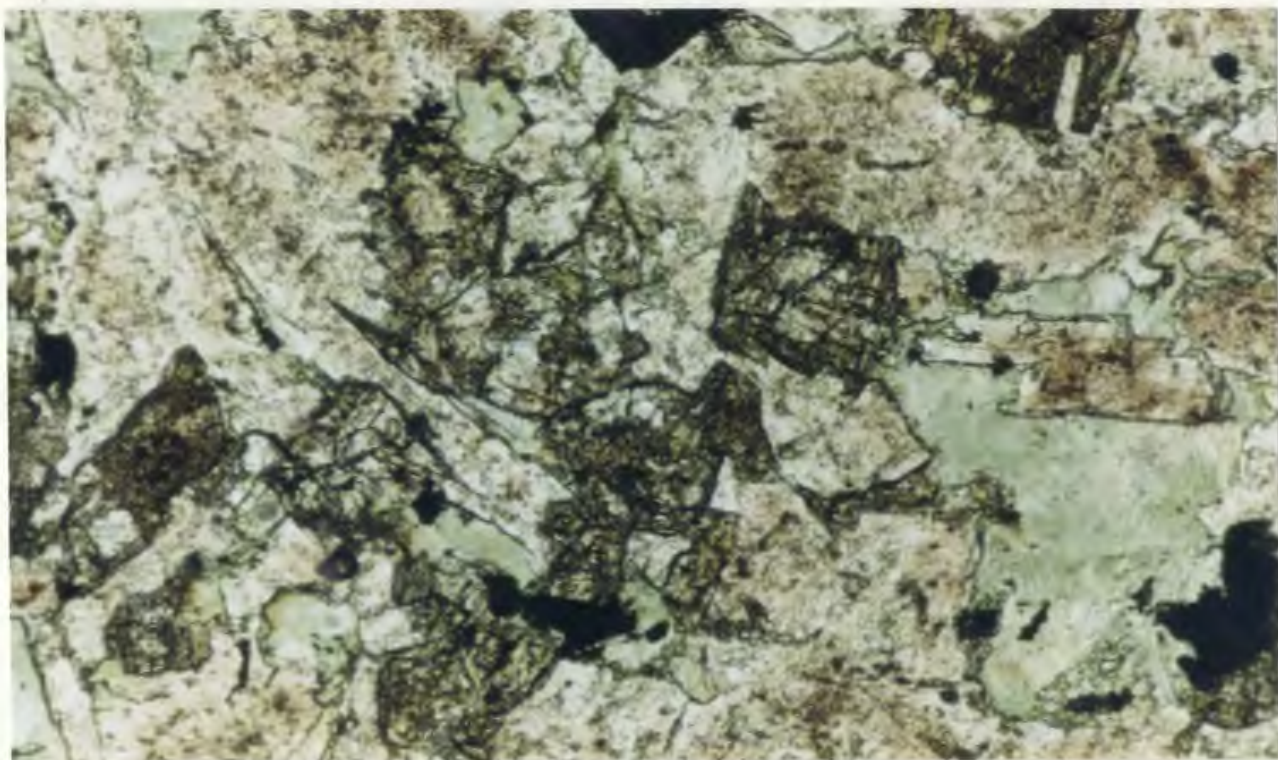
**Plate 4.21** Microphotograph of amphibolitized gabbro with brown pleochroic hornblende (an inclusion within a sheared serpentinite fault zone, Lee River area, T-288). Plane-polarized light, x50.



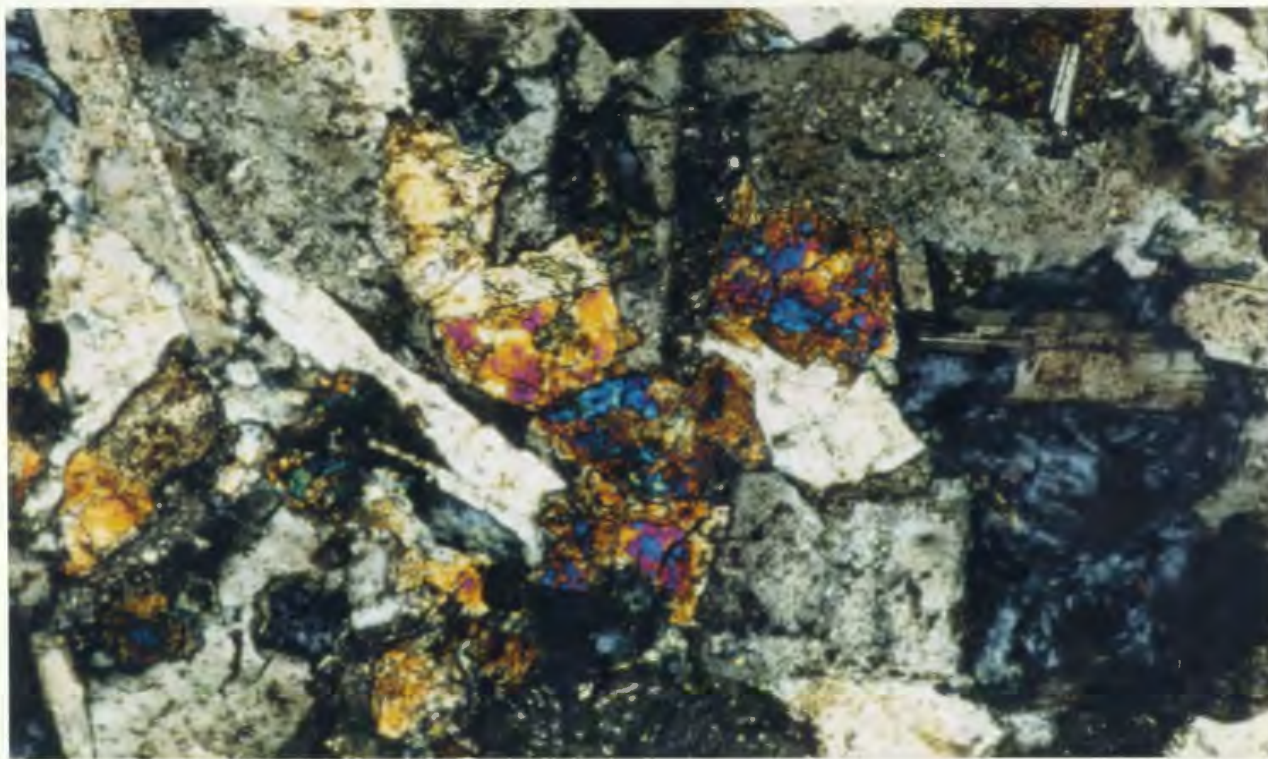
crystal boundaries.

Rocks of the plagioclase porphyritic suite are easily recognized in the field and are estimated to represent less than 5 percent of the Lee River Group subvolcanic sequence. Although these rocks are relatively rare and were only observed in outcrop along the Tinline River section (Figure 3.2.5); they are not considered to represent a suite of rocks unique to the Tinline River area as boulders of similar plagioclase porphyritic diabase were observed in Champion Creek (Figure 3.2.4) approximately 17 kilometres southwest of the Tinline River section. Rocks of this suite are considered to be generally younger in age than those of the aphyric suite as plagioclase porphyritic diabase dykes are observed intruding dykes and gabbros of the aphyric suite.

Rocks of the third suite of Lee River Group subvolcanics are composed of undeformed, nonamphibolitized, medium- to fine-grained, intergranular, clinopyroxene-phyric gabbro and diabase dykes (Plates 4.24a,b to 4.27) and closely resemble the clinopyroxene-phyric flows of the Lee River Group volcanics (ie. Dun Mountain Track and Taipare Bay sections). Although these rocks are easily identified in thin section they could not be distinguished from rocks of the aphyric suite in outcrop. Rocks of this suite are predominantly composed of non-amphibolitized clinopyroxene, weakly to moderately saussuritized plagioclase, minor amounts of iron-titanium oxides, and pyrite. Within these rocks clinopyroxene is typically partially altered to chlorite and occurs as zoned, subhedral, intergranular, phenocrysts (less than 1 millimetre in diameter) in which cores and/or rims are generally chloritized (Plate 4.26a).

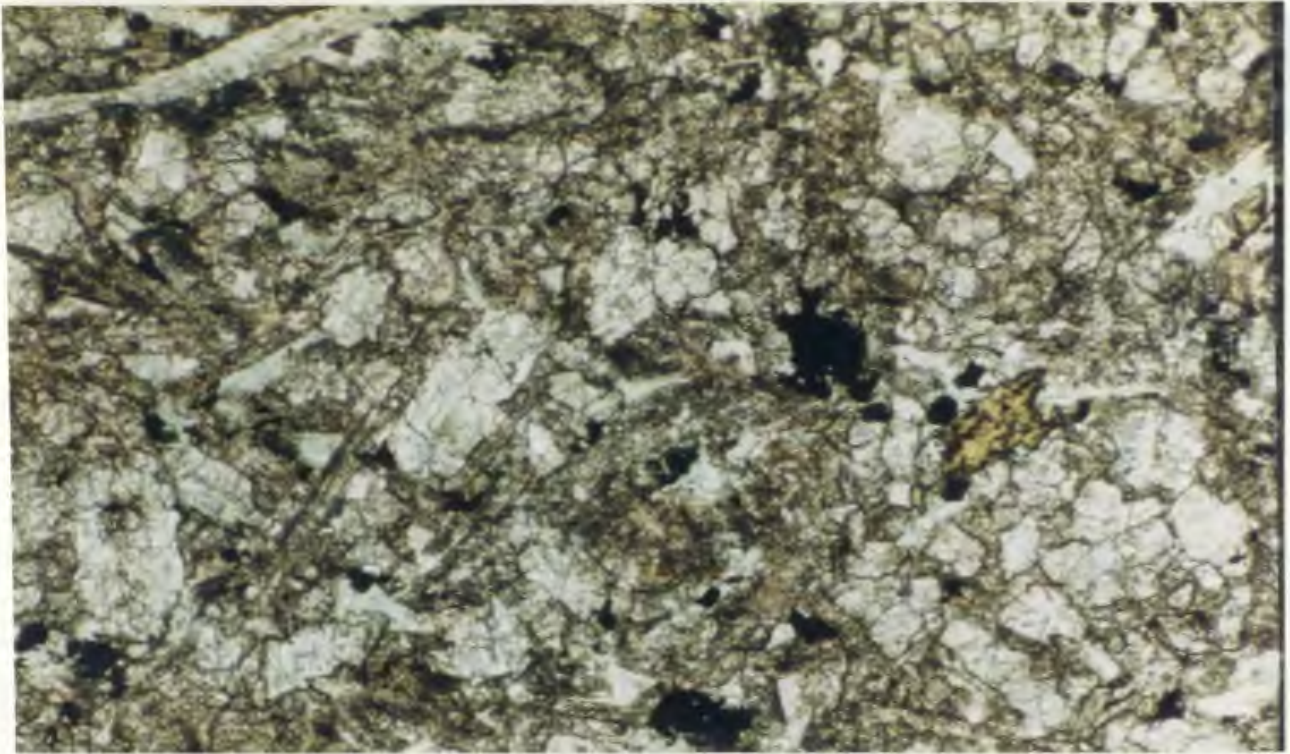


**Plate 4.24a** Microphotograph of medium-grained Lee River Group gabbro (Lee River area, T-290). Note abundant intersertal chloritized glass material. Plane-polarized light, x100.

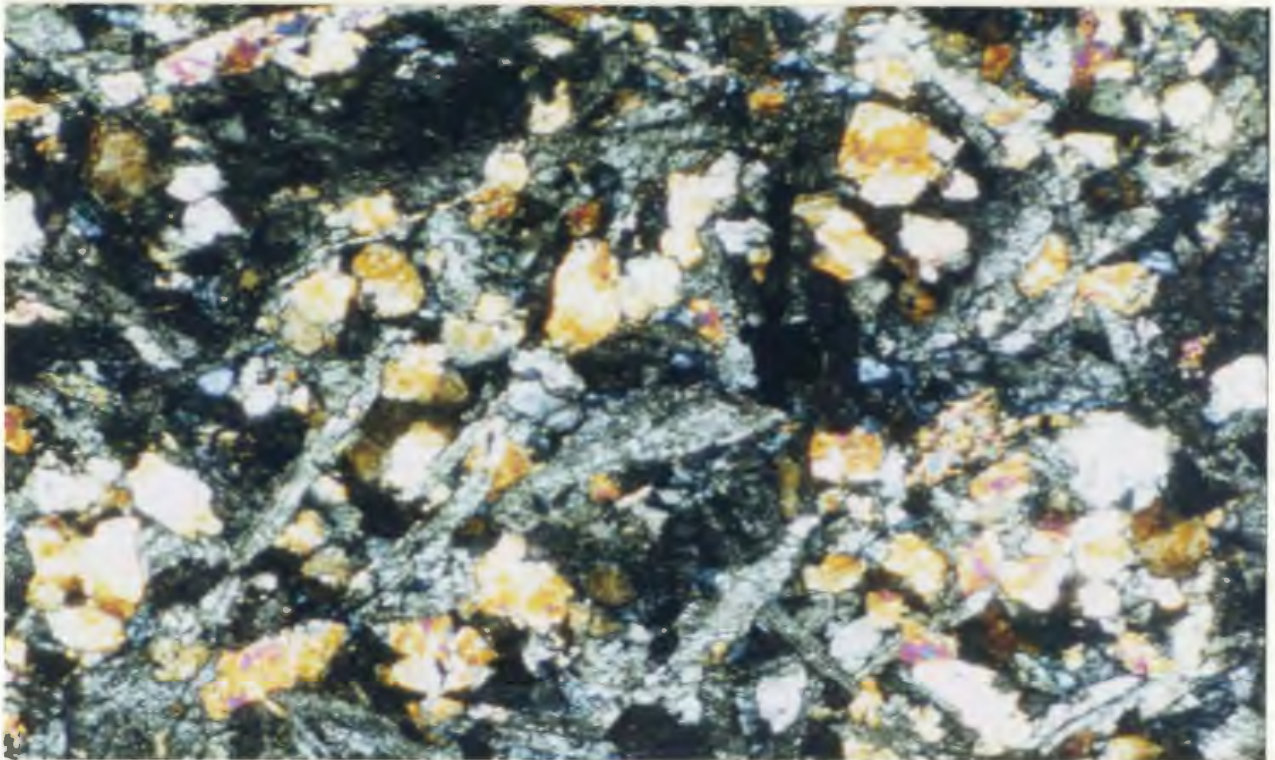


**Plates 4.24b** Microphotograph of medium-grained Lee River Group gabbro (Lee River area, T-290). Note abundant intersertal chloritized glass material. Crossed nicols, x100.



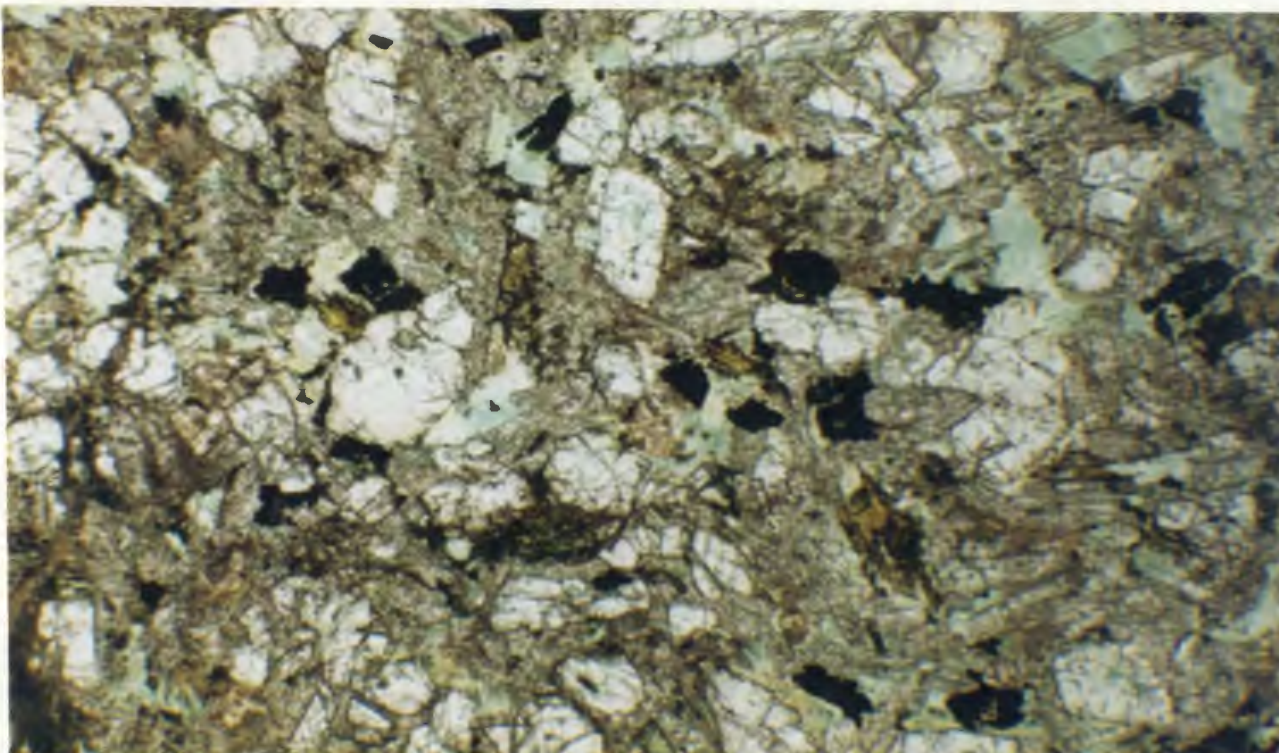


**Plate 4.25a** Microphotograph of weakly altered Lee River diabase (United Creek, Roding river area, U-767). Clinopyroxene is unaltered. Note minor amounts of chloritized interstitial glass. Plane-polarized light, x50.

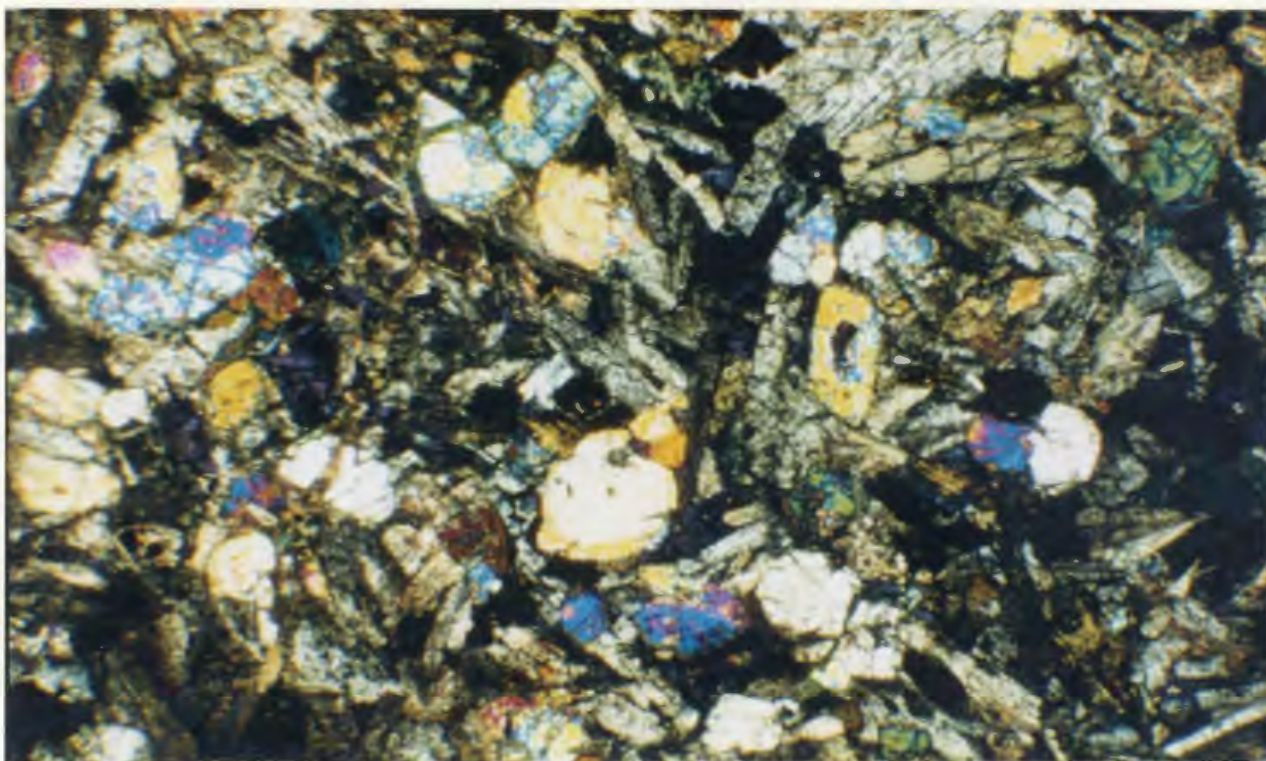


**Plate 4.25b** Microphotograph of weakly altered Lee River diabase (United Creek, Roding river area, U-767). Clinopyroxene is unaltered. Note minor amounts of chloritized interstitial glass. Crossed nicols, x50.



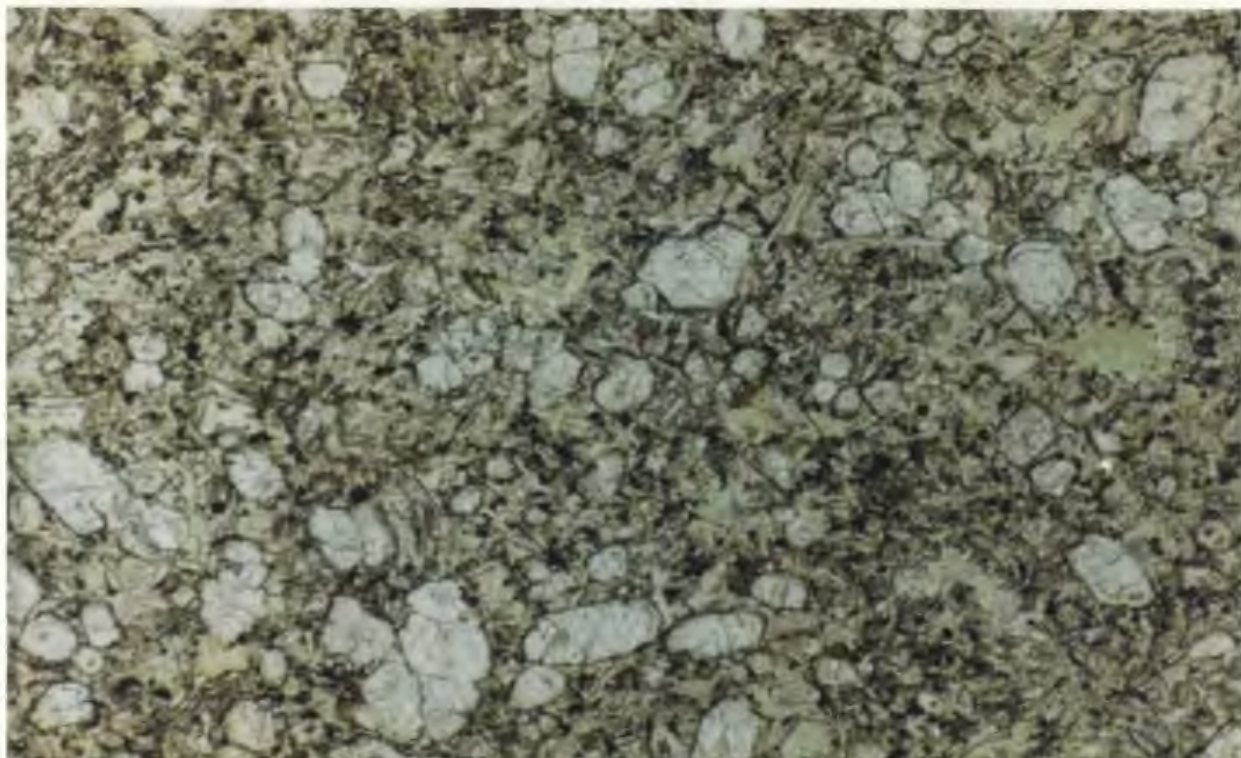


**Plate 4.26a** Microphotograph of weakly altered, intergranular to subophitic Lee River Group gabbro (Tinline River area, TL-526). Note clinopyroxene is partially chloritized and zoned with some crystals having chloritized cores. Plane-polarized light, x25.

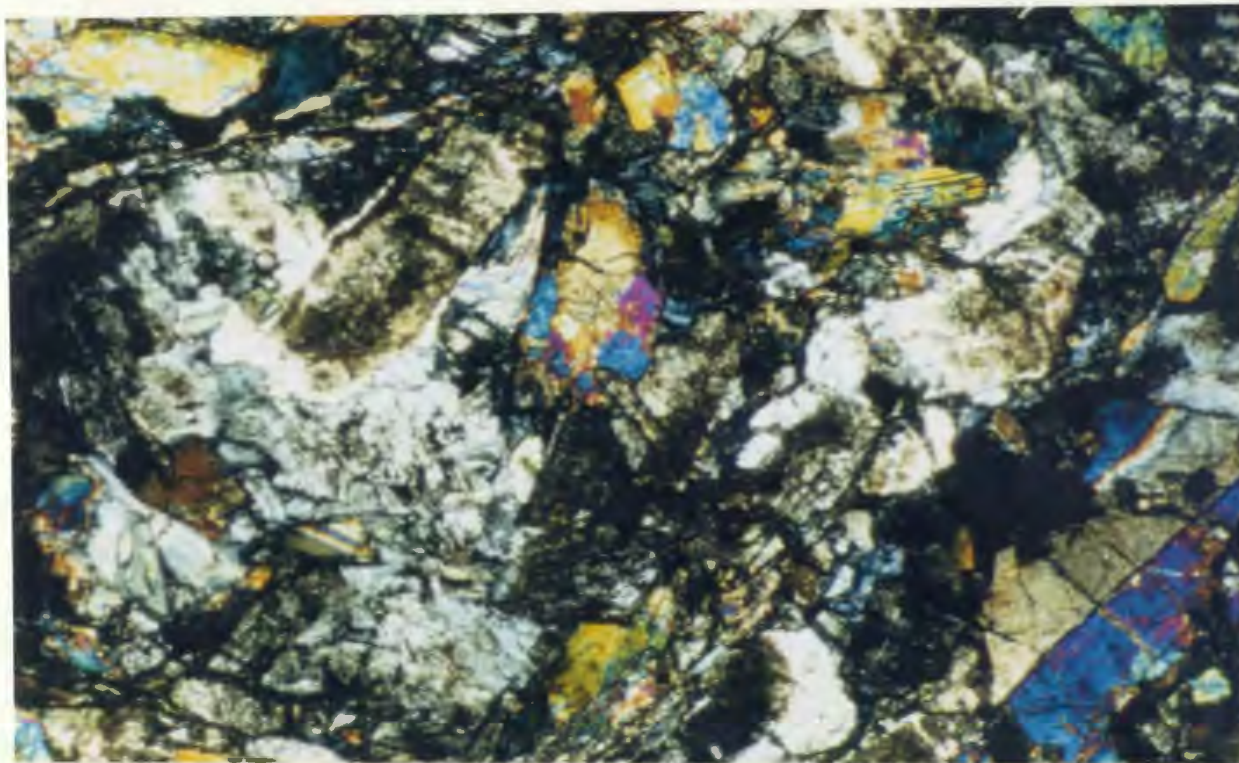


**Plate 4.26b** Microphotograph of weakly altered, intergranular to subophitic Lee River Group gabbro (Tinline River area, TL-526). Crossed nicols, x25.





**Plate 4.27** Microphotograph of weakly altered, intergranular Lee River Group diabase (Tinline River area, TL-530b). Note abundant chloritized intersertal glass. Plane-polarized light, x50.



**Plate 4.28** Microphotograph of a medium-grained gabbro inclusion (a block within the Sheared Serpentinite Complex Zone, Red Hills, R-926f). Clinopyroxene is altered to actinolitic amphibole while plagioclase is saussuritized. Note preserved gabbroic texture. Crossed nicols, x50.

Plagioclase typically occurs as abundant, weakly to moderately saussuritized interstitial laths surrounding subhedral phenocrysts or intergranular crystals of clinopyroxene and minor amounts of chloritized intersertal glass (eg. 4.27).

It is worth noting here that rocks of the non-amphibolitized, intergranular, clinopyroxene-phyric suite are likely younger than those of the other two suites as they are not amphibolitized and are relatively undeformed.

Rocks of the clinopyroxene-phyric and aphyric suites likely represent minor variations of the same suite, as, if amphibolitized, clinopyroxene-phyric suite rocks would resemble those of the aphyric suite.

Secondary minerals ubiquitously observed in each of the three suites include albite, epidote, prehnite, pumpellyite, chlorite and quartz in veins. Pyrite is also locally observed within these rocks as fine disseminations and rare micro-veinlets (less than 0.5 millimetres wide).

#### 4.3.3 Sheared Serpentinite Complex (Red Hills)

In the Red Hills area subvolcanic rocks of the Lee River Group are observed as tectonic inclusions in a large (generally less than 600 metres wide) serpentinite shear zone (Sheared Serpentinite Complex). The field relationships of this complex were discussed in the previous chapter (Figure 3.2.1). In earlier studies this complex was not considered a major fault zone; but, had been interpreted as part of an intrusive contact metamorphic aureole (Challis, 1965a,b).

Here the petrography of these rocks is described with some emphasis being placed on the metamorphism of the Lee River Group subvolcanic inclusions as well as the petrography of layered series plutonic rocks (tectonic inclusions) which represent vestiges of cumulate gabbroic sequences of the Lee River Group subvolcanics.

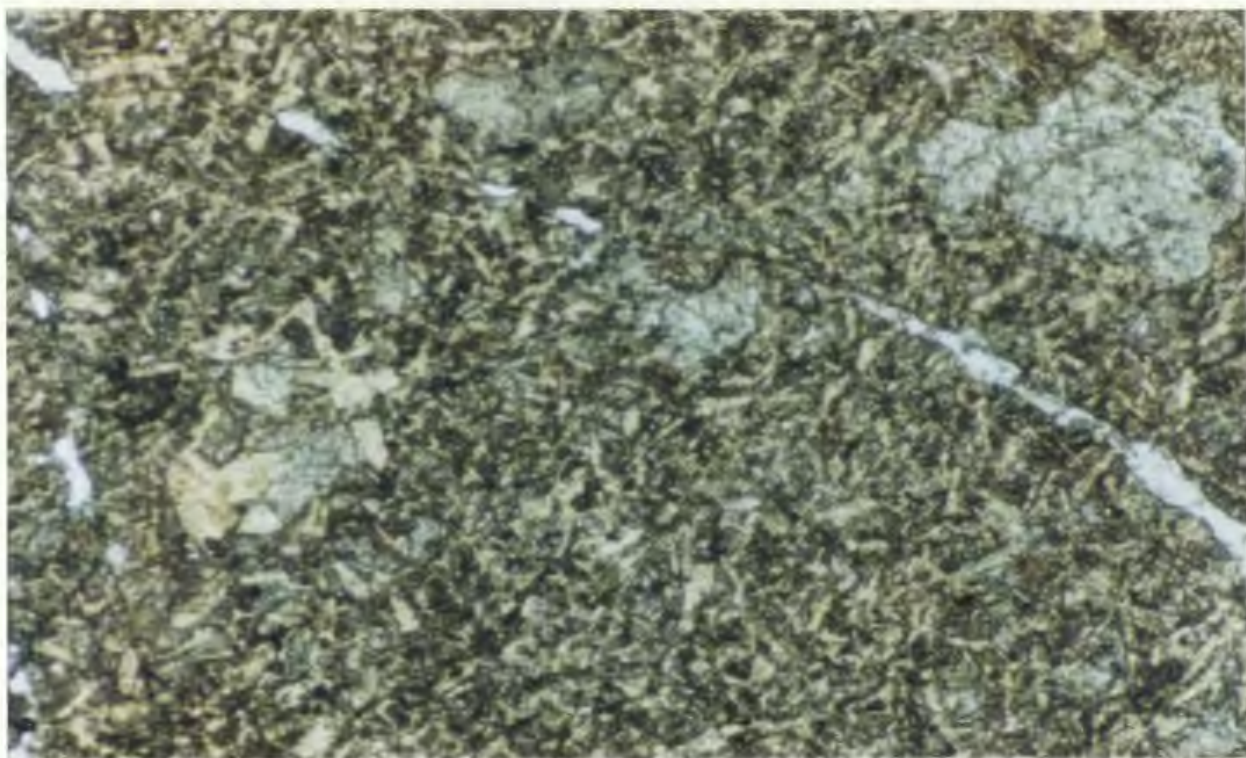
Tectonic inclusions within the Red Hills Sheared Serpentinite Complex (unit Ir/dm, Figure 3.2.1) range from Lee River Group fine-grained diabase and medium-grained gabbro to layered series gabbros and ultramafic rocks of the Dun Mountain Ultramafics Group. Although many of these rocks are strongly foliated and metamorphosed a significant number were observed in which primary igneous textures remain intact (Plates 4.28 and 4.29).

#### 4.3.3.1 Lee River Group Diabase and Gabbro Inclusions

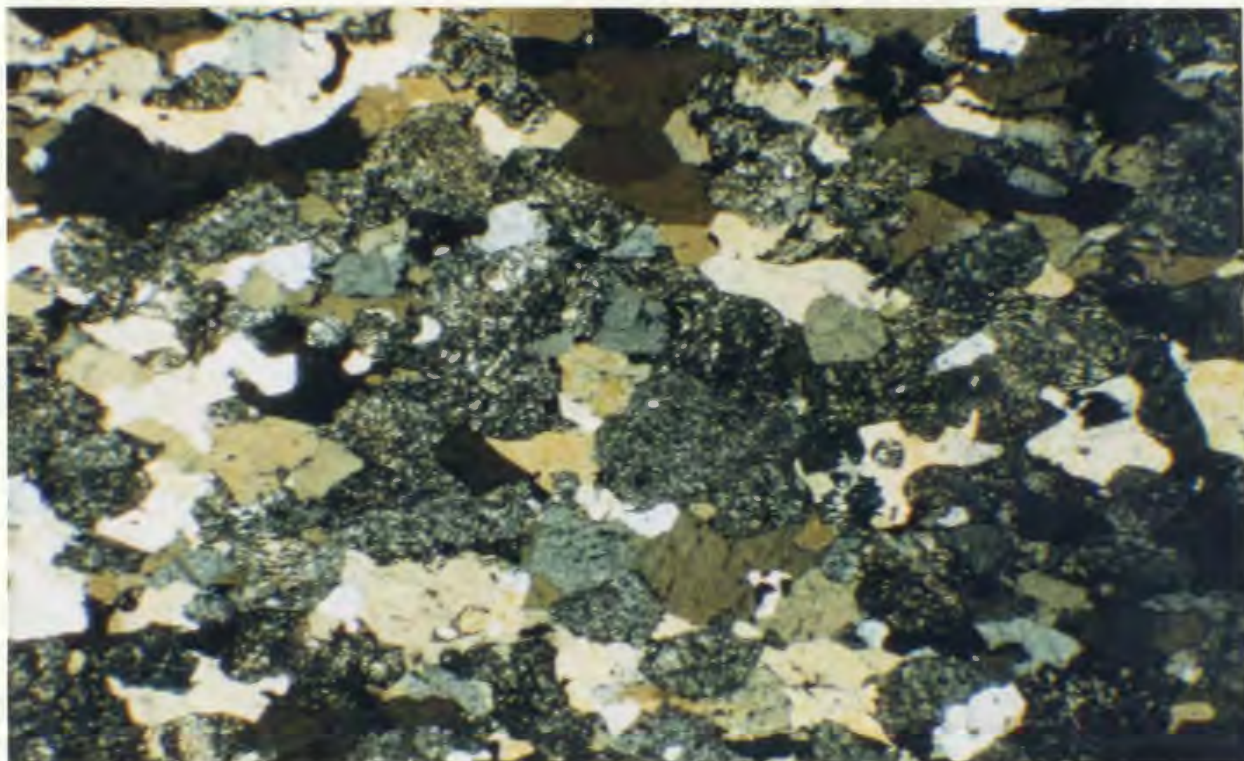
Within the Sheared Serpentinite Complex many gabbro and diabase blocks are rodingitized. Plagioclase is replaced by hydrogrossular while green pleochroic amphibole (produced by the earlier greenschist metamorphism of clinopyroxene) is replaced by weakly pleochroic tremolite. Primary grain sizes and textures are often well preserved in the cores of many of these inclusions, allowing original rock types to be identified (eg. Plate 4.29).

Less altered blocks are only partially rodingitized on their margins. In such cases a white-coloured rim or metasomatic reaction zone of rodingitized material surrounds the block and the mineralogy of the core material is unaffected. These reaction zones are similar to those described by Coleman (1977) who suggests that rodingites are low-temperature metasomatic by-





**Plate 4.29** Rodingitized fine-grained diabase (block within Sheared Serpentinite Complex Zone, Red Hills, R-902b). Although primary intergranular texture is preserved, the rock is now entirely composed of hydrogrossular and tremolitic amphibole. Plane-polarized light, x25.



**Plate 4.30** Microphotograph of foliated, brown hornblende amphibolitized, medium-grained gabbro (a block within the Sheared Serpentinite Complex Zone, Red Hills, R-966). Note metamorphism has obliterated original gabbroic texture. Crossed nicols, x25.

products of serpentinization.

Many gabbroic inclusions derived from the Lee River Group are strongly foliated and consist of brown pleochroic hornblende and saussuritized plagioclase. In these rocks hornblende crystals often show curved, sutured crystal boundaries while plagioclase crystal boundaries are jagged and were likely not recrystallized (Plate 4.30). Although no analytical data is available, this brown hornblende was likely produced by metamorphic recrystallization of clinopyroxene at higher temperatures than those under which clinopyroxene altered to green pleochroic amphibole within higher levels of the Lee River Group gabbros. Challis (1965a,b) considered these strongly amphibolitized gabbroic inclusions to represent amphibolite produced by high-temperature contact metamorphism of spilitic volcanics and tuffs along the contact of an alpine-type ultramafic intrusion (the Red Hills ultramafic massif). As these blocks of amphibolitized gabbroic material are similar in grain size and composition to nearby Lee River Group gabbros (Red Hills) and other amphibolitized gabbros (containing brown pleochroic hornblende) observed within lower levels of the Lee River Group sequence (eg., Champion and United Creek sections of the Roding River area and the Tinline River area); they are interpreted as blocks of metamorphosed Lee River Group gabbro incorporated into the Sheared Serpentine Complex during faulting along the contact between the Lee River Group and Dun Mountain Ultramafics Group. In support of this conclusion is the inclusion of blocks of "critical zone" (layered series) cumulate gabbros within the Sheared Serpentine Complex. These rocks are similar to cumulate gabbro sequences observed in other

ophiolites (eg. Bay of Islands, Smith, 1958; Malpas, 1977) and the deformation and metamorphism of these rocks is considered analogous to that produced during active spreading on the ocean floor (eg. Girardeau et al., 1982); therefore suggesting that it is not a late metamorphic event.

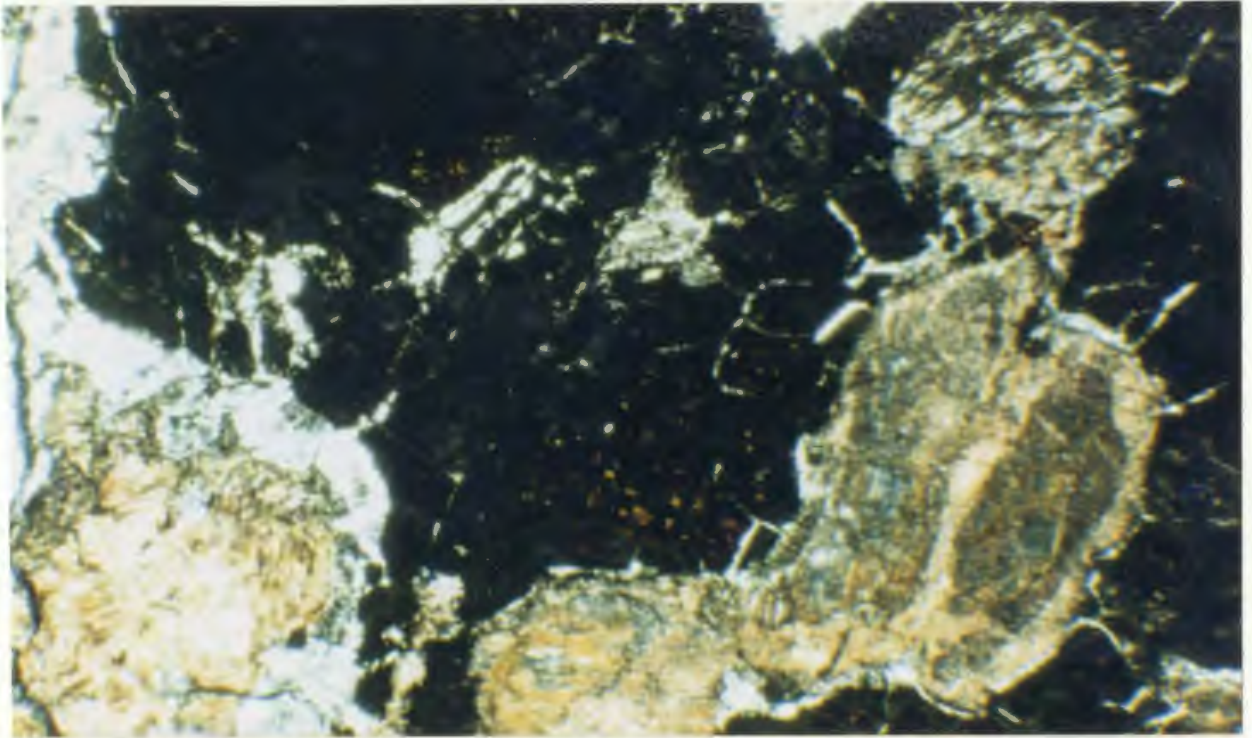
#### 4.3.3.2 Layered Series Gabbro Inclusions

Cumulate gabbro inclusions are composed of gabbroic to ultramafic bands or layers and bear a close resemblance to "critical zone" rocks or "layered series" rocks observed at the base of layer 3 gabbros in other ophiolites (eg., Bay of Islands, Newfoundland; Troodos, Cyprus; and Semail, Oman). In other ophiolites these rocks generally make up layered sequences consisting of variable amounts of plagioclase, clinopyroxene, orthopyroxene, olivine and spinel.

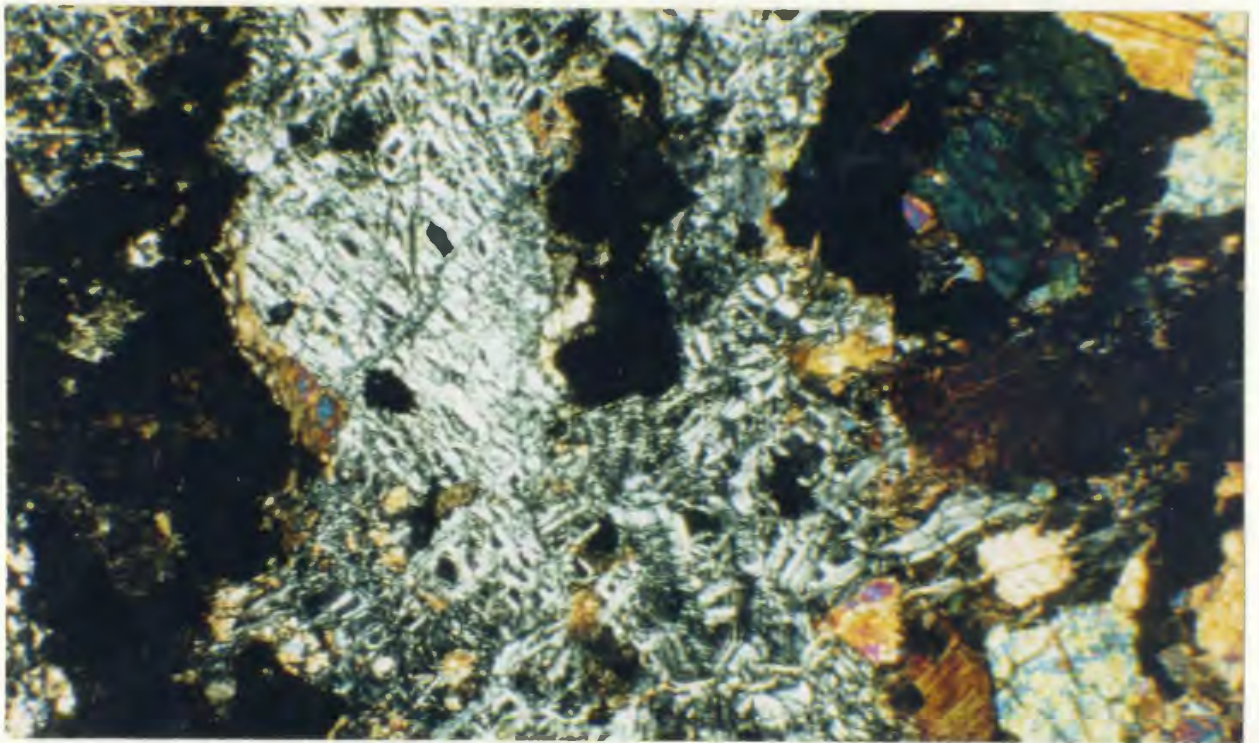
As similar rocks were not recognised from other sections of the Dun Mountain Ophiolite, the inclusions of layered series material observed within the Sheared Serpentinite Complex of the Red Hills area were studied in detail. There, inclusions are highly serpentinized and rodingitized (Plates 4.31 and 4.32).

Within these rocks olivine is typically completely altered to serpentine, although kernels are rarely preserved. Plagioclase is replaced by hydrogrossular, orthopyroxene is generally altered to bastite, and primary clinopyroxene is replaced by metamorphic diopside. Although these rocks are altered and commonly strongly foliated, some blocks contain well preserved igneous layered sequences up to 10 metres thick (10 metres being the





**Plate 4.31** Orthopyroxene and plagioclase rich band within a band of transition series rock (inclusion in the Sheared Serpentinite Complex Zone, Red Hills, R-904). Orthopyroxene is altered to bastite while plagioclase is replaced by isotropic hydrogrossular. Crossed nicols, x25.



**Plate 4.32** Olivine rich layer in transition series rock (inclusion in the Sheared Serpentinite Complex Zone, R-926d). Olivine is serpentinized; but, small kernels of unaltered olivine survive in the left half of the photo. Plagioclase is replaced by hydrogrossular. Crossed nicols, x25.

largest block of layered series rock observed). Individual layers within these rocks represent a large variety of compositions including: dunite, harzburgite, wehrlite, leuco-norite, gabbro, and anorthosite (eg., Plates 4.31 and 4.32). Layers are typically less than 20 centimetres thick and range from being strongly foliated to relatively undeformed.

Alteration tends to be less penetrative within thicker bands of gabbroic material (greater than 0.5 metres) where rodingitization has not completely penetrated the rock. These less altered bands are composed of weakly to moderately saussuritized plagioclase, green pleochroic amphibole (alteration of clinopyroxene), and iron-titanium oxides. Pleochroic brown amphibole is also observed within some of these rocks partially replacing clinopyroxene and in some samples is partially replaced by green pleochroic amphibole. This suggests that these rocks have undergone retrograde metamorphism as they cooled beneath the ocean floor.

Layered series rocks preserved here are considered to represent basal cumulate sequences of the Lee River Group gabbros.

#### 4.3.4 Dun Mountain Ultramafics Group

Although a detailed petrographic study of ultramafic rocks from the Dun Mountain Ultramafics Group was not undertaken, a number of these rocks were examined in thin section from the Red Hills massif (Figure 3.2.1) and Lee River areas (Figure 3.2.2).

At these localities, ultramafic rocks of the Dun Mountain Ultramafics Group range in composition from foliated harzburgite and pyroxene peridotite,

to banded dunite with minor concentrations of chromite.

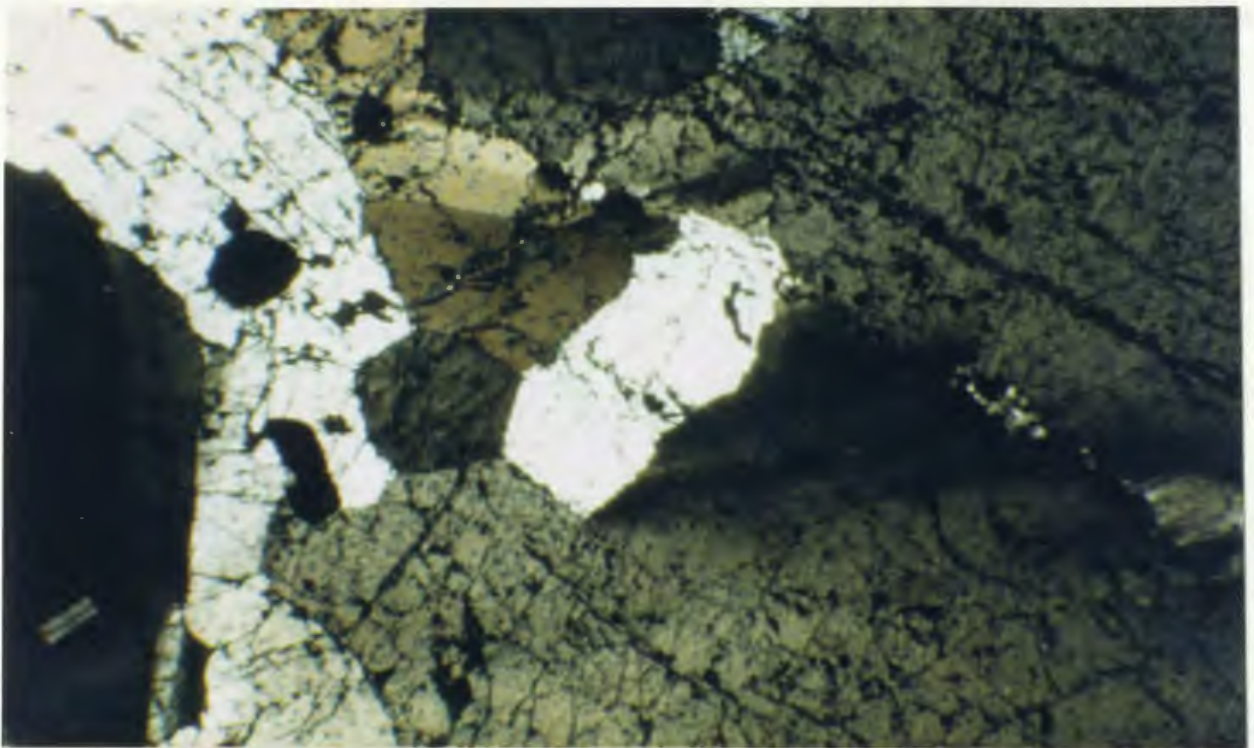
Primary mineral phases include: olivine, orthopyroxene, clinopyroxene, and spinel (Plates 4.33 to 4.36). Olivine is generally fractured and is partially altered to serpentine and for the most part, both ortho- and clinopyroxenes are fresh and commonly contain exsolution lamellae. Spinel is typically observed as interstitial euhedral to anhedral crystals.

In terms of deformation, rocks of the Dun Mountain Ultramafics Group are generally foliated and, in areas other than the Red Hills massif, commonly disrupted by numerous serpentinite shear zones. In areas directly adjacent to these shear zones, ultramafic rocks are strongly serpentinized and relict crystals of pyroxene and spinel are preserved in fine-grained, mesh-textured serpentine. The degree of serpentinization within these rocks appears to vary directly with the amount of faulting, and sheared rocks are more intensely serpentinized than undeformed and unsheared rocks.

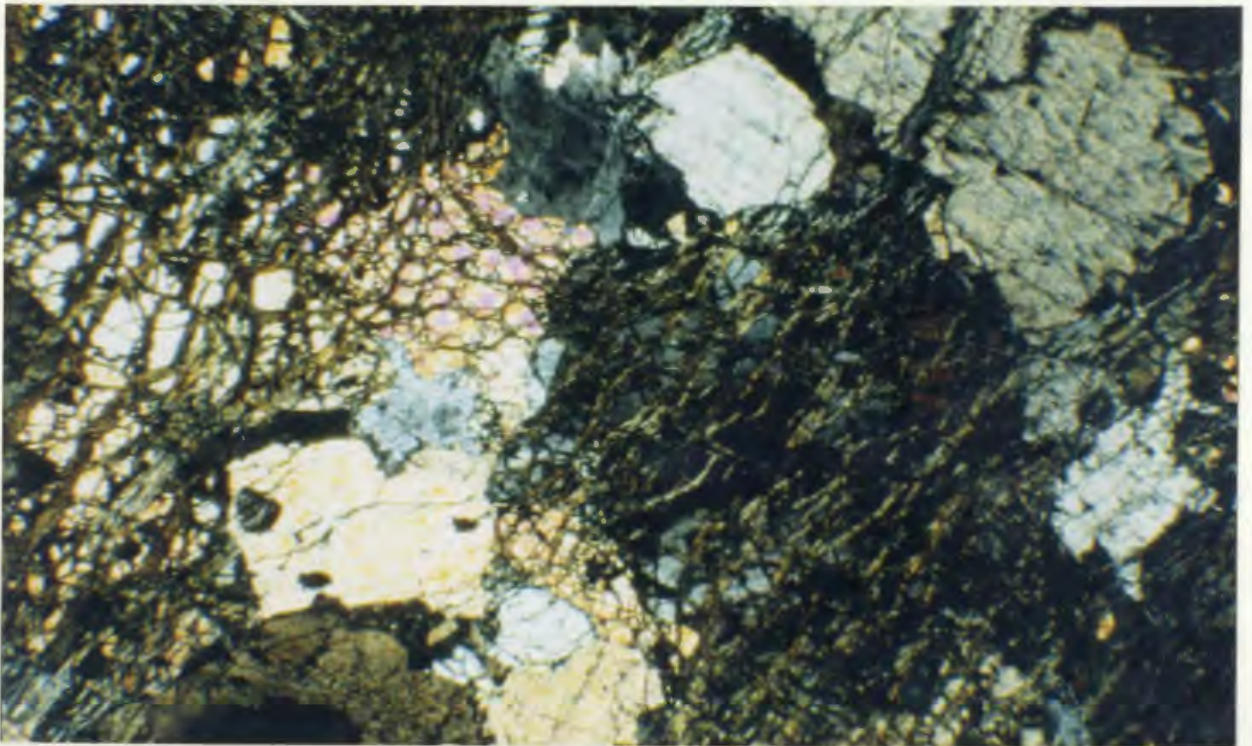
Within less serpentinized and deformed samples, grain boundaries between individual crystals are strained and irregular and larger orthopyroxene grains often display undulatory extinction (eg. Plate 4.33). Granulation of crystals is rarely observed in the samples studied here; however, Walcott (1969) has described porphyroclastic textures within similar rocks of the Red Hills massif. For the most part, this deformation is likely the result of mantle tectonism, and similar textures have been identified and interpreted within other ophiolites (eg., Nicolas et al., 1973; Mercier and Nicolas, 1975).

For the most part, harzburgitic rocks of the Dun Mountain Ultramafics Group are composed of partially serpentinized and fractured olivine as well as



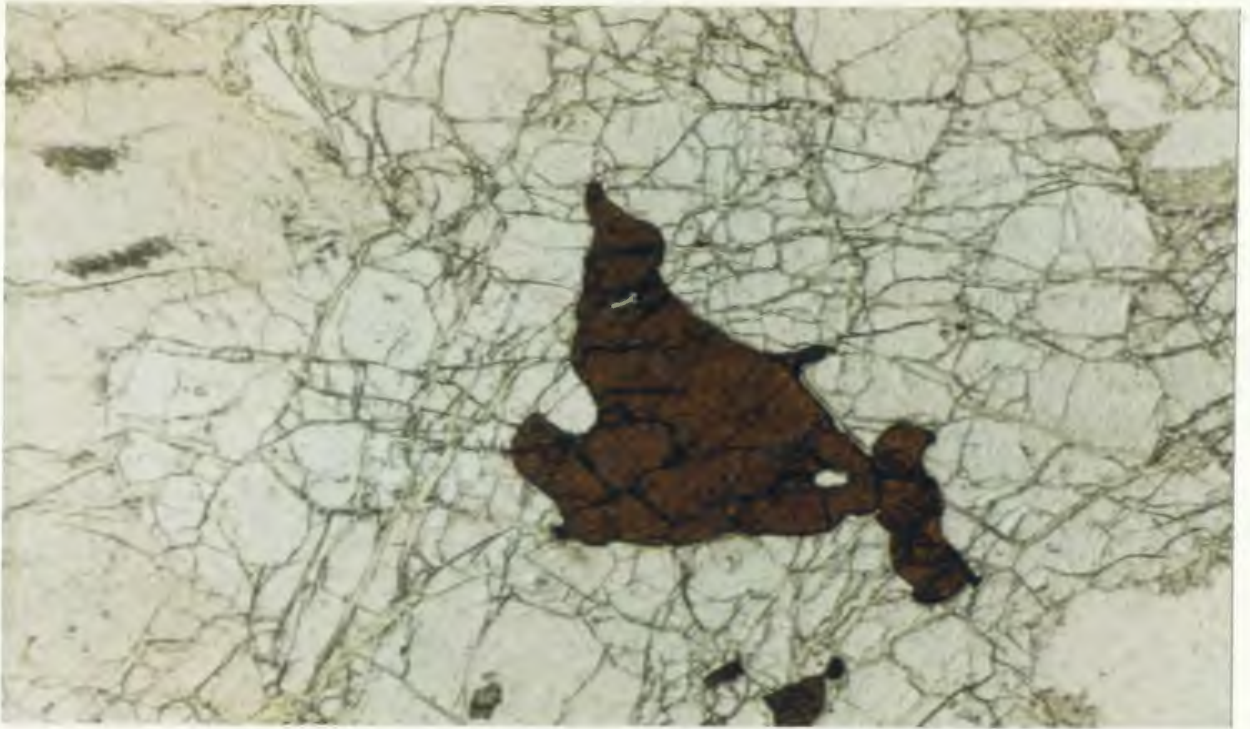


**Plate 4.33** Microphotograph of strained and granulated texture within an orthopyroxenite band within the Red Hills massif (Dun Mountain Ultramafics Group, Red Hills, R-953). Crossed nicols, x25.

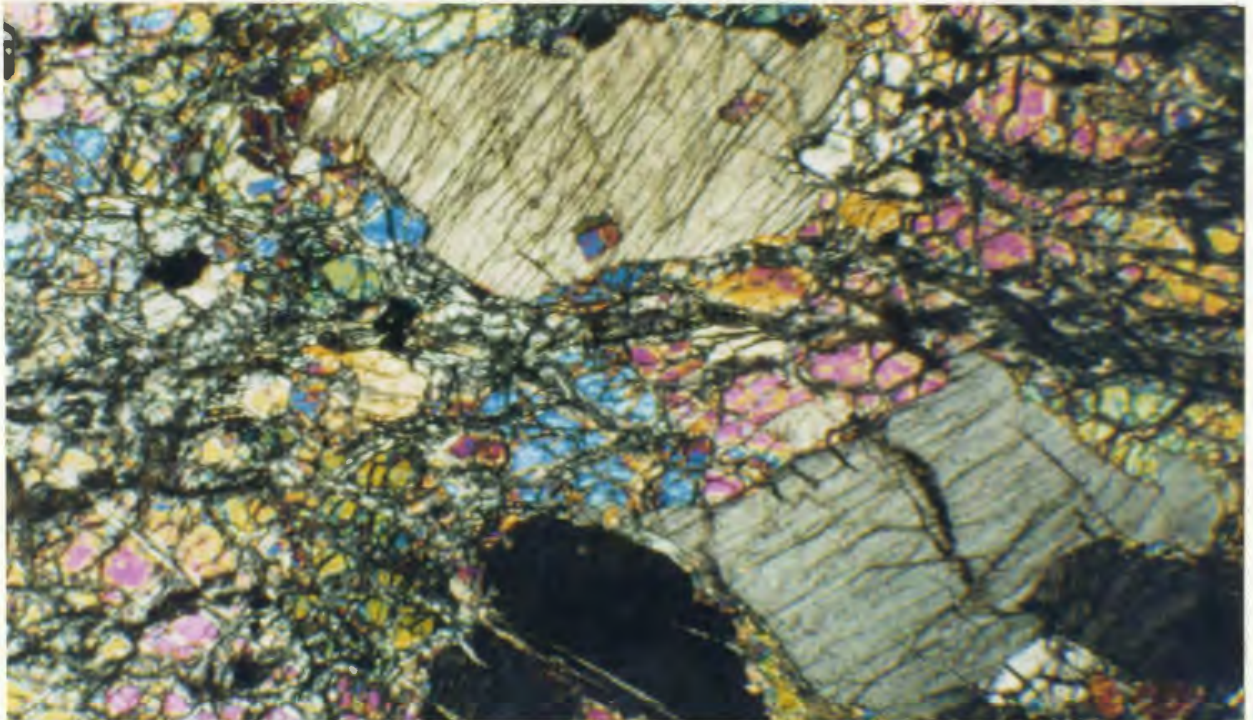


**Plate 4.34** Microphotograph of partially serpentinized harzburgite from the Red Hills ultramafic massif (Dun Mountain Ultramafics Group, Red Hills, R-958a). Crossed nicols, x25.





**Plate 4.35** Microphotograph of brown-coloured spinel in orthopyroxenite band of the Red hills ultramafic massif (Dun Mountain Ultramafics Group, Red Hills, R-972). Note resorbed crystal boundaries. Plane-polarized light, x50.



**Plate 4.36** Partially serpentinized harzburgite of the Dun Mountain Ultramafics Group (Lee River area, T-336). Crossed nicols, x25.

abundant orthopyroxene which occurs as large strained crystals that display undulose extinction in thin section. Dunitic rocks; however, are more intensely serpentinized than harzburgitic rocks but trails of chromiferous spinel crystals in places preserve the foliation.

In the Red Hills area (Red Hills massif), ultramafic rocks of the Dun Mountain Ultramafics Group are relatively unserpentinized and unaffected by deformation associated with the Sheared Serpentine Complex along the massif's western contact. The contact between these two units is quite sharp with relatively unsheared and unserpentinized ultramafic rocks of the massif outcropping within 5 metres of the Sheared Serpentine Complex's eastern fault contact.

#### 4.4. Patuki mélange

Rocks of the Patuki mélange were encountered in three of the study areas: (i) the Lee River area (Figure 3.2.2); (ii) the Serpentine River area (Figure 3.2.3); and (iii) the Tinline River area (Figure 3.2.5). Volcanic and subvolcanic rocks of the Patuki mélange are discussed with reference to petrographic samples collected in each of these areas.

##### 4.4.1 Patuki Volcanics

Basaltic rocks of the Patuki mélange outcrop as locally vesicular, glassy to fine-grained, pillowed to massive flows. For the most part these basalts are hematite-stained; however, rare unoxidized outcrops weather a greyish-green colour.



Basalts of the Patuki mélange can petrographically be divided into two fundamental suites. The first and most common of these consists of quenched intersertal to intergranular, olivine-poor basalts. Rocks of the second suite are generally glassier than those of the first and typically contain markedly more abundant olivine microphenocrysts.

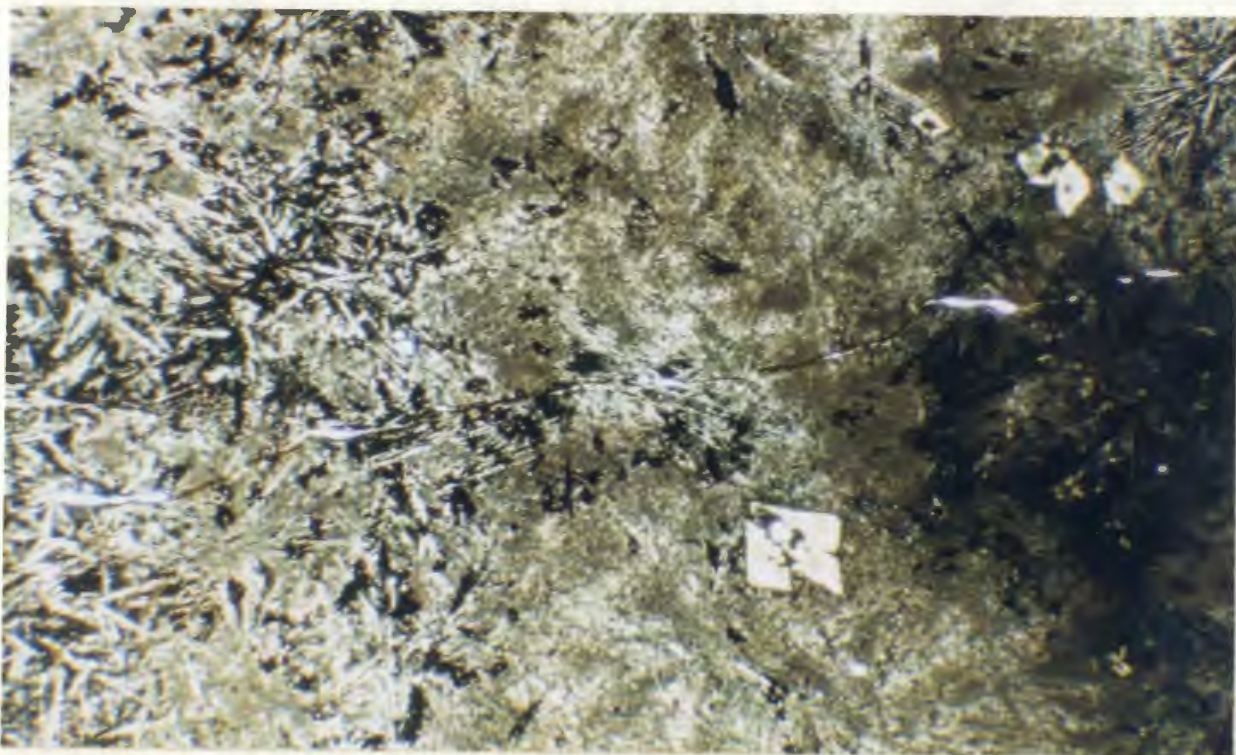
Basalts of the first suite, the "olivine-poor" suite, are predominantly composed of plagioclase and clinopyroxene with rare microphenocrysts of plagioclase, clinopyroxene, and olivine (less than 1 % olivine; Plates 4.37 to 4.39).

Basalts of the second suite, the "olivine-rich" suite, are generally glassier than those of the first and typically contain higher proportions of subhedral, crudely equant olivine microphenocrysts (less than 5% volume) set in a matrix of variolitic plagioclase and clinopyroxene (Plates 4.40 to 4.45).

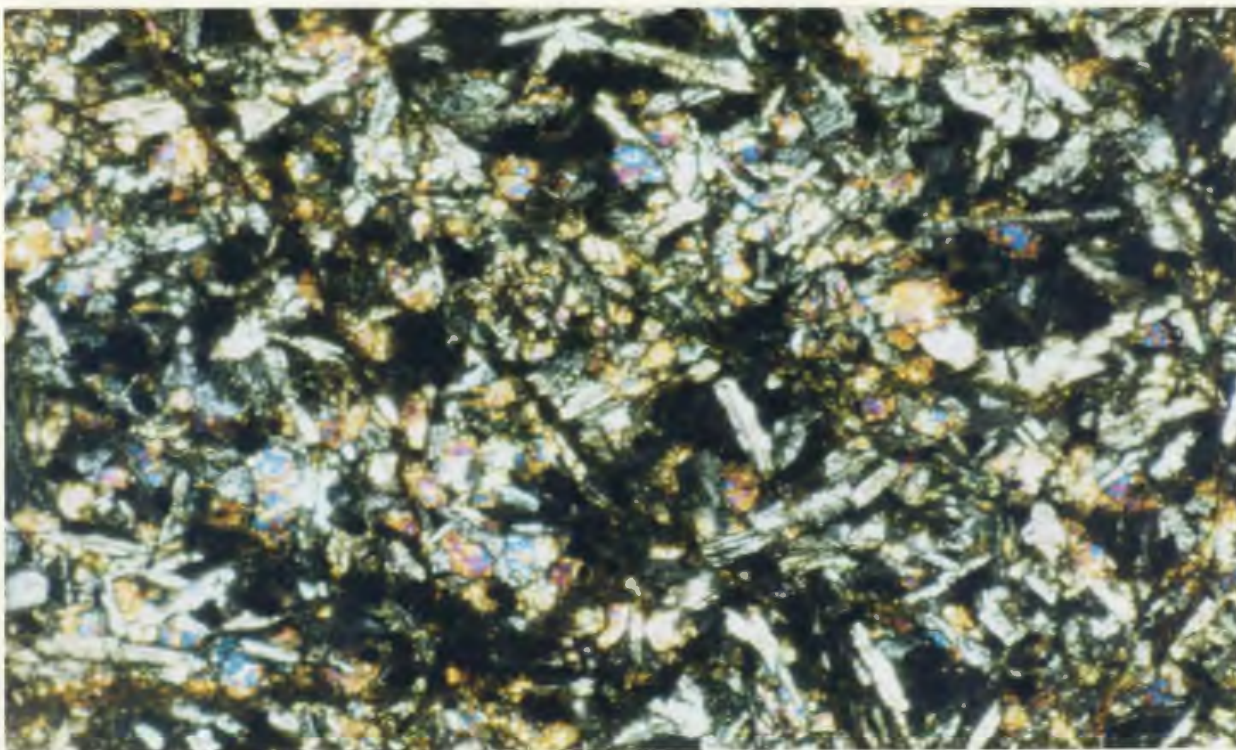
Although these groups are generally distinguishable in thin section, definite discrimination is only possible on the basis of geochemical composition as petrographic variations within rocks of both suites make absolute identification in thin section difficult. Geochemical differences between these respective basaltic suites are presented in the following chapter.

Locally, seemingly homogeneous outcrops were later found to contain both basalt suites upon petrographic and geochemical analysis.

At some localities (eg. Serpentine River area) minor thicknesses of basaltic breccia (generally less than 2 metres thick) are observed associated with pillowed flows. Within these breccia units basalt clasts are typically



**Plate 4.37** Microphotograph of altered olivine microphenocryst in quenched textured variolitic Patuki basalt (Lee River area, T-515). Plane-polarized light, x25.

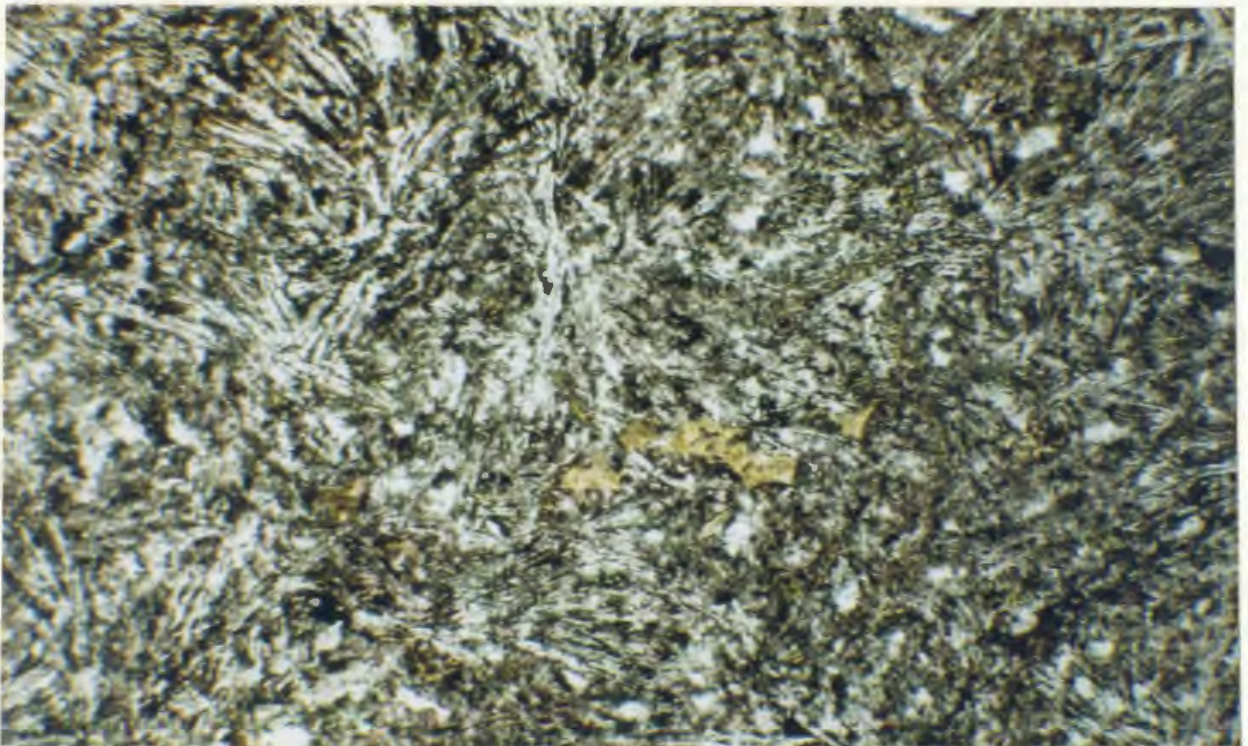


**Plate 4.38** Microphotograph of fresh intergranular, fine-grained Patuki basalt (Lee River area, B-159). Crossed nicols, x50.



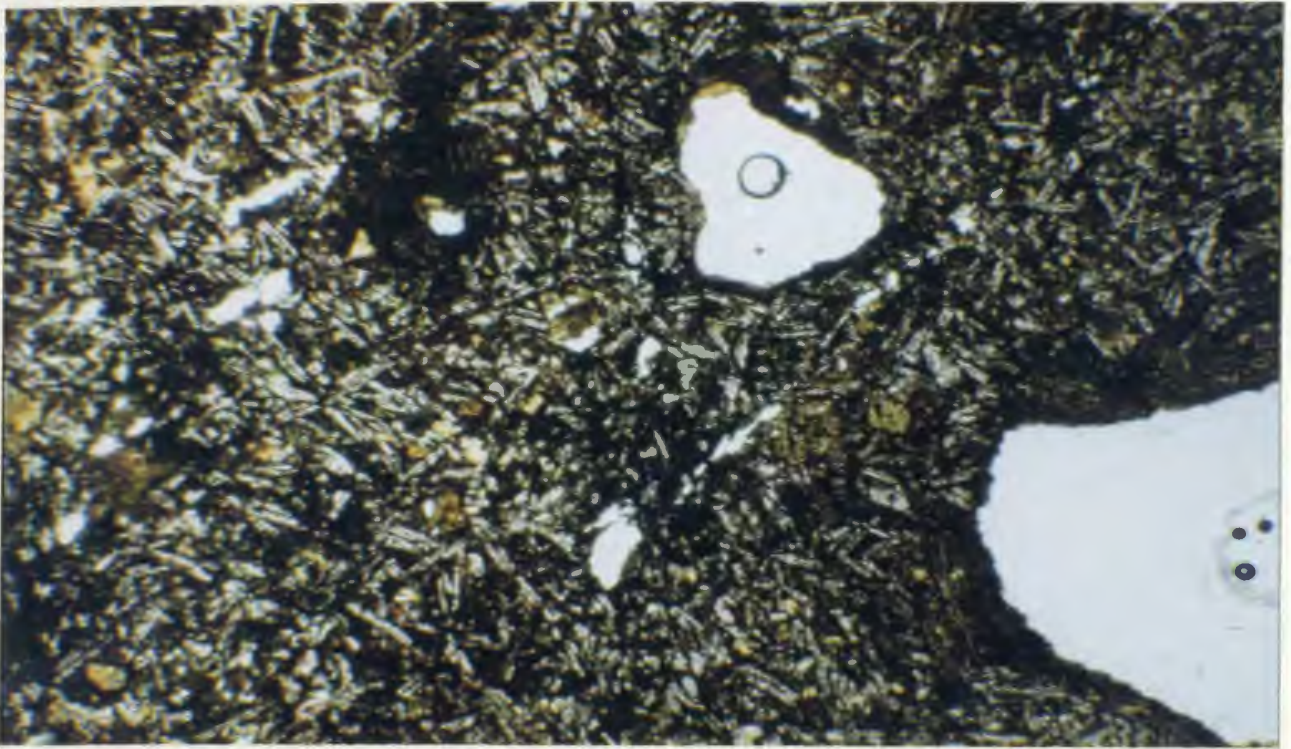


**Plate 4.39** Microphotograph of plagioclase phenocrysts in Patuki basalt (Lee River area, B-132). Crossed nicols, x25.

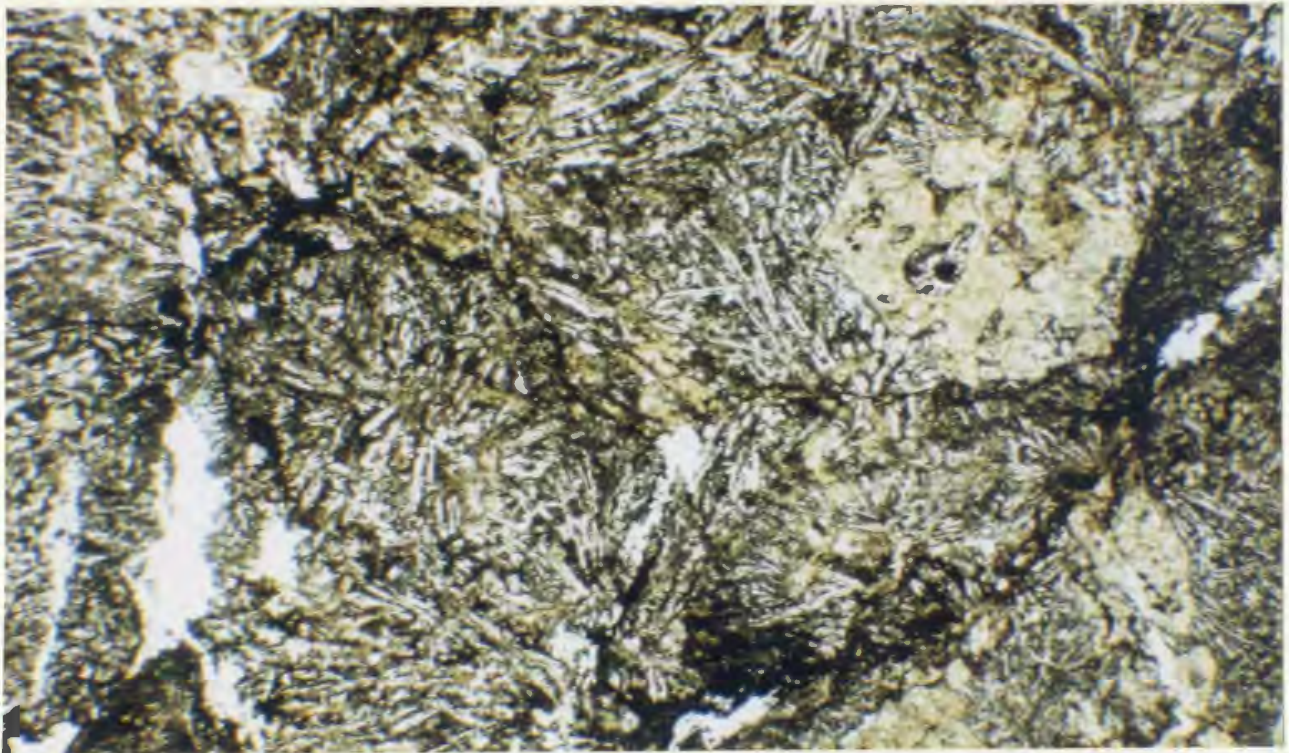


**Plate 4.40** Quenched textured variolitic Patuki basalt (Lee River area, T-492). Plane-polarized light, x25.



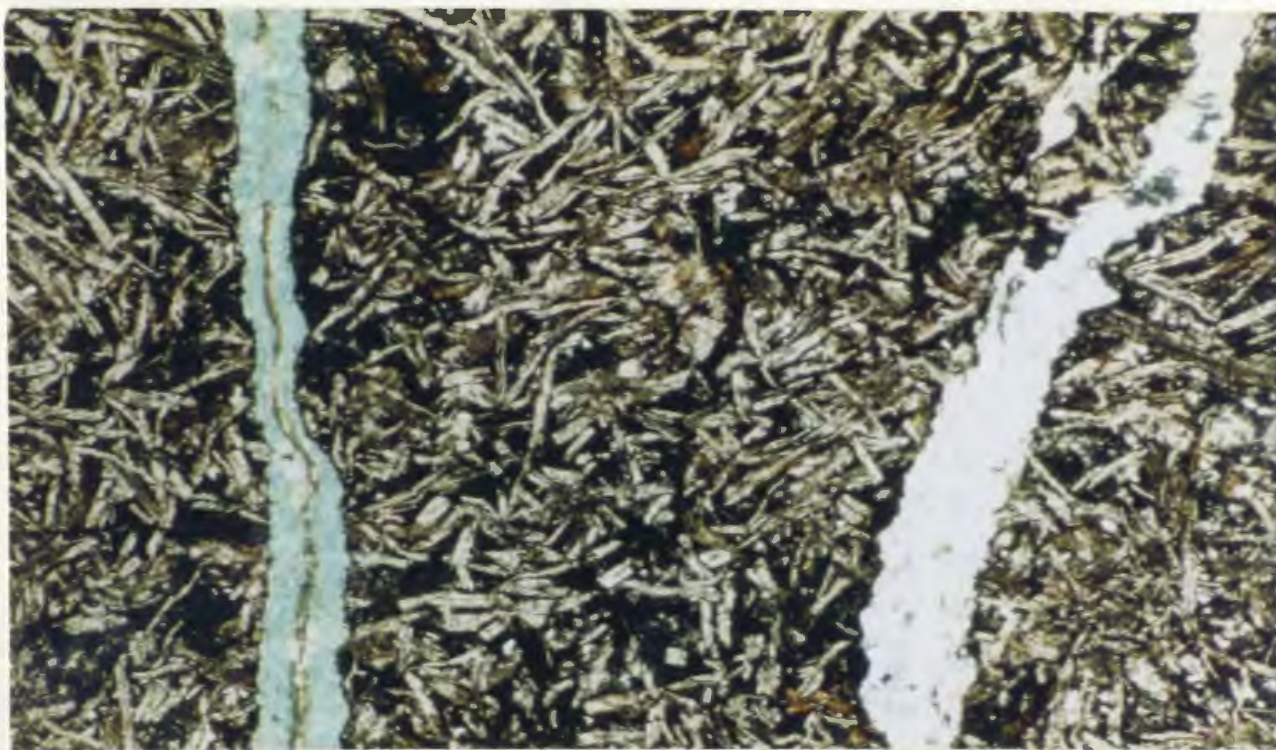


**Plate 4.41** Microphotograph of olivine microphenocrysts within quenched, vesicular Patuki Basalt (Lee River area, B-158). Olivine phenocrysts have been pseudomorphed by pale green pleochroic cryptocrystalline olivine. Plane-polarized light, x25.

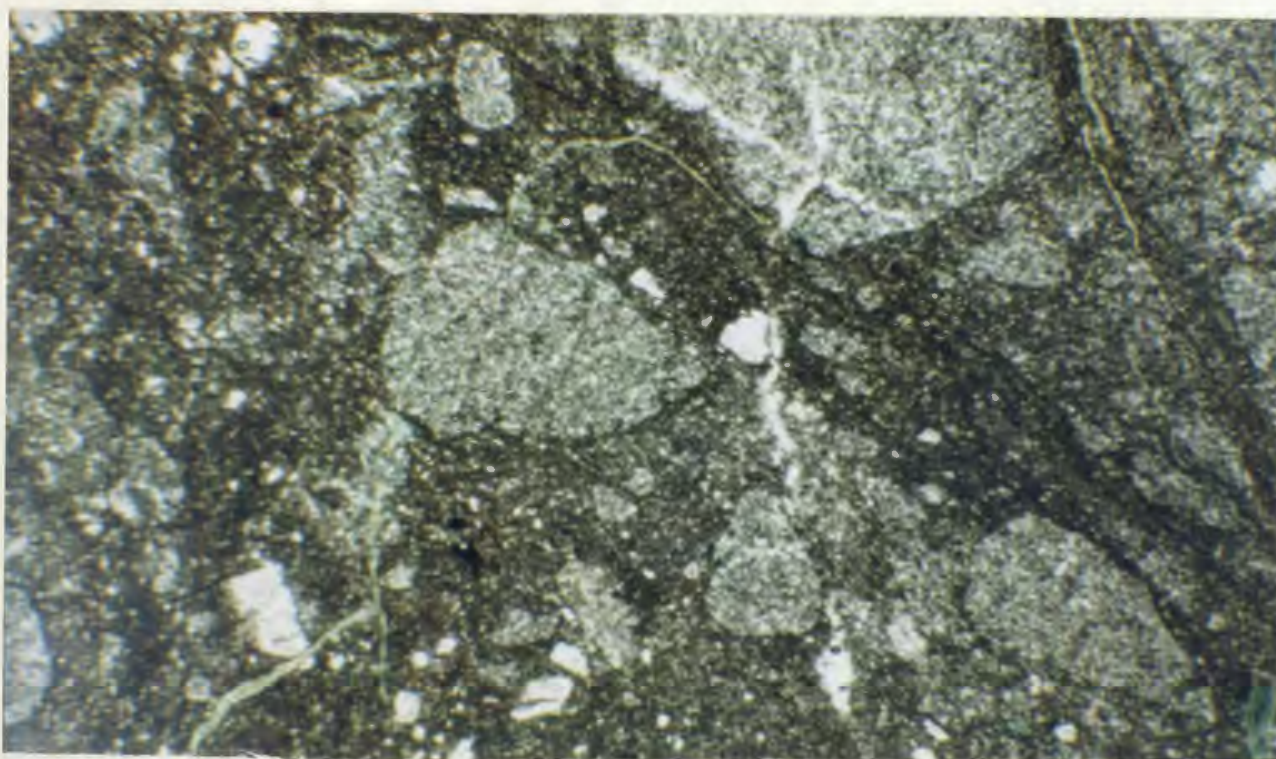


**Plate 4.42** Microphotograph of quenched texture, olivine porphyritic Patuki basalt (Lee River area, B-157). Olivine phenocrysts are replaced by pale green pleochroic chlorite. Plane-polarized light, x25.



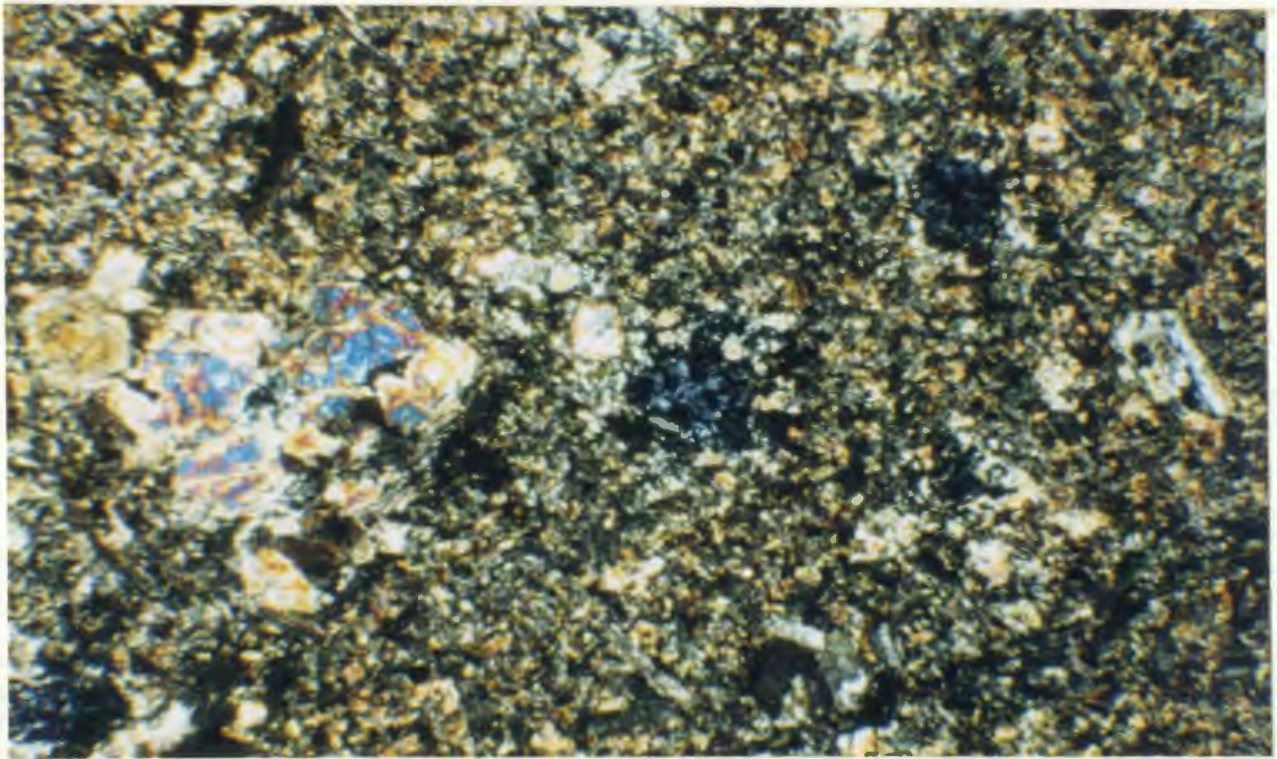


**Plate 4.43** Microphotograph of fine-grained, quenched Patuki basalt cut by veinlets of pumpellyite and prehnite (Serpentine River area, S-16). Plane-polarized light, x50.

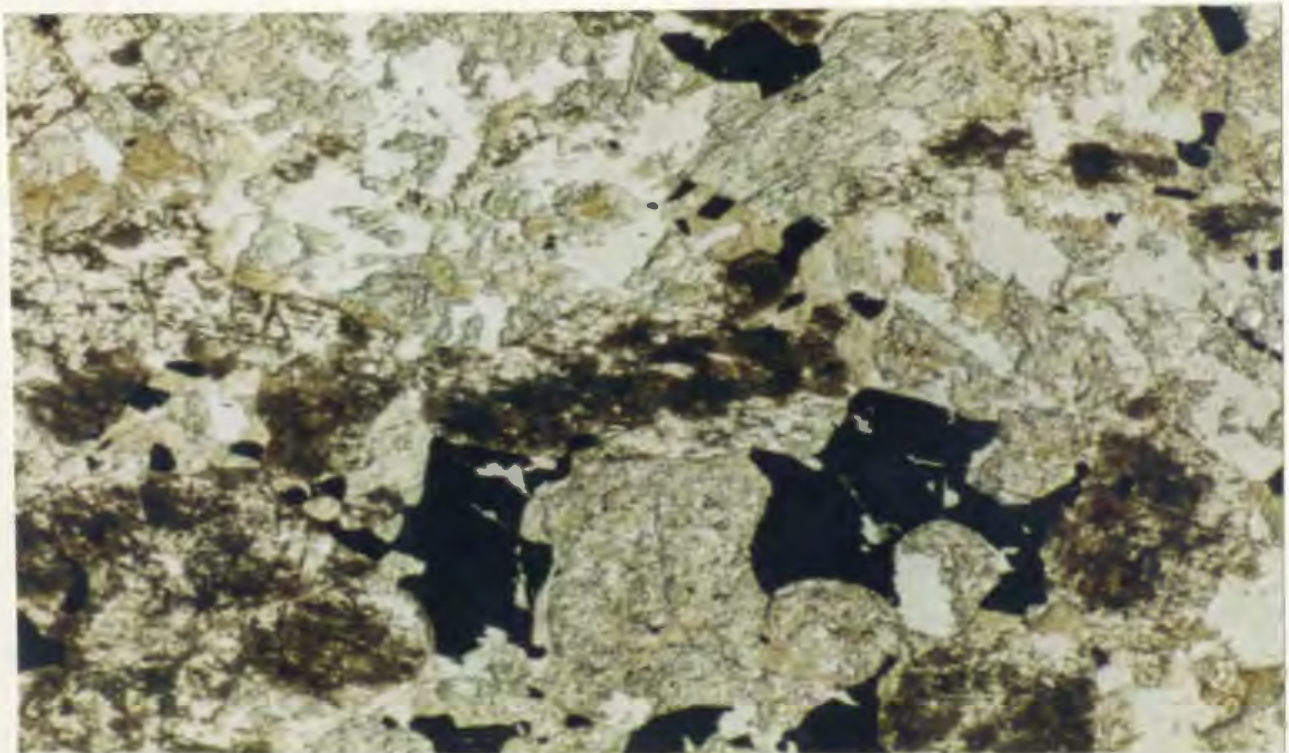


**Plate 4.44** Microphotograph of Patuki basaltic breccia (Serpentine River area, S-14). Rock is cut by small veinlets of green pleochroic pumpellyite. Plane-polarized light, x25.





**Plate 4.45** Microphotograph of Patuki diabase with partially amphibolitized clinopyroxene phenocrysts (Lee River area, L-37). Crossed nicols, x25.



**Plate 4.46** Microphotograph of partially amphibolitized, medium-grained Patuki gabbro (Lee River area, B-90). Clinopyroxene is partially altered to brown pleochroic hornblende. Plane-polarized light, x50.



broken into centimetre sized pieces surrounded by fine detrital sand composed of altered clinopyroxene and plagioclase (Plate 4.44). In addition, clasts of intergranular basalt are observed which contain weakly altered clinopyroxene (pale green pleochroic amphibole). Alteration of the suites varies in intensity from outcrop to outcrop, although plagioclase is generally strongly saussuritized while clinopyroxene is relatively unaltered. In both suites, olivine phenocrysts are pseudomorphed by cryptocrystalline, pale-green chlorite containing minor amounts of disseminated oxides; while glassy mesostasis material is generally replaced by chlorite.

Secondary mineral phases observed in these rocks include calcite, pumpellyite, prehnite, quartz and epidote which commonly occur in veinlets and amygdules.

Metamorphism of the Patuki volcanics appears to have taken place in at least two stages including both lower greenschist and sub-greenschist facies metamorphic events. Greenschist facies metamorphism is considered to have taken place on the sea floor, while prehnite and pumpellyite facies metamorphism has been attributed to later regional metamorphism associated with the Rangitata orogeny (eg., Coombs et al., 1976; Sivell and Rankin, 1982).

#### 4.4.2 Patuki Subvolcanics

Gabbroic rocks of the Patuki mélange closely resemble those of the Lee River Group and are generally observed as medium-grained isotropic gabbros cut by rare diabase dykes. These rocks are comprised of strongly

saussuritized plagioclase, amphibolitized clinopyroxene, and minor amounts of magnetite and sphene (Plates 4.45 to 4.48).

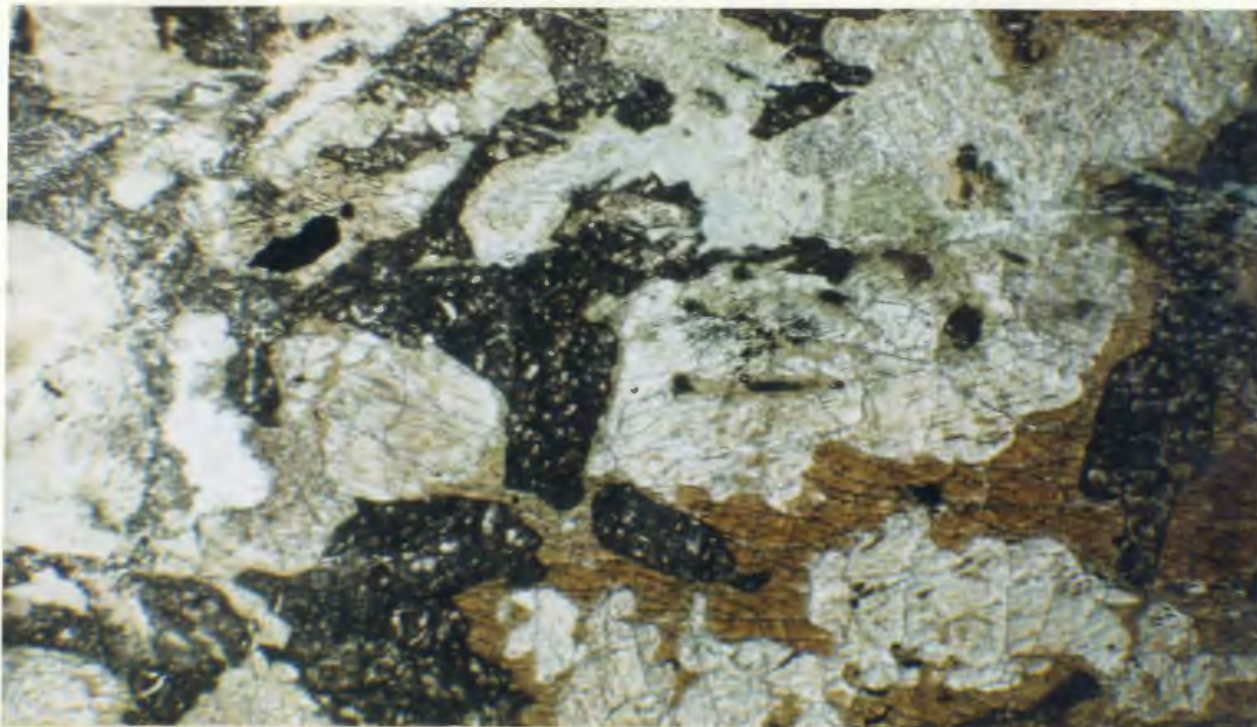
Plagioclase is strongly saussuritized within these rocks (remnant albite and Carlsbad twinning are rarely observed in thin section), while clinopyroxene is typically partially or completely altered to green pleochroic amphibole or pale-brown hornblende.

Dykes within the Patuki mélange are generally composed of aphyric intergranular diabase and have a similar mineralogy to that of the Patuki gabbros. Some of these dykes however, also contain rare olivine and clinopyroxene phenocrysts. The olivine phenocrysts are invariably pseudomorphed by pale-green, cryptocrystalline chlorite while clinopyroxene is relatively unaltered.

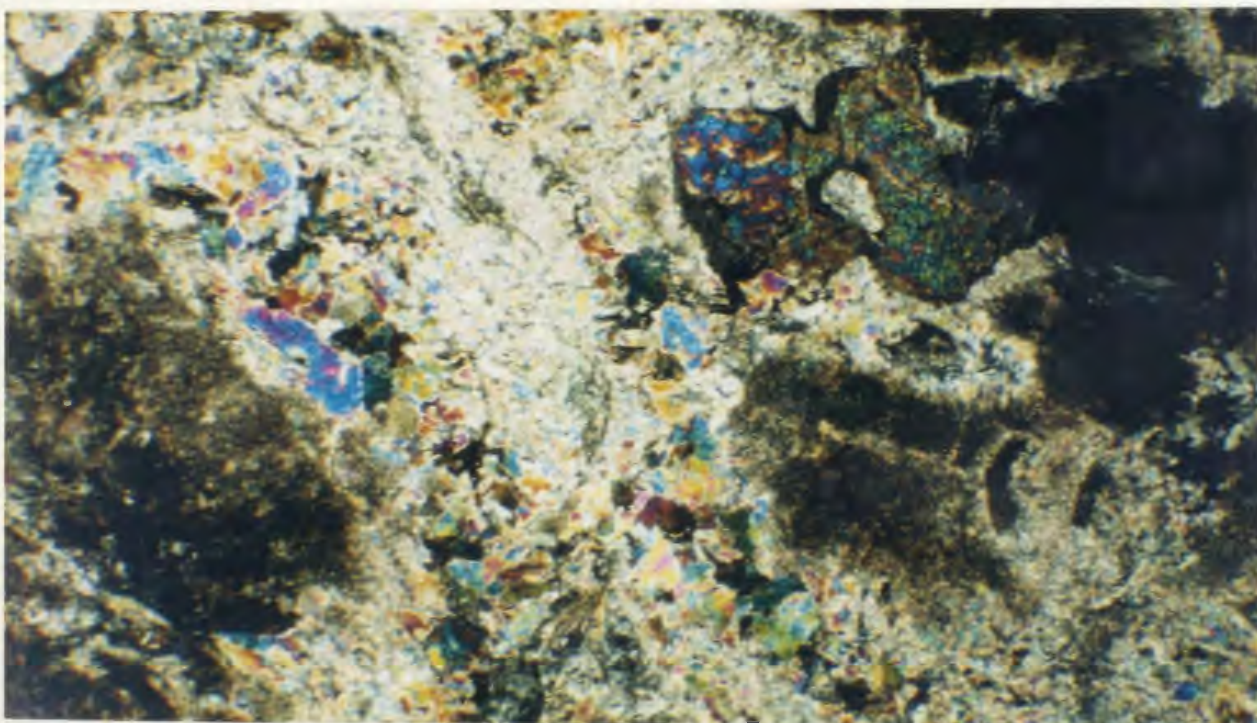
For the most part, subvolcanic rocks of the Patuki mélange are weakly foliated; although, local outcrops of strongly foliated gabbros are observed as small wedges or blocks along the mélange's eastern fault contact. At these localities Patuki gabbros are associated with ultramafic material and contain greater amounts of clinopyroxene and serpentine (after olivine). These strongly foliated gabbros are typically somewhat rodingitized and plagioclase is altered to prehnite while clinopyroxene is altered to a very faint pleochroic pale-brown to colourless tremolitic amphibole.

#### 4.5 Croisilles Mélange

During this study rocks of the Croisilles mélange were examined and sampled along a segment of the mélange which stretches from Ronga Saddle



**Plate 4.47** Microphotograph of partially amphibolitized, medium-grained Patuki gabbro (Lee River area, L-36). Clinopyroxene crystals are rimmed by brown pleochroic hornblende. Plane-polarized light, x25.



**Plate 4.48** Microphotograph of rodingitized orthopyroxene-bearing, Patuki gabbro (Lee River area, B-167). Orthopyroxene is in the top right corner of the photo (at extinction). Plagioclase has been replaced by hydrogrossular and prehnite. Crossed nicols, x25.



to Elaine Bay south of Croisilles Harbour (Figure 3.2.6). In this section mafic volcanic and subvolcanic rocks as well as ultramafic plutonic rocks of the Croisilles mélange are discussed with reference to petrographic samples collected in the Croisilles Harbour area.

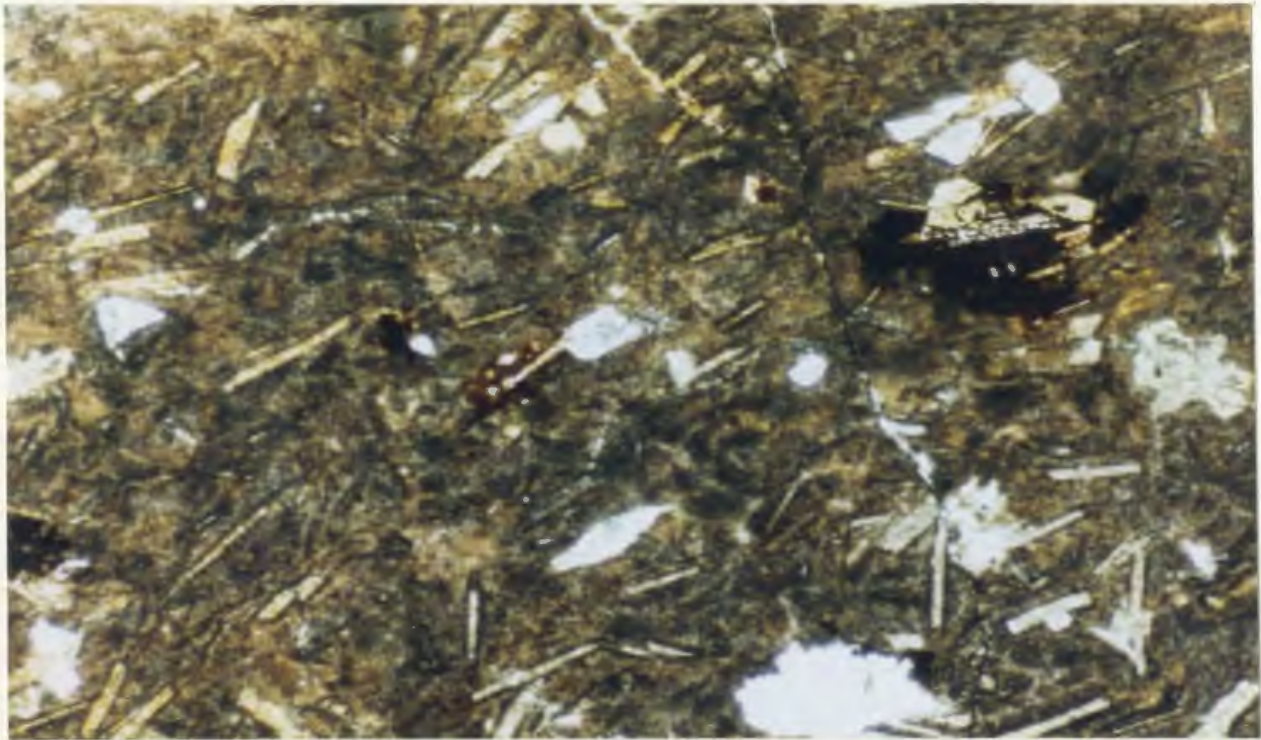
In the Croisilles Harbour area ophiolitic rocks of the Croisilles mélange are composed of: glassy to fine-grained pillowed mafic flows and breccias; medium-grained gabbros; and pyroxene peridotite and dunite.

#### 4.5.1 Croisilles Volcanics

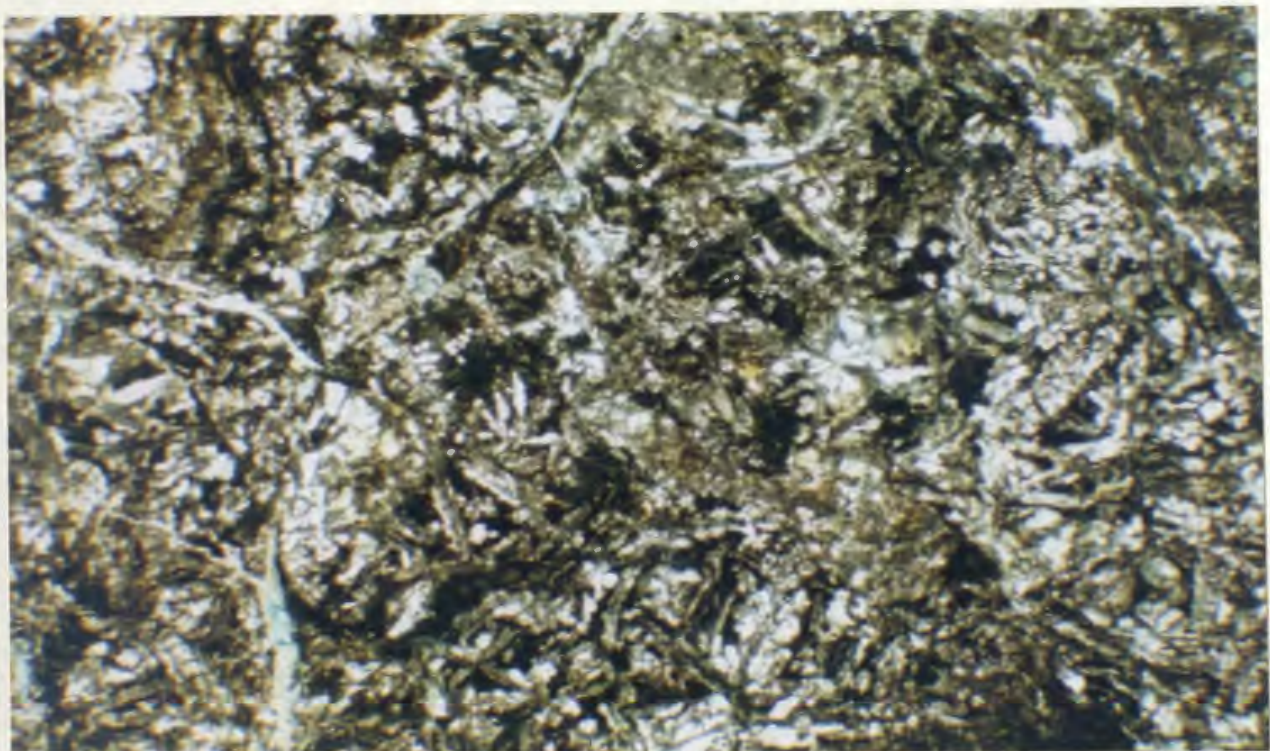
Basaltic rocks of the Croisilles mélange range in composition from quenched glassy, variolitic basalts to fine-grained, intergranular basalts (Plates 4.49 and 4.50). For the most part, these rocks are similar to basalts of the "olivine poor" suite of the Patuki mélange. Although these rocks occur in a variety of petrographic compositions they appear to represent variations within a single basaltic suite and in places are observed grading into each other within single pillows.

A small number of the glass-rich basalts sampled contain rare euhedral phenocrysts of plagioclase and clinopyroxene; however most appear to be composed of strongly hematized, aphyric, quench-textured (variolitic) basalt. The less glassy fine-grained basalts are typically aphyric in character and are generally composed of subhedral plagioclase laths and equidimensional, intergranular to subophitic crystals of clinopyroxene.

Plagioclase is weakly to strongly saussuritized and is often replaced by green to yellow pleochroic pumpellyite; however clinopyroxene is relatively



**Plate 4.49** Microphotograph of hyalopilitic, glassy Croisilles basalt (Croisilles Harbour, C-721b). Note some plagioclase microlites are replaced by pumpellyite and vesicles are infilled by chlorite. Plane-polarized light, x50.



**Plate 4.50** Microphotograph of variolitic to subophitic Croisilles basalt (Croisilles Harbour, C-721a). Plagioclase is altered while clinopyroxene is fresh (clear bladed, variolitic crystals). Plane-polarized light, x25.

unaltered and fresh crystals are occasionally rimmed by minor amounts of chlorite and or pumpellyite. Iron-titanium oxides occur as small grains separated along grain boundaries or as fine disseminations suspended within altered (hematized) glass.

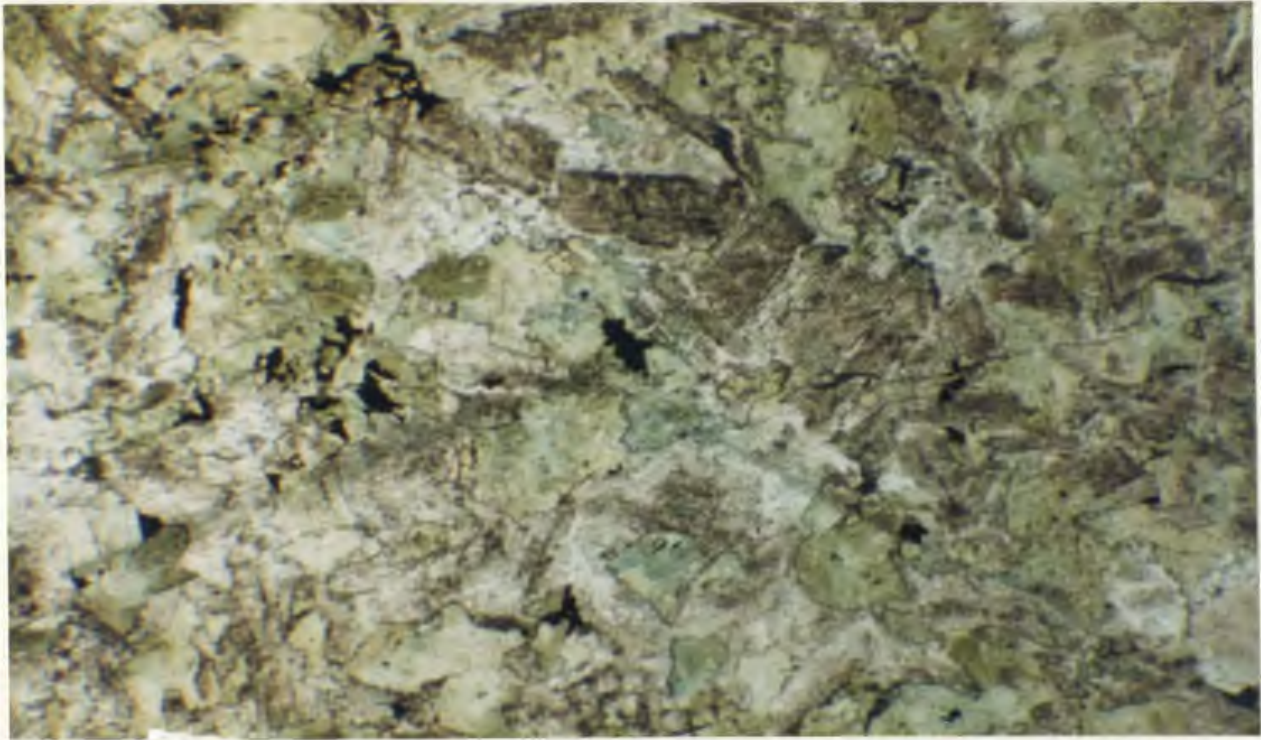
Vesiculated flows are common in the Croisilles volcanics and vesicles are generally infilled by secondary pumpellyite or albite. Other secondary minerals observed in these rocks include minor amounts of epidote (in vugs and cavities) as well as numerous veinlets of pumpellyite and albite, and later veinlets of carbonate and quartz.

#### 4.5.2 Croisilles Subvolcanics

For the most part, gabbroic rocks of the Croisilles mélange are composed of aphyric medium-grained, intergranular gabbro. These occur as variably deformed and metamorphosed rocks which range from weakly metamorphosed and undeformed intergranular gabbro (Plates 4.51a and b) to strongly foliated amphibolitized gabbro (amphibolite) in which all primary igneous textures have been destroyed (Plate 4.52).

The less deformed and less metamorphosed gabbros are predominantly composed of weakly to moderately saussuritized plagioclase and amphibolitized clinopyroxene (pale-green to green pleochroic amphibole), while strongly foliated amphibolitized gabbros (amphibolites) are composed of green to blueish-green pleochroic amphibole (amphibolitized clinopyroxene) and strongly saussuritized plagioclase. Both contain minor amounts of iron-titanium oxides and some of the more strongly foliated gabbros or



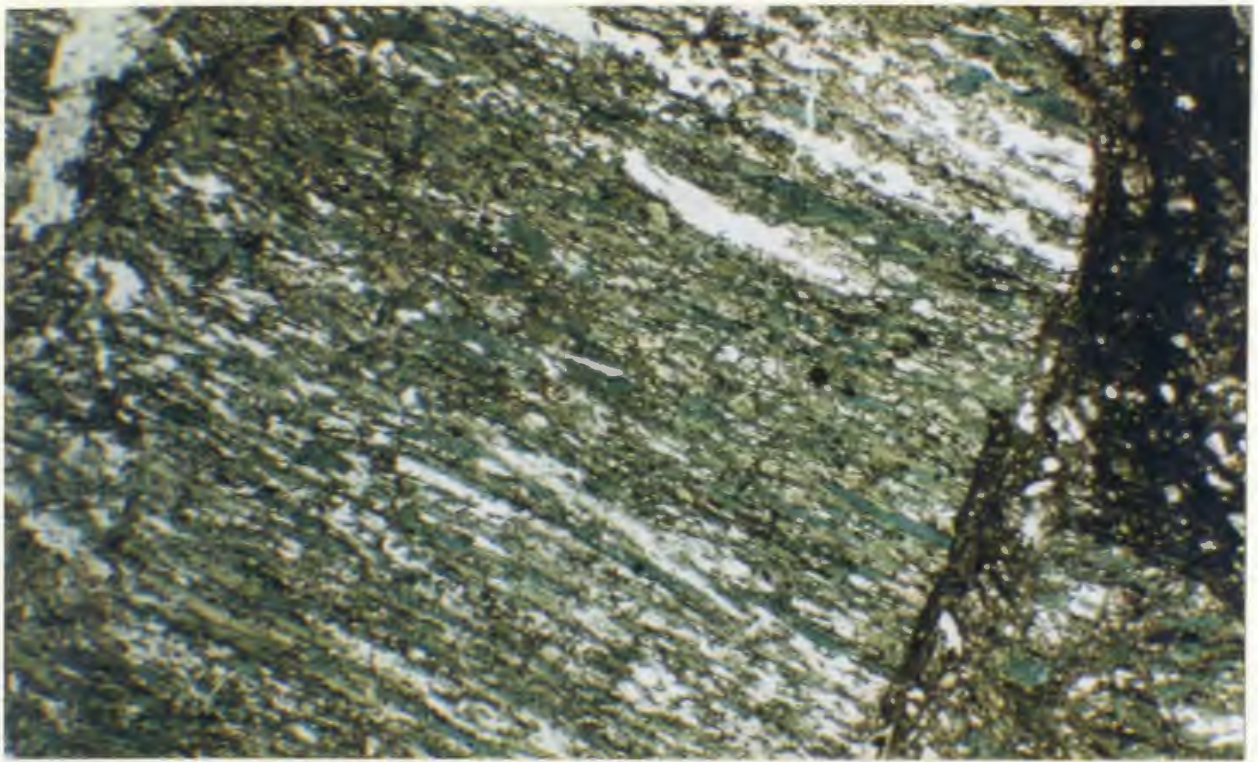


**Plate 4.51a** Microphotograph of nonfoliated, medium-grained Croisilles gabbro (Croisilles Harbour, C-715). Clinopyroxene is altered to green-blue pleochroic amphibole. Note well preserved intergranular texture. Plane-polarized light, x25.



**Plate 4.51b** Microphotograph of nonfoliated, medium-grained Croisilles gabbro (Croisilles Harbour, C-715). Note well preserved intergranular texture. Crossed nicols, x25.





**Plate 4.52** Microphotograph of intensely foliated and amphibolitized Croisilles gabbro (Croisilles Harbour, C-708). Plane-polarized light, x25.



**Plate 4.53** Microphotograph of partially resorbed spinel crystals in serpentinized dunite (Croisilles Harbour, C-721c). Crossed nicols, x25.

amphibolites also contain significant amounts of quartz and epidote as thin bands aligned parallel to the foliation (eg. Plate 4.52). These strongly amphibolitized rocks also contain minor amounts of sphene (euhedral needles) and albite.

#### 4.5.3 Croisilles Ultramafics

Ultramafic rocks of the Croisilles mélange appear, for the most part, to be comprised of intensely serpentized dunite and pyroxene peridotite. Within the Croisilles Harbour area these rocks are observed as serpentized blocks within a matrix of sheared serpentinite (Plates 3.48b and 3.48c). Many of these rocks, particularly those of dunitic composition, are associated with minor concentrations of chromiferous spinel preserved as small anhedral crystals suspended in a matrix of fine, mesh-textured serpentine (Plate 4.53).

#### 4.6 Summary

From petrographic relationships observed in ophiolitic rocks of the East Nelson ophiolites, mafic volcanic and subvolcanic rocks of each of the East Nelson ophiolites (Dun Mountain Ophiolite, Patuki mélange and Croisilles mélange) can be subdivided into a number of distinctive petrologic suites.

Ophiolitic rocks of the Upukerora Formation are preserved as clasts of basalt and gabbro suspended in a hematite-stained, mud and sand matrix. For the most part these clasts resemble basaltic and gabbroic compositions observed within volcanic and subvolcanic rocks of the underlying Dun Mountain Ophiolite particularly the clinopyroxene-phyric as well as glassy



basalt flows of the Lee River Group. Mafic clasts within the Upukerora conglomerates are generally relatively unaltered; however, evidence of weak, lower greenschist and sub-greenschist facies metamorphism is observed as chloritized glass and olivine micro-phenocrysts and as secondary veinlets of pumpellyite.

Volcanic rocks of the Dun Mountain Ophiolite (Lee River Group) occur in a variety of compositions; each of which appear to represent variations of one petrologic suite. These basalts are predominantly composed of glassy to fine-grained, clinopyroxene-phyric, pillowed and massive flows and have undergone moderate degrees of lower greenschist and sub-greenschist facies metamorphism. Lower greenschist facies metamorphism is exemplified by chloritized glass and olivine micro-phenocrysts, albitized and saussuritized plagioclase and vuggy chlorite, epidote, and albite. Evidence of sub-greenschist facies metamorphism is observed as secondary veinlets of pumpellyite.

Subvolcanic rocks of the Lee River Group (Dun Mountain Ophiolite) outcrop as three distinctive petrographic suites of diabase dykes and gabbros. These include:

(i) an aphyric suite predominantly composed of weakly to strongly foliated, intergranular diabase and gabbro in which clinopyroxene is typically partly to completely altered to a pale-green pleochroic amphibole while plagioclase is saussuritized. Locally, along the lower contact of Lee River Group's subvolcanic sequence, rocks of the aphyric suite are intensely amphibolitized and foliated and likely represent subvolcanic material deformed

and metamorphosed at greater temperatures and pressures than the overlying, pale-green pleochroic amphibole bearing aphyric suite rocks. Gabbros and diabase dykes of the aphyric suite are estimated to make up approximately 90 percent of the Lee River Group's subvolcanic sequence and likely represent the oldest rocks of the sequence.

(ii) a plagioclase porphyritic suite predominantly composed of weakly to strongly foliated, intergranular diabase and gabbro in which clinopyroxene is typically partly to completely altered to a pale-green pleochroic amphibole while plagioclase is strongly saussuritized and often partially replaced by prehnite. These rocks are estimated to represent less than 5 percent of the Lee River Group's subvolcanic sequence and are considered to be generally younger than rocks of the aphyric suite which they typically intrude.

(iii) a relatively unaltered clinopyroxene-phyric suite composed of fine- to medium-grained, relatively undeformed, intergranular to clinopyroxene porphyritic, diabase dykes and gabbros. Within this suite of rocks, clinopyroxene is well-preserved and not altered to amphibole but rather, is occasionally partially replaced by chlorite. Rocks of this suite bear a close resemblance to basaltic rocks of the Upukerora Formation and Lee River Group and are considered to represent their subvolcanic equivalents.

Subvolcanic rocks of the Dun Mountain Ophiolite (Lee River Group) have undergone at least two phases of metamorphism; a primary, lower greenschist facies event which took place on the sea-floor and a later regional, sub-greenschist facies event in which rocks of the ophiolite were cut through by veinlets of prehnite, pumpellyite, quartz, and carbonate.

On the basis of petrographic observations, rocks of the plagioclase porphyritic and clinopyroxene-phyric suites may represent minor variations of the more plentiful aphyric suite, particularly those of the later which, if amphibolitized, would closely resemble rocks of the aphyric suite. Geochemical data presented in the following chapter suggests; however, that plagioclase porphyritic suite rocks may represent a compositionally distinct suite.

Also included within the Dun Mountain Ophiolite's subvolcanic rocks are layered series gabbros preserved as blocks of mafic to ultramafic gabbro in the Sheared Serpentine Complex separating rocks of the Lee River Group and the Red Hills ultramafic massif. These gabbros are considered to be cumulate in origin and are composed of gabbroic to ultramafic bands or layers containing varying proportions of olivine, ortho- and clinopyroxene, plagioclase and spinel produced during crystallization of the Lee River Group gabbros. These layered series rocks are similar to "critical zone" or "layered series" rocks observed at the base of layer 3 gabbros in other ophiolites.

Volcanic rocks of the Patuki mélange are unlike those of the Dun Mountain Ophiolite and Upukerora Formation and can be subdivided into two petrographically distinct suites. Subdivision of these basalts into two suites is based on the marked difference in olivine phenocryst abundance within the basalts such that there is an "olivine-poor" suite which generally contains less than 1 percent olivine phenocrysts, and a second "olivine-rich" suite composed of basalts containing generally up to 5 percent olivine phenocrysts. Basalts of these suites are generally glassy to fine-grained and typically have



a quenched, variolitic to intersertal texture. In outcrop, basalts of both suites were in places encountered next to one another without faulted contacts. This suggests that these suites were extruded in close proximity to one another and have not been tectonically juxtaposed.

Metamorphism of the Patuki volcanics appears to have taken place in at least two stages including both lower greenschist and sub-greenschist facies metamorphic events. Greenschist facies metamorphism is considered to have taken place on the sea floor, while prehnite and pumpellyite facies metamorphism has been attributed to later regional metamorphism associated with the Rangitata orogeny.

Subvolcanic rocks of the Patuki *mélange* closely resemble those of the Lee River Group's aphyric suite and are generally observed as medium-grained isotropic gabbros cut by rare diabase dykes. For the most part; however, these subvolcanic rocks are generally more strongly foliated than those of the Lee River Group.

Volcanic rocks of the Croisilles *mélange* are generally similar to "olivine poor" basalts of the Patuki *mélange* and possibly represent material derived from the same oceanic crust as the Patuki *mélange*. These rocks have also undergone at least two phases of metamorphism (lower greenschist and sub-greenschist facies) similar to that experienced by volcanic rocks of the Patuki *mélange*.

Subvolcanic rocks of the Croisilles *mélange* are similar in character to those of the Patuki *mélange* but are generally more strongly deformed and less abundant in outcrop.

From petrographic examination it appears that mafic volcanic and subvolcanic rocks of the Dun Mountain Ophiolite are unlike those of the Patuki and Croisilles mélanges but are somewhat similar to basaltic and gabbroic clasts observed within the Upukerora Formation. This suggests that conglomerates of the Upukerora Formation were derived from submarine erosion of the Dun Mountain Ophiolite, and that ophiolitic rocks of the tectonic mélanges were not derived from the same ocean crust as the Dun Mountain Ophiolite. In the following chapters geochemical evidence is presented to test these hypotheses.

## CHAPTER 5

### GEOCHEMISTRY OF VOLCANIC AND SUBVOLCANIC ROCKS OF THE EAST NELSON OPHIOLITES

#### 5.1 Introduction

114 whole rock samples of mafic volcanic and subvolcanic rocks from all three ophiolitic assemblages of the East Nelson ophiolites (Dun Mountain Ophiolite, Patuki mélange, and Croisilles mélange) were collected and analyzed for major and 14 trace elements (ie. Ga, Zn, Cu, Ni, Ti, Ba, Sc, Cr, V, Rb, Sr, Y, Zr, and Nb). 82 samples were selected on the basis of these initial results for further analyses for additional trace elements (ie. Li, Mo, Cs, Hf, Ta, W, Tl, Pb, Th, and U) and rare earth elements (REE's). Microprobe analyses of relict primary clinopyroxenes were also obtained from 27 basaltic rocks of the various ophiolitic suites.

Sampling and sample preparation methods are described in Appendix A. Samples were collected so as to obtain representative suites of mafic ophiolitic rocks from each of the areas studied. Sample locations are shown on Figures 3.2.1 to 3.2.7 and whole rock chemical analyses are presented in Appendix C.

As this thesis is primarily concerned with the geochemistry and petrogenesis of basaltic rocks of the East Nelson ophiolites, most of the rocks analyzed here are of basaltic and diabasic compositions. These rock types are generally considered representative of liquid compositions and can be



directly compared to other liquid compositions (basalts) of known tectonic setting assuming compositions were unaffected by metamorphism. In this way these rocks can be compositionally classified into their respective suites and the original eruptive setting(s) for each of the "basaltic" suites of the East Nelson ophiolites can be inferred.

In cases where pillowed basalts were sampled, samples were taken from the crystalline interiors of pillows (unless otherwise stated) and selected where possible, to minimize effects of weathering, alteration, and vesiculation. Subvolcanic rocks sampled and analyzed other than the previously mentioned aphanitic to fine-grained diabase dykes include fine- to medium-grained gabbros of variable composition and varying degrees of metamorphism.

All sample preparation and chemical analyses were carried out at Memorial University of Newfoundland. Major elements have been determined by atomic absorption spectrophotometry while the trace elements: Rb, Sr, V, Zr, Y, Cr, Ni, Zn, Ga, Cu, and Sc were determined by X-ray fluorescence spectrometry on pressed powder pellets. Additional trace and rare earth elements were determined by inductively coupled plasma-mass spectrometry (ICP-MS) on whole rock samples dissolved by HF nitrate digestion using the procedures of Jenner et al. (1990). Details of analytical methods and data handling procedures used here are presented in Appendix B.

## 5.2 Presentation of Data

Within this and other studies, basaltic (and diabasic) rocks of the East Nelson ophiolites have been mapped as portions of three different ophiolite

assemblages (eg., Coombs et al. 1976; Davis et al. 1980; Johnston, 1981; Dickins et al. 1986; Landis and Blake, 1987; and Sivell, 1988). These are: the Dun Mountain Ophiolite, the Patuki mélange, and the Croisilles mélange. Within these assemblages basaltic rocks have been further classified here into five petrographic suites (previous chapter) whereby the Dun Mountain Ophiolite (Lee River Group) consists of three distinct basaltic suites and the Patuki and Croisilles ophiolitic mélanges comprise the other two.

As basaltic rocks of the East Nelson ophiolites include these different ophiolitic assemblages as a number of petrographically distinct basaltic suites, it is possible that these rocks represent oceanic crust produced in more than one tectonic environment. In this chapter the compositional characteristics of each suite are described and magmatic affinities and eruptive settings are proposed.

Before describing the compositional characteristics of each suite it is first necessary to assess the effects alteration may have had on the rocks sampled. Once this is complete, basaltic rocks of the East Nelson ophiolites can be defined on the basis of elemental concentrations which have not been affected by alteration and metamorphism.

In this and following chapters, all major and trace elements have been recalculated to 100 percent anhydrous on all diagrams.

#### 5.2.1 Effects of Alteration

The use of geochemical data to interpret magmatic histories of igneous rocks is based on the assumption that some of the original geochemical

characteristics of the rocks are preserved. Field and petrographic evidence; however, clearly indicate that all mafic volcanic rocks of the East Nelson ophiolites have been metamorphosed under greenschist and sub-greenschist facies conditions. In particular, major elements appear to have been somewhat mobilized and veins, vesicles, and vuggy cavities are commonly infilled by secondary minerals such as chlorite, pumpellyite, albite, quartz, prehnite, and epidote.

As part of this study 47 basalts, 22 diabbases, 30 gabbros, and 1 plagiogranite sample were analyzed, as well as a small number of other variously altered samples of less consistent compositions including: fine-grained clastic sediments, rodingitized mafic and ultramafic rocks, and serpentized ultramafic rocks.

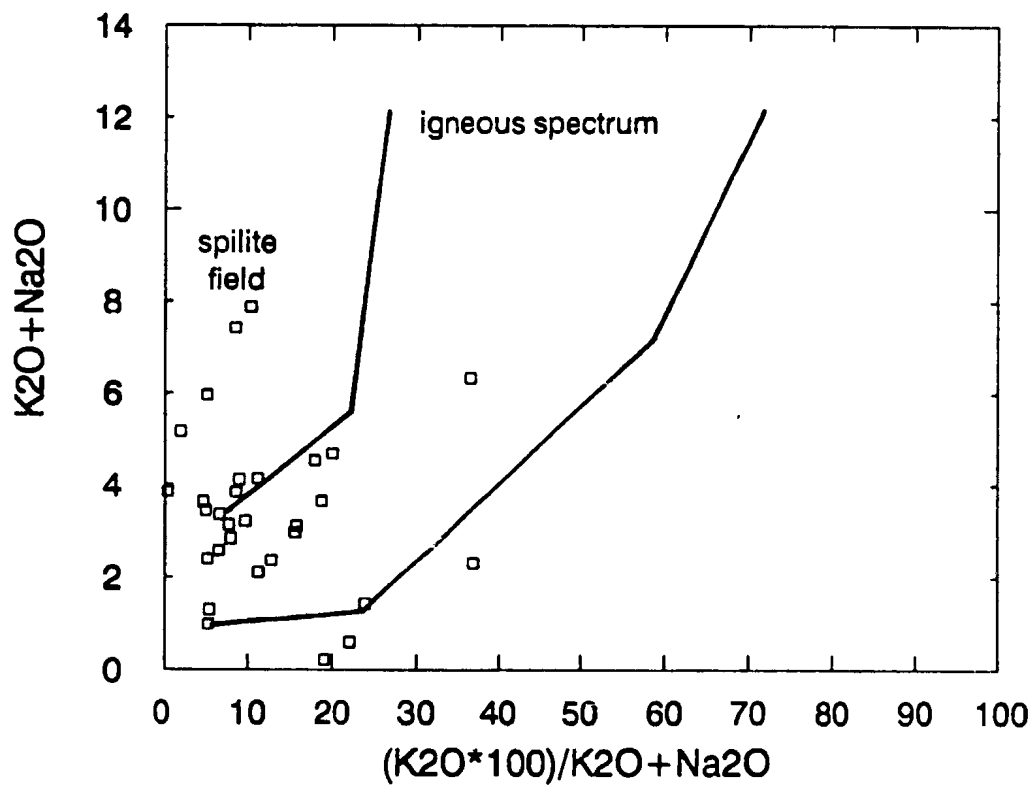
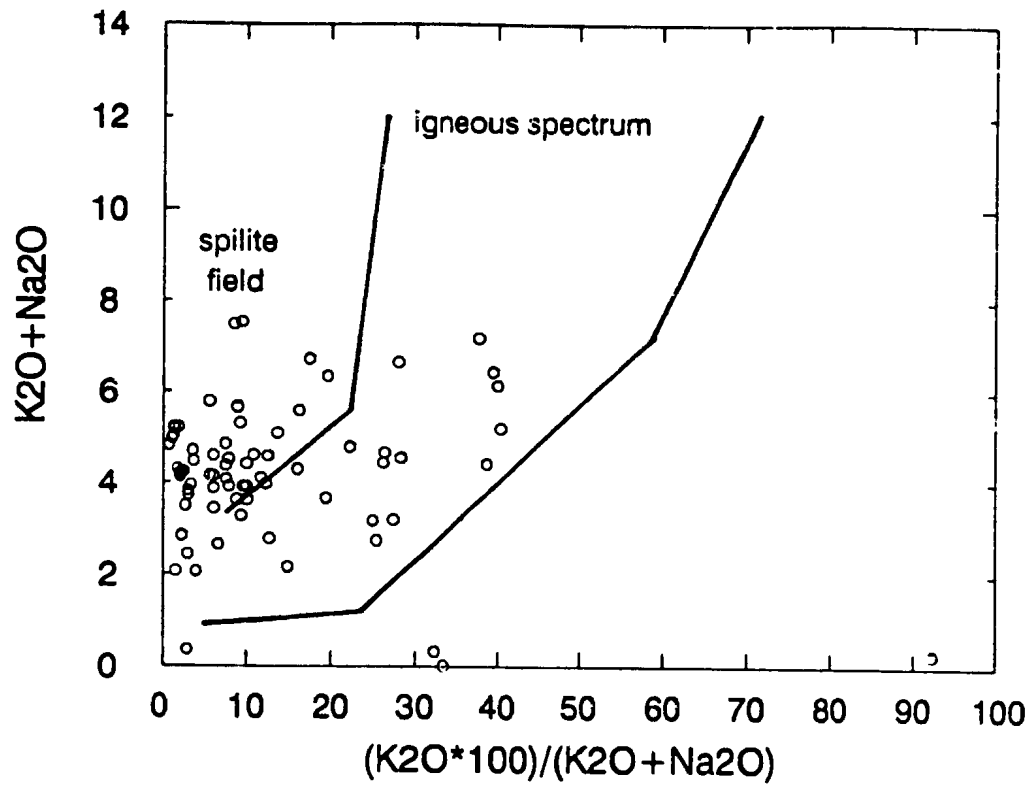
#### 5.2.1.1 Major Elements

Mobility of the alkali elements (Na and K) in mafic igneous rocks can be appraised using the "igneous spectrum" of Hughes (1972), on which the fields of normal igneous rocks including: spilites, keratophyres (Hughes, 1972) and island-arc tholeiites (after Stauffer et al. 1975) are defined. On this diagram (Figures 5.1a) approximately 70 percent of the mafic volcanic rocks plot outside the "igneous spectrum" with approximately 55 percent plotting in or near the spilite field. As 65 percent of these basaltic samples plot above the "igneous spectrum" it can be suggested that significant and pervasive alkali metasomatism has taken place within volcanic rocks of the East Nelson ophiolites. This alteration involved the addition of Na relative to K during



**Figure 5.1a** Modified Hughes (1972) igneous spectrum diagram after Stauffer et al. (1975). Samples plotted are basaltic rocks of the East Nelson ophiolites. Oxides are in weight percent.

**Figure 5.1b** Modified Hughes (1972) igneous spectrum diagram after Stauffer et al. (1975). Samples plotted are gabbroic rocks of the East Nelson ophiolites. Oxides are in weight percent.



metamorphism. Samples plotting below the "igneous spectrum" on the other hand, are considerably replaced by chlorite and pumpellyite; but, are devoid of secondary albite. Although approximately 30 percent of the samples plot within the "igneous spectrum", it is possible that many of these samples may have been altered such that changes in the relative proportions of  $K_2O$  and  $Na_2O$  have moved the samples' bulk rock compositions parallel to the "igneous spectrum" boundaries.

Intrusive mafic rocks of the ophiolites are also assessed using Hughes's diagram in Figure 5.1b and appear to have been slightly less affected by alkali metasomatism as approximately 58 percent of the gabbroic samples plot within the "igneous spectrum". Despite this observation it is assumed here that changes in the relative abundances of  $SiO_2$ ,  $CaO$ , and the alkali elements has taken place as many of these rocks are weakly to strongly amphibolitized and often weakly rodingitized.

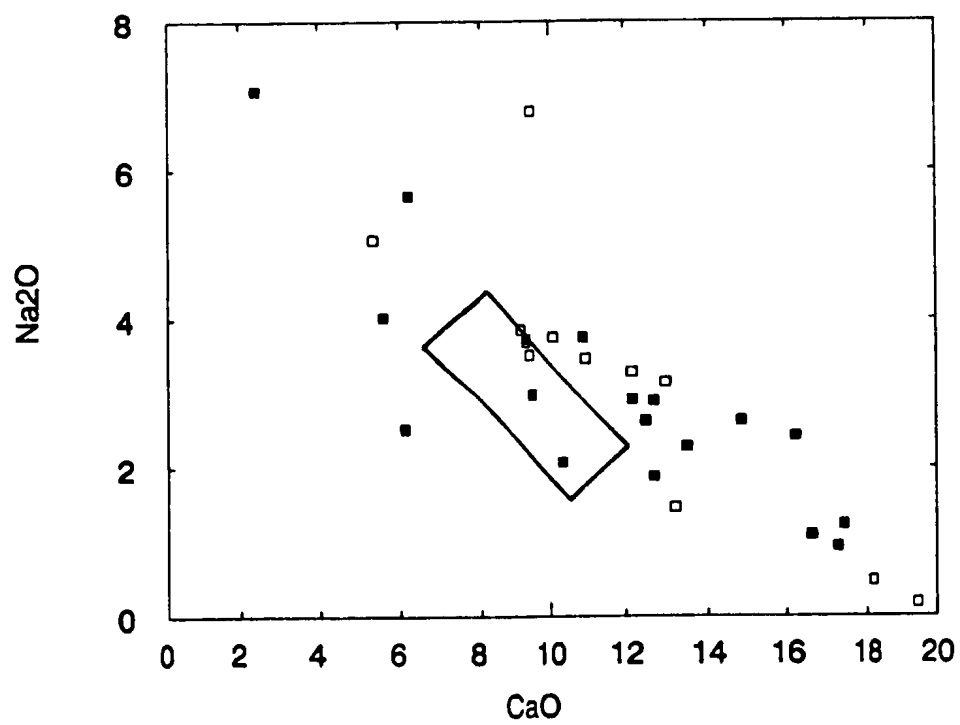
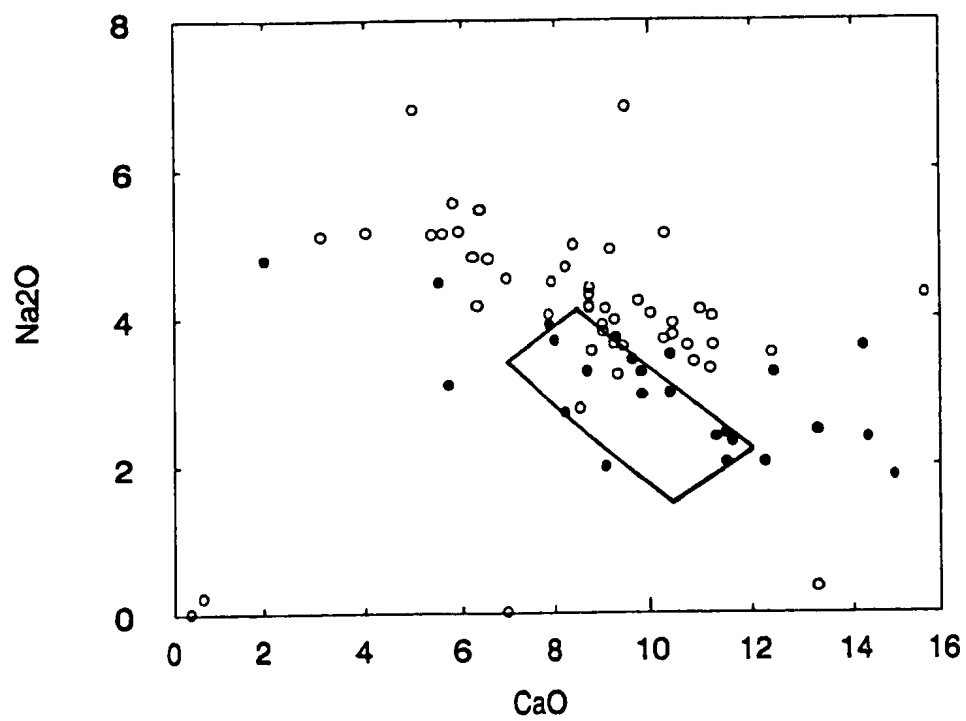
Like the alkali elements,  $CaO$  mobility can also be appraised in terms of an igneous spectrum or field. Stephens (1982) uses a binary plot  $CaO$  against  $Na_2O$  in which a rectangular field outlines the distribution of normal igneous mafic rock compositions. On this diagram, Figure 5.2a, samples which plotted within the "igneous spectrum" of Hughes's diagram (Figure 5.1a) are plotted as solid symbols.

Of the mafic volcanic rocks plotted, only 35 percent plot within the igneous spectrum of Stephens (1982) while most of the remaining samples plot above and to the left. This suggests that these rocks have been depleted in  $CaO$  and enriched in  $Na_2O$  relative to unaltered mafic igneous



**Figure 5.2a** Igneous spectrum diagram after Stephens (1982). The igneous field is defined by the rectangular field in the centre of the diagram. Samples plotted are basaltic rocks of the East Nelson ophiolites. Solid symbols represent samples which plot in the igneous spectrum in Figure 5.1a (Hughes igneous spectrum diagram). Oxides are in weight percent.

**Figure 5.2b** Igneous spectrum diagram after Stephens (1982). Samples plotted are gabbroic rocks of the East Nelson ophiolites. Solid symbols represent samples which plot in the igneous spectrum in Figure 5.1b (Hughes igneous spectrum diagram). Oxides are in weight percent.



rocks. Samples plotting to the right of the igneous field were generally found to contain anomalous amounts of secondary calcite and/or prehnite.

Intrusive rocks also display considerable scatter on Stephen's diagram (Figure 5.2b) whereby less than 40 percent of the gabbro samples plot within the igneous field.

It can thus be implied that within the majority of the mafic, volcanic and subvolcanic rocks of the East Nelson ophiolites,  $\text{Na}_2\text{O}$ ,  $\text{K}_2\text{O}$ , and  $\text{CaO}$  have been redistributed as only 20 percent of the rocks plot within normal igneous fields on both the Hughes and Stephens diagrams (Figures 5.1a, 5.1b, 5.2a, and 5.2b). As these elements appear to have been remobilized it can be inferred here that many of the low field strength elements (eg., Rb, Sr, and Ba) have been redistributed as well. The concentrations of these elements are therefore considered to be unreliable as discriminants between rocks of the various suites or as petrogenetic indicators, and are not discussed further.

Although the processes of primary low grade hydrothermal alteration (on the sea floor) and later burial metamorphism are known to have affected these rocks, further investigation of the affects produced by these individual processes was not carried out within this study.

Another element of some importance to petrogenetic evaluation of basaltic rocks is  $\text{SiO}_2$ . This element is commonly used to discriminate between basalts, basaltic andesites, and other volcanic rock types. It is generally accepted that  $\text{SiO}_2$  is mobile during greenschist facies and sub-greenschist facies metamorphism as well as during hydrothermal alteration on the seafloor. Within the ophiolites described here it is apparent that

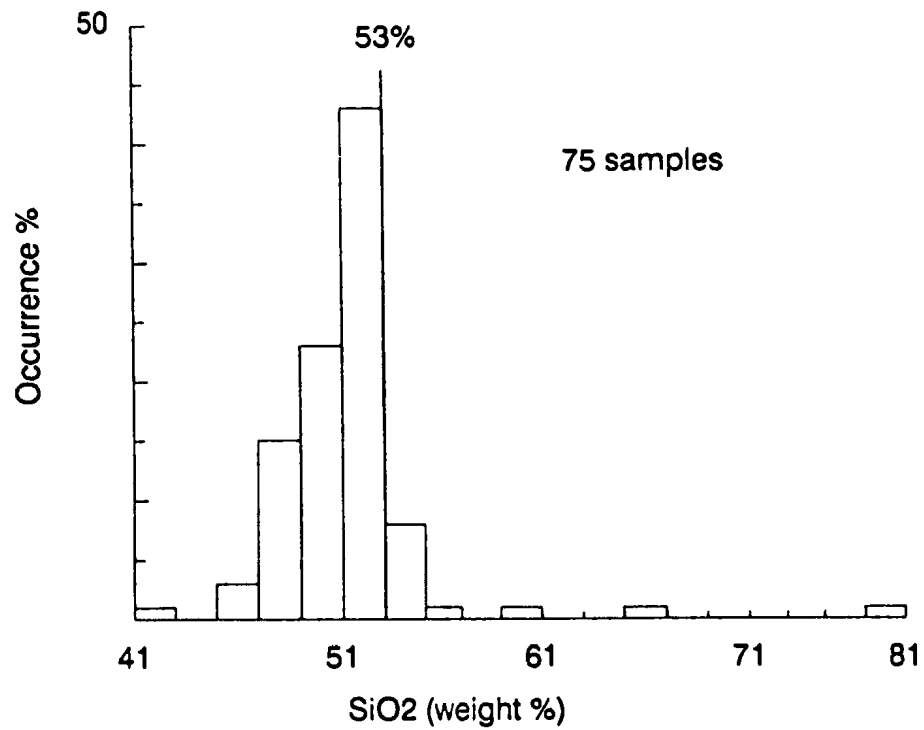


mobilization of  $\text{SiO}_2$  has occurred as quartz veins and quartz-filled vesicles and vuggy cavities are commonly observed. Despite this, the majority of the samples analyzed can be classified as basalts on the basis of their  $\text{SiO}_2$  content (Figure 5.3). Only 10 percent of the volcanic rocks sampled contain greater than 53 percent  $\text{SiO}_2$  (the basalt-basaltic andesite boundary as accepted by the Basaltic Volcanism Study Project, 1981) with values ranging between 45 and 57 weight percent (Figure 5.3). Although these values suggest that some of the samples are basaltic andesite most of the higher  $\text{SiO}_2$  samples are either slightly silicified and/or contain amygdaloidal quartz. It is therefore proposed that the high  $\text{SiO}_2$  samples represent basaltic rocks which have been enriched in  $\text{SiO}_2$  through the addition of secondary quartz. This proposal is supported by the observation that rocks of similar petrographic suites which do not contain secondary silica contain less than 53 percent  $\text{SiO}_2$ .

Magnesium and iron are also important in petrogenetic studies of mafic igneous rocks, particularly basalts, as the ratio of these elements is commonly used as a differentiation index.

Many authors have previously shown that  $\text{MgO}$  is a major reactant during hydrothermal alteration of basaltic rocks, whereby  $\text{MgO}$  concentrations can be directly correlated with the water/rock ratio of an altered rock while iron concentrations are essentially preserved (eg., Seyfried et al., 1978; Mottl and Seyfried, 1980; Mottl, 1983).

As water/rock ratios are the dominant factors in the mobility of  $\text{MgO}$ , it is apparent that the relative amounts of  $\text{MgO}$  redistribution are dependent on



**Figure 5.3** Histogram of SiO<sub>2</sub> contents within basaltic rocks of the East Nelson ophiolites. Samples with greater than 59 percent SiO<sub>2</sub> were found to be strongly altered and contain abundant secondary SiO<sub>2</sub>.

the permeability of the rock being altered. Spooner et al., (1977) proposed that pillowed flows and highly fractured basalts are significantly more permeable than massive unfractured flows and that mass transfer (water/rock interaction) primarily occurs along pillow margins, fractures, and joint surfaces.

In agreement with Spooner et al. (1977), other workers (eg., Humphris and Thompson, 1978 and Coish, 1977) have shown mass transfer of MgO between basaltic rocks and seawater to be more extensive within pillow rims than crystalline cores. They observed altered rims to generally be significantly more enriched in MgO than crystalline pillow interiors.

From these studies it is evident that pillow rims should be excluded from geochemical sampling of basaltic rocks which have undergone lower greenschist facies metamorphism. It should also be noted here however, that other studies (eg. Alt and Emmermann, 1985; Seyfried et al., 1978) suggest changes in MgO concentrations produced under low water/rock ratios during the alteration of fresh basalt to greenschist facies metabasalt may be only slight.

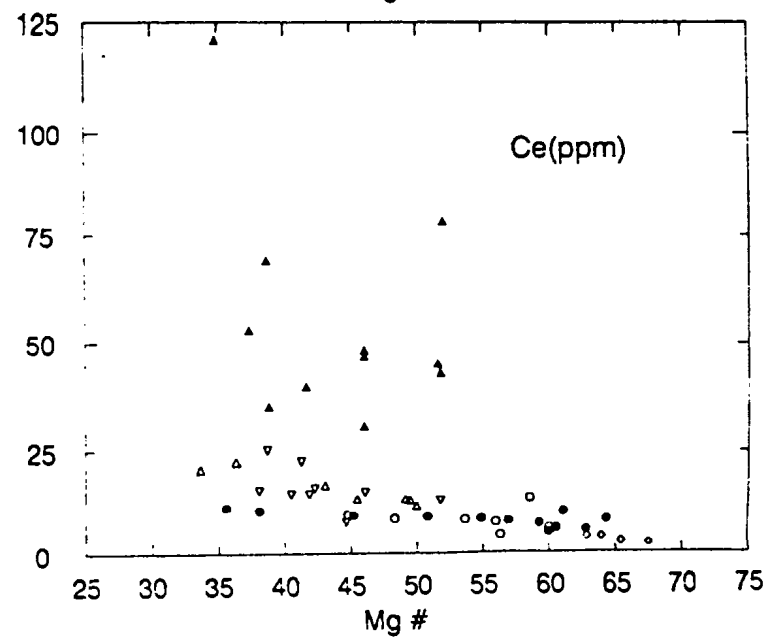
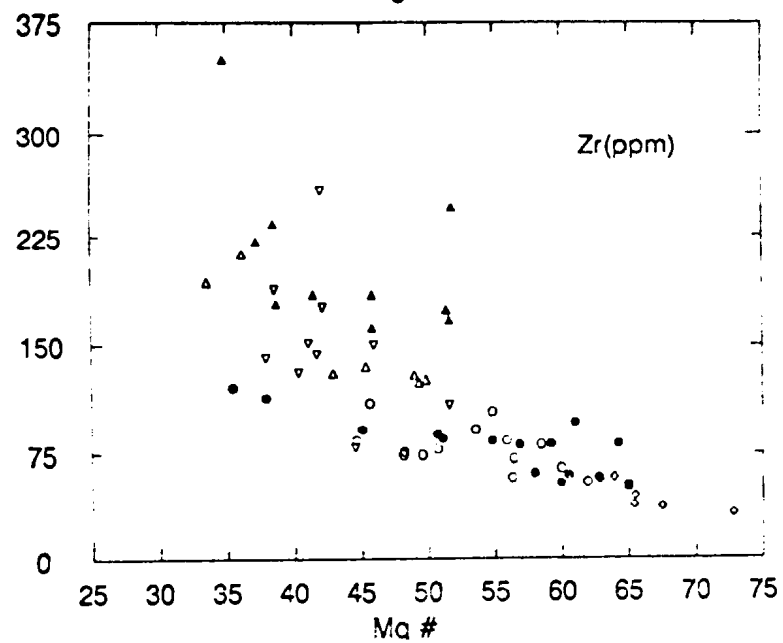
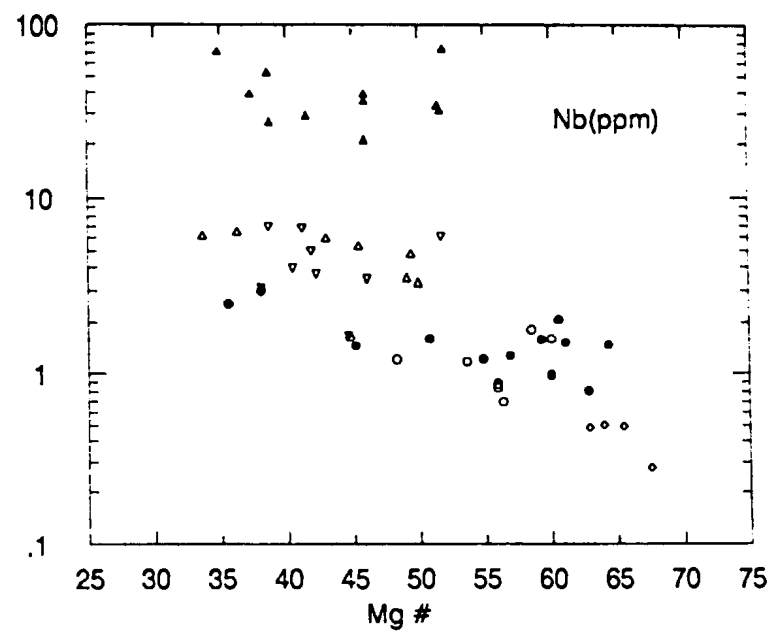
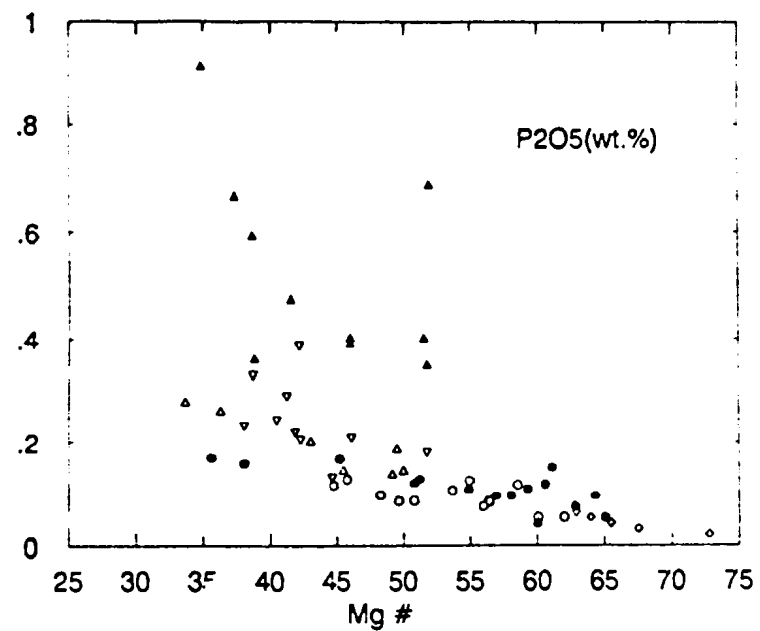
As MgO and FeO\* are particularly valuable as indicators of differentiation of basaltic rocks an attempt was made within this study to use these elements as a fractionation index. It was therefore necessary to limit sampling to the less altered cores of pillows and centres of flows in order to avoid, as much as possible, problems associated with the use of Mg# for basaltic rocks that have undergone greenschist facies metamorphism as indicated in the previous paragraphs.



Figures 5.4a,b,c Variation diagrams of selected trace, rare earth and major elements plotted against Mg# (fractionation index). Samples plotted are basalts. All elements have been recalculated anhydrous. Oxides are plotted as weight percent; other elements in parts per million (ppm). Field boundaries for various suites have been drawn on some of the diagrams.

Symbols:

- aphyric suite rocks
- clinopyroxene-phyric suite rocks
- plagioclase porphyritic suite rocks
- ▲ "olivine-poor" suite basalts (Patuki mélange)
- ▼ "olivine-poor" suite basalts (Croisilles mélange)
- ▲ "olivine-rich" suite basalts (Patuki mélange)



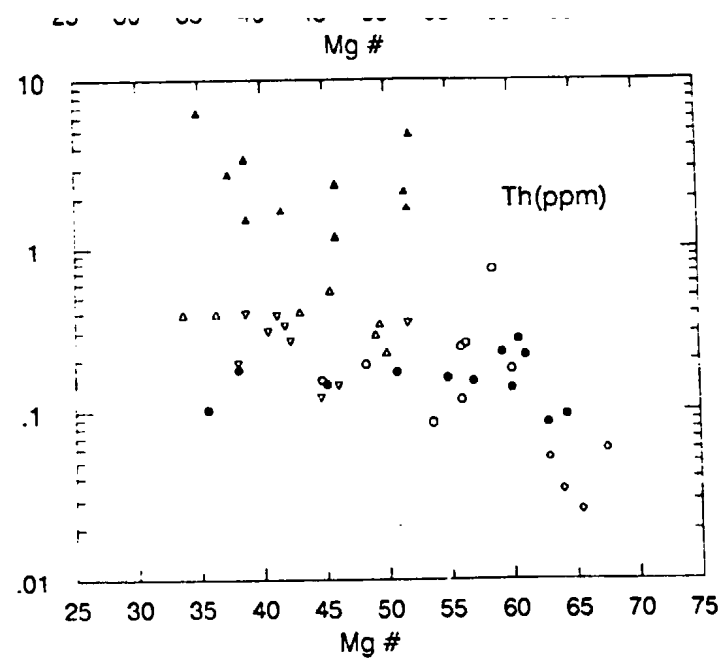
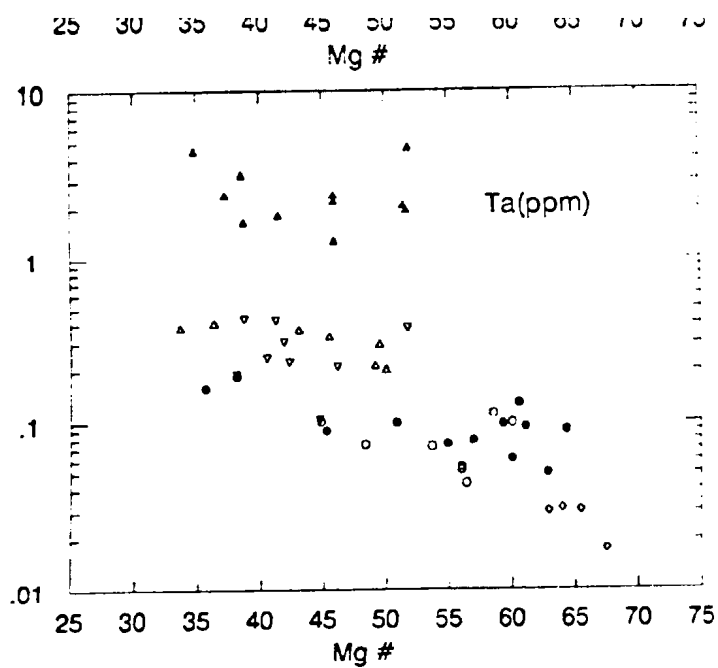
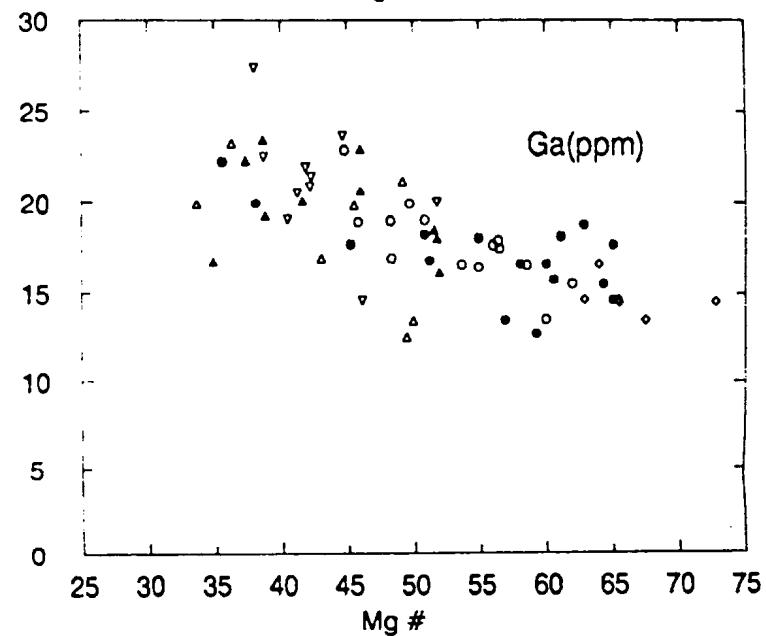
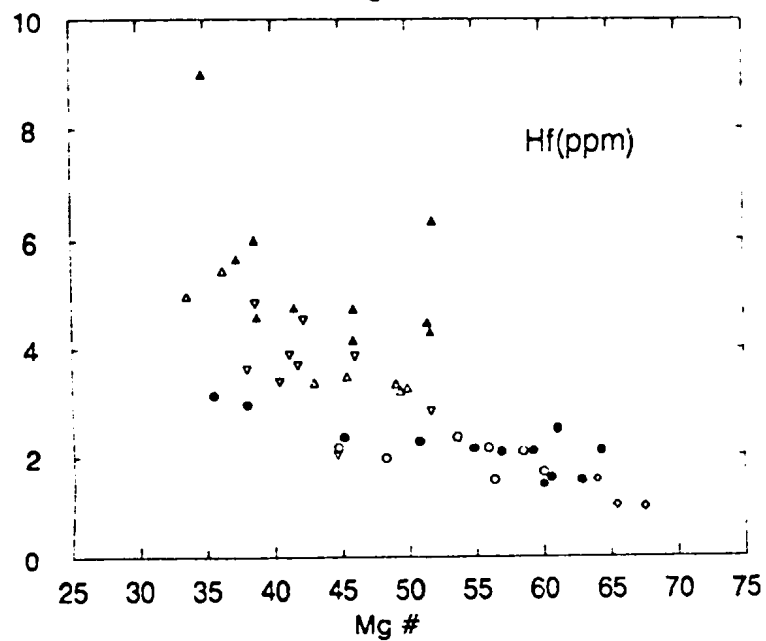
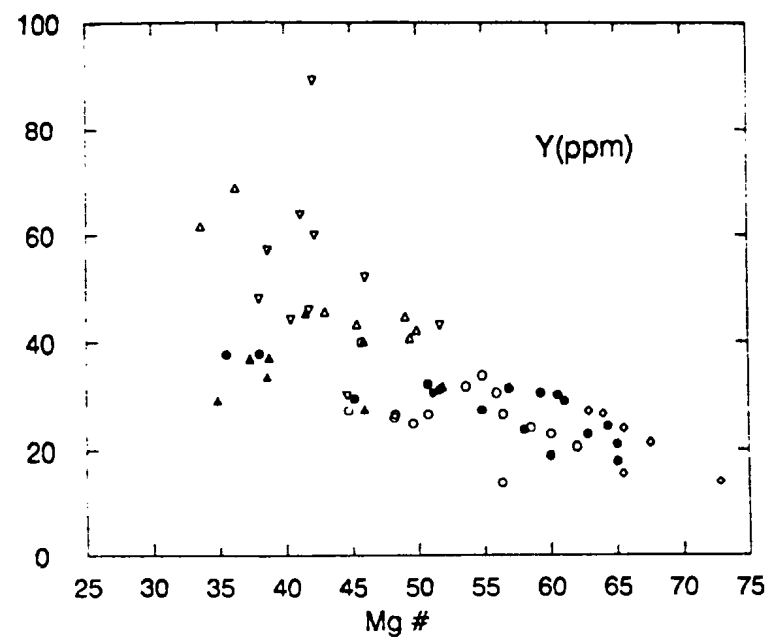
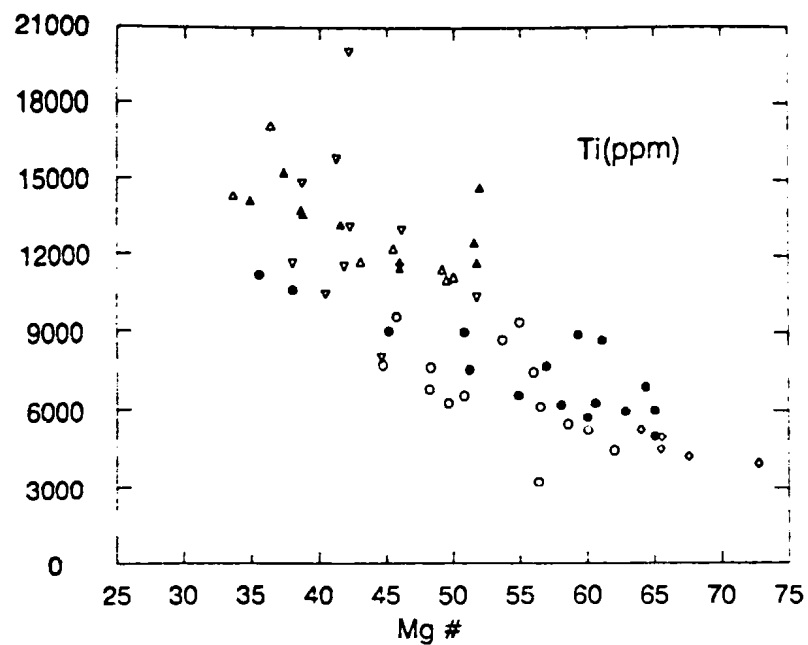


Figure 5.4a Immobile trace elements plotted against Mg#.





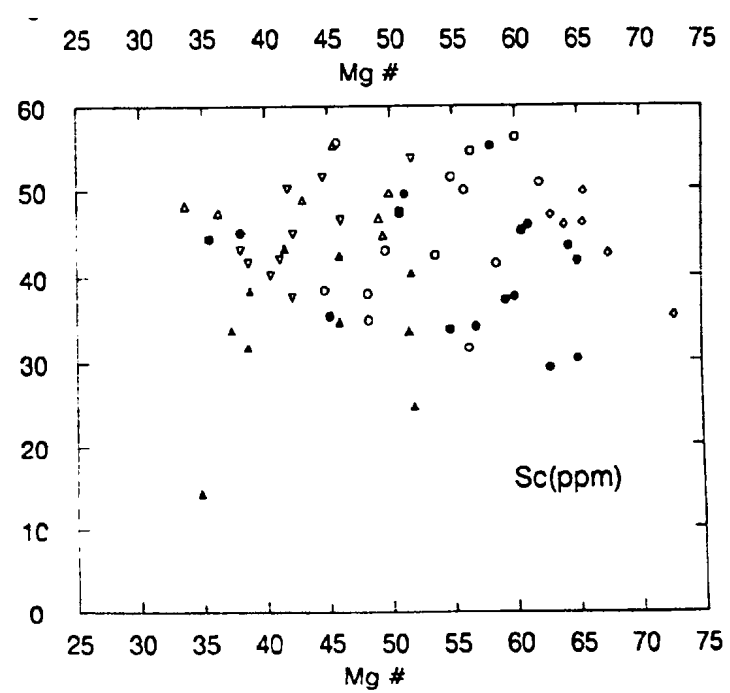
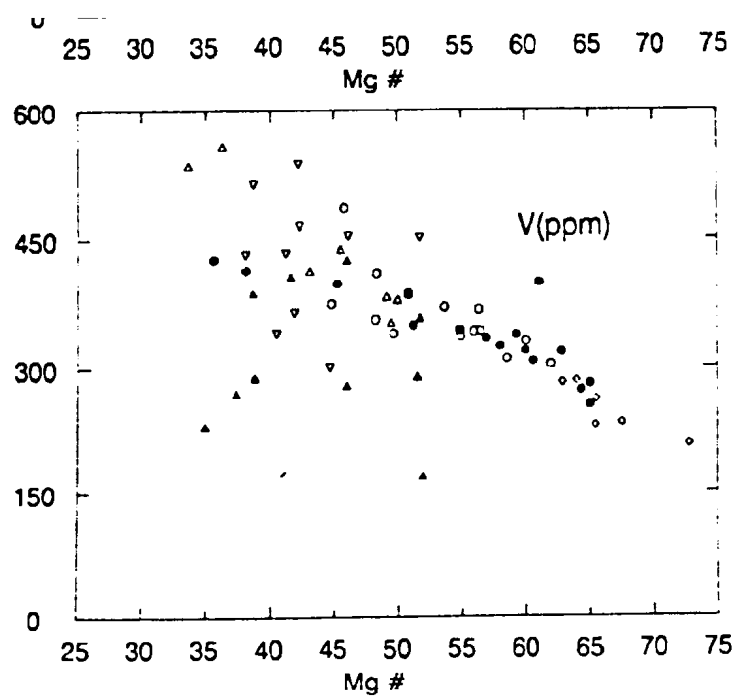


Figure 5.4a (continued) Immobile trace elements plotted against Mg#.

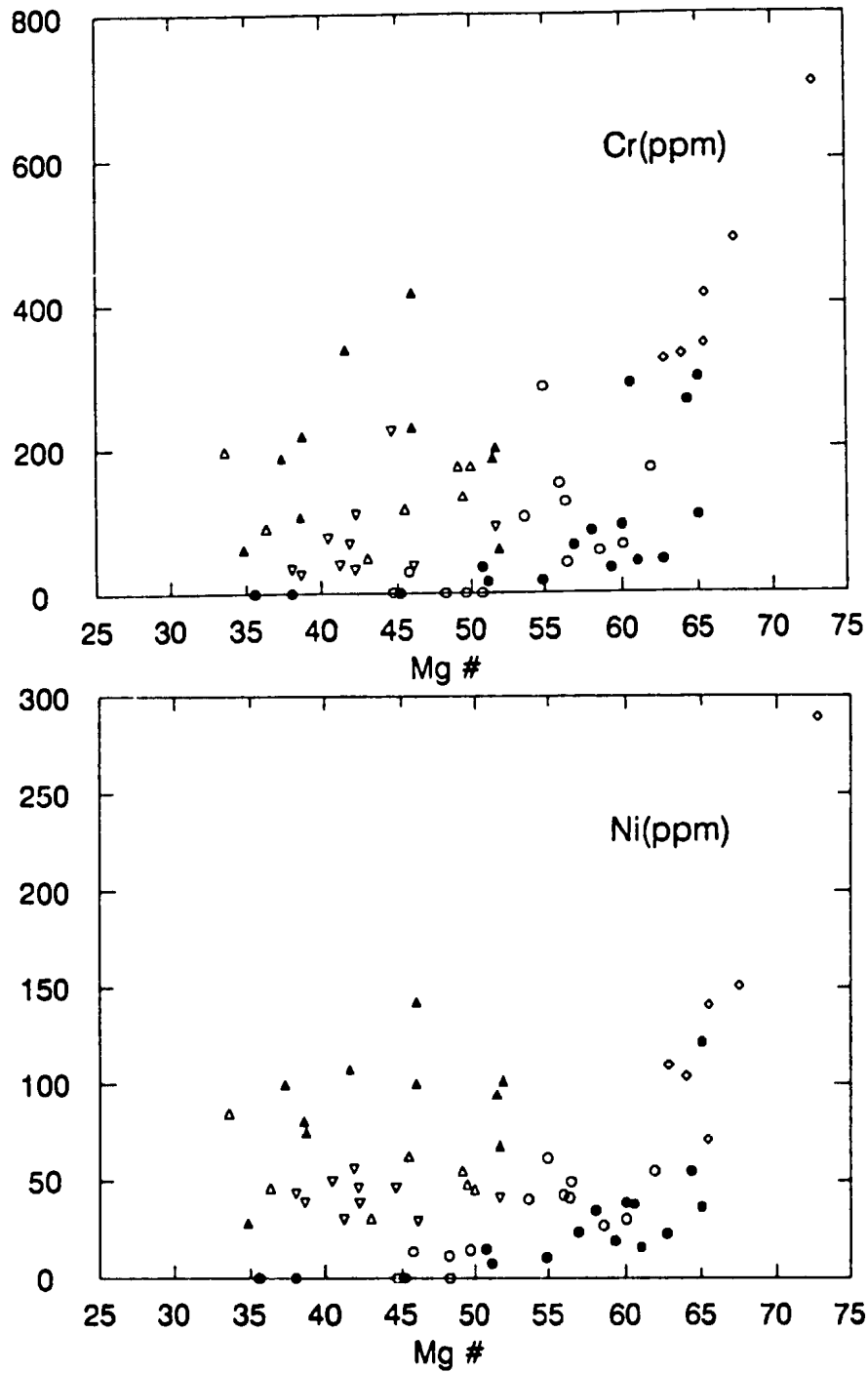
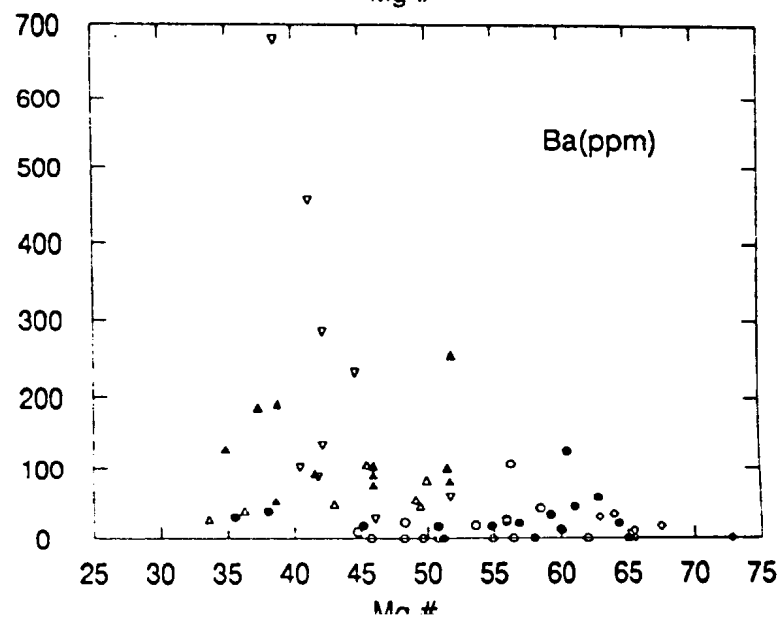
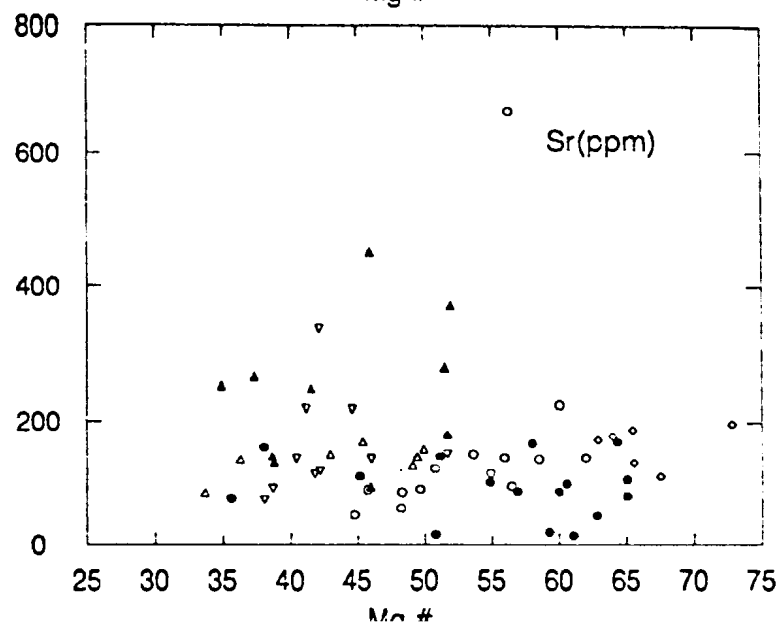
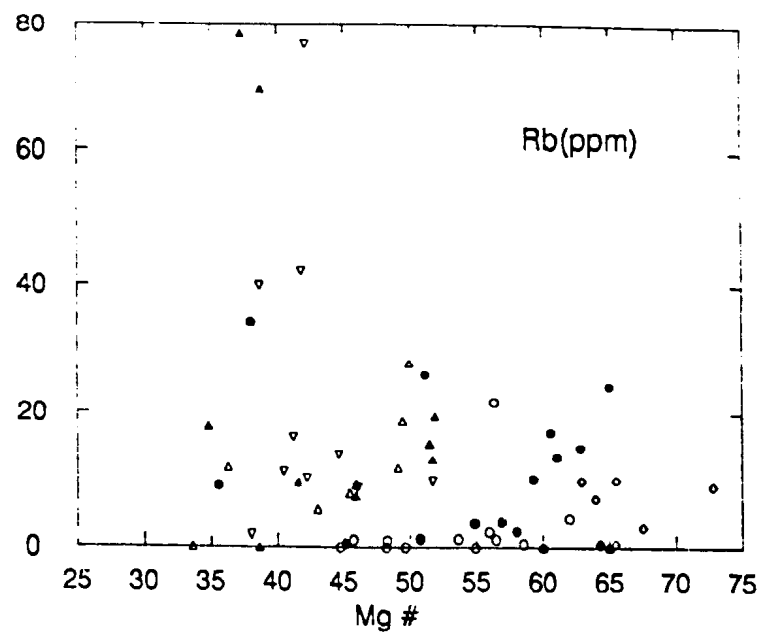
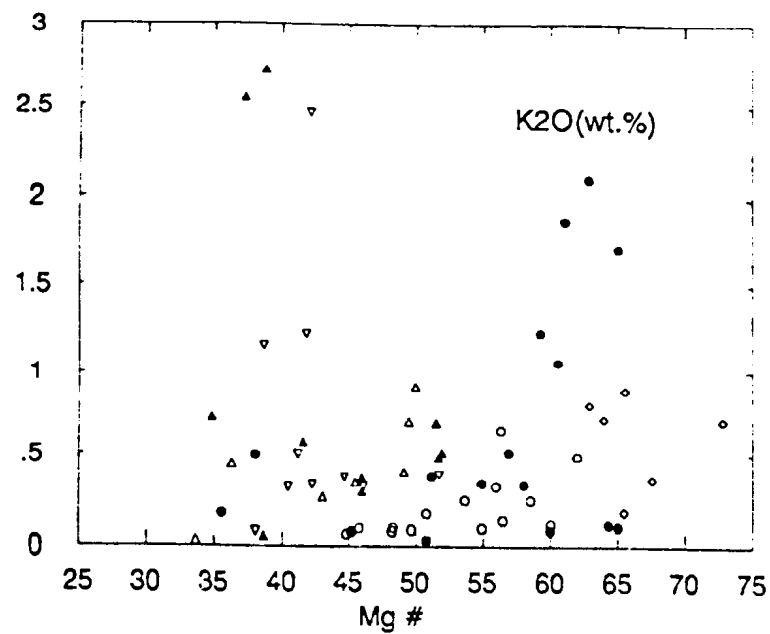


Figure 5.4b Cr and Ni plotted against Mg#.





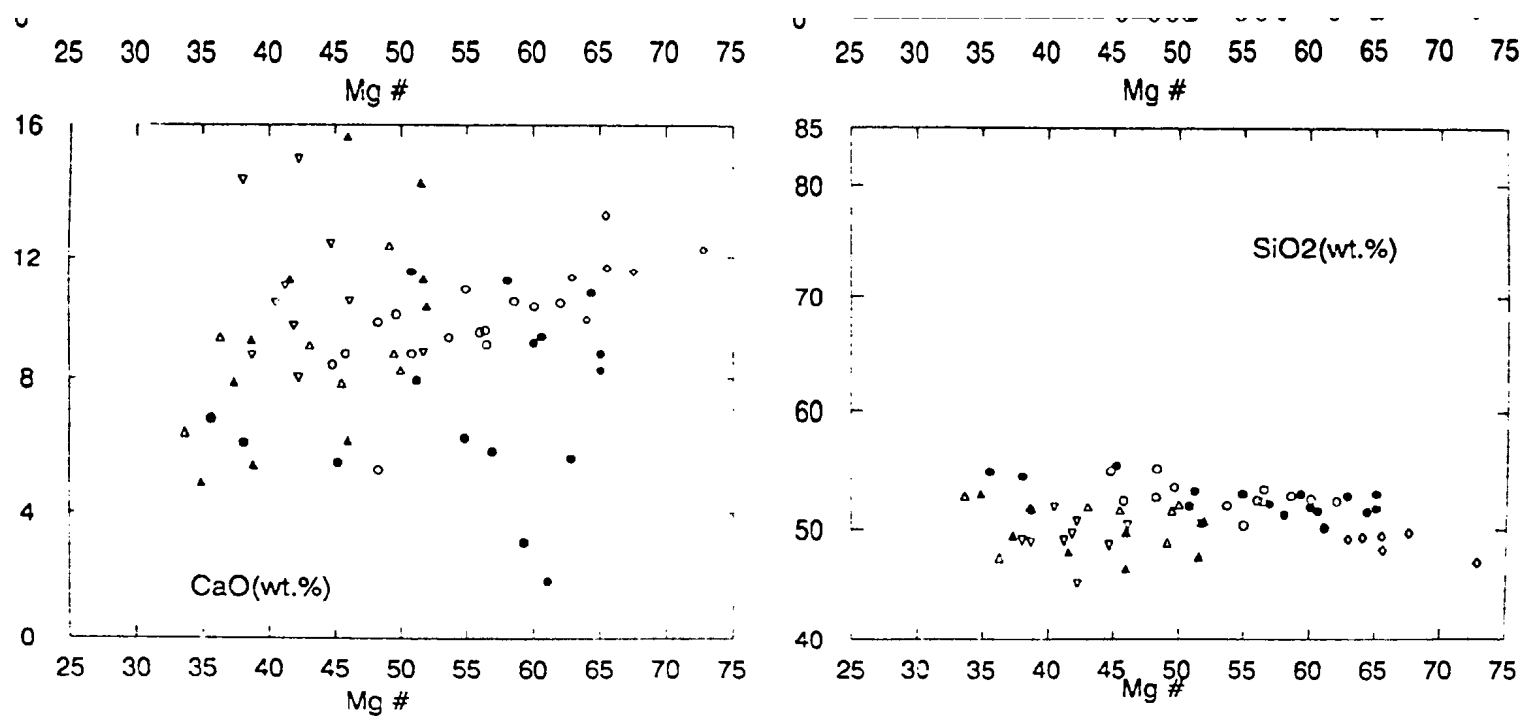


Figure 5.4c Mobile trace elements and major oxides plotted against Mg#.

Within this study Mg# is defined as:

$$\text{Mg} \times 100 / [\text{Mg} + \text{Fe}^{2+}]^1,$$

where Mg and Fe are the molecular proportions of magnesium and ferrous iron respectively.

Use of Mg# as a differentiation index appears permissible within this study as a correlation between high field strength elements and Mg#'s is generally observed (Figures 5.4a and 5.4b); while the more mobile elements (alkali, alkaline earth, and low field strength elements as well as SiO<sub>2</sub>) show very limited correlation (Figure 5.4c).

#### 5.2.1.2 Trace Elements

In this section susceptibilities of selected trace elements to mobilization during seafloor hydrothermal alteration and low-grade metamorphic conditions (greenschist facies) are reviewed for basaltic rocks. As a detailed and complete review of previous trace element mobility studies is beyond the scope of this thesis, reference is made only to some of the principle studies carried out over the past 25 years.

To date many studies have shown that a select number of trace elements are only slightly mobile under greenschist facies conditions and can be used effectively in petrogenetic discrimination of altered basaltic rocks (eg., Frey et al., 1968; Cann, 1970; Kay et al., 1970; Thompson, 1973; Hart et al., 1974; Pearce, 1975; Floyd and Winchester, 1975; Wood et al., 1976; Wood et

---

<sup>1</sup> Fe<sup>2+</sup> has been calculated from Fe<sub>2O3</sub>\* by using a ratio of FeO/Fe<sub>2O3</sub> of 0.85 after Brooks (1976).



al., 1979; Coish, 1977). These elements include: P, Nb, Y, Zn, Zr, Ti, Hf, Ta, Th, and the heavy rare earth elements. In addition: Ce, Ga, Sc, V, Cr, Co, Ni and the light rare earth elements are also generally considered to be sufficiently immobile under greenschist facies conditions that they can be used in making petrogenetic interpretations on basaltic rocks. It is important to note here; however, that this later group of elements are prone to minor to major remobilization with increasing metamorphism, particularly within altered basaltic glasses, and must be used with caution (eg., Frey et al., 1974; Coish, 1977; Garcia, 1978; Shervais, 1982).

Although some of the basalt samples contain large percentages of glass, care was taken during sampling and sample preparation to avoid (as much as possible) involvement of pillow rims and other altered glassy material unless otherwise stated.

### 5.3 Basalt Geochemistry

#### 5.3.1 Introduction

In this section data for trace and rare earth elements considered to be immobile under greenschist facies conditions as well as relict pyroxene compositions are presented. Using these, compositional characteristics of the various suites of the East Nelson ophiolites are defined and magmatic affinities and eruptive settings are inferred on the basis of rare earth elements and relict pyroxene compositions.

As previously described in chapters 3 and 4, basaltic rocks (diabase dykes and lavas) of the East Nelson ophiolites (volcanics and dykes of the

Dun Mountain Ophiolite; Patuki volcanics of the Patuki mélange; and, Croisilles volcanics of the Croisilles mélange) can be subdivided into 5 petrographic groups or suites. Three of these groups occur within the Lee River Group of the Dun Mountain Ophiolite and include:

(Group i); an aphyric suite of diabase dykes in which clinopyroxene is partly to completely altered to amphibole;

(Group ii); a clinopyroxene-phyric suite of basaltic flows and diabase dykes within which clinopyroxene is relatively fresh and occasionally partially altered to chlorite; and

(Group iii); a plagioclase porphyritic suite predominantly composed of diabase dykes and basalts containing up to 30 percent altered plagioclase phenocrysts.

The other two basaltic suites of the East Nelson ophiolites occur within the Patuki and Croisilles ophiolitic mélanges. These suites include:

(Group iv); a suite of "olivine-poor" basalts which contain less than 1 percent olivine phenocrysts, and

(Group v); a suite of "olivine-rich" basalts which contain less than 5 percent olivine phenocrysts.

The basalts of groups iv and v are glassy to fine-grained and have quenched, variolitic to intersertal textures.

### 5.3.2 Trace Elements

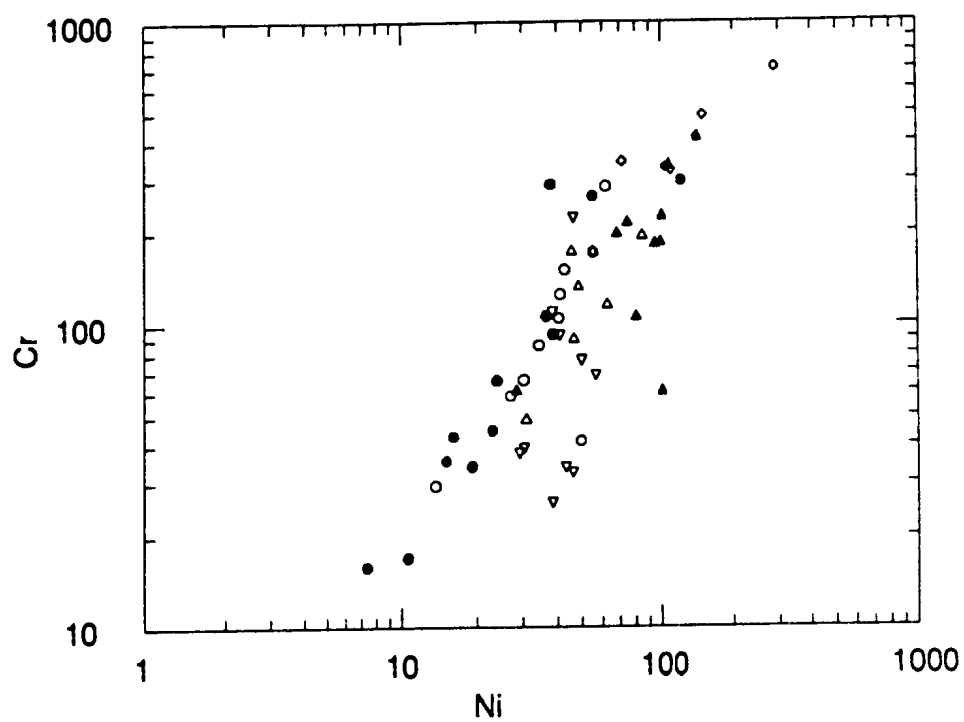
Trace element abundances in volcanic rocks of the five petrographic suites can be assessed through the use of variation diagrams in which trace

element concentrations are plotted against a differentiation index (Mg#). In this way characteristic trace element abundances for the various suites are observed while rocks produced through varying degrees of fractionation within individual suites group together along fractionation trends.

On these diagrams (Figures 5.4a and 5.4b) the elements  $P_2O_5$ , Nb, Zr, Ce, Th, Ta, and to a lesser extent Hf, Ga, Ti, Y and V, exhibit higher concentrations with decreasing Mg# while Ni and Cr decrease markedly.

This first group of elements ( $P_2O_5$  to V; Figure 5.4a) are considered to be incompatible in basaltic rocks and therefore have greater affinities for the liquid phase than basaltic "rock-forming" minerals. Ni and Cr, on the other hand (Figure 5.4b), are considered to be somewhat compatible as they are typically enriched in olivine and spinel (respectively) during crystallization. As a result, Ni and Cr concentrations decrease within the basaltic rocks as the degree of fractionation increases. A plot of Cr versus Ni (Figure 5.5) shows an overall positive correlation between these elements; however, basalts of the "olivine-poor" and "olivine-rich" suites of the Patuki and Croisilles mélanges tend to contain slightly higher Ni values than rocks of similar Cr content from other suites (Lee River Group). This may in part, be attributed to the greater abundance of olivine phenocrysts and lesser abundance of clinopyroxene phenocrysts within Patuki and Croisilles lavas, as Ni is typically strongly enriched in olivine while Cr tends to be taken up in other phases, particularly spinel and clinopyroxene.

From data presented in the above variation diagrams (Figures 5.4a and 5.4b) it is apparent that many of the petrographically defined rock suites of





the East Nelson ophiolites can be discriminated on the basis of their trace element abundances.

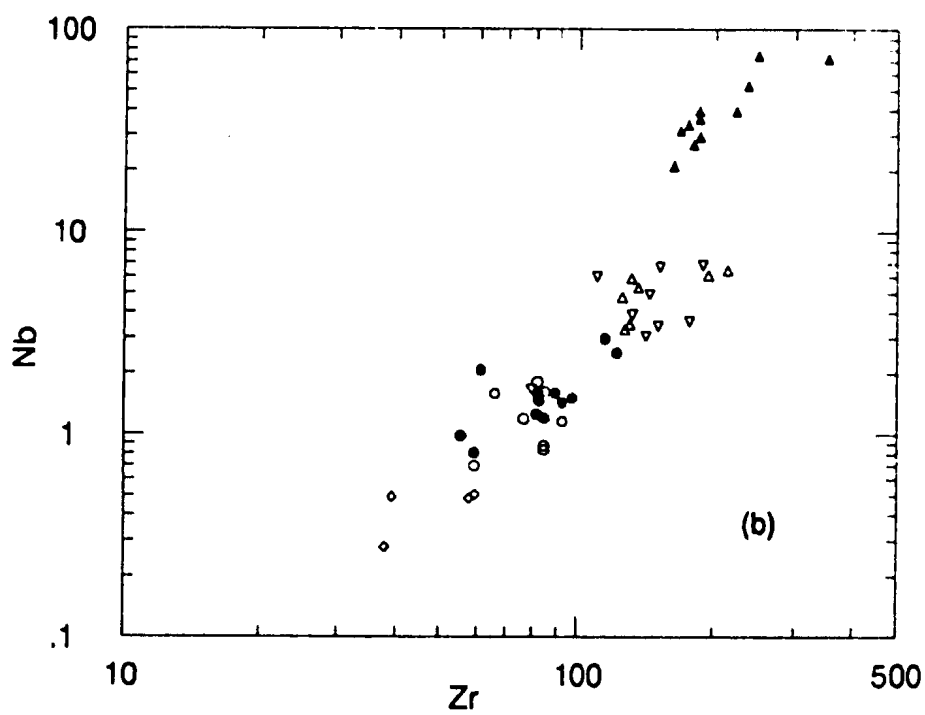
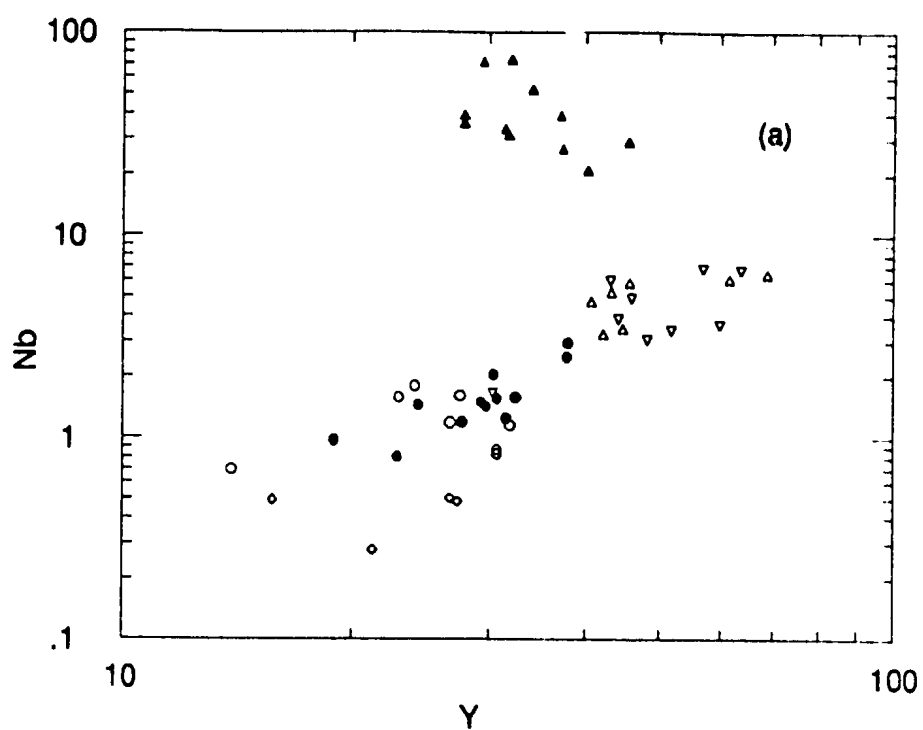
"Olivine-rich" suite basalts (Patuki volcanics) tend to contain higher concentrations of  $P_2O_5$ , Nb, Zr, Cr, Ni, Ce, Th, and Ta than rocks of other suites of similar Mg#'s. Hf, Ga, and Ti concentrations, on the other hand, overlap with those observed within "olivine-poor" suite basalts, while Y and V concentrations are generally lower than that observed in "olivine-poor" suite basalts.

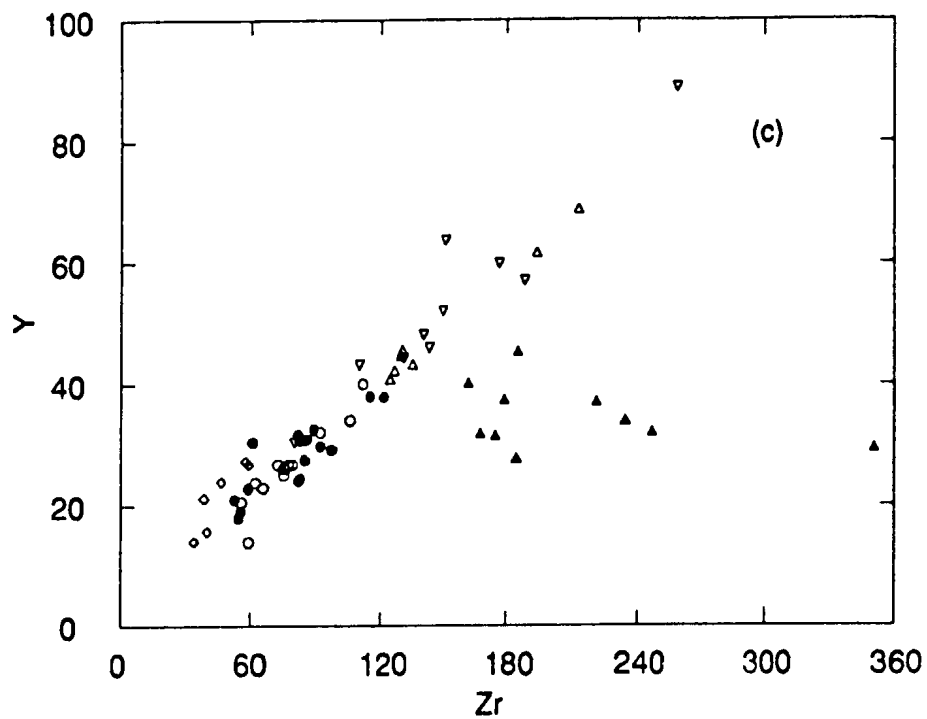
"Olivine-poor" suite basalts do not appear to be selectively enriched in any of the trace elements used here and consistently contain higher concentrations of  $P_2O_5$ , Nb, Zr, Cr, Ni, Ce, Th, Ta, Hf, Ti, V, and Y than in rocks of the Lee River Group suites (of similar Mg#).

As for rocks of the Lee River Group suites (Dun Mountain Ophiolite), only two of the three petrographic suites of the Lee River Group can be discriminated using trace elements. Rocks of the aphyric and clinopyroxene-phyric suites generally contain similar trace element abundances and Mg#'s and are therefore compositionally indistinguishable. Rocks of the plagioclase porphyritic suite; however, possess higher Mg#'s than rocks of other suites and contain the lowest concentrations of  $P_2O_5$ , Nb, Zr, Ce, Th, Ta, Hf, Ti, V, and Y of all the suites studied, while containing higher concentrations of Cr and Ni.

As all five suites fail to plot along a single fractionation trend produced by different degrees of fractionation of a liquid (Figures 5.4a and 5.4b), it is unlikely that these suites represent rocks derived from a common mantle

**Figures 5.6a,b and c Immobile trace element variation diagrams  
(concentrations in ppm) for basaltic rocks of the East Nelson ophiolites.  
Symbols as in Figure 5.4.**







source. This suggestion is supported here through the comparison of trace element ratios as "olivine-rich" suite basalts contain markedly higher Nb/Y, Nb/Zr, and Y/Zr ratios than rocks of the other suites (Figures 5.6a,b, and c).

In lieu of the evidence presented here it is considered likely that the various suites of the East Nelson ophiolites were derived from a number of different, chemically distinct mantle sources. It should be noted here; however, that the evidence presented thus far is somewhat inconclusive and a more in depth petrogenetic evaluation of the trace element chemistry of these rocks is presented in a later section using trace element discrimination diagrams (section 5.4).

### 5.3.3 Rare Earth Elements

Averaged rare earth element (REE) contents of representative samples of the various basaltic suites are presented in Table 5.1 while chondrite normalized REE plots of these values are presented in Figure 5.7.

Representative rare earth element patterns for rocks of the various suites range from being highly light rare earth element enriched to strongly light rare earth element depleted.

Although these rocks have undergone greenschist and sub-greenschist facies metamorphism, variations in light rare earth element concentrations suggest that significant remobilization of the light rare earth elements has not taken place. This suggestion is supported by the observation within some outcrops of samples with different rare earth element compositions (light rare earth element enriched and depleted) collected within 3 metres of each other

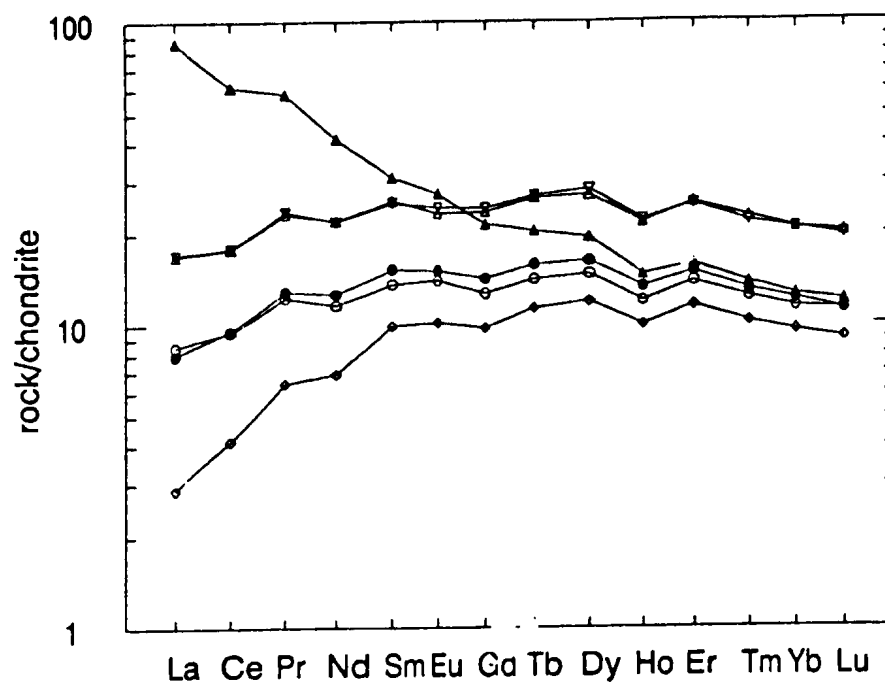
	aphyric suite	range	clinopyroxene- aphyric suite	range	"olivine-rich" suite	range	Patuki "olivine-poor" suite	range	Croisilles "olivine-poor" suite	range	plagioclase porphyritic suite	range
La	2.75	2.19-5.35	2.56	1.71-3.22	27.19	13.03-69.46	5.48	3.50-7.34	5.51	3.21-8.83	0.93	0.65-1.10
Ce	8.29	8.35-13.71	8.29	6.27-10.89	52.15	28.62-115.4	15.58	11.64-21.58	15.45	7.32-23.68	3.61	2.70-4.31
Pr	1.43	1.47-2.13	1.49	0.96-2.04	6.59	4.20-13.38	2.70	2.09-3.77	2.72	1.47-3.81	0.75	0.59-0.93
Nd	7.16	7.24-9.75	7.74	4.76-10.98	24.82	17.57-43.89	13.54	11.02-18.93	13.34	7.62-18.13	4.24	3.27-5.18
Sm	2.57	2.57-3.57	2.84	1.79-3.93	5.63	4.61-7.28	4.82	3.96-6.73	4.68	2.82-6.23	1.86	1.42-2.27
Eu	0.98	0.93-1.27	1.05	0.8-1.44	1.86	1.49-2.35	1.63	1.34-2.21	1.69	1.10-2.20	0.71	0.61-0.81
Gd	3.17	3.12-4.26	3.52	2.57-4.52	5.22	4.32-5.97	5.88	4.92-8.71	5.99	3.71-7.72	2.44	1.90-2.94
Tb	0.64	0.60-0.86	0.71	0.52-0.92	0.90	0.76-1.06	1.18	1.00-1.63	1.19	0.71-1.53	0.51	0.41-0.60
Dy	4.25	3.80-5.89	4.65	3.50-5.84	5.46	4.68-6.64	7.70	6.47-10.59	7.98	4.70-10.90	3.45	2.67-4.06
Ho	0.90	0.79-1.23	0.99	0.77-1.18	1.07	0.75-1.21	1.63	1.44-2.25	1.64	1.01-2.16	0.75	0.58-0.88
Er	2.68	2.30-3.64	2.86	2.10-3.42	2.97	1.84-3.52	4.85	4.14-6.76	4.73	1.01-5.95	2.23	1.76-2.57
Tm	0.38	0.32-0.50	0.40	0.31-0.47	0.41	0.25-0.54	0.69	0.59-0.95	0.66	0.42-0.83	0.31	0.24-0.37
Yb	2.41	2.09-3.25	2.54	1.91-2.98	2.59	1.50-3.36	4.38	3.77-6.04	4.32	2.75-5.52	2.01	1.52-2.32
Lu	0.37	0.31-0.48	0.36	0.28-0.42	0.38	0.19-0.51	0.66	0.56-0.91	0.63	0.40-0.79	0.29	0.22-0.34
# of samples	6		11		11		4		9		4	

Table 5.1 Averaged rare earth element abundances (parts per million) for basaltic suites of the East Nelson ophiolites. Values shown here are not recalculated anhydrous, although anhydrous values are plotted in Figures 5.7a and 5.7b. Number of samples averaged and ranges are indicated.

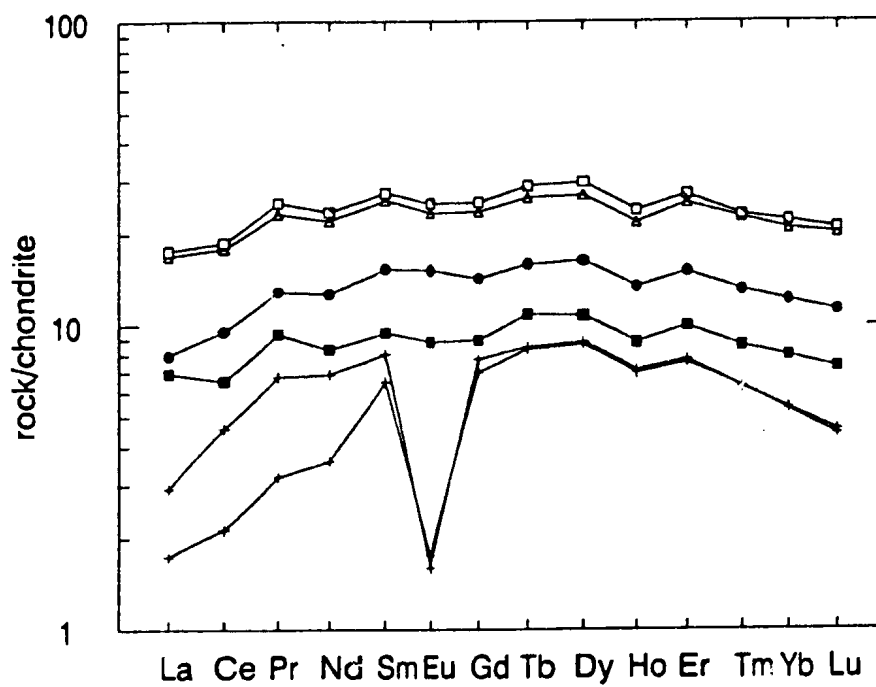
**Figure 5.7a** Chondrite normalized rare earth element patterns for average basaltic suite compositions of the East Nelson ophiolites. Data is normalized using average chondrite values of Wakita et al. (1971).

**Figure 5.7b** Chondrite normalized rare earth element patterns for altered basaltic samples of the "olivine-poor" suite (samples B-80 and B-80b) and the aphyric suite (SD-807a and SD-810). Average suite compositions are plotted for comparison.

○ aphyric    ● cpx-phyric    ▲ olv-rich    △ olv-poor(p)    ▼ olv-poor(c)    ◇ plg-phyric



● cpx-phyric    △ olv-poor(p)    □ B-80    ■ B-80b    + SD-807a    + SD-810





with no visible difference in alteration intensity observed between sample sites. Further evidence of rare earth element immobility within these rocks is provided by the observation of highly consistent rare earth element concentrations within samples of each suite, especially as some suites contain samples collected from outcrops separated by distances of 75 kilometres or more.

Although the majority of samples analyzed here appear to have been unaffected by rare earth element remobilization during alteration, a small number of intensely altered samples were found to have been affected. These samples include SD-807a, SD-810, and B-80b, each of which contains anomalously low rare earth element concentrations (Figure 5.7b). Samples SD-807a and SD-810 display well defined convex-downward patterns and strong negative Eu anomalies. Within these samples light rare earth elements were likely lost during intense chloritization while the strong Eu anomalies indicate alteration and or depletion of plagioclase. Sample B-80b is strongly silicified and contains abundant secondary quartz. The rare earth element pattern of this sample mimics the pattern of an unaltered sample from the same outcrop (B-80a); however, rare earth element abundances within the altered sample (B-80b) are noticeably lower than that observed within B-80a. It is therefore suggested that rare earth element concentrations within B-80b have been diluted by the addition of secondary silica as selective depletion of the more susceptible light rare earth elements has not taken place.

Each of the five basaltic suites of the East Nelson ophiolites display characteristic chondrite normalized rare earth element patterns; however, not

with no visible difference in alteration intensity observed between sample sites. Further evidence in support of rare earth element immobility within these rocks is provided through the observation of highly consistent rare earth element concentrations within samples of each suite, especially as some suites contain samples collected from outcrops separated by distances of 75 kilometres or more.

Although the majority of samples analyzed here appear to have been unaffected by rare earth element remobilization during alteration, a small number of intensely altered samples were found to have been affected. These samples include SD-807a, SD-810, and B-80b, each of which contains anomalously low rare earth element concentrations (Figure 5.7b). Samples SD-807a and SD-810 display well defined convex-downward patterns and strong negative Eu anomalies. Within these samples it is likely that some of the light rare earth elements were lost during intense, localized replacement of the rocks by chlorite. B-80b on the other hand, is strongly silicified and contains abundant secondary quartz. The rare earth element pattern of this sample mimics the pattern of an unaltered sample from the same outcrop (B-80a); however, rare earth element abundances within the altered sample (B-80b) are noticeably lower than that observed within B-80a. It is therefore suggested here that rare earth element concentrations within sample B-80b have been diluted by the addition of secondary silica as selective depletion of the more susceptible light rare earth elements has not taken place.

Each of the five basaltic suites of the East Nelson ophiolites display characteristic chondrite normalized rare earth element patterns; however, not

all of the suites can be discriminated on this basis as patterns for two of the Lee River Group suites (clinopyroxene-phyric and aphyric suites) appear to be identical.

Patterns for Lee River Group aphyric suite rocks are flat and slightly depleted in the light rare earth elements La and Ce except sample H-761b which is slightly light rare earth element enriched. For the most part, rocks of this suite contain 10 times average chondritic rare earth element abundances (chondritic values of Wakita et al., 1971).

Patterns for clinopyroxene-phyric suite basalts (Lee River Group) are also flat in appearance (excluding samples SD-807a and SD-810) and closely resemble patterns exhibited by aphyric suite rocks.

Patterns displayed by plagioclase porphyritic suite basalts are generally similar to those displayed by rocks of the other Lee River Group suites but are more strongly light rare earth element depleted and contain lower rare earth element abundances.

Basalts of the Patuki and Croisilles mélanges consistently contain greater rare earth element abundances than rocks of the Lee River Group. Patterns for these basalts clearly discriminate between the "olivine-poor" and "olivine-rich" basaltic suites of the mélanges.

"Olivine-poor" suite basalts display flat patterns slightly depleted in La and Ce and consistently contain greater rare earth element abundances than rocks of the Lee River Group suites (greater than 20 times chondritic concentrations).

"Olivine-rich" suite basalts, on the other hand, are strongly light rare earth element enriched and consistently contain lower heavy rare earth elements abundances (Ho to Lu) than "olivine-poor" suite rocks.

Through observation of the above rare earth element patterns it is apparent that the various basaltic suites of the East Nelson ophiolites were not derived from a common source magma.

For the most part, rocks of the Lee River Group suites (Dun Mountain Ophiolite) and "olivine-poor" suite (Patuki/Croisilles mélanges) are relatively flat and display only slight light rare earth element depletion. Of these suites; however, rocks of the plagioclase porphyritic suite (Lee River Group) are significantly more light rare earth element depleted and contain the lowest concentrations of rare earth elements of all the suites analyzed.

These patterns closely resemble rare earth element patterns displayed by mid-ocean ridge (MORB) basalts and the rocks are considered to have been produced from a mantle source similar to that which is considered to produce mid-ocean ridge basalts.

Despite close similarities of these patterns, field and petrographic evidence suggest that "olivine-poor" suite basalts of the Patuki and Croisilles mélanges and basalts of the Lee River Group suites within the Dun Mountain Ophiolite are distinct and may not represent basalts derived from a common mantle source through varying degrees of partial melting or fractionation.

"Olivine-rich" suite basalts, on the other hand, display markedly different rare earth element patterns than those exhibited by rocks of the other suites. Chondrite normalized patterns for these rocks closely resemble



those of "within-plate" and "enriched mid-ocean ridge" (E-type MORB) basalts (Saunders and Tarney, 1984) as these basalts are strongly light rare earth element enriched and slightly heavy rare earth element depleted.

#### 5.3.4 Pyroxene Chemistry

Results of electron microprobe analyses of relict clinopyroxene grains from representative thin sections of the various basaltic suites are presented in Table 5.1. In total, twenty-seven samples were analyzed including two samples from the Upukerora Formation. Unfortunately, pyroxene analyses could not be obtained from the plagioclase porphyritic suite as all primary pyroxene is replaced by metamorphic amphibole.

The majority of pyroxenes analyzed here can be classified within the pyroxene quadrilateral as Ca-rich augites (Figure 5.8); however, a small number of samples straddle the augite field boundary to plot as endiopside (2) and salite (1). In terms of end-member compositions, wollastonite, clinoenstatite, and clinoferrosilite; clinopyroxenes of the various suites show very little compositional variation and all analyses plot within a narrowly defined field on the pyroxene quadrilateral. As a result, clinopyroxene crystallization trends are not well defined for any of the suites analyzed.

In the past, previous workers have determined that chemical compositions of clinopyroxene phenocrysts and groundmass crystals are typical of the magma type from which they crystallize (Kushiro, 1960; Le Bas, 1962; Coombs, 1963). Therefore it has been suggested that relict clinopyroxene compositions can be used to determine magmatic affinities of

**Table 5.2 Average clinopyroxene analyses from basaltic rocks of the East Nelson ophiolites. Numbers in parentheses represent the number of analyses used in each average. FeO\* is total iron expressed as FeO\*. Fe\* is the sum of Fe<sup>2+</sup> and Fe<sup>3+</sup>. Suite #1 = aphyric and clinopyroxene-phyric suites; suite #2 = "olivine-poor" suite (Patuki and Croisilles mélanges); suite #3 = "olivine-rich" suite; suite #4 = Upukerora Formation.**

	37(6)	76(6)	128(7)	132C(5)	159(16)	160(14)	267(7)	290(7)	291(12)	467(14)
SiO <sub>2</sub>	51.69	46.21	48.85	51.37	50.54	48.25	50.29	50.40	50.82	50.06
TiO <sub>2</sub>	0.62	2.86	1.92	1.09	1.12	1.98	0.57	0.83	0.47	1.47
Al <sub>2</sub> O <sub>3</sub>	3.21	6.84	3.69	3.93	3.18	4.77	2.94	3.52	3.73	3.77
Cr <sub>2</sub> O <sub>3</sub>	0.43	0.14	0.11	0.69	0.10	0.18	0.00	0.06	0.10	0.14
FeO*	5.60	7.58	13.21	6.96	9.94	7.70	11.13	9.88	6.92	10.07
MnO	0.14	0.13	0.25	0.21	0.26	0.18	0.25	0.24	0.19	0.23
NiO	0.03	0.04	0.03	0.05	0.01	0.02	0.03	0.02	0.03	0.02
MgO	15.46	12.44	14.19	16.13	15.45	13.59	13.57	15.02	14.83	14.43
CaO	22.74	22.79	17.26	19.96	18.58	22.38	20.30	19.90	22.39	19.83
Na <sub>2</sub> O	0.28	0.37	0.37	0.28	0.37	0.35	0.37	0.27	0.29	0.34
K <sub>2</sub> O	0.01	-	0.05	0.04	0.03	0.01	0.02	0.01	0.01	0.01
Total	100.21	99.40	99.93	100.71	99.58	99.41	99.47	100.15	99.78	100.37

Number of ions on the basis of 6 oxygen.

Si IV	1.90	1.75	1.85	1.88	1.89	1.82	1.90	1.88	1.89	1.87
Al IV	0.10	0.25	0.15	0.12	0.11	0.18	0.10	0.12	0.11	0.13
Ti IV	0.00	0.00	0.00	0.00	0.00	0.00	0.00	0.00	0.00	0.00
Fe IV	0.00	0.00	0.00	0.00	0.00	0.00	0.00	0.00	0.00	0.00
T site	2.00	2.00	2.00	2.00	2.00	2.00	2.00	2.00	2.00	2.00
Al VI	0.04	0.05	0.01	0.05	0.03	0.03	0.03	0.04	0.05	0.03
Ti	0.02	0.08	0.05	0.03	0.03	0.06	0.02	0.02	0.01	0.04
Cr	0.01	0.00	0.00	0.02	0.00	0.01	0.00	0.00	0.00	0.00
Fe +3	0.00	0.00	0.00	0.00	0.00	0.00	0.00	0.00	0.00	0.00
Fe +2	0.17	0.24	0.42	0.21	0.31	0.24	0.35	0.31	0.22	0.31
Mn +2	0.00	0.00	0.01	0.01	0.01	0.01	0.01	0.01	0.01	0.01
Ni	0.00	0.00	0.00	0.00	0.00	0.00	0.00	0.00	0.00	0.00
Mg	0.85	0.70	0.80	0.88	0.86	0.76	0.77	0.84	0.82	0.80
Ca	0.90	0.92	0.70	0.78	0.74	0.90	0.82	0.80	0.89	0.79
Na	0.02	0.03	0.03	0.02	0.03	0.03	0.03	0.02	0.02	0.02
K	0.00	0.00	0.00	0.00	0.00	0.00	0.00	0.00	0.00	0.00
M1,M2	2.01	2.03	2.03	2.01	2.02	2.03	2.03	2.03	2.03	2.02
Mg	44.14	37.53	41.56	46.75	44.75	39.86	39.28	42.91	42.48	41.87
Fe*+Mn	9.20	13.05	22.12	11.66	16.58	12.97	18.49	16.22	11.43	16.77
Ca	46.66	49.42	36.33	41.58	38.68	47.17	42.23	40.86	46.09	41.36
Suite#	1	3	2	2	2	3	1	1	4	2

Table 5.2 (continued) Average clinopyroxene analyses from basaltic rocks of the East Nelson ophiolites. Numbers in parentheses represent the number of analyses used in each average. FeO\* is total iron expressed as FeO\*. Fe\* is the sum of Fe<sup>2+</sup> and Fe<sup>3+</sup>. Suite #1 = aphyric and clinopyroxene-phyric suites; suite #2 = "olivine-poor" suite (Patuki and Croisilles mélanges); suite #3 = "olivine-rich" suite; suite #4 = Upukerora Formation.

	525b(9)	530b(10)	702(12)	712C(8)	718A(13)	721A(14)	764(10)	767(11)	770(7)	802(1)
SiO <sub>2</sub>	52.87	53.13	50.05	50.84	50.66	49.40	52.55	51.88	50.83	50.49
TiO <sub>2</sub>	0.49	0.34	1.44	0.96	1.33	1.61	0.41	0.59	0.79	1.01
Al <sub>2</sub> O <sub>3</sub>	2.43	2.54	3.62	3.35	3.36	4.81	2.76	3.56	2.90	4.35
Cr <sub>2</sub> O <sub>3</sub>	0.35	0.34	0.13	0.20	0.13	0.15	0.09	0.39	0.02	0.17
FeO*	5.94	5.49	11.34	8.38	10.67	10.29	6.96	5.00	11.05	6.81
MnO	0.21	0.14	0.29	0.19	0.26	0.22	0.18	0.13	0.27	0.11
NiO	0.05	0.03	0.04	0.03	0.03	0.02	0.01	0.04	0.02	0.00
MgO	15.67	17.71	15.62	16.18	15.20	13.64	16.80	17.11	15.18	16.08
CaO	21.44	20.63	17.12	19.11	18.28	19.41	20.51	21.03	18.77	20.14
Na <sub>2</sub> O	0.39	0.15	0.30	0.32	0.38	0.45	0.21	0.26	0.28	0.27
K <sub>2</sub> O	0.02	0.01	0.01	0.01	0.01	0.05	0.01	0.00	0.01	0.00
Total	99.86	100.51	99.96	99.57	100.31	100.05	100.49	99.99	100.12	99.43
Number of ions on the basis of 6 oxygen.										
Si IV	1.94	1.93	1.87	1.89	1.89	1.85	1.92	1.90	1.90	1.87
Al IV	0.06	0.07	0.13	0.11	0.11	0.15	0.08	0.10	0.10	0.13
Ti IV	0.00	0.00	0.00	0.00	0.00	0.00	0.00	0.00	0.00	0.00
Fe IV	0.00	0.00	0.00	0.00	0.00	0.00	0.00	0.00	0.00	0.00
T site	2.00	2.00	2.00	2.00	2.00	2.00	2.00	2.00	2.00	2.00
Al VI	0.05	0.04	0.03	0.04	0.03	0.06	0.04	0.05	0.03	0.06
Ti	0.01	0.01	0.04	0.03	0.04	0.05	0.01	0.02	0.02	0.03
Cr	0.01	0.01	0.00	0.01	0.00	0.00	0.00	0.01	0.00	0.00
Fe +3	0.00	0.00	0.00	0.00	0.00	0.00	0.00	0.00	0.00	0.00
Fe +2	0.18	0.17	0.35	0.26	0.33	0.32	0.21	0.15	0.35	0.21
Mn +2	0.01	0.00	0.01	0.01	0.01	0.01	0.01	0.00	0.01	0.00
Ni	0.00	0.00	0.00	0.00	0.00	0.00	0.00	0.00	0.00	0.00
Mg	0.86	0.96	0.87	0.90	0.84	0.76	0.92	0.93	0.85	0.89
Ca	0.85	0.80	0.69	0.76	0.73	0.78	0.80	0.82	0.75	0.80
Na	0.03	0.01	0.02	0.02	0.03	0.03	0.01	0.02	0.02	0.02
K	0.00	0.00	0.00	0.00	0.00	0.00	0.00	0.00	0.00	0.00
M1,M2	2.00	2.01	2.02	2.02	2.02	2.01	2.01	2.01	2.02	2.01
Mg	45.38	49.61	45.34	46.60	44.09	40.73	47.26	48.74	43.34	46.69
Fe*+Mn	10.00	8.85	18.94	13.85	17.79	17.61	11.27	8.20	18.14	11.27
Ca	44.62	41.54	35.72	39.55	38.11	41.66	41.47	43.06	38.52	42.03
Suite#	1	1	2	2	2	2	2	2	1	1

Table 5.2 (continued) Average clinopyroxene analyses from basaltic rocks of the East Nelson ophiolites. Numbers in parentheses represent the number of analyses used in each average. FeO\* is total iron expressed as FeO\*. Fe\* is the sum of Fe<sup>2+</sup> and Fe<sup>3+</sup>. Suite #1 = aphyric and clinopyroxene-phyric suites; suite #2 = "olivine-poor" suite (Patuki and Croisilles mélanges); suite #3 = "olivine-rich" suite; suite #4 = Upukerora Formation.

	803(11)	809(10)	912A(7)	961d(12)	1002(5)	1005(12)	1007(10)
SiO <sub>2</sub>	52.38	51.47	51.21	52.31	50.88	51.66	51.12
TiO <sub>2</sub>	0.64	0.63	0.69	0.24	0.81	0.69	0.82
Al <sub>2</sub> O <sub>3</sub>	3.13	3.50	3.97	2.62	4.97	2.35	2.48
Cr <sub>2</sub> O <sub>3</sub>	0.19	0.13	0.07	0.09	0.38	0.04	0.04
FeO*	6.86	7.52	7.47	8.78	6.10	9.30	11.01
MnO	0.19	0.19	0.21	0.21	0.14	0.25	0.26
NiO	0.03	0.02	0.04	0.04	0.03	0.03	0.02
MgO	17.09	16.93	15.28	16.67	16.03	15.43	14.93
CaO	19.59	19.61	20.55	19.20	20.75	20.12	19.01
Na <sub>2</sub> O	0.24	0.22	0.31	0.23	0.23	0.25	0.26
K <sub>2</sub> O	0.01	0.01	0.00	0.01	0.01	0.00	0.02
Total	100.35	100.23	99.80	100.40	100.33	100.12	99.97

Number of ions on the basis of 6 oxygen.

Si IV	1.92	1.89	1.90	1.93	1.86	1.92	1.91
Al IV	0.08	0.11	0.10	0.07	0.14	0.08	0.09
Ti IV	0.00	0.00	0.00	0.00	0.00	0.00	0.00
Fe IV	0.00	0.00	0.00	0.00	0.00	0.00	0.00
T site	2.00	2.00	2.00	2.00	2.00	2.00	2.00
Al VI	0.05	0.04	0.07	0.04	0.08	0.02	0.02
Ti	0.02	0.02	0.02	0.01	0.02	0.02	0.02
Cr	0.01	0.00	0.00	0.00	0.01	0.00	0.00
Fe +3	0.00	0.00	0.00	0.00	0.00	0.00	0.00
Fe +2	0.21	0.23	0.23	0.27	0.19	0.29	0.34
Mn +2	0.01	0.01	0.01	0.01	0.00	0.01	0.01
Ni	0.00	0.00	0.00	0.00	0.00	0.00	0.00
Mg	0.93	0.93	0.84	0.92	0.88	0.86	0.83
Ca	0.77	0.77	0.81	0.76	0.81	0.80	0.76
Na	0.02	0.02	0.02	0.02	0.02	0.02	0.02
K	0.00	0.00	0.00	0.00	0.00	0.00	0.00
M1,M2	2.01	2.02	2.01	2.02	2.01	2.02	2.02
Mg	48.65	47.89	44.47	46.94	46.54	43.77	42.76
Fe*+Mn	11.26	12.24	12.54	14.20	10.17	15.20	18.11
Ca	40.08	39.87	42.99	38.86	43.30	41.02	39.13
Suite#	1	1	4	1	1	1	1



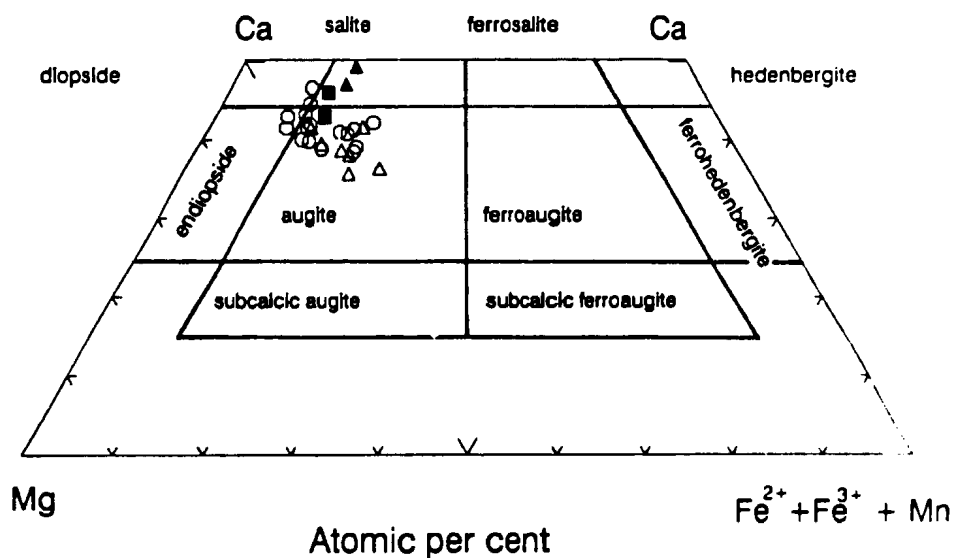


Figure 5.8 Pyroxene quadrilateral diagram of averaged clinopyroxene analysis from basaltic rocks of the East Nelson ophiolites. Field boundaries are after Poldervaart and Hess (1951). Symbols are as follows:

- aphyric and clinopyroxene-phyric suites
- △ "olivine-poor" suite
- ▲ "olivine-rich" suite
- Upukerora Formation

altered basaltic rocks in which whole rock analyses may be unreliable (eg., Vallance, 1969; Nisbet and Pearce, 1977). Nisbet and Pearce (1977) have also been able to classify basaltic rocks on the basis of relict clinopyroxene compositions into: ocean floor basalts, volcanic arc basalts, within-plate tholeiites, and within-plate alkali basalts. More recently, Leterrier et al. (1982) and Beccaluva et al. (1989) have classified ophiolitic lavas in terms of magma types and original tectonic setting using discrimination diagrams based on relict augitic clinopyroxene compositions. In this section, basaltic rocks of the East Nelson ophiolites are discriminated using relict clinopyroxene compositions and an attempt is made to suggest magmatic affinities and original tectonic settings of formation for the various basaltic suites.

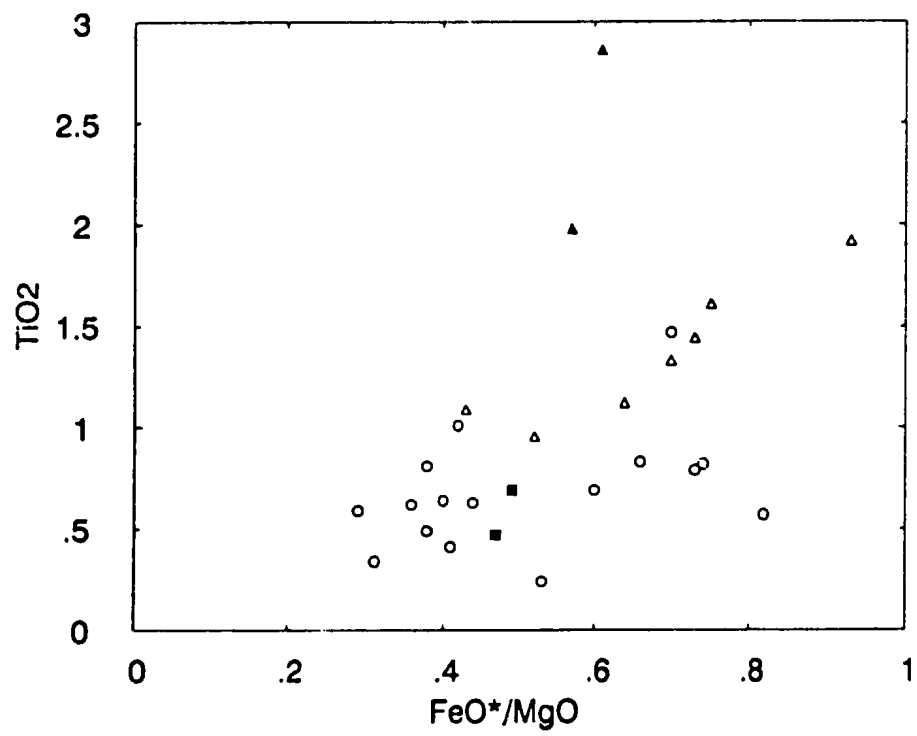
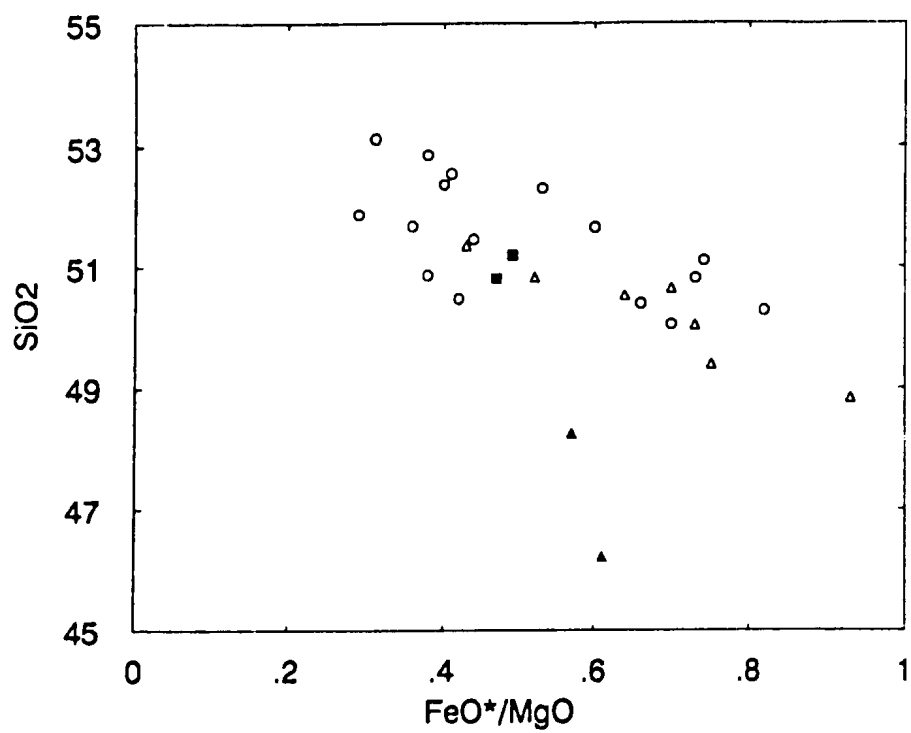
Despite some overlap, clinopyroxenes from the various suites can be partially discriminated through the use of variation diagrams involving the elements  $\text{TiO}_2$ ,  $\text{SiO}_2$ ,  $\text{Al}_2\text{O}_3$ , and the ratio  $\text{FeO}^*/\text{MgO}$ .

In Figure 5.9a it can be observed that clinopyroxenes of the "olivine-rich" suite contain markedly lower  $\text{SiO}_2$  concentrations than pyroxenes of other suites. On this diagram clinopyroxenes of the "olivine-poor" suite, Dun Mountain Ophiolite suites, and the Upukerora Formation contain similar concentrations of  $\text{SiO}_2$  and  $\text{FeO}^*/\text{MgO}$  whereby  $\text{SiO}_2$  values tend to increase with decreasing  $\text{FeO}^*/\text{MgO}$ .

Figure 5.9b, however, shows pyroxenes of the "olivine-rich" suite to be characterized by anomalously high concentrations of  $\text{TiO}_2$  while pyroxenes of the "olivine-poor" suite contain slightly higher  $\text{TiO}_2$  concentrations than pyroxenes of the Upukerora Formation and the Lee River Group's suites.

**Figure 5.9a**  $\text{SiO}_2$  versus  $\text{FeO}^*/\text{MgO}$  (weight percent) plot of pyroxenes from various basaltic suites of the East Nelson ophiolites. Symbols as in Figure 5.8.

**Figure 5.9b**  $\text{TiO}_2$  versus  $\text{FeO}^*/\text{MgO}$  (weight percent) plot of pyroxenes from various basaltic suites of the East Nelson ophiolites. Symbols as in Figure 5.8.





From this figure it can be seen that pyroxenes of the Lee River Group suites show very little variation in  $\text{TiO}_2$  concentrations with increasing  $\text{FeO}^*/\text{MgO}$  while pyroxenes of the "olivine-poor" suite plot along a positive sloping trend in which  $\text{TiO}_2$  concentrations increase with increasing  $\text{FeO}^*/\text{MgO}$ .

Figures 5.10a and 5.10b also discriminate between pyroxenes of the various basaltic suites. On Figure 5.10a "olivine-rich" suite pyroxenes are characterized by low  $\text{MgO}$  and high  $\text{Al}_2\text{O}_3$  concentrations while pyroxenes of the "olivine-poor" suite generally contain slightly higher concentrations of  $\text{Al}_2\text{O}_3$  and  $\text{TiO}_2$  than those of the Upukerora Formation<sup>2</sup> and Lee River Group suites (Figure 5.10b).

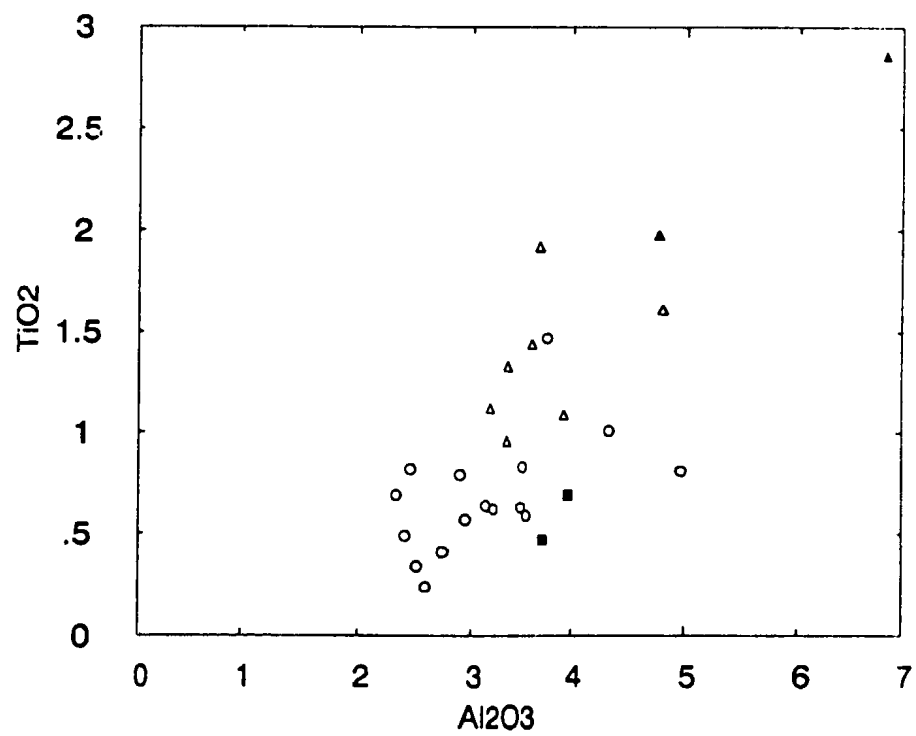
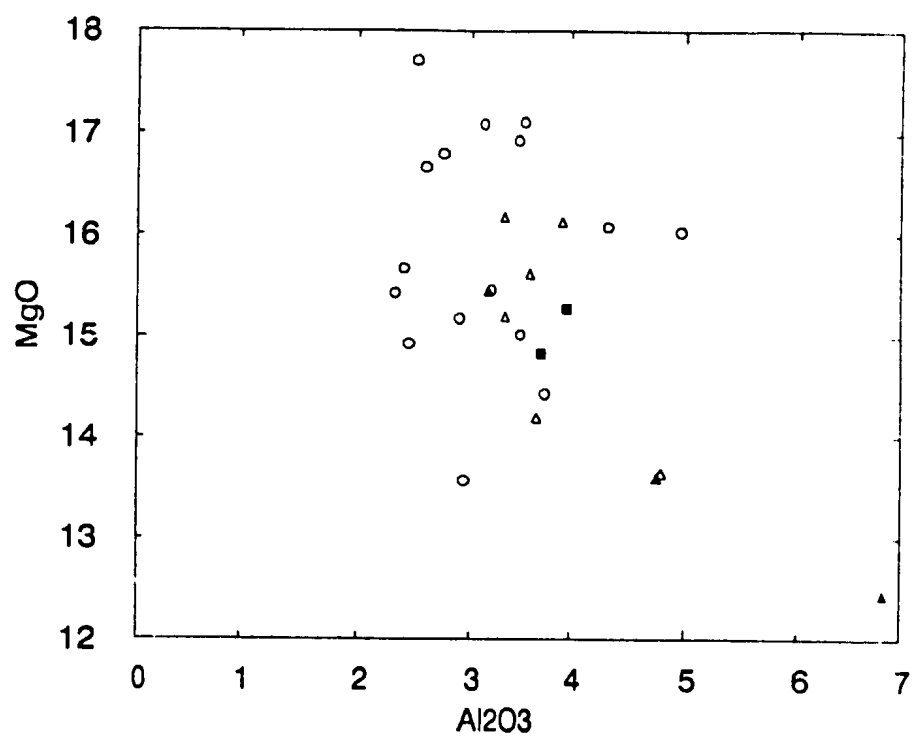
Through comparison of concentrations of the elements discussed above, pyroxenes from the different suites of the East Nelson ophiolites can be compared. Pyroxenes of the Lee River Group suites (aphyric and clinopyroxene-phyric suites) and the Upukerora Formation are indistinguishable from one another and therefore provide further evidence that the clinopyroxene-phyric and aphyric suites of the Lee River Group are compositionally identical to each other while also suggesting that the Upukerora Formation is likely composed of material eroded off the underlying Dun Mountain Ophiolite. Pyroxenes of the "olivine-poor" suite are compositionally quite similar to those analyzed from the Lee River Group suites; however, these pyroxenes typically contain higher concentrations of

---

<sup>2</sup> Although pyroxene compositions from the Upukerora Formation contain similar aluminium concentrations to those of the "olivine poor" suite, it is possible that Upukerora pyroxenes have been partially altered to chlorite.

**Figure 5.10a** MgO versus  $\text{Al}_2\text{O}_3$  (weight percent) plot for pyroxenes of the various basaltic suites of the East Nelson ophiolites. Symbols as used in Figure 5.8.

**Figure 5.10b**  $\text{TiO}_2$  versus  $\text{Al}_2\text{O}_3$  (weight percent) plot for pyroxenes of the various basaltic suites of the East Nelson ophiolites. Symbols as used in Figure 5.8.



$\text{Al}_2\text{O}_3$  and  $\text{TiO}_2$  than pyroxenes of similar  $\text{FeO}^*/\text{MgO}$  values from rocks of the Lee River Group suites. Fractionation trends suggest that fractionation proceeded along different paths than experienced by Lee River Group rocks whereby  $\text{TiO}_2$  concentrations tend to increase with higher degrees of fractionation within the "olivine-poor" suite while  $\text{TiO}_2$  concentrations within Lee River Group pyroxenes show little variation.

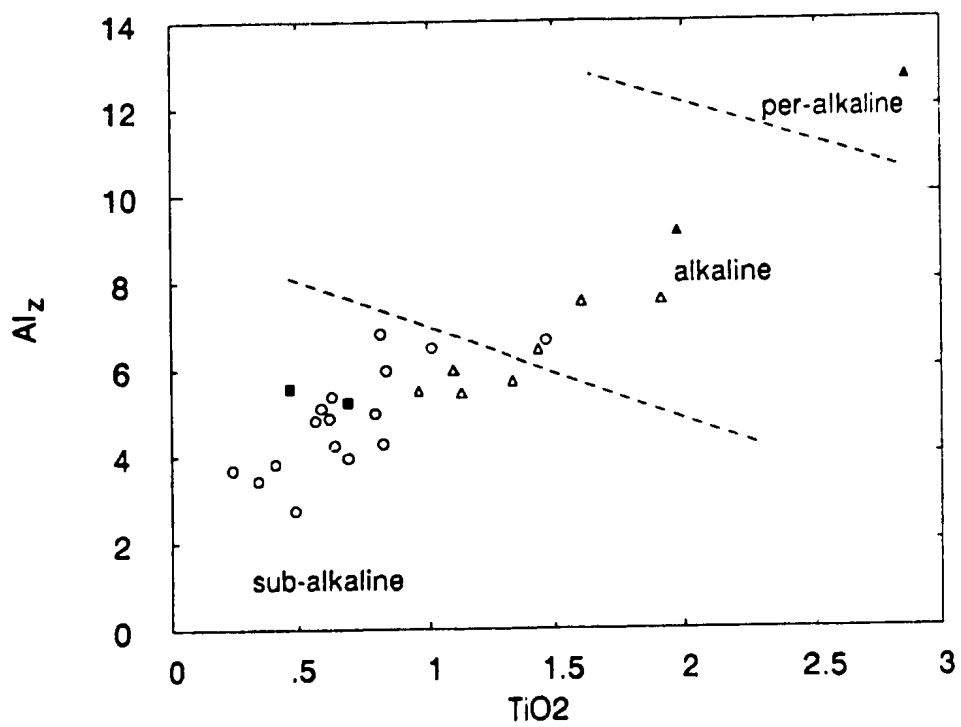
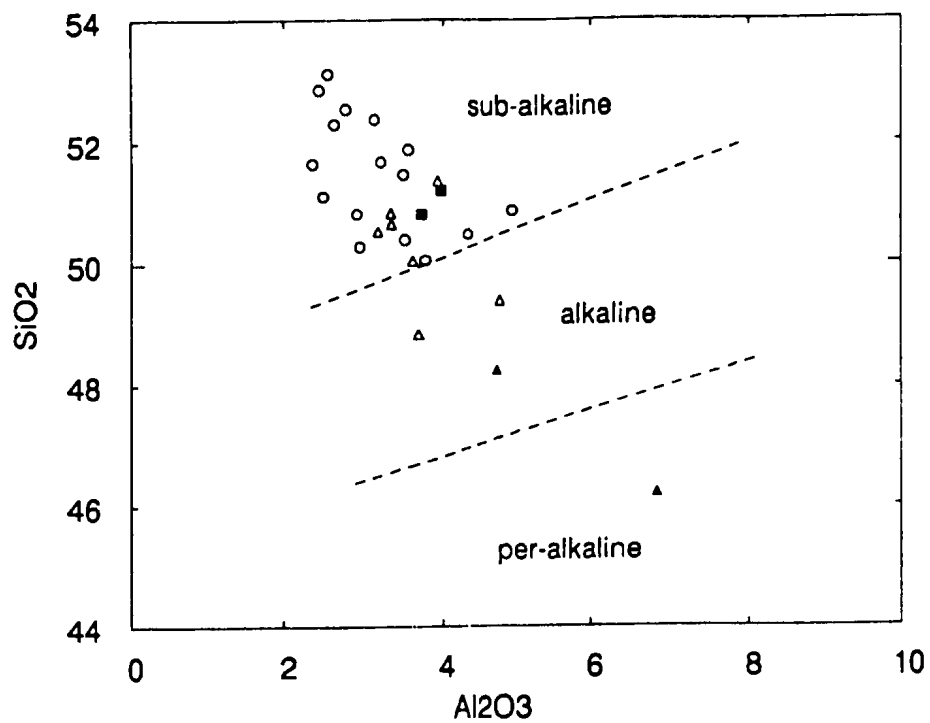
"Olivine-rich" suite pyroxenes are compositionally quite distinct from pyroxenes of other suites and are characterized by higher concentrations of  $\text{TiO}_2$  and  $\text{Al}_2\text{O}_3$  and lower  $\text{SiO}_2$  concentrations. Although the number of analyses obtained for pyroxenes of this suite are too limited to produce well defined fractionation trends it is obvious that these pyroxene compositions lie off trends defined by pyroxenes of other suites. It is therefore considered here that this suite was derived from a fundamentally different source magma composition.

Through comparison of the above pyroxene compositions to those of known magmatic affinity, Le Bas (1962) was able to discriminate between basalts of different alkalinity. To do this he defined compositional fields on variation diagrams involving the elements  $\text{SiO}_2$ ,  $\text{Al}_2\text{O}_3$ , elemental Al, and  $\text{TiO}_2$ . On these diagrams (Figures 5.11a and 5.11b) it is evident that pyroxenes of the "olivine-poor" suite, Upukerora Formation, and Lee River Group suites are similar to those which occur within sub-alkaline igneous rocks. Pyroxenes of the "olivine-rich" suite, on the other hand, contain low  $\text{SiO}_2$  and high  $\text{TiO}_2$  concentrations and are therefore compositionally similar to those observed within more alkaline rocks.



**Figure 5.11a**  $\text{SiO}_2$  versus  $\text{Al}_2\text{O}_3$  (weight percent) plot for pyroxenes of the various basaltic suites of the East Nelson ophiolites. Compositional boundaries as defined by Le Bas (1962). Symbols as used in Figure 5.8.

**Figure 5.11b**  $\text{Al}_2$  (total aluminum ions on the basis of 6 oxygen) versus  $\text{TiO}_2$  (weight percent) plot for pyroxenes of the various basaltic suites of the East Nelson ophiolites. Compositional boundaries as defined by Le Bas (1962). Symbols as used in Figure 5.8.



Leterrier et al. (1982) uses discrimination diagrams involving Ti, Cr, Ca, Al, and Na contents to discriminate between basalts of three major basaltic types. These types are: "the alkali basalt group" (including alkali basalts, basanites and related rocks from oceanic or continental intra-plate and island-arc volcanism), "tholeiites from spreading zones" (including tholeiites and transitional basalts from ridges, ocean basins, oceanic islands, back-arc basins and passive continental margins), and "orogenic-type basalts" (including island-arc tholeiites, calc-alkali basalts from active continental margins and island-arcs, and shoshonitic lavas). On these diagrams, despite considerable overlap, Leterrier et al. (1982) were able to classify basalts of these types with a level of confidence of near or better than 80 percent.

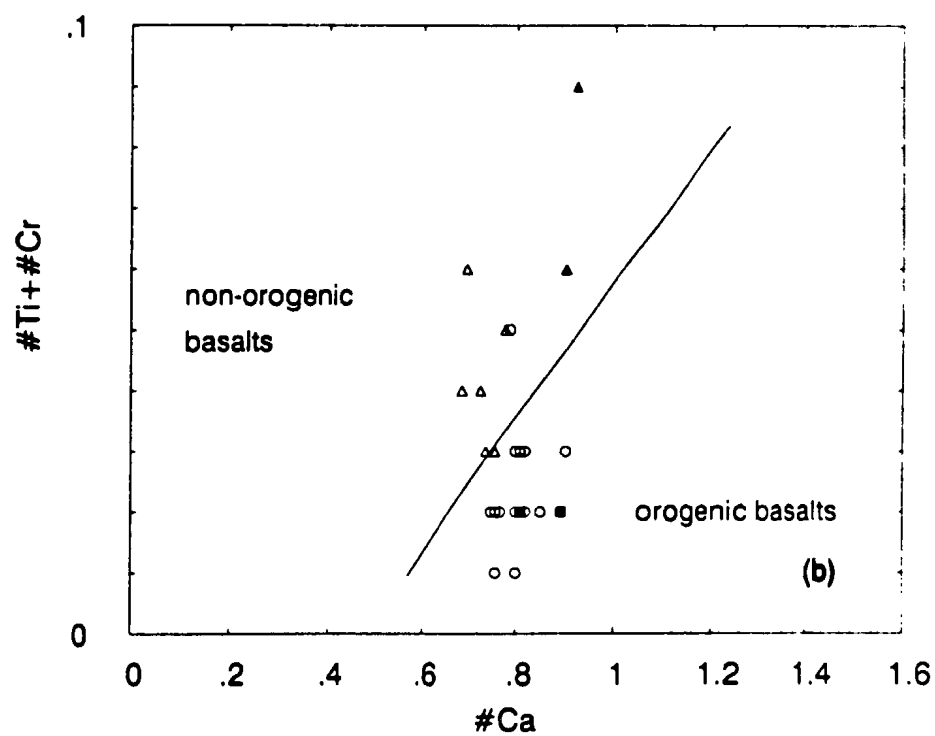
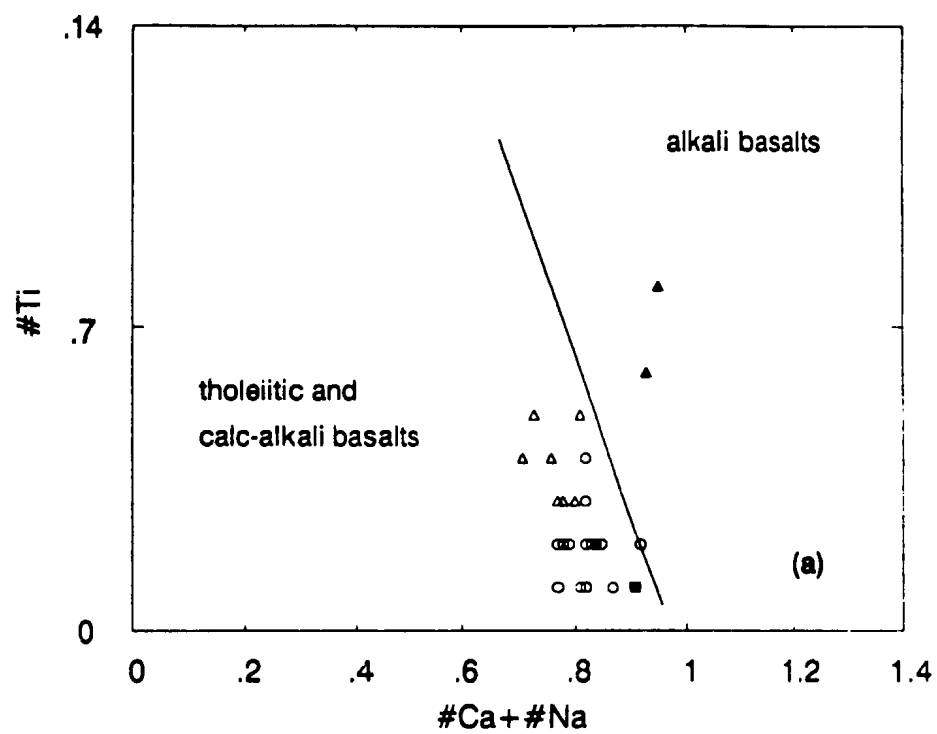
Using the diagrams of Leterrier et al. (Figures 5.12a,b and c), basaltic rocks of the East Nelson ophiolites were found to include alkali and tholeiitic (and/or calc-alkali) basalts, whereby basalts of the "olivine-rich" suite are alkalic and rocks of the other suites (including the Upukerora Formation) have tholeiitic or possibly calc-alkali affinities<sup>3</sup>. From Figure 5.12b basalts of the various suites were also classified into orogenic and non-orogenic basalts whereby basalts of the ophiolitic mélanges (Patuki and Croisilles mélanges) plot as non-orogenic basalts while basalts of the Lee River Group suites and Upukerora formation plot as orogenic-type basalts.

---

<sup>3</sup> Although most pyroxenes of the Lee River Group suites plot as calc-alkali basalts on figure 5.12c most of the analyses straddle the calc-alkali-tholeiitic basalt boundary and thus no definitive identification can be proposed.

Figure 5.12a,b and c Discriminant diagrams of Leterrier et al. (1982) for determining the tectonic character of host volcanic rocks based on cationic proportions within clinopyroxenes. Symbols as used in Figure 5.8. "#"= number of ions on the basis of 6 oxygen.





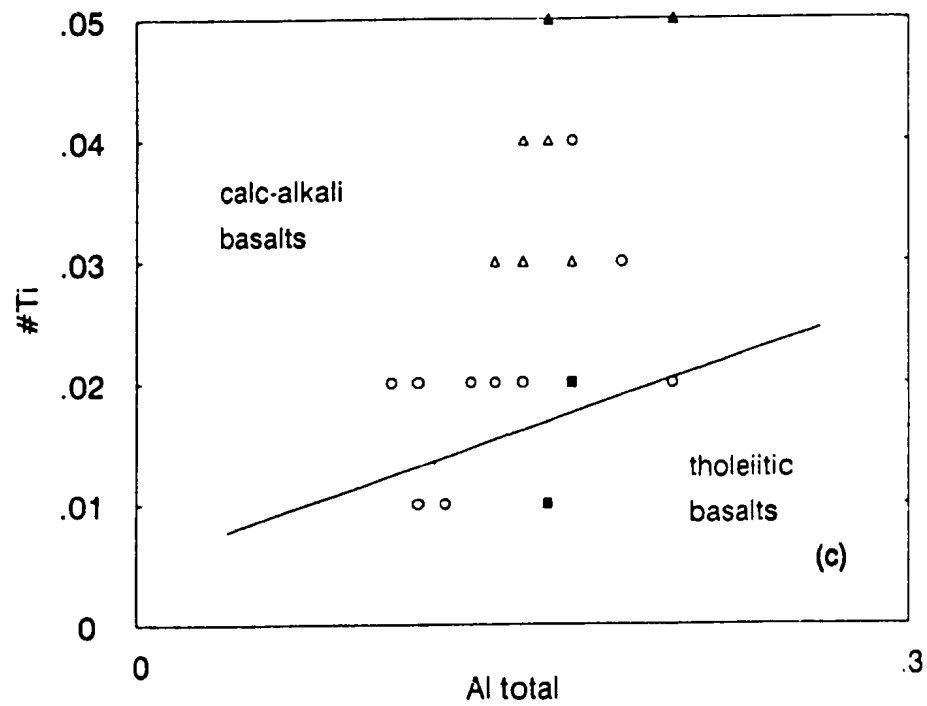
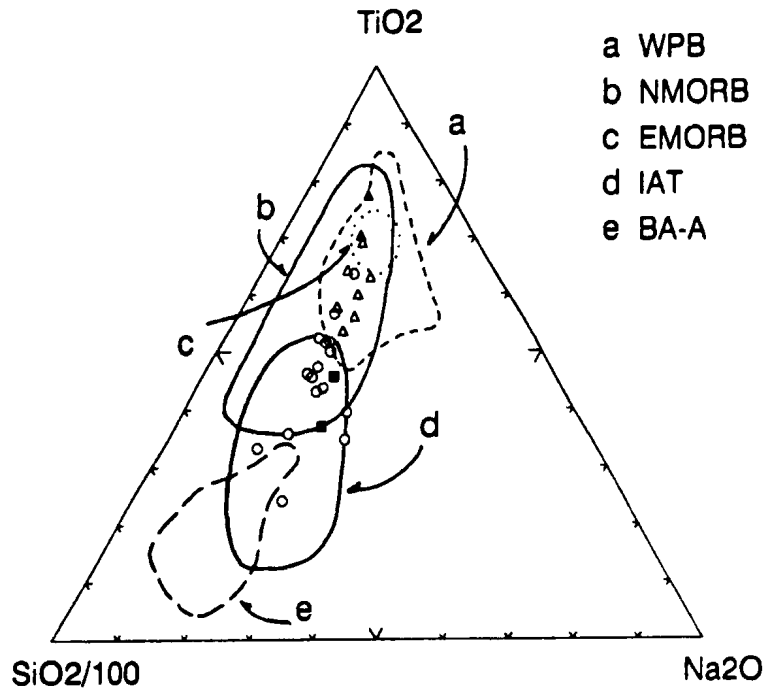


Figure 5.12 (continued) Ti versus Al discrimination diagram of Leterrier et al. (1982).

The discrimination diagrams of Leterrier et al. (1982) suggest that "olivine-rich" and "olivine-poor" suite basalts of the Patuki and Croisilles mélanges represent alkali and tholeiitic basalts produced within a non-orogenic environment. This implies that these suites were produced at oceanic islands and MORB-like spreading ridges analogous to that which produce within-plate alkali basalts and mid-ocean ridge tholeiitic basalts respectively. Analyses of pyroxenes from the Lee River Group and Upukerora Formation; however, plot within the orogenic basalt field (Figure 5.12b) and were likely produced within an arc-related, or possibly supra-subduction zone environment.

Beccaluva et al. (1989) have recently used relict clinopyroxene compositions to discriminate between different suites of metabasalt in Phanerozoic ophiolites. By their method, variation diagrams involving the elements Si, Al, Ti, Na, and Al(iv) are plotted and compositional fields are defined on the basis of augitic pyroxenes from present day oceanic settings.

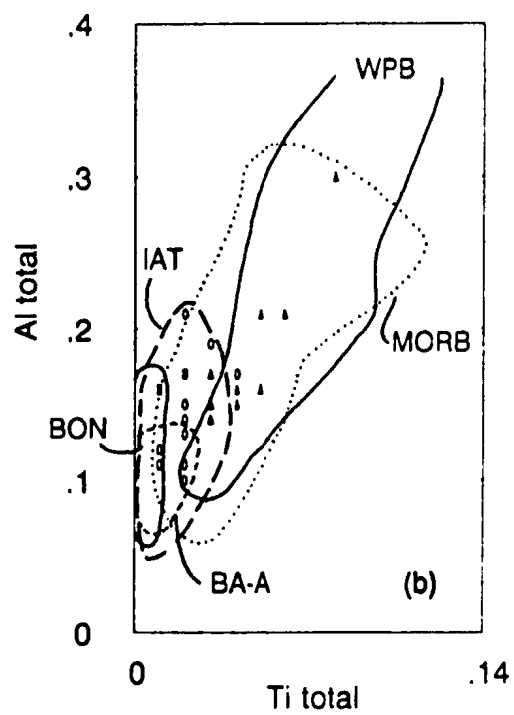
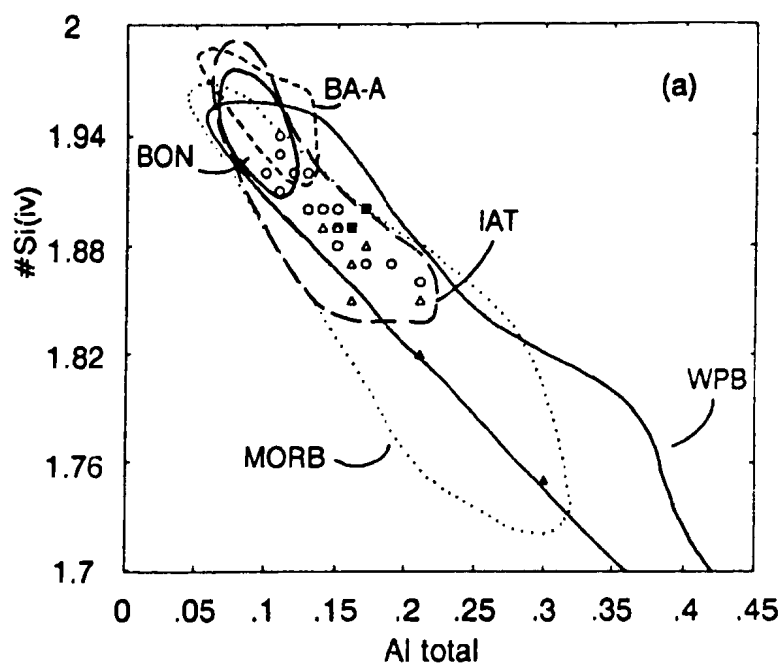
On these diagrams (Figures 5.13 and 5.14a,b,c and d) pyroxenes of the Lee River Group suites and Upukerora Formation consistently plot as island-arc tholeiites while "olivine-poor" suite basalts typically plot as mid-ocean ridge basalts (MORB). Although only two analyses of "olivine-rich" suite pyroxenes are available, these samples tend to plot as mid-ocean ridge and/or within-plate basalts and are compositionally quite distinct from subduction related basalts (ie. island-arc tholeiites; boninites; and quartz tholeiites, basaltic andesites, and andesites from intra-oceanic fore-arc regions). As the previously mentioned diagrams of Leterrier et al. (Figure



**Figure 5.13** Tectonic discrimination diagram of Beccaluva et al. (1989). This diagram discriminates between calcic pyroxenes of basalts from different ophiolite types and present day oceanic settings. Symbols as in Figure 5.8. WPB= within-plate basalts; NMORB= normal mid-ocean ridge basalts; EMORB= enriched mid-ocean ridge basalts; IAT= island-arc tholeiitic basalts; BA-A= quartz tholeiites, basaltic andesites and andesites from intra-oceanic fore-arc settings. Oxides are in weight percent.



Figures 5.14a,b,c and d Tectonic discrimination diagrams of Beccaluva et al. (1989). These diagrams discriminate between calcic pyroxenes of basalts from different ophiolite types and present day oceanic settings. Symbols as in Figure 5.8. WPB= within-plate basalts; NMORB= normal mid-ocean ridge basalts; EMORB= enriched mid-ocean ridge basalts; IAT= island-arc tholeiitic basalts; BA-A= quartz tholeiites, basaltic andesites and andesites from intra-oceanic fore-arc settings; BON= boninitic basalts.  $^{iv}\text{Si}$ = number of Si ions tetrahedrally coordinated. Al total= total number of aluminum ions on the basis of 6 oxygen. Ti total= total number of titanium ions on the basis of 6 oxygen. Al(iv)= number of Si ions tetrahedrally coordinated.



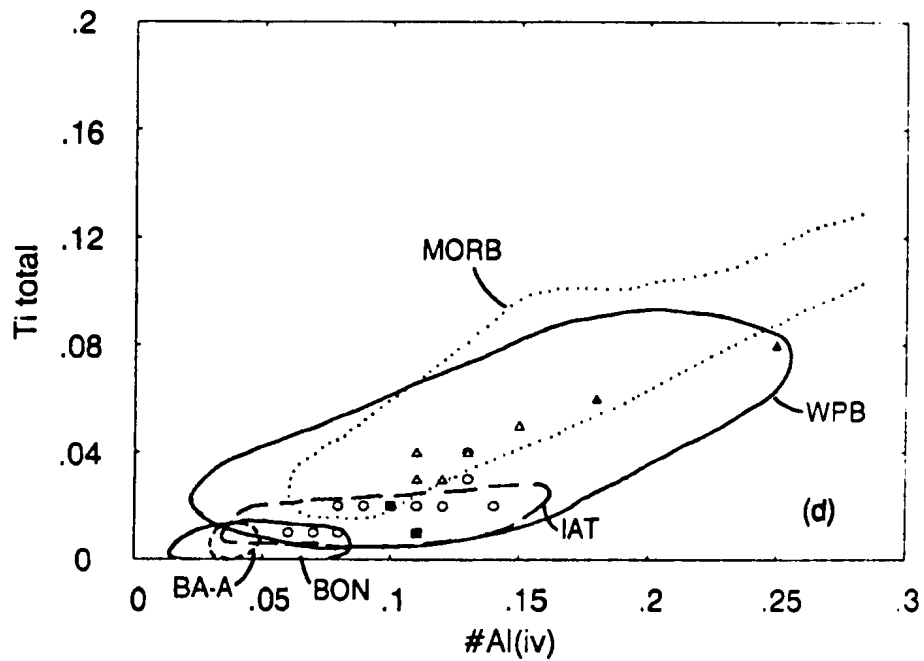
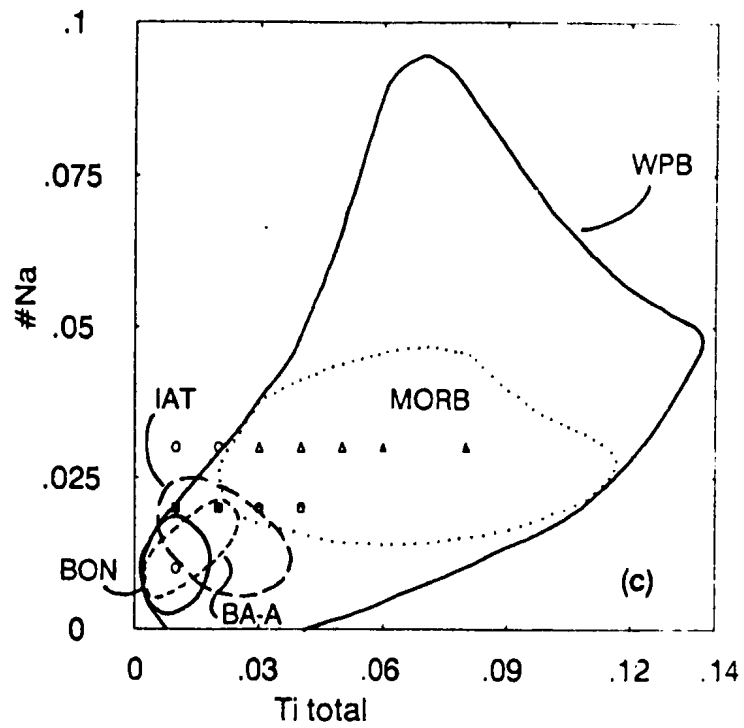


Figure 5.14 (continued) Tectonic discrimination diagrams of Beccaluva et al. (1989).

5.12a) and Le Bas (Figures 5.11a and 5.11b) classify these rocks as having an alkaline affinity, it is suggested here that "olivine-rich" suite basalts represent within-plate alkali basalts as opposed to mid-ocean ridge tholeiitic basalts. This suggestion is also supported by the discrimination diagram of Nisbet and Pearce (1977) (ternary plot of  $\text{MnO-TiO}_2\text{-Na}_2\text{O}$  concentrations within augitic pyroxenes) whereby "olivine-rich" suite basalts plot within the within-plate alkali basalt field (Figure 5.15).

Through examination of relict pyroxene compositions, basaltic rocks of the Dun Mountain Ophiolite can be classified as follows. Basalts of the "olivine-poor" suite are representative of typical mid-ocean ridge basalts (MORB); "olivine-rich" suite rocks resemble alkaline basalts produced at within-plate ocean islands; and, basalts of the Lee River Group aphyric and clinopyroxene-phyric suites are representative of orogenic basalts of island-arc tholeiite affinity. Compositional similarities displayed between Lee River Group and Upukerora Formation pyroxenes also suggest that the mafic basaltic component of the Upukerora conglomerate is composed of eroded material derived from the underlying Dun Mountain Ophiolite (Lee River Group).

### 5.3.5 Geochemical Discrimination Diagrams

In this section, a number of commonly used trace element discrimination plots are used to discriminate between different basaltic suites of the East Nelson ophiolites and define tectonic environments of formation.



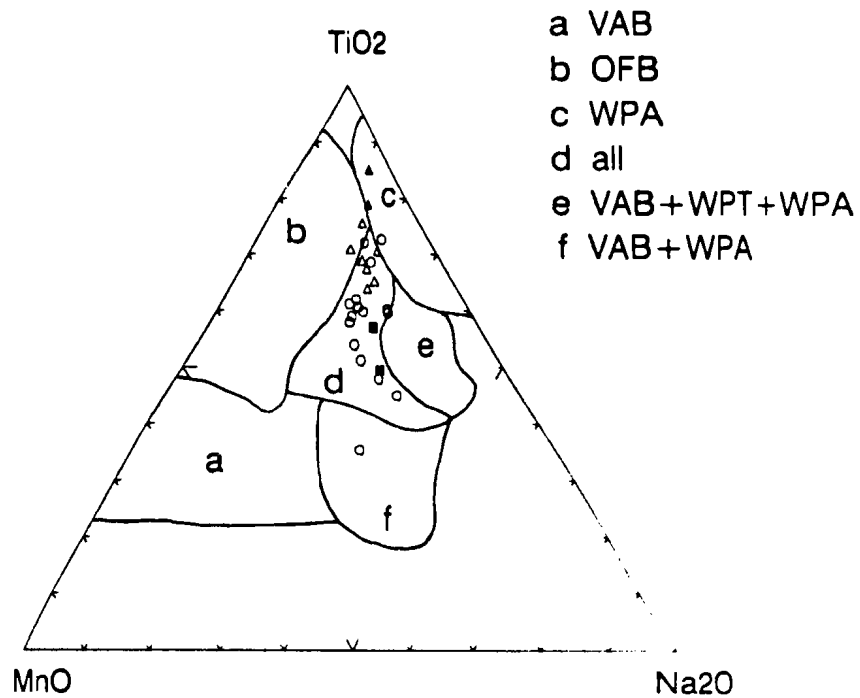


Figure 5.15 Tectonic discrimination diagram of Pearce and Nisbet (1977). Tectonic settings are discriminated using weight percent oxide contents of pyroxenes. Symbols as in Figure 5.8. VAB= volcanic arc basalts; OFB= ocean floor basalts; WPA= within-plate alkali basalts; WPT= within-plate tholeiitic basalts.

Through observation of the data presented thus far it is apparent that basaltic rocks of the various suites of the East Nelson ophiolites were likely produced within a range of tectonic environments including: mid-ocean ridges and oceanic islands ("olivine-rich" and "olivine-poor" suites respectively), and above a subduction zone (Lee River Group suites). Within supra-subduction zone environments and island-arcs, both tholeiitic and calc-alkaline series basalts are commonly observed, whereby tholeiitic series lavas are typically associated with early stages of arc evolution and late stages of arc rifting (eg. Miyashiro, 1974). Basalts of these different series can be discriminated using a number of diagrams; however, all rely on the observation of differing fractionation trends exhibited by these rock series. Calc-alkaline series rocks are characterized by depletions in iron ( $\text{FeO}^*$ ) and titanium ( $\text{TiO}_2$ ) while tholeiitic rocks typically display enrichment of these elements during the early and middle stages of fractional crystallization.

Through observation of Figures 5.16a and 5.16b (after Miyashiro, 1974) it can be observed that all sub-alkaline basaltic suites (as previously defined by pyroxene compositions) of the East Nelson ophiolites exhibit tholeiitic fractionation trends whereby  $\text{FeO}^*$  and  $\text{TiO}_2$  concentrations increase with increased degrees of fractionation. Basalts of the alkaline "olivine-rich" suite; however, show little variation in the concentrations of these oxides with varying degrees of fractionation.

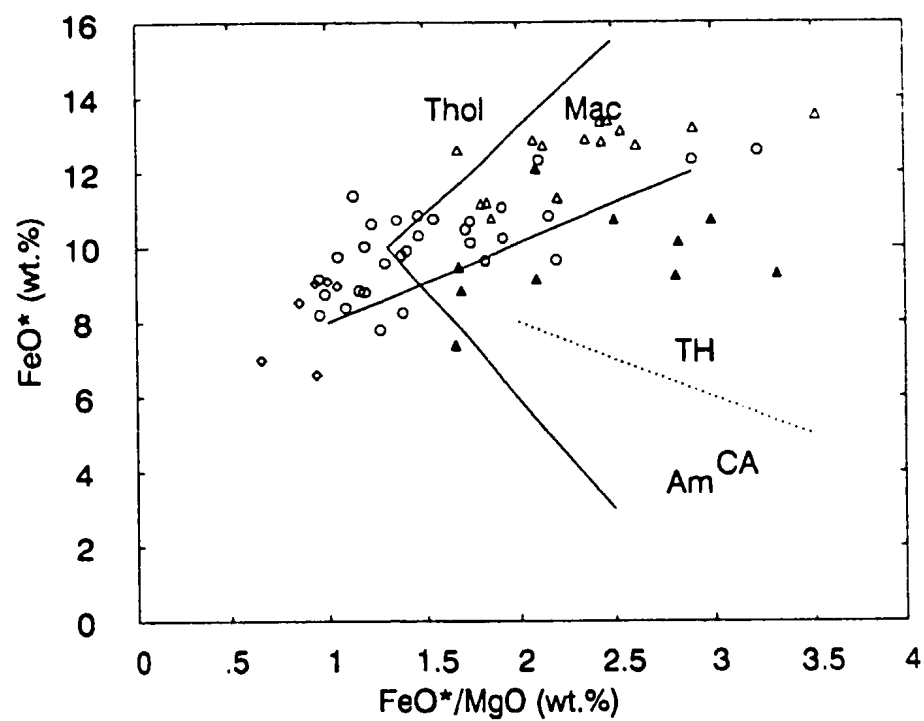
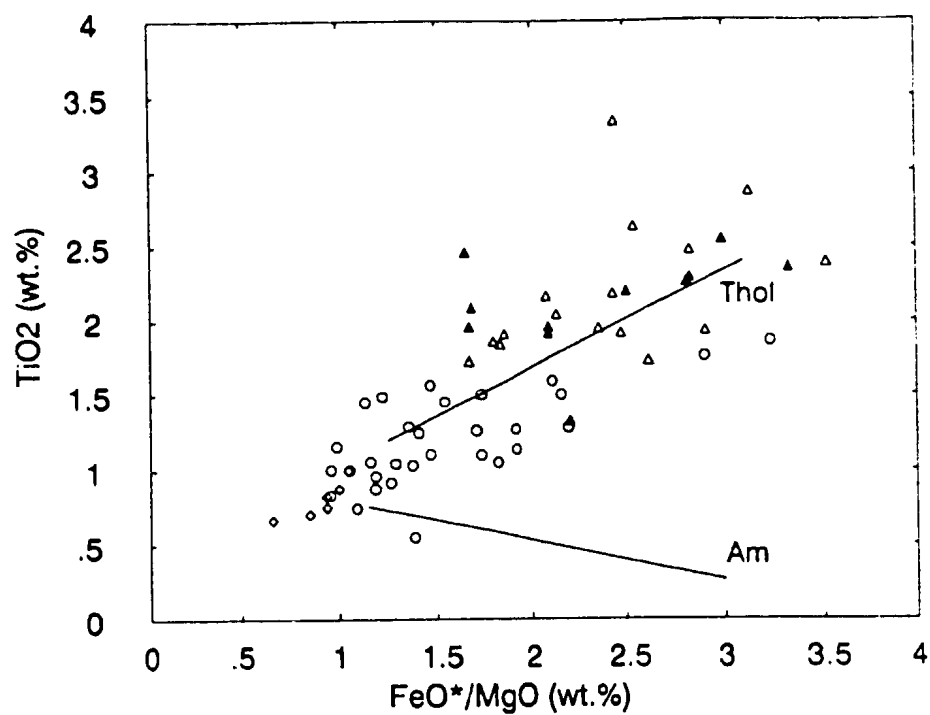
Another diagram which relies on these less mobile elements (and  $\text{Al}_2\text{O}_3$ ) and discriminates between calc-alkaline and tholeiitic series lavas is that of Jensen (1976). On this diagram, Figure 5.17, basalts of the various

**Figure 5.16a** Plot of  $\text{TiO}_2$  versus  $\text{FeO}^*/\text{MgO}$  for basaltic rocks of the East Nelson ophiolites. Fractionation trends have been drawn for comparison after Miyashiro (1973); Thol= estimated tholeiitic fractionation trend; Am= estimated calc-alkali fractionation trend from Amagi.

**Symbols:**

- aphyric/clinopyroxene-phyric suite basalts
- plagioclase porphyritic basalts
- △ "olivine-poor" suite basalts
- ▲ "olivine-rich" suite basalts

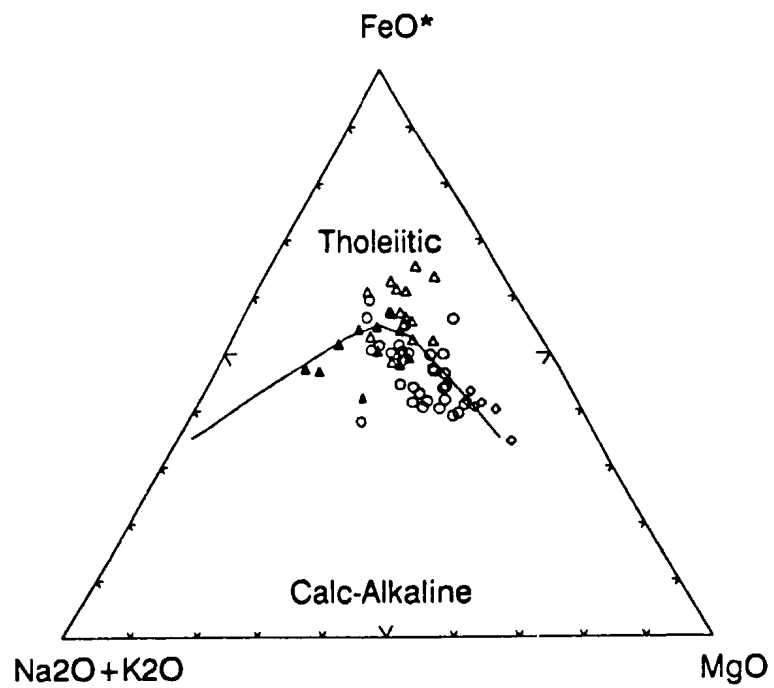
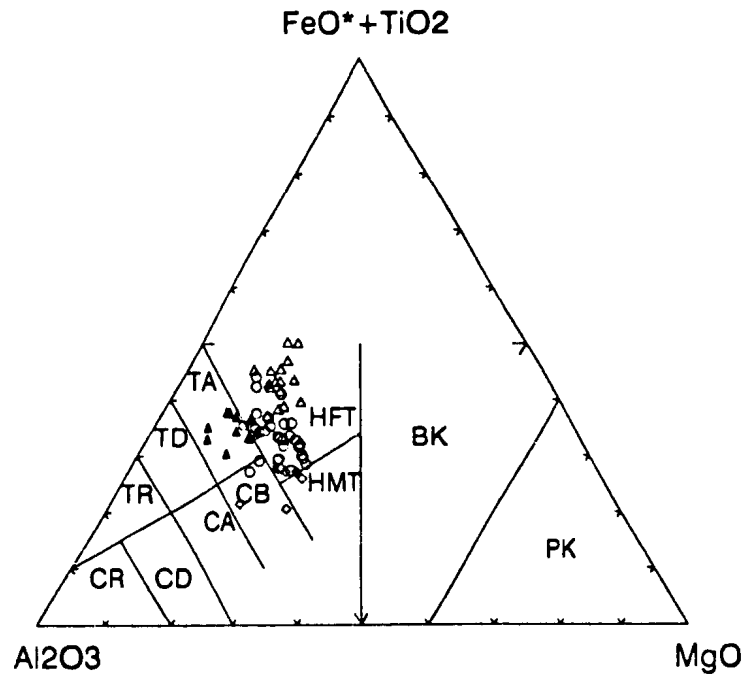
**Figure 5.16b** Plot of  $\text{FeO}^*$  versus  $\text{FeO}^*/\text{MgO}$  for basaltic rocks of the East Nelson ophiolites. Fractionation trends have been drawn for comparison after Miyashiro (1973); Thol= estimated tholeiitic fractionation trend (Skaergaard); Am= estimated calc-alkali fractionation trend from Amagi; Mac= Macauley. Th/Ca= tholeiitic/calc-alkali compositional boundary. Symbols as in Figure 5.16a.





**Figure 5.17** Basaltic discrimination diagram after Jensen (1976). Fields: PK= picritic komatiite; BK= basaltic komatiite; HFT= high iron tholeiite; TA= tholeiitic andesite; TD= tholeiitic dacite; TH= tholeiitic rhyolite; HMT= high magnesium tholeiite; CB= calc-alkali basalt; CA= calc-alkali andesite; CD= calc-alkali dacite; CR= calc-alkali rhyolite. Symbols as used in Figure 5.16. Oxides in weight percent.

**Figure 5.18** AFM plot of basaltic rocks of the East Nelson ophiolites.  $\text{FeO}^*$  = total iron expressed as FeO. Tholeiitic/calc-alkali dividing line from Irvine and Baragar (1971). Symbols as used in Figure 5.16. Oxides in weight percent.



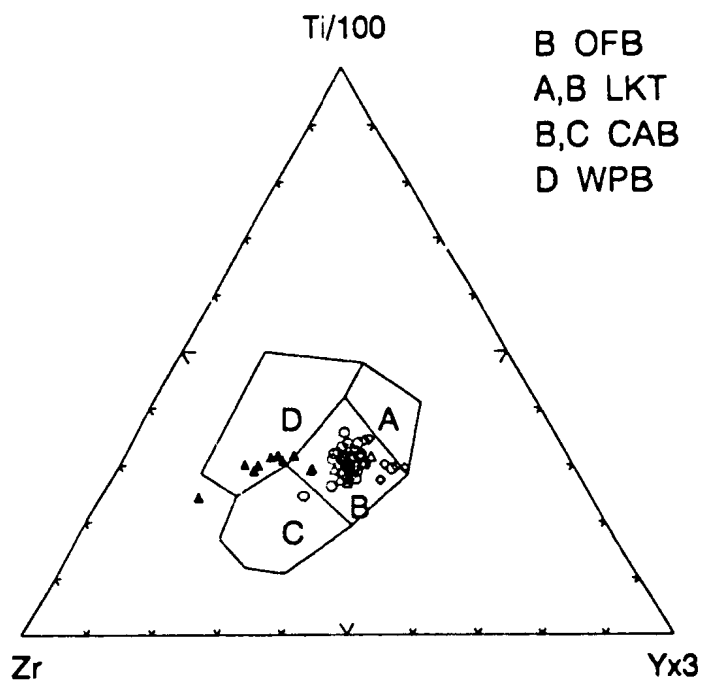
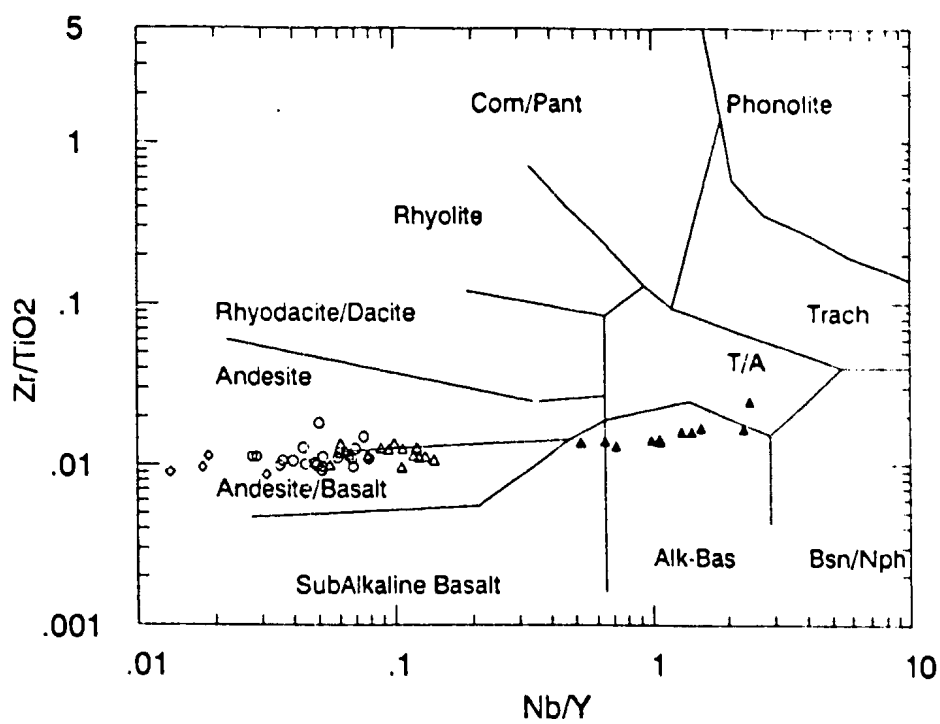
suites of the East Nelson ophiolites plot almost entirely in the "high iron tholeiitic basalt" field while only a small number of plagioclase porphyritic suite rocks plot within the "calc-alkaline basalt" field. Although these anomalous samples indicate rocks of the plagioclase porphyritic suite may be of calc-alkaline affinity, the well defined  $\text{TiO}_2$  enrichment trend displayed by these rocks in Figure 5.16a shows them to actually be tholeiitic in character. It should also be noted here that although  $\text{K}_2\text{O}$  and  $\text{Na}_2\text{O}$  are considered to have been mobilized during alteration, most samples from the various sub-alkaline suites still plot along a tholeiitic fractionation trend on a  $(\text{Na}_2\text{O}+\text{K}_2\text{O}-\text{FeO}^{\cdot}-\text{MgO})$  triangular diagram (Figure 5.18) as  $\text{FeO}^{\cdot}/\text{MgO}$  ratios are virtually unaffected by alkali element concentrations.

In the previous section, discrimination diagrams that rely on relict pyroxene compositions were presented. From these diagrams (eg., Figures 5.11a, 5.11b, 5.12a, 5.15) it is suggested that basalts of the "olivine-rich" suite are alkaline in character while rocks of the other suites are sub-alkaline. Discrimination between different rock series by this method is found to agree well with whole rock compositions plotted on the  $\text{Zr}/\text{TiO}_2$ -Nb/Y diagram of Winchester and Floyd (1977). This diagram (Figure 5.19) discriminates between various types of common volcanic rocks on the basis of immobile trace elements whereby the  $\text{Zr}/\text{TiO}_2$  ratio acts as a differentiation index while the Nb/Y ratio acts as an alkalinity index. The "olivine-rich" suite basalts plot predominantly within the "alkaline basalt" field while 95 percent of the basalts from the other suites plot in the sub-alkaline "andesite/basalt" field.

**Figure 5.19**  $\text{Zr/TiO}_2$  versus  $\text{Log Nb/Y}$  (ppm) discrimination diagram of Winchester and Floyd (1977). Symbols as used in Figure 5.16.

**Figure 5.20** Basalt tectonic discrimination diagram of Pearce and Cann (1973). Symbols as used in Figure 5.16. Concentrations are in (ppm).





The remaining discrimination diagrams are dedicated to discriminating between tectonic environments of formation for each of the basaltic suites of the East Nelson ophiolites. On these diagrams, rocks of the clinopyroxene-phyric and aphyric suites are plotted as one suite as they have been found to be compositionally indistinguishable and therefore likely represent variably metamorphosed equivalents of a single petrographic suite. Strongly altered samples previously shown to have been compositionally affected by alteration processes as indicated by rare earth element compositions and petrography are not plotted (ie. SD-807a, SD-810, B-80b, and D-1003).

Two "immobile trace element" discrimination diagrams commonly used to determine tectonic environments of formation are the Zr-Ti-Y triangular diagram and log Zr/Y-log Zr diagram of Pearce and Cann (1973) and Pearce and Norry (1979) respectively. On these diagrams (Figures 5.20 and 5.21) compositional fields for basalts erupted at a number of different tectonic settings have been defined by plotting large numbers of samples from known tectonic environments.

On the Zr-Ti-Y diagram (Figure 5.20) basaltic rocks of the East Nelson ophiolites plot predominantly within two fields, whereby "olivine-rich" suite rocks plot within the "within-plate basalt" field while samples from the remaining suites plot as "ocean floor basalts".

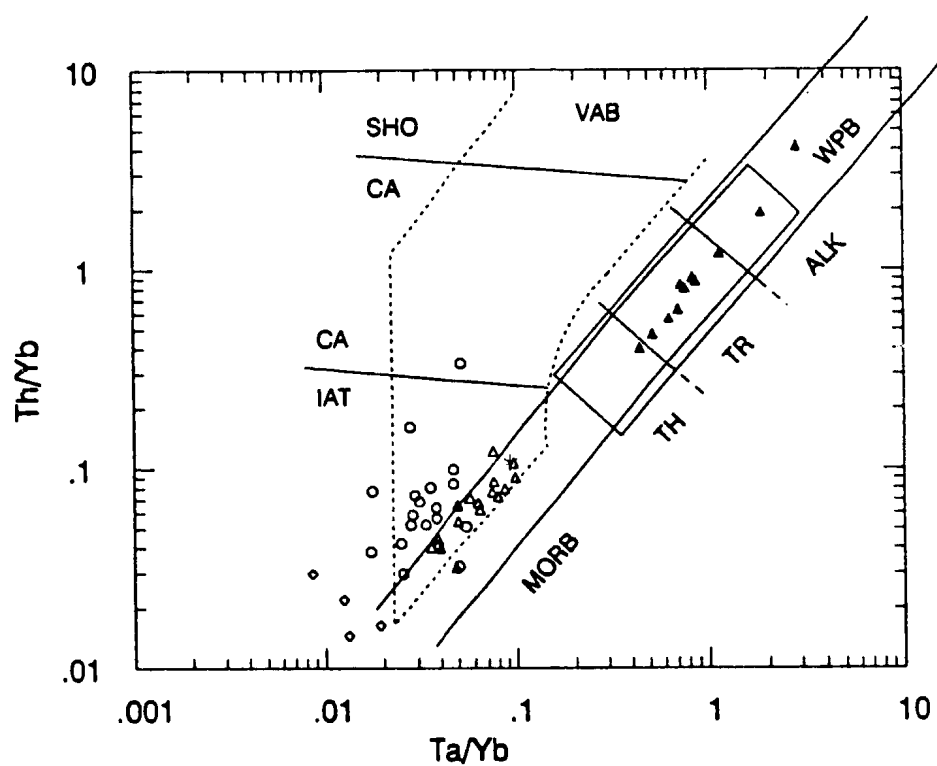
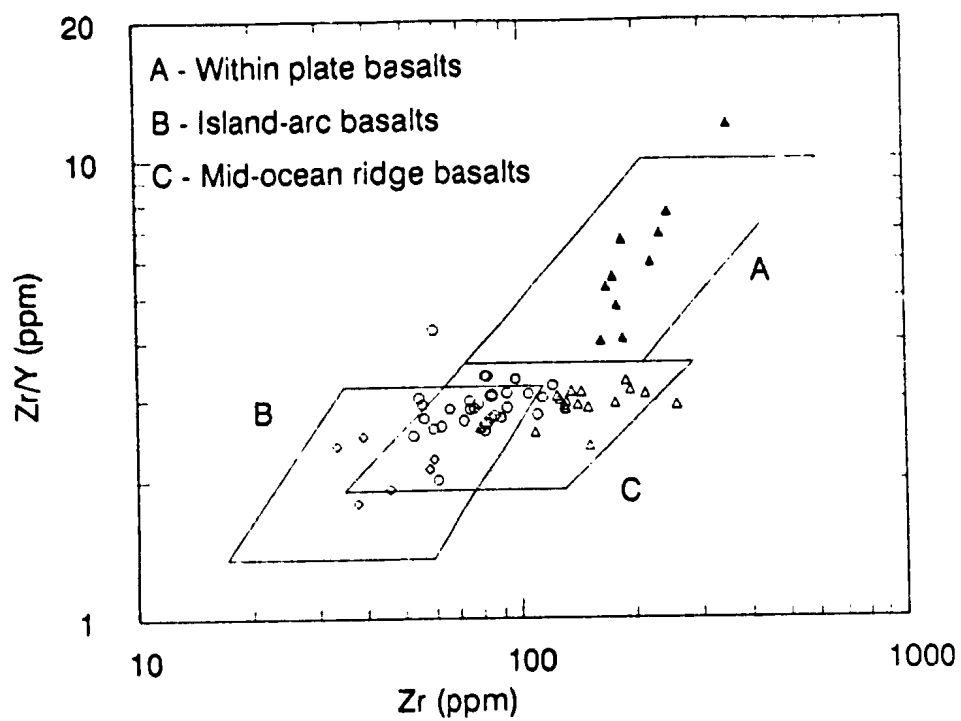
On the log Zr/Y-log Zr plot (Figure 5.21) "olivine-rich" suite rocks again plot within the field defined for within-plate basalts. Rocks of the remaining

---

<sup>1</sup> The "ocean floor basalt" field defined on figure 5.20 includes mid-ocean ridge basalts, low-potassium tholeiites, and calc-alkali basalts (Pearce and Cann, 1973).

**Figure 5.21** Basalt tectonic discrimination diagram of Pearce and Norry (1979). Symbols as used in Figure 5.16.

**Figure 5.22** Th/Yb versus Ta/Yb (ppm) covariation diagram of Pearce et al. (1981) based on the work of Wood et al. (1979). Asterisk indicates estimated primordial mantle composition of Alabaster et al. (1982). MORB= mid-ocean ridge basalt; WPB= within-plate basalt; VAB= volcanic arc basalt; TH= tholeiitic; TR= transitional; ALK= alkalic; CA= calc-alkalic; SHO= shoshonitic; IAT= island-arc tholeiite.





suites; however, are further discriminated whereby "olivine-poor" suite basalts plot almost entirely within the mid-ocean ridge basalt field while rocks of the Lee River Group suites plot predominantly within a field of overlap between mid-ocean ridge basalts and island-arc basalts.

From these plots (Figures 5.20 and 5.21) it can be suggested that basalts of the "olivine-rich" suite are likely representative of within-plate basalts while "olivine-poor" suite basalts are representative of mid-ocean ridge or MORB basalts. These proposals agree well with both rare earth element data and relict pyroxene compositions and suggest that rocks sampled from the Patuki and Croisilles mélanges are representative of oceanic crust produced in large ocean basins independent of orogenic or subduction zone influences. Basaltic rocks of the Lee River Group suites; however, are not clearly discriminated using these diagrams as they plot almost entirely within the overlapping field of island-arc and mid-ocean ridge basalts.

As this is the case, discrimination diagrams which discriminate between basalts erupted within island-arc and at mid-ocean ridge settings must now be employed. Such discrimination diagrams rely on a very limited group of immobile trace elements including Th, Ta, Nb, Zr, Ti, Y, V, Cr, and the rare earth elements.

One such diagram is the Th/Yb-Ta/Yb covariation diagram of Pearce et al (1981). This diagram (Figure 5.22) distinguishes between arc-related basalts and various ocean basin basalts by identifying basaltic compositions that contain a "subduction component". This component is identified as a selective enrichment of Th over Ta whereby Th is believed to be preferentially

driven off the subducted slab during subduction causing enrichment within the mantle wedge above a subduction zone. Both Th and Ta are plotted as ratios to Yb on this diagram to eliminate compositional variations caused by differing degrees of partial melting and fractional crystallization. On Figure 5.22, basalts of the Patuki and Croisilles mélanges do not appear to contain a "subduction component" as basalts of the "olivine-poor" suite plot within the field of normal mid-ocean ridge basalts (MORB) while "olivine-rich" suite basalts plot as "transitional"<sup>5</sup> to alkaline within-plate basalts. Rocks of the Lee River Group suites; however, plot within the compositional field of island-arc tholeiites whereby 90 percent of the samples plot above the compositional boundaries of normal mid-ocean ridge basalts. Of these rocks, those of the plagioclase porphyritic suite appear to have been derived from a strongly depleted mantle source as they contain noticeably lower Th/Yb and Ta/Yb ratios than other Lee River Group rocks.

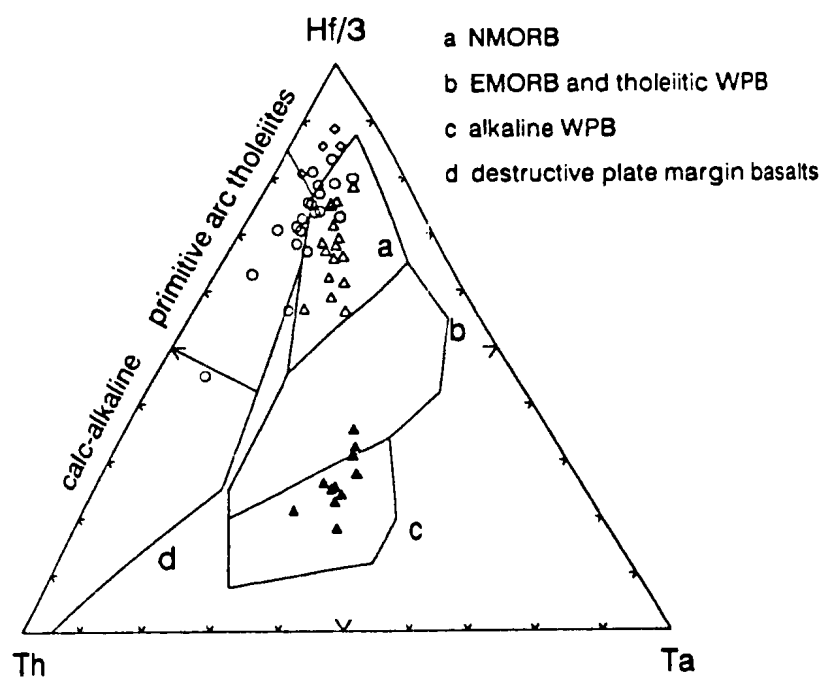
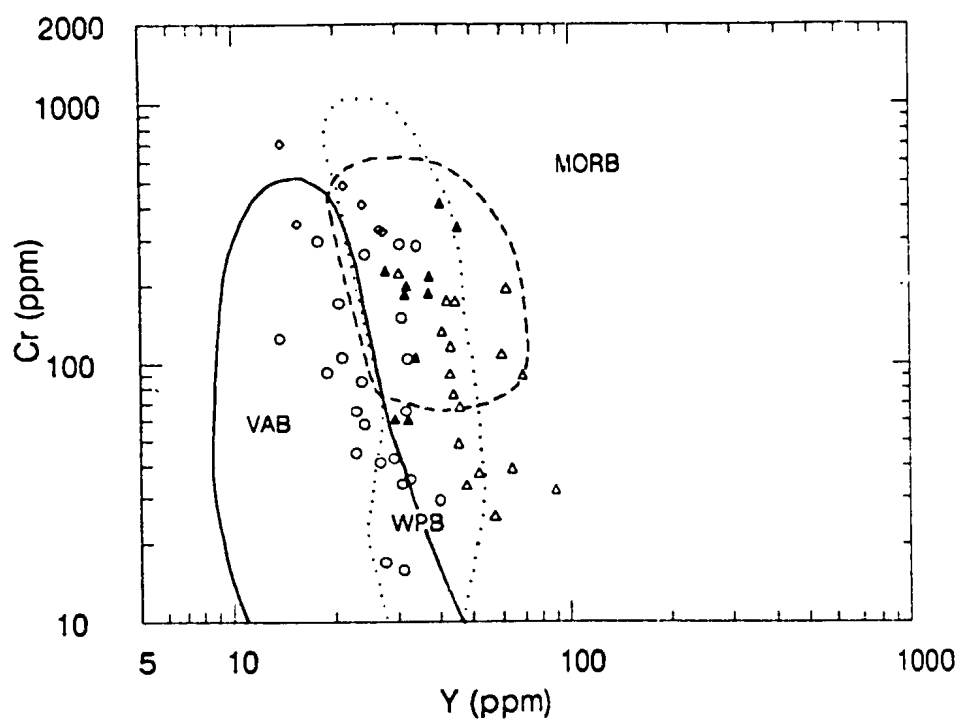
Another valuable diagram in the discrimination of island-arc tholeiites from basalts of major ocean basins is the Cr-Y variation diagram of Pearce (1980). This diagram (Figure 5.23) relies upon the observation that at a given Cr content, elements of high ionic potential are depleted in island-arc lavas more so than in lavas produced at mid-ocean ridges (eg., Pearce, 1975; Garcia, 1978). Explanations for this phenomenon are varied and controversial; however, it is generally considered that addition of aqueous fluids driven off subducted oceanic crust is required (eg., Pearce and Norry, 1979; Green, 1973; Dixon and Batiza, 1979).

---

<sup>5</sup> Transitional between tholeiitic and alkaline within-plate basalts.

**Figure 5.23 Cr versus Y variation diagram of Pearce (1980), Pearce et al. (1981) and Pearce et al. (1984). MORB= mid-ocean ridge basalt; VAB= volcanic arc basalt; WPB= within-plate basalt. Symbols as used in Figure 5.16.**

**Figure 5.24 Th-Hf/3-Ta (ppm) basalt tectonic discrimination diagram of Wood (1980). Symbols as used in Figure 5.16. NMORB= normal mid-ocean ridge basalts; EMORB= enriched mid-ocean ridge basalts; WPB= within-plate basalts.**





On the Cr-Y variation diagram of Pearce (1980), despite some overlap within the compositional fields defined for mid-ocean ridge and within-plate basalts, basaltic rocks of the Lee River Group suites tend to plot within the field of island-arc tholeiites as they are typically more depleted in Y than the Patuki and Croisilles lavas of similar Cr concentrations (Figure 5.23). This observation agrees well with the classification of Lee River Group rocks on Figure 5.22 as island-arc tholeiites and also further discriminates "olivine-poor" suite basalts from island-arc tholeiites as all "olivine-poor" suite samples plot outside the compositional field defined for island-arc tholeiites on the Cr-Y variation diagram (Figure 5.23). "Olivine-rich" suite basalts plot predominantly within the within-plate basalt field although a small number of samples contain slightly higher Y concentrations and plot to the right of the within-plate basalt field. On this diagram the rocks of each suite tend to plot within specific fields; however, many samples contain slightly higher Y concentrations than expected for the respective rock suites. This feature may be attributable to high degrees of fractional crystallization involving olivine, spinel, clinopyroxene, and plagioclase (Pearce, 1980).

Another diagram which discriminates between basalts erupted at supra-subduction zones and major ocean basins is that of Wood et al. (1979) and Wood (1980). This ternary diagram (Figure 5.24) relies on the relative proportions of Th, Ta, and Hf within basaltic rocks whereby subduction zone influenced basalts are typically enriched in Th and depleted in Ta compared to rocks erupted in major ocean basins. This diagram also discriminates between basalts erupted at mid-ocean ridges and within-plate settings as

within-plate basalts are relatively enriched in high field strength elements such as Hf compared to basalts erupted at mid-ocean ridges (Wood et al, 1979; Wood, 1980). A particularly useful feature of this diagram is that it discriminates between calc-alkaline and tholeiitic series basalts erupted above subduction zones.

In Figure 5.24, basaltic rocks of the Lee River Group suites overlap the compositional fields defined for primitive arc tholeiites and mid-ocean ridge basalts and are characterized by relatively high Hf/Th ratios. This suggests that these rocks may be transitional in composition between island-arc tholeiites and mid-ocean ridge basalts, a feature commonly displayed by basalts erupted in large marginal basins of back-arc derivation (eg. Tarney et al., 1977; Wood et al, 1982; Tarney et al. 1981; Taylor and Kerner, 1983). As for basaltic rocks of the Patuki and Croisilles mélanges, all "olivine-poor" suite basalts plot within the compositional field defined for normal mid-ocean ridge basalts, while basaltic rocks of the "olivine-rich" suite plot as within-plate basalts whereby 75 percent of the samples plot as within-plate alkali basalts while the remainder plot as being transitional between within-plate tholeiites and within-plate alkali basalts. This observation agrees well with the classification of the various basaltic suites on the basis of pyroxene compositions and other trace element discrimination diagrams and is particularly useful here as it distinguishes between tholeiitic and alkaline within-plate basalts.

Servais (1982), has shown that Ti/V ratios can also be used as a diagnostic tool in determining tectonic settings of eruption for modern volcanic

rocks as well as for volcanic rocks from ancient ophiolites. Through the observation of Ti/V ratios from different tectonic environments Shervais has shown:

(i) volcanic rocks from modern island-arcs typically have Ti/V ratios of less than or equal to 20; however, calc-alkaline series rocks are effected by significant magnetite fractionation and therefore contain inconsistent Ti/V ratios whereby Ti/V ratios increase with increased degrees of fractionation;

(ii) mid-ocean ridge and continental flood basalts have Ti/V ratios of about 20 to 50;

(iii) alkaline rocks have Ti/V ratios which are typically greater than 50; and,

(iv) volcanic rocks of back-arc basins generally have either arc-like or mid-ocean ridge-like Ti/V ratios whereby rocks from individual back-arc basins may have Ti/V ratios ranging from 10 to 50.

Through comparison of Ti/V ratios from rocks of various basaltic suites of the East Nelson ophiolites to those of known tectonic setting (Figure 5.25), eruptive settings can be inferred. Rocks of the East Nelson ophiolites plot within three distinct, slightly overlapping groups, whereby basaltic rocks of the Lee River Group suites have Ti/V ratios which range between 14 and 26, while basalts of the "olivine-poor" and "olivine-rich" suites contain values ranging between 23 and 37, and 32 and 88 respectively. These ratios suggest that rocks of the Lee River Group are transitional in composition between rocks erupted at island-arcs and mid-ocean ridges, while "olivine-poor" and "olivine-rich" suite basalts have similar Ti/V ratios to those observed

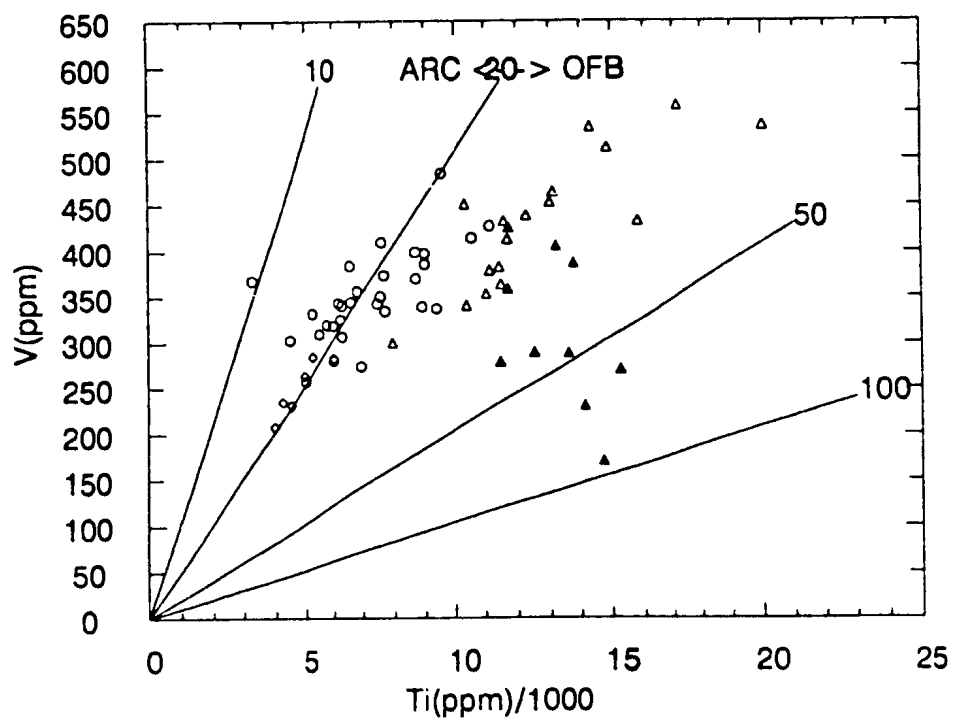


Figure 5.25 V versus Ti/1000 basalt tectonic discrimination diagram of Shervais (1982). ARC= arc related rocks; OFB= ocean floor basalts. Symbols as used in Figure 5.16.



within tholeiitic basalts erupted at mid-ocean ridges and alkaline basalts from oceanic islands and seamounts.

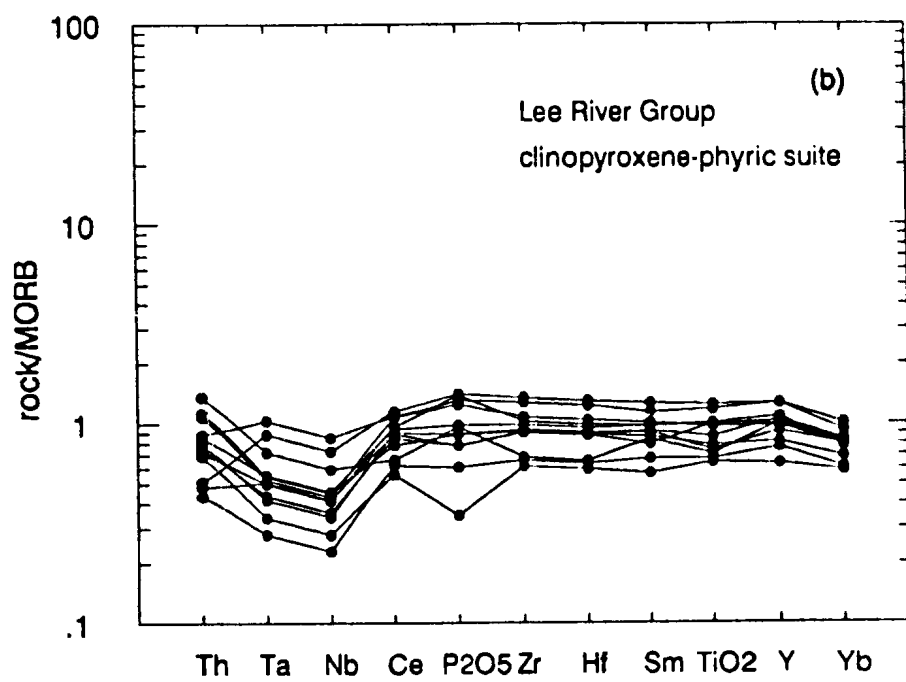
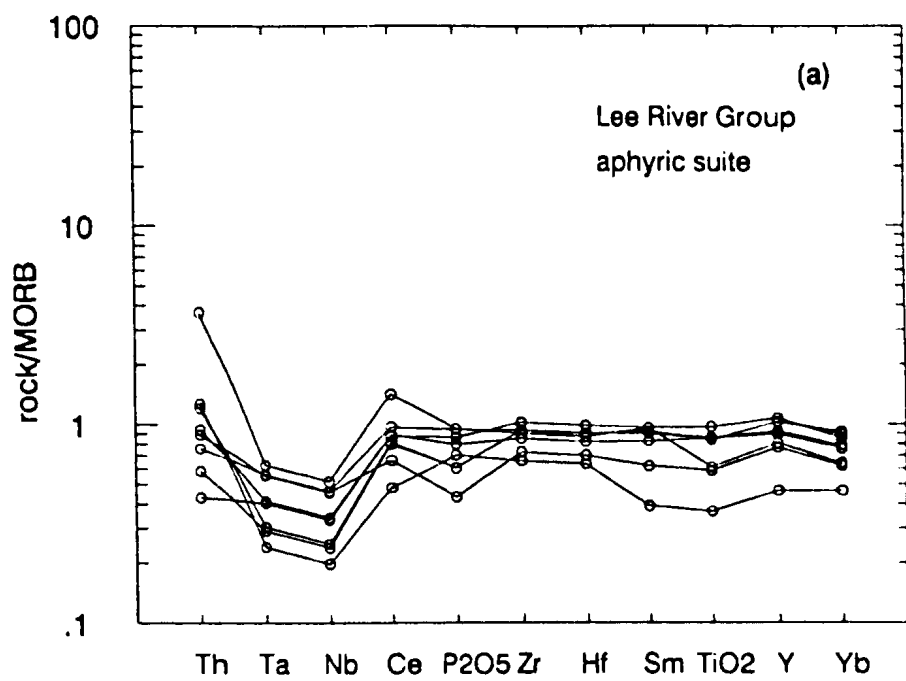
### 5.3.6 MORB Normalized Trace Element Diagrams

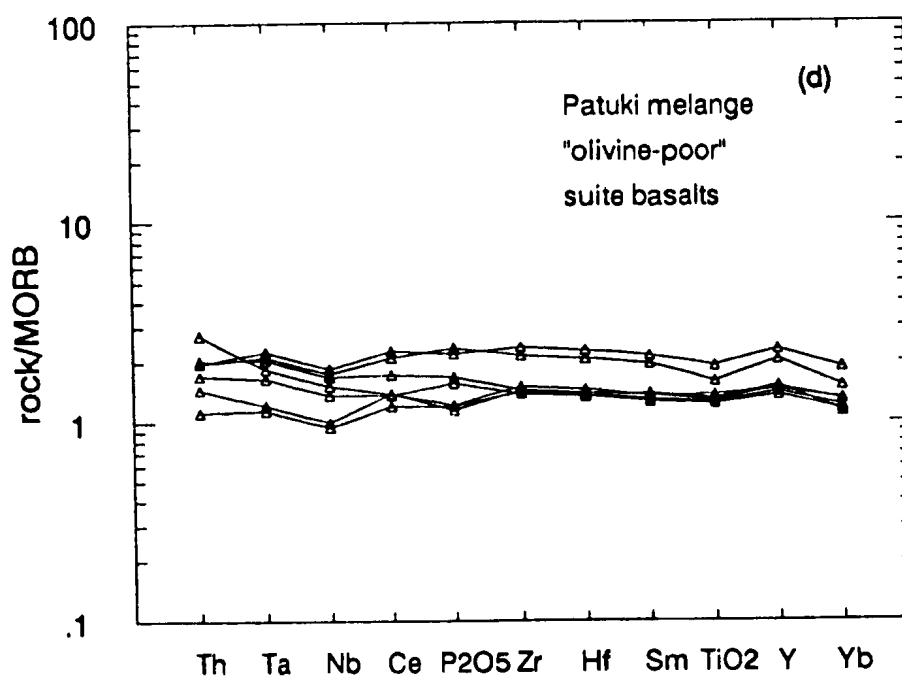
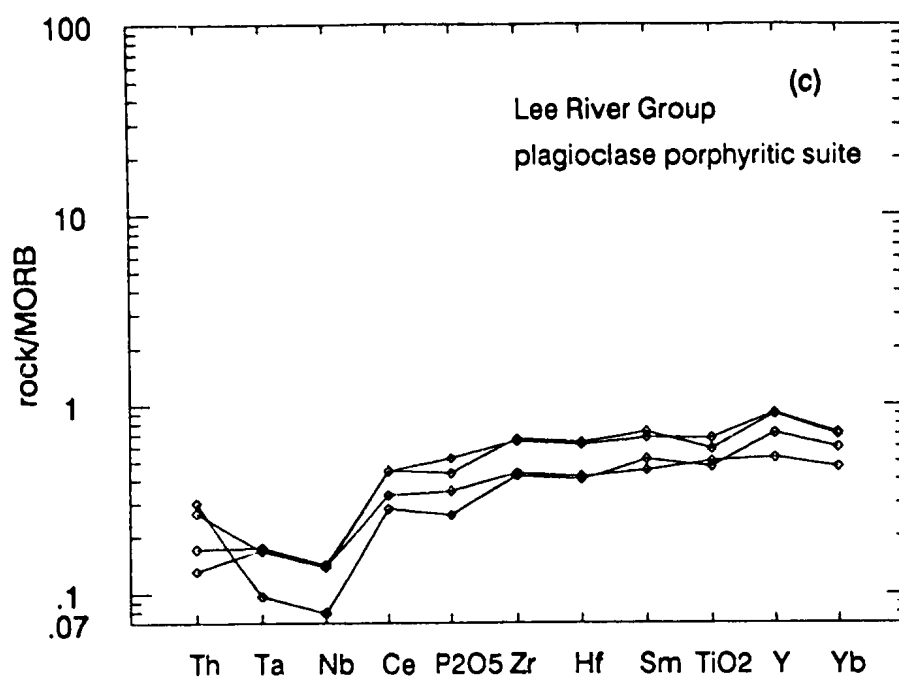
In this section, rocks of the various basaltic suites of the East Nelson ophiolites are described and compared to mid-ocean ridge basalts using MORB (average mid-ocean ridge basalt) normalized geochemical patterns. All samples plotted here are normalized to average mid-ocean ridge basalt (MORB) concentrations as estimated by Pearce et al. (1981) and normalized geochemical patterns for rocks of the respective suites are presented in Figures 5.26a to 5.26f. As basaltic rocks of the East Nelson ophiolites have been affected by greenschist and sub-greenschist facies metamorphism, only trace elements previously outlined as being immobile under greenschist facies conditions are plotted on these diagrams.

From these figures (5.26a to 5.26f) it can be observed that a number of suites display geochemical patterns which are virtually indistinguishable from those of other suites while some suites are compositionally quite distinct.

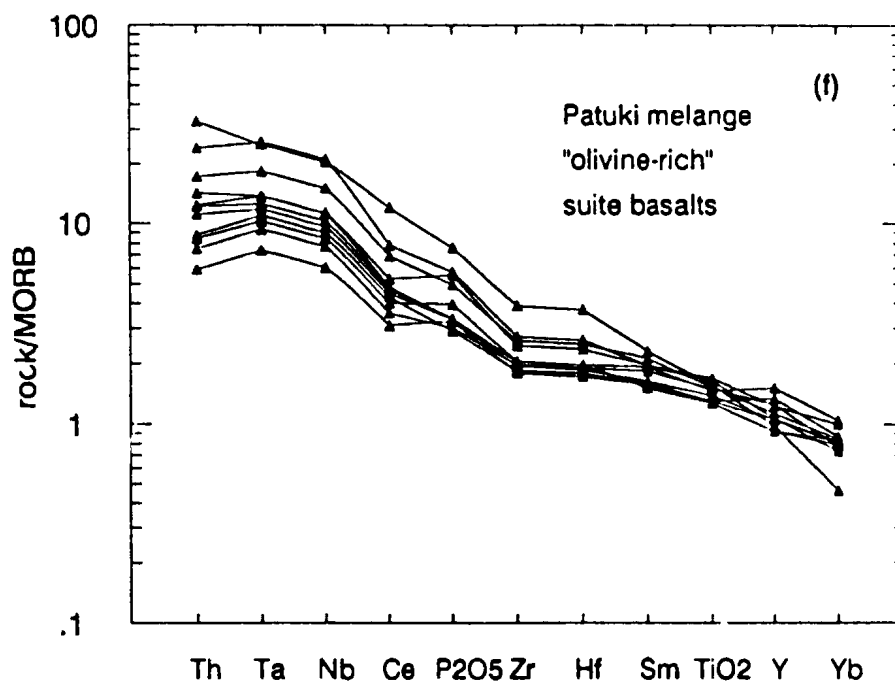
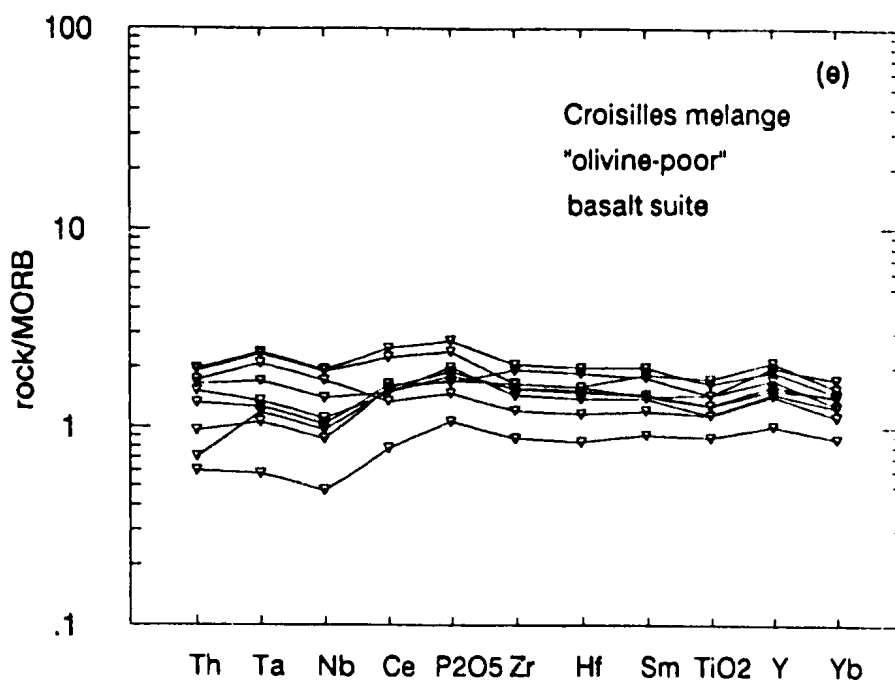
Of the Lee River Group rocks, aphyric and clinopyroxene-phyric suite samples (Figures 5.26a and 5.26b) exhibit similar patterns whereby rocks of both suites are relatively flat; but, contain consistent Nb depletions, and normalized Th/Nb ratios greater than 1. As these geochemical patterns are indistinguishable, these rocks likely represent variably metamorphosed samples of a single compositional suite. Geochemical patterns for plagioclase porphyritic suite samples are also somewhat similar to those of aphyric and

Figures 5.26a,b,c,d,e and f MORB normalized geochemical patterns for basalts of the East Nelson ophiolites. Samples have been normalized to average mid-ocean ridge basalt values of Pearce et al. (1981). Symbols as used in Figure 5.4.









clinopyroxene-phyric suite rocks but generally contain lower elemental abundances and marked light rare earth element depletions (Figure 5.26c).

Patterns produced for rocks of the Patuki and Croisilles "olivine-poor" suites are also quite flat (MORB-like) but do not display Nb depletions (Figures 5.26d and 5.26e). From these patterns it can be seen that these rock suites are compositionally indistinguishable from one another and likely belong to a single suite. The rocks of these suites generally contain greater elemental abundances than average mid-ocean ridge basalt (ie. normalized values are greater than 1).

Rocks of the "olivine-rich" suite exhibit geochemical patterns markedly different from those of the forementioned suites (Figure 5.26e). Compared to average mid-ocean ridge basalt these rocks are enriched in Th, Nb, and the light rare earth elements and are slightly heavy rare earth element depleted.

Through comparison of the geochemical patterns mentioned above and other previously discussed geochemical characteristics (eg., trace and rare earth element data and relict pyroxene compositions), petrographically defined basaltic suites of the East Nelson ophiolites can be compositionally redefined. Aphyric and clinopyroxene-phyric suite rocks are compositionally indistinguishable and are therefore considered to represent a single suite, the "aphyric/clinopyroxene-phyric" suite. "Olivine-poor" suite rocks of the Patuki and Croisilles mélanges are also compositionally indistinguishable and therefore might represent a single suite of rocks which has been tectonically severed and incorporated into two discrete units of mélange material (the Patuki and Croisilles tectonic mélanges). Average mid-ocean ridge basalt

normalized patterns for each of these compositionally defined basaltic suites of the East Nelson ophiolites are presented in Figure 5.27.

By comparing these normalized patterns to those of basalts erupted at known tectonic settings, tectonic settings of eruption for each of the basaltic suites of the East Nelson ophiolites can be inferred. On Figure 5.28 a number of representative samples (basalts) from mid-ocean ridges, ocean islands and island-arcs have been plotted for comparison to those of the East Nelson ophiolites suites. These representative samples were selected from Sun (1980) and are based on least fractionated samples (see Sun, 1980 p.301). Through comparison of these geochemical patterns it can be observed that:

(i) the geochemical pattern for the "olivine-rich" suite is analogous to that of an ocean island alkali basalt;

(ii) "olivine-poor" suite basalts are similar to mid-ocean ridge basalts; but, display relatively flat patterns, therefore showing a closer resemblance to depleted or normal mid-ocean ridge basalts as there is no selective enrichment in Th, Ta, Nb, Ce, or  $P_2O_5$ , as is typically observed within enriched mid-ocean ridge basalts;

(iii) the aphyric/clinopyroxene-phyric suite pattern is somewhat transitional between that of depleted mid-ocean ridge basalts and island-arc tholeiites as it contains similar elemental abundances to that observed within depleted mid-ocean ridge basalts but also shows a pronounced depletion in Nb and Ta; a feature considered to be somewhat diagnostic of arc-related basalts (eg., Gill, 1981; Pearce, 1982); and,

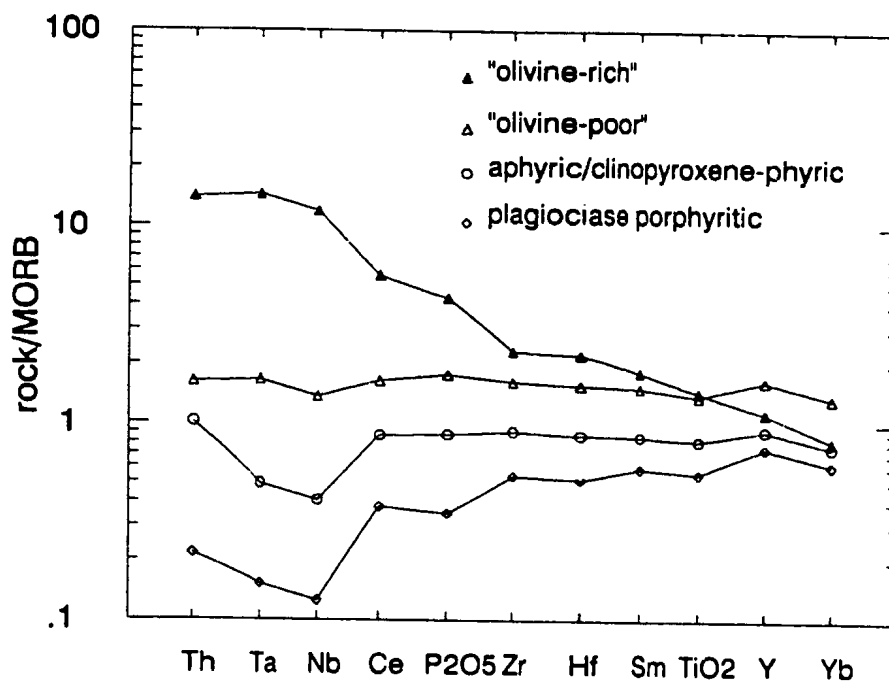
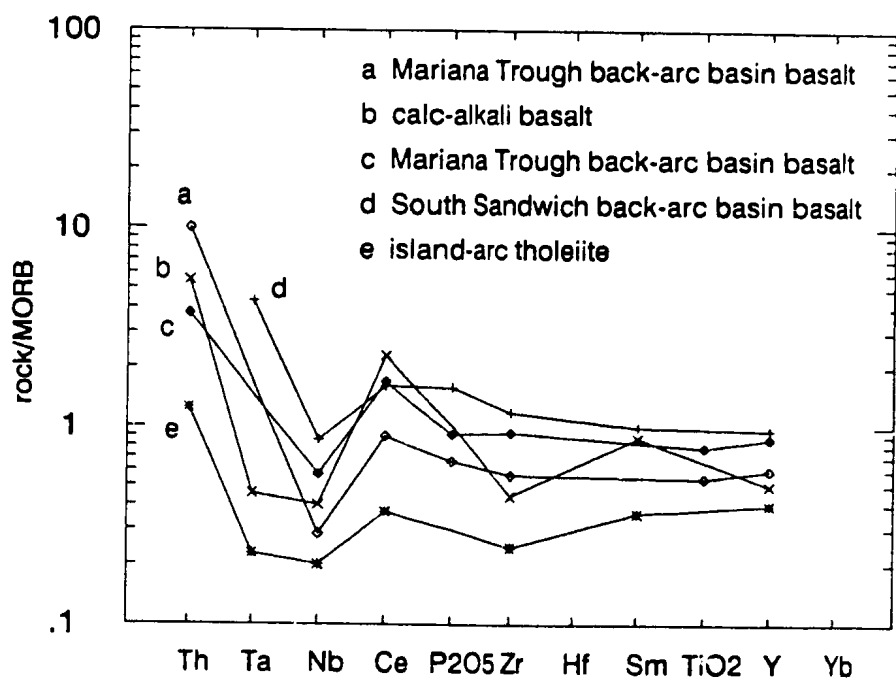
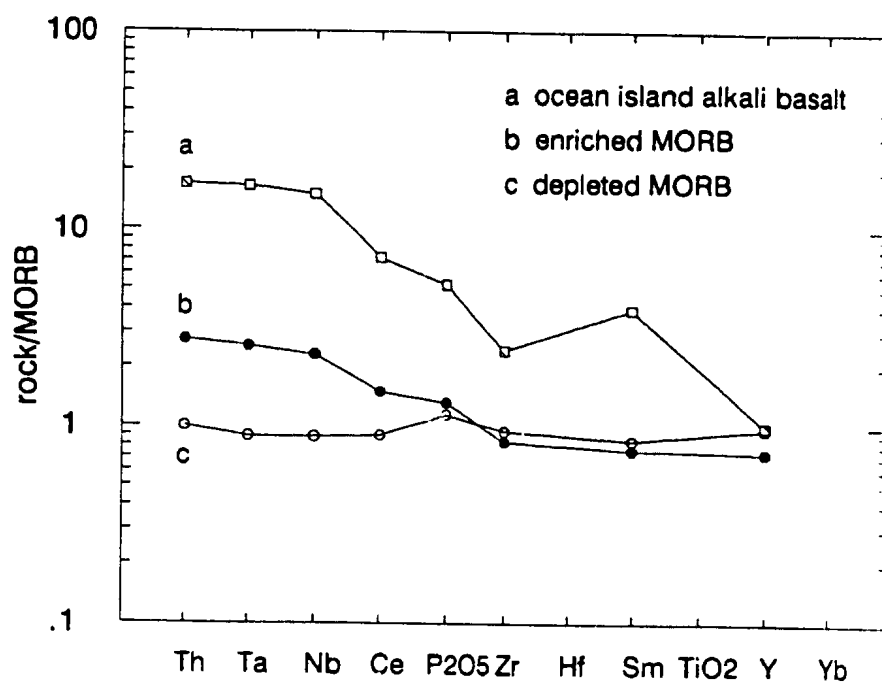


Figure 5.27 MORB normalized average basaltic suite geochemical patterns for basaltic suites of the East Nelson ophiolites. Samples have been normalized to average mid-ocean ridge basalt values of Pearce et al. (1981).

**Figures 5.28a MORB normalized geochemical patterns for basalts of known, non-arc related tectonic settings. Samples have been normalized to average mid-ocean ridge basalt values of Pearce et al. (1981). Sample a= estimated ocean island alkali basalt after Sun (1980); b= estimated enriched mid-ocean ridge basalt after Sun (1980); c= depleted mid-ocean ridge basalt after Sun (1980).**

**Figure 5.28b MORB normalized geochemical patterns for basalts of known, arc related tectonic settings. Samples have been normalized to average mid-ocean ridge basalt values of Pearce et al. (1981). Sample a= Mariana Trough back-arc basin basalt (DSDP hole 454A, Sample 5-4) after Wood et al. (1982); b= estimated calc-alkali basalt after Sun (1980); c= Mariana Trough back-arc basin basalt (DSDP hole 456A, sample 13-1) after Wood et al. (1982); d= South Sandwich back-arc basin basalt (sample D20.43B) after Saunders and Tarney, 1979; e= estimated island-arc tholeiite after Sun (1980).**





(iv) rocks of the plagioclase porphyritic suite resemble island-arc tholeiite but lack a pronounced positive Th anomaly commonly observed within island-arc tholeiitic basalts.

From the above diagrams (Figures 5.27 and 5.28) it is clear that the relative elemental abundances observed within some suites, particularly the "olivine-poor" and aphyric/clinopyroxene-phyric suites, are relatively high compared to those observed within mid-ocean ridge basalts and island-arc tholeiitic basalts. These features may be explained when the effects of differentiation are considered, as most trace element concentrations typically increase within basaltic melts with increased degrees of fractional crystallization. When this effect is taken into account, elemental abundances observed within basalts of the "olivine-poor" suite probably compare favourably with that of normal mid-ocean ridge basalts, while elemental abundances observed within rocks of the aphyric/clinopyroxene-phyric suite better resemble those observed within island-arc tholeiites.

Despite the absence of pronounced positive Th anomalies within basalts of the Lee River Group suites (aphyric/clinopyroxene-phyric and plagioclase porphyritic suites), it can be suggested on the basis of the negative Nb anomalies, that these suites have supra-subduction zone or arc related geochemical signatures.

#### 5.4 Summary

As a result of ocean floor and regional metamorphic events of greenschist and sub-greenschist facies, mobilization of many trace and major

elements has taken place including the alkalis, alkaline earths, and to some extent,  $\text{SiO}_2$ . As this is the case, basaltic rocks of the East Nelson ophiolites have been discriminated using immobile trace elements, rare earth elements, and relict pyroxene compositions.

Examination of these criteria within basaltic rocks of the various petrographic suites have shown that Lee River Group basaltic rocks are composed of two chemically distinct suites whereby the petrographically defined aphyric and clinopyroxene-phyric suites represent variably metamorphosed equivalents of a single suite, the "aphyric/clinopyroxene-phyric" suite, while rocks of the plagioclase porphyritic suite represent a more depleted/less fractionated suite of rocks of similar affinity.

Basaltic rocks of the Patuki and Croisilles mélanges also consist of two chemically distinct suites whereby "olivine-poor" suite basalts of both the Patuki and Croisilles mélanges are compositionally identical, therefore making up one suite, the "olivine-poor" suite; while "olivine-rich" suite basalts of the Patuki mélange represent the other.

Discrimination of these basaltic rocks through the use of chondrite normalized rare earth element patterns, relict pyroxene compositions, trace element discrimination diagrams, and average mid-ocean ridge normalized geochemical patterns suggest;

(i) basaltic rocks of the Lee River Group suites are tholeiitic in character and contain a compositional component similar to that observed within island-arc tholeiites and therefore were likely erupted above a subduction zone;

- (ii) basalts of the "olivine-poor" suite (Patuki and Croisilles mélange) are similar to tholeiitic basalts erupted at normal mid-ocean ridges; and
- (iii) "olivine-rich" suite basalts resemble alkaline basalts erupted at within-plate oceanic islands.

Although rocks of the Lee River Group suites contain an arc compositional component, a number of previously mentioned trace element discrimination diagrams suggest that these rocks have compositional characteristics that are somewhat transitional between normal mid-ocean ridge basalts and island-arc tholeiites (Figures 5.21, 5.24, 5.25). The subduction zone compositional component is observed in these rocks as:

- (i) a selective enrichment of Th over Ta relative to mid-ocean ridge basalts (as observed from MORB normalized geochemical patterns);
- (ii) a relative depletion in elements of high ionic potential compared to basalts erupted at mid-ocean ridges and within-plate settings of similar Cr content (eg. Figure 5.23);
- (iii) low Ti/V ratios (eg. Figure 5.25); and,
- (iv) relict pyroxene compositions whereby Lee River Group pyroxenes plot as orogenic basalts and island-arc tholeiites on pyroxene composition based discrimination diagrams (eg., Figure 5.12b, and Figures 5.14a,d).

## CHAPTER 6

PETROGENESIS OF THE BASALTIC ROCKS OF THE  
EAST NELSON OPHIOLITES

## 6.1 Introduction

It is evident from examination of petrographic and geochemical characteristics of basaltic rocks of the Dun Mountain Ophiolite Belt (East Nelson ophiolites) that at least two distinct ophiolite suites occur within the belt. These suites include the Dun Mountain Ophiolite (composed of mafic rocks of the Lee River Group and ultramafic rocks of the Dun Mountain Ultramafics Group) and the Patuki and Croisilles *mélanges* (highly disrupted, ophiolitic, tectonic *mélanges*). Through geochemical evaluation of these rocks, it has been proposed that the Dun Mountain Ophiolite was produced above a subduction zone while ophiolitic rocks of the Patuki and Croisilles *mélanges* are considered to have formed as mid-ocean ridge basalts.

This chapter attempts to evaluate the petrogenetic processes involved in the formation of these ophiolitic rocks and reviews a number of models for their formation and emplacement. To provide constraints on the models presented here, field evidence as well as petrographic and geochemical evidence are used as much as possible; but, a number of additional assumptions are made on the basis of evidence collected from ophiolites of similar tectonic affinity which occur elsewhere in the world.



Rocci et al. (1975) and Pearce et al. (1984) have previously reviewed some of the fundamental differences between ophiolites produced within supra-subduction zone and "normal" ocean basin environments. These differences can be outlined as follows.

(i) Supra-subduction zone (SSZ) ophiolites and mid-ocean ridge (MORB) ophiolites generally display dissimilar crystallization sequences. Within SSZ ophiolites, clinopyroxene (and sometimes orthopyroxene) typically crystallizes before plagioclase, while plagioclase usually crystallizes before clinopyroxene in MORB ophiolites. This distinction can be observed through the examination of cumulate sequences from different ophiolites, whereby basal cumulate dunites in SSZ ophiolites are generally succeeded up sequence by lherzolites, wehrlites, norites and gabbros; while in MORB ophiolites, basal dunites are followed up sequence by troctolites and gabbros. In present day oceanic settings; boninitic lavas are considered to have formed by fractionation of olivine → orthopyroxene → clinopyroxene; island-arc tholeiites by olivine → clinopyroxene → plagioclase; and, mid-ocean ridge basalts by olivine → plagioclase → clinopyroxene.

(ii) SSZ ophiolites tend to contain larger volumes and more numerous occurrences of cumulate chromite-dunite bodies within their mantle sequences than do MORB ophiolites.

(iii) The mantle sequences of SSZ ophiolites tend to be dominated by harzburgite (typically between 80 and 90 percent) while mantle sequences of MORB ophiolites are usually composed of both harzburgites and lherzolites where abundance of lherzolite may even surpass that of harzburgite, as in

many Western Mediterranean ophiolite complexes (Pearce et al., 1984).

On the basis of these criteria, the Dun Mountain Ophiolite should be classified as a SSZ ophiolite, the evidence being:

(i) The mantle sequence of the Dun Mountain Ultramafics Group is dominated by foliated harzburgite and contains only rare wehrlite (Davis et al., 1980). The bulk composition of these rocks has been approximated by Walcott (1968) to be: olivine Fo91, 70 percent; orthopyroxene, En88, 22 percent; clinopyroxene, 5 percent; plagioclase, An96, less than 0.2 percent; and spinel, 2 percent. These rocks are therefore considered to be highly refractory and have likely undergone high degrees of partial melting.

(ii) Numerous cumulus lenses of dunite containing significant amounts of chrome spinel are observed within upper portions of the mantle sequence. This suggests that crystallization of olivine and chrome spinel took place within the upper mantle prior to the ascent of partial melts into overlying magma chambers of the gabbroic complex.

(iii) Although only upper portions of the gabbroic complex of the Dun Mountain Ophiolite are well preserved (except for rare occurrences of "critical zone" plutonic rocks found along faulted contacts between the gabbroic and ultramafic complexes), the cumulate mineralogy of these rocks suggests the following fractional crystallization sequence. Initial crystallization of olivine and chrome spinel, followed by olivine, clinopyroxene and chrome spinel ( $\pm$  orthopyroxene), and finally olivine, clinopyroxene, plagioclase ( $\pm$  chrome spinel). This sequence of crystallization agrees well with that determined by Challis (1965a) in which olivine and chrome spinel crystallization is overlapped

and followed by crystallization of clinopyroxene, and later, plagioclase. Other evidence which supports this sequence of crystallization is the phenocryst assemblage within the lavas (aphyric/clinopyroxene-phyric suite) of the Dun Mountain Ophiolite. Clinopyroxene is the dominant phenocryst phase while plagioclase is typically observed as interstitial to intergranular crystals within the groundmass and only rarely as phenocrysts.

The Patuki and Croisilles mélanges (ophiolites) are somewhat more problematical because of their poor preservation. The only clear evidence of their tectonic affinity is their MORB-like geochemical signatures.

## 6.2 Petrogenetic Modelling

### 6.2.1 Introduction

In this section, processes involved in the magmatic evolution of basaltic rocks of the Dun Mountain Ophiolite and the Patuki and Croisilles mélanges are evaluated on the basis of field relationships, petrographic and geochemical evidence.

Although it can clearly be argued that these rocks are somewhat altered it has clearly been shown that primary geochemical variations exist within each of the basaltic suites. On this basis an attempt is here made to evaluate possible genetic relationships between these suites; but it is necessary to first explain the cause(s) of the "within-suite" variations.

A number of petrogenetic variables commonly considered to be involved in the production of basaltic rocks are:

- (i) source heterogeneities;

(ii) the degree and nature of partial melting;

(iii) the degree and nature of fractional crystallization (eg. Alabaster et al., 1982); and,

(iv) mixing of magmas from partial melting of different mantle sources or mixing of mantle sources prior to melting (Langmuir et al., 1978).

A number of methods used to evaluate the affects of such processes on the composition of basalts are those of Treuil and Varet (1973), Pearce and Norry (1979), Pearce (1982); Alabaster et al. (1982) and Pearce et al. (1984). In this approach, geochemical data is plotted on key covariation diagrams in which theoretical trends are illustrated for comparison with the trends defined by actual data. The present study uses an approach similar to this involving a number of trace element discrimination diagrams shown in the preceding chapter. To put constraints on the theoretical trends modelled here, field and petrographic evidence have been used as much as possible.

#### 6.2.2 Source Variations

As the East Nelson ophiolites are considered to have formed in two tectonic environments, two types of source variations must be considered:

(i) those which existed prior to subduction and involved mantle enrichment and depletion events unrelated to supra-subduction zone processes; and,

(ii) those that have been directly caused by subduction and involve the transfer of a compositional component from subducted oceanic crust into an overlying mantle wedge.

These types of variations can be evaluated through the examination of particular trace element concentrations (eg. Pearce and Norry, 1979).

Processes related to pre-subduction activity are considered to only affect elements that are mobile in  $\text{CO}_2$ -rich fluids or interstitial melts (eg., Frey and Green, 1974; Wood et al., 1979) and which are also considered to be incompatible with garnet lherzolite (Pearce, 1980). Of these elements, those that are the most incompatible and show the greatest variations include: Th, La, Ta, and Nb, while the less incompatible elements: K, Sr, Sm, Zr, and Ti show moderate variations. The compatible elements: Y, Yb, Cr, and Sc show very little variation (eg. Pearce, 1982). Elements considered to be involved in subduction-related processes, on the other hand, are considered mobile in  $\text{H}_2\text{O}$ -rich fluids (eg. Hawkesworth et al. 1979) and include a large number of elements including: K, Rb, Ba, Sr as well as Th, P and the light rare earth elements (eg., Pearce, 1982; Alabaster et al., 1982).

Through careful selection and comparison of the elements mentioned above, a number of trace element covariation diagrams capable of discriminating source variations caused by pre-subduction and subduction related processes have been devised. Two such diagrams are the Th/Yb-Ta/Yb covariation diagram of Pearce et al. (1981) and the Th-Hf-Ta diagram of Wood et al. (1979). These diagrams are particularly useful as they are somewhat independent of compositional variations caused by other processes including partial melting and fractional crystallization and use elements that are immobile under greenschist facies conditions.

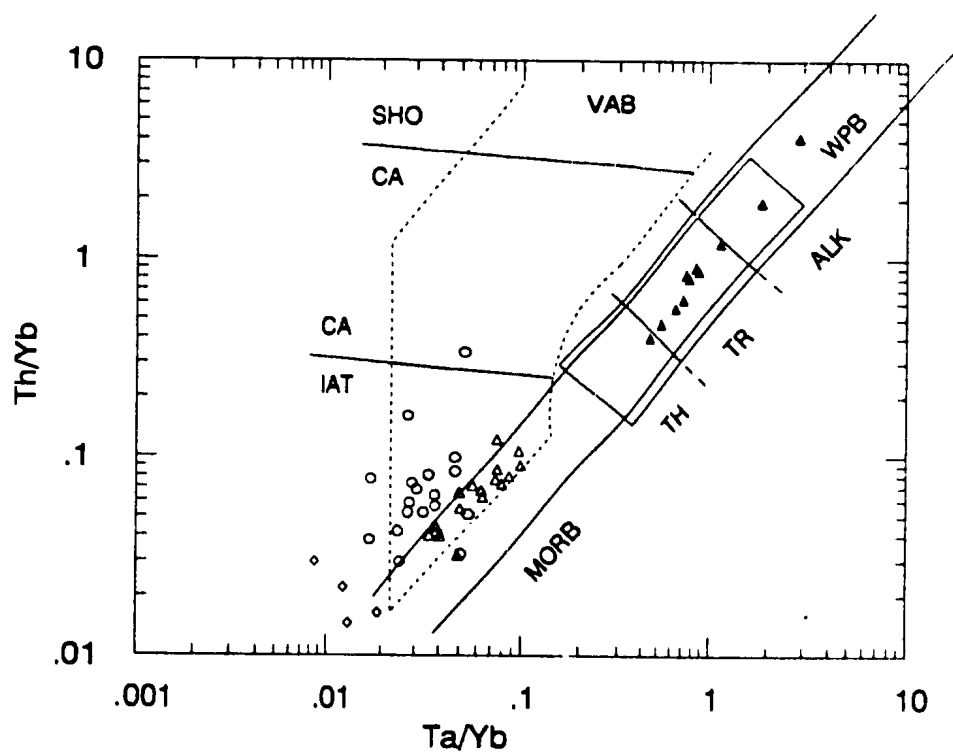
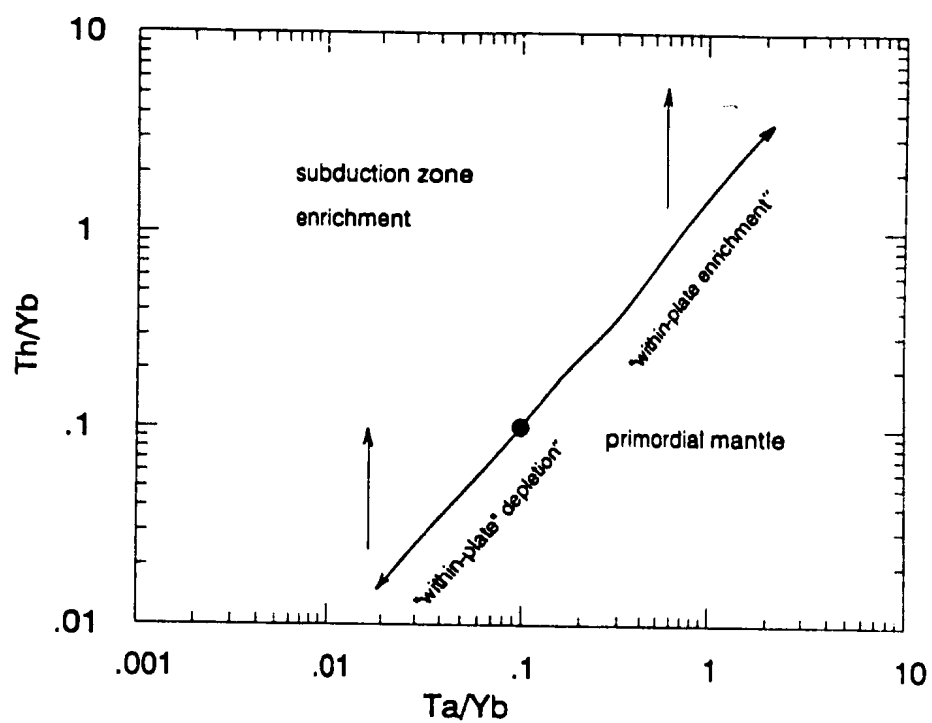


The Th/Yb-Ta/Yb covariation diagram (Figures 6.1a and 6.1b) discriminates between basalts derived from mantle sources affected by within-plate and supra-subduction processes by modelling trends or paths of evolution from basaltic compositions back to a primordial mantle source composition (Pearce, 1981). On this diagram, mantle compositional variations produced by within-plate processes plot along a "within-plate" vector which passes through a primordial mantle composition and has a slope of unity (Figure 6.1a). Mantle compositions are directed upwards for source enrichment and downwards for source depletion. By contrast, mantle enrichments caused by the addition of a supra-subduction zone component plot along a "subduction vector" which is directed vertically upwards (Figure 6.1a).

From a Th/Yb-Ta/Yb plot (Figures 6.1b) it appears that rocks of the Dun Mountain Ophiolite were derived from a depleted mantle source and that rocks of the plagioclase porphyritic suite were likely produced from a more depleted mantle source than that which produced the aphyric/clinopyroxene-phyric suite rocks. Basalts of the Patuki and Croisilles mélanges, on the other hand, involve both depleted and enriched mantle sources. The "olivine-poor" or MORB suite basalts appear to have been derived from a less depleted mantle source than that which produced the Dun Mountain Ophiolite rocks, and basalts of the "olivine-rich" or within-plate suite were derived from an enriched mantle source. From this diagram it can also be noted that only rocks of the Dun Mountain Ophiolite exhibit a subduction zone component.

**Figure 6.1a** Th/Yb versus Ta/Yb covariation diagram showing vectors of within-plate enrichment and depletion as well as supra-subduction zone enrichment. Primordial mantle composition is estimated after Alabaster et al. (1982).

**Figure 6.1b** Th/Yb versus Ta/Yb covariation diagram of Pearce et al. (1984). MORB= mid-ocean ridge basalt; WPB= within-plate basalt; VAB= volcanic arc basalt; TH= tholeiitic; TR= transitional; ALK= alkalic; CA= calc-alkalic; SHO= shoshonitic; IAT= island-arc tholeiite. Symbols as used in Figure 5.16.



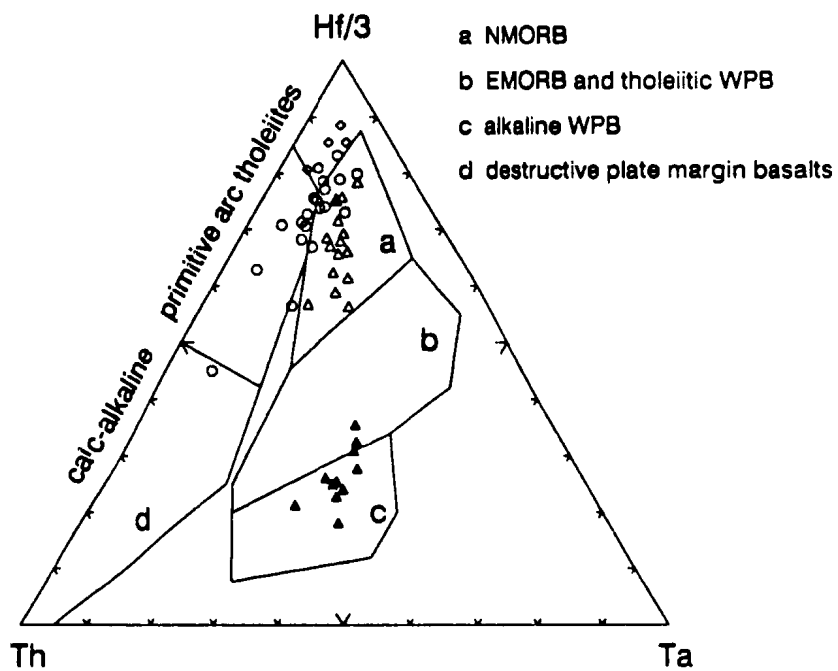
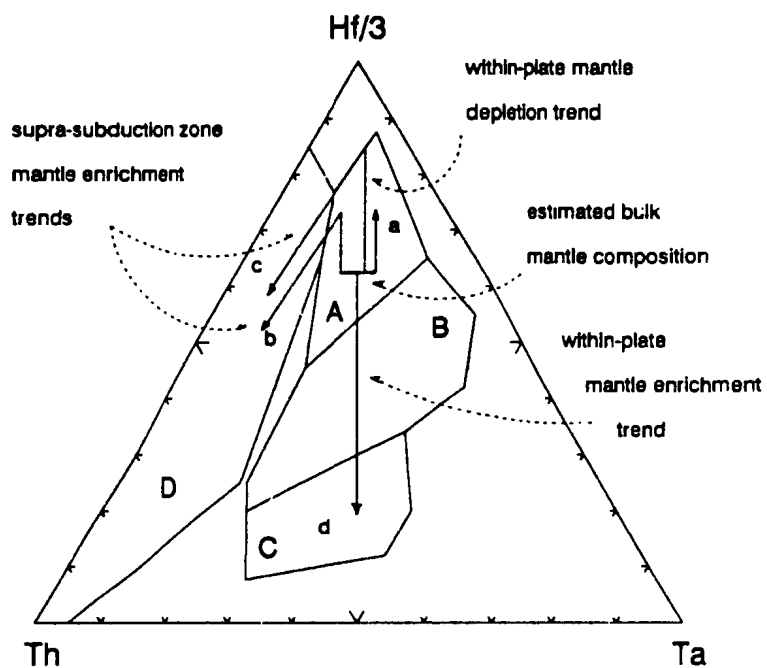
A similar diagram is the redefined (Wood, 1980) ternary diagram of Wood et al. (1979). Using this diagram, within-plate and subduction zone related mantle variations can again be modelled with reference to a theoretical mantle composition along "within-plate" and "subduction zone" vectors (Pearce et al., 1984). Within-plate mantle variations plot along a vertical vector which passes through an estimated bulk mantle composition and is directed downwards by within-plate enrichment and upwards by within-plate depletion (Figure 6.2a). Thus a "petrogenetic pathway" for a normal MORB basalt (path A) would involve within-plate depletion while the petrogenetic pathway for a within-plate basalt would involve within-plate enrichment (pathway D). Subduction related mantle enrichment vectors, on the other hand, are inclined and directed towards the Th apex of the diagram. Thus, island-arc tholeiites would be produced along a pathway similar to that of "path B" while the petrogenetic pathway for boninitic compositions would follow a path similar to that of "path C" as additional depletion is necessary to produce a more depleted composition prior to the addition of a subduction zone component.

From the Wood (1980) ternary plot (Figure 6.2b) it can be seen that rocks of the Dun Mountain Ophiolite exhibit only a small subduction zone component and were likely derived from a depleted mantle source. It is also worth noting here that rocks of the plagioclase porphyritic suite appear to have been derived from a source more depleted than that which produced the aphyric/clinopyroxene-phyric suite rocks; and, that they have likely evolved along a petrogenetic pathway similar to that suggested for boninitic lavas

**Figure 6.2a Petrogenetic pathways on a Th-Hf/3-Ta diagram for ophiolites of different tectonic affinities. Pathway "a" = ophiolites of mid-ocean ridge affinity; pathway "b" = ophiolites of island-arc tholeiitic affinities; pathway "c" = ophiolites of boninitic affinities; pathway "d" = within-plate mantle enrichment trend.**

**Figure 6.2b Th-Hf/3-Ta basalt tectonic discrimination diagram of Wood (1980). Symbols as used in Figure 5.16. NMORB= normal mid-ocean ridge basalts; EMORB= enriched mid-ocean ridge basalts; WPB= within-plate basalts.**





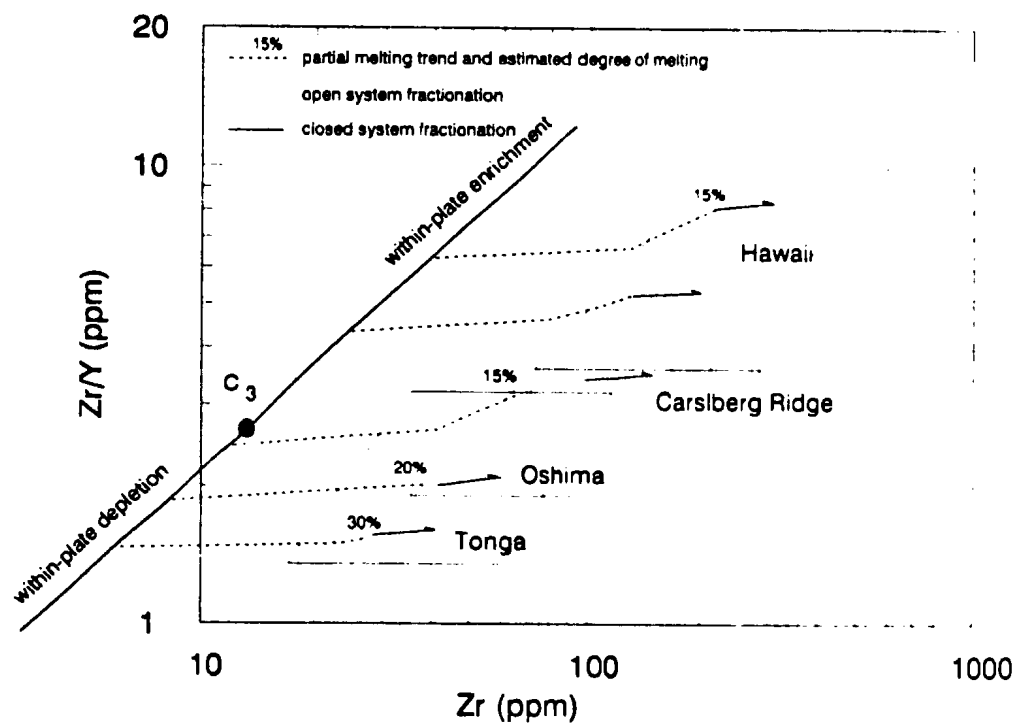
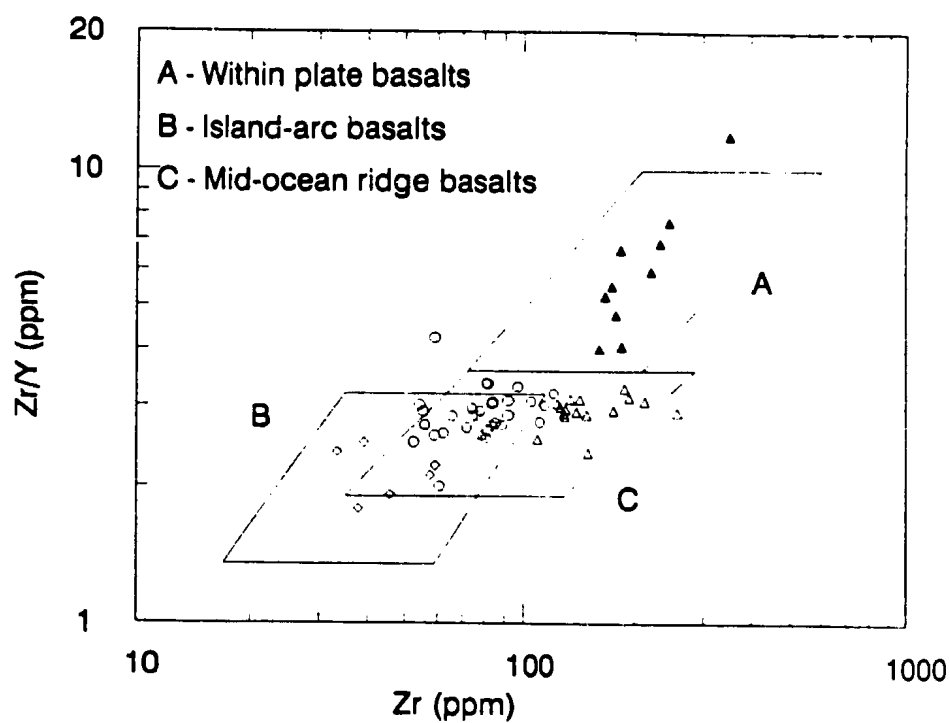
(path "C"). Basalts of the Patuki and Croisilles mélanges, on the other hand, again plot as two distinct suites along a within-plate vector.

In addition to the diagrams mentioned above, further information on pre-subduction mantle variations can be gained from plotting basaltic compositions on a Zr/Y-Zr diagram (Figure 6.3a) whereby basalts derived from an enriched mantle source contain greater Zr/Y ratios than those derived from depleted mantle. From this diagram, it was previously determined that rocks of the aphyric/clinopyroxene-phyric suite of the Dun Mountain Ophiolite and the "olivine-poor" (MORB) suite of the Patuki and Croisilles mélanges were derived from a depleted mantle source similar to that which is considered to produce mid-ocean ridge basalts. Also on this diagram it was determined that rocks of the plagioclase porphyritic suite of the Dun Mountain Ophiolite appear to have been derived from a somewhat depleted source while basalts of the "olivine-rich" (within-plate) suite of the Patuki mélange appear to have been derived from enriched mantle.

Pre-subduction related mantle variations can be evaluated by comparing basalt compositions to a primordial mantle composition and modelling petrogenetic paths of evolution (Figure 6.3b). These petrogenetic pathways have been taken from Pearce and Norry (1979) and are based on the observation that Zr and not Y is affected by processes which cause mantle source heterogeneities (Pearce and Norry, 1979). On this diagram, the vector for within-plate source variations is defined by a line with a slope of unity that passes through an estimated primordial mantle composition. Along this vector, within-plate source enrichments are directed upwards while

**Figure 6.3a Basalt tectonic discrimination diagram of Pearce and Norry (1979). Symbols as used in Figure 5.16.**

**Figure 6.3b Petrogenetic pathways for basaltic rocks from some typical volcanic suites plotted on a Zr/Y versus Zr diagram after Pearce and Norry (1979). Full details of components of pathways and method of modelling are documented in Pearce and Norry (1979).  $C_0$  = estimated primordial mantle composition after Pearce and Norry (1979).**



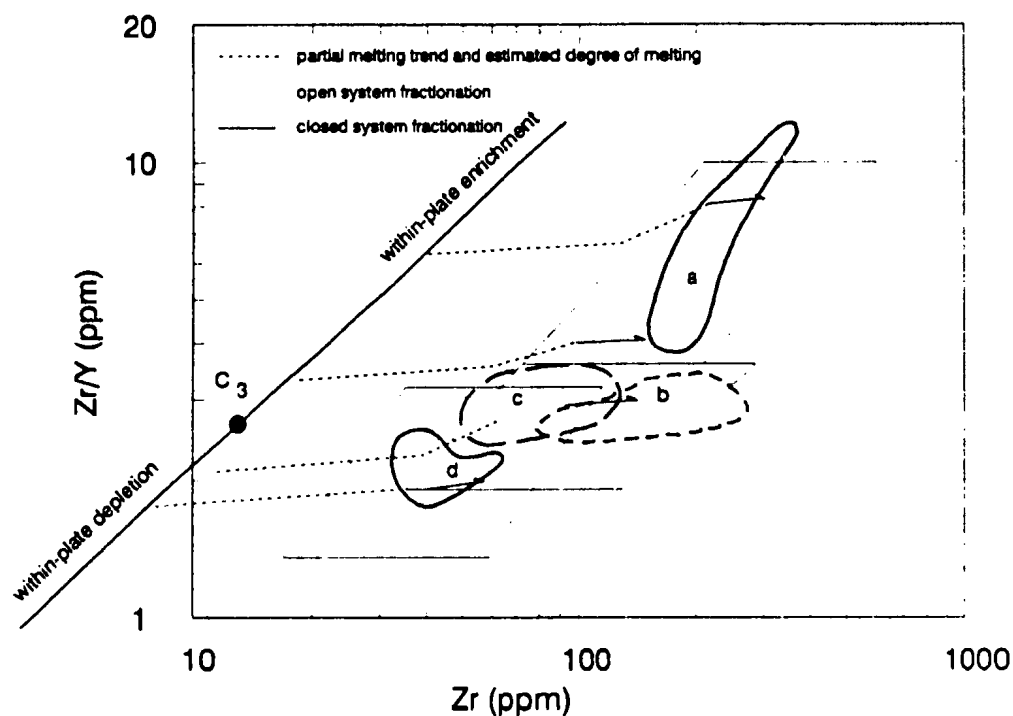


Figure 6.3c Estimated petrogenetic pathways for basaltic suites of the East Nelson ophiolites plotted on a  $Zr/Y$  versus  $Zr$  diagram. Lettered fields ("a-d") have been drawn for the various suites; field "a" = "olivine-rich" within-plate basalt suite; field "b" = "olivine-poor" mid-ocean ridge basalt suite; field "c" = aphyric/clinopyroxene-phyric suite island-arc tholeiites of the Dun Mountain Ophiolite; and, field "d" = plagioclase porphyritic suite island-arc tholeiites of the Dun Mountain Ophiolite. Tectonic discrimination field boundaries from Pearce and Norry (1979) have also been drawn for comparison.  $C_3$  = estimated primordial mantle composition after Pearce and Norry (1979).



depletions are directed downwards. To model basalt compositions back to a source composition, lava compositions are projected back towards a point of intersection with the within-plate source variation line along trends of fractional crystallization and partial melting.

The trends shown on Figure 6.3b have been modelled for an average crystallizing assemblage of olivine, 90 percent and chrome spinel, 10 percent followed by olivine, 20 percent, clinopyroxene, 30 percent, and plagioclase, 50 percent, while partial melting trends are modelled assuming a source composition equivalent to olivine, 60 percent, orthopyroxene, 20 percent, clinopyroxene, 10 percent and plagioclase 10 percent in which the phases enter the melt in the ratio 3:1:4:4 respectively (after Pearce and Norry, 1979). These trends can be modelled for different degrees of open and closed system fractionation and partial melting. They do not however, produce compositions with marked differences in Zr/Y ratios when small changes are made to the petrogenetic variables involved (ie. degree of partial melting, open versus closed system fractionation, and the proportions of the phases involved) (Pearce and Norry, 1979). Hence, significant differences in Zr/Y ratios observed between different rock suites can, for the most part, be well explained only by varying degrees of within-plate related mantle depletion or enrichment.

From Figure 6.3c it can be therefore be suggested that:

(i) Rocks of the plagioclase porphyritic suite were derived from a more depleted mantle source than that which produced aphyric/clinopyroxene-phyric suite rocks of the Dun Mountain Ophiolite or MORB basalts of the Patuki and

**Croisilles mélanges.**

(ii) Aphyric/clinopyroxene-phyric suite basalts of the Dun Mountain Ophiolite and MORB basalts of the Patuki and Croisilles mélanges may have been derived from mantle sources which have undergone similar degrees of within-plate related depletion, but may have undergone different degrees of open system fractionation.

(iii) Basalts of the within-plate ("olivine-rich") suite of the Patuki mélange were derived from an enriched mantle source. The apparent range of mantle compositions associated with within-plate basalts may however, be explained in a number of ways including: systematic source heterogeneities; variations in the degree of partial melting of a garnet lherzolite source; progressive melting of a single source; fractional crystallization involving garnet as an important crystallizing phase (eg., Pearce and Flower, 1977; Pearce and Norry, 1979); and, partial melting of an upper mantle source which has been enriched in incompatible elements by CO<sub>2</sub>-rich fluids or undersaturated melts derived from the asthenosphere or low-velocity zone (LVZ) (eg., Green, 1971; McCulloch et al., 1983; Hart, 1988; Nelson et al., 1988). As assessment of such processes is beyond the scope of the present study they are not evaluated further.

As for the difference in Zr/Y ratios observed between MORB and within-plate basalts, Pearce and Norry (1979) have concluded that these differences are likely the result of "long-lived" source heterogeneities rather than recent progressive melting variations.

### 6.2.3 Partial Melting and Fractional Crystallization

One method of modelling the nature and degree of fractional crystallization, partial melting, and to some extent, magma mixing, is to use diagrams which plot a compatible element against an incompatible element. One such diagram that has been widely used and found to be effective in evaluation of these processes is the Cr-Y diagram of Pearce (1980). These elements are plotted (Figure 6.4a) as they are not significantly affected by processes which cause mantle heterogeneities. As a result, two assumptions can be made:

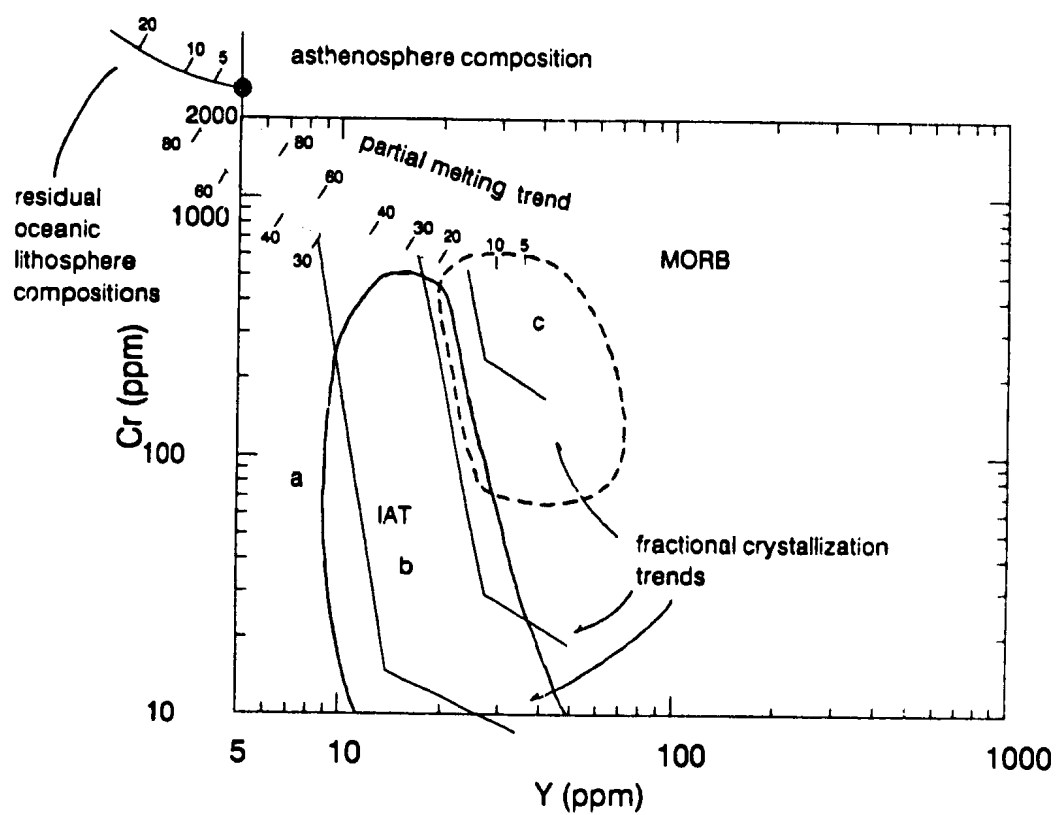
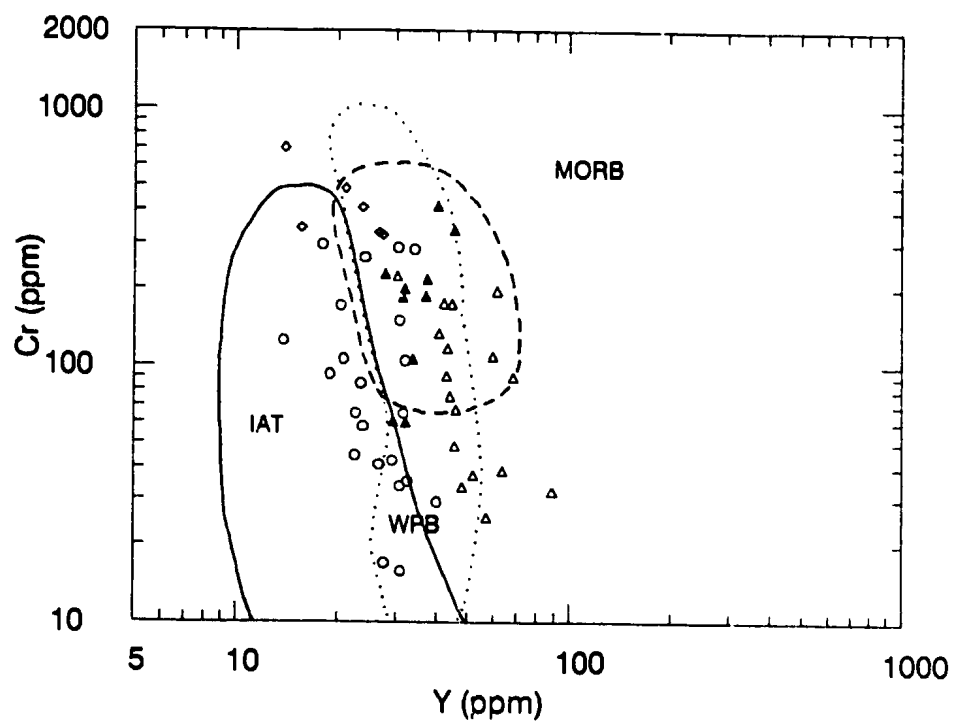
- (i) The mantle sources for basalts erupted from different tectonic settings probably contain Cr and Y abundances similar to primordial mantle concentrations (Pearce, 1980).
- (ii) Certain compositional variations observed between different basaltic suites can be attributed to differences in partial melting and fractional crystallization histories rather than mantle source heterogeneities (Pearce, 1980).

Another important feature of this diagram is that, unlike the previously described diagrams, trends defined for fractional crystallization and partial melting are quite distinct, and can therefore be discriminated from one another (Figure 6.4b).

Figure 6.4b displays petrogenetic trends involved in the partial melting of a mantle source (after Pearce et al., 1984) composed of olivine, 60 percent, orthopyroxene, 20 percent, clinopyroxene, 10 percent and plagioclase, 10 percent in which the phases melt in the ratio 3:1:4:4 (as

**Figure 6.4a** Cr versus Y variation diagram of Pearce (1980), Pearce et al. (1981) and Pearce et al. (1984). MORB= mid-ocean ridge basalt; VAB= volcanic arc basalt; WPB= within-plate basalt. Symbols as used in Figure 5.16.

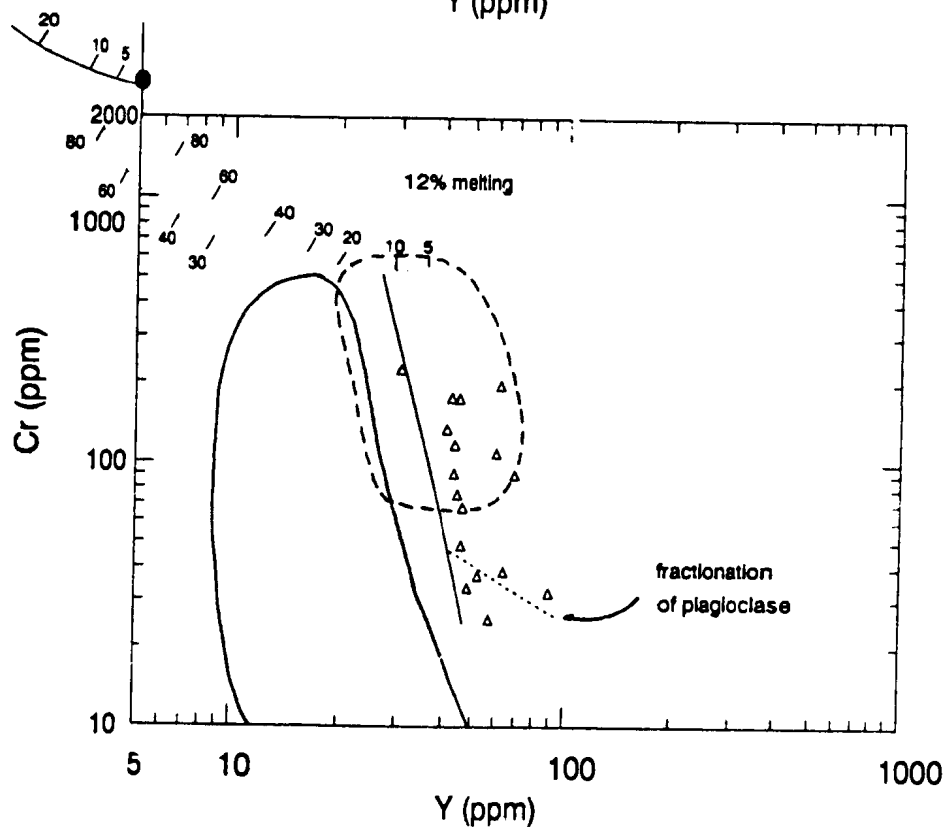
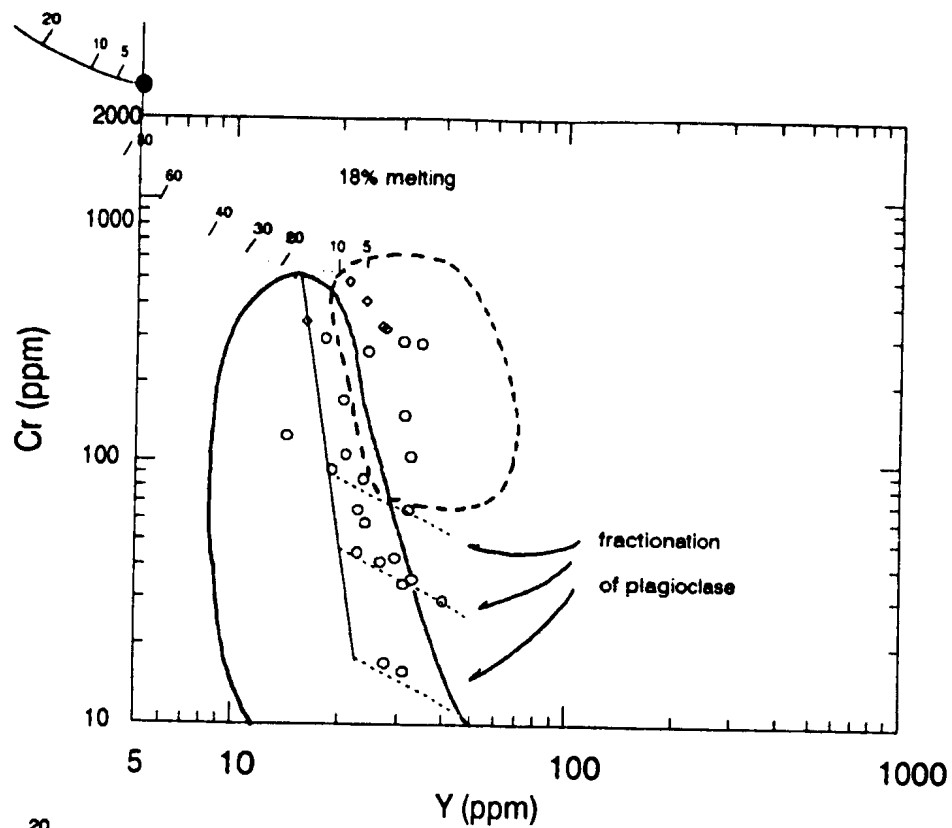
**Figure 6.4b** Petrogenetic pathways for ophiolites of different tectonic affinities plotted on a Cr versus Y diagram after Pearce et al. (1984). Pathway "a" = mid-ocean ridge ophiolites; pathway "b" = supra-subduction zone ophiolites of island-arc tholeiitic affinities; pathway "c" = supra-subduction zone ophiolites of boninitic affinities. Full details of components of pathways and method of modelling are documented in Pearce et al. (1984). Estimated asthenosphere composition after Pearce et al. (1984).





**Figure 6.4c** Estimated petrogenetic trends for basaltic rocks of the Dun Mountain Ophiolite plotted on a Cr versus Y diagram. Symbols as used in Figure 5.16. Field boundaries have been taken from Pearce et al. (1984). On this diagram basaltic rocks of Dun Mountain Ophiolite are suggested to have been produced by partial melting of an previously depleted mantle source.

**Figure 6.4d** Estimated petrogenetic trends for "olivine-poor" suite basaltic rocks of the Patuki and Croisilles mélanges plotted on a Cr versus Y diagram. Symbols as used in Figure 5.16. Field boundaries and partial melting trends taken from Pearce et al. (1984).



modelled in the Zr/Y-Zr diagram earlier in this chapter). From this diagram, it can be observed that during partial melting Y concentrations decrease within the melt with increased degrees of melting, while Cr concentrations are virtually unchanged. It can also be observed that melting trends run subparallel to the yttrium axis for smaller degrees of partial melting, as a result of residual phases such as chrome spinel, olivine, and pyroxene which act to buffer Cr concentrations (Pearce, 1980).

In contrast to the partial melting trends, fractional crystallization trends are more linear, and tend to be steeper depending on the mineral phases involved. In Figure 6.4b, the steeper trends represent crystallization of olivine + chrome spinel  $\pm$  clinopyroxene, while the shallower trends represent crystallization of olivine + chrome spinel + clinopyroxene + plagioclase.

The petrogenetic paths used here are those of Pearce et al. (1984) and have been modelled for basalts of different tectonic affinity including boninite, island-arc tholeiite and MORB compositions. The pathways have also been drawn in accordance with criteria obtained through observations of field and petrographic relationships from ophiolites produced in different tectonic settings. Pathway "c" represents the pathway for typical basalts from MORB ophiolites. Projection of MORB basalt compositions back to the partial melting trend suggests that basalts of this type are typically derived from 15 percent partial melting followed by fractional crystallization of olivine + chrome spinel, followed by plagioclase and pyroxene. Pathway "b" represents the pathway for basalts from typical supra-subduction zone (SSZ) ophiolites. Projection of these compositions back to the partial melting trend indicates

that one method of producing SSZ basalts is by higher degrees of partial melting of a similar source than that required for the production of MORB ophiolites (approximately 30 percent), and that the involvement of plagioclase as an important crystallizing phase likely takes place later in the crystallization history. Pathway "a" represents the pathway of a typical boninitic composition from an ophiolite complex. Unlike the other pathways, projection of the boninitic composition back to the primordial mantle partial melting trend involves approximately 80 percent partial melting. As this situation is considered to be highly unlikely, a previously depleted mantle source is favoured by Pearce et al. (1984). The partial melting of a previously depleted mantle is indicated on Figure 6.4b.

Through comparison of the pathways modelled by Pearce et al. (1984) for other ophiolites, the degree and nature of partial melting and fractional crystallization can now be evaluated for rocks of the East Nelson ophiolites. In Figures 6.4c and 6.4d data is plotted for rocks of the Dun Mountain Ophiolite and the "olivine-poor" (MORB) suite of the Patuki and Croisilles mélanges. On these figures, petrogenetic paths can be defined by the data for each of the suites plotted and suggest:

(i) Tholeiitic rocks of the Dun Mountain Ophiolite (Figure 6.4c) were likely produced by processes similar to those thought to be involved in the production of island-arc tholeiitic basalts from typical SSZ ophiolites.

(ii) "Olivine-poor" suite basalts of the Patuki and Croisilles mélanges (Figure 6.4d) were likely produced by processes similar to those thought to be involved in the production of MORB.

In addition to these observations, other, more detailed observations can also be made from the data plotted.

Rocks of the plagioclase porphyritic suite appear to have fractionated and possibly accumulated plagioclase relatively early in their petrogenetic history, while rocks of the aphyric/clinopyroxene-phyric suite appear to have crystallized plagioclase after various degrees of fractional crystallization of olivine + chrome spinel  $\pm$  clinopyroxene. This suggests that closed system fractionation operated during the production of these rocks as the initiation of plagioclase crystallization appears to have taken place at a variety of points along the olivine + chrome spinel  $\pm$  clinopyroxene crystallization path (Figure 6.4c). As a result, a steady-state basalt composition was not maintained during the spreading history of the Dun Mountain Ophiolite, a feature commonly associated with slow spreading ridges (eg. Alabaster et al., 1982).

In contrast to the rocks of the Dun Mountain Ophiolite, MORB basalts of the Patuki and Croisilles mélanges tend to plot along a fractional crystallization trend involving crystallization of olivine + chrome spinel, and therefore suggest that open system fractional crystallization may have operated during production of these MORB basalts, a feature often associated with fast spreading ridges (eg. Alabaster et al., 1982).

Since the degree of partial melting approximated for production of the island-arc tholeiitic suites from Pearce et al.'s estimated asthenosphere source composition is quite high (approximately 35 percent); it is proposed that these suites were likely produced by smaller degrees of partial melting involving an already depleted mantle source (here estimated to have undergone 10



percent partial melting prior to production of the Dun Mountain Ophiolite as indicated in Figure 6.4c). This explanation for the depleted character of these rocks follows those of previously proposed models that seek to explain the petrogenesis of supra-subduction zone basalts including island-arc tholeiites and boninitic lavas (eg. Green et al., 1987).

The petrogenetic history of "olivine-rich" (within-plate) suite basalts of the Patuki mélange is not assessed on the above Cr-Y diagrams. However it is proposed that basalts of this nature are produced by:

- (i) partial melting of a heterogeneous mantle source in which garnet may be involved as a major phase (eg. Pearce and Flower, 1977); or,
- (ii) partial melting of an upper mantle source which has been enriched in incompatible elements by CO<sub>2</sub>-rich fluids or undersaturated melts derived from the asthenosphere or low-velocity zone (LVZ) (eg., Green, 1971; McCulloch et al., 1983; Hart, 1988; Nelson et al., 1988).

Such partial melting and fractional crystallization trends are not modelled here as it is difficult to place realistic constraints on source compositions and paths of petrogenetic evolution.

### 6.3 Summary

It appears that as many as four compositionally distinct mantle sources may have been involved in the production of basaltic rocks of the East Nelson ophiolites. Within the Dun Mountain Ophiolite, rocks of the plagioclase porphyritic suite appear to have been derived from a highly depleted mantle source, which in some ways, resembles that which is

considered to produce lavas of boninitic compositions. Rocks of the aphyric/clinopyroxene-phyric suite; however, appear to have been derived from a less depleted source which is slightly more depleted than mantle compositions which are believed to produce normal mid-ocean ridge basalts. As for basalts of the Patuki and Croisilles mélanges, rocks of the "olivine-poor" or MORB suite appear to have been derived from a depleted mantle source similar to that which is considered to produce normal MORB basalts while basalts of the "olivine-rich" or within-plate alkali basalt suite appear to have been derived from an enriched mantle source. This enriched source appears to have included a broad range of compositions as suggested by the spread of the geochemical data.

In terms of partial melting and fractional crystallization processes, rocks of the Dun Mountain Ophiolite and "olivine-poor" (MORB) suite appear to have followed petrogenetic paths similar to those defined for island-arc tholeiites and mid-ocean ridge basalts respectively. Rocks of the Dun Mountain Ophiolite appear to have formed by closed system fractionation, while "olivine-poor" (MORB) suite basalts may have formed by open system fractionation.

## CHAPTER 7

### TECTONIC MODELS

#### 7.1 Introduction

Tectonic modelling of the formation and emplacement of the Dun Mountain Ophiolite Belt has in the past been hampered as tectonic reconstructions of Gondwana's late Palaeozoic "Pacific" margin were proposed in the absence of knowledge of the number, polarity and nature of arcs, subduction zones, and crustal types involved. In the absence of such constraints the tectonic evolution of the East Nelson ophiolites has become the topic of much debate. This study attempts to provide additional constraints for models of the evolution of the rocks. These constraints are the result of examination of new geochemical and petrographic data as well as observation of field relationships from ophiolites of the Nelson segment of the Dun Mountain Ophiolite Belt (East Nelson ophiolites). In this section, the implications of this work are discussed in light of previously proposed models and a number of possible models are reviewed.

#### 7.2 Previous Tectonic Models

Previously proposed tectonic models for the formation of the Dun Mountain Ophiolite Belt (including the ophiolites of East Nelson) can be

divided into three distinct groups:

(i) those that suggest the Dun Mountain Ophiolite represents spreading in a fore-arc basin east of the Brook Street volcanic arc above a westward-dipping subduction zone (eg., Coombs et al., 1976; Davis et al., 1980);

(ii) those that suggest the Dun Mountain Ophiolite represents oceanic crust formed in a mid-ocean ridge type basin that has been juxtaposed against rocks of the Brook Street volcanic arc by subduction (eg. Coombs et al., 1976); and,

(iii) those which propose the Dun Mountain Ophiolite was formed by back-arc spreading behind the Brook Street volcanic arc above an eastward-dipping subduction zone (eg. Coombs et al., 1976).

Until recently, the Brook Street and Murihiku terranes were considered to share a sedimentary contact, with a number of workers suggesting the Brook Street terrane may have been involved as a source of detritus for sedimentary rocks of the Murihiku and Maitai terranes (eg., Coombs et al., 1976; Howell, 1980; MacKinnon, 1983; and Bishop et al., 1985). Landis et al. (1987) and Landis (1987) have however, shown that the Brook Street and Murihiku terranes share only faulted contacts. Frost and Coombs (1987) and Coombs (1988; see Haston et al., 1989) have also suggested on the basis of neodymium isotope data that the Brook Street terrane has a mantle source, while the Murihiku terrane has a continental origin. These observations, coupled with palaeomagnetic evidence presented by Haston et al. (1989) suggests the Brook Street and Murihiku terranes are genetically distinct, and indicate that there are no clearly demonstrable links between the Brook

Street and other terranes of New Zealand's Eastern Province prior to Late Cretaceous time (see Haston et al., 1989). In light of these observations, models which do not propose genetic links between the Dun Mountain Ophiolite and the Brook Street terrane are discussed here for the origin of the Dun Mountain Ophiolite and the other East Nelson ophiolites.

Models proposed for formation of the Dun Mountain Ophiolite and its incorporation within the Dun Mountain Ophiolite Belt are constrained by a number of features observed within the ophiolite and the associated Patuki and Croisilles mélanges. These constraints include: (i) the relative ages of the ophiolites and their associated sediments; (ii) field relationships exhibited by rocks of the belt; (iii) the distinct geochemical characteristics of rocks of the Dun Mountain Ophiolite and the Patuki and Croisilles mélanges; and, (iv) the regional setting of the East Nelson ophiolites.

#### 7.2.1 Age Dates

Age dates for rocks of the East Nelson ophiolites have been produced both radiometrically and by fossil dating. These ages suggest that:

(i) the Dun Mountain Ophiolite is of Lower Permian age (268 Ma by U-Pb; Kimbrough and Coombs, 1988);

(ii) the oldest sedimentary rocks (dated) which overly the Dun Mountain Ophiolite, the Wooded Peak Limestones, are late Middle Permian (Punjabian) age (Waterhouse, 1979);

(iii) ophiolitic rocks of the Croisilles mélange are of Lower Permian age (280-283 Ma, U-Pb; 265-272 Ma, K-Ar; Dickins et al., 1986); and,



(iv) sedimentary blocks within the Croisilles mélange that likely represent sedimentary material deposited on the Croisilles ophiolite are considered to be Upper Permian in age (Dickins et al., 1986).

Relative ages of these rocks suggest that ophiolitic rocks and associated sediments of the Dun Mountain Ophiolite and the Patuki and Croisilles mélanges are of similar age<sup>1</sup>.

Ages of what may be subduction related metamorphic events, formation of shear zone associated amphibolite within the Patuki/Croisilles mélanges, indicate these events as having occurred 202-216 Ma ago (K-Ar; Sivell, 1988). This suggests that tectonic emplacement of the mélanges may have occurred by Middle Triassic time.

Another point worth noting here is that it is generally accepted that rocks of the East Nelson ophiolites were juxtaposed against rocks of the Caples-Pelorus terrane prior to deposition of Late Jurassic Torlesse sediments (eg., Coombs et al., 1976; Carter et al., 1978).

The above chronological information suggests rocks of the Dun Mountain Ophiolite and the Patuki and Croisilles mélanges are of similar age and that they were juxtaposed by Middle Triassic times, possibly earlier.

#### 7.2.2 Field Relationships

Rocks of the Dun Mountain Ophiolite are unconformably overlain by the basal formation of the Maitai Group, the Upukerora Formation.

---

<sup>1</sup> It is proposed here that the Croisilles and Patuki ophiolitic mélanges represent vestiges of the same ocean crust and are of similar age.

Conglomerates of the Upukerora Formation appear to have been derived from material eroded from upper levels of the ophiolite and were likely deposited during a period of extensive uplift and erosion as they in places, directly overlie gabbros of the ophiolite. Upukerora conglomerates are in turn overlain by limestones of the Wooded Peak Formation. These limestones are considered to be Punjabiian age (late Middle Permian) and were likely deposited after a depositional hiatus, as clasts of Wooded Peak Limestones are not observed within the Upukerora Formation. Unfortunately, the author is unaware of any reliable age dates for the Upukerora Formation but it is likely Middle Permian age. It is also worth noting here that sheeted dyke sequences are in places orientated sub-parallel to the Maitai Group-ophiolite contact, suggesting extensive listric faulting and block rotation may have occurred prior to deposition of Maitai Group sediments.

Rocks of the Patuki *mélange* are separated from those of the Dun Mountain Ophiolite by a faulted contact situated at the base of the Dun Mountain Ultramafics Group. As a result, rocks of the Patuki *mélange* are considered to structurally underlie the Dun Mountain Ophiolite.

Both the Patuki and Croisilles *mélanges* are considered to represent vestiges of oceanic crusts (ophiolites) preserved as tectonic *mélanges*. Both consist of blocks of ophiolitic material suspended in matrices of sheared serpentinite (and locally sheared sediments). Unfortunately, no internal order could be consistently established within these units; although at some localities, blocks appear to be arranged in a semi-ordered sequence as sedimentary and volcanic rocks outcrop along the *mélange*'s western margin

while blocks of ultramafic material outcrop along the eastern contact.

In terms of structural and metamorphic relationships, rocks of the Dun Mountain Ophiolite Belt appear to have undergone two major episodes of deformation and metamorphism. The first episode is credited with deformation and greenschist grade metamorphism of the ophiolites on the ocean floor while the second episode is attributed to regional tectonism and sub-greenschist grade metamorphism of the ophiolites during and after emplacement.

While on the sea-floor, rocks of the Dun Mountain Ophiolite appear to have undergone extensive deformation which produced zones of ductile deformation at the base of the high level gabbros. Within these zones gabbroic rocks are amphibolitized and have a flazered appearance. Locally, these zones are intruded by rare, relatively undeformed diabase dykes suggesting deformation within the zones occurred on the sea-floor. These amphibolitized zones are typically observed along the fault contact between gabbros and ultramafics rocks of the Dun Mountain Ophiolite and may have acted as early planes of weakness which were utilized during initial obduction events.

### 7.2.3 Petrological and Geochemical Data

Petrographic and geochemical relationships observed within mafic rocks of the East Nelson ophiolites suggest the Dun Mountain Ophiolite and the Patuki and Croisilles mélanges represent two distinct ophiolitic assemblages, the Dun Mountain Ophiolite being composed of oceanic crust produced in a

marginal basin above a subduction zone, while the *mélanges* represent vestiges of ocean crust(s) produced within a normal ocean basin at a mid-ocean ridge and within-plate volcanoes. Trace element concentrations observed within basaltic rocks of the Dun Mountain Ophiolite suggest spreading occurred above a subduction zone in which oceanic crust was subducted below oceanic crust as there is no evidence of contamination by continental crustal material (as suggested by the ophiolites low Zr/Y ratios).

As basaltic rocks of the Patuki and Croisilles *mélanges* are compositionally indistinguishable (aside from the absence of within-plate alkali basalts within the Croisilles *mélange*), it is suggested here that the *mélanges* represent highly disrupted portions of the same ocean basin.

Since initiation of this study, Sivell (1988) has described the occurrence of an additional suite of mafic rocks within the Croisilles *mélange*. These rocks consist of a younger suite of cross-cutting dykes and irregular intrusions which are compositionally similar to island-arc tholeiites. Sivell (1988) suggests these rocks were produced as a result of partial melting of depleted mantle above a subduction zone after oceanward stepping-out of a westward-dipping subduction zone.

#### 7.2.4 Regional Setting

It has been proposed by previous workers (eg., Coombs et al., 1976; Davis et al., 1980) that rocks of the East Nelson ophiolites were involved in the evolution of a westward-dipping subduction zone, now represented by the faulted contact at the base of the Dun Mountain Ophiolite. Previously

presented evidence which supports the existence of a remnant subduction zone at this location is based upon:

- (i) the observation of the positive Junction Magnetic Anomaly (Hatherton, 1969) which has been traced by Hatherton (1969) and Hatherton and Sibson (1970) for a distance of 670 kilometres and possibly 1100 kilometres (see Coombs et al., 1976);
- (ii) observed differences in structural and metamorphic styles between rocks of the Dun Mountain-Maitai terrane and the adjacent Caples-Pelorus terrane (eg., Coombs et al., 1976);
- (iii) the tectonic position and facing direction of the Dun Mountain Ophiolite (eg. Coombs et al., 1976).

### 7.3 Tectonic Models

In light of the geological evidence outlined above a number of assumptions can be made about the formation and emplacement of the East Nelson ophiolites.

The ophiolites represent oceanic crusts produced in at least two different ocean basins during the Lower Permian and were likely juxtaposed against one another by Middle Triassic time, possibly earlier.

The Dun Mountain Ophiolite appears to have undergone a period of extensive uplift and erosion prior to late Middle Permian Time.

The base of the Dun Mountain Ophiolite represents a major structural discontinuity which is regional in extent and likely represents the hanging wall of a once active subduction zone.



Rocks of the Patuki *mélange* are considered to structurally underlie those of the Dun Mountain Ophiolite and are likely representative of oceanic crust subducted prior to Middle Triassic time.

In light of these considerations it is proposed here that the Dun Mountain Ophiolite was produced by igneous activity above a westward-dipping subduction zone in which normal ocean crust, represented by the Patuki and Croisilles *mélanges*, was subducted during Lower Permian times (Figure 7.1a). Although the crusts involved are of similar age, it is suggested that subducted ocean crust was produced at a mid-ocean spreading ridge east of the trench and therefore older crust was initially subducted<sup>2</sup>. Subduction of this older crust induced partial melting of depleted mantle material above the subduction zone after hydration of the mantle and variable enrichment in hygromagmatophile elements such as Th had taken place. This melting produced intrusion and volcanism at a spreading ridge or ridges similar to those associated with early stages of arc volcanism at an incipient island-arc (eg. Natland and Tarney, 1981). At this ridge (or ridges) tholeiitic basalts of the Dun Mountain Ophiolite were extruded (Figure 7.1b).

At some time prior to late Middle Permian time (Punjabian), rocks of the Dun Mountain Ophiolite underwent a period of extensive uplift and erosion which produced conglomeratic deposits of the Upukerora Formation and later deposition of limestones of the Wooded Peak Formation (Figure 7.1c). This period of uplift and erosion may have resulted from jamming (possibly due to

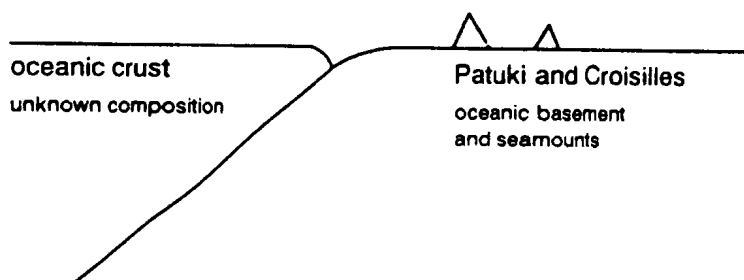
---

<sup>2</sup> Radiometric age dates suggest that it is likely that ophiolitic rocks of the Patuki and Croisilles *mélanges* are slightly older than those of the Dun Mountain Ophiolite.

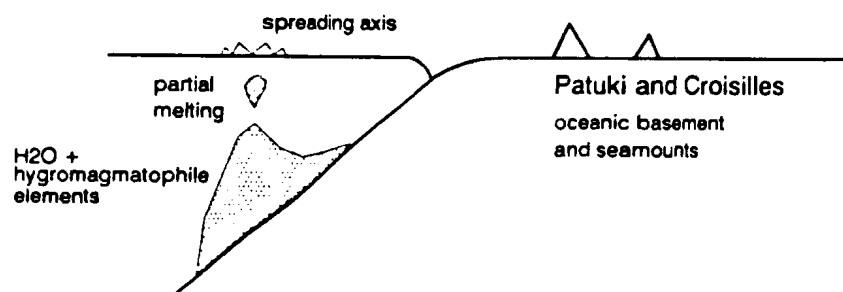
**Figure 7.1** Schematic tectonic model for evolution of the East Nelson ophiolites. During the Early Permian, subduction of oceanic basement material took place (diagram "A") beneath other oceanic crust of unknown composition (possibly similar to that being subducted). This activity induced partial melting of the overlying crusts due to hydration of mantle material above the subducted slab (diagram "B"). As a result active sea-floor spreading was initiated and oceanic crustal material of the Dun Mountain Ophiolite was formed. By the late Middle Permian the subduction zone is considered to have jammed; possibly due to failed subduction of seamounts associated with the Patuki mélange (diagram "C"). This resulted in oceanward stepping out of subduction, uplift and erosion of the Dun Mountain Ophiolite, and later deposition of Maltai Group Limestones. By Late Permian (possibly Early Triassic) this second episode of subduction may have produced partial melting and intrusive activity within "trapped" oceanic crust (diagram "D") above the subduction zone (as represented by stage III plutonic rocks of Sivell, 1988; see text). By the Early Cretaceous the East Nelson ophiolites are considered to have been juxtaposed against rocks of the Caples-Pelorus terrane and largely destroyed by subsequent tectonic activity. See text for details.

**A**

initial subduction

Early Permian  
(or earlier)**B**sea-floor spreading above subduction zone  
production of Dun Mountain Ophiolite

Early Permian



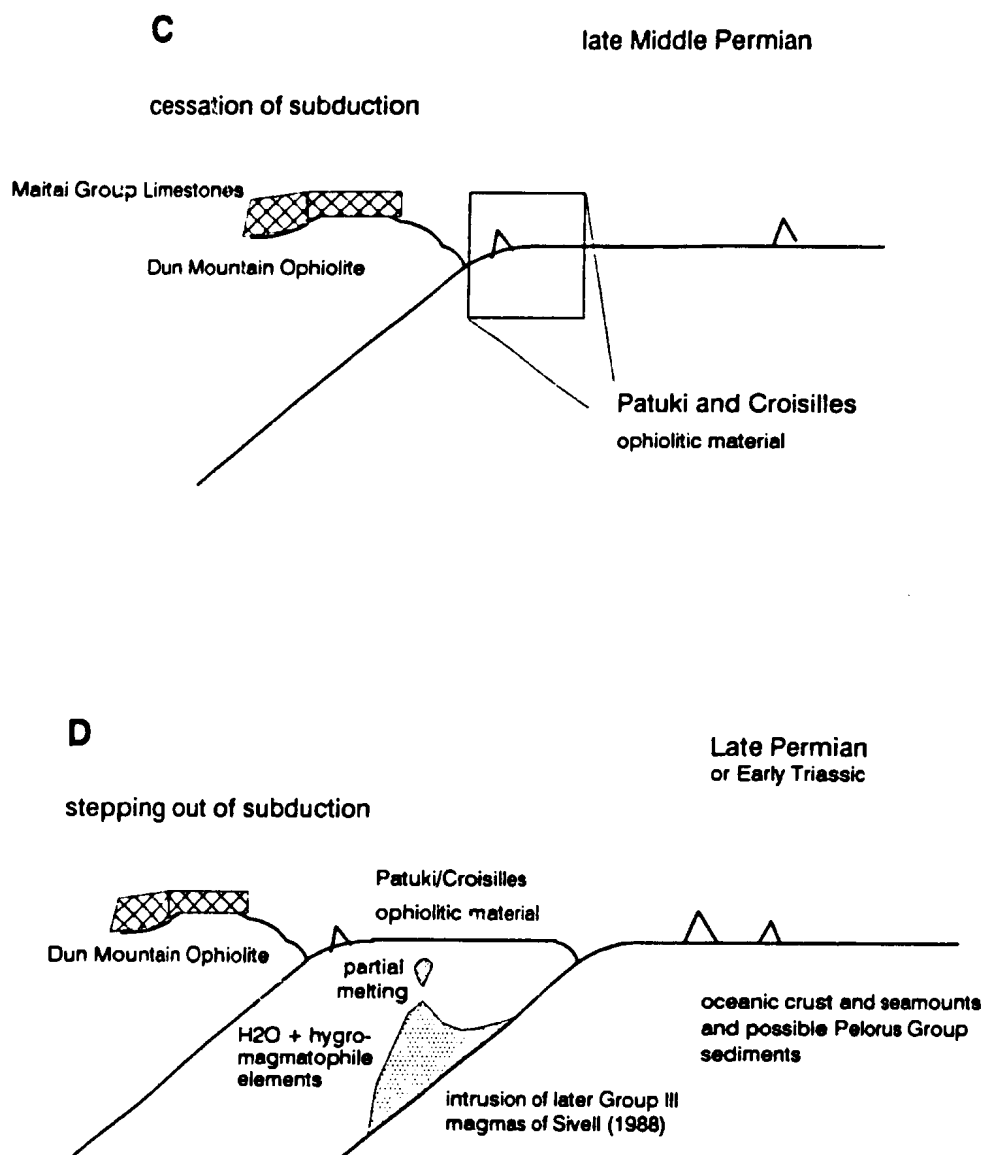


Figure 7.1 (continued) Tectonic model for the evolution of the East Nelson ophiolites.

**E**

Early Cretaceous

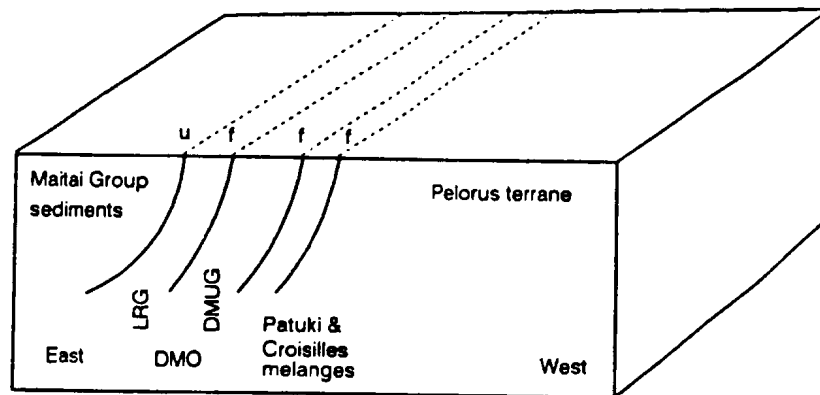


Figure 7.1 (continued) Tectonic model for the evolution of the East Nelson ophiolites.



subduction of oceanic seamounts on Patuki oceanic crust) and possible oceanward stepping-out of the subduction zone. Cessation of subduction likely marked the end of igneous activity within the marginal basin (the Dun Mountain Ophiolite) as basaltic rocks of the ophiolite are not observed intruding limestones of the Wooded Peak Formation.

Stepping-out of the subduction zone likely induced arc related igneous activity to the east of the Dun Mountain Ophiolite within trapped normal ocean basin crusts of the Patuki and Croisilles mélanges (Figure 7.1d), as indicated by the presence of island-arc tholeiitic intrusive rocks within the Croisilles mélange as observed by Sivell (1988). Sivell suggests this igneous activity likely took place prior to or during Triassic time. Such activity may also explain the separation of rocks of the Croisilles mélange from those of the Patuki mélange as tectonic activity related to the cessation of subduction may have caused deformation and uplift of blocks of the oceanic basement material of the subducting plate outboard (oceanward) of the subduction zone. It should be noted here however, that other explanations for emplacement of the Croisilles mélange exist. It is possible that rocks of the Croisilles mélange represent portions of Patuki mélange that have been displaced by strike-slip movements along faults during the Rangitata and Kaikoura orogenies.

#### 7.4 Discussion

Although a fore-arc model for formation of the Dun Mountain Ophiolite is favoured here, a number of alternative models can also be proposed to

explain formation of the Dun Mountain Ophiolite and its relationship to the other East Nelson ophiolites.

Coombs et al. (1976) posed the possibility that the Dun Mountain Ophiolite may represent oceanic crust produced within a back-arc basin. If this was the case, it is likely that arc related calc-alkaline crusts would be preserved within or along side rocks of the Dun Mountain Ophiolite, particularly if island-arc tholeiites of the ophiolite were produced during initial stages of formation of a back-arc basin. Such rocks were not observed. If, on the other hand, the Dun Mountain Ophiolite represents oceanic crust produced within an evolved back-arc basin; it is likely basaltic rocks similar to mid-ocean ridge basalt would be observed similar to those observed within the Lau Basin (eg. Hawkins and Melchoir, 1985). Such compositions were not observed within the Dun Mountain Ophiolite. Other complications to such a model include the existence of an eastward-dipping subduction zone to the west of the Dun Mountain Ophiolite during the Lower Permian and a reversal of subduction zone polarity. Due to the complexity of such a model a fore-arc model is favoured here; however, it is possible that rock types diagnostic of a back-arc basin were destroyed or displaced during subduction or later tectonic events.

Aside from the model's simplicity, evidence which may support fore-arc formation of the Dun Mountain Ophiolite includes the existence of the highly depleted, plagioclase porphyritic suite diabase dykes and gabbro within the ophiolite. The highly depleted nature and supra-subduction zone chemistry of these rocks suggest they may have been produced by processes similar to

those believed to be responsible for the genesis of boninitic or "low-Ti" lavas. Basaltic rocks of this nature are commonly associated with initial stages of fore-arc spreading in supra-subduction environments (eg. Mariana fore-arc; Natland and Tarney, 1981) or ophiolite complexes (eg. western Tasmania, Brown and Jenner, 1989).

Although the existence and location of adjacent island-arcs are not indicated within the model proposed here, it has been suggested that oceanic crusts of the Dun Mountain Ophiolite and Patuki and Croisilles mélanges are overlain by sediments which may have an arc signature (eg., Davis et al., 1980; Dickins et al., 1986; Landis and Blake, 1987). As a result, it has previously been proposed that an island-arc or island-arcs had existed in the vicinity of East Nelson ophiolites. If such was the case, it is likely that ocean crusts of the East Nelson ophiolites were formed along an oceanic-oceanic plate boundary in the vicinity of evolved island-arcs. A modern analogy of such an environment may include ocean crusts of the Philippine Sea or Lau Basin where marginal basin crusts occur along destructive plate boundaries involving crusts of the Pacific Plate. These boundary areas are characterized by fore-arc crusts of the Mariana fore-arc and fore-arc regions of the Tonga Ridge.

Although stepping-out of a westward-dipping subduction zone is suggested in the model presented here, other hypotheses have been proposed to explain the existence of arc related intrusive rocks within the Patuki mélange of north D'Urville Island. As the Patuki mélange consists of highly disrupted ophiolitic blocks suspended in a matrix of sheared

serpentinite, and rocks of the East Nelson ophiolites have been disrupted by faults related to movements along the Alpine Fault during the Rangitata and Kaikoura orogenies (eg. Johnston, 1981); it is possible that tectonic blocks of gabbroic material of the Dun Mountain Ophiolite may have been tectonically incorporated within the Patuki mélange. Such occurrences are likely rare but may explain the existence of arc related rocks within the Patuki mélange as well as the noted resemblance (Sivell, 1988) of these rocks to those of the Dun Mountain Ophiolite.

## CHAPTER 8

### SUMMARY AND CONCLUSIONS

In the East Nelson area, the East Nelson ophiolites comprise potentially three separate ophiolite suites; the Dun Mountain Ophiolite, the Patuki mélange and the Croisilles mélange.

The Dun Mountain Ophiolite represents an ophiolite suite comprised of mafic volcanic and plutonic rocks of the Lee River Group and underlying ultramafic rocks of the Dun Mountain Ultramafics Group. The contact between these units is marked by faulting along which basal gabbros of the Lee River Group are commonly highly deformed and amphibolitized taking on a flasered appearance. Diabase intrusive relationships suggest that initiation of this deformation took place while the ophiolite was evolving on the sea floor.

Rocks of the Dun Mountain Ophiolite, for the most part, lack cumulate gabbroic sequences commonly observed in other ophiolites such as Troodos in Cyprus or the Bay of Islands in Newfoundland. It is probable that these rocks were tectonically removed during obduction and later tectonism of the ophiolite; however, local occurrences of critical zone gabbros are observed in places as fault bounded blocks along the faulted contact between mafic rocks of the Lee River Group and Dun Mountain Ultramafics Group (eg. Red Hills



western margin). These rocks are considered to represent crystal fractionates of the overlying Lee River Group high level gabbros.

Overlying mafic volcanic and plutonic rocks of the Lee River Group are local accumulations of conglomeratic material composed of clasts of mafic volcanic and plutonic rocks suspended in a sand and mud matrix. This sedimentary unit is known as the Upukerora Formation. Clasts within this formation closely resemble lithologies observed within higher levels of the Dun Mountain Ophiolite (Lee River Group) and a number of pyroxenes analyzed from clasts were found to be compositionally similar to those observed within volcanic and subvolcanic rocks of the Lee River Group.

The Patuki and Croisilles ophiolitic mélanges lie in fault contact with, and structurally underlie rocks of the Dun Mountain Ophiolite, but are separated from one another by sedimentary rocks of the Rai terrane. The mélanges consist of blocks of sedimentary, mafic to ultramafic volcanic and plutonic rocks suspended in matrices of sheared serpentinite and locally sheared sediments. Although these rocks are highly disrupted they are considered to represent vestiges of true ophiolitic assemblages as the various lithologies of an ophiolite are observed within blocks of the mélanges. As the mélanges are highly tectonized and disrupted it is suggested that these rocks represent fragments of oceanic crust which have been subducted beneath the Dun Mountain Ophiolite.

Petrographic and geochemical evidence suggests the Dun Mountain Ophiolite consists of two distinct mafic suites of island-arc tholeiite composition; a plagioclase porphyritic suite and an aphyric/clinopyroxene-

phyric suite. Rocks of the aphyric/clinopyroxene-phyric suite represent more than 95 percent of the diabasic and volcanic rocks of the ophiolite while rocks of the plagioclase porphyritic suite are estimated to make up less than 5 percent. Field relationships suggest rocks of the plagioclase porphyritic suite were intruded intermittently during the ophiolite's evolution.

Both suites of the Dun Mountain Ophiolite appear to have been derived from a depleted mantle source above a subduction zone, and contain a supra-subduction zone compositional component. Rocks of the plagioclase porphyritic suite; however, appear to have been derived from a slightly more depleted source than rocks of the aphyric/clinopyroxene-phyric suite. The chemical compositions of these suites suggest the Dun Mountain Ophiolite was formed by sea-floor spreading above a subduction zone in a marginal basin.

Basaltic rocks of the Patuki and Croisilles mélanges can also be divided into two petrographically and geochemically defined suites, an "olivine-poor" suite and an "olivine-rich" suite. Both suites are petrographically similar but can be roughly distinguished by the relative abundances of olivine phenocrysts. Basalts of the "olivine-poor" suite generally contains less than 1 percent olivine phenocrysts while basalts of the "olivine-rich" suite generally contain more than 5 percent olivine phenocrysts. Both suites are observed within ophiolitic blocks of the Patuki mélange however, only basalts of the "olivine-poor" suite are recognized within the Croisilles mélange. Due to the identical petrographic and compositional nature of "olivine-poor" suite rocks from the Patuki and Croisilles mélanges, it is proposed that these rocks

represent vestiges of oceanic crusts from the same ocean basin and may represent disrupted portions of a single ophiolite sequence.

Chemical evidence suggests the "olivine-poor" and "olivine-rich" suites were produced in two distinct tectonic environments; basalts of the "olivine-rich" suite being compositionally similar to alkaline basalts erupted at within-plate ocean islands, while "olivine-poor" suite basalts resemble basalts erupted at mid-ocean ridge type settings. This suggests rocks of the Patuki and Croisilles mélanges were produced within a normal ocean basin similar to that of the Pacific Plate as oceanic basement and superimposed seamounts.

Petrogenetic evaluation of basaltic rocks of the East Nelson ophiolites suggest rocks of the Dun Mountain Ophiolite were produced by closed system fractionation at what was likely a slow spreading ridge, while "olivine-poor" suite basalts were more likely produced by open system fractionation at a faster spreading ridge.

A fore-arc environment of formation is favoured here for the origin of the Dun Mountain Ophiolite in which oceanic crust was subducted beneath oceanic crust and incipient arc related volcanism was induced above a westward-dipping subduction zone to produce the Dun Mountain Ophiolite. By this model the Patuki and Croisilles mélanges are considered to represent fragments of normal ocean crusts sheared off the subducted slab during subduction and separated either by tectonic movements related to cessation of subduction or later faulting associated with the Rangitata and Kaikoura orogenies. This model does not suggest any direct genetic links between the East Nelson ophiolites and island-arc rocks of the Brook Street terrane. It

should be noted however, that until palaeomagnetic studies are conducted on rocks of the East Nelson ophiolites, the possibility remains that these terranes are related and that they may have been brought into contact with rocks of the Murihiku terrane during tectonic movements associated with the Rangitata or Kaikoura orogenies.

Confirmation of the model presented here requires further detailed work, particularly in the areas of palaeomagnetic reconstructions and dating of petrogenetic and sedimentary events within terranes of New Zealand's Eastern Province. Such information may enhance knowledge of the number, polarity and nature of arcs, subduction zones, and ocean basins involved in the evolution of Gondwana's late Palaeozoic "Pacific" margin. In the absence of such tectonic constraints, relationships between various terranes of New Zealand's Eastern Province remain a mystery.

## REFERENCES

- Abbey, S., 1983: Studies in "standard samples" of silicate rocks and minerals, 1969-1982. Geological Survey of Canada Paper 83-15, 114p.
- Adams, C. J. D., 1975: Discovery of Precambrian rocks in New Zealand: Age relations of the Greenland Group and Constant Gneiss, West Coast, South Island. *Earth and Planetary Science Letters*, 28: pp.98-104.
- Adams, C. J. D., Morris, P. A. and Beggs, J. M., 1979: Age and correlation of volcanic rocks of Campbell Island and metamorphic basement of the Campbell Plateau, South-west Pacific. *New Zealand Journal of Geology and Geophysics*. vol.22: pp.679-962.
- Afifi, A. M. and Essene, E. J.,: Minfile user manual, Version 3-88. Unpublished. Department of Geological Sciences, University of Michigan, Ann Arbor Michigan.
- Anonymous, 1972: Penrose field conference on ophiolites. *Geotimes*, 17: pp.24-25.
- Alabaster, T., Pearce, J. A., and Malpas, J., 1982: The volcanic stratigraphy and petrogenesis of the Oman Ophiolite Complex. *Contributions to Mineralogy and Petrology*, 81: pp.168-183.
- Alt, J. C. and Emmermann, R., 1985: Geochemistry of hydrothermally altered basalts: Deep Sea Drilling Project Hole 504B, Leg 83. In: Initial Reports of the Deep Sea Drilling Project, volume.83, U.S. Government Printing Office, Washington, pp.249-262.
- Basaltic Volcanism Study Project (1981): Basaltic Volcanism on the Terrestrial Planets. Pergamon Press, Inc., New York. p.1286.
- Beccaluva, L., Macciotta, G., Piccardo, G. B. and Zeda, O., 1989: Clinopyroxene composition of ophiolite basalts as petrogenetic indicator. *Chemical Geology*, 77: pp.165-182.
- Beck, A. C., 1964: Sheet 14, Marlborough Sounds. Geological map of New Zealand 1:250 000 (1st edition). Wellington, New Zealand Department of Scientific and Industrial Research.
- Beggs, J. M., 1980: Sedimentology and paleogeography of some Kaihikuan Torlesse rocks in mid Canterbury. *New Zealand Journal of Geology and Geophysics*. vol.23: 439-445.



- Benson, W. N., 1926: The tectonic conditions accompanying the intrusion of basic and ultrabasic igneous rocks. *National Academy of Science Memoirs*. vol.19, No. 1, 90p.
- Bishop, D. G., Bradshaw, J. D., Landis, C. A., and Turnbull, I. M., 1976: Lithostratigraphy and structure of the Caples terrane of the Humbolt Mountains. *New Zealand Journal of Geology and Geophysics*. vol. 19: pp.827-848.
- Bishop, D. G., Bradshaw, J. D., and Landis, C. A., 1985: Provisional Terrane map of South Island, New Zealand. *In: Tectonostratigraphic Terranes*. D.G.Howell (editor), Circumpacific Council for Energy and Minerals Resources. Earth Sciences Series, No.1. Houston, Texas.
- Blake, Jr., M. C. and Landis, C. A., 1973: The Dun Mountain Ultramafic Belt. Permian oceanic crust and upper mantle in New Zealand. *Journal of Research, U.S. Geological Survey* 1: No.5, pp.529-534.
- Blake, Jr., M. C., Jones, D. L., and Landis, C. A., 1974: Active continental margins: contrasts between California and New Zealand. *In: C. A. Burk and C. L. Drake (editors), The Geology of Continental Margins*. Springer-Verlag, New York, pp.853-872.
- Boles, J. R., 1974: Structure, stratigraphy, and petrology of mainly Triassic rocks, Hokonui Hills, Southland, New Zealand. *New Zealand Journal of Geology and Geophysics*. vol.17, pp.337-374.
- Boudier, F. and Nicolas, A., 1982: Peridotite microtextures (II): In tectonites from Ultramafic sequences in ophiolites. *In: Atlas of deformational and metamorphic rock fabrics*. G.J. Borradaile, M.B. Bayly, and C. Powell, McA. (editors), Springer-Verlag, Berlin Heidelberg. 550p.
- Bradshaw, J. D., 1972: Stratigraphy and structure of the Torlesse Supergroup (Triassic-Jurassic) in the foothills of the Southern Alps near Hawarden. *New Zealand Journal of Geology and Geophysics*. vol.15, pp.71-87.
- Bradshaw, J. D., 1973: Allochthonous Mesozoic fossil localities in mélange within the Torlesse rocks of North Canterbury. *Journal of the Royal Society of New Zealand*, vol.3, pp.161-167.
- Bradshaw, J. D., 1989: Cretaceous geotectonic patterns in the New Zealand region. *Tectonics*, vol.8, No.4, pp.803-820.
- Bradshaw, J. D., and Andrews, P. B., 1973: Geotectonics and the New Zealand Geosyncline. *Nature*, 241: pp.14-16.
- Brooks, C.K., 1976: The  $\text{Fe}^2\text{O}^3/\text{FeO}$  ratio of basaltic analyses: an appeal for a standardized procedure. *Geological Society of Denmark, Bulletin* 25: pp.117-120.

- Brown, A. V. and Jenner, G. A., 1989: Geological setting, petrology and chemistry of Cambrian boninite and low-Ti tholeiite lavas in western Tasmania. In: A. Crawford (editor), *Boninites and related rocks*. Unwin Hyman, pp.232-263.
- Bruce, J. G., 1962: The geology of the Nelson city area. *Transactions of the Royal Society of New Zealand, Geology*, vol.1, No.11, pp.157-158.
- Cann, J. R., 1970: Rb, Sr, Y, Zr, and Nb in some ocean floor basaltic rocks. *Earth and Planetary Science Letters*, 10: pp.7-11.
- Campbell, J. D., (editor), 1975: *Gondwana Geology*. (Proceedings, 3rd Gondwana Symposium, Canberra, 1973). ANU Press, Canberra.
- Campbell, J. D. and Coombs, D. S., 1966: Murihiku Supergroup (Triassic-Jurassic) of Southland and South Otago. *New Zealand Journal of Geology and Geophysics*. vol.9, pp.393-398.
- Carter, R. M., Landis, C. A., Norris, R. J., and Bishop, D. G., 1974: Suggestions toward a high-level nomenclature for New Zealand rocks. *Journal of the Royal Society of New Zealand*, vol.4, pp.5-18.
- Carter, R. M., Hicks, M. D., Norris, R. J., Turnbull, I. M. 1978: Sedimentation patterns in an ancient arc-trench-ocean basin complex: Carboniferous to Jurassic Rangitata Orogen, New Zealand. pp.340-361, In: *Sedimentation in submarine canyons, fans, and trenches*. D.J. Stanley and G. Kelling (editors). Dowden, Hutchinson, and Ross, Stroudsburg, Pennsylvania.
- Cawood, P. A., 1984: The development of the SW Pacific margin of Gondwana: correlations between the Rangitata and New England Orogens. *Tectonics*, 3: pp.539-553.
- Challis, G. A., 1965a: The origin of New Zealand ultramafic intrusions. *Journal of Petrology*. vol.6, No.2, pp.332-364.
- Challis, G. A., 1965b: High-temperature contact metamorphism at the Red Hills ultramafic intrusion, Wairau Valley, New Zealand. *Journal of Petrology*. vol.6, No.3, pp.365-419.
- Challis, G. A., 1968: The K<sub>2</sub>O/Na<sub>2</sub>O ratios of ancient volcanic arcs in New Zealand. *New Zealand Journal of Geology and Geophysics*. vol.11 pp.200-211.
- Challis, G. A., 1969: Discussion on the paper "the origin of ultramafic and ultrabasic rocks" by P. J. Wyllie. *Tectonophysics*, vol.7, No. 5-6, pp.495-505.

- Challis, G. A., and Lauder, W. R., 1966: The genetic position of "alpine" type ultramafic rocks. *Bulletin of Volcanology*. 29: pp.283-304.
- Coish, R. A., 1977: Ocean floor metamorphism in the Betts Cove ophiolite, Newfoundland. *Contributions to Mineralogy and Petrology*, 60: pp.255-270.
- Coleman, R. G., 1962: Metamorphic aragonite as evidence relating emplacement of ultramafic rocks to thrust faulting in New Zealand. *Transactions, American Geophysical Union*. 43: pp.447.
- Coleman, R. G., 1966: New Zealand serpentinites and associated metasomatic rocks. *New Zealand Geological Survey Bulletin*. 76: 102p.
- Coleman, R. G., 1977: *Ophiolites: Ancient Oceanic Lithosphere?* Springer-Verlag, Berlin, 229p.
- Coombs, D. S., 1963: Trends and affinities of basaltic magmas and pyroxenes as illustrated on the diopside-olivine-silica diagram. *Mineralogical Society of America, Special Paper* 1, pp.227-250.
- Coombs, D. S., Landis, C. A., Sinton, J. M., Borns, D. J. and Nakamura, Y., 1973: The Dun Mountain Ophiolite belt, New Zealand. *In: Ophiolites in the Earth's Crust*, U.S.S.R., Nauka Press, Acad. Sci.
- Coombs, D. S., Landis, C. A., Norris, R. J., Sinton, J. M., Borns, D. J., and Craw, D., 1976: The Dun Mountain Ophiolite Belt, New Zealand, its tectonic setting, constitution, and origin, with special reference to the southern portion. *American Journal of Science*. 276: pp.561-603.
- Cooper, A. F., 1976: Concentrically zoned ultramafic pods from the Haast schist zone, South Island, New Zealand. *New Zealand Journal of Geology and Geophysics*. vol.19, pp.603-623.
- Crook, K. A. W. and Feary, D. A., 1982: Development of New Zealand according to the fore-arc model of crustal evolution. *Tectonophysics*, 87: pp.65-107.
- Davis, T. E., Johnston, M. R., Rankin, P. C., Stull, R. J. 1980: The Dun Mountain Ophiolite Belt in East Nelson, New Zealand. A. Panayiotou (editor), *In: Ophiolites. Proceedings of the International Ophiolite Symposium, Cyprus, 1979*. Cyprus, Ministry of Agriculture and Natural Resources, Geological Survey Department, pp.480-498.
- Dickins, J. M., Johnston, M. R., Kimrough, D. L., and Landis C. A., 1986: The stratigraphic and structural position and age of the Croisilles Mélange, East Nelson, New Zealand. *New Zealand Journal of Geology and Geophysics*, vol.29, pp.291-301.

- Dickinson, W. R., 1971: Detrital modes of New Zealand graywackes. *Sedimentary Geology*, 5: pp.37-56.
- Dickinson, W. R., 1982: Compositions of sandstone in Circum-Pacific Subduction Complexes and fore-arc basins. *American Association of Petroleum Geology, Bulletin*. 66: pp.121-137.
- Dixon, T. H., and Batiza, R., 1979: Chemistry and petrology of recent lavas in the northern Marianas: Implications for the origin of island-arc basalts. *Contributions to Mineralogy and Petrology*, 70: pp.167-181.
- Flanagan, F. J., 1973: 1972 values for internal geochemical reference standards. *Geochimica et Cosmochimica Acta*, 37: pp.1189-1200.
- Fleming, C. A. (Transl. and Ed.), 1959: *Geology of New Zealand: Contributions to the Geology of the provinces of Auckland and Nelson by Ferdinand von Hochstetter*. New Zealand Government Printer, Wellington.
- Floyd, P. A. and Winchester, J. A., 1975: Magma type and tectonic setting discrimination using immobile elements. *Earth and Planetary Science Letters*, 27: pp.211-218.
- Frey, F. A., Haskin, M. A., Poetz, J. A., and Haskin, L. A., 1968: Rare earth abundances in some basic rocks. *Journal of Geophysical Research*, 73: pp.6085-6098.
- Frey, F. A., Bryan, W. B. and Thompson, G., 1974: Atlantic ocean floor: geochemistry and petrology of basalts from Legs 2 and 3 of the Deep Sea Drilling Project. *Journal of Geophysical Research*, 79: pp.5507-5527.
- Frey, F. A. and Green, D. H., 1974: The mineralogy, geochemistry and origin of lherzolite inclusions in Victorian basanites. *Geochimica et Cosmochimica Acta*, 38: pp.1023-1059.
- Frost, C. D. and Coombs, D. S., 1987: Neodymium isotope analysis of New Zealand terranes. *Annual Meeting, Abstract and Proceedings*, vol.19, 669p. Geological Society of America, Boulder, Colorado, U.S.A.
- Garcia, M. O., 1978: Criteria for the identification of ancient volcanic arcs. *Earth-Science Reviews*, 14: pp.147-165.
- Gill, J. B., 1981: *Orogenic andesites and plate tectonics*. Springer-Verlag, Heidelberg, 390p.
- Grapes, R. H., and Palmer, K., 1984: Magma type and tectonic setting of metabasites, Southern Alps, New Zealand, using immobile elements. *New Zealand Journal of Geology and Geophysics*. vol.27: pp.21-25.

- Green, D. H., 1971: Composition of basaltic magmas as indicator of conditions of origin: application to oceanic volcanism. *Philosophical transactions of the Royal Society of London*, A268: pp.707-725.
- Green, D. H., 1973: Conditions of melting of basanite magma from garnet peridotite. *Earth and Planetary Sciences Letters*, 17: pp.456-465.
- Green, D. H.; Falloon, T. J. and Taylor, W. R., 1987: Mantle-derived magmas-roles of variable source peridotite and variable C-H-O fluid compositions. *In: Magmatic Processes: Physicochemical Principles*. B.O. Mysen (editor), The Geochemical Society, Special Publication Number 1, Lancaster Press, Washington.
- Grikurov, G. E. and Lopatin, B. G., 1975: Structure and evolution of the West Antarctica part of the Circum-Pacific Mobile Belt. *In: K. S. W. Campbell (editor), Gondwana Geology*. ANU Press, Canberra, A.C.T., pp.639-650.
- Grindley, G. W., 1958: The geology of the Eglinton Valley, Southland, parts of Eglinton (S131) and Mavora (S141) sheet districts. *New Zealand Geological Survey Bulletin*, 58: pp.68.
- Hart, S. R., 1988: Heterogeneous mantle domains: signatures, genesis and mixing chronologies. *Earth and Planetary Science Letters*, 90: pp.273-296.
- Hart, S. R., Erlank, A. J., and Kable, E. J. D., 1974: Sea floor basalt alteration: some chemical and Sr isotope effects. *Contributions to Mineralogy and Petrology*, 44: pp.219-240.
- Haston, R. B., Luyendyk, B. P., Landis, C. A. and Coombs, D. S., 1989: Paleomagnetism and question of original location of the Permian Brook Street terrane, New Zealand. *Tectonics*, vol.8, No.4, pp.791-801.
- Hatherton, T., 1969: Geophysical anomalies over the eu- and miogeosynclinal systems of California and New Zealand. *Geological Society of America Bulletin*, 80: pp.213-230.
- Hawkesworth, C. J., O'Nions, R. K. and Arculus, R. J., 1979: Nd and Sr isotope geochemistry of island-arc volcanics, Grenada, Lesser Antilles. *Earth and Planetary Science Letters*, 45: pp.237-248.
- Hawkins J. W. and Melchoir, J. T., 1985: Petrology of Mariana Trough and Lau Basin basalts. *Journal of Geophysical Research*, 90: pp.11,431-11,468.
- Hochsetter, F. von, 1864a: Dunit, korniger Olivinfels vom Dun Mountain bei Nelson, Neu-Seeland. *Deutsche geol. Gesell. Zeitschr.*, 16: pp.341-344.



- Howell, D. G., 1980: Mesozoic accretion of exotic terranes along the New Zealand segment of Gondwanaland. *Geology*, 8: pp.487-491.
- Hsü, K. J., 1968: Principles of mélanges and their bearing on the Franciscan-Knoxville paradox. *Geological Society of America Bulletin*, 79: pp.1063-1074.
- Hughes, C. J., 1972: Spilites, keratophyres, and the igneous spectrum. *Geological Magazine*, 109: pp.513-527.
- Humphris, S. E. and Thompson, G., 1978: Hydrothermal alteration of oceanic basalts by seawater. *Geochimica et Cosmochimica Acta*, 42: pp.107-125.
- Hunt, T. M., 1974: Rock magnetism in the alpine-peridotite body at Dun Mountain, New Zealand. *Journal of the Royal Society of New Zealand*, vol.4, pp.433-445.
- Hunt, T. M., 1978: Interpretation of gravity anomalies over the Dun Mountain ultramafic body. *New Zealand Journal of Geology and Geophysics*. vol.21, pp.413-417.
- Irvine, T. N. and Baragar, W. R. A., 1971: A guide to the chemical classification of the common volcanic rocks. *Canadian Journal of Earth Science*, 8: pp.523-548.
- Jenner, G. A., Longerich, H. P., Jackson, S. E., and Fryer, B. J., 1990: ICP - MS: a powerful tool for high precision trace element analysis in earth sciences. *Chemical Geology* (in press).
- Jensen, L. S., 1976: A new cation plot for classifying subalkaline volcanic rocks. Ontario Ministry of Natural Resources, Miscellaneous Paper No. 66, 22p.
- Johnston, M. R. 1977: The Rai Sandstone in the Dun Mountain area, east Nelson. *Journal of the Royal Society of New Zealand*, 7: pp.113-117.
- Johnston, M. R. 1981: Sheet 027BD Dun Mountain. Geological map of New Zealand, 1:50 000. Department of Scientific and Industrial Research, Wellington, New Zealand.
- Johnston, M. R. 1982: Sheet N28BD Red Hills. Geological map of New Zealand, 1:50 000. Department of Scientific and Industrial Research, Wellington, New Zealand.
- Jones, D. L. et al., 1982: Recognition, character, and analysis of tectonostratigraphic terranes in western North America. In: Oji Seminar volume, Centre for Academic Publications Japan.

- Kawachi, Y., 1974: Geology and petrochemistry of weakly metamorphosed rocks in the Upper Wakatipu district, southern New Zealand. *New Zealand Journal of Geology and Geophysics*, vol.17, pp.169-208.
- Kay, R., Hubbard, N. J. and Gast, P. W., 1970: Chemical characteristics and origin of oceanic ridge volcanic rocks. *Journal of Geophysical Research*, 75: pp.1584-1614.
- Kingma, J. T., 1959: The tectonic history of New Zealand. *New Zealand Journal of Geology and Geophysics*. vol.2, pp.1-55.
- Korsh, R. J. and Wellman, H.W., 1988: The geological evolution of New Zealand and the New Zealand region. *In: The Ocean Basins and Margins. Volume 7B: The Pacific Ocean.* A.M. Nairn, F.G. Stehli and S. Uyeda (editors), pp.411-482. Plenum Press, New York.
- Kushiro, I., 1960: Si-Al relations in clinopyroxenes from igneous rocks. *American Journal of Science*, 258: pp.548-554.
- Landis, C. A., 1974a: Stratigraphy, lithology, structure, and metamorphism of Permian, Triassic, and Tertiary rocks between the Mararoa River and Mount Snowdon, western Southland, New Zealand. *Journal of the Royal Society of New Zealand*, vol.4, pp.229-251.
- Landis, C. A., 1974b: Palaeocurrents and composition of lower Bryneira strata (Permian) at Barrington Peak, north-west Otago. *New Zealand Journal of Geology and Geophysics*, vol.17, pp.799-806.
- Landis, C. A., 1980: Little Ben Sandstone, Maitai Group (Permian): nature and extent in the Hollyford-Eglinton region, South Island, New Zealand. *New Zealand Journal of Geology and Geophysics*, vol.23, pp.551-567.
- Landis, C. A., 1987: Permian-Jurassic rocks at Productus Creek-Letham Ridge, Southland. *Geological Society of New Zealand, Miscellaneous Publication*, 37c: pp.89-110.
- Landis, C. A. and Coombs, D. S., 1967: Metamorphic belts and orogenesis in New Zealand. *Tectonophysics*, 4: pp.501-518.
- Landis, C. A. and Blake, M. C. Jr., 1987: Tectonostratigraphic terranes of the Croisilles Harbour region, South Island, New Zealand. *In: Terrane Accretion and Orogenic Belts Geodynamic Series, Volume 19.* E.C. Leitch and E. Scheiber (editors), AGU Washington, D.C., pp.179-198.
- Langmuir, C. H., Vocke, R. D., Hanson, G. N. and Hart, S. R., 1978: A general mixing equation with applications to Icelandic basalts. *Earth and Planetary Science Letters*, 37: pp.380-392.

- Lauder, W. R., 1965a: The geology of Dun Mountain, Nelson, New Zealand; Pt. I, The petrology and structure of the sedimentary and volcanic rocks of the Te Anau and Maitai Groups. *New Zealand Journal of Geology and Geophysics*, vol. 8, pp. 3-34.
- Lauder, W. R., 1965b: The geology of Dun Mountain, Nelson, New Zealand; Part 2, The petrology, structure, and origin of the ultrabasic rocks. *New Zealand Journal of Geology and Geophysics*, vol. 8, pp. 475-504.
- Le Bas, M. J., 1962: The role of aluminum in igneous clinopyroxenes with relation to their parentage. *American Journal of Science*, 260: pp. 267-288.
- Leterrier, J., Maury, R. C., Thonon, P., Girard, D. and Marchal, M., 1982: Clinopyroxene compositions as a method of identification of the magmatic affinities of paleo-volcanic series. *Earth and Planetary Science Letters*, 59: pp. 139-154.
- Lillie, A. R. and Gunn, B. M., 1964: Steeply plunging folds in the Sealy Range, Southern Alps. *New Zealand Journal of Geology and Geophysics*, vol. 7, pp. 403-423.
- Longerich, H. P., Jenner, G. A., Fryer, B. J., and Jackson, S. E., 1990: Inductively coupled plasma-mass spectrometric analysis of geological samples: a critical evaluation based on case studies. *Chemical Geology* (in press).
- MacKinnon, T. C., 1983: Origin of the Torlesse terrane and coeval rocks, South Island, New Zealand. *Geological Society of America Bulletin*, 94: pp. 969-985.
- Macpherson, E. O., 1946: An outline of Late Cretaceous and Tertiary diastrophism in New Zealand. *New Zealand Geological Survey, Memoir*, 6, pp. 32.
- Malpas, J. G., 1977: Petrology and tectonic significance of Newfoundland ophiolites, with examples from the Bay of Islands. In: *North American Ophiolites*. R.G. Coleman and W.P. Irwin (editors), *Oreg., Dep. Geol., Miner. Ind., Bull.* 95, pp. 13-24.
- McKay, A., 1879: The district between the Wairau and Motueka Valleys. *New Zealand Geological Survey Rept. Geol. Explor.* 1878-79, vol. 12, pp. 97-121.
- McCulloch, M. T., Jacques, A. L., Nelson, D. R. and Lewis, J. D., 1983: Nd and Sr isotopes in kimberlites and lamproites from Western Australia: an enriched mantle origin. *Nature (London)*, 302: pp. 400-403.

- McQueen, D. R., 1954: Upper Paleozoic plant fossils from South Island, New Zealand. *Transactions of the Royal Society of New Zealand*, 82: pp.231-235.
- Mildenhall, D. C., 1976: *Glossopteris ampla* Dana from New Zealand Permian Sediments. *New Zealand Journal of Geology and Geophysics*, vol.19, pp.130-132.
- Miyashiro, A., 1974: Volcanic rocks series in island-arcs and active continental margins. *American Journal of Science*, 274: pp.321-355.
- Molnar, P., Atwater, Tanya, Mammerickx, Jacqueline, and Smith, S. M., 1975: Magnetic anomalies, bathymetry and the tectonic evolution of the South Pacific since the late Cretaceous. *Royal Astron. Soc. Geophys. Jour.*, vol.60, pp.383-420.
- Mossman, D. J. and Force, L. M., 1969: Permian fossils from the Greenhills Group, Bluff, Southland, New Zealand. *New Zealand Journal of Geology and Geophysics*, vol.12, pp.659-672.
- Mossman, D. J., 1973: Geology of the Greenhills ultramafic complex, Bluff Peninsula, Southland, New Zealand. *Geological Society of America Bulletin*, 84: pp.39-62.
- Mottl, M. J., 1983: Metabasalts, axial hot springs, and the structure of hydrothermal systems at mid-ocean ridges. *Geological Society of America Bulletin*, 94: pp.161-180.
- Mottl, M. J. and Seyfried, W. E. 1980: Sub-seafloor hydrothermal systems: Rock-vs. seawater-dominated. In: *Seafloor Spreading Centers: Hydrothermal Systems*. P.A. Rona and R.P. Lowell (editors), Dowden, Hutchinson and Ross Inc., Stroudsburg, Pennsylvania, pp.869-884.
- Natland, J. H. and Tarney, J., 1981: Petrologic evolution of the Mariana arc and back-arc basin system: a synthesis of drilling results in the South Philippine Sea. In: *Hussong, D. M., Uyeda, S., et al., 1981. Initial Reports of the Deep Sea Drilling Project*, 60: pp.877-908.
- Nelson, D. R., Chivas, A. R., Chappel, B. W. and McCulloch, M. T., 1988: Geochemical and isotopic systematics in carbonatites and implications for the evolution of oceanic-island sources. *Geochimica et Cosmochimica Acta*, 53: pp.1-17.
- Nicolas, A., Bouchez, J-L., Boudier, F., and Mercier, J-C., 1971: Textures, structures and fabrics due to solid-state flow in some European lherzolites. *Tectonophysics*, 12: pp.55-86.

- Nisbet, E. G. and Pearce, J. A., 1977: Clinopyroxene composition in mafic lavas from different tectonic settings. *Contributions to Mineralogy and Petrology*, 63: pp.149-160.
- Park, J., 1887: On the district between the Dart and Big Bay. New Zealand Colonial Museum Geological Survey Department Geological Explor. 1886-87, pp.121-137.
- Park, J., 1921: Geology and mineral resources of Western Southland. New Zealand Geological Survey Bulletin, 23: pp.88.
- Pearce, J. A., 1975: Basalt geochemistry used to investigate past tectonic environments on Cyprus. *Tectonophysics*, 25: pp.41-67.
- Pearce, J. A., 1980: Geochemical evidence for the genesis and eruptive setting of lavas from Tethyan ophiolites. *In: Ophiolites, Proceedings of the international Ophiolite Symposium, Cyprus, 1979. A. Panayiotou (editor). pp.261-272.*
- Pearce, J. A., 1982: Trace element characteristics of lavas from destructive plate boundaries. *In: Andesites: orogenic andesites and related rocks. R.S. Thorpe (editor), John Wiley and Sons, Chichester. pp.525-548.*
- Pearce, J. A., 1983: Role of sub-continental lithosphere in magma genesis at active continental margins. *In: Continental Basalts and Mantle Xenoliths. C.J. Hawkesworth and M.J. Norry (editors), Shiva Publishing, Nantwich. pp.230-249.*
- Pearce, J. A. and Cann, J. R., 1973: Tectonic setting of basic volcanic rocks determined using trace element analyses. *Earth and Planetary Science Letters*, 19: pp.290-300.
- Pearce, J. A. and Flower, M. F. J., 1977: The relative importance of petrogenetic variables in magma genesis at accreting plate margins: a preliminary investigation. *Journal of the Geological Society of London*, 134: pp.103-127.
- Pearce, J. A. and Norry, M. J., 1979: Petrogenetic implications of Ti, Zr, Y, and Nb variations in volcanic rocks. *Contributions to Mineralogy and Petrology*, 69: pp.33-47.
- Pearce, J. A., Alabaster, T., Shelton, A. W., and Searle, M. P., 1981: The Oman ophiolite as a Cretaceous arc-basin complex: evidence and implications. *Philosophical Transactions of the Royal Society of London. A 300: pp.299-317.*



- Pearce, J. A., Lippard, S. J. and Roberts, S., 1984: Characteristics and tectonic significance of supra-subduction zone ophiolites. *In*: Marginal Basin Geology. B.P. Kokelaar and M.F. Howells (editors), Geological Society of London Special Publication Number 16, Blackwell Scientific Publications, Oxford. pp.77-94.
- Poldervaart, A. and Hess, H.H., 1951: Pyroxenes in the crystallization of basaltic magmas. *Journal of Geology*, 59: p.472-489.
- Pringle, I. J., 1980: Petrology, geochemistry, and igneous and metamorphic mineralogy of low-grade metamorphosed basalts of the Torlesse terrane, South Island, New Zealand. [Ph.D. thesis]: Dunedin, New Zealand, University of Otago, 440p.
- Reed, J. J., 1957: Petrography of the lower Mesozoic rocks of the Wellington district. *New Zealand Geological Survey Bulletin*, No.57, 60p.
- Rigg, T.; Chittenden, E. T.; Hodgson, L., 1957: A survey of soils, vegetation and agriculture of the eastern hills, Waimea County, Nelson. Nelson, Cawthorn Institute.
- Rocci, G., Ohnenstetter, D. and Ohnenstetter, M., 1975: La dualité des ophiolites tethysiennes. *Petrologie*, vol.1, pp.172-174.
- Ross, C. S., Foster, M. D., Myers, A. T., 1954: Origin of Dunites and of Olivine-rich Inclusions in Basaltic Rocks. *American Mineralogist*, 39: pp.693-737.
- Saunders, A. D. and Tarney, J., 1979: The geochemistry of basalts from a back-arc spreading centre in the East Scotia Sea. *Geochimica et Cosmochimica Acta*, 43: pp.555-572.
- Saunders, A. D. and Tarney, J., 1984: Geochemical characteristics of basaltic volcanism within back-arc basins. *In*: Marginal basin geology: volcanic and associated sedimentary and tectonic processes in modern and ancient marginal basins. B.P. Kokelaar and M.F. Howells (editors), Geological Society of London Special Publication 16, pp.59-76.
- Seyfried, W.E., Mottl, M. J., and Bischoff, J. L., 1978: Seawater/basalt ratio effects on the chemistry and mineralogy of spilites from the ocean floor. *Nature*, vol.275: No.5677, pp.211-213.
- Seyfried, W. E. and Bischoff, J. L. 1981: Experimental seawater-basalt interaction at 300° and 500 bars: chemical exchange, secondary mineral formation and implications for the transport of heavy metals. *Geochimica et Cosmochimica Acta*, 45: pp.135-147.

- Shervais, J. W., 1982: Ti-V plots and the petrogenesis of modern and ophiolitic lavas. *Earth and Planetary Science Letters*, 59: pp.101-118.
- Sinton, J. M., 1980: Petrology and evolution of the Red Mountain ophiolite complex, New Zealand. *American Journal of Science*, 280: pp.296-328.
- Sivell, W. J. and Rankin, P. C. 1982: Discrimination between ophiolitic metabasalts, north D'Urville Island, New Zealand. *New Zealand Journal of Geology and Geophysics*, vol.25, pp.275-293.
- Sivell, W. J. and Waterhouse, J. B., 1984a: The Patuki Intrusive suite: closed-system fractionation beneath a slow-spreading ridge. *Lithos*, 17: pp.1-17.
- Sivell, W. J. and Waterhouse, J. B., 1984b: Oceanic ridge metamorphism of the Patuki Volcanics, D'Urville Island, New Zealand. *Lithos*, 17: pp.19-36.
- Sivell, W. J. and Waterhouse, J. B., 1986: The geochemistry, origin and tectonic significance of rodingites from the Dun Mountain Ultramafics, D'Urville Island, New Zealand. *New Zealand Journal of Geology and Geophysics*, vol.29, pp.9-27.
- Sivell, W. J., 1988: Geochemical constraints on the origin of Croisilles and Patuki ophiolites: implications for late Paleozoic-Mesozoic tectonics in New Zealand. *Tectonics*, 7: pp.1015-1032.
- Smith, C. H., 1958: Bay of Islands igneous complex, western Newfoundland. *Geological Survey of Canada Memoir*, 290: pp.1-132.
- Spooner, E.T.C., Beckinsdale, R.D., England, P.C. and Senior A., 1977: Hydration,  $^{18}\text{O}$  enrichment and oxidation during ocean floor hydrothermal metamorphism of ophiolitic metabasic rocks from E. Liguria, Italy. *Geochimica et Cosmochimica Acta*, 41: pp.857-871.
- SpÖrli, K. B., 1975: Waiheke and Manaia Hill Groups, east Auckland. *New Zealand Journal of Geology and Geophysics*, vol. 18, pp.757-762.
- SpÖrli, K. B., 1978: Mesozoic tectonics, North Island, New Zealand. *Geological Society of America Bulletin*, 89: pp.415-425.
- Stauffer, Mel. R., Mukherjee, A. C., and Koo, J., 1975: The Amisk Group: An Aphebian(?) Island-Arc Deposit. *Canadian Journal of Earth Sciences*, 12: pp.2021-2035.
- Stephens, M. B., 1982: Field relationships, petrochemistry and petrogenesis of the Stenerjokk Volcanites, central Swedish Caledonides. *Sveriges Geologiska Undersökning, Series C*, 111p.

- Stevens, G. R. and Speden, I. G., 1978: New Zealand. In: M. Moullade, and A.F.M. Nairn, (editors), The Mesozoic, the Phanerozoic geology of the world. Volume II. Elsevier, Amsterdam, pp.251-328.
- Stipp, J. J., 1968: The geochronology and petrogenesis of the Cenozoic volcanics of North Island, New Zealand. [Ph.D. thesis], Australian National University, Canberra, Australia.
- Suggate, R. P., Stevens, G. R., Te Punga, M. T. (editors), 1978: "The Geology of New Zealand". Government Printer, Wellington. 2 volumes, 820p.
- Sun, S.-S., 1980: Lead isotopic study of young volcanic rocks from mid-ocean ridges, ocean islands and island-arcs. Philosophical Transactions of the Royal Society of London, A297: pp.409-445.
- Tarney, J., Saunders, A. D. and Weaver, S. D., 1977: Geochemistry of volcanic rocks from the island arcs and marginal basins of the Scotia Arc region. In: Island Arcs, Deep Sea Trenches and Back-Arc Basins. American Geophysical Union, Maurice Ewing Series 1, pp.367-377.
- Tarney, J., Saunders, A. D., Mathey, D. P., Wood, D. A. and Marsh, N. G., 1981: Geochemical aspects of back-arc spreading in the Scotia Sea and western Pacific. Philosophical Transactions of the Royal Society of London, A300, pp.263-285.
- Taylor, B. and Karner, G. D., 1983: On the evolution of marginal basins. Reviews of Geophysics and Space Physics, vol.21, No.8, pp.1727-1741.
- Thayer, T. P., 1963: Flow Layering in Alpine-type Peridotite-gabbro Complexes. Mineralogical Society of America Special Paper, No.1, pp.55-61.
- Thompson, G., 1973: A geochemical study of the low-temperature interaction of sea water and oceanic igneous rocks. EOS Transactions, American Geophysical Union, 54: pp.1015-1019.
- Treuil, M. and Varet, J., 1973: Critère volcanologiques, pétrologiques et géochimiques de la genèse et de la différenciation des magmas basaltiques. Exemple de l'Afar. Bull. Soc. Géol. fr., 15, pp.506-540.
- Turnbull, I. M., 1979: Petrography of the Caples terrane of the Thompson Mountains, northern Southland, New Zealand. New Zealand Journal of Geology and Geophysics, vol.22: pp.709-727.
- Turnbull, I. M., 1980: Structure and interpretation of the Caples terrane of the Thompson Mountains, northern Southland, New Zealand. New Zealand Journal of Geology and Geophysics, vol.23: pp.43-62.

- Turner, F. J., 1930: The Metamorphic and ultrabasic rocks of the lower Cascade Valley, South Westland. New Zealand Institute Transactions, vol.61, pp.170-201.
- Vallance, T. G., 1969: Spilites again: some consequences of the degradation of basalts. Proceedings of the Linnean Society, New South Wales, 94: pp.8-51.
- Vitaliano, C. J., 1968: Petrology and structure of the south-eastern Marlborough Sounds, New Zealand. New Zealand Geological Survey Bulletin, 74: 40p.
- Wakita, H., Rey, P. and Schmitt, R. A., 1971: Abundances of the 14 rare earth elements and 12 other trace elements in Apollo 12 samples: five igneous and one breccia rocks and four soils. Proceedings of the 2nd Lunar Science Conference, pp.1319-1329.
- Walcott, R. I., 1969: Geology of the Red Hills complex, Nelson, New Zealand. Transactions of the Royal Society of New Zealand, Earth Sciences, vol.7, No.5, pp.57-88.
- Waterhouse, J. B., 1959: Stratigraphy of the lower part of the Maitai Group, Nelson. New Zealand Journal of Geology and Geophysics, vol.2, pp.944-953.
- Waterhouse, J. B. 1964: Permian stratigraphy and faunas of New Zealand. New Zealand Geological Survey Bulletin, 72: 101p.
- Waterhouse, J. B., 1966: The age of the Croisilles Volcanics, eastern Nelson. Transactions of Royal Society of New Zealand, Geology, vol.3, pp.175-181.
- Waterhouse, J. B., 1979: The debated age of the ammonoid *Durvilleoceras* Waterhouse. Geological Magazine, 116: pp.385-392.
- Waterhouse, J. B., 1982: The Early Permian age of the Rai Sandstone, east Nelson, New Zealand. New Zealand Journal of Geology and Geophysics, vol.25, pp.359-362.
- Wellman, H. W., 1952: The Permian-Jurassic stratified rocks. In: Symposium sur les séries de Gondwana (Nouvelle-Zélande). 19th International Geological Congress, Algiers, 1952, pp.13-24.
- Wellman, H. W., 1956: Structural outline of New Zealand. New Zealand Department of Science and Industrial Research Bulletin, vol.121, 36p.
- Winchester, J. A. and Floyd, P. A., 1977: Geochemical discrimination of different magma series and their differentiation products using immobile elements. Chemical Geology, 20: pp.325-343.

- Wood, D. A., 1980: The application of a Th-Hf-Ta diagram to problems of tectonomagmatic classification and to establishing the nature of crustal contamination of basaltic lavas of the British Tertiary Volcanic Province. *Earth and Planetary Science Letters*, 50: pp.11-30.
- Wood, D. A., Gibson, I. L., and Thompson, R. N., 1976: Elemental mobility during zeolite facies metamorphism of the Tertiary basalts of eastern Iceland. *Contributions to Mineralogy and Petrology*, 55: pp.241-254.
- Wood, D. a., Joron, J-L, and Treuil, M., 1979: A re-appraisal of the use of trace elements to classify and discriminate between magma series erupted in different tectonic settings. *Earth and Planetary Science Letters*, 45: pp.326-336.
- Wood, D. A., Marsh, N. G., Tarney, J., Joron, J-L, Fryer, P. and Treuil, M., 1982: Geochemistry of igneous rocks recovered from a transect across the Mariana Trough, Arc, Fore-arc, and Trench sites 453 to 461, DSDP leg 60. In: Initial Reports of the Deep Sea Drilling Project 60. Washington, D.C.; U.S. Government Printing Office, pp.611-645.



## APPENDIX A

### ANALYTICAL METHODS

#### A.1 Sampling Procedure

Specimens chosen for analyses were selected with the aim of obtaining a representative sampling of the various rock types studied. In order to overcome, as much as possible, problems associated with alteration; efforts were made to avoid sampling rocks which showed any obvious macroscopic evidence of alteration (eg., veining, oxidation, amygdules, altered pillow margins). Further screening of specimens was done during petrographic study of the rocks prior to analysis.

#### A.2 Sample Preparation

After removing weathered surfaces, samples were broken into 3 to 4 centimetre pieces using hammer. These were then crushed to chips (less than 0.5 centimetres) using a Braun "chipmunk" jaw-crusher. The contact plates of this machine were brushed and scrubbed between processing of each samples so as to minimize contamination. A portion of these smaller chips were then pulverised in one of two ways, (i) in an agate bowl or (ii) a tungsten-carbide bowl. To clean these bowls between samples, silica sand was pulverised and discarded and then the bowls were cleaned with using water and methanol.

## APPENDIX B

### ANALYTICAL METHODS

#### B.1 Major Elements

Major and minor oxides were determined by atomic absorption. By this process 0.1000 grams of 100 mesh rock powder from each sample was weighed into a flask. 5 millilitres of a concentrated hydrofluoric acid and 50 millilitres saturated boric acid solution was added to each flask to dissolve the sample. This mixture was then diluted by adding 145 millilitres of distilled water and further diluted with lanthanum oxide and distilled water. Samples were then compared to standards of known amounts of major oxides. Initial readings for percent absorption were obtained for the standards, then for the sample and for the standards just lower and just higher than the samples. The formula presented below was then applied to the readings to calculate the amount of a particular oxide:

$$\begin{aligned} \text{percent oxide} = & \text{percent low standard} + (\text{percent sample} - \\ & \text{percent absorption low standard}) / (\text{percent absorption high} \\ & \text{standard} - \text{percent absorption low standard}) * (\text{percent high} \\ & \text{standard} - \text{percent low standard}) * 2 \end{aligned}$$

Loss on ignition (LOI) was determined by weighing a known amount of rock powder in a crucible before and after ignition at 1000 degrees Celsius.

## B.2 Trace Elements (XRF)

A number of trace elements were determined by X-ray fluorescence using a Phillips 1450 fully automated sequential X-ray fluorescence spectrometer using a rhodium target X-ray tube.

Pellets used for these analyses were prepared by combining 10 grams of rock powder with 1.5 grams of binder (Bakelite brand phenyl resin) using a mechanical shaker. The mixtures were then pressed into pellets and baked for approximately 20 minutes at 200 degrees Celsius.

The elements Ni, Sc, V, Cu, Zn, and Ga were analyzed using a standard package designated TRACEF and the elements Rb, Sr, Zr and Y were determined using a separate program known as REPEAT. The standards BCR-1 and W-1 were analyzed with the samples to give estimates of precision and accuracy (Table B.1).

## B.3 Trace and Rare Earth Elements (ICP-MS)

Rare earth elements and selected trace elements were analyzed by ICP using the following procedure. Approximately 0.1 grams of a sample were weighed into a 100 millilitre teflon beaker. 10 to 15 millilitres of HF and 10 to 15 millilitres of concentrated  $\text{HNO}_3$  were added to the beaker and evaporated. 10 millilitres of 8N  $\text{HNO}_3$  were then added and evaporated. If residue was observed, equal volumes of 8N  $\text{HNO}_3$  and 6N HCL were added and evaporated. An additional evaporation with 8N  $\text{HNO}_3$  was then carried out. The samples were then taken into solution by adding about 10 millilitres of 0.2N  $\text{HNO}_3$  and heated for a few minutes if necessary. The samples were

## TRACE ELEMENTS (PPM) XRF

	BCR-1	mean S.D	Pub.			
Rb	47.9	0.6	47			
Sr	339.3	2.1	330			
Y	36.8	0.7	40			
Zr	198.6	2.2	185			
	n=19			W-1	mean S.D.	Pub.
Ga	24	1.1	22	19	1.3	16
Zn	130	3.1	125	96	2.6	86
Cu	31	2.5	16	111	1.5	110
Ni	23	4.0	10	83	3.6	76
V	422	3.4	420	257	2.9	240
Cr	24	8.2	15	108	5.5	120
Sc	30	1.9	33	34	1.8	-
	n=9				n=7	

Table B.1 Precision and accuracy estimates for trace element analyses by XRF. "n" refers to the number of times the standard was analysed. "S.D." is the standard deviation; "Pub." refers to the published value for the analysis from Abbey (1983) for BCR-1 and Flanagan (1973) for W-1.

then taken to a final volume of 90 millilitres in 0.2N HNO<sub>3</sub>. If the sample did not contain silicate minerals, an initial dissolution with 6N HCL and 8N HNO<sub>3</sub> was used instead of the HF/HNO<sub>3</sub> dissolution.

Two tubes were used in the final analysis. Tube No. 1 contained 9 grams of sample solution and 1 gram of 0.2N HNO<sub>3</sub>. Tube No. 2 contained 9 grams of the sample solution and 1 gram of a mixed spike solution.

Precision and accuracy estimates for the runs are based on the standard SY-2 and are listed in Table B.2.

#### B.4 Mineral Analysis

Representative thin sections containing relict clinopyroxene grains were polished and then coated with carbon. Analysis of relict pyroxenes was then carried out using an automated JEOL JXA-50A electron probe microanalyser, equipped with Krisel Control through a PDP-11 computer. Operating conditions consisted of an acceleration potential of 15 kV and a beam current of 20 microamperes. The width of the electron beam was approximately 1 micron. Compositions of the analyzed pyroxenes were computer calculated by reference to calibration curves based on analysis of established standard materials.



## TRACE ELEMENTS (PPM) ICP

	SY-2	mean S.D	Pub.
Li	92	3.5	96
Be	23	0.4	24
Nb	31	1.8	30
Mo	0.8	0.1	0.8
Cs	2.60	0.2	2.68
Ba	437	11.7	447
La	67	1.5	69
Ce	154	3.2	157
Pr	19.2	0.3	19.6
Nd	69	1.5	72
Sm	15.1	0.3	15.5
Eu	2.25	0.1	2.27
Gd	14.4	0.3	14.9
Tb	2.82	0.1	2.86
Dy	19.3	0.5	19.5
Ho	4.4	0.1	4.5
Er	14.8	0.4	15.0
Tm	2.36	0.1	2.40
Yb	17.0	0.6	17.3
Lu	2.79	0.1	2.89
Hf	8.1	0.3	8.5
Ta	2.2	0.5	1.8
W	12	12.8	6
Tl	1.56	0.1	1.54
Pb	81	1.1	80
Th	380	18.4	390
U	300	10.7	295

Table B.2 Precision and accuracy estimates for trace element analyses by ICP. Estimates based on analyses of the standard SY-2. Published values are those of Abbey (1983.)

**APPENDIX C**  
**GEOCHEMICAL ANALYSES**

### C.1 Major and Trace Element Analyses

Note: Ta has been calculated using the accepted Nb/Ta = 16 ratio for basaltic rocks of Wood et al. (1979). Hf has been calculated using a ratio of Zr/Hf = 39 after Wood et al. (1979). Where shown FeO and Fe<sub>2</sub>O<sub>3</sub> have been calculated from total iron expressed as Fe<sub>2</sub>O<sub>3</sub>\* using a ratio of FeO/Fe<sub>2</sub>O<sub>3</sub> = 0.85 after Brooks (1976).

**C.1a Basaltic Rocks**

Sample Name	L-37	T-267	T-290	TL-525b*	TL-525b	TL-527	TL-528
Figure #	3.2.2	3.2.2	3.2.2	3.2.5	3.2.5	3.2.5	3.2.5
Rock Suite	aphyric/CPX	aphyric/CPX	aphyric/CPX	aphyric/CPX	aphyric/CPX	aphyric/CPX	aphyric/CPX
Rock Type	diabase	microgabbro	diabase	diabase	diabase	diabase	diabase
Mg#	65.03	48.30	54.87	55.96	55.96	49.64	50.80
SiO <sub>2</sub> (wt.%)	50.80	52.30	50.08	50.50	50.50	51.20	49.30
TiO <sub>2</sub>	0.96	1.20	1.04	1.20	1.20	1.00	1.04
Al <sub>2</sub> O <sub>3</sub>	15.10	14.50	14.90	14.80	14.80	14.90	15.40
Fe <sub>2</sub> O <sub>3</sub>	1.30	1.74	1.62	1.59	1.59	1.53	1.69
FeO	6.65	8.87	8.26	8.09	8.09	7.79	8.61
MnO	0.13	0.16	0.17	0.17	0.17	0.15	0.18
MgO	8.16	5.47	6.63	6.79	6.79	5.07	5.87
CaO	8.38	5.08	5.96	9.10	9.10	9.56	8.30
Na <sub>2</sub> O	3.95	4.83	5.14	3.47	3.47	3.86	4.08
K <sub>2</sub> O	0.10	0.09	0.31	0.30	0.30	0.08	0.16
P <sub>2</sub> O <sub>5</sub>	0.05	0.09	0.10	0.07	0.07	0.08	0.08
LOI	3.10	3.47	2.99	1.99	1.99	4.08	3.30
Cr (ppm)	284	0	16	145	145	0	0
Ni	116	0	10	41	41	14	14
Sc	40	33	32	48	48	41	45
V	269	387	325	330	330	325	364
Cu	48	11	12	40	40	24	24
Pb	n.a.	1	1	3	2	n.a.	n.a.
Zn	42	75	75	60	60	100	65
W	n.a.	34.36	58.02	4.95	39.28	n.a.	n.a.
Mo	n.a.	0.21	0.47	0.38	0.34	n.a.	n.a.
Rb	0	1	3	2	2	0	1
Cs	n.a.	0.74	0.34	0.38	0.38	n.a.	n.a.
Ba	n.a.	22	17	26	23	n.a.	n.a.
Sr	76	80	96	136	136	85	117
Tl	n.a.	0.02	0.00	0.01	0.06	n.a.	n.a.
Ga	14	16	17	17	17	19	18
Li	n.a.	6.12	5.77	2.18	2.42	n.a.	n.a.
Ta	n.a.	0.07	0.07	0.05	0.05	n.a.	n.a.
Nb	n.a.	1.1	1.1	0.8	0.8	n.a.	n.a.
Hf	1.33	1.85	2.03	2.07	2.07	1.82	1.91
Zr	52	72	79	81	81	71	74
Y	17	25	26	30	30	24	25
Th	n.a.	0.18	0.15	0.23	0.11	n.a.	n.a.
U	n.a.	0.10	0.08	0.08	0.05	n.a.	n.a.
La	n.a.	2.78	2.70	2.19	2.24	n.a.	n.a.
Ce	n.a.	8.35	8.47	7.84	7.65	n.a.	n.a.
Pr	n.a.	1.46	1.53	1.47	1.40	n.a.	n.a.
Nd	n.a.	7.24	7.82	7.29	7.42	n.a.	n.a.
Sm	n.a.	2.57	2.81	2.93	2.88	n.a.	n.a.
Eu	n.a.	0.93	1.00	1.11	1.11	n.a.	n.a.
Gd	n.a.	3.12	3.40	3.71	3.66	n.a.	n.a.
Tb	n.a.	0.63	0.67	0.78	0.76	n.a.	n.a.
Dy	n.a.	4.23	4.40	5.19	5.03	n.a.	n.a.
Ho	n.a.	0.89	0.94	1.11	1.10	n.a.	n.a.
Er	n.a.	2.68	2.79	3.46	3.16	n.a.	n.a.
Tm	n.a.	0.38	0.39	0.47	0.45	n.a.	n.a.
Yb	n.a.	2.42	2.52	3.00	2.91	n.a.	n.a.
Lu	n.a.	0.35	0.36	0.48	0.44	n.a.	n.a.

Sample Name	TL-530b	TL-531	TL-532	H-756b	H-757	H-758a	H-761b
Figure #	3.2.5	3.2.5	3.2.5	3.2.4	3.2.4	3.2.4	3.2.4
Rock Suite	aphyric/CPX	aphyric/CPX	aphyric/CPX	aphyric/CPX	aphyric/CPX	aphyric/CPX	aphyric/CPX
Rock Type	diabase	diabase	diabase	diabase	diabase	diabase	diabase
Mg#	60.00	48.23	53.64	58.04	44.75	61.99	58.52
SiO <sub>2</sub> (wt.%)	49.80	50.20	50.20	49.20	53.30	50.60	51.00
TiO <sub>2</sub>	0.92	1.08	1.40	1.00	1.24	0.72	0.88
Al <sub>2</sub> O <sub>3</sub>	14.30	15.10	14.50	14.80	15.00	15.40	16.50
Fe <sub>2</sub> O <sub>3</sub>	1.60	1.62	1.73	1.53	1.55	1.35	1.25
FeO	8.17	8.26	8.81	7.81	7.91	6.86	6.39
MnO	0.16	0.18	0.20	0.16	0.16	0.14	0.13
MgO	8.09	5.08	6.73	7.13	4.23	7.39	5.95
CaO	8.74	9.30	8.96	10.74	8.12	10.04	10.08
Na <sub>2</sub> O	3.95	4.01	3.51	3.17	4.80	3.37	3.78
K <sub>2</sub> O	0.08	0.07	0.23	0.31	0.06	0.47	0.23
P <sub>2</sub> O <sub>5</sub>	0.04	0.09	0.10	0.09	0.11	0.05	0.11
LOI	3.25	2.77	1.99	2.14	2.79	2.13	2.74
Cr (ppm)	89	0	101	82	1	166	56
Ni	37	11	39	33	0	53	26
Sc	36	36	41	53	37	49	40
V	307	339	357	313	361	292	299
Cu	45	34	40	64	15	46	3
Pb	0	n.a.	1	n.a.	1	n.a.	1
Zn	54	102	74	49	47	41	22
W	53.52	n.a.	47.00	n.a.	88.46	n.a.	58.46
Mo	0.28	n.a.	0.33	n.a.	0.55	n.a.	0.29
Rb	0	0	'	2	0	4	1
Cs	0.36	n.a.	0.14	n.a.	0.28	n.a.	0.64
Ba	12	n.a.	18	n.a.	9	n.a.	41
Sr	83	56	142	160	46	137	135
Tl	0.00	n.a.	0.00	n.a.	0.01	n.a.	0.00
Ga	16	18	16	16	22	15	16
Li	4.63	n.a.	2.01	n.a.	3.64	n.a.	3.59
Ta	0.06	n.a.	0.07	n.a.	0.10	n.a.	0.11
Nb	0.9	n.a.	1.1	n.a.	1.6	n.a.	1.7
Hf	1.36	1.82	2.27	1.53	2.09	1.38	2.01
Zr	53	71	89	60	81	54	78
Y	18	25	31	23	27	20	23
Th	0.13	n.a.	0.08	n.a.	0.15	n.a.	0.71
U	0.07	n.a.	0.13	n.a.	0.07	n.a.	0.24
La	1.71	n.a.	2.54	n.a.	3.04	n.a.	5.35
Ce	5.36	n.a.	8.43	n.a.	9.41	n.a.	13.71
Pr	0.96	n.a.	1.63	n.a.	1.58	n.a.	2.13
Nd	4.76	n.a.	8.22	n.a.	8.45	n.a.	9.75
Sm	1.79	n.a.	3.06	n.a.	2.87	n.a.	3.04
Eu	0.80	n.a.	1.23	n.a.	1.18	n.a.	1.05
Gd	2.57	n.a.	3.95	n.a.	3.53	n.a.	3.18
Tb	0.52	n.a.	0.81	n.a.	0.68	n.a.	0.60
Dy	3.50	n.a.	5.31	n.a.	4.57	n.a.	3.80
Ho	0.77	n.a.	1.09	n.a.	0.97	n.a.	0.79
Er	2.10	n.a.	3.29	n.a.	2.84	n.a.	2.30
Tm	0.31	n.a.	0.47	n.a.	0.42	n.a.	0.32
Yb	1.91	n.a.	2.79	n.a.	2.58	n.a.	2.09
Lu	0.28	n.a.	0.43	n.a.	0.38	n.a.	0.31



Sample Name	H-762	H-764	H-766	H-767	H-770	SD-802	*SD-803
Figure #	3.2.4	3.2.4	3.2.4	3.2.4	3.2.4	3.2.6 inset	3.2.6 inset
Rock Suite	aphyric/CPX	aphyric/CPX	aphyric/CPX	aphyric/CPX	aphyric/CPX	aphyric/CPX	aphyric/CPX
Rock Type	diabase	diabase	diabase	diabase	diabase	basalt	basalt
Mg#	45.74	54.90	56.47	64.33	45.18	56.90	59.28
SiO <sub>2</sub> (wt.%)	50.07	48.90	52.00	49.70	53.40	50.30	50.00
TiO <sub>2</sub>	1.52	1.52	1.00	1.12	1.44	1.24	1.40
Al <sub>2</sub> O <sub>3</sub>	13.50	14.40	14.60	14.30	14.90	15.20	15.20
Fe <sub>2</sub> O <sub>3</sub>	1.96	1.75	1.58	1.41	1.73	1.72	1.67
FeO	9.99	8.95	8.07	7.17	8.82	8.78	8.50
MnO	0.20	0.28	0.18	0.17	0.19	0.14	0.15
MgO	5.56	7.19	6.91	8.54	4.80	7.65	8.17
CaO	8.56	10.56	8.80	10.38	5.38	5.72	2.98
Na <sub>2</sub> O	3.96	3.30	3.70	3.49	4.92	4.97	4.80
K <sub>2</sub> O	0.09	0.09	0.13	0.11	0.07	0.49	1.17
P <sub>2</sub> O <sub>5</sub>	0.12	0.12	0.08	0.09	0.16	0.09	0.10
LOI	2.02	1.41	2.51	2.66	2.77	3.34	3.49
Cr (ppm)	28	277	40	256	0	63	32
Ni	13	60	48	53	0	23	18
Sc	53	50	53	42	34	33	35
V	462	328	334	265	381	323	320
Cu	32	29	36	43	14	0	0
Pb	n.a.	n.a.	n.a.	0	2	1	0
Zn	80	98	54	42	64	55	67
W	n.a.	n.a.	n.a.	26.16	34.20	13.26	8.38
Mo	n.a.	n.a.	n.a.	0.37	0.42	0.59	0.46
Rb	1	0	1	1	1	3	9
Cs	n.a.	n.a.	n.a.	1.30	0.81	0.16	0.33
Ba	n.a.	n.a.	n.a.	20	17	21	31
Sr	84	113	92	163	106	83	19
Tl	n.a.	n.a.	n.a.	0.00	0.00	0.02	0.05
Ga	18	16	17	15	17	13	12
Li	n.a.	n.a.	n.a.	7.59	9.10	11.55	12.07
Ta	n.a.	n.a.	n.a.	0.09	0.09	0.08	0.09
Nb	n.a.	n.a.	n.a.	1.4	1.4	1.2	1.5
Hf	2.72	2.62	1.79	2.03	2.26	2.00	1.97
Zr	106	102	70	79	88	78	77
Y	38	33	26	24	29	31	29
Th	n.a.	n.a.	n.a.	0.09	0.14	0.14	0.21
U	n.a.	n.a.	n.a.	0.05	0.08	0.09	0.10
La	n.a.	n.a.	n.a.	2.58	2.87	2.56	2.13
Ce	n.a.	n.a.	n.a.	8.57	9.26	8.12	7.35
Pr	n.a.	n.a.	n.a.	1.50	1.65	1.45	1.26
Nd	n.a.	n.a.	n.a.	7.60	8.47	7.44	6.97
Sm	n.a.	n.a.	n.a.	2.73	3.05	2.93	2.45
Eu	n.a.	n.a.	n.a.	1.04	1.18	1.09	0.94
Gd	n.a.	n.a.	n.a.	3.23	3.78	3.59	3.40
Tb	n.a.	n.a.	n.a.	0.65	0.72	0.74	0.68
Dy	n.a.	n.a.	n.a.	4.14	4.85	4.76	4.82
Ho	n.a.	n.a.	n.a.	0.87	1.02	1.07	1.05
Er	n.a.	n.a.	n.a.	2.69	2.97	3.05	2.78
Tm	n.a.	n.a.	n.a.	0.34	0.43	0.43	0.40
Yb	n.a.	n.a.	n.a.	2.25	2.60	2.75	2.64
Lu	n.a.	n.a.	n.a.	0.32	0.38	0.35	0.36

Sample Name	SD-804a	SD-805	SD-807a	SD-809	SD-810	*R-907	R-961d
Figure #	3.2.6 inset	3.2.6 inset	3.2.6 inset	3.2.6 inset	3.2.6 inset	3.2.1	3.2.1
Rock Suite	aphyric/CPX	aphyric/CPX	aphyric/CPX	aphyric/CPX	aphyric/CPX	aphyric/CPX	aphyric/CPX
Rock Type	basalt	altrd. bslt.	altrd. bslt.	basalt	altrd. bslt.	diabase	microgabbro
Mg#	61.08	54.26	37.50	62.82	26.56	60.03	56.36
SiO <sub>2</sub> (wt.%)	47.00	46.80	49.20	50.80	46.50	50.60	49.80
TiO <sub>2</sub>	1.36	1.28	0.60	0.96	0.80	0.84	0.52
Al <sub>2</sub> O <sub>3</sub>	16.70	17.30	12.90	15.10	14.00	15.10	14.60
Fe <sub>2</sub> O <sub>3</sub>	1.78	1.87	3.57	1.56	3.99	1.41	1.30
FeO	9.06	9.51	18.20	7.94	20.36	7.18	6.64
MnO	0.13	0.21	0.25	0.16	0.23	0.16	0.14
MgO	9.39	7.45	7.21	8.86	4.86	7.12	5.66
CaO	1.90	3.76	0.64	5.50	0.36	9.88	9.04
Na <sub>2</sub> O	4.48	4.80	0.21	2.97	0.02	3.56	6.49
K <sub>2</sub> O	1.75	0.06	0.10	2.01	0.24	0.11	0.61
P <sub>2</sub> O <sub>5</sub>	0.14	0.11	0.06	0.07	0.17	0.05	0.08
LOI	5.83	5.43	5.35	3.90	5.12	2.84	3.99
Cr (ppm)	40	30	54	43	0	63	119
Ni	15	14	14	22	0	29	39
Sc	43	39	37	28	42	54	30
V	374	383	302	306	390	319	349
Cu	0	139	0	57	0	31	68
Pb	2	0	0	1	1	0	;
Zn	80	95	58	54	59	56	52
W	12.76	23.58	19.75	23.24	23.00	3.10	23.58
Mo	0.29	0.29	0.24	0.25	0.24	0.69	1.04
Rb	12	0	1	14	3	0	21
Cs	0.79	0.12	0.15	0.30	0.19	0.49	5.60
Ba	42	8	5	56	10	12	101
Sr	14	27	2	45	1	216	636
Tl	0.00	0.02	0.01	0.00	0.00	0.00	0.04
Ga	17	18	11	18	13	13	17
Li	15.64	7.05	16.55	2.67	15.97	4.89	38.87
Ta	0.09	0.43	0.04	0.05	0.16	0.10	0.04
Nb	1.4	6.8	0.6	0.8	2.5	1.5	0.7
Hf	2.33	2.37	0.97	1.45	2.86	1.62	1.44
Zr	91	92	38	57	112	63	56
Y	27	33	15	22	30	22	13
Th	0.20	0.21	0.09	0.08	0.17	0.17	0.24
U	0.18	0.22	0.07	0.07	0.06	0.05	0.14
La	3.22	3.00	0.92	1.85	0.54	2.13	1.75
Ce	10.10	9.96	3.87	5.96	1.78	6.37	4.56
Pr	1.76	1.81	0.76	1.07	0.35	1.08	0.70
Nd	8.85	9.27	4.09	5.62	2.09	5.47	3.46
Sm	3.11	3.57	1.46	2.12	1.16	1.96	1.22
Eu	0.94	1.27	0.11	0.87	0.12	0.84	0.42
Gd	3.64	4.26	1.86	2.39	1.66	2.64	1.61
Tb	0.76	0.86	0.37	0.53	0.36	0.54	0.32
Dy	4.99	5.89	2.46	3.53	2.38	3.65	2.24
Ho	1.06	1.23	0.52	0.76	0.50	0.78	0.49
Er	3.04	3.64	1.43	2.21	1.38	2.16	1.54
Tm	0.42	0.50	0.19	0.31	0.19	0.31	0.22
Yb	2.51	3.25	1.10	1.97	1.07	2.01	1.50
Lu	0.30	0.43	0.14	0.29	0.14	0.29	0.24

Sample Name	D-1001	D-1002	D-1003	D-1004	D-1005	D-1006	D-1007
Figure #	3.2.4	3.2.4	3.2.4	3.2.4	3.2.4	3.2.4	3.2.4
Rock Suite	aphyric/CPX	aphyric/CPX	aphyric/CPX	aphyric/CPX	aphyric/CPX	aphyric/CPX	aphyric/CPX
Rock Type	basalt	basalt	altrd. bslt.	basalt	basalt	basalt	basalt
Mg#	65.04	60.57	42.00	50.80	51.18	35.54	38.04
SiO <sub>2</sub> (wt.%)	49.70	49.00	63.10	48.50	50.70	52.10	52.10
TiO <sub>2</sub>	0.80	1.00	0.32	1.40	1.20	1.76	1.68
Al <sub>2</sub> O <sub>3</sub>	14.90	15.50	12.60	15.30	14.60	13.60	14.20
Fe <sub>2</sub> O <sub>3</sub>	1.46	1.40	0.88	1.57	1.66	1.98	1.96
FeO	7.45	7.14	4.50	8.01	8.45	10.11	9.99
MnO	0.18	0.16	0.09	0.16	0.19	0.21	0.17
MgO	9.15	7.24	2.15	5.46	5.85	3.68	4.05
CaO	7.90	8.86	8.10	10.72	7.52	6.48	5.90
Na <sub>2</sub> O	2.60	3.54	2.62	1.90	4.25	4.28	4.59
K <sub>2</sub> O	1.64	1.01	0.06	0.03	0.35	0.16	0.47
P <sub>2</sub> O <sub>5</sub>	0.05	0.11	0.07	0.11	0.12	0.16	0.15
LOI	3.95	3.07	3.08	5.29	3.15	3.26	2.85
Cr (ppm)	102	275	59	33	15	0	0
Ni	35	36	3	14	7	0	0
Sc	29	43	25	44	47	42	43
V	247	292	137	360	333	404	395
Cu	74	23	6	0	0	32	10
Pb	n.a.	2	n.a.	1	n.a.	1	1
Zn	44	69	30	36	42	45	90
W	n.a.	53.49	n.a.	42.58	n.a.	68.15	54.57
Mo	n.a.	0.35	n.a.	0.54	n.a.	0.36	0.79
Rb	23	16	0	1	25	8	33
Cs	n.a.	1.05	n.a.	0.07	n.a.	0.21	0.73
Ba	n.a.	120	n.a.	16	n.a.	29	37
Sr	102	94	71	15	137	70	150
Tl	n.a.	0.08	n.a.	0.00	n.a.	0.00	0.03
Ga	17	15	15	17	16	21	19
Li	n.a.	29.00	n.a.	32.30	n.a.	20.44	17.32
Ta	n.a.	0.12	n.a.	0.09	n.a.	0.15	0.18
Nb	n.a.	2.0	n.a.	1.5	n.a.	2.4	2.8
Hf	1.29	1.48	1.22	2.12	2.08	2.95	2.80
Zr	50	58	47	83	81	115	109
Y	20	29	18	30	29	36	36
Th	n.a.	0.26	n.a.	0.16	n.a.	0.10	0.17
U	n.a.	0.14	n.a.	0.12	n.a.	0.08	0.17
La	n.a.	2.18	n.a.	2.75	n.a.	3.10	3.13
Ce	n.a.	6.27	n.a.	8.74	n.a.	10.89	10.38
Pr	n.a.	1.26	n.a.	1.52	n.a.	2.04	1.87
Nd	n.a.	6.54	n.a.	8.17	n.a.	10.98	9.65
Sm	n.a.	2.62	n.a.	2.98	n.a.	3.93	3.60
Eu	n.a.	0.82	n.a.	1.17	n.a.	1.44	1.34
Gd	n.a.	3.45	n.a.	3.59	n.a.	4.52	4.69
Tb	n.a.	0.69	n.a.	0.71	n.a.	0.92	0.90
Dy	n.a.	4.62	n.a.	4.48	n.a.	5.84	5.87
Ho	n.a.	1.02	n.a.	0.94	n.a.	1.18	1.24
Er	n.a.	3.06	n.a.	2.67	n.a.	3.42	3.60
Tm	n.a.	0.40	n.a.	0.38	n.a.	0.47	0.50
Yb	n.a.	2.60	n.a.	2.46	n.a.	2.98	3.25
Lu	n.a.	0.39	n.a.	0.37	n.a.	0.48	0.47

Sample Name	*S-16	B-74*	B-74	*B-76	B-157	*B-158	*B-160
Figure #	3.2.3	3.2.2	3.2.2	3.2.2	3.2.2	3.2.2	3.2.2
Rock Suite	olivine-rich	olivine-rich	olivine-rich	olivine-rich	olivine-rich	olivine-rich	olivine-rich
Rock Type	basalt	basalt	basalt	basalt	basalt	basalt	basalt
Mg#	37.31	45.96	45.96	51.52	41.55	38.63	51.71
SiO <sub>2</sub> (wt.%)	46.70	43.10	43.10	44.10	45.70	48.90	47.60
TiO <sub>2</sub>	2.40	1.76	1.76	1.92	2.08	2.16	1.84
Al <sub>2</sub> O <sub>3</sub>	17.20	15.30	15.30	15.30	16.80	16.00	15.30
Fe <sub>2</sub> O <sub>3</sub>	1.69	1.40	1.40	1.36	1.69	1.59	1.48
FeO	8.60	7.12	7.12	6.91	8.63	8.11	7.57
MnO	0.16	0.15	0.15	0.14	0.17	0.14	0.15
MgO	3.38	4.00	4.00	4.85	4.05	3.37	5.35
CaO	7.42	14.38	14.38	13.08	10.62	8.68	10.58
Na <sub>2</sub> O	3.68	3.96	3.96	3.32	3.80	4.63	3.41
K <sub>2</sub> O	2.40	0.26	0.26	0.63	0.54	0.05	0.45
P <sub>2</sub> O <sub>5</sub>	0.63	0.37	0.37	0.37	0.45	0.56	0.33
LOI	3.86	7.14	7.14	6.24	4.27	3.95	3.95
Cr (ppm)	177	211	211	171	319	100	189
Ni	94	92	92	87	102	76	64
Sc	32	32	32	31	41	30	38
V	256	257	257	267	384	365	338
Cu	27	13	13	26	26	25	20
Pb	2	3	3	1	2	3	2
Zn	112	79	79	54	94	78	71
W	1.76	15.63	42.65	1.29	47.46	2.48	5.10
Mo	2.31	1.31	1.38	1.45	1.75	1.48	1.21
Rb	74	7	7	14	9	0	12
Cs	1.67	0.60	0.53	1.47	0.49	0.13	0.81
Ba	177	84	72	94	89	51	78
Sr	248	413	413	255	234	135	170
Tl	0.50	0.05	0.03	0.11	0.08	0.02	0.10
Ga	21	21	21	17	19	22	17
Li	8.16	13.04	14.79	16.19	20.50	31.34	25.92
Ta	2.34	2.28	2.08	1.96	1.75	3.12	1.86
Nb	37.5	36.4	33.3	31.3	28.0	49.9	29.8
Hf	5.36	4.35	4.35	4.13	4.50	5.67	4.05
Zr	209	170	170	161	175	221	158
Y	35	25	25	29	43	32	30
Th	2.69	2.28	2.25	2.05	1.60	3.28	1.66
U	0.59	0.51	0.49	0.42	0.38	1.04	0.63
La	24.16	21.41	21.45	20.30	20.69	32.96	19.56
Ce	50.17	44.41	43.19	41.64	38.12	65.14	40.67
Pr	6.67	5.29	5.40	5.17	5.89	7.87	5.11
Nd	26.02	20.16	19.97	20.61	23.65	29.88	20.30
Sm	6.14	4.61	4.67	4.97	6.03	6.64	5.00
Eu	2.13	1.49	1.53	1.63	1.97	2.04	1.63
Gd	5.97	4.52	4.32	4.66	5.84	5.63	4.79
Tb	1.01	0.77	0.76	0.83	1.06	0.97	0.86
Dy	6.50	4.68	4.70	5.22	6.64	5.72	5.14
Ho	1.27	0.97	0.96	1.05	1.32	1.09	1.03
Er	3.52	2.76	2.82	2.92	3.94	3.20	2.88
Tm	0.49	0.40	0.41	0.41	0.54	0.41	0.42
Yb	3.20	2.60	2.48	2.54	3.36	2.72	2.63
Lu	0.46	0.38	0.38	0.38	0.51	0.40	0.39

Sample Name	T-257	*T-467	*T-482	*T-492	*T-514b	*T-572
Figure #	3.2.2	3.2.2	3.2.2	3.2.2	3.2.2	3.2.2
Rock Suite	olivine-rich	olivine-poor	olivine-poor	olivine-rich	olivine-rich	olivine-rich
Rock Type	basalt	basalt	basalt	basalt	basalt	basalt
Mg#	51.95	47.89	34.46	34.86	45.96	38.78
SiO <sub>2</sub> (wt.%)	47.10	48.20	50.50	50.50	45.80	48.40
TiO <sub>2</sub>	2.28	1.84	2.32	2.24	1.80	2.12
Al <sub>2</sub> O <sub>3</sub>	16.70	14.00	13.60	17.80	17.10	18.80
Fe <sub>2</sub> O <sub>3</sub>	1.14	1.94	2.08	1.47	1.85	1.44
FeO	5.83	9.89	10.60	7.50	9.44	7.34
MnO	0.13	0.21	0.18	0.15	0.23	0.19
MgO	4.16	6.00	3.68	2.65	5.30	3.07
CaO	9.56	9.46	5.54	4.74	5.76	5.18
Na <sub>2</sub> O	4.76	3.13	5.28	6.48	3.82	4.19
K <sub>2</sub> O	0.47	1.24	1.11	0.68	0.33	2.54
P <sub>2</sub> O <sub>5</sub>	0.64	0.13	0.22	0.87	0.36	0.34
LOI	5.45	2.43	2.55	2.73	6.06	4.67
Cr (ppm)	56	131	24	58	383	204
Ni	94	45	39	27	131	70
Sc	23	45	40	14	39	36
V	158	407	421	220	391	271
Cu	8	40	25	0	6	19
Pb	3	2	1	3	1	1
Zn	44	120	139	109	158	172
W	24.58	2.26	1.62	1.74	0.94	2.22
Mo	0.79	9.32	0.67	0.76	1.07	0.98
Rb	18	37	27	17	8	65
Cs	5.95	1.37	1.11	0.81	0.95	2.52
Ba	235	59	269	123	96	180
Sr	346	107	12*	238	86	125
Tl	0.19	0.59	0.22	0.15	0.08	0.59
Ga	15	18	13	16	19	18
Li	53.07	16.22	5.59	24.20	51.25	33.73
Ta	4.32	0.25	0.20	4.28	1.22	1.58
Nb	69.1	4.1	3.1	68.5	19.4	25.3
Hf	5.86	3.08	3.87	8.56	3.82	4.31
Zr	229	120	151	334	149	168
Y	30	47	56	28	37	35
Th	4.47	0.24	0.34	6.24	1.09	1.40
U	1.17	0.07	0.18	0.95	0.20	0.39
La	40.29	4.17	7.64	69.46	13.03	15.79
Ce	72.76	12.52	18.43	115.41	28.62	33.56
Pr	8.46	2.29	3.61	13.38	4.20	5.04
Nd	29.75	11.49	17.70	43.89	17.57	21.18
Sm	6.03	4.15	5.91	7.28	4.80	5.70
Eu	2.02	1.52	1.97	2.35	1.74	1.92
Gd	5.05	5.28	7.34	5.40	5.41	5.86
Tb	0.84	1.07	1.48	0.79	0.97	1.00
Dy	4.96	7.22	9.62	4.69	6.13	5.70
Ho	0.97	1.50	1.97	0.75	1.21	1.12
Er	2.67	4.64	5.89	1.84	3.22	2.91
Tm	0.38	0.65	0.81	0.25	0.43	0.39
Yb	2.31	4.25	4.94	1.50	2.70	2.47
Lu	0.35	0.59	0.72	0.19	0.41	0.34

Sample Name	*B-80	*B-80b	*B-127	B-128	B-132cr	B-132rm	*B-159
Figure #	3.2.2	3.2.2	3.2.2	3.2.2	3.2.2	3.2.2	3.2.2
Rock Suite	olivine-poor	olivine-poor	olivine-poor	olivine-poor	olivine-poor	olivine-poor	olivine-poor
Rock Type	altrd. bslt.	altrd. bslt.	basalt	basalt	basalt	basalt	basalt
Mg#	33.98	33.55	49.48	36.27	49.12	49.96	43.03
SiO <sub>2</sub> (wt.%)	57.30	77.90	49.30	45.40	46.20	50.50	48.90
TiO <sub>2</sub>	2.00	0.72	1.76	2.72	1.80	1.80	1.84
Al <sub>2</sub> O <sub>3</sub>	11.00	6.15	14.10	12.90	14.70	13.70	13.10
Fe <sub>2</sub> O <sub>3</sub>	1.74	0.66	1.78	2.55	1.69	1.80	2.02
FeO	8.89	3.36	9.08	13.02	8.63	9.18	10.31
MnO	0.18	0.07	0.19	0.20	0.20	0.20	0.19
MgO	3.02	1.12	5.87	4.89	5.50	6.05	5.14
CaO	8.66	6.64	8.38	8.84	11.70	7.98	8.52
Na <sub>2</sub> O	1.88	0.02	4.20	3.77	3.32	4.53	3.67
K <sub>2</sub> O	0.08	0.01	0.66	0.42	0.37	0.87	0.24
P <sub>2</sub> O <sub>5</sub>	0.20	0.07	0.18	0.25	0.13	0.14	0.19
LOI	2.85	2.32	2.38	2.47	3.01	1.54	3.40
Cr (ppm)	23	20	128	86	165	170	46
Ni	24	5	46	44	52	44	29
Sc	31	16	43	45	44	48	46
V	340	198	338	530	361	367	389
Cu	20	15	55	17	41	35	45
Pb	3	1	1	3	3	2	1
Zn	90	29	91	137	79	71	100
W	0.79	1.04	1.38	72.31	72.75	75.60	0.92
Mo	0.62	0.76	0.75	0.85	0.60	0.61	0.74
Rb	3	0	18	11	11	27	5
Cs	0.10	0.03	0.94	0.36	0.31	0.44	0.24
Ba	28	7	45	38	53	81	46
Sr	733	170	137	131	122	152	139
Tl	0.04	0.00	0.21	0.08	0.08	0.13	0.10
Ga	15	10	12	22	20	13	16
Li	5.71	2.57	9.47	6.49	4.58	4.30	18.51
Ta	0.16	0.10	0.29	0.39	0.21	0.20	0.35
Nb	2.6	1.6	4.6	6.2	3.3	3.2	5.6
Hf	4.18	1.44	3.05	5.18	3.14	3.14	3.15
Zr	163	56	119	202	122	123	123
Y	51	18	39	66	42	41	43
Th	0.29	0.13	0.33	0.38	0.28	0.22	0.38
U	0.17	0.05	0.18	0.27	0.12	0.09	0.19
La	5.69	2.28	4.72	7.34	4.50	3.50	6.72
Ce	16.20	5.76	13.04	21.58	13.10	11.64	16.29
Pr	2.92	1.10	2.24	3.77	2.31	2.09	2.75
Nd	14.40	5.16	11.29	18.93	11.63	11.02	13.16
Sm	5.08	1.78	3.96	6.73	4.22	4.13	4.30
Eu	1.75	0.62	1.39	2.21	1.53	1.34	1.51
Gd	6.29	2.25	4.92	8.17	5.24	5.02	5.16
Tb	1.28	0.49	1.00	1.63	1.08	1.02	1.02
Dy	8.45	3.12	6.47	10.59	7.11	6.78	6.46
Ho	1.78	0.66	1.43	2.25	1.50	1.44	1.36
Er	5.14	1.92	4.14	6.73	4.52	4.41	4.06
Tm	0.71	0.27	0.59	0.95	0.67	0.63	0.57
Yb	4.65	1.69	3.77	6.04	4.15	3.95	3.59
Lu	0.68	0.24	0.56	0.91	0.64	0.60	0.53



Sample Name	B-199	*T-514	T-515
Figure #	3.2.2	3.2.2	3.2.2
Rock Suite	olivine-poor	olivine-poor	olivine-poor
Rock Type	basalt	altrd. bslt.	basalt
Mg#	45.46	32.35	33.62
SiO <sub>2</sub> (wt.%)	49.50	49.50	50.50
TiO <sub>2</sub>	1.96	1.92	2.28
Al <sub>2</sub> O <sub>3</sub>	14.10	14.10	14.60
Fe <sub>2</sub> O <sub>3</sub>	2.03	2.03	2.15
FeO	10.36	10.36	10.98
MnO	0.24	0.23	0.20
MgO	5.70	3.27	3.67
CaO	7.52	8.78	6.18
Na <sub>2</sub> O	3.87	3.02	4.57
K <sub>2</sub> O	0.32	0.20	0.03
P <sub>2</sub> O <sub>5</sub>	0.14	0.22	0.27
LOI	3.49	3.76	2.99
Cr (ppm)	112	63	188
Ni	60	34	81
Sc	53	41	46
V	420	427	511
Cu	10	11	27
Pb	3	1	2
Zn	128	128	119
W	94.61	3.43	79.36
Mo	1.04	8.76	0.73
Rb	7	5	0
Cs	0.47	0.59	0.27
Ba	101	40	26
Sr	161	57	80
Tl	0.11	0.09	0.00
Ga	19	19	19
Li	23.58	30.73	29.44
Ta	0.32	0.27	0.37
Nb	5.1	4.3	5.9
Hf	3.32	3.62	4.75
Zr	130	141	185
Y	42	51	59
Th	0.52	0.37	0.38
U	0.18	0.40	0.16
La	4.72	6.06	6.86
Ce	13.29	17.19	20.12
Pr	2.35	2.90	3.42
Nd	11.78	14.31	17.00
Sm	4.25	4.97	6.14
Eu	1.51	1.68	1.94
Gd	5.31	5.95	7.35
Tb	1.08	1.22	1.45
Dy	7.16	7.99	9.30
Ho	1.48	1.65	1.94
Er	4.62	4.78	5.51
Tm	0.68	0.66	0.77
Yb	4.26	4.36	4.93
Lu	0.64	0.63	0.72

Sample Name	C-702	C-709	C-710	*C-712A	C-712c	*C-718a	C-718b
Figure #	3.2.6	3.2.6	3.2.6	3.2.6	3.2.6	3.2.6	3.2.6
Rock Suite	Croisilles	olivine-poor	olivine-poor	olivine-poor	olivine-poor	olivine-poor	olivine-poor
Rock Type	basalt	basalt	basalt	basalt	basalt	basalt	basalt
Mg#	42.14	40.46	41.81	46.08	38.00	41.16	38.65
SiO <sub>2</sub> (wt.%)	48.60	49.10	47.60	48.40	46.70	45.50	45.90
TiO <sub>2</sub>	3.20	1.64	1.84	2.08	1.84	2.44	2.32
Al <sub>2</sub> O <sub>3</sub>	12.40	13.60	14.00	12.70	13.10	12.60	11.90
Fe <sub>2</sub> O <sub>3</sub>	2.05	2.01	2.13	2.06	2.09	2.02	2.50
FeO	10.44	10.23	10.88	10.49	10.65	10.31	12.74
MnO	0.18	0.20	0.22	0.20	0.19	0.20	0.28
MgO	5.02	4.59	5.16	5.92	4.31	4.76	5.30
CaO	7.66	9.84	9.26	10.04	13.60	10.18	8.16
Na <sub>2</sub> O	3.53	2.81	3.28	3.61	2.25	3.80	3.06
K <sub>2</sub> O	2.35	0.29	1.18	0.30	0.07	0.46	1.09
P <sub>2</sub> O <sub>5</sub>	0.37	0.23	0.21	0.20	0.22	0.27	0.31
LOI	2.58	4.13	3.68	2.38	3.44	4.99	4.01
Cr (ppm)	31	72	65	36	32	36	24
Ni	44	47	54	28	41	28	36
Sc	36	38	48	45	41	39	39
V	514	323	349	435	411	401	480
Cu	1	61	47	9	15	0	8
Pb	n.a.	2	3	0	1	1	4
Zn	93	117	117	71	50	124	132
W	n.a.	69.07	38.89	1.57	105.35	2.35	32.81
Mo	n.a.	0.66	0.36	0.87	0.65	0.70	0.68
Rb	73	10	40	8	2	15	37
Cs	n.a.	1.82	2.15	0.58	0.26	1.31	8.02
Ba	n.a.	97	85	26	36	421	639
Sr	321	132	109	134	69	203	84
Tl	n.a.	0.07	0.26	0.04	0.00	0.04	0.08
Ga	20	18	21	14	26	19	21
Li	n.a.	17.27	16.72	11.23	7.91	15.74	12.74
Ta	n.a.	0.23	0.30	0.20	0.18	0.39	0.40
Nb	n.a.	3.7	4.7	3.3	2.9	6.3	6.4
Hf	6.35	3.18	3.52	3.69	3.43	3.59	4.53
Zr	248	124	137	144	134	140	177
Y	85	42	44	50	46	59	54
Th	n.a.	0.29	0.32	0.14	0.18	0.36	0.37
U	n.a.	0.38	0.31	0.24	0.21	0.81	0.75
La	n.a.	5.44	4.75	4.67	4.95	7.45	8.83
Ce	n.a.	14.15	14.44	14.95	15.15	21.05	23.68
Pr	n.a.	2.54	2.54	2.63	2.70	3.50	3.81
Nd	n.a.	12.35	12.86	13.23	13.52	16.99	18.13
Sm	n.a.	4.38	4.54	4.57	4.59	5.67	6.23
Eu	n.a.	1.48	1.63	1.73	1.63	2.18	1.94
Gd	n.a.	5.17	6.13	5.66	5.69	7.70	7.38
Tb	n.a.	1.07	1.21	1.18	1.14	1.47	1.43
Dy	n.a.	6.99	8.02	7.68	7.87	10.26	8.97
Ho	n.a.	1.47	1.72	1.55	1.60	2.05	1.83
Er	n.a.	4.47	4.96	4.54	4.74	5.47	5.31
Tm	n.a.	0.61	0.71	0.62	0.70	0.76	0.75
Yb	n.a.	4.02	4.68	4.21	4.53	4.91	4.65
Lu	n.a.	0.60	0.69	0.64	0.68	0.71	0.68

Sample Name	*C-721a	C-721b	C-726
Figure #	3.2.6	3.2.6	3.2.6
Rock Suite	olivine-poor	olivine-poor	olivine-poor
Rock Type	basalt	basalt	basalt
Mg#	42.22	44.63	51.72
SiO <sub>2</sub> (wt.%)	42.60	45.50	48.00
TiO <sub>2</sub>	2.04	1.24	1.64
Al <sub>2</sub> O <sub>3</sub>	14.60	15.70	13.50
Fe <sub>2</sub> O <sub>3</sub>	2.08	1.76	1.99
FeO	10.59	8.96	10.17
MnO	0.20	0.19	0.20
MgO	5.11	4.77	7.19
CaO	13.96	11.62	8.38
Na <sub>2</sub> O	1.73	3.04	3.37
K <sub>2</sub> O	0.30	0.34	0.36
P <sub>2</sub> O <sub>5</sub>	0.19	0.12	0.17
LOI	4.22	4.19	2.54
Cr (ppm)	102	209	87
Ni	36	43	39
Sc	42	48	51
V	434	280	429
Cu	41	94	46
Pb	1	1	1
Zn	121	87	116
W	3.03	55.29	20.29
Mo	0.84	0.63	0.66
Rb	9	13	9
Cs	4.03	2.94	0.27
Ba	266	215	57
Sr	111	204	141
Tl	0.03	0.13	0.04
Ga	20	22	19
Li	13.65	10.15	13.47
Ta	0.21	0.10	0.36
Nb	3.4	1.6	5.7
Hf	4.23	1.89	2.67
Zr	165	74	104
Y	56	28	41
Th	0.25	0.11	0.33
U	0.16	1.24	0.14
La	5.54	3.21	4.73
Ce	15.47	7.32	12.86
Pr	3.14	1.47	2.11
Nd	15.01	7.62	10.36
Sm	5.53	2.82	3.81
Eu	2.20	1.10	1.30
Gd	7.72	3.71	4.75
Tb	1.53	0.71	0.95
Dy	10.90	4.70	6.44
Ho	2.16	1.01	1.40
Er	5.95	3.01	4.13
Tm	0.83	0.42	0.58
Yb	5.52	2.75	3.63
Lu	0.79	0.40	0.52

Sample Name	TL-782	TL-783	TL-784	TL-785	TL-786	U-823a
Figure #	3.2.5	3.2.5	3.2.5	3.2.5	3.2.5	3.2.5
Rock Suite	plag. porph.	plag. porph.	plag. porph.	plag. porph.	plag. porph.	plag. porph.
Rock Type	diabase	diabase	diabase	diabase	diabase	diabase
Mg#	62.90	65.51	72.80	63.99	67.52	65.44
SiO <sub>2</sub> (wt.%)	47.20	46.80	45.60	47.40	47.90	47.30
TiO <sub>2</sub>	0.96	0.80	0.64	0.84	0.68	0.72
Al <sub>2</sub> O <sub>3</sub>	16.60	16.30	18.40	16.90	15.80	18.90
Fe <sub>2</sub> O <sub>3</sub>	1.43	1.45	1.12	1.45	1.37	1.05
FeO	7.29	7.42	5.71	7.40	6.97	5.36
MnO	0.18	0.15	0.13	0.16	0.15	0.14
MgO	8.16	9.30	10.09	8.68	9.57	6.70
CaO	10.82	11.22	11.80	9.46	11.06	12.74
Na <sub>2</sub> O	2.28	2.24	1.96	2.83	2.34	2.36
K <sub>2</sub> O	0.76	0.85	0.67	0.68	0.34	0.17
P <sub>2</sub> O <sub>5</sub>	0.06	0.04	0.02	0.05	0.03	0.04
LOI	2.48	2.48	3.51	3.26	3.52	3.22
Cr (ppm)	309	399	678	316	471	329
Ni	105	136	278	100	145	68
Sc	45	48	34	44	41	44
V	271	255	200	273	226	221
Cu	43	53	29	41	69	31
Pb	1	n.a.	n.a.	1	1	1
Zn	54	56	26	59	45	36
W	35.79	n.a.	n.a.	61.65	17.60	89.80
Mo	0.16	n.a.	n.a.	0.13	0.22	0.24
Rb	9	9	8	7	3	1
Cs	0.89	n.a.	n.a.	0.97	0.33	1.40
Ba	29	n.a.	n.a.	32	16	11
Sr	164	129	190	170	107	179
Tl	0.00	n.a.	n.a.	0.00	0.01	0.01
Ga	14	14	14	16	13	14
Li	8.21	n.a.	n.a.	6.83	5.83	2.25
Ta	0.03	n.a.	n.a.	0.03	0.02	0.03
Nb	0.5	n.a.	n.a.	0.5	0.3	0.5
Hf	1.42	1.14	0.82	1.46	0.93	0.96
Zr	55	44	32	57	36	37
Y	26	23	14	26	20	15
Th	0.05	n.a.	n.a.	0.03	0.06	0.03
U	0.03	n.a.	n.a.	0.02	0.02	0.01
La	1.07	n.a.	n.a.	1.10	0.65	0.91
Ce	4.26	n.a.	n.a.	4.31	2.70	3.17
Pr	0.86	n.a.	n.a.	0.93	0.59	0.60
Nd	4.98	n.a.	n.a.	5.18	3.52	3.27
Sm	2.12	n.a.	n.a.	2.27	1.63	1.42
Eu	0.81	n.a.	n.a.	0.77	0.66	0.61
Gd	2.77	n.a.	n.a.	2.94	2.16	1.90
Tb	0.57	n.a.	n.a.	0.60	0.47	0.41
Dy	3.80	n.a.	n.a.	4.07	3.26	2.67
Ho	0.84	n.a.	n.a.	0.88	0.70	0.58
Er	2.45	n.a.	n.a.	2.57	2.13	1.76
Tm	0.35	n.a.	n.a.	0.37	0.30	0.24
Yb	2.32	n.a.	n.a.	2.26	1.95	1.52
Lu	0.34	n.a.	n.a.	0.34	0.27	0.22

**C.1b Gabbroic Rocks**

Sample Name	S-7	T-267	T-288	T-393	TL-523	TL-524	TL-525
Figure #	3.2.3	3.2.2	3.2.2	3.2.2	3.2.5	3.2.5	3.2.5
Rock Suite	aphyric/CPX	aphyric/CPX	aphyric/CPX	aphyric/CPX	aphyric/CPX	aphyric/CPX	aphyric/CPX
Rock Type	gabbro	microgabbro	gabbro	gabbro	metagabbro	metagabbro	gabbro
Mg Number	61.93	48.29	67.09	57.50	76.90	59.38	58.46
SiO <sub>2</sub> (wt.%)	49.70	52.30	44.50	44.50	47.00	49.50	51.90
TiO <sub>2</sub>	1.04	1.20	1.08	0.88	0.36	1.40	1.04
Al <sub>2</sub> O <sub>3</sub>	14.20	14.50	15.20	14.70	17.60	14.60	15.60
Fe <sub>2</sub> O <sub>3</sub> *	9.35	11.60	8.91	9.75	5.55	10.23	9.19
MnO	0.17	0.16	0.13	0.15	0.09	0.16	0.14
MgO	7.68	5.47	9.17	6.66	9.33	7.55	6.53
CaO	11.86	5.08	16.00	18.62	12.84	10.74	9.08
Na <sub>2</sub> O	3.20	4.83	1.05	0.17	2.16	3.39	3.60
K <sub>2</sub> O	0.17	0.09	0.33	0.04	0.12	0.17	0.45
P <sub>2</sub> O <sub>5</sub>	0.08	0.09	0.00	0.06	0.00	0.12	0.10
LOI	2.73	3.47	3.62	3.63	3.72	1.58	2.25
Cr (ppm)	165	0	179	22	684	238	150
Ni	53	0	47	15	690	56	61
Sc	52	33	86	36	51	53	46
V	269	387	448	237	154	334	297
Cu	15	11	107	9	149	51	35
Pb	n.a.	1	0	0	1	n.a.	n.a.
Zn	28	75	30	26	46	71	30
W	n.a.	34.36	73.20	60.47	39.76	n.a.	n.a.
Mo	n.a.	0.21	0.43	0.33	0.37	n.a.	n.a.
Rb	1	1	5	0	1	1	4
Cs	n.a.	0.74	0.58	0.14	0.18	n.a.	n.a.
Ba	n.a.	22	31	4	5	n.a.	n.a.
Sr	201	80	368	55	163	193	147
Tl	n.a.	0.02	0.00	0.00	0.00	n.a.	n.a.
Ga	14	16	12	14	38	16	18
Li	n.a.	6.12	3.52	1.31	0.90	n.a.	n.a.
Ta	n.a.	0.07	0.91	0.12	0.01	n.a.	n.a.
Nb	n.a.	1.1	14.6	1.9	0.2	n.a.	n.a.
Hf	n.a.	1.85	0.82	1.46	0.41	n.a.	n.a.
Zr	60	72	32	57	16	111	76
Y	22	25	27	20	7	34	25
Th	n.a.	0.18	0.07	0.14	0.05	n.a.	n.a.
U	n.a.	0.10	0.01	0.04	0.12	n.a.	n.a.
La	n.a.	2.78	0.25	1.75	0.37	n.a.	n.a.
Ce	n.a.	8.35	1.42	5.78	1.28	n.a.	n.a.
Pr	n.a.	1.46	0.39	1.00	0.25	n.a.	n.a.
Nd	n.a.	7.24	2.91	5.03	1.35	n.a.	n.a.
Sm	n.a.	2.57	1.64	1.89	0.60	n.a.	n.a.
Eu	n.a.	0.93	0.69	0.69	0.41	n.a.	n.a.
Gd	n.a.	3.12	2.91	2.51	0.93	n.a.	n.a.
Yb	n.a.	0.63	0.64	0.48	0.19	n.a.	n.a.
Dy	n.a.	4.23	4.68	3.41	1.33	n.a.	n.a.
Ho	n.a.	0.89	1.07	0.74	0.29	n.a.	n.a.
Er	n.a.	2.68	2.86	1.97	0.75	n.a.	n.a.
Tm	n.a.	0.38	0.39	0.28	0.10	n.a.	n.a.
Yb	n.a.	2.42	2.42	1.92	0.64	n.a.	n.a.
Lu	n.a.	0.35	0.36	0.28	0.10	n.a.	n.a.



Sample Name	TL-526	TL-530a	H-754a	H-754b	H-756	H-758c	H-763
Figure #	3.2.5	3.2.5	3.2.5	3.2.5	3.2.5	3.2.5	3.2.5
Rock State	aphyric/CPX	aphyric/CPX	aphyric/CPX	aphyric/CPX	aphyric/CPX	aphyric/CPX	aphyric/CPX
Rock Type	gabbro	gabbro	Rodingitized	gabbro	gabbro	gabbro	gabbro
Mg Number	64.76	54.85	83.60	74.83	56.06	70.23	75.62
SiO <sub>2</sub> (wt.%)	49.10	52.00	43.50	49.40	50.00	49.40	46.90
TiO <sub>2</sub>	0.96	0.84	0.12	0.44	1.28	0.56	0.60
Al <sub>2</sub> O <sub>3</sub>	15.50	13.70	25.40	14.40	14.50	15.20	13.50
Fe <sub>2</sub> O <sub>3</sub>	9.30	12.52	2.47	5.89	10.29	7.27	8.94
MnO	0.15	0.20	0.05	0.12	0.17	0.13	0.15
MgO	8.63	7.68	6.36	8.84	6.63	8.66	14.00
CaO	9.08	5.88	12.10	14.26	9.76	12.04	9.98
Na <sub>2</sub> O	3.39	2.41	2.93	2.52	3.63	2.53	1.99
K <sub>2</sub> O	0.32	0.44	0.21	0.22	0.36	0.47	0.29
P <sub>2</sub> O <sub>5</sub>	0.05	0.05	0.02	0.00	0.12	0.00	0.04
LOI	3.66	3.74	5.43	2.57	2.30	2.49	2.74
Cr	120	43	302	506	161	446	975
Ni	59	32	158	86	40	90	420
Sc	36	47	15	66	46	61	35
V	281	342	36	231	379	241	229
Cu	136	630	0	87	49	85	27
Pb	n.a.	n.a.	n.a.	n.a.	n.a.	n.a.	n.a.
Zn	42	61	13	20	60	33	49
W	n.a.	n.a.	n.a.	n.a.	n.a.	n.a.	n.a.
Mo	n.a.	n.a.	n.a.	n.a.	n.a.	n.a.	n.a.
Rb	2	3	2	1	3	3	3
Cs	n.a.	n.a.	n.a.	n.a.	n.a.	n.a.	n.a.
Ba	n.a.	n.a.	n.a.	n.a.	n.a.	n.a.	n.a.
Sr	137	89	340	153	164	130	104
Tl	n.a.	n.a.	n.a.	n.a.	n.a.	n.a.	n.a.
Ga	12	14	12	12	16	12	13
Li	n.a.	n.a.	n.a.	n.a.	n.a.	n.a.	n.a.
Ta	n.a.	n.a.	n.a.	n.a.	n.a.	n.a.	n.a.
Nb	n.a.	n.a.	n.a.	n.a.	n.a.	n.a.	n.a.
Hf	n.a.	n.a.	n.a.	n.a.	n.a.	n.a.	n.a.
Zr	50	48	15	20	72	18	36
Y	17	17	1	11	25	13	20
Th	n.a.	n.a.	n.a.	n.a.	n.a.	n.a.	n.a.
U	n.a.	n.a.	n.a.	n.a.	n.a.	n.a.	n.a.
La	n.a.	n.a.	n.a.	n.a.	n.a.	n.a.	n.a.
Ce	n.a.	n.a.	n.a.	n.a.	n.a.	n.a.	n.a.
Pr	n.a.	n.a.	n.a.	n.a.	n.a.	n.a.	n.a.
Nd	n.a.	n.a.	n.a.	n.a.	n.a.	n.a.	n.a.
Sm	n.a.	n.a.	n.a.	n.a.	n.a.	n.a.	n.a.
Eu	n.a.	n.a.	n.a.	n.a.	n.a.	n.a.	n.a.
Gd	n.a.	n.a.	n.a.	n.a.	n.a.	n.a.	n.a.
Tb	n.a.	n.a.	n.a.	n.a.	n.a.	n.a.	n.a.
Dy	n.a.	n.a.	n.a.	n.a.	n.a.	n.a.	n.a.
Ho	n.a.	n.a.	n.a.	n.a.	n.a.	n.a.	n.a.
Er	n.a.	n.a.	n.a.	n.a.	n.a.	n.a.	n.a.
Tm	n.a.	n.a.	n.a.	n.a.	n.a.	n.a.	n.a.
Yb	n.a.	n.a.	n.a.	n.a.	n.a.	n.a.	n.a.
Lu	n.a.	n.a.	n.a.	n.a.	n.a.	n.a.	n.a.

Sample Name	H-769	R-902c	R-961b	R-961d	R-966	R-967
Figure #	3.2.5	3.2.1	red hills	red hills	red hills	3.2.1
Rock Suite	aphyric/CPX	aphyric/CPX	aphyric/CPX	aphyric/CPX	aphyric/CPX	aphyric/CPX
Rock Type	gabbro	metagabbro	rodingitized	microgabbro	metagabbro	metagabbro
Mg Number	56.40	61.35	82.89	56.36	59.96	59.18
SiO <sub>2</sub> (wt.%)	50.50	50.80	42.70	49.80	47.10	44.30
TiO <sub>2</sub>	0.84	0.44	0.28	0.52	1.28	1.32
Al <sub>2</sub> O <sub>3</sub>	15.70	13.80	14.10	14.60	15.40	15.60
Fe <sub>2</sub> O <sub>3</sub>	10.15	9.83	6.03	8.68	10.46	10.49
MnO	0.19	0.16	0.10	0.14	0.17	0.16
MgO	6.63	7.88	14.75	5.66	7.91	7.68
CaO	8.84	10.70	16.40	9.04	12.44	17.00
Na <sub>2</sub> O	3.72	3.68	0.89	6.49	2.84	1.20
K <sub>2</sub> O	0.01	0.92	0.05	0.61	0.24	0.07
P <sub>2</sub> O <sub>5</sub>	0.05	0.04	0.01	0.08	0.10	0.08
LOI	3.20	2.01	3.61	3.99	1.71	2.48
Cr	50	232	890	119	285	254
Ni	23	56	570	39	63	58
Sc	34	50	42	30	53	42
V	305	335	157	349	335	307
Cu	29	116	94	68	45	245
Pb	n.a.	n.a.	0	1	n.a.	3
Zn	73	43	16	52	48	44
W	n.a.	n.a.	30.42	23.58	n.a.	88.52
Mo	n.a.	n.a.	0.20	1.04	n.a.	0.37
Rb	0	21	2	21	2	0
Cs	n.a.	n.a.	0.13	5.60	n.a.	0.36
Ba	n.a.	n.a.	21	101	n.a.	15
Sr	141	2200	428	636	664	420
Tl	n.a.	n.a.	0.02	0.04	n.a.	0.00
Ga	14	14	10	17	20	19
Li	n.a.	n.a.	21.61	38.87	n.a.	1.99
Ta	n.a.	n.a.	0.00	0.04	n.a.	0.28
Nb	n.a.	n.a.	0.1	0.7	n.a.	4.4
Hf	n.a.	n.a.	0.49	1.44	n.a.	1.85
Zr	47	113	19	56	82	72
Y	15	5	6	13	28	28
Th	n.a.	n.a.	0.04	0.24	n.a.	0.23
U	n.a.	n.a.	0.01	0.14	n.a.	0.09
La	n.a.	n.a.	0.07	1.75	n.a.	1.81
Ce	n.a.	n.a.	0.27	4.56	n.a.	6.95
Pr	n.a.	n.a.	0.09	0.70	n.a.	1.35
Nd	n.a.	n.a.	0.64	3.46	n.a.	7.41
Sm	n.a.	n.a.	0.44	1.22	n.a.	2.96
Eu	n.a.	n.a.	0.22	0.42	n.a.	1.17
Gd	n.a.	n.a.	0.65	1.61	n.a.	3.75
Tb	n.a.	n.a.	0.15	0.32	n.a.	0.72
Dy	n.a.	n.a.	1.05	2.24	n.a.	4.68
Ho	n.a.	n.a.	0.24	0.49	n.a.	0.99
Er	n.a.	n.a.	0.71	1.54	n.a.	2.92
Tm	n.a.	n.a.	0.10	0.22	n.a.	0.40
Yb	n.a.	n.a.	0.62	1.50	n.a.	2.64
Lu	n.a.	n.a.	0.09	0.24	n.a.	0.40

Sample Name	L-36	B-81	B-90	T-516
Figure #	3.2.2	3.2.2	3.2.2	3.2.2
Rock Suite	Patuki	Patuki	Fatuki	Patuki
Rock Type	gabbro	gabbro	gabbro	rodingitized gabbro
Mg Number	68.48	44.81	42.96	73.72
SiO <sub>2</sub> (wt.%)	47.60	43.90	40.80	42.10
TiO <sub>2</sub>	0.96	1.00	2.32	0.04
Al <sub>2</sub> O <sub>3</sub>	15.90	14.60	13.30	22.50
Fe <sub>2</sub> O <sub>3</sub>	7.95	13.71	18.88	4.54
MnO	0.13	0.19	0.17	0.05
MgO	8.72	5.62	7.18	6.43
CaO	11.72	17.72	12.32	15.14
Na <sub>2</sub> O	2.80	0.46	1.82	2.25
K <sub>2</sub> O	0.30	0.13	0.23	0.16
P <sub>2</sub> O <sub>5</sub>	0.04	0.04	0.00	0.00
LOI	2.93	2.53	1.99	6.07
Cr	413	0	25	516
Ni	114	3	65	205
Sc	48	54	69	12
V	271	534	1059	27
Cu	59	87	79	25
Pb	n.a.	n.a.	1	0
Zn	35	60	42	0
W	n.a.	n.a.	40.58	52.61
Mo	n.a.	n.a.	0.50	0.35
Rb	3	0	3	3
Cs	n.a.	n.a.	0.50	0.06
Ba	n.a.	n.a.	22	34
Sr	182	50	429	106
Tl	n.a.	n.a.	0.00	0.00
Ga	15	15	20	13
Li	n.a.	n.a.	5.10	15.21
Ta	n.a.	n.a.	0.05	0.04
Nb	n.a.	n.a.	0.9	0.6
Hf	n.a.	n.a.	0.77	0.14
Zr	81	35	30	5
Y	27	15	11	1
Th	n.a.	n.a.	0.07	0.25
U	n.a.	n.a.	0.03	0.03
La	n.a.	n.a.	0.30	0.13
Ce	n.a.	n.a.	1.14	0.37
Pr	n.a.	n.a.	0.26	0.06
Nd	n.a.	n.a.	1.69	0.34
Sm	n.a.	n.a.	0.94	0.15
Eu	n.a.	n.a.	0.51	0.23
Gd	n.a.	n.a.	1.53	0.22
Tb	n.a.	n.a.	0.33	0.05
Dy	n.a.	n.a.	2.24	0.43
Ho	n.a.	n.a.	0.50	0.10
Er	n.a.	n.a.	1.34	0.27
Tm	n.a.	n.a.	0.18	0.04
Yb	n.a.	n.a.	1.09	0.31
Lu	n.a.	n.a.	0.15	0.04

Sample Name	C-704	C-714	C-715	C-717	C-727
Figure #	3.2.6	3.2.6	3.2.6	3.2.6	3.2.6
Rock Suite	Croisilles	Croisilles	Croisilles	Croisilles	Croisilles
Rock Type	metagabbro	gabbro	gabbro	plagiogranite	gabbro
Mg Number	51.12	46.01	52.03	46.60	40.20
SiO <sub>2</sub> (wt.%)	49.40	48.30	53.10	65.00	50.00
TiO <sub>2</sub>	1.36	1.00	0.88	0.76	1.56
Al <sub>2</sub> O <sub>3</sub>	12.80	16.60	14.80	14.10	14.10
Fe <sub>2</sub> O <sub>3</sub>	13.84	12.92	10.37	4.88	13.73
MnO	0.22	0.43	0.15	0.05	0.19
MgO	7.31	5.56	5.68	2.15	4.66
CaO	9.30	5.38	6.04	2.36	9.12
Na <sub>2</sub> O	2.92	3.88	5.47	6.87	3.65
K <sub>2</sub> O	0.67	2.24	0.30	0.79	0.79
P <sub>2</sub> O <sub>5</sub>	0.16	0.20	0.08	0.26	0.12
LOI	1.43	2.82	2.07	1.22	1.82
Cr	48	51	0	0	1
Ni	41	71	8	0	0
Sc	46	34	38	16	48
V	398	332	393	17	500
Cu	48	130	0	0	29
Pb	n.a.	7	0	0	n.a.
Zn	130	161	16	0	71
W	n.a.	17.40	44.13	106.86	n.a.
Mo	n.a.	58.19	0.35	1.53	n.a.
Rb	14	59	5	12	17
Cs	n.a.	2.62	0.26	1.17	n.a.
Ba	n.a.	309	317	496	n.a.
Sr	150	245	161	138	273
Tl	n.a.	0.38	0.00	0.06	n.a.
Ga	19	23	14	17	18
Li	n.a.	18.72	14.60	3.14	n.a.
Ta	n.a.	0.29	0.30	0.21	n.a.
Nb	n.a.	4.7	4.8	3.4	n.a.
Hf	n.a.	3.54	1.23	4.46	n.a.
Zr	100	138	48	174	68
Y	38	38	19	43	26
Th	n.a.	3.83	0.17	0.17	n.a.
U	n.a.	0.45	0.05	0.11	n.a.
La	n.a.	15.03	2.12	6.23	n.a.
Ce	n.a.	38.58	6.24	15.55	n.a.
Pr	n.a.	4.77	1.08	2.94	n.a.
Nd	n.a.	19.08	5.35	13.86	n.a.
Sm	n.a.	5.63	1.93	4.57	n.a.
Eu	n.a.	1.57	0.90	1.37	n.a.
Gd	n.a.	6.13	2.55	5.53	n.a.
Tb	n.a.	1.13	0.48	1.01	n.a.
Dy	n.a.	7.21	3.13	6.67	n.a.
Ho	n.a.	1.48	0.69	1.41	n.a.
Er	n.a.	4.48	1.98	4.02	n.a.
Tm	n.a.	0.63	0.29	0.55	n.a.
Yb	n.a.	4.16	1.88	3.37	n.a.
Lu	n.a.	0.63	0.29	0.49	n.a.

## C.2 Mineral Analyses

Note: Number of cations have been calculated using MINFILE (version 3-88), a program package by A. M. Afifi and E. J. Essene. Cations have been calculated on the basis of 6 oxygens, ferric and ferrous iron have been calculated using a charge balance procedure (see Afifi and Essene (1988) for details. Suite numbers are indicated: suite #1 = aphyric/clinopyroxene-phyric suite; suite #2 = "olivine-poor" suite (Patuki and Croisilles mélanges); suite #3 = "olivine-rich" suite (Patuki and Croisilles mélanges); suite #4 = Upukerora Formation (pyroxenes in mafic clasts).

	3a 37	3b 37	4a 37	4b 37	5a 37	5b 37	1a 76	1b 76	2a 76	2b 76
SiO <sub>2</sub>	53.33	50.30	51.95	52.23	51.31	51.00	45.88	45.84	46.26	46.08
TiO <sub>2</sub>	0.47	0.75	0.46	0.60	0.55	0.89	3.10	3.24	2.96	2.66
Al <sub>2</sub> O <sub>3</sub>	1.85	4.17	2.24	2.60	4.16	4.25	6.35	6.85	6.80	6.95
Cr <sub>2</sub> O <sub>3</sub>	0.32	0.51	0.10	0.12	0.72	0.79	0.16	0.11	0.18	0.10
FeO	5.34	5.89	5.56	6.24	5.61	4.94	9.05	8.34	6.82	7.30
MnO	0.10	0.14	0.23	0.16	0.09	0.11	0.14	0.14	0.10	0.19
NiO	0.06	0.03	-	0.04	0.02	0.02	0.05	0.03	0.04	-
MgO	16.88	15.54	14.75	14.32	15.53	15.75	11.62	11.93	12.96	12.45
CaO	21.78	22.11	23.62	24.13	22.14	22.64	22.13	22.55	22.63	23.60
Na <sub>2</sub> O	0.18	0.23	0.46	0.42	0.19	0.18	0.47	0.27	0.38	0.39
K <sub>2</sub> O	0.01	-	-	0.01	-	0.03	-	-	-	-
Total	100.32	99.67	99.37	100.87	100.31	100.60	98.95	99.30	99.13	99.72
#Si IV	1.95	1.86	1.93	1.92	1.88	1.87	1.75	1.74	1.75	1.74
#Al IV	0.05	0.14	0.07	0.08	0.12	0.13	0.25	0.26	0.25	0.26
#Ti IV	-	-	-	-	-	-	-	-	-	-
#Fe IV	-	-	-	-	-	-	-	-	-	-
T site	2.00	2.00	2.00	2.00	2.00	2.00	2.00	2.00	2.00	2.00
#Al VI	0.03	0.05	0.03	0.03	0.06	0.05	0.04	0.05	0.05	0.05
#Ti	0.01	0.02	0.01	0.02	0.02	0.02	0.09	0.09	0.08	0.08
#Cr	0.01	0.01	0.00	0.00	0.02	0.02	0.00	0.00	0.01	0.00
#Fe +3	-	0.00	0.00	0.00	0.00	-	-	0.00	-	-
#Fe +2	0.16	0.18	0.17	0.19	0.17	0.15	0.29	0.26	0.22	0.23
#Mn +2	0.00	0.00	0.01	0.00	0.00	0.00	0.00	0.00	0.00	0.01
#Ni	0.00	0.00	-	0.00	0.00	0.00	0.00	0.00	0.00	-
#Mg	0.92	0.86	0.82	0.79	0.85	0.86	0.66	0.67	0.73	0.70
#Ca	0.85	0.88	0.94	0.95	0.87	0.89	0.91	0.92	0.92	0.95
#Na	0.01	0.02	0.03	0.03	0.01	0.01	0.03	0.02	0.03	0.03
#K	0.00	-	-	0.00	-	0.00	-	-	-	-
M1, M2	2.00	2.02	2.02	2.02	2.01	2.01	2.03	2.02	2.03	2.04
%Mg	47.43	44.64	42.17	40.62	44.83	45.19	35.56	36.27	39.15	37.04
%Fe+Mn	8.58	9.72	9.29	10.19	9.23	8.13	15.78	14.46	11.73	12.50
%Ca	43.99	45.64	48.54	49.19	45.94	46.68	48.67	49.27	49.13	50.46
Suite #	1	1	1	1	1	1	3	3	3	3



	3a 76	3b 76	1a 128	1b 128	2a 128	2b 128	3a 128	4a 128	4b 128	1a 132cr
SiO2	46.71	46.49	47.60	48.17	49.30	49.97	49.73	48.67	48.50	51.20
TiO2	2.44	2.74	2.49	2.10	2.01	1.83	1.20	1.84	1.95	1.23
Al2O3	7.22	6.89	3.57	3.73	4.05	3.75	3.11	3.61	3.98	4.17
Cr2O3	0.12	0.20	0.02	0.04	0.10	0.05	0.41	0.07	0.05	0.88
FeO	7.13	6.82	14.12	15.05	12.65	11.99	10.21	14.58	13.89	6.45
MnO	0.11	0.10	0.31	0.18	0.24	0.19	0.17	0.37	0.30	0.20
NiO	0.05	0.05	0.03	0.04	0.03	-	0.05	0.01	0.02	0.05
MgO	12.81	12.87	12.84	13.67	13.70	15.34	16.47	14.18	13.14	15.74
CaO	23.34	22.49	18.07	16.46	16.85	17.32	18.40	15.73	18.02	20.70
Na2O	0.32	0.38	0.44	0.40	0.34	0.37	0.31	0.34	0.36	0.20
K2O	-	0.01	-	0.01	0.16	0.02	-	0.03	0.12	0.02
Total	100.25	99.04	99.49	99.85	99.43	100.83	100.06	99.43	100.33	100.84
#Si IV	1.75	1.75	1.83	1.84	1.86	1.86	1.86	1.85	1.84	1.87
#Al IV	0.25	0.25	0.16	0.16	0.14	0.14	0.14	0.15	0.16	0.13
#Ti IV	-	-	0.01	-	-	-	0.00	-	-	-
#Fe IV	-	-	-	-	-	-	-	-	-	-
T site	2.00	2.00	2.00	2.00	2.00	2.00	2.00	2.00	2.00	2.00
#Al VI	0.06	0.06	-	0.00	0.05	0.02	-	0.02	0.02	0.05
#Ti	0.07	0.08	0.06	0.06	0.06	0.05	0.03	0.05	0.06	0.03
#Cr	0.00	0.01	0.00	0.00	0.00	0.00	0.01	0.00	0.00	0.03
#Fe +3	0.00	-	-	0.00	0.00	0.00	0.00	0.00	0.00	0.00
#Fe +2	0.22	0.22	0.45	0.48	0.40	0.37	0.32	0.46	0.44	0.20
#Mn +2	0.00	0.00	0.01	0.01	0.01	0.01	0.01	0.01	0.01	0.01
#Ni	0.00	0.00	0.00	0.00	0.00	-	0.00	0.00	0.00	0.00
#Mg	0.71	0.72	0.73	0.78	0.77	0.85	0.92	0.81	0.74	0.86
#Ca	0.93	0.91	0.74	0.67	0.68	0.69	0.74	0.64	0.73	0.81
#Na	0.02	0.03	0.03	0.03	0.02	0.03	0.02	0.03	0.03	0.01
#K	-	0.00	-	0.00	0.01	0.00	-	0.00	0.01	0.00
M1,M2	2.04	2.03	2.04	2.03	2.00	2.02	2.04	2.02	2.03	2.00
%Mg	38.07	39.10	37.85	40.15	41.46	44.31	46.37	41.86	38.59	45.82
%Fe*+Mn	12.07	11.80	23.87	25.10	21.89	19.74	16.40	24.77	23.38	10.86
%Ca	49.85	49.11	38.28	34.75	36.65	35.95	37.23	33.37	38.03	43.31
Suite #	3	3	2	2	2	2	2	2	2	2

[illegible]



[illegible]

	7b 160	1a 257	1a 267	1b 267	2a 267	2b 267	3a 267	4a 267	4b 267	1b 290
SiO2	49.02	51.28	51.25	49.66	49.31	50.61	50.09	51.30	49.79	51.66
TiO2	1.70	0.59	0.63	0.54	0.77	0.05	0.59	0.68	0.70	0.64
Al2O3	3.79	3.55	3.29	3.74	3.48	2.32	2.03	2.64	3.11	2.44
Cr2O3	0.04	0.23	0.03	-	-	-	-	-	-	0.02
FeO	8.70	7.60	8.88	9.03	11.07	13.63	14.82	10.67	9.79	10.68
MnO	0.22	0.20	0.20	0.10	0.34	0.39	0.44	0.01	0.26	0.21
NiO	0.01	0.01	0.02	0.04	0.05	0.05	0.01	0.01	0.03	0.01
MgO	13.74	16.63	15.34	15.60	14.24	10.08	10.48	14.79	14.49	15.60
CaO	21.49	20.16	20.28	20.05	19.98	22.45	19.69	19.65	19.99	19.17
Na2O	0.31	0.25	0.28	0.31	0.29	0.42	0.47	0.52	0.31	0.30
K2O	0.01	-	0.02	0.01	-	0.02	0.04	0.03	0.01	0.01
Total	99.03	100.50	100.22	99.08	99.53	100.02	98.66	100.30	98.48	100.74
#Si IV	1.85	1.89	1.90	1.87	1.87	1.94	1.94	1.91	1.89	1.92
#Al IV	0.15	0.11	0.10	0.13	0.13	0.06	0.06	0.09	0.11	0.08
#Ti IV	-	-	-	-	-	-	-	-	-	-
#Fe IV	-	-	-	-	-	-	-	-	-	-
T site	2.00	2.00	2.00	2.00	2.00	2.00	2.00	2.00	2.00	2.00
#Al VI	0.02	0.04	0.04	0.03	0.02	0.04	0.04	0.03	0.03	0.02
#Ti	0.05	0.02	0.02	0.02	0.02	0.00	0.02	0.02	0.02	0.02
#Cr	0.00	0.01	0.00	-	-	-	-	-	-	0.00
#Fe +3	0.00	-	0.00	-	-	0.00	-	0.00	0.00	0.00
#Fe +2	0.28	0.23	0.28	0.28	0.35	0.44	0.48	0.33	0.31	0.33
#Mn +2	0.01	0.01	0.01	0.00	0.01	0.01	0.01	0.00	0.01	0.01
#Ni	0.00	0.00	0.00	0.00	0.00	0.00	0.00	0.00	0.00	0.00
#Mg	0.77	0.91	0.85	0.88	0.80	0.58	0.61	0.82	0.82	0.86
#Ca	0.87	0.79	0.81	0.81	0.81	0.92	0.82	0.79	0.81	0.76
#Na	0.02	0.02	0.02	0.02	0.02	0.03	0.04	0.04	0.02	0.02
#K	0.00	-	0.00	0.00	-	0.00	0.00	0.00	0.00	0.00
M1, M2	2.02	2.03	2.02	2.04	2.04	2.02	2.01	2.03	2.03	2.02
%Mg	40.19	46.85	43.82	44.40	40.68	29.58	31.57	42.37	42.00	43.96
%Fe*+Mn	14.64	12.33	14.55	14.58	18.29	23.08	25.80	17.17	16.35	17.22
%Ca	45.17	40.82	41.63	41.02	41.02	47.34	42.63	40.46	41.65	38.82
Suite #	3	3	1	1	1	1	1	1	1	1

	2a 290	2b 290	3a 290	3b 290	4a 290	4b 290	1a 291	1b 291	2a 291	2b 291
SiO <sub>2</sub>	49.28	51.18	50.27	49.44	50.73	50.24	51.39	51.88	49.21	50.12
TiO <sub>2</sub>	0.87	0.51	1.01	1.02	0.81	0.96	0.22	0.20	0.42	0.43
Al <sub>2</sub> O <sub>3</sub>	3.87	3.74	3.30	3.14	3.79	4.37	3.08	2.74	4.02	3.85
Cr <sub>2</sub> O <sub>3</sub>	0.04	0.27	0.03	-	0.02	0.05	0.13	0.09	0.03	-
FeO	9.41	7.20	11.38	11.88	9.40	9.18	5.77	5.79	7.63	7.38
MnO	0.18	0.14	0.27	0.37	0.24	0.25	0.06	0.15	0.14	0.16
NiO	0.03	0.02	0.01	0.03	0.04	-	0.04	0.05	0.05	0.03
MgO	15.25	16.63	14.36	13.98	14.96	14.39	15.71	15.90	14.30	14.60
CaO	20.00	20.63	19.91	19.34	20.11	20.14	23.25	22.61	22.87	22.07
Na <sub>2</sub> O	0.25	0.23	0.32	0.20	0.29	0.33	0.18	0.14	0.32	0.32
K <sub>2</sub> O	-	0.02	-	0.01	0.02	-	-	0.01	0.01	-
Total	99.18	100.57	100.86	99.41	100.35	99.91	99.83	99.56	99.00	98.96
#Si IV	1.86	1.88	1.88	1.88	1.88	1.87	1.90	1.92	1.86	1.88
#Al IV	0.14	0.12	0.12	0.12	0.12	0.13	0.10	0.08	0.14	0.12
#Ti IV	-	-	-	-	-	-	-	-	-	-
#Fe IV	-	-	-	-	-	-	-	-	-	-
T site	2.00	2.00	2.00	2.00	2.00	2.00	2.00	2.00	2.00	2.00
#Al VI	0.03	0.04	0.02	0.02	0.05	0.06	0.04	0.04	0.04	0.05
#Ti	0.02	0.01	0.03	0.03	0.02	0.03	0.01	0.01	0.01	0.01
#Cr	0.00	0.01	0.00	-	0.00	0.00	0.00	0.00	0.00	-
#Fe +3	-	0.00	0.00	-	0.00	-	0.00	-	-	-
#Fe +2	0.30	0.22	0.36	0.38	0.29	0.29	0.18	0.18	0.24	0.23
#Mn +2	0.01	0.00	0.01	0.01	0.01	0.01	0.00	0.00	0.00	0.01
#Ni	0.00	0.00	0.00	0.00	0.00	-	0.00	0.00	0.00	0.00
#Mg	0.86	0.91	0.80	0.79	0.82	0.80	0.87	0.88	0.81	0.82
#Ca	0.81	0.81	0.80	0.79	0.80	0.80	0.92	0.90	0.93	0.89
#Na	0.02	0.02	0.02	0.01	0.02	0.02	0.01	0.01	0.02	0.02
#K	-	0.00	-	0.00	0.00	-	-	0.00	0.00	-
M1, M2	2.04	2.03	2.03	2.03	2.02	2.02	2.03	2.02	2.05	2.03
%Mg	43.57	46.75	40.79	40.23	42.86	42.13	44.02	44.81	40.74	42.08
%Fe+Mn	15.37	11.58	18.57	19.78	15.56	15.49	9.16	9.39	12.42	12.20
%Ca	41.06	41.68	40.64	39.99	41.58	42.38	46.82	45.80	46.83	45.72
Suite #	1	1	1	1	1	1	4	4	4	4



[illegible]

[illegible]

	7b 467	7c 467	1a 525b	2a 525b	5a 525b	5c 525b	6a 525b	6b 525b	7a 525b	7b 525b
SiO <sub>2</sub>	50.33	50.27	52.40	52.64	53.65	51.56	53.42	53.67	52.21	53.43
TiO <sub>2</sub>	1.23	1.30	0.49	0.49	0.43	0.77	0.38	0.33	0.52	0.54
Al <sub>2</sub> O <sub>3</sub>	3.02	3.11	2.73	2.80	1.49	4.41	2.10	2.30	2.13	2.32
Cr <sub>2</sub> O <sub>3</sub>	0.08	0.07	0.57	0.49	0.20	0.13	0.32	0.19	0.45	0.45
FeO	10.84	12.39	4.74	4.96	5.32	8.43	4.77	4.58	8.66	6.99
MnO	0.27	0.28	0.09	0.09	0.33	0.22	0.14	0.16	0.36	0.32
NiO	0.03	-	0.02	0.04	0.14	0.05	0.07	0.02	-	0.12
MgO	14.14	13.71	15.20	14.87	15.70	15.48	17.34	17.12	14.94	15.72
CaO	19.23	19.38	24.26	23.76	23.39	16.93	21.25	21.66	19.04	19.29
Na <sub>2</sub> O	0.39	0.33	0.29	0.29	0.29	1.23	0.15	0.18	0.38	0.43
K <sub>2</sub> O	0.01	0.05	0.02	0.01	-	0.09	0.01	0.01	0.02	-
Total	99.57	100.89	100.81	100.44	100.44	99.30	99.95	100.22	98.71	99.61
#Si IV	1.90	1.88	1.92	1.93	1.97	1.91	1.95	1.95	1.96	1.97
#Al IV	0.10	0.12	0.08	0.07	0.03	0.09	0.05	0.05	0.04	0.03
#Ti IV	-	-	-	-	-	-	-	-	-	-
#Fe IV	-	-	-	-	-	-	-	-	-	-
T site	2.00	2.00	2.00	2.00	2.00	2.00	2.00	2.00	2.00	2.00
#Al VI	0.03	0.02	0.03	0.05	0.03	0.10	0.04	0.05	0.05	0.07
#Ti	0.03	0.04	0.01	0.01	0.01	0.02	0.01	0.01	0.01	0.01
#Cr	0.00	0.00	0.02	0.01	0.01	0.00	0.01	0.01	0.01	0.01
#Fe +3	-	-	0.00	0.00	-	0.00	0.00	-	-	-
#Fe +2	0.34	0.39	0.14	0.15	0.16	0.26	0.15	0.14	0.27	0.22
#Mn +2	0.01	0.01	0.00	0.00	0.01	0.01	0.00	0.00	0.01	0.01
#Ni	0.00	-	0.00	0.00	0.00	0.00	0.00	0.00	-	0.00
#Mg	0.79	0.77	0.83	0.81	0.83	0.85	0.94	0.93	0.83	0.86
#Ca	0.78	0.78	0.95	0.93	0.92	0.67	0.83	0.84	0.76	0.76
#Na	0.03	0.02	0.02	0.02	0.02	0.09	0.01	0.01	0.03	0.03
#K	0.00	0.00	0.00	0.00	-	0.00	0.00	0.00	0.00	-
M1,M2	2.02	2.02	2.01	2.00	2.00	2.02	2.00	1.99	1.99	1.98
%Mg	41.35	39.46	43.00	42.75	43.20	47.63	49.03	48.43	44.35	46.67
%Fe*+Mn	18.23	20.46	7.67	8.15	9.02	14.93	7.79	7.53	15.03	12.18
%Ca	40.42	40.08	49.33	49.10	47.78	37.44	43.18	44.04	40.62	41.15
Suite #	2	2	1	1	1	1	1	1	1	1

[illegible]

[illegible]

[illegible]



[illegible]

[illegible]

[illegible]

[illegible]

[illegible]

[illegible]



[illegible]

[illegible]

	1b 912a	2a 912a	2b 912a	3a 912a	4a 912a	1a 961d	1b 961d	2a 961d	3a 961d	3b 961d
SiO2	50.63	51.07	51.47	52.17	48.86	51.49	51.84	52.27	53.40	53.73
TiO2	0.80	0.56	0.57	0.69	1.04	0.13	0.25	0.26	0.20	0.17
Al2O3	4.60	3.03	3.02	3.84	6.77	3.20	3.38	2.98	2.43	1.91
Cr2O3	0.05	0.01	-	0.19	0.05	0.16	0.13	0.40	0.09	0.05
FeO	7.17	9.38	9.25	5.91	7.25	7.97	6.98	6.76	7.40	7.81
MnO	0.20	0.34	0.28	0.14	0.14	0.19	0.14	0.16	0.20	0.27
NiO	0.03	0.11	-	0.04	0.02	0.05	0.08	0.04	0.04	0.04
MgO	14.35	14.46	14.78	16.69	13.35	17.88	17.10	17.32	17.93	17.96
CaO	22.14	19.98	20.01	19.88	22.20	18.68	20.29	20.53	18.53	18.35
Na2O	0.30	0.33	0.37	0.25	0.40	0.21	0.30	0.17	0.23	0.16
K2O	-	0.01	0.01	-	-	0.07	-	0.01	-	-
Total	100.27	99.28	99.76	99.80	100.08	100.03	100.49	100.90	100.45	100.45
#Si IV	1.87	1.92	1.92	1.91	1.81	1.90	1.90	1.91	1.95	1.96
#Al IV	0.13	0.08	0.08	0.09	0.19	0.10	0.10	0.09	0.05	0.04
#Ti IV	-	-	-	-	-	-	-	-	-	-
#Fe IV	-	-	-	-	-	-	-	-	-	-
T site	2.00	2.00	2.00	2.00	2.00	2.00	2.00	2.00	2.00	2.00
#Al VI	0.07	0.05	0.05	0.08	0.11	0.04	0.05	0.03	0.05	0.04
#Ti	0.02	0.02	0.02	0.02	0.03	0.00	0.01	0.01	0.01	0.00
#Cr	0.00	0.00	-	0.01	0.00	0.00	0.00	0.01	0.00	0.00
#Fe +3	-	0.00	0.00	-	-	-	0.00	0.00	-	0.00
#Fe +2	0.22	0.29	0.29	0.18	0.23	0.25	0.21	0.21	0.23	0.24
#Mn +2	0.01	0.01	0.01	0.00	0.00	0.01	0.00	0.00	0.01	0.01
#Ni	0.00	0.00	-	0.00	0.00	0.00	0.00	0.00	0.00	0.00
#Mg	0.79	0.81	0.82	0.91	0.74	0.98	0.93	0.94	0.97	0.98
#Ca	0.88	0.80	0.80	0.78	0.88	0.74	0.80	0.80	0.72	0.72
#Na	0.02	0.02	0.03	0.02	0.03	0.02	0.02	0.01	0.02	0.01
#K	-	0.00	0.00	-	-	0.00	-	0.00	-	-
M1,M2	2.02	2.01	2.01	1.99	2.02	2.04	2.03	2.02	2.00	2.00
%Mg	41.72	42.19	42.83	48.56	39.91	49.83	47.93	48.17	50.49	50.33
%Fe+Mn	12.02	15.92	15.50	9.88	12.40	12.76	11.20	10.80	12.01	12.71
%Ca	46.26	41.90	41.67	41.57	47.70	37.41	40.87	41.03	37.50	36.96
Suite #	4	4	4	4	4	1	1	1	1	1

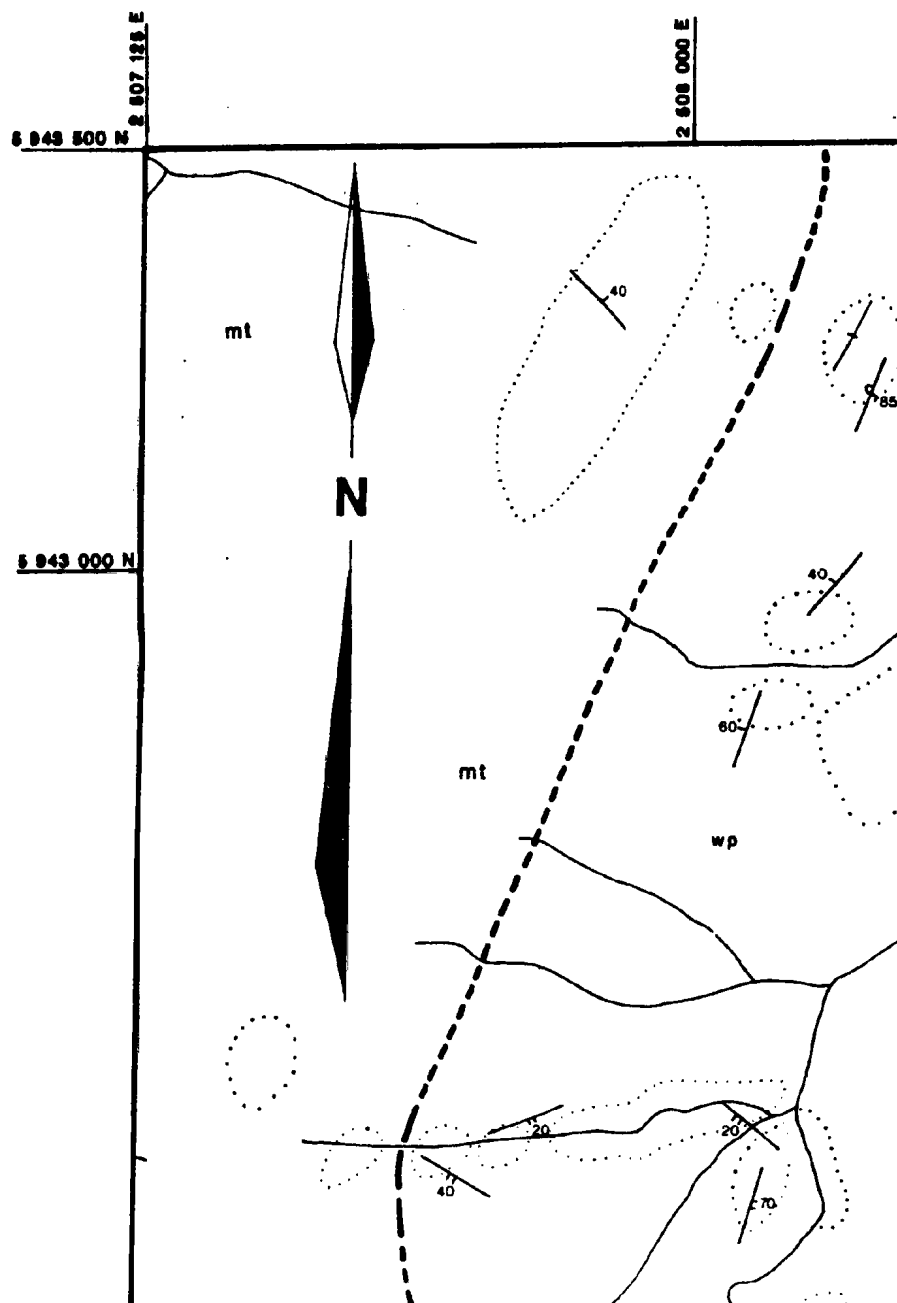
[illegible]

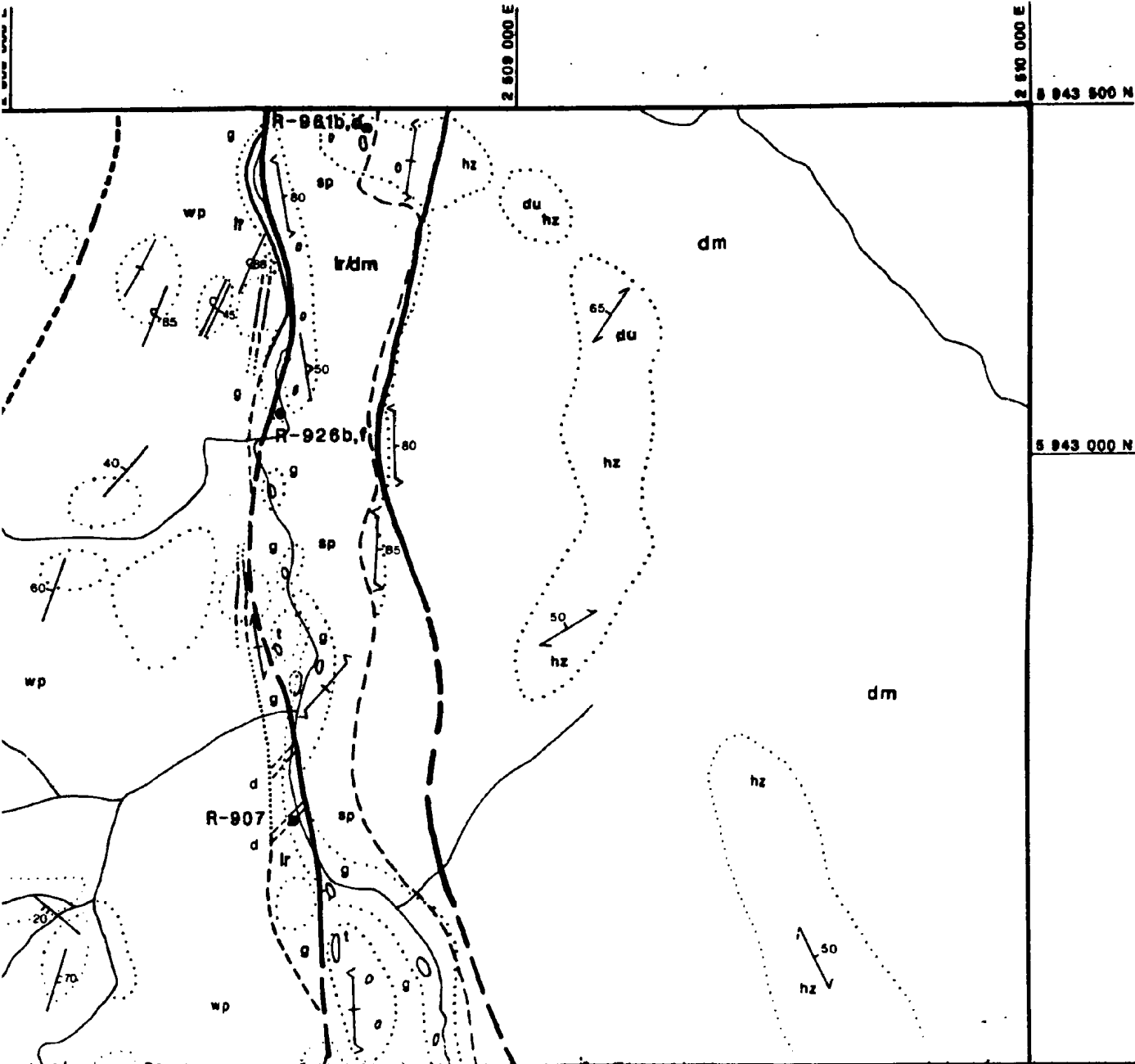
[illegible]

[illegible]



	4a	4b	5a	5b
	1007	1007	1007	1007
SiO <sub>2</sub>	50.81	49.57	52.41	51.83
TiO <sub>2</sub>	1.07	1.01	0.63	0.64
Al <sub>2</sub> O <sub>3</sub>	3.18	3.31	2.13	1.57
Cr <sub>2</sub> O <sub>3</sub>	0.04	0.05	0.04	0.07
FeO	11.07	11.40	9.96	10.95
MnO	0.21	0.23	0.15	0.25
NiO	0.04	-	0.03	-
MgO	14.81	14.14	15.85	15.93
CaO	18.54	19.86	18.78	18.71
Na <sub>2</sub> O	0.30	0.16	0.21	0.25
K <sub>2</sub> O	-	0.02	-	0.03
Total	100.07	99.75	100.19	100.23
#Si IV	1.90	1.87	1.94	1.93
#Al IV	0.10	0.13	0.06	0.07
#Ti IV	-	-	-	-
#Fe IV	-	-	-	-
T site	2.00	2.00	2.00	2.00
#Al VI	0.04	0.02	0.03	0.00
#Ti	0.03	0.03	0.02	0.02
#Cr	0.00	0.00	0.00	0.00
#Fe +3	-	0.00	0.00	0.00
#Fe +2	0.35	0.36	0.31	0.34
#Mn +2	0.01	0.01	0.00	0.01
#Ni	0.00	-	0.00	-
#Mg	0.82	0.80	0.88	0.89
#Ca	0.74	0.80	0.75	0.75
#Na	0.02	0.01	0.02	0.02
#K	-	0.00	-	0.00
M1, M2	2.01	2.03	2.00	2.02
%Mg	42.97	40.47	45.26	44.67
%Fe+Mn	18.37	18.68	16.20	17.62
%Ca	38.66	40.85	38.54	37.71
Suite #	1	1	1	1

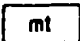

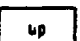





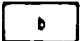



5 943 500 N

## GEOLOGICAL LEGEND

### MAITAI GROUP


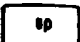
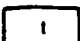
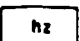

-  undifferentiated (bedded to poorly bedded, green to grey sandstones, grey siltstones, and dark grey to purple mudstones).
-  Wooded Peak Formation (bedded to poorly bedded, grey fine grained limestone with minor units of fine-grained green sandstone).
-  Upukerora Formation (purple to grey conglomerates and breccias consisting of mafic volcanic and plutonic clasts supported in a grey to purple sand and mud matrix).

### LEE RIVER GROUP

-  undifferentiated
-  basaltic breccia (often in a hematite-stained mud matrix)
-  pillowed/massive flows (aphyric to augite and/or plagioclase phytic).
-  diabase dykes (aphyric to augite and/or plagioclase phytic).
-  gabbro (typically isotropic, locally foliated and amphibolized).

5 943 000 N

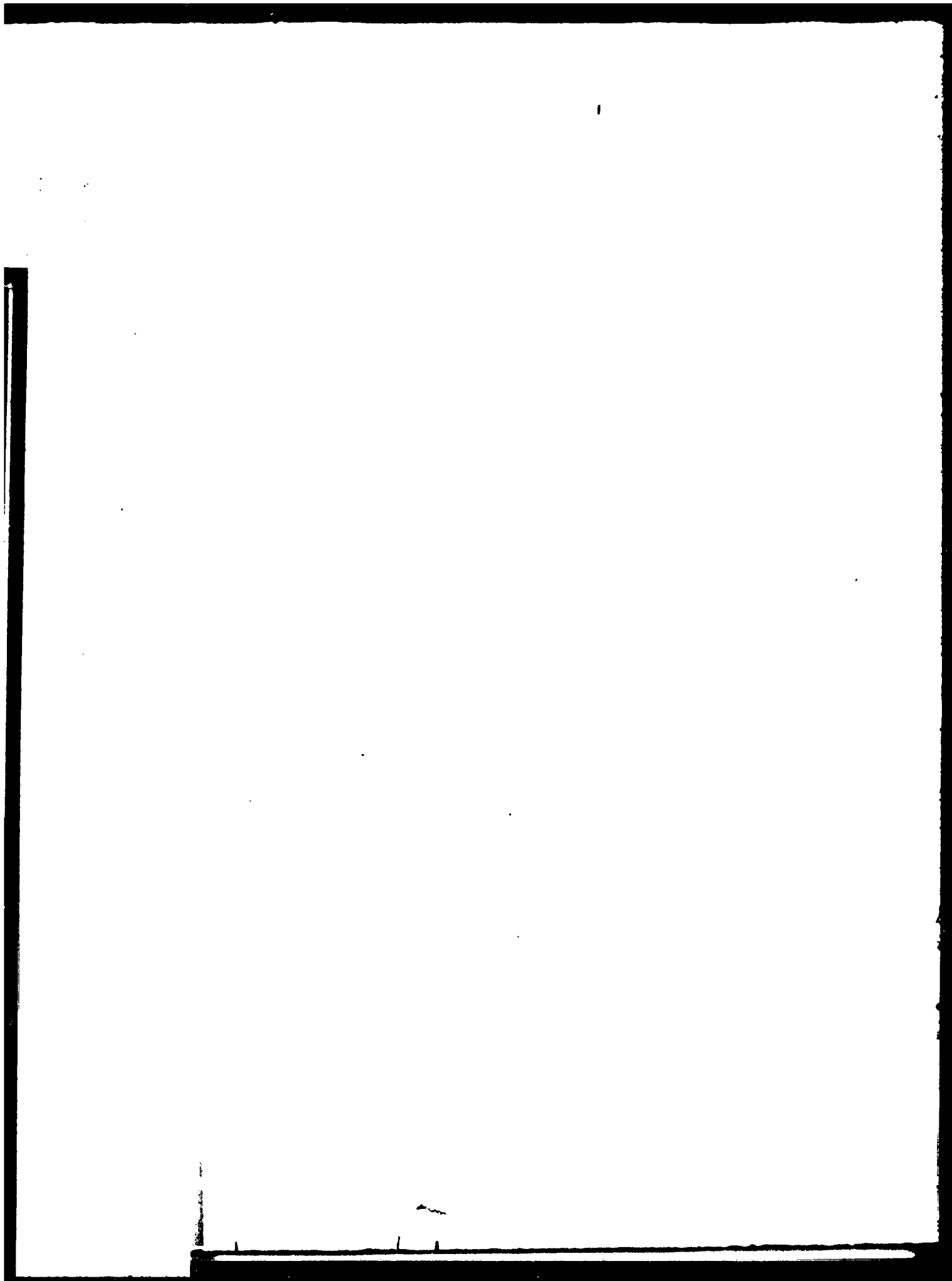
### DUN MOUNTAIN ULTRAMAFICS

-  undifferentiated
-  serpentinite
-  transition zone series (banded plutonic sequence of gabbroic and ultramafic rocks)
-  harzburgite (with minor chromite pods and lenses).
-  dunite (with minor chromite pods and lenses).

### PELORUS GROUP

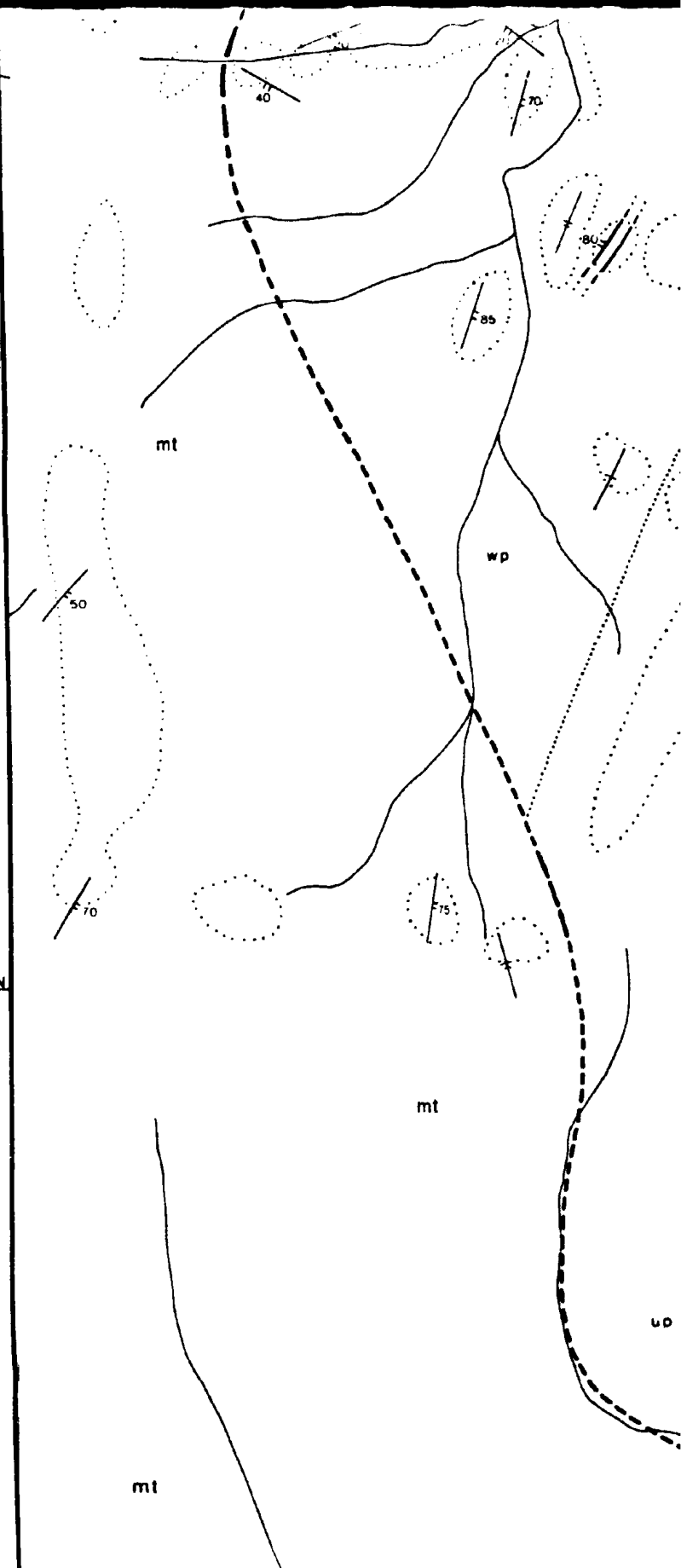
-  sediments (undifferentiated grey siltstones, sandstones and mudstones).

### PATUKI MÉLANGE

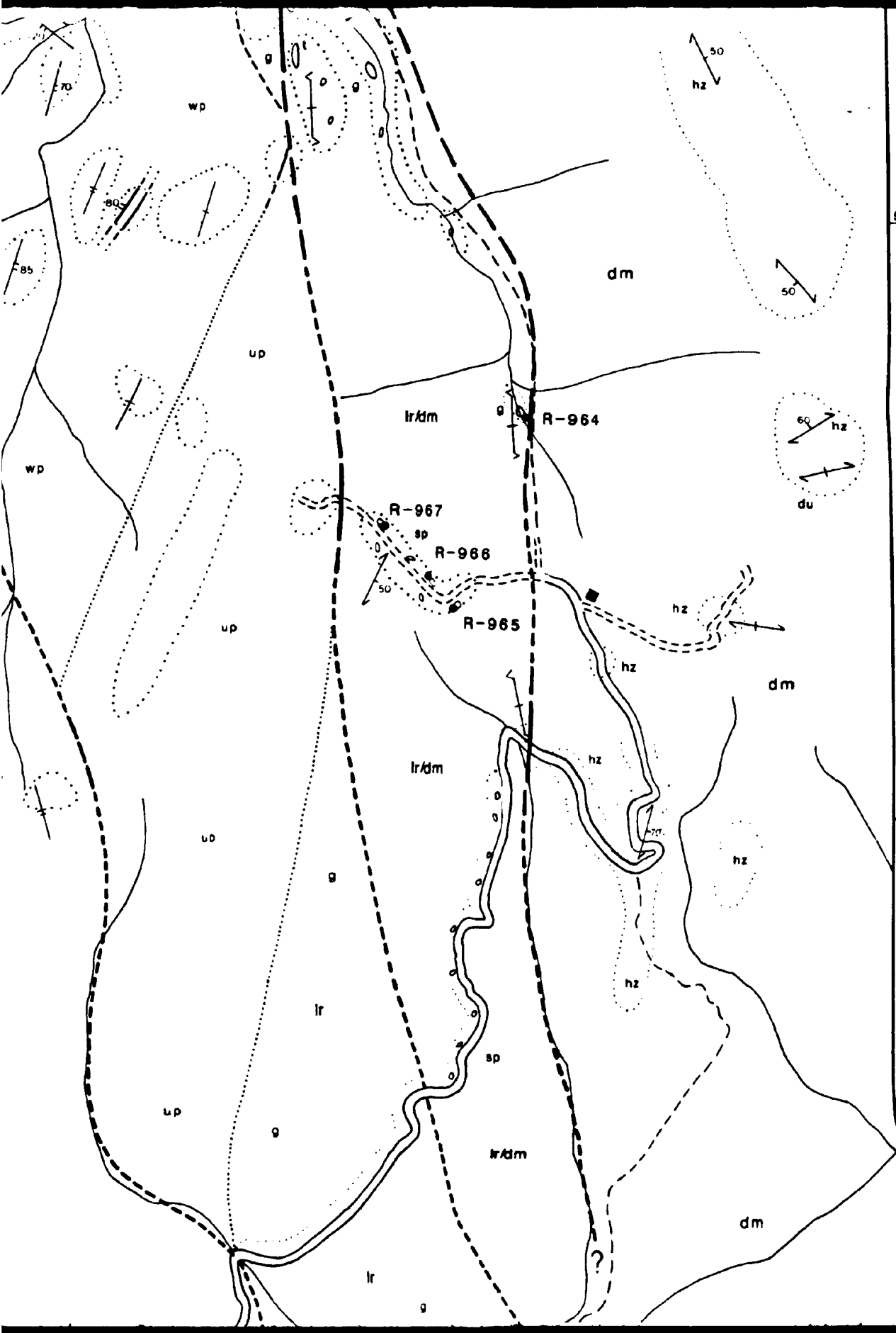


5 942 000 N

5 941 000 N







5 942 000 N

5 941 000 N

## PELORUS GROUP



sediments (undifferentiated gray siltstones, sandstones and mudstones).

## PATUKI MÉLANGE



undifferentiated



sediments (undifferentiated gray to purple sandstones, siltstones and mudstones).



pillowed/massive basaltic flows (typically aphyric to olivine porphyritic).



diabase dykes (aphyric).



gabbro (typically isotropic, locally amphibolized).



ultramafic rocks (undifferentiated)

## CROISILLES MÉLANGE



undifferentiated



sediments (undifferentiated gray to purple sandstones siltstones and mudstones)



pillowed/massive basaltic flows (typically aphyric to olivine porphyritic)



diabase dykes (aphyric)



gabbro (typically isotropic, often amphibolized)



ultramafic rocks (undifferentiated)

## MISCELLANEOUS



sheared serpentinite



sediments (undifferentiated)

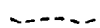
## SYMBOL LEGEND

### GEOLOGICAL SYMBOLS

#### Geological Contact



defined (dip 30°)



approximate (vertical)



assumed

#### Bedding



tops known



horizontal



vertical



dipping 40° southwest



overturned 50° northwest

#### Fabrics

#### Fault



defined



approximate



assumed



tops unknown



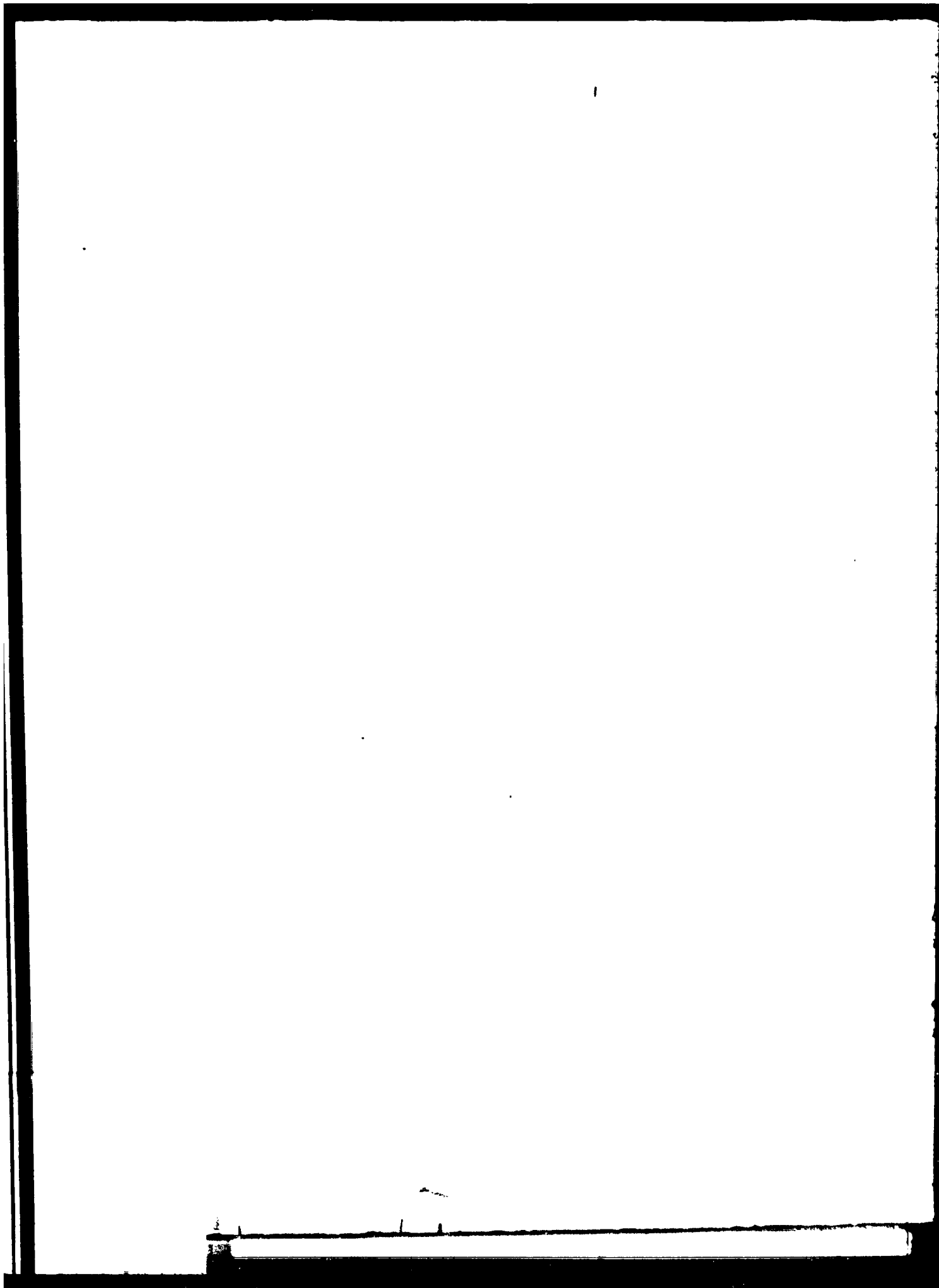
horizontal



vertical



dipping 40° southwest



5 940 000 N

2 507 125 E

2 508 000 E

mt

Topographic

# GEOLOGY OF THE RED HILLS WESTERN MARGIN

By Paul J. Moore

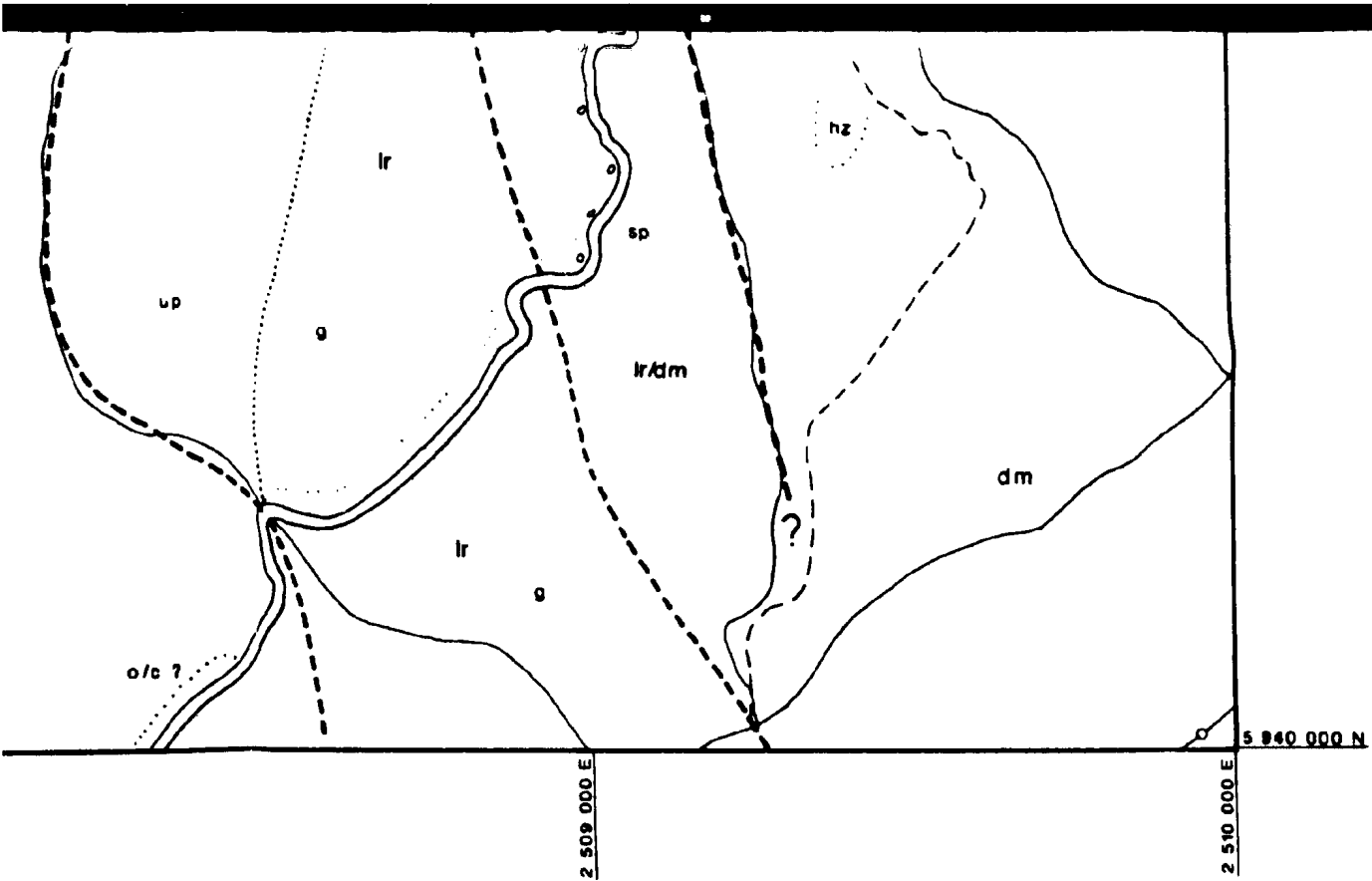
1988

SCALE 1: 10 000

0 m

500 m

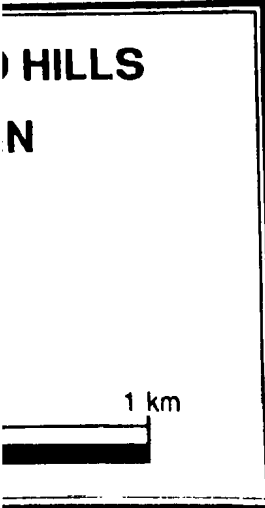
1



Topographic data taken from map sheets N.Z.M.S. 270 027, N28, and N29 of the New Zealand Department of Lands and Survey.




Grid references are in reference to the New Zealand Map Grid.

Elevations in metres. Elevations in metres.






## GEOLOGICAL SYMBOLS






## Geological Contact




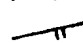
-  defined (dip 30°)  
 approximate (verdict)  
 assumed

## Fault





-  defined  
 approximate  
 assumed

## Bedding

-  top known  
 horizontal  
 vertical  
 dipping 40° southwest  
 overturned 50° northwest

-  top unknown  
 horizontal  
 vertical  
 dipping 40° southwest

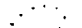

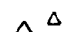
## Fabrics

-  cleavage (strike and dip)  
 foliation (strike and dip)  
 lineation (strike and plunge)  
 shearing (strike and dip)



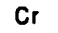


## Sample location

-  B-74 location and number








## Outcrop

-  area of outcrop  
 questionable outcrop  
 boulders

## Miscellaneous

-  quarry  
 prospecting shaft or abandoned mine  
 chromite  
 copper  
 serpentine

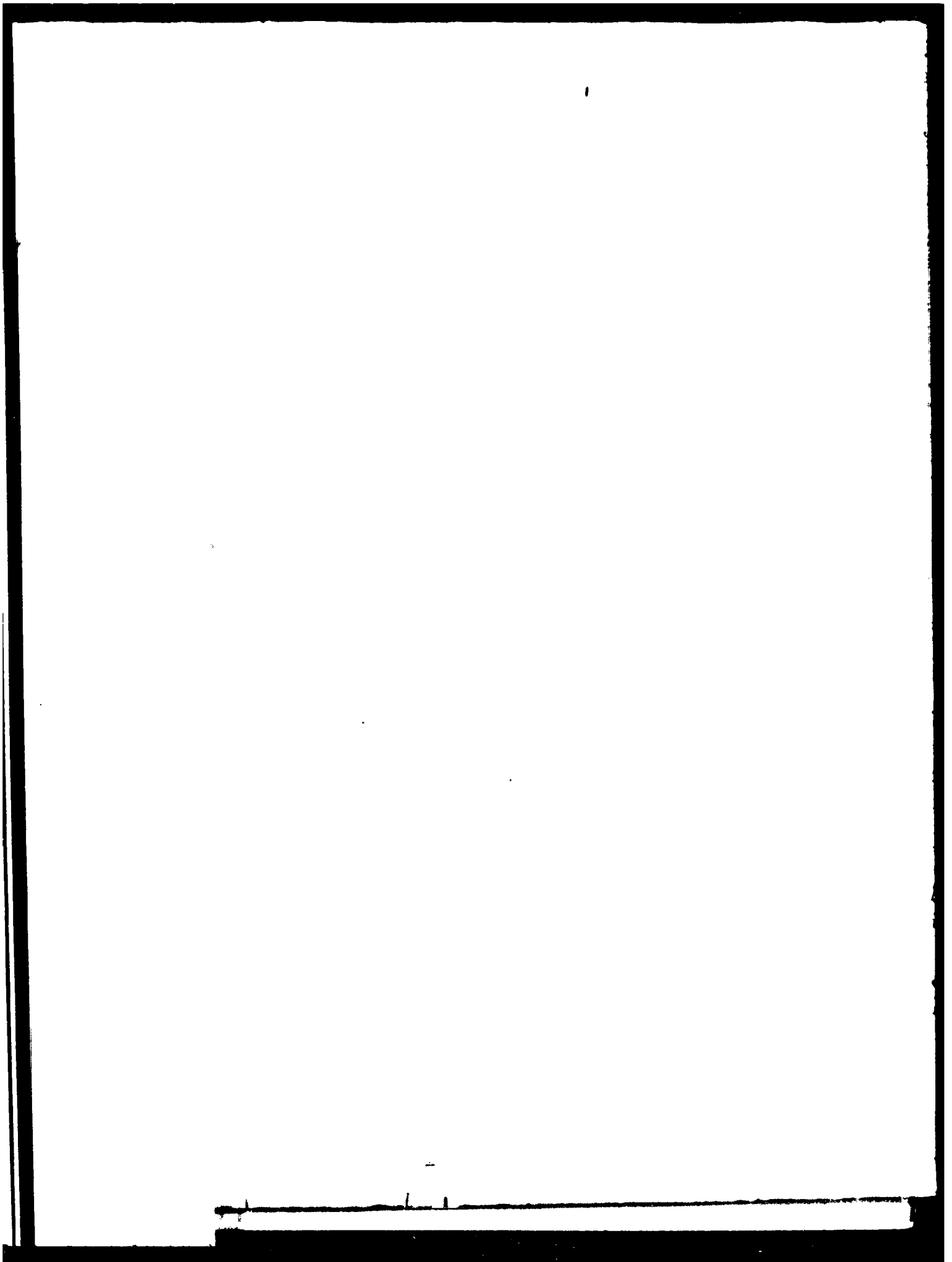
## TOPOGRAPHICAL REFERENCE

-  road  
 four wheel drive track  
 foot track  
 power lines  
 building  
 trig. station  
 spot elevation

S 940 000 N

ds and Survey.



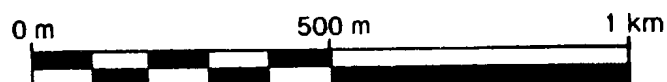


**GEOLOGY OF THE RED HILLS  
WESTERN MARGIN**

**By Paul J. Moore**

**1988**

**SCALE 1: 10 000**

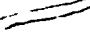
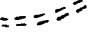

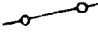

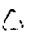



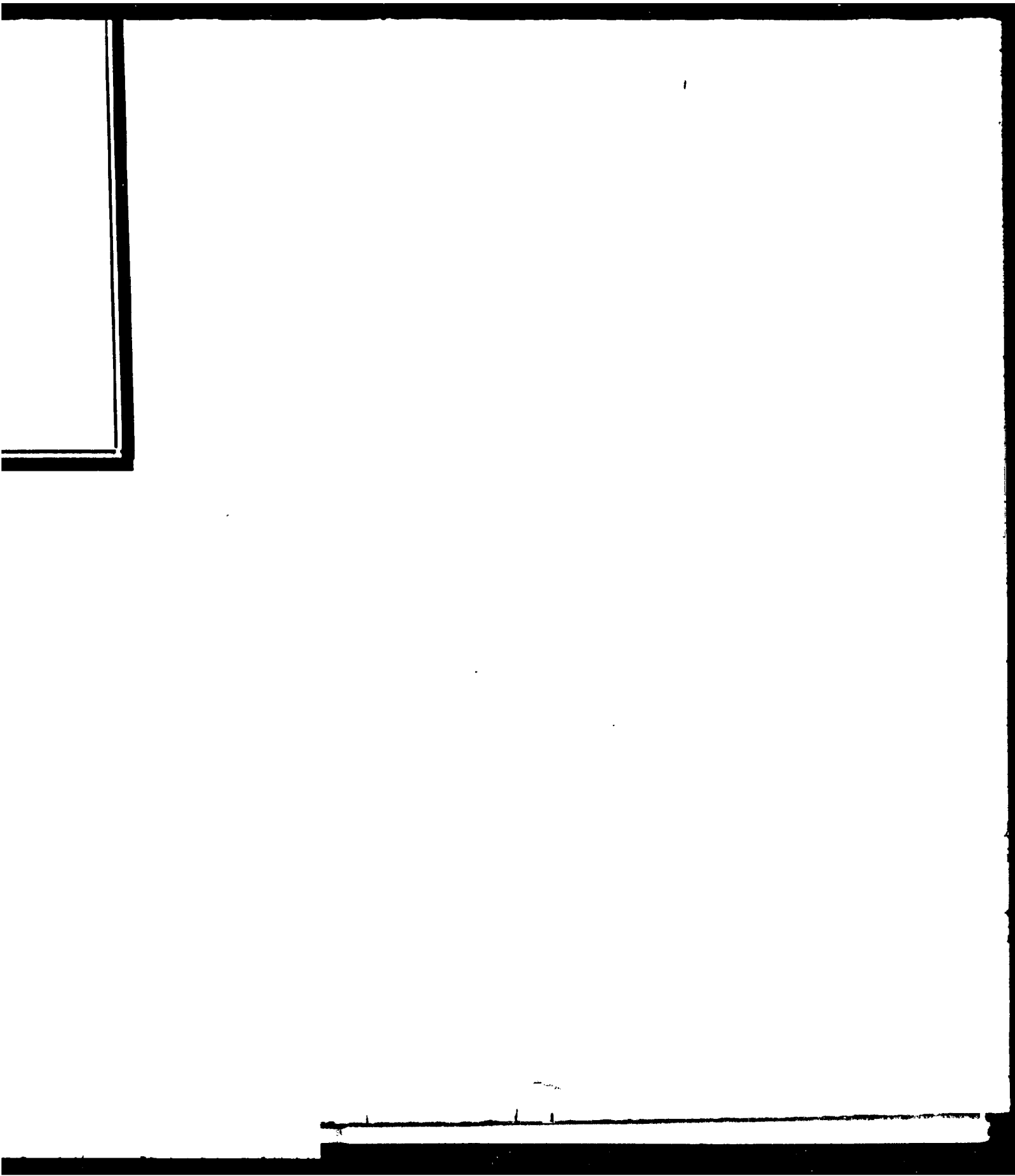
**Figure 3.2.1 Geology of the Red Hill**

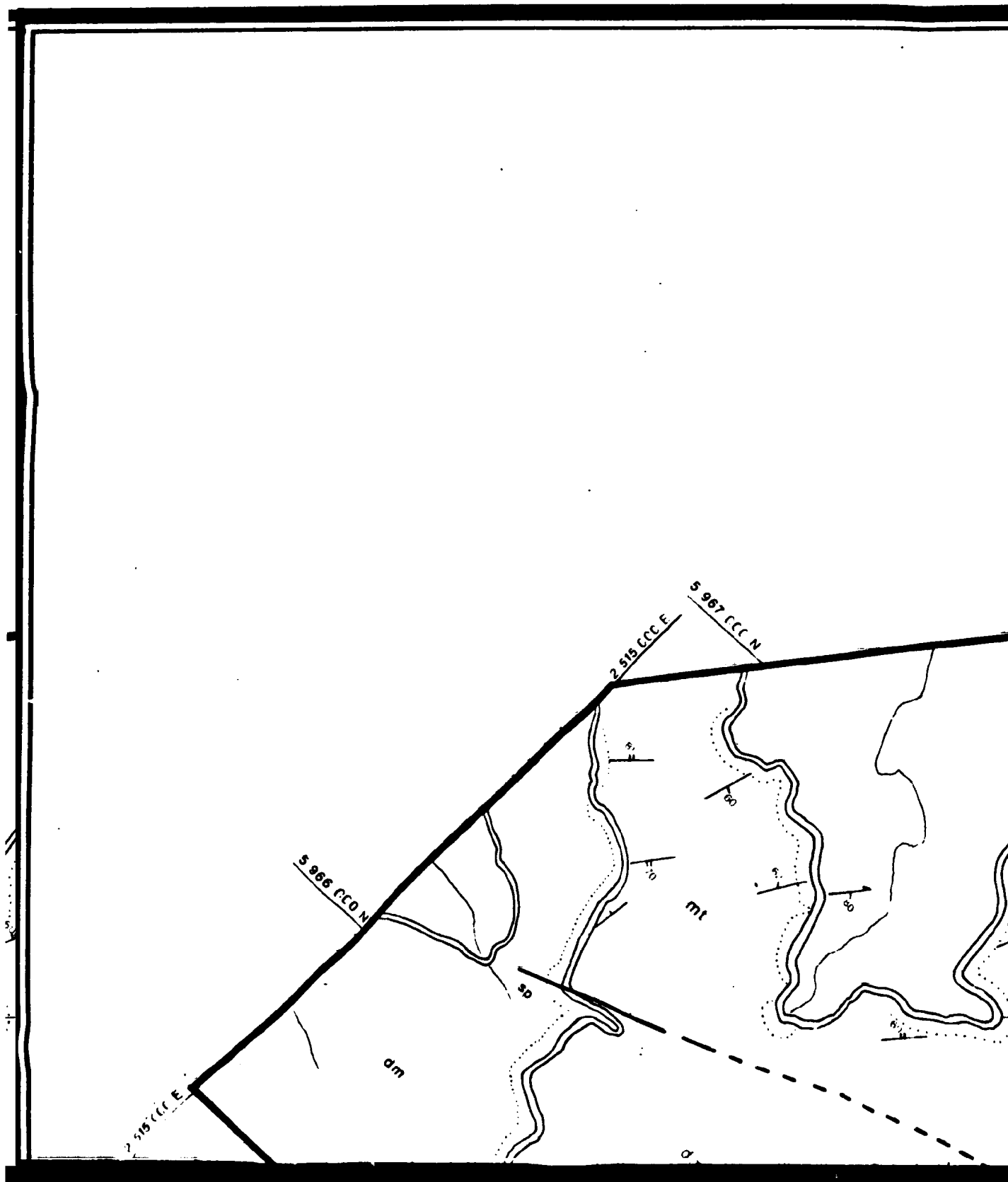
D HILLS  
IN

1 km

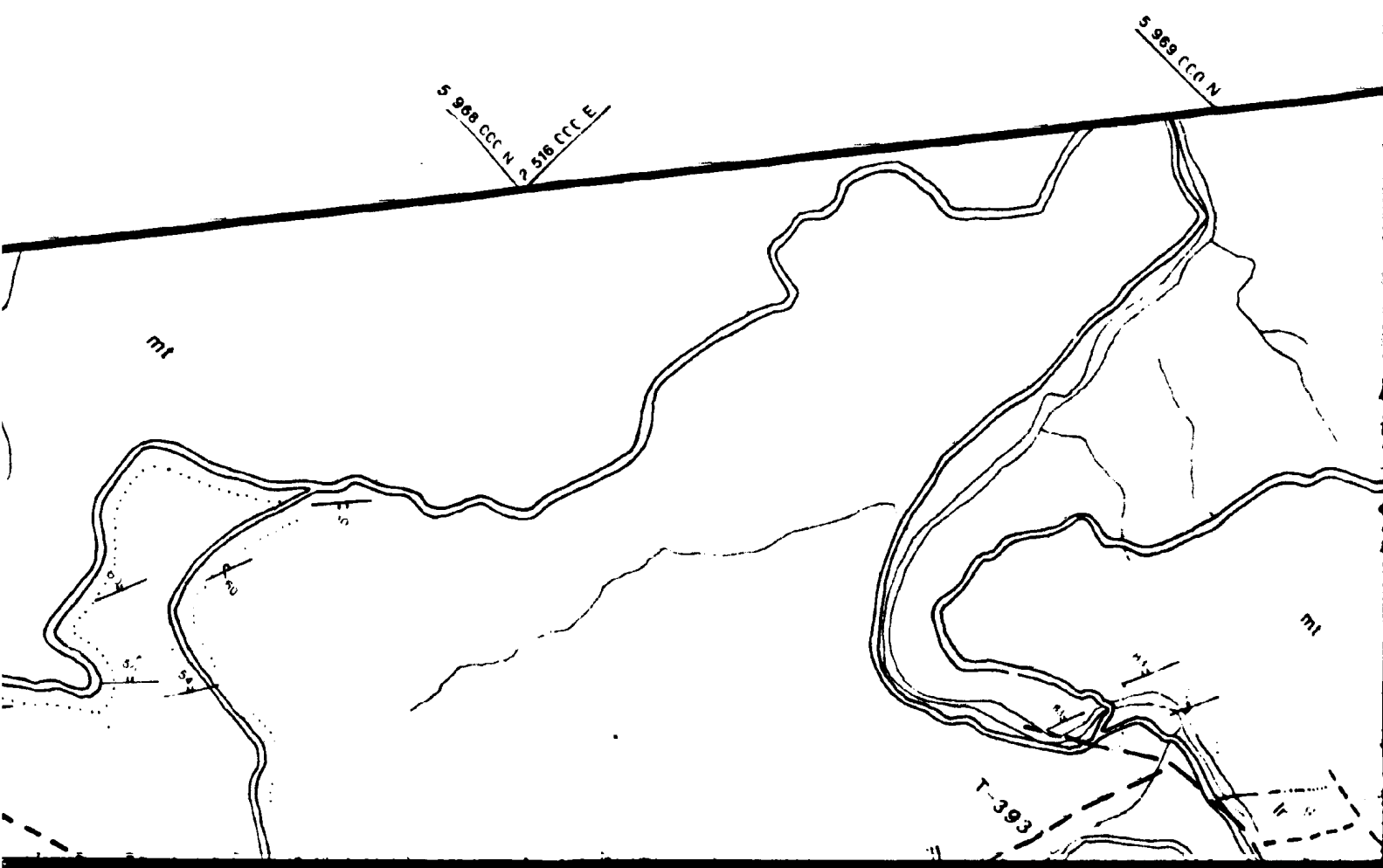
ie Red Hills western margin.

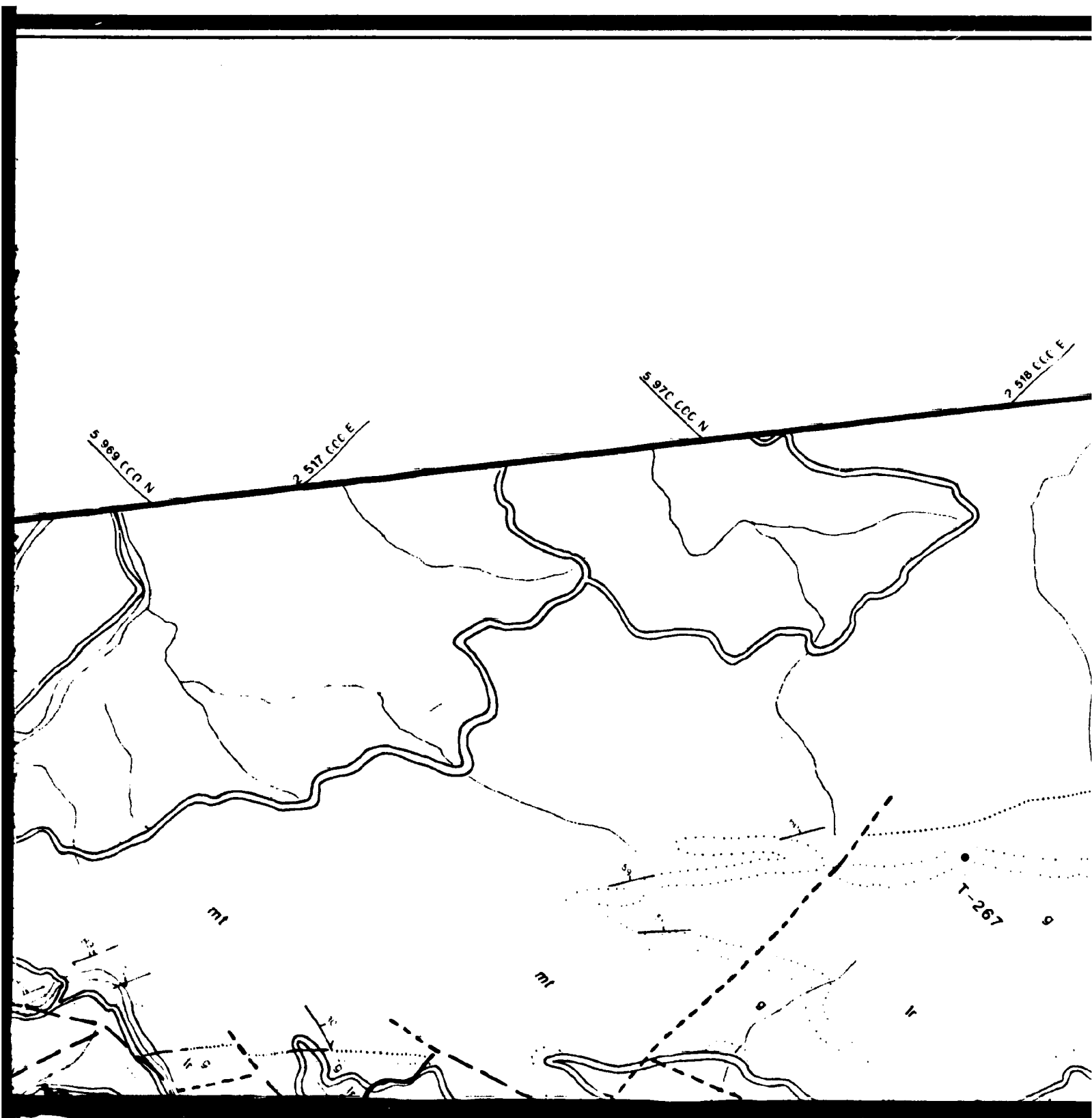
-  road
-  four wheel drive track
-  foot track
-  power lines
-  building
-  trig station
-  spot elevation

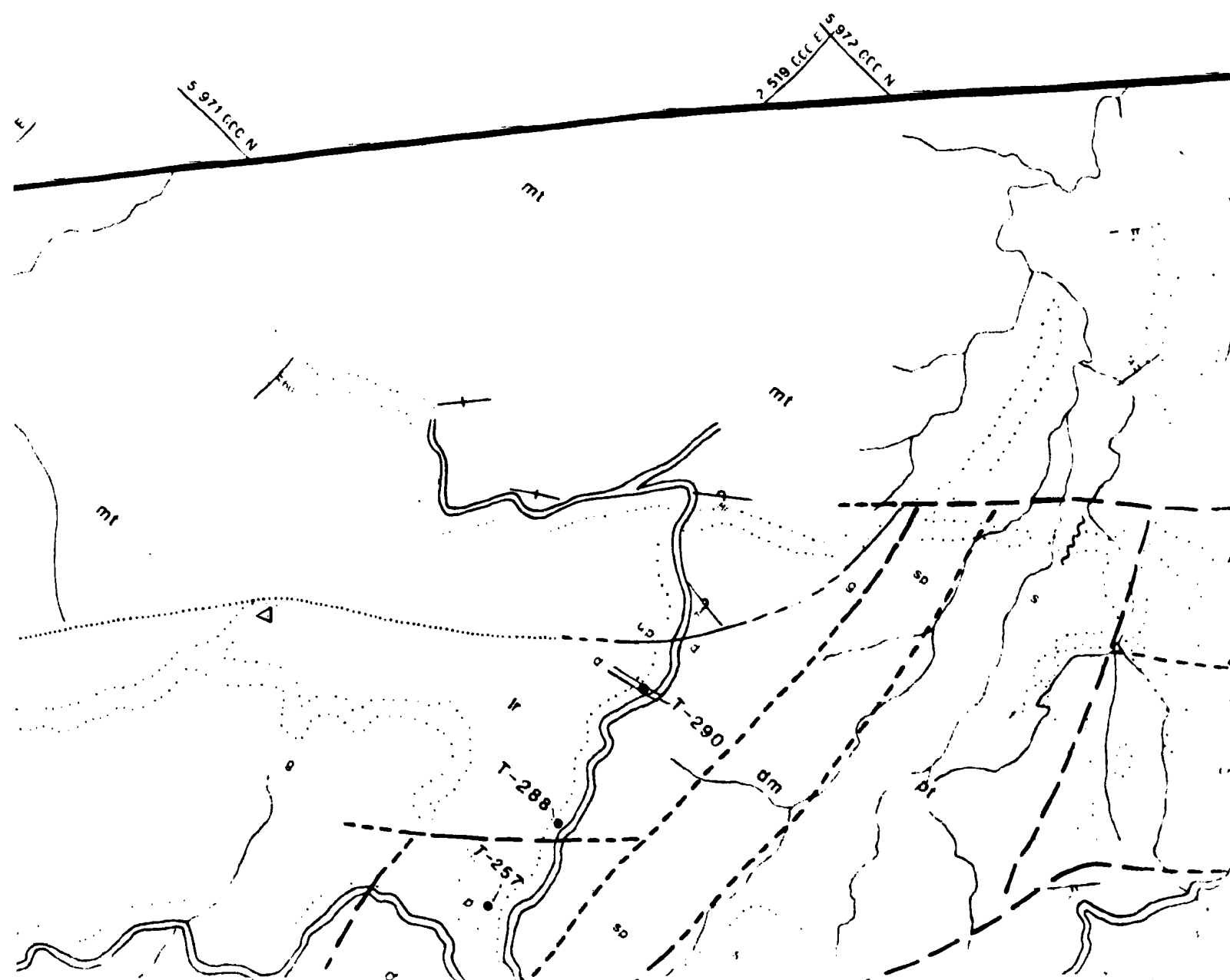


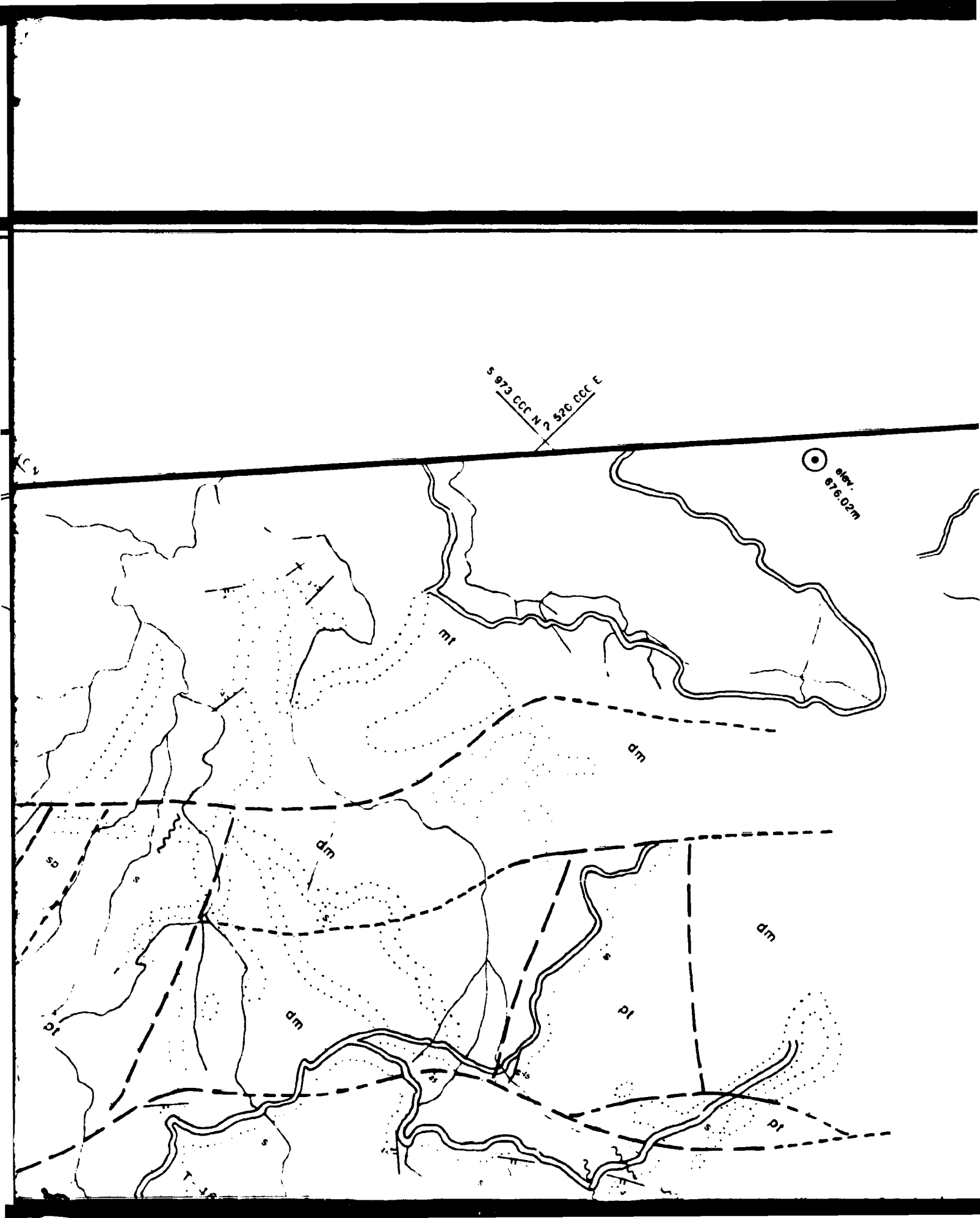


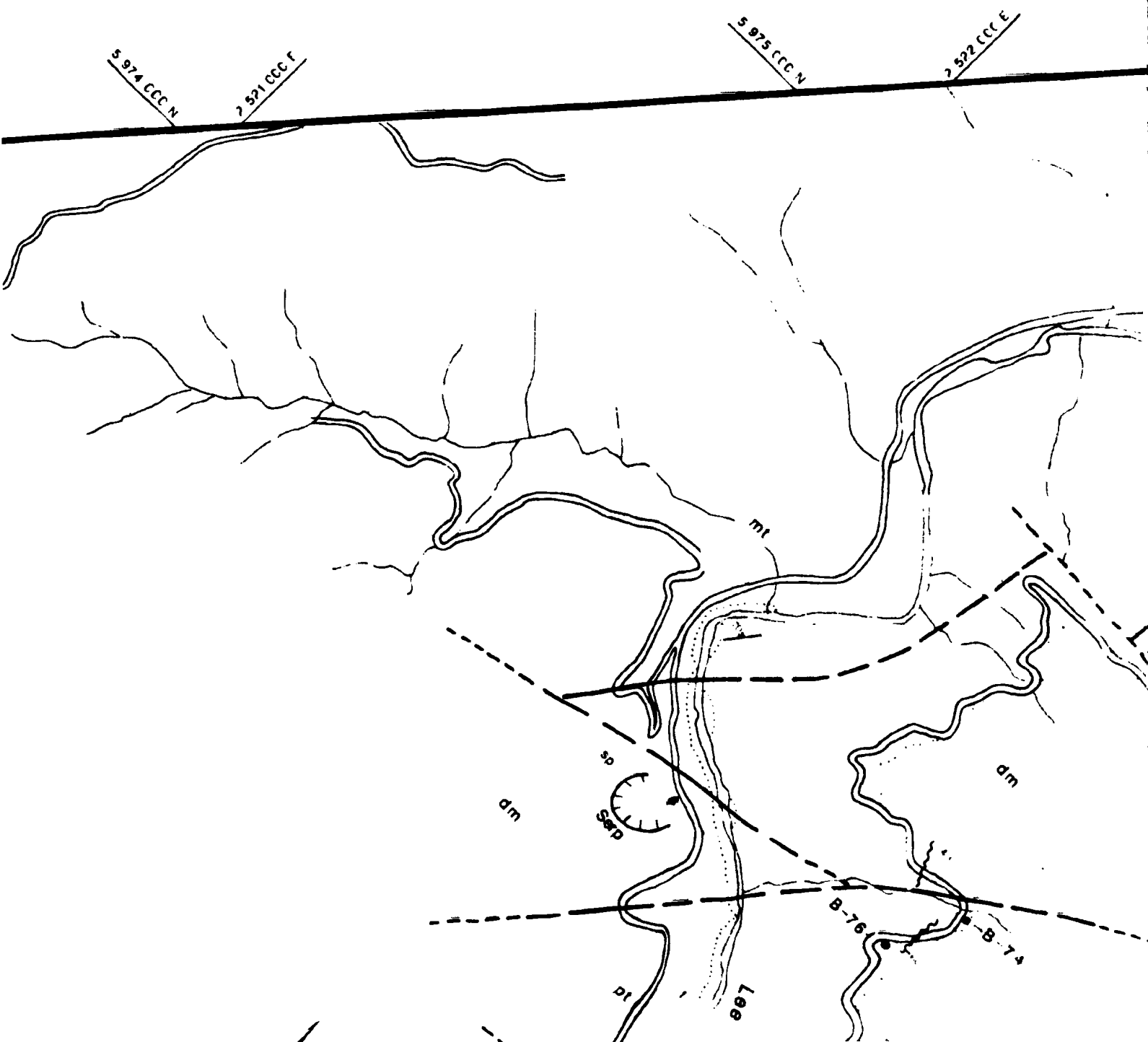












5 974 CCC N

2 521 CCC F

5 975 CCC N

2 522 CCC E

mt

dm



dm

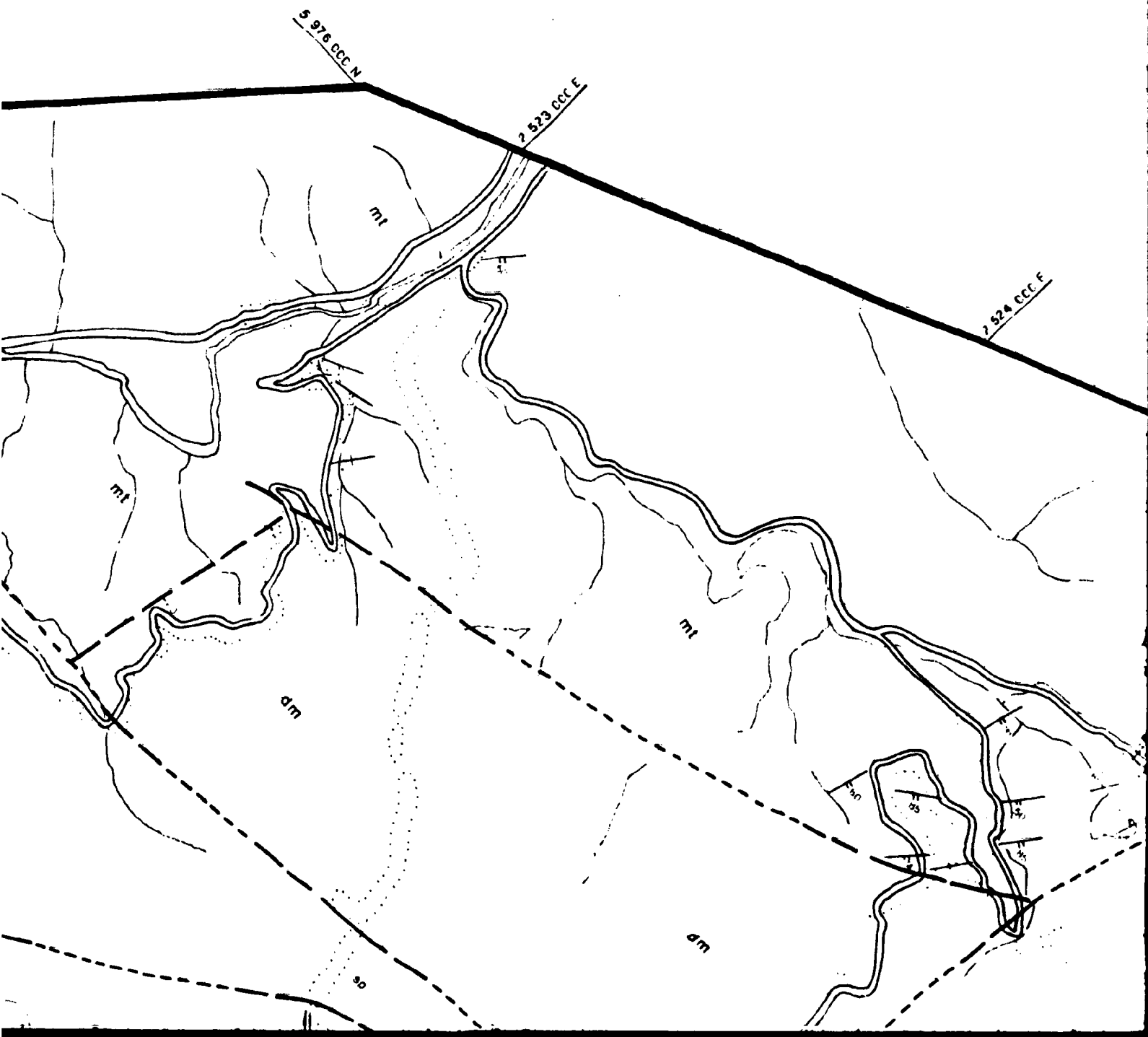
B-76

B-74

to

Le





2 524 CCC F

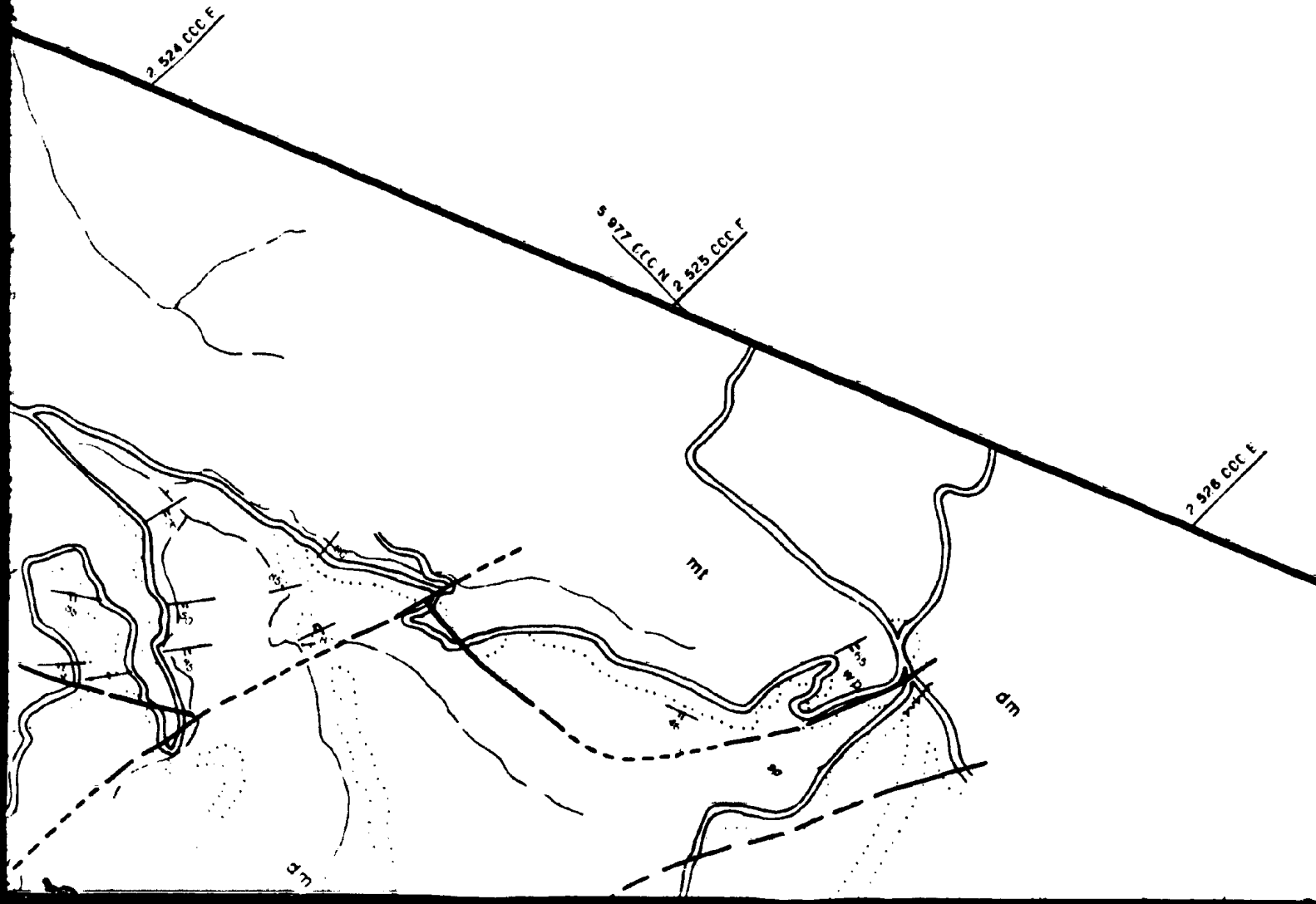
5 977 CCC N 2 525 CCC F

2 526 CCC E

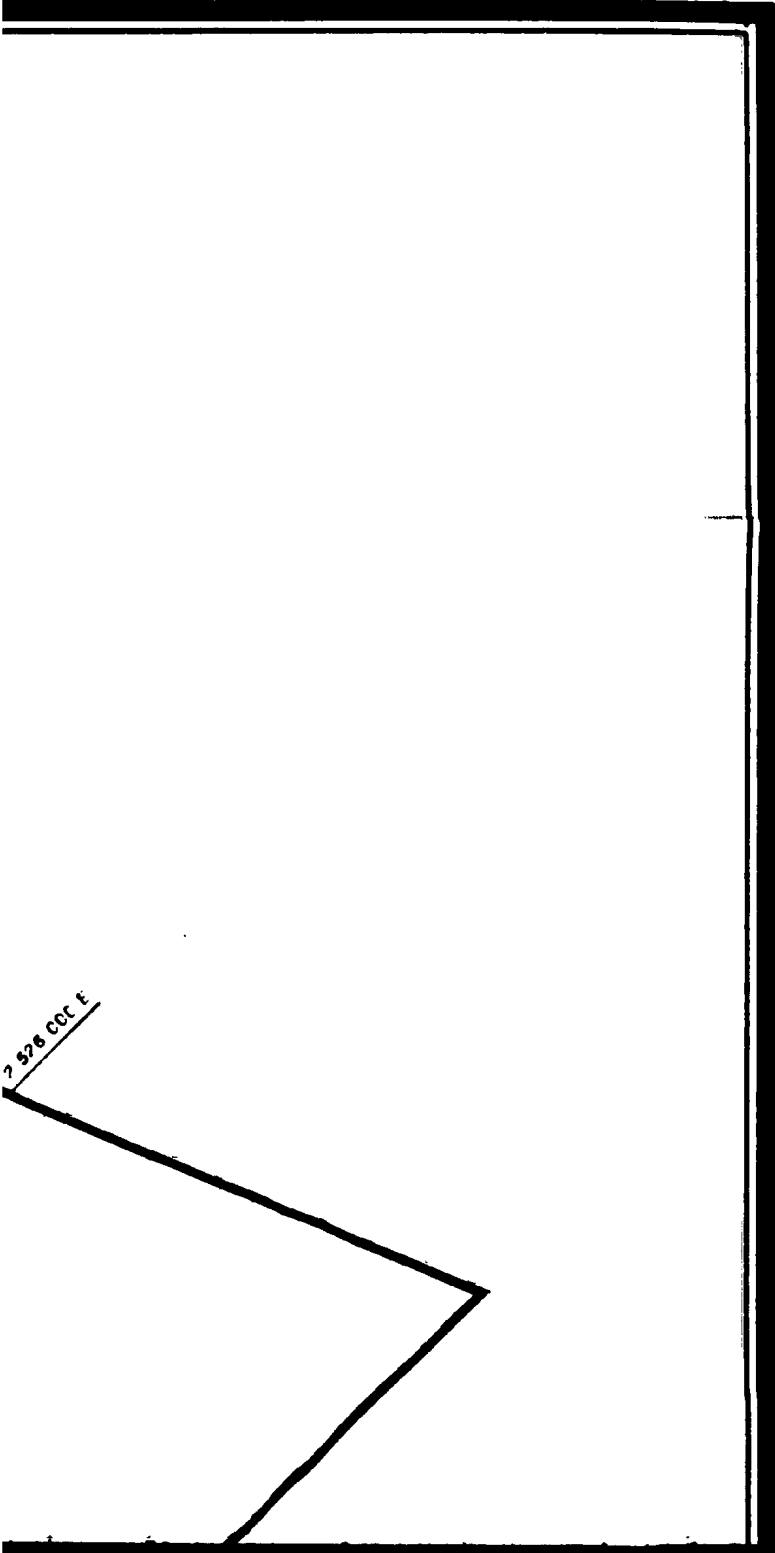
mt

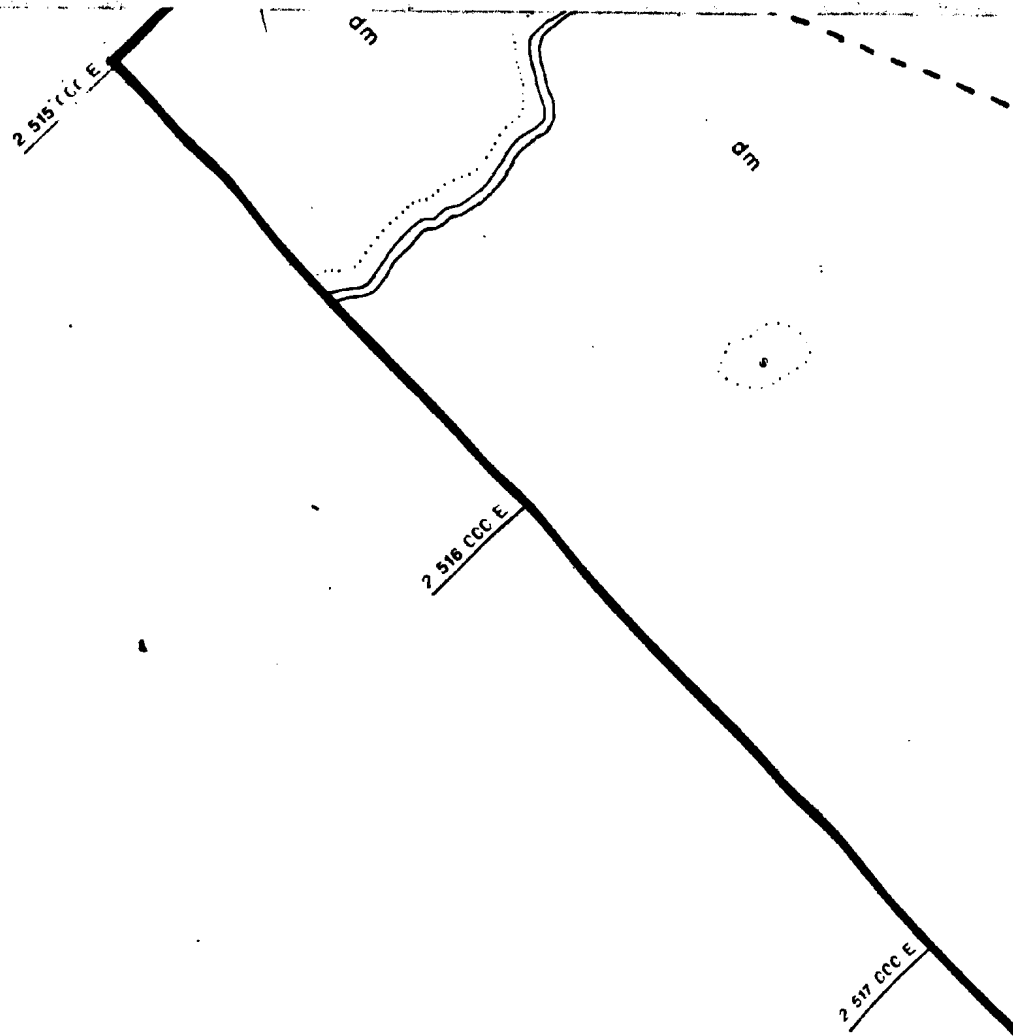
dm

dm

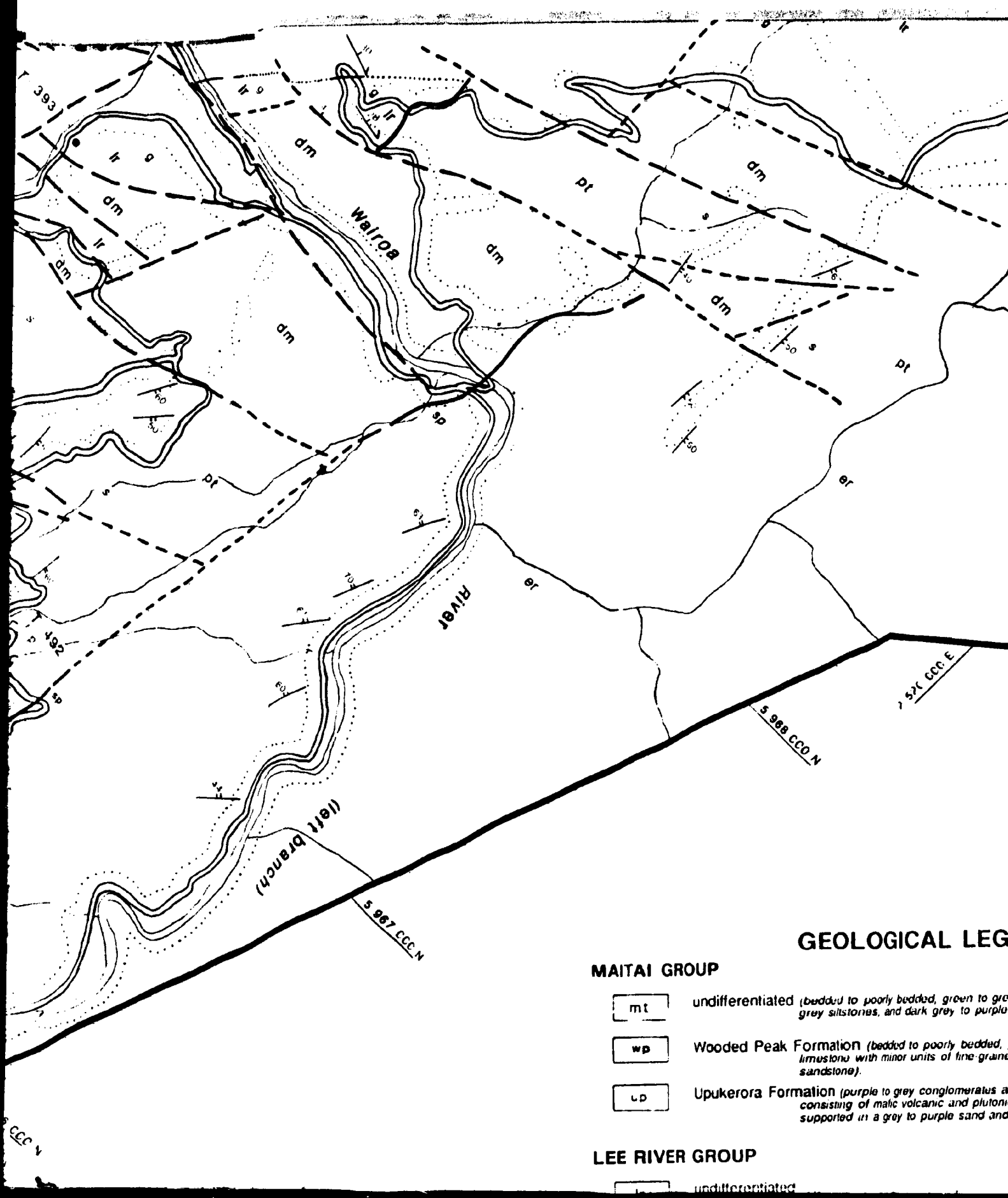


2 526 COT E









# GEOLOGICAL LEG

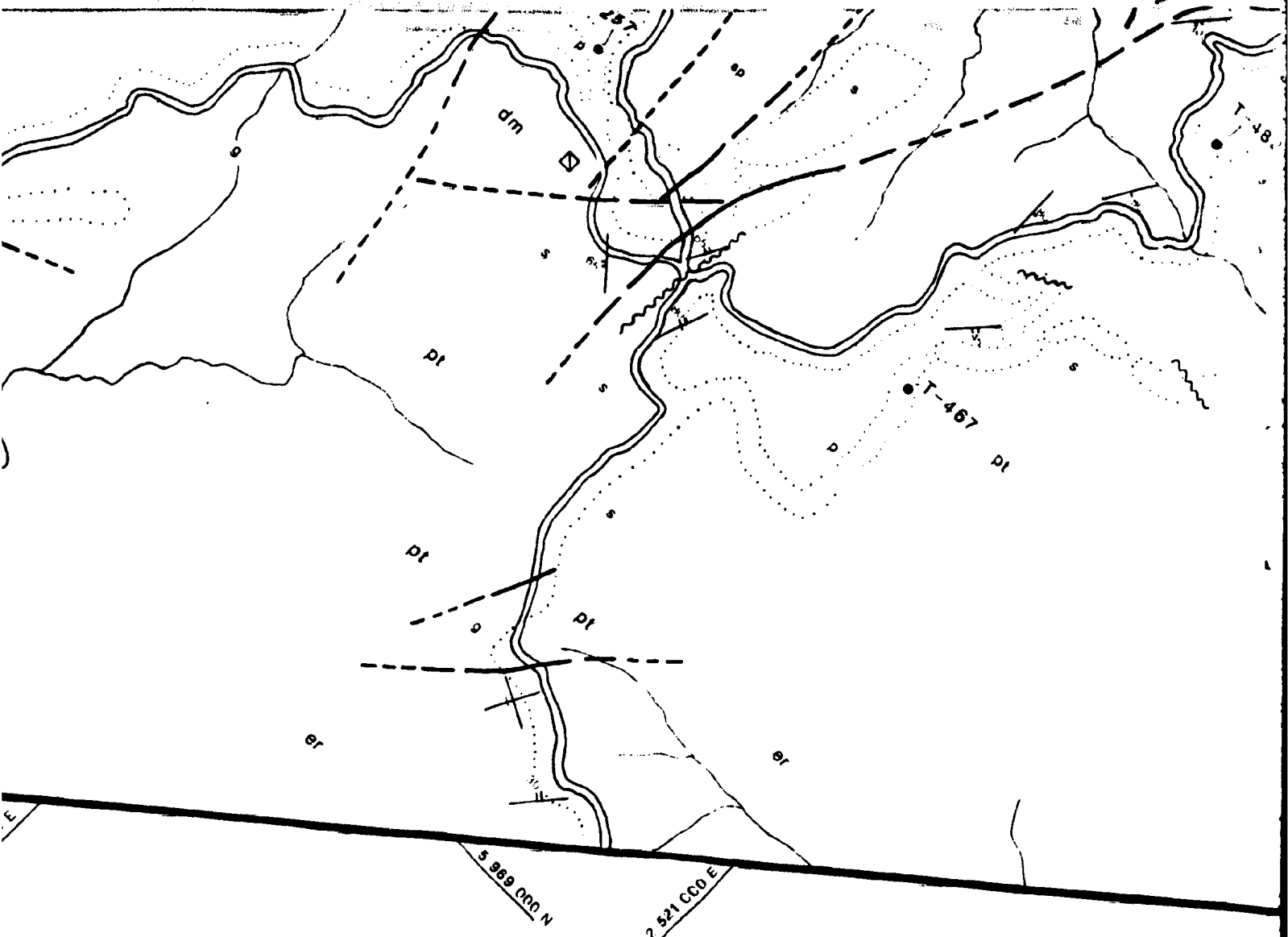
## MAITAI GROUP

- mt undifferentiated (bedded to poorly bedded, green to grey grey siltstones, and dark grey to purple)
- wp Wooded Peak Formation (bedded to poorly bedded, & limestone with minor units of fine-grained sandstone).
- up Upukerora Formation (purple to grey conglomerates or consisting of mafic volcanic and plutonic supported in a grey to purple sand and

## LEE RIVER GROUP

- undifferentiated





# LEGEND

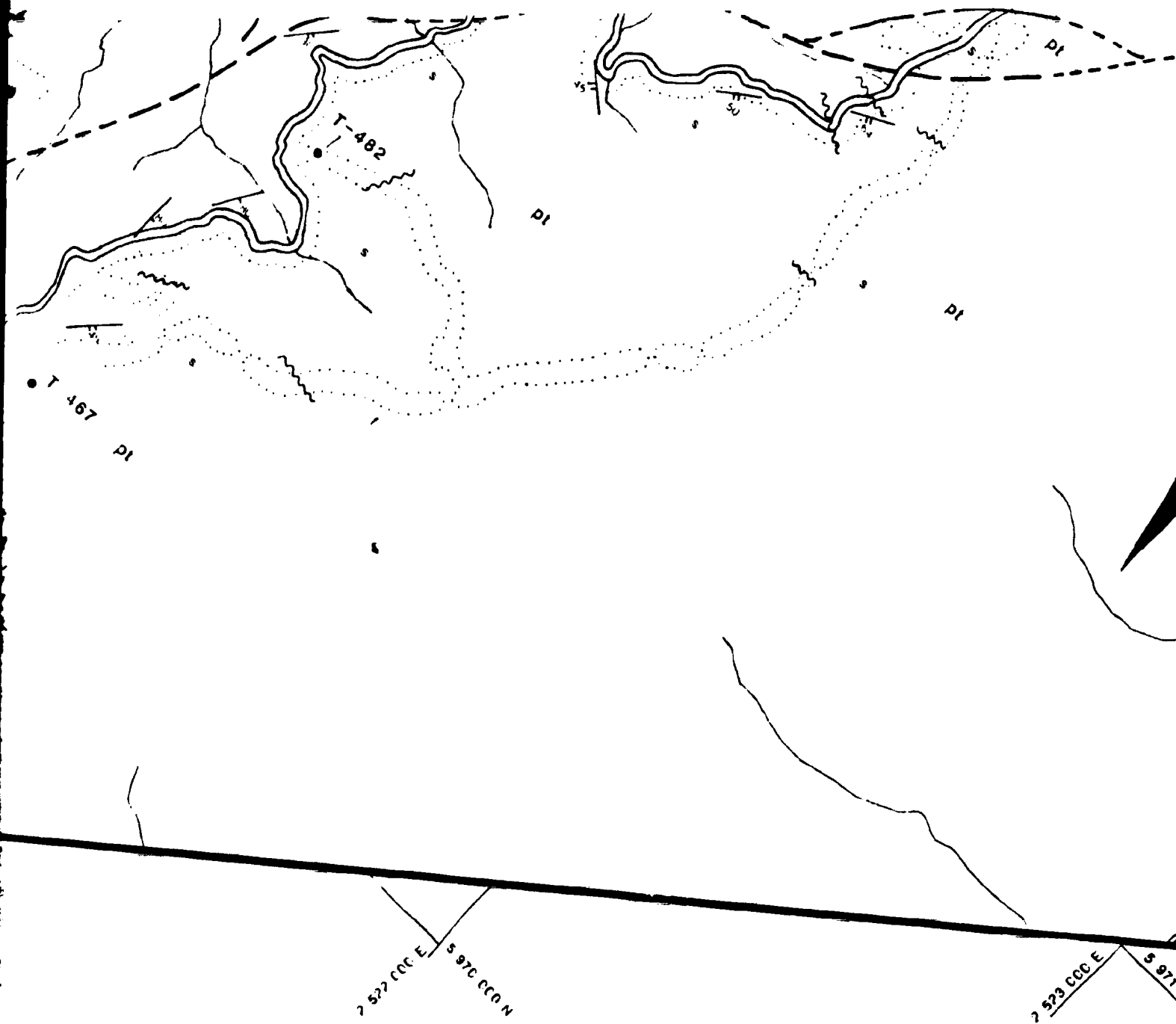
green to grey sandstones,  
 ey to purple mudstones).

ily bedded, gray fine grained  
 of fine-grained green

glomerates and breccias  
 (and plutonic clasts  
 (k) sand and mud matrix)

## GEOLOGICAL SYM

Geological Cor  
 bedded ro  
 app



## SYMBOL LEGEND

### GEOLOGICAL SYMBOLS

Geological Contact

— defined (dip 30°)

- - - approximate (vertical)

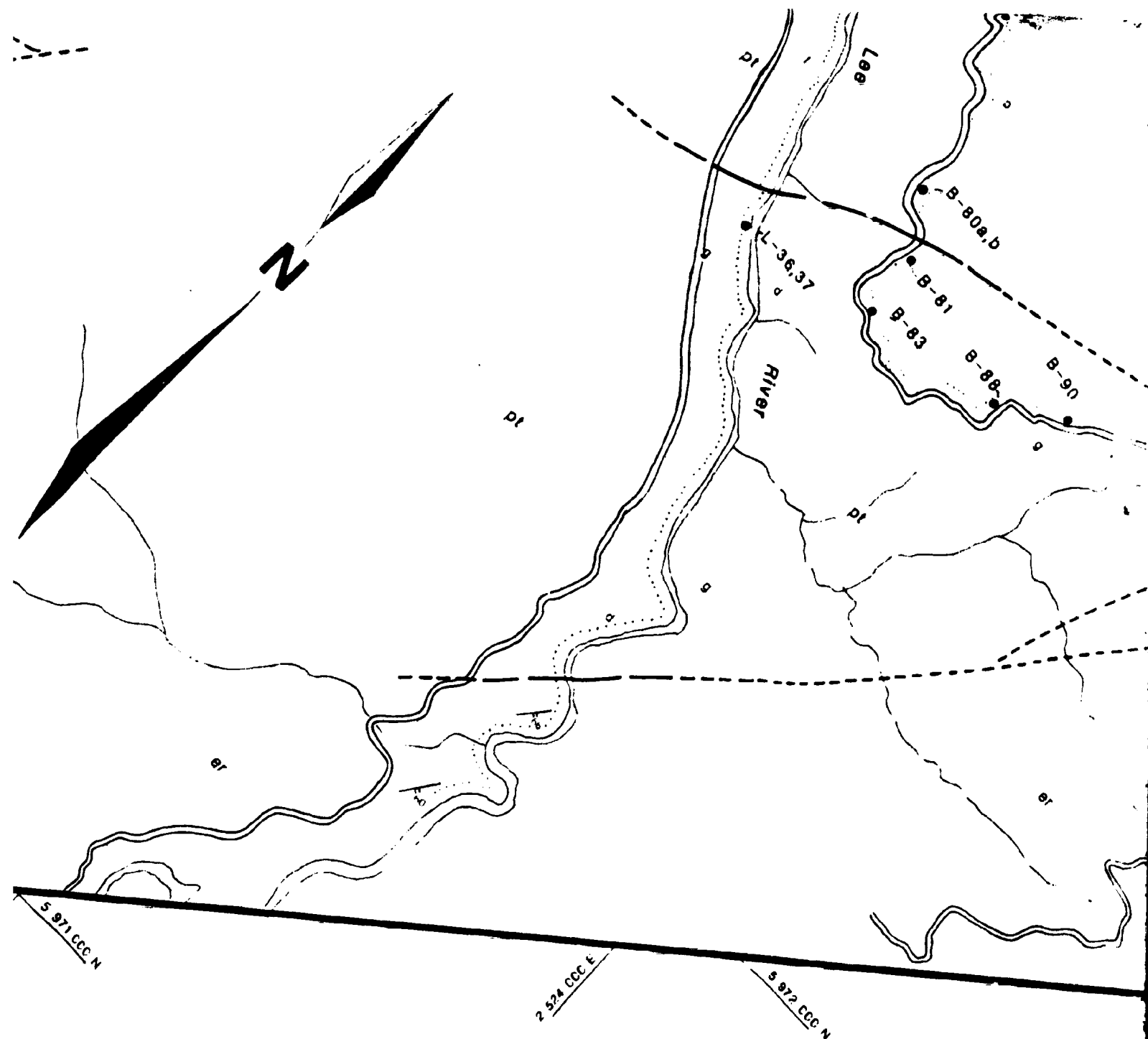
... assumed

Fault

— defined

- - - approximate

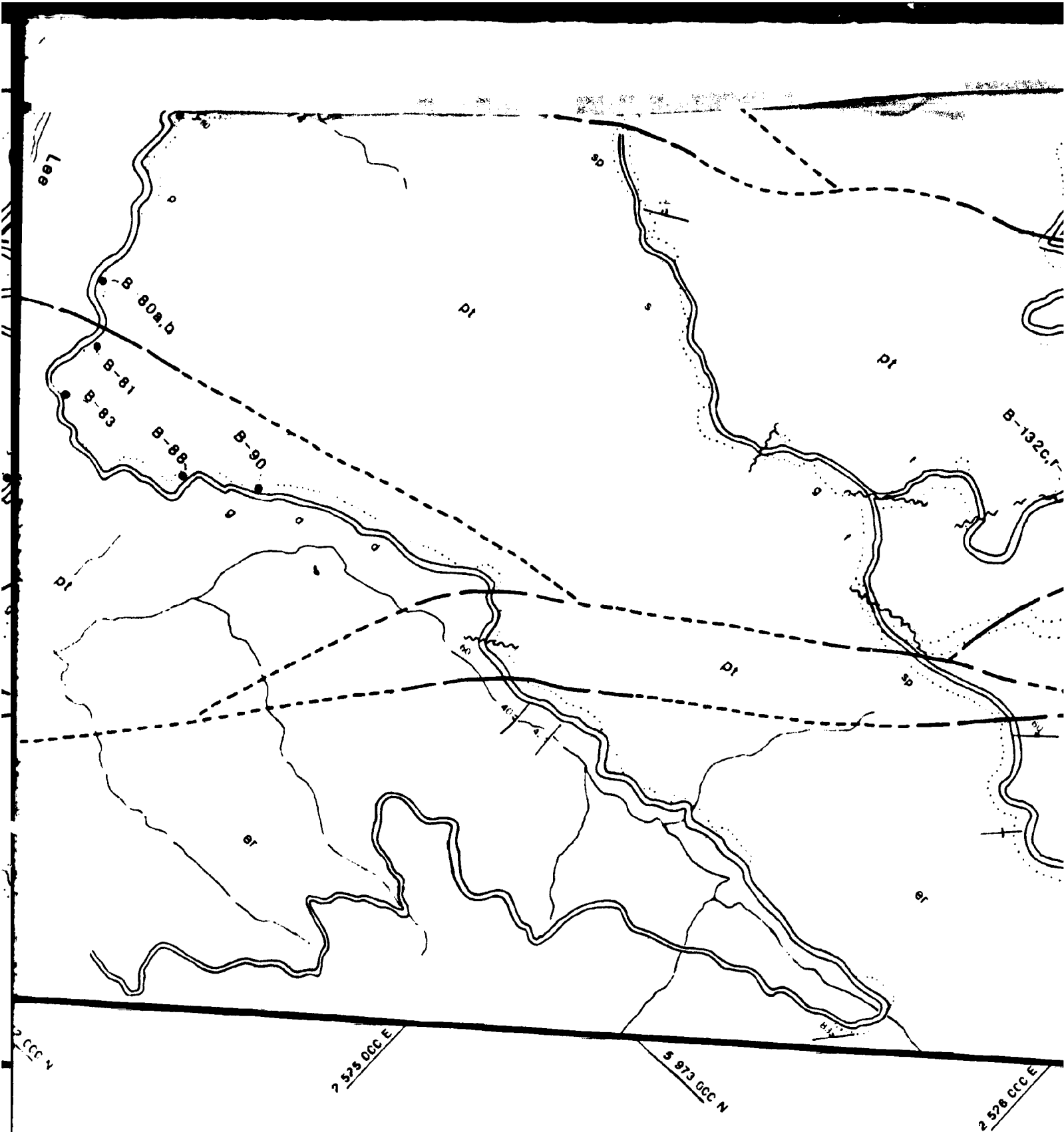
... assumed



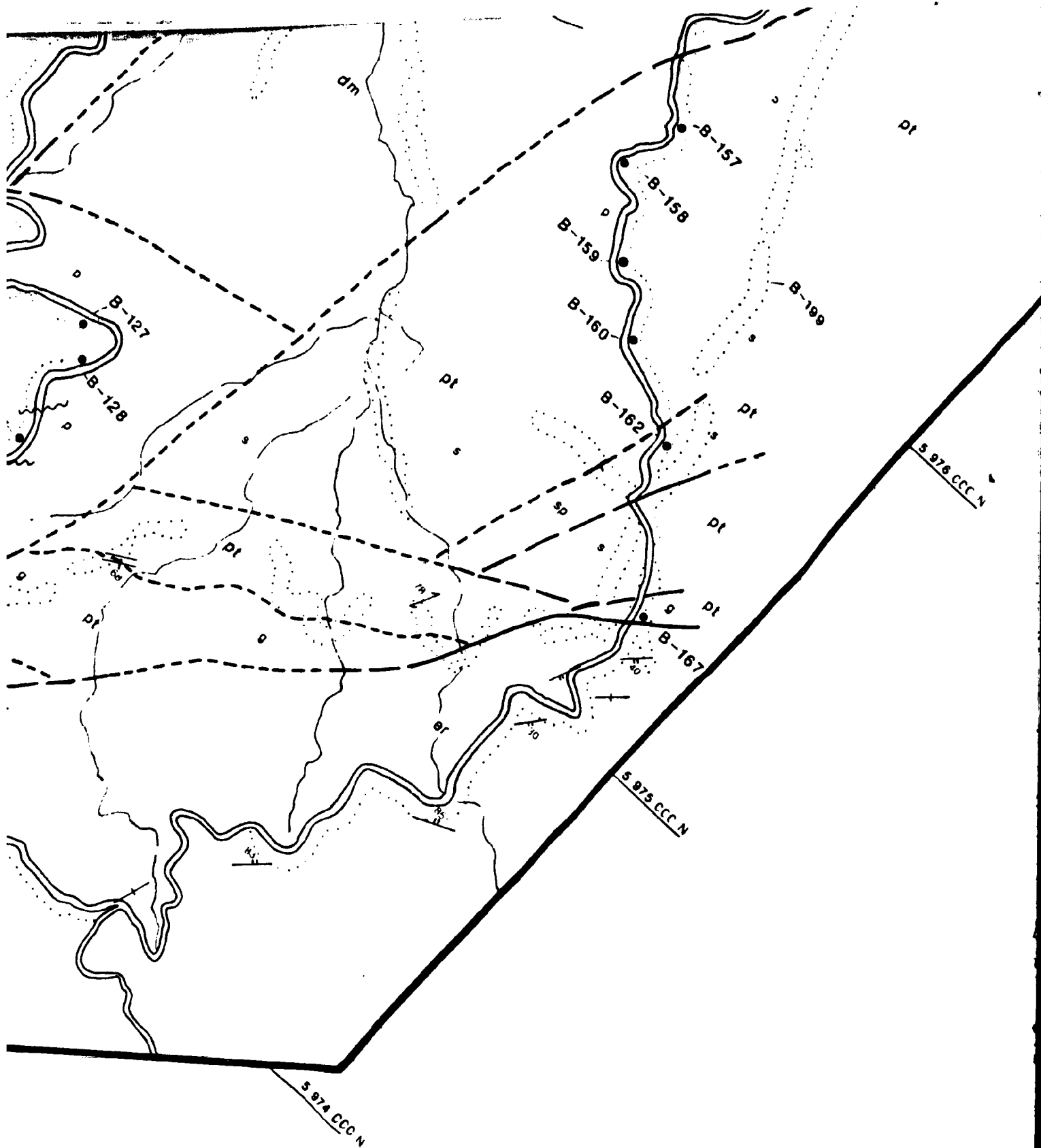
Topographic data taken from base maps of H. Baigents and Sons Ltd. Nelson

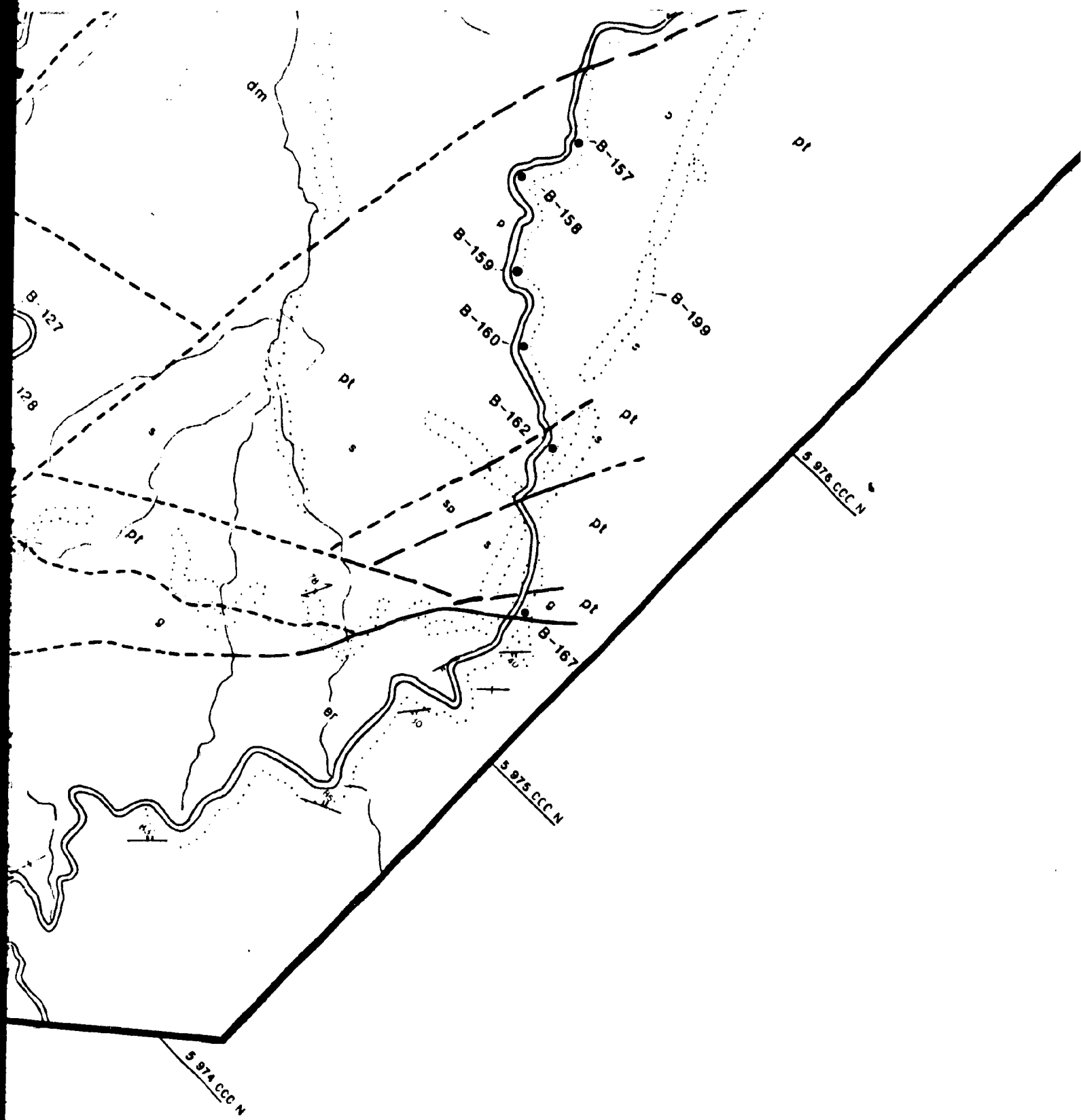
Grid references are in reference to the New Zealand Map Grid.

Elevations in metres.



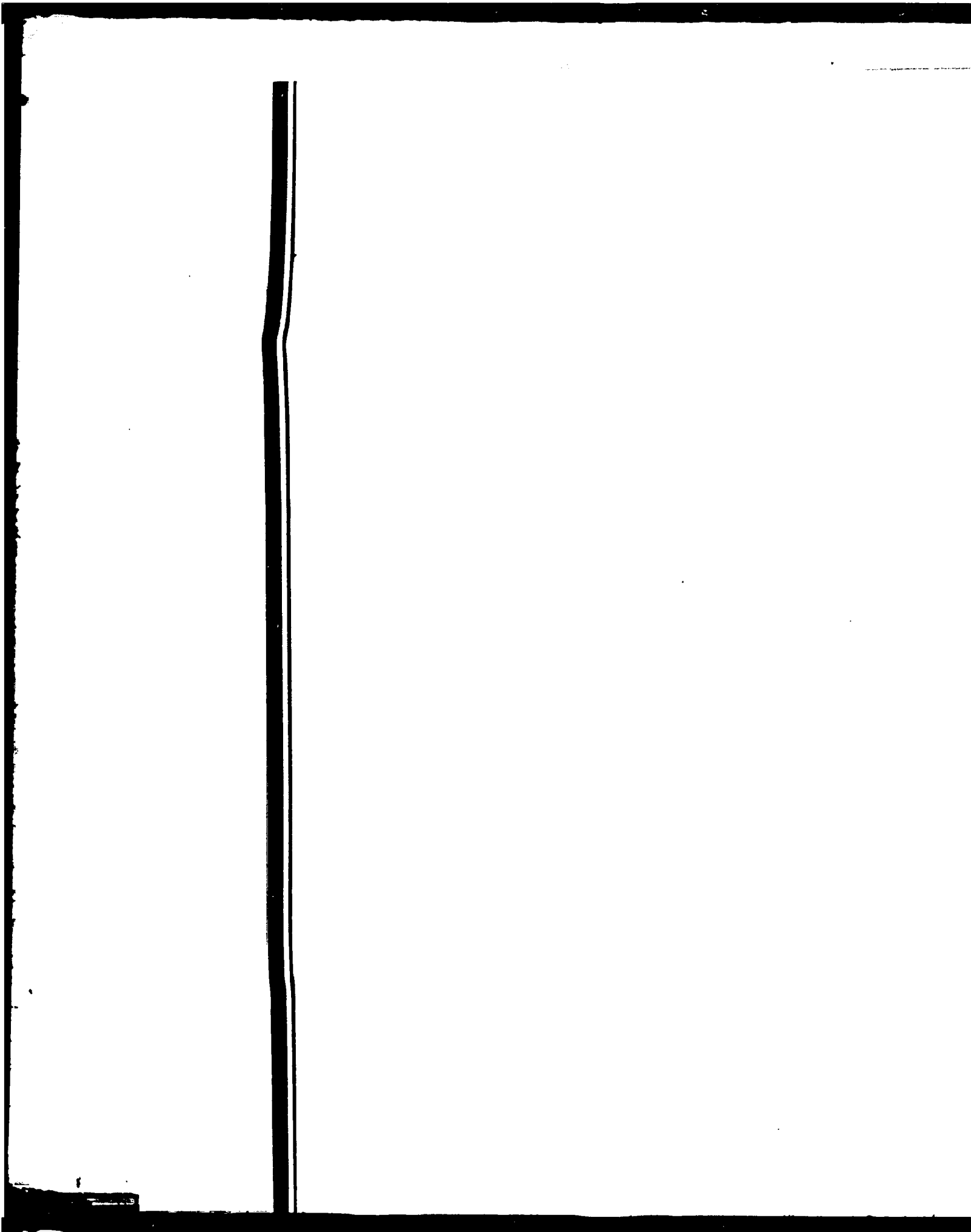
maps of H. Baigents and Sons Ltd. Nelson and Timberlands Ltd.  
the New Zealand Map Grid.





5-977 CCC N





2 519 CCC E  
5 988 CCC N

1

wp

Wooded Peak Formation (bedded to poorly bedded limestone with minor units of fine sandstone)

up

Upukerora Formation (purple to grey conglomerate consisting of mafic volcanic and f. supported in a grey to purple sandstone)

### LEE RIVER GROUP

lr

undifferentiated

b

basaltic breccia (often in a hematite-stained mudstone)

p

pillowed/massive flows (aphyric to augite and/or plagioclase)

d

diabase dykes (aphyric to augite and/or plagioclase)

g

gabbro (typically isotropic, locally foliated and amphibolized)

### DUN MOUNTAIN ULTRAMAFICS

dm

undifferentiated

sp

serpentinite

t

transition zone series (banded plutonic sequence and ultramafic rocks)

hz

harzburgite (with minor chromite pods and lenses)

du

dunite (with minor chromite pods and lenses)

### PELORUS GROUP

er

sediments (undifferentiated grey siltstones, sandstones and mudstones)

### PATUKI MÉLANGE

pt

undifferentiated

s

sediments (undifferentiated grey to purple sandstone and mudstones)

p

pillowed/massive basaltic flows (typically aphyric porphyritic)

d

diabase dykes (aphyric)

g

gabbro (typically isotropic, locally amphibolized)

u

ultramafic rocks (undifferentiated)

### CROISILLES MÉLANGE

cr

undifferentiated

s

sediments (undifferentiated grey to purple sandstone and mudstones)

p

pillowed/massive basaltic flows (typically aphyric porphyritic)

d

diabase dykes (aphyric)

g

gabbro (typically isotropic, often amphibolized)

u

ultramafic rocks (undifferentiated)

### MISCELLANEOUS

sp

sheared serpentinite

loosely bedded, grey fine grained  
s of fine grained green

conglomerates and breccias  
mic and plutonic clasts  
purple sand and mud matrix)

red mud matrix)  
to and/or plagioclase phytic).  
plagioclase phytic).  
and amphibolized).

sequence of gabbroic  
lenses)  
s).

sandstones and

sandstones, siltstones  
lly aphyric to olivine  
ized).

sandstones siltstones  
lly aphyric to olivine  
od)

GEOLOGICAL SYMBOLS

Geological Contact

- defined
- approximate
- assumed

Bedding

- tops known
- horizontal
- vertical
- dipping 40° south
- overturned 50°

Fabrics

- cleavage (strike)
- foliation (strike)
- lineation (strike)
- shearing (strike)

Sample location

- B-74 location and number

Outcrop

- area of outcrop
- o/c ? questionable outcrop
- △ △ boulders

Miscellaneous

- quarry
- prospecting shaft
- Cr chromite
- Cu copper
- Serp serpentine

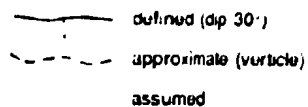
TOPOGRAPHICAL

- road
- four wheel drive
- foot track
- power lines
- building
- trig station
- spot elevation

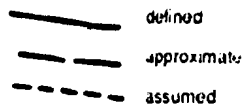
# SYMBOL LEGEND

## GEOLOGICAL SYMBOLS

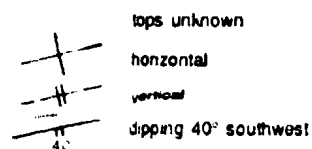
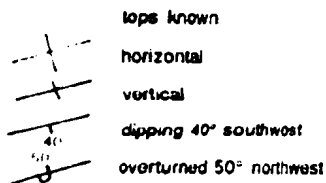
### Geological Contact



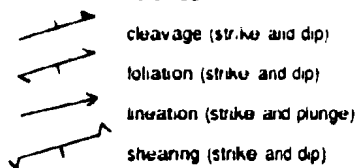
### Fault



### Bedding



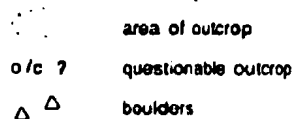
### Fabrics



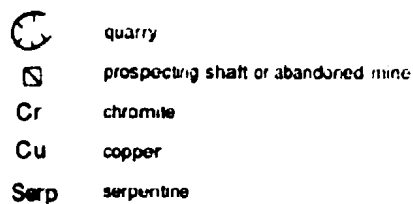
### Sample location



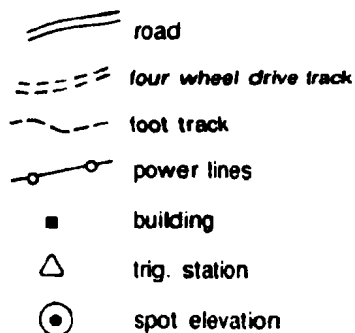
### Outcrop



### Miscellaneous



## TOPOGRAPHICAL REFERENCE



Topographic data taken from base maps of H. Baigents and Sons Ltd.

Grid references are in reference to the New Zealand Map Grid.

Elevations in metres.

2578

base maps of H. Baigents and Sons Ltd. Nelson and Timberlands Ltd.

ence to the New Zealand Map Grid.



2 520 CCC

5 874 CCC N

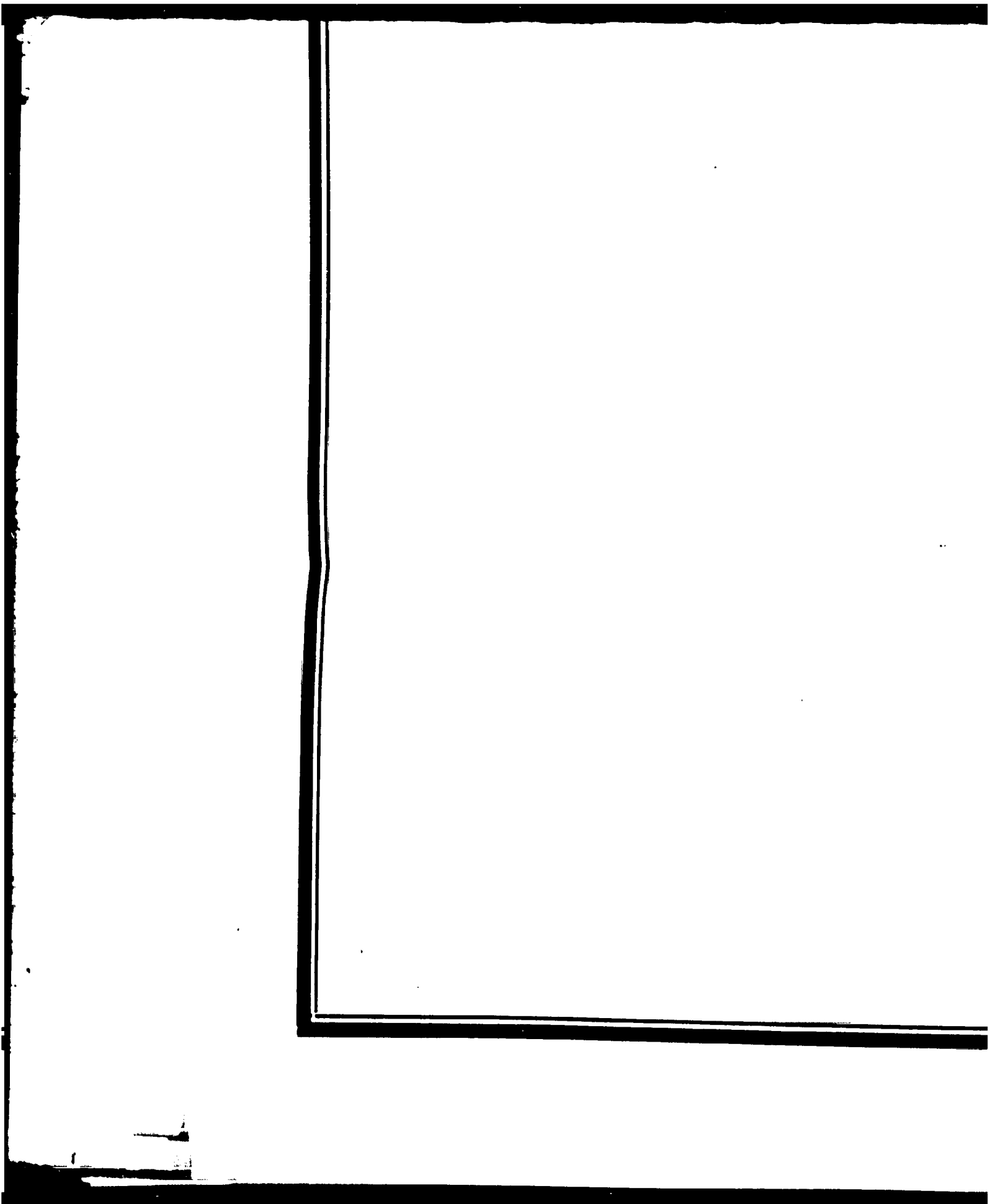
16



S 974 CCC N

GEOLOG  
RIV

**OLOGY OF THE LEE**  
**RIVER AREA**



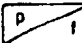


sp	serpentinite
t	transition zone series (banded plutonic sequence and ultramafic rocks)
hz	harzburgite (with minor chromite pods and lenses)
du	dunite (with minor chromite pods and lenses)


## PELORUS GROUP

er	sediments (undifferentiated grey siltstones, sandstone mudstones)
----	---

## PATUKI MÉLANGE

pt	undifferentiated
s	sediments (undifferentiated grey to purple sandstone and mudstones)
	pillowed/massive basaltic flows (typically aphy. porphyritic)
d	diabase dykes (aphyric)
g	gabbro (typically isotropic, locally amphibolitized)
u	ultramafic rocks (undifferentiated)

## CROISILLES MÉLANGE

cr	undifferentiated
s	sediments (undifferentiated grey to purple sandstone and mudstones)
	pillowed/massive basaltic flows (typically aphy. porphyritic)
d	diabase dykes (aphyric)
g	gabbro (typically isotropic, often amphibolitized)
u	ultramafic rocks (undifferentiated)

## MISCELLANEOUS

sp	sheared serpentinite
s	sediments (undifferentiated)

2 sequence of gabbroic

nd lenses)

ies)

's, sandstones and

'o sandstones, siltstones

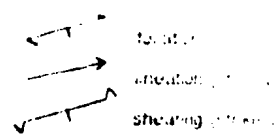
ically aphyric to olivine

olitized).

le sandstones siltstones

ically aphyric to olivine

olitized)

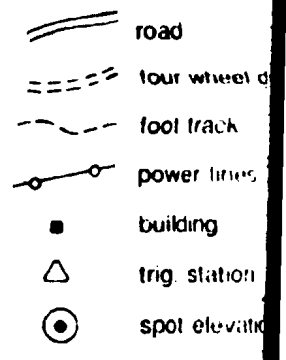


Sample location  
location and name

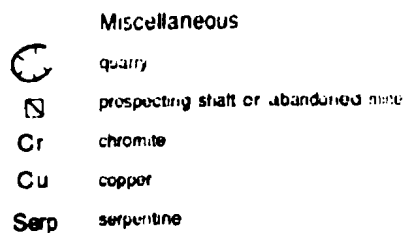
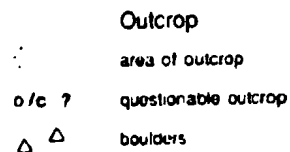
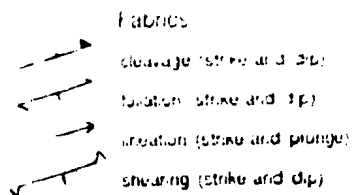
Outcrop  
area of outcrop  
questionable outcrop  
boulders

Miscellaneous  
quarry  
prospecting shaft  
Cr chromite  
Cu copper  
Serp serpentine

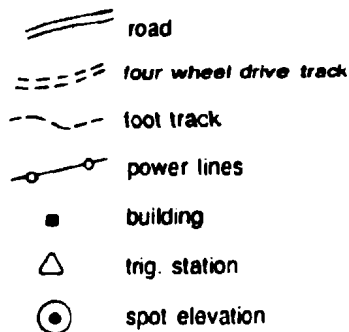
TOPOGRAPHICAL





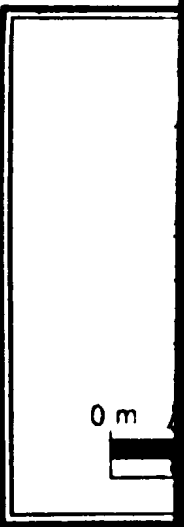


## TOPOGRAPHICAL REFERENCE









**Figure 3**

**GEOLOGY OF THE  
RIVER AREA**

**By Paul J. Moon**

**1988**

**SCALE 1: 10 000**

0 m 500 m

**Figure 3.2.2 Geology of 1**

**OGY OF THE LEE  
RIVER AREA**

**by Paul J. Moore**

**1988**

**SCALE 1: 10 000**

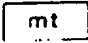
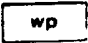
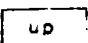
**500 m**

**1 km**

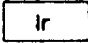
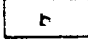

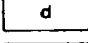
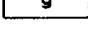
**ology of the Lee River area.**

## GEOLOGIC

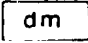
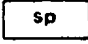

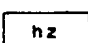
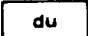
### MAITAI GROUP

	undifferentiated (bedded to poorly bedded grey siltstones, and clay)
	Wooded Peak Formation (bedded to limestone with minor or sandstone).
	Upukerora Formation (purple to grey, consisting of mafic volcanic rocks supported in a grey to light grey sandstone).

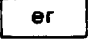
### LEE RIVER GROUP

	undifferentiated
	basaltic breccia (often in a hematite-stained matrix)
	pillowed/massive flows (aphyric to augite and/or olivine)
	diabase dykes (aphyric to augite and/or olivine)
	gabbro (typically isotropic, locally foliated)

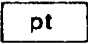
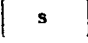
### DUN MOUNTAIN ULTRAMAFICS

	undifferentiated
	serpentinite
	transition zone series (banded pyroxene and ultramafic rocks)
	harzburgite (with minor chromite pods and lenses)
	dunite (with minor chromite pods and lenses)

### PELORUS GROUP

	sediments (undifferentiated grey siltstone and mudstones).
---	--

### PATUKI MÉLANGE

	undifferentiated
	sediments (undifferentiated grey to purple mudstones and siltstones).



LOGICAL LEGEND

poorly bedded, green to gray sandstones,  
es, and dark grey to purple mudstones).

(bedded to poorly bedded, grey fine grained  
ith minor units of fine-grained green

ble to grey conglomerates and breccias  
f mafic volcanic and plutonic clasts  
t a grey to purple sand and mud matrix)

hematite-stained mud matrix)

phyric to augite and/or plagioclase phyric).

ugite and/or plagioclase phyric).

ally foliated and amphibolitized).

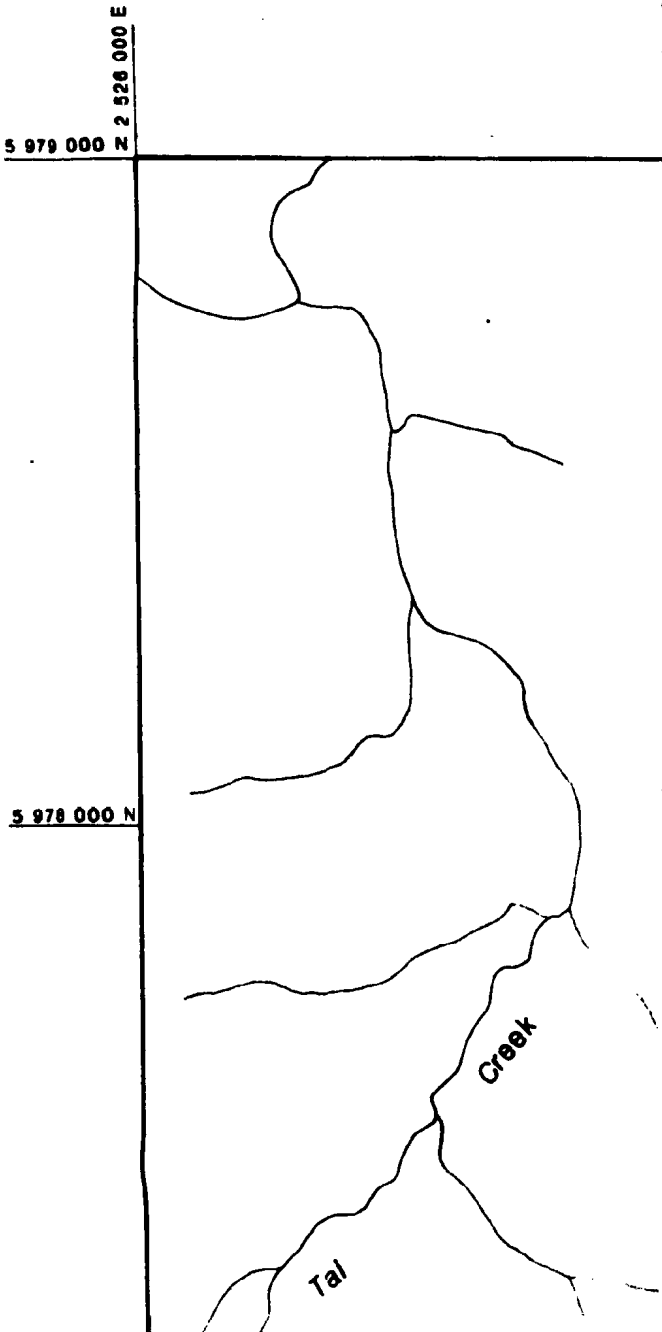
ided plutonic sequence of gabbroic  
the rocks;

mite pods and lenses).

ods and lenses)

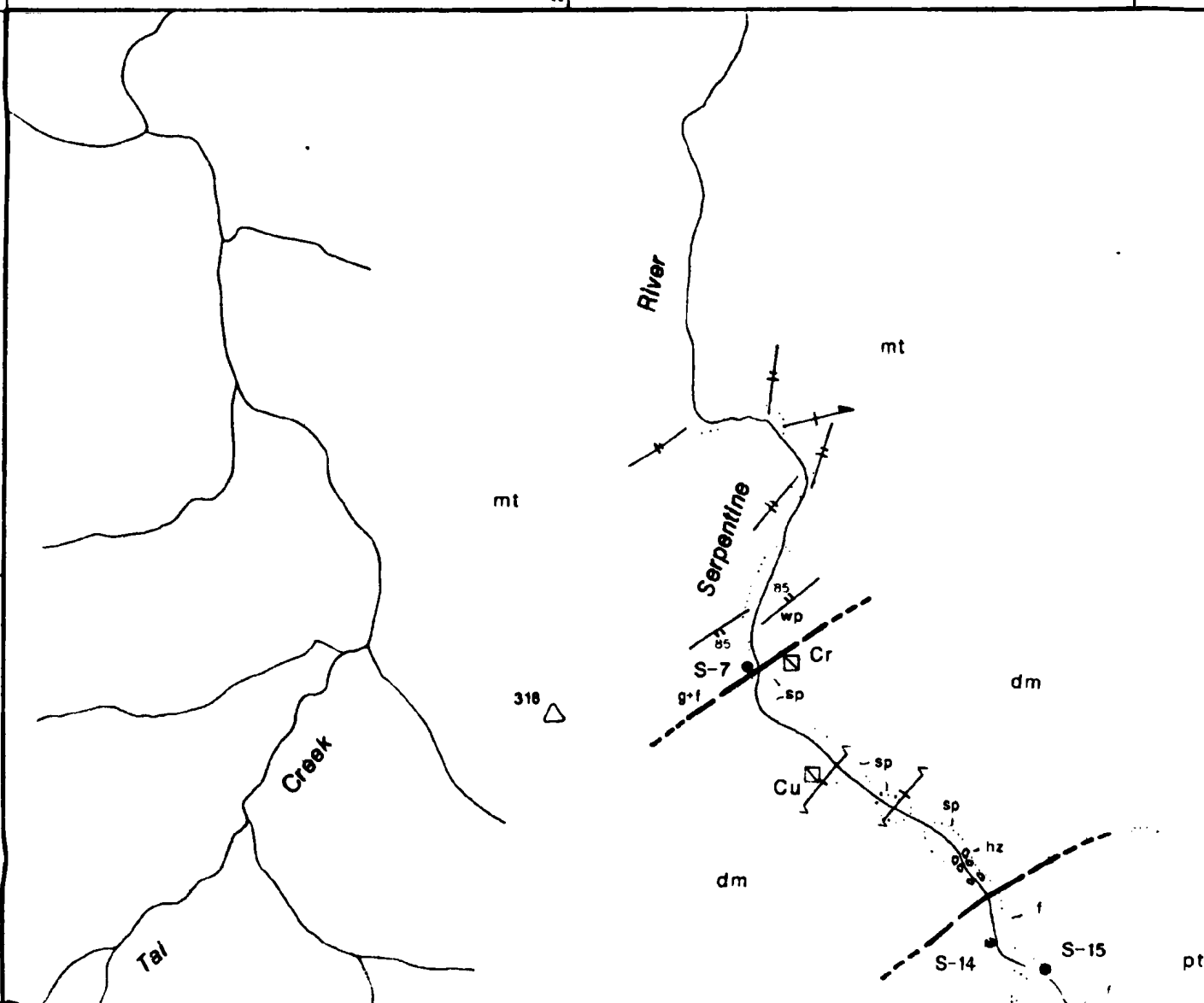
grey siltstones, sandstones and

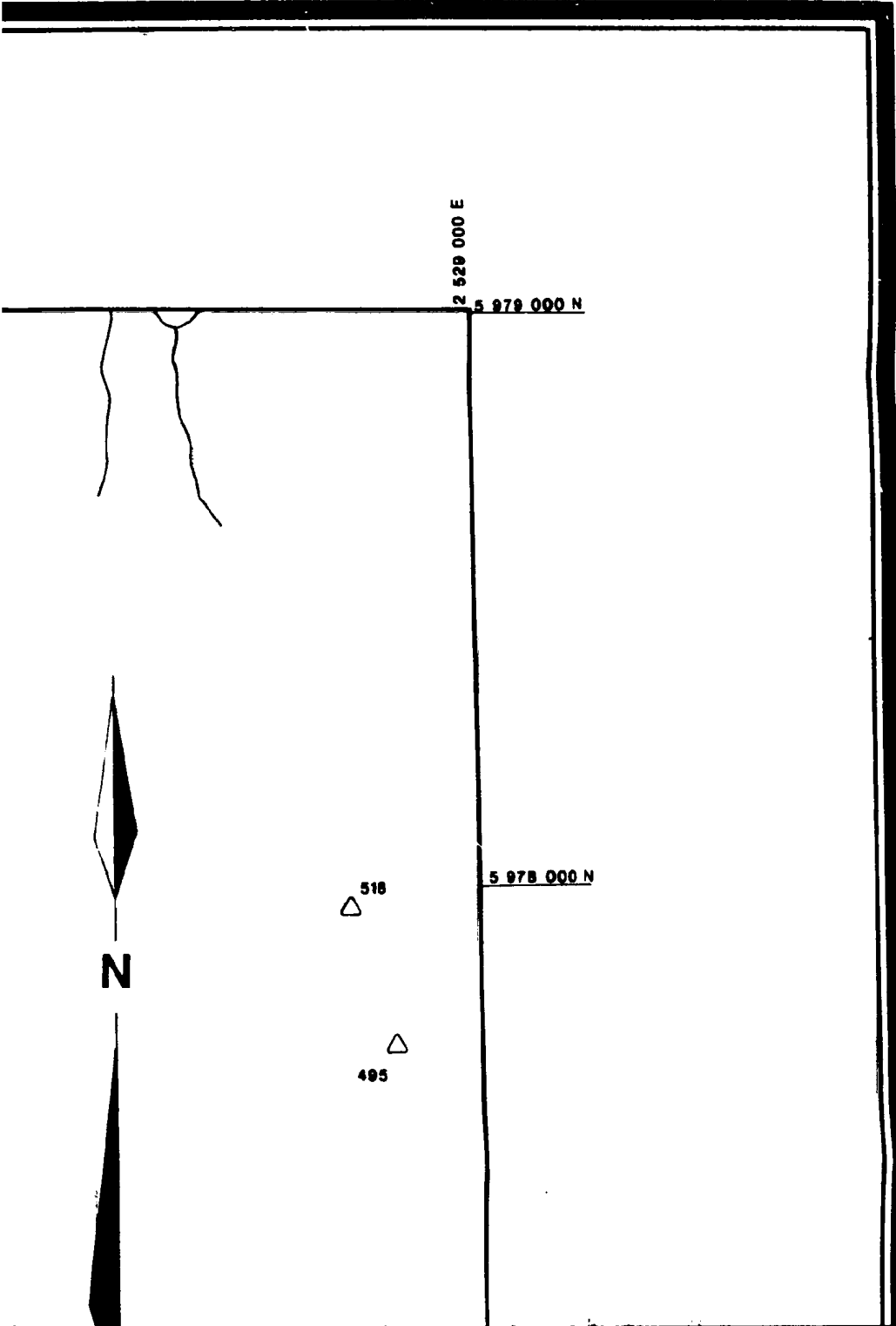
grey to purple sandstones, siltstones  
and



**2 528 000 E**

000 N



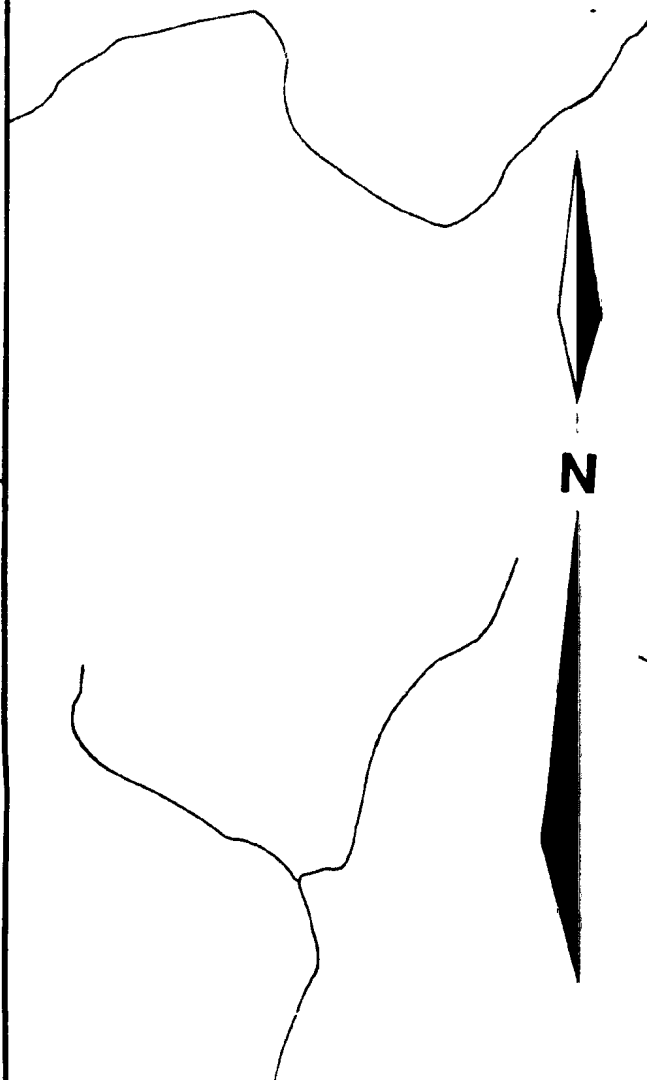


5 986 000 N

2 533 000 E

5 985 000 N

N



2 534 000 E

2 535 000 E

2 536 000 E

Hilton

Creek

Roding

2 536 000 E

2 537 000 E

2 538 000 E

Dun Mountain Track

mt

wp

amygdol

lr

Coads

River

2 539 000 E

5 986 000 N

1111



Wooded Peak

mt

wp

D-1007

D-1006

D-1005

D-1004

D-1003

D-1002

D-1001

Creek

Windy Point

## GEOLOGY

### MAITAI GROUP



undifferentiated (bedded to poorly bedded grey silstone)



Wooded Peak Formation (limestone with sandstone)



Upukerora Formation (purple consisting of thin supported in a)

### LEE RIVER GROUP



undifferentiated



basaltic breccia (often in a thin)



pillowed/massive flows (sp. l.)



diabase dykes (aphytic to aug. l.)



gabbro (typically isotropic local)

### DUN MOUNTAIN ULTRAMAFICS



undifferentiated



serpentinite



transition zone series (banded and ultramafic)



harzburgite (with minor chromite)



dunite (with minor chromite pods)

### PELORUS GROUP



sediments (undifferentiated and grey silstone)



2 539 000 E

5 986 000 N

1111



Wooded Peak

wp

7

1006

lr

5 985 000 N

hz

Windy Point

## GEOLOGICAL LEGEND

### MAITAI GROUP



undifferentiated (bedded to poorly bedded, green to grey sandstone, grey siltstones, and dark grey to purple mudstones).



Wooded Peak Formation (bedded to poorly bedded, grey fine grained limestone with minor units of fine-grained green sandstone)



Upukerora Formation (purple to grey conglomerates and breccias consisting of mafic volcanic and plutonic clasts supported in a grey to purple sand and mud matrix).

### LEE RIVER GROUP



undifferentiated



basaltic breccia (often in a hematite-stained mud matrix)



pillowed/massive flows (aphynic to augite and/or plagioclase phynic).



diabase dykes (aphynic to augite and/or plagioclase phynic).



gabbro (typically isotropic, locally foliated and amphibolized).

### DUN MOUNTAIN ULTRAMAFICS



undifferentiated



serpentinite



transition zone series (banded plutonic sequence of gabbroic and ultramafic rocks)



harzburgite (with minor chromite pods and lenses).



dunite (with minor chromite pods and lenses)

### PELORUS GROUP



sediments (undifferentiated grey siltstones, sandstones and mudstones)

### PATUKI MÉLANGE

D

lstoner  
'ones).

ne grained  
in

coals  
s  
matrix).

phyrac).

## PATUKI MÉLANGE

pt	undifferentiated
s	sediments (undifferentiated grey t and mudstones)
p / i	pillowed/massive basaltic flow (porphyritic)
d	diabase dykes (aphytic)
g	gabbro (typically isotropic, locally)
u	ultramafic rocks (undifferentiated)

## CROISILLES MÉLANGE

cr	undifferentiated
s	sediments (undifferentiated grey and mudstones)
p / i	pillowed/massive basaltic flow (porphyritic)
d	diabase dykes (aphytic)
g	gabbro (typically isotropic, often a)
u	ultramafic rocks (undifferentiated)



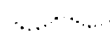
## MISCELLANEOUS

sp	sheared serpentinite
s	sediments (undifferentiated)






## SYMBOL LEG

### GEOLOGICAL SYMBOLS




#### Geological Contact

	defined (dip 30°)
	approximate (vortice)
	assumed

#### Bedding

	tops known
	horizontal
	vortical
	dipping 40° southwest
	overturned 50° northwest

#### Fabrics

	cleavage (strike and dip)
	foliation (strike and dip)
	lineation (strike and plunge)

ed

ndifferentiated grey to purple sandstones, siltstones  
and mudstones)

sive basaltic flows (typically aphyric to olivine  
porphyritic)

es (aphyric)

ally isotropic, locally amphibolized.

cks (undifferentiated)

E

led

ndifferentiated grey to purple sandstones siltstones  
and mudstones)

ssive basaltic flows (typically aphyric to olivine  
porphyritic)

es (aphyric)

ally isotropic, often amphibolized)

cks (undifferentiated)

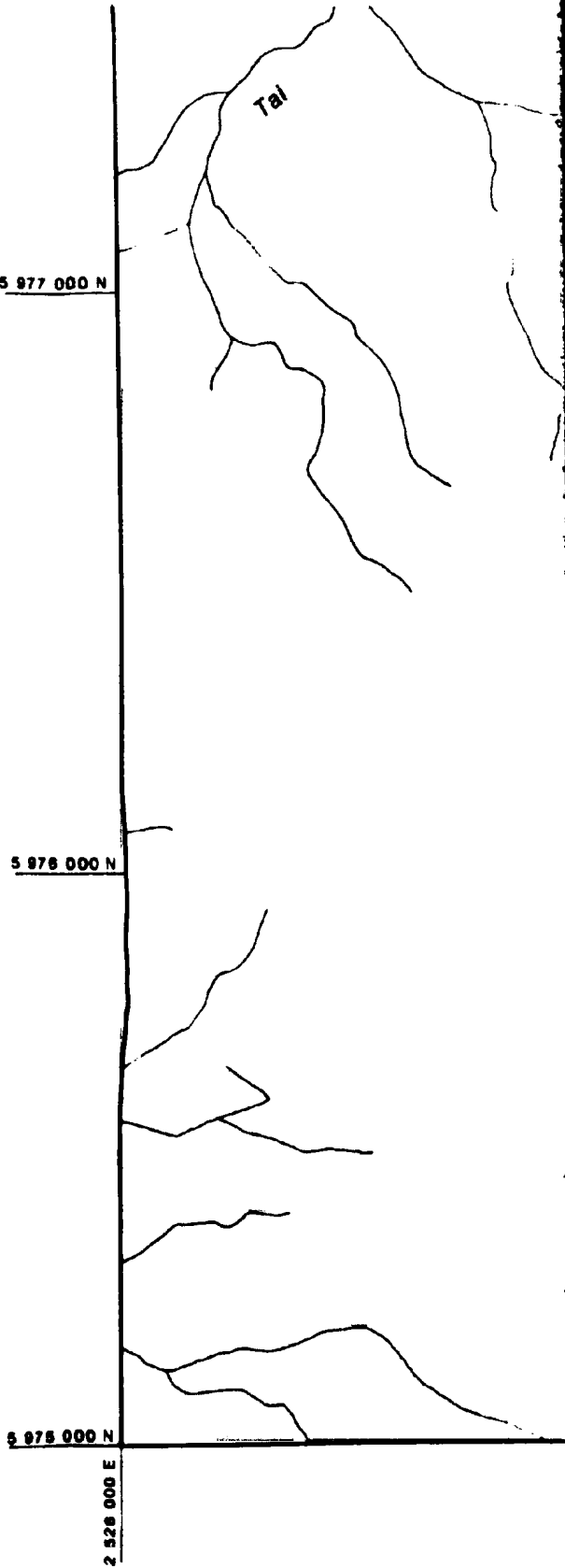
pentinite

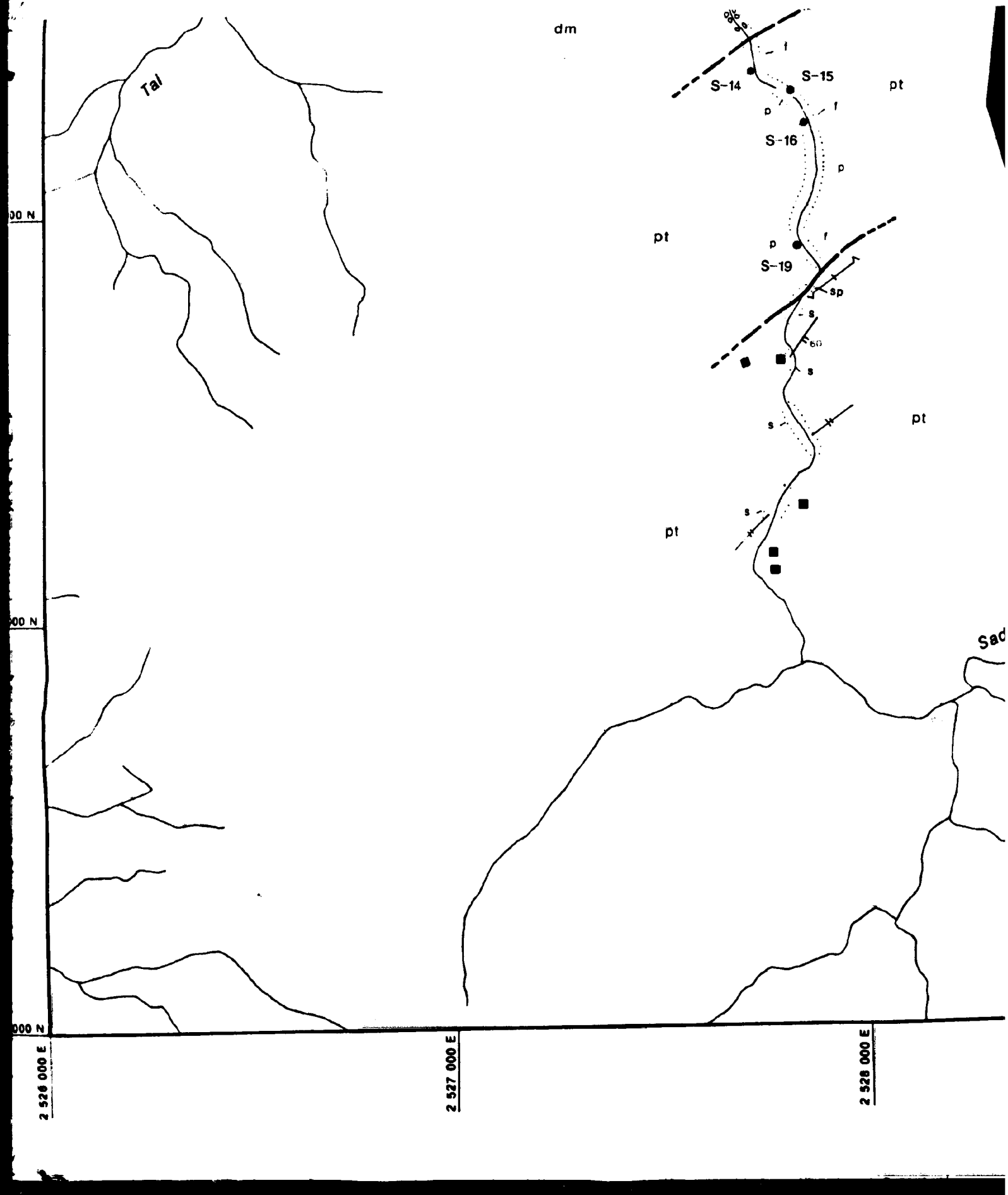
undifferentiated)

MBOL LEGEND

LS

Fault	
( )	defined
orcle)	approximate
	assumed
	tops unknown
	horizontal
	vertical
	dipping 40° southwest





5 977 000 N

△  
434

Creek

Saddle

5 978 000 N

5 979 000 N

2 829 000 E

5 984 000 N

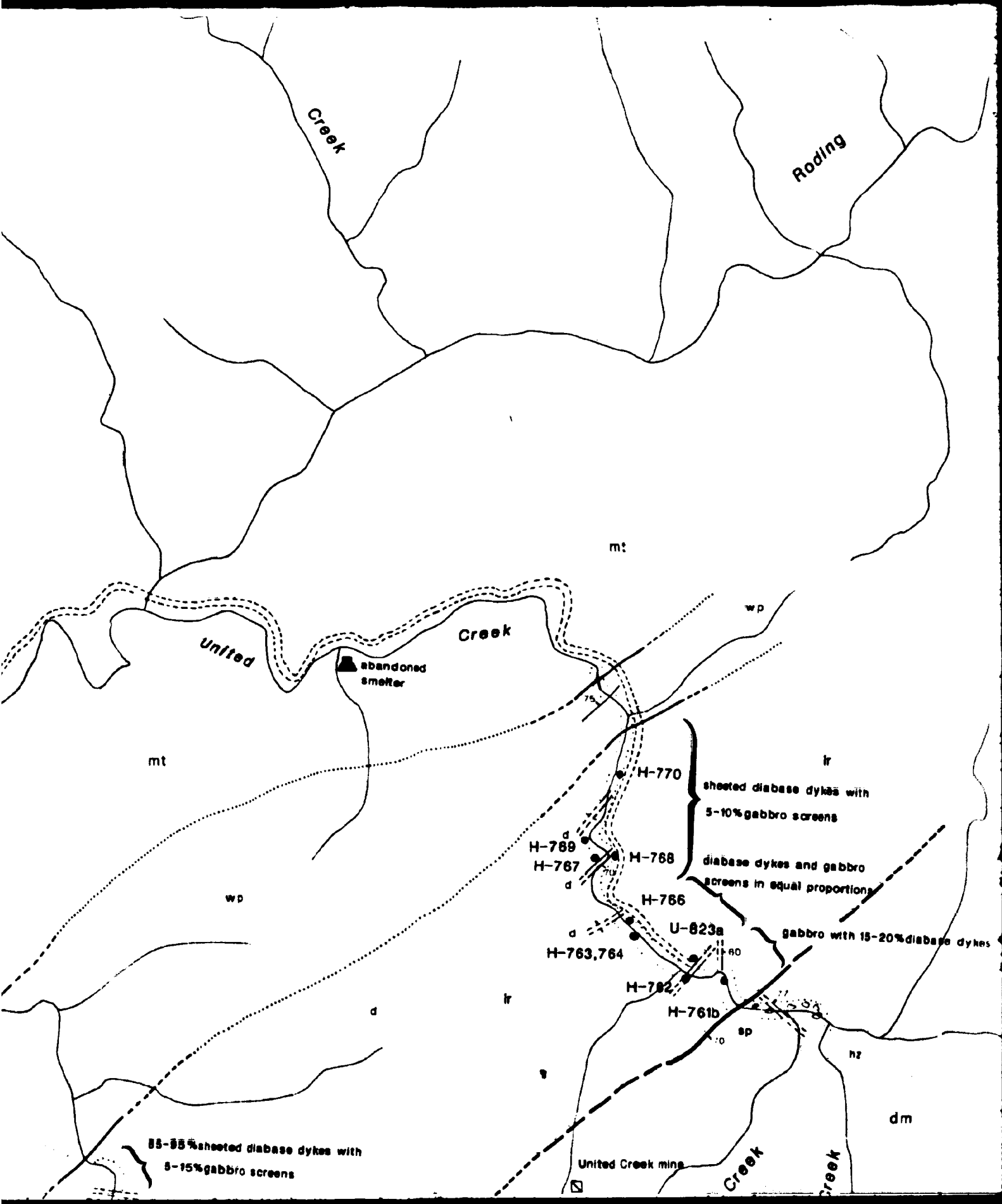
5 983 000 N

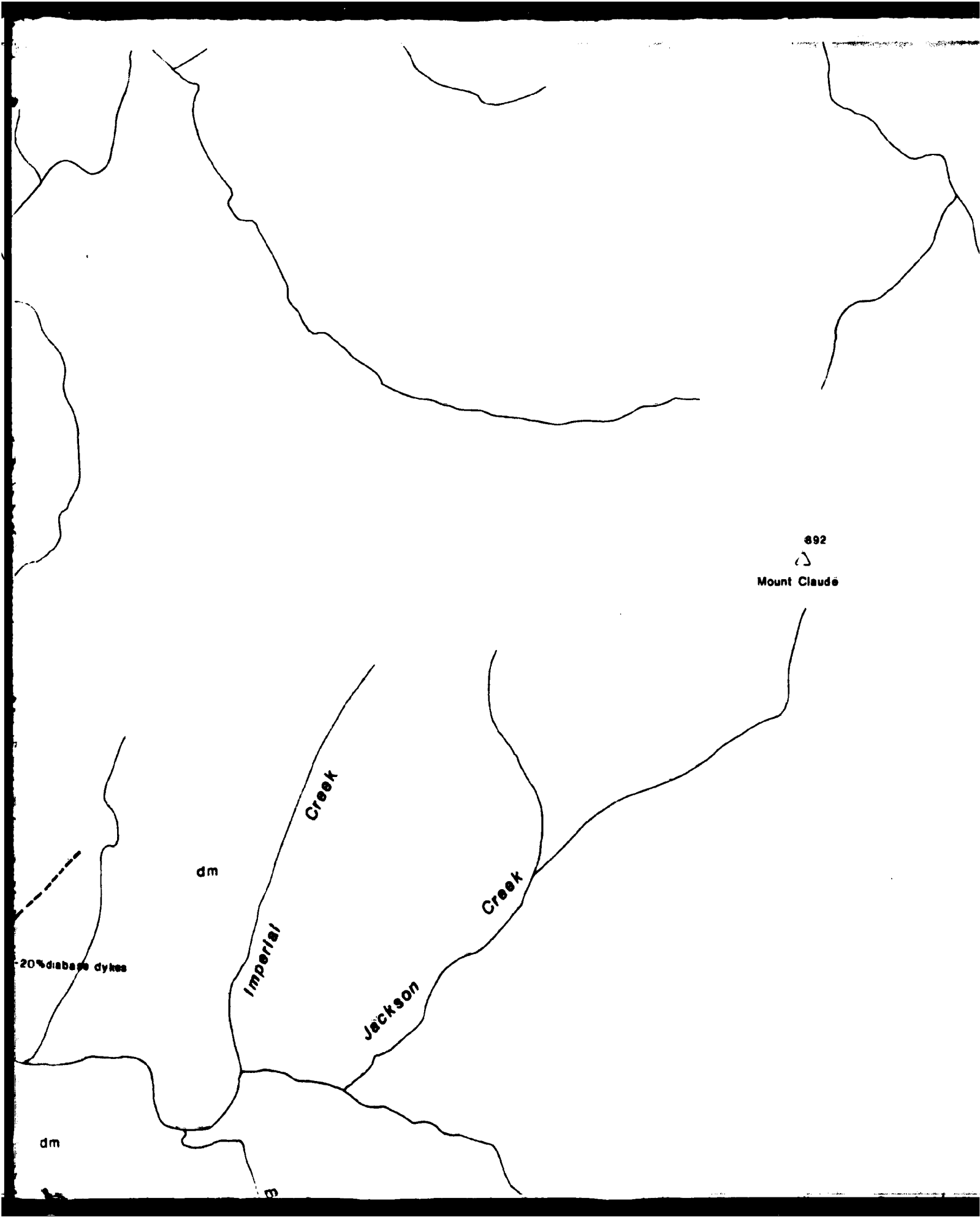
5 982 000 N

Champion  
Creek

mt







892



Mount Claude

Creek

dm

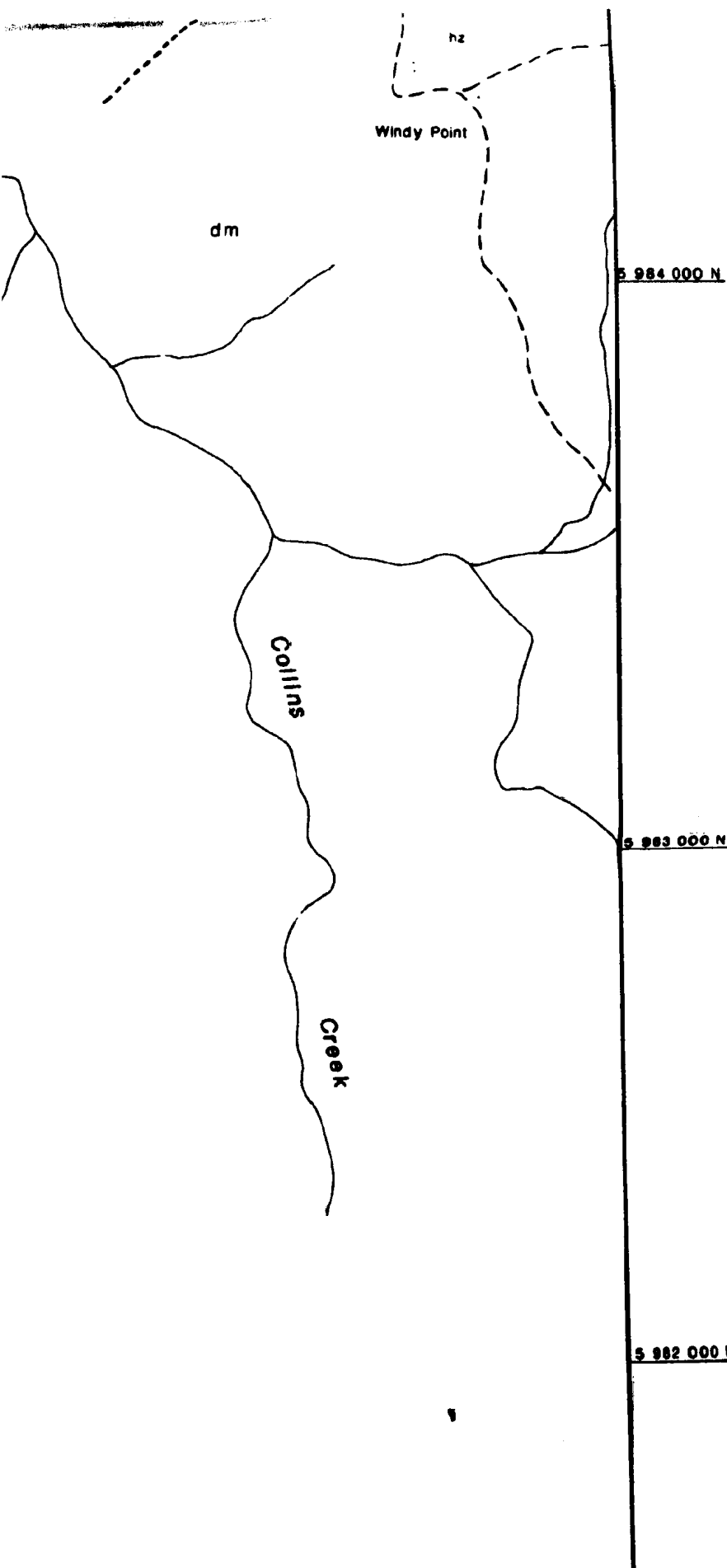
Creek

Imperial

Jackson

20% diabase dykes

dm



# PELORUS GROUP

er sediments (undifferentiated and mudstone)

## PATUKI MÉLANGE

pt undifferentiated  
s sediments (undifferentiated and mudstone)  
p/i pillowed/massive basaltic porphyries  
d diabase dykes (aphytic)  
g gabbro (typically isotropic)  
u ultramafic rocks (undifferentiated)

## CROISILLES MÉLANGE

cr undifferentiated  
s sediments (undifferentiated and mudstone)  
p/i pillowed/massive basaltic porphyries  
d diabase dykes (aphytic)  
g gabbro (typically isotropic)  
u ultramafic rocks (undifferentiated)

## MISCELLANEOUS

sp sheared serpentinite  
s sediments (undifferentiated)

## SYMB

### GEOLOGICAL SYMBOLS

**Geological Contact**  
— defined (dip 30°)  
--- approximate (vertical)  
... assumed

**Bedding**  
+ tops known  
— horizontal  
— vertical  
— dipping 40° southwest  
— overturned 50° northwest

**Fabrics**

Creek

Windy Point

S 984 000 N

S 983 000 N

S 982 000 N

# PELORUS GROUP

er sediments (undifferentiated grey siltstones, sandstones and mudstones)

# PATUKI MÉLANGE

pt undifferentiated

s sediments (undifferentiated grey to purple sandstones, siltstones and mudstones)

p/i pillowed/massive basaltic flows (typically aphyric to olivine porphyritic)

d diabase dykes (aphyric)

g gabbro (typically isotropic, locally amphibolized)

u ultramafic rocks (undifferentiated)

# CROISILLES MÉLANGE

cr undifferentiated

s sediments (undifferentiated grey to purple sandstones siltstones and mudstones)

p/i pillowed/massive basaltic flows (typically aphyric to olivine porphyritic)

d diabase dykes (aphyric)

g gabbro (typically isotropic, often amphibolized)

u ultramafic rocks (undifferentiated)

# MISCELLANEOUS

sp sheared serpentinite

s sediments (undifferentiated)

# SYMBOL LEGEND

## GEOLOGICAL SYMBOLS

Geological Contact		Fault	
	defined (dip 30°)		defined
	approximate (veritic)		approximate
	assumed		assumed
Bedding			
	top known		top unknown
	horizontal		horizontal
	vertical		vertical
	dipping 40° southwest		dipping 40° southwest
	overturned 50° northwest		

ones

ine

ones

vine

lined

proximate

summed

is unknown

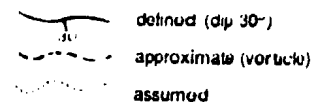
horizontal

ritical

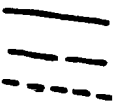
eping 40° southwest

## GEOLOGICAL SYMBOLS

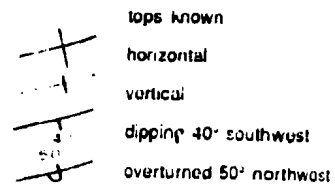
### Geological Contact



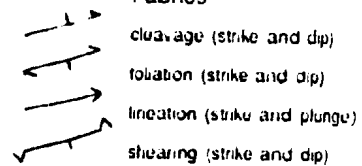
### Fault



### Bedding



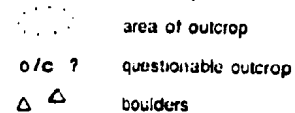
### Fabrics



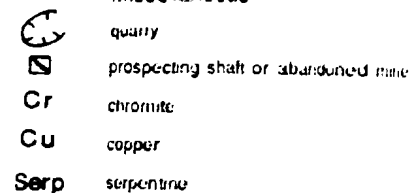
### Sample location



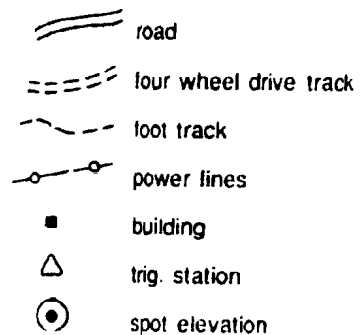
### Outcrop

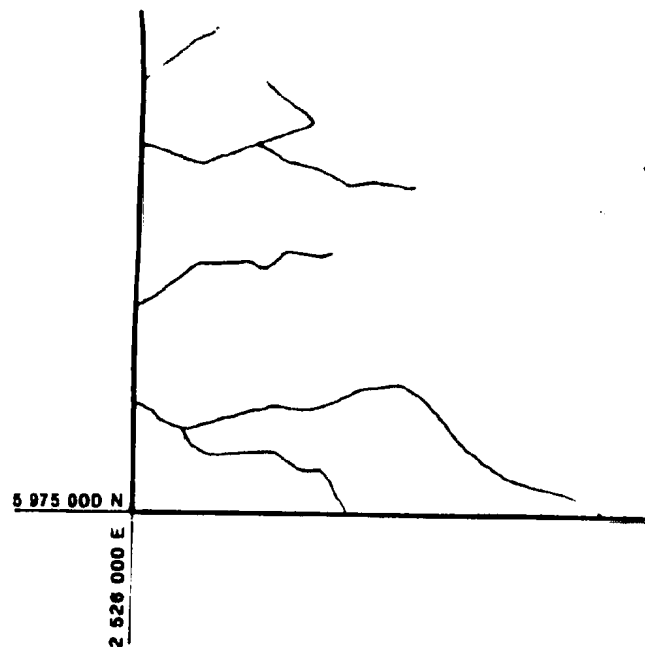
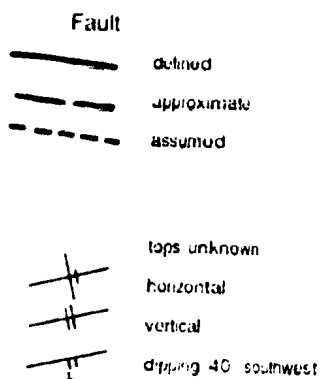


### Miscellaneous



## TOPOGRAPHICAL REFERENCE



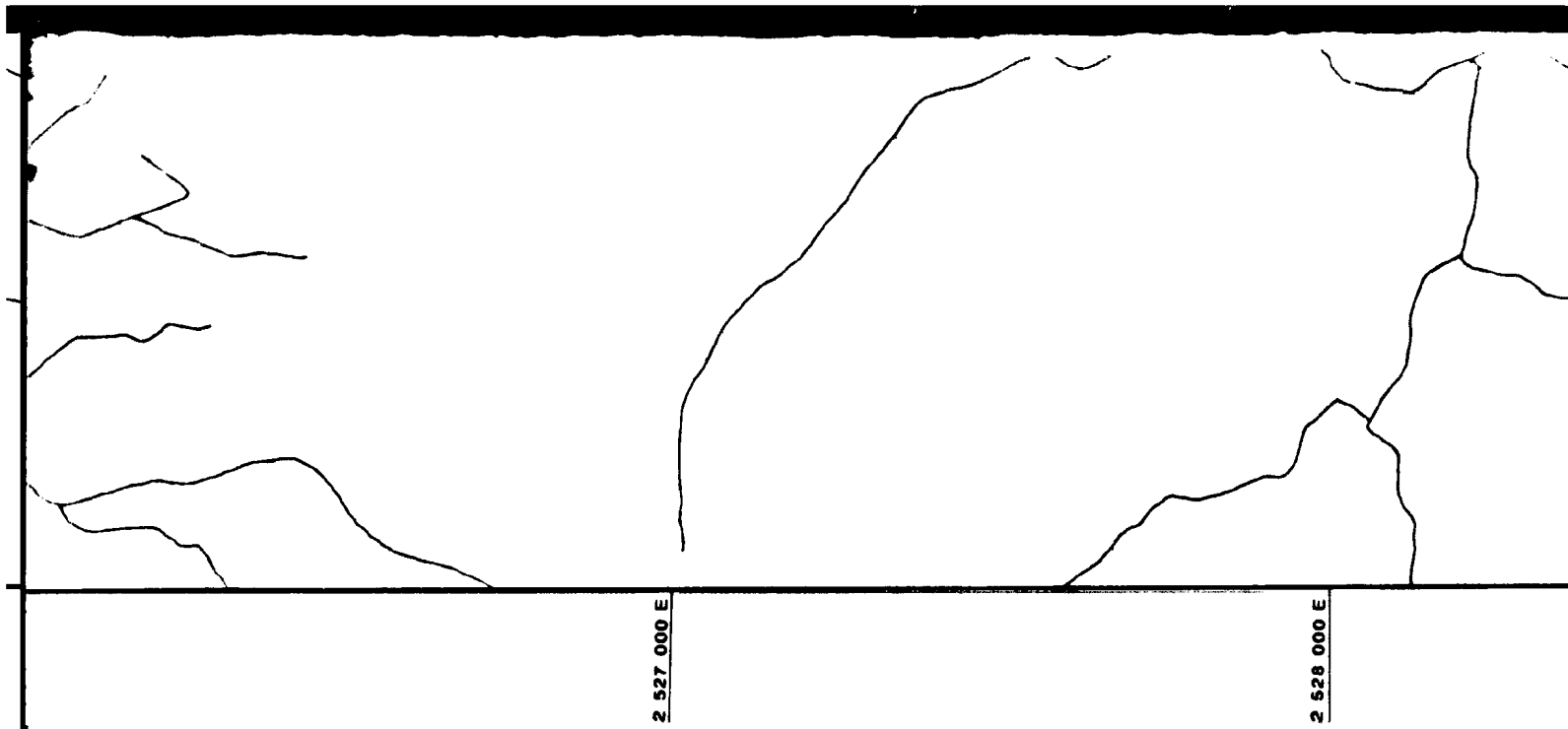


Topographic data taken from map sheets N.Z.M.S. 270 027, N28, and N29 of the New Zealand Map Grid.

Grid references are in reference to the New Zealand Map Grid.

Elevations in metres.





ets N.Z.M.S. 270 O27, N28, and N29 of the New Zealand Department of Lands and Survey.

New Zealand Map Grid.

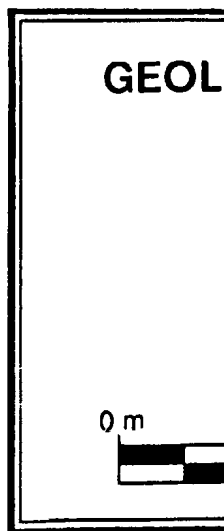
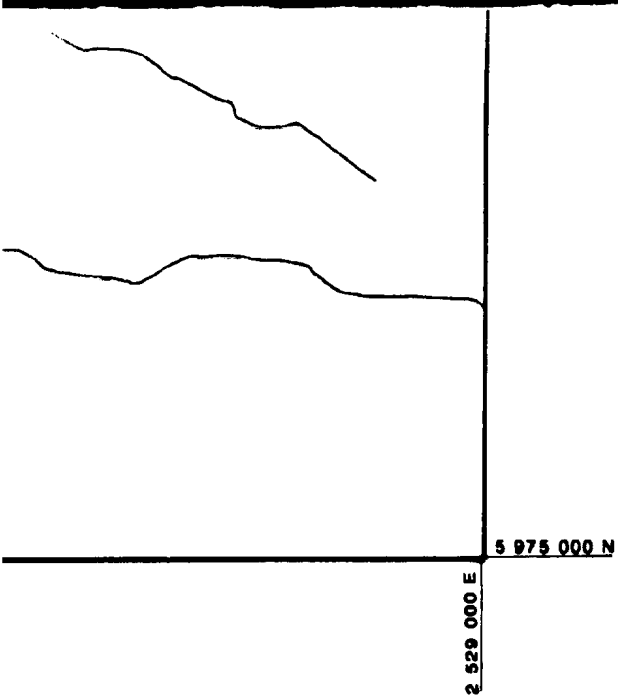


Figure 3.2.3 Geol



**GEOLOGY OF THE SERPENTINE  
RIVER**

By Paul J. Moore

1988

SCALE 1: 10 000

500 m 1 km

**Geology of the Serpentine River area.**

5 882 000 N

5 881 000 N

Mount Malite



2 533 000 E

mt

wp

d  
H-758a,c  
H-75

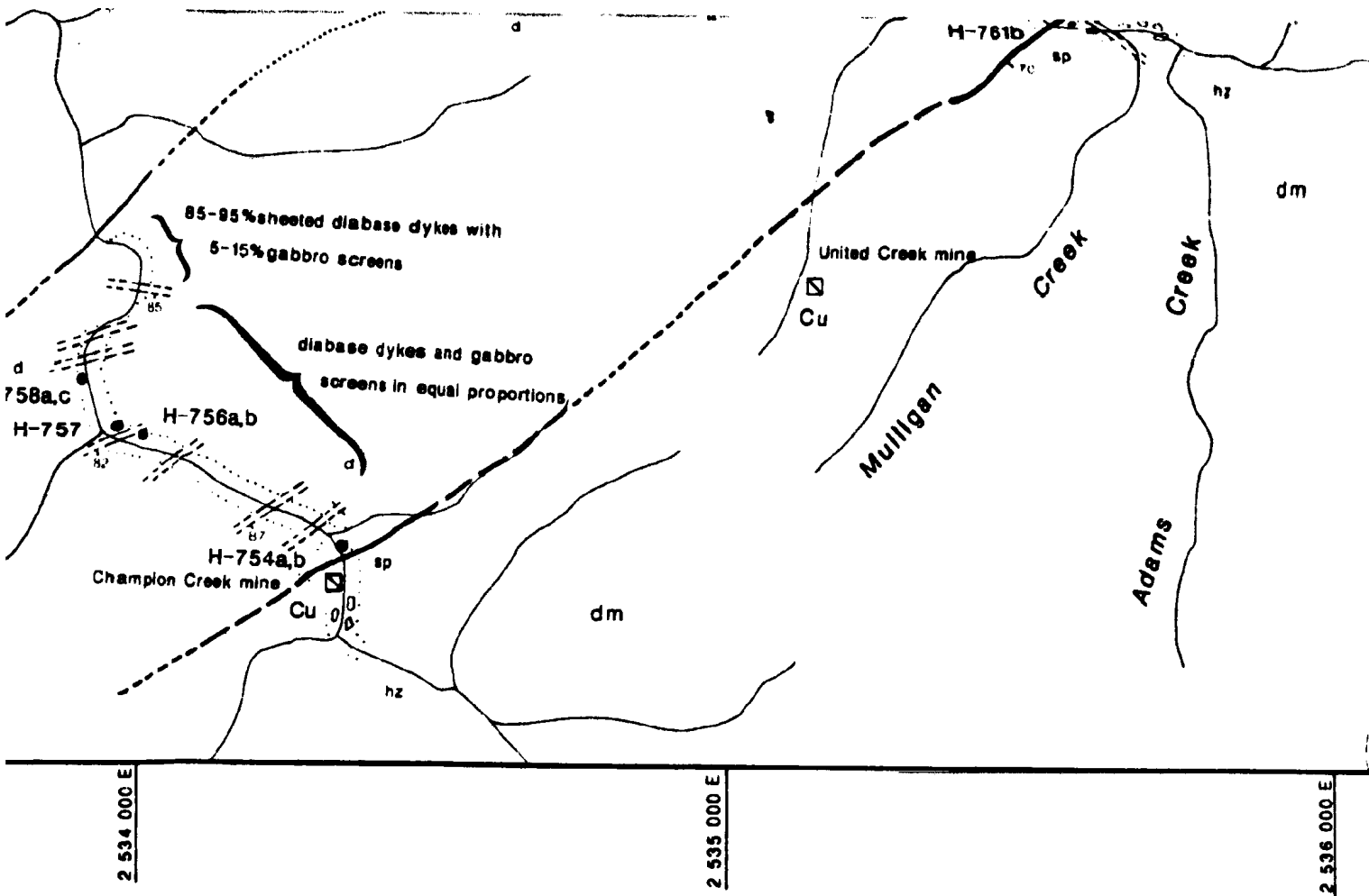
lr

## GEOLOGY OF RODING RIVER

By Paul J. Moore

1988

SCALE 1:10 000

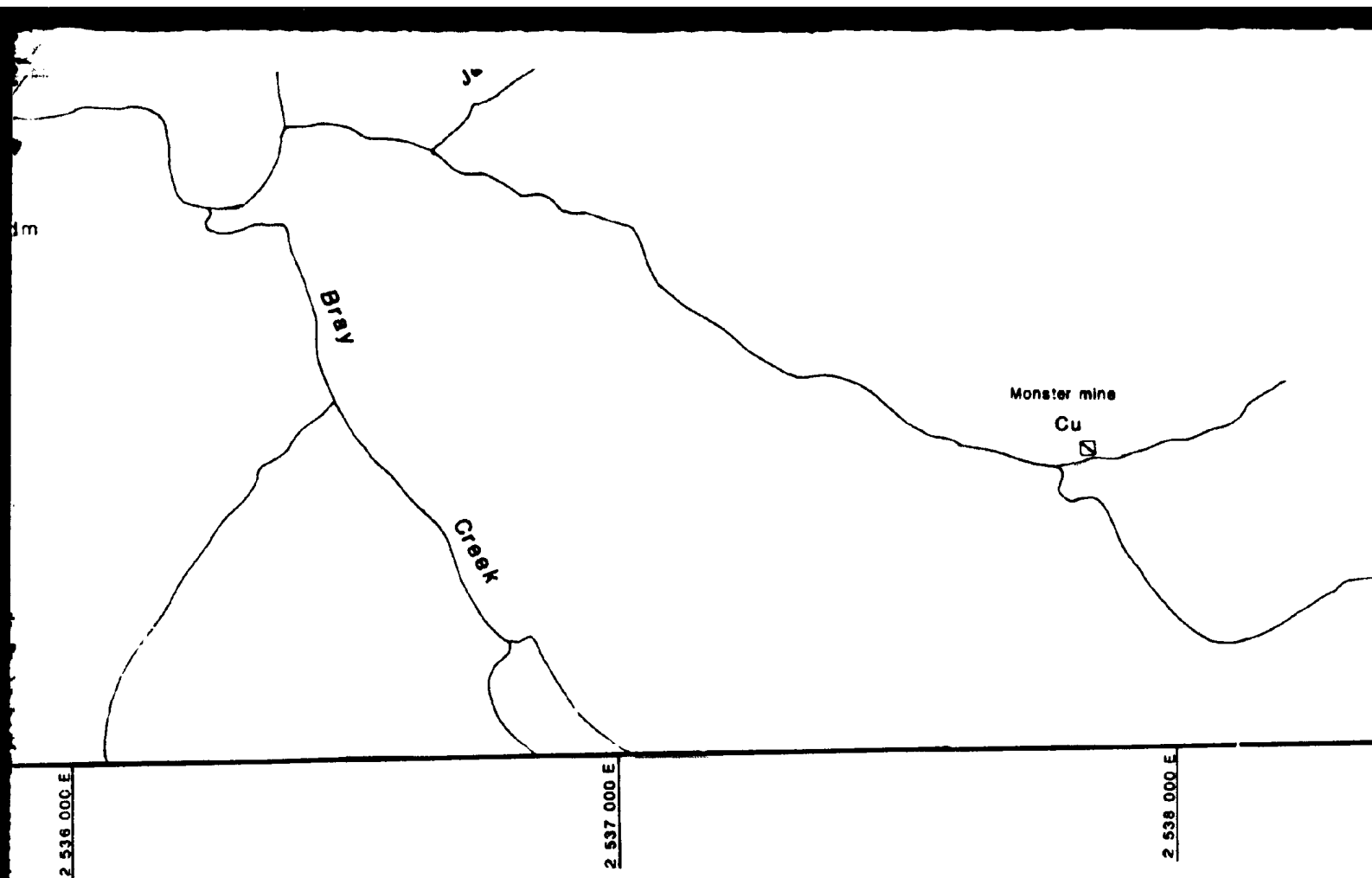


Topographic data taken from map sheets N.Z.M.S. 270

Grid references are in reference to the New Zealand Ma

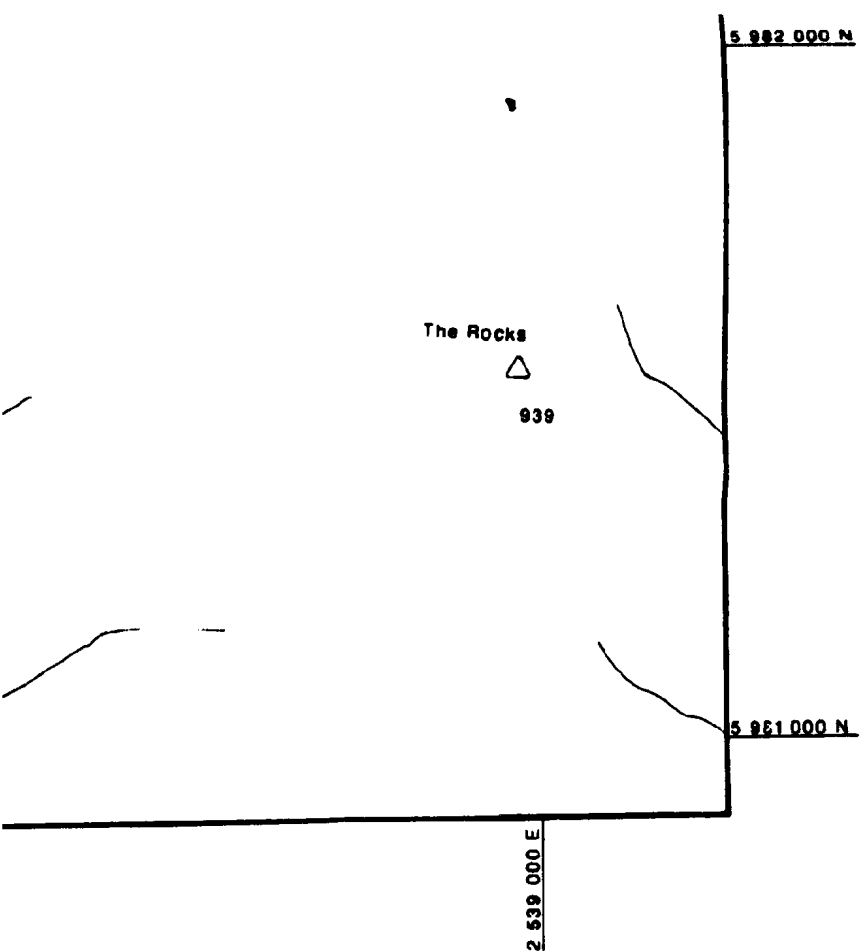
Elevations in metres.

R



ts N.Z.M.S. 270 027, N28, and N29 of the New Zealand Department of Lands and Survey.

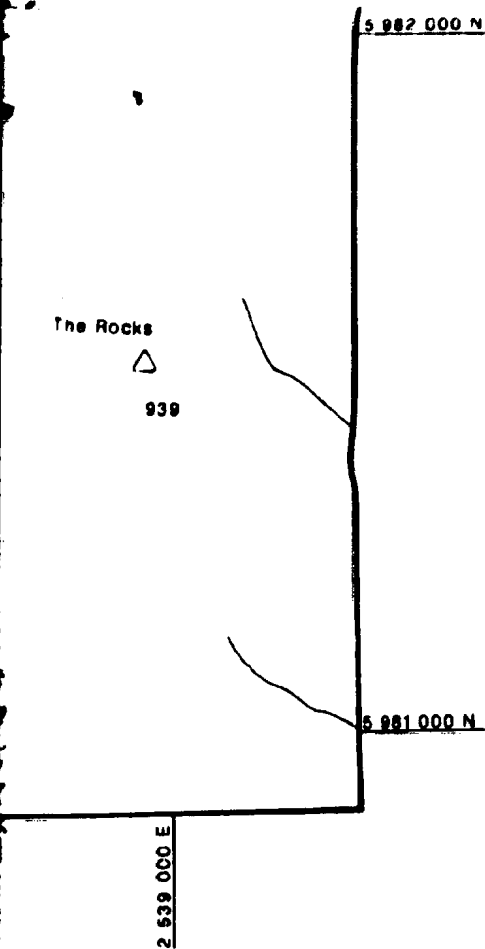
New Zealand Map Grid.



- Bedding**
- type known
  - horizontal
  - vertical
  - dipping 40° southwest
  - overturned 50° northwest
- Fabrics**
- cleavage (strike and dip)
  - foliation (strike and dip)
  - lineation (strike and plunge)
  - shearing (strike and dip)
- Sample location**
- B-74 location and number
- Outcrop**
- area of outcrop
  - o/c ? questionable outcrop
  - △ △ boulders
- Miscellaneous**
- quarry
  - prospecting shaft or abandoned mine
  - Cr chromite
  - Cu copper
  - Serp serpentine

**TOPOGRAPHICAL REFERENCE**

- road
- four wheel drive track
- foot track
- power lines
- building
- △ trig station
- spot elevation



### Bedding

- tops known
- horizontal
- vertical
- dipping 40° southwest
- overturned 50° northwest

- tops unknown
- horizontal
- vertical
- dipping 40° southwest

### Fabrics

- cleavage (strike and dip)
- foliation (strike and dip)
- lineation (strike and plunge)
- shearing (strike and dip)

### Sample location

- B-74 location and number

### Outcrop

- area of outcrop
- o/c ? questionable outcrop
- boulders

### Miscellaneous

- quarry
- prospecting shaft or abandoned mine
- Cr chromite
- Cu copper
- Serp serpentine



### TOPOGRAPHICAL REFERENCE

- road
- four wheel drive track
- foot track
- power lines
- building
- △ trig. station
- ⊙ spot elevation


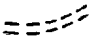







down

3" southwest

Miscellaneous	
	quarry
	prospecting shaft or abandoned mine
Cr	chromite
Cu	copper
Serp	serpentine

# TOPOGRAPHICAL REFERENCE

	road
	four wheel drive track
	foot track
	power lines
	building
	trig. station
	spot elevation

1 abandoned mine

## REFERENCE

3 track

GEC

0 m



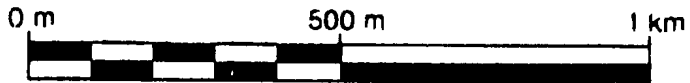
Figure 3.2.3 G

# **GEOLOGY OF THE SERPENTINE RIVER**

**By Paul J. Moore**

**1988**

**SCALE 1: 10 000**



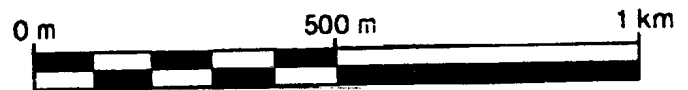
## **3 Geology of the Serpentine River area.**

# **GEOLOGY OF RODING RIVER**

**By Paul J. Moore**

**1988**

**SCALE 1: 10 000**



**Figure 3.2.4 Geology of the Roding**

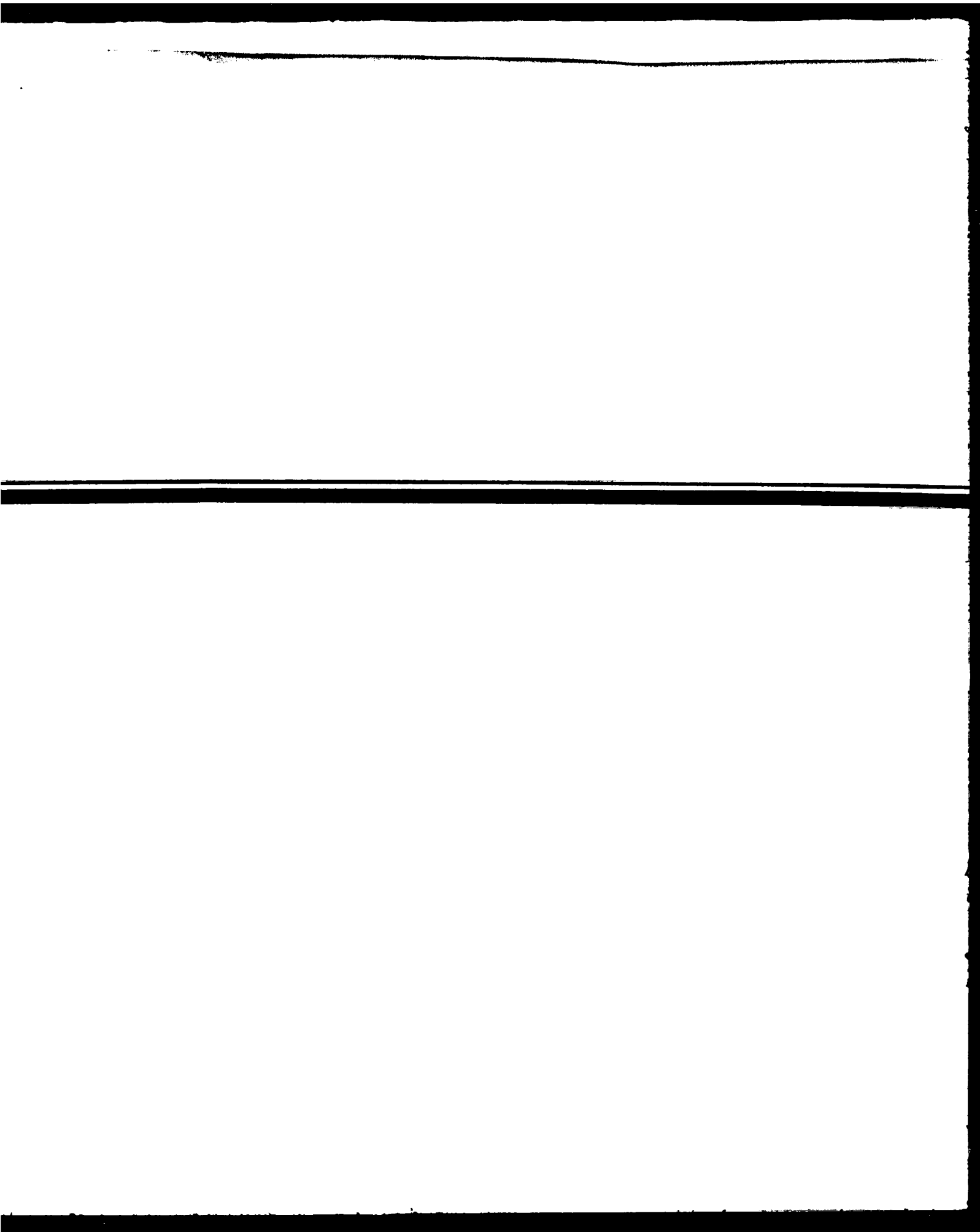
R

1 km

oding River area.









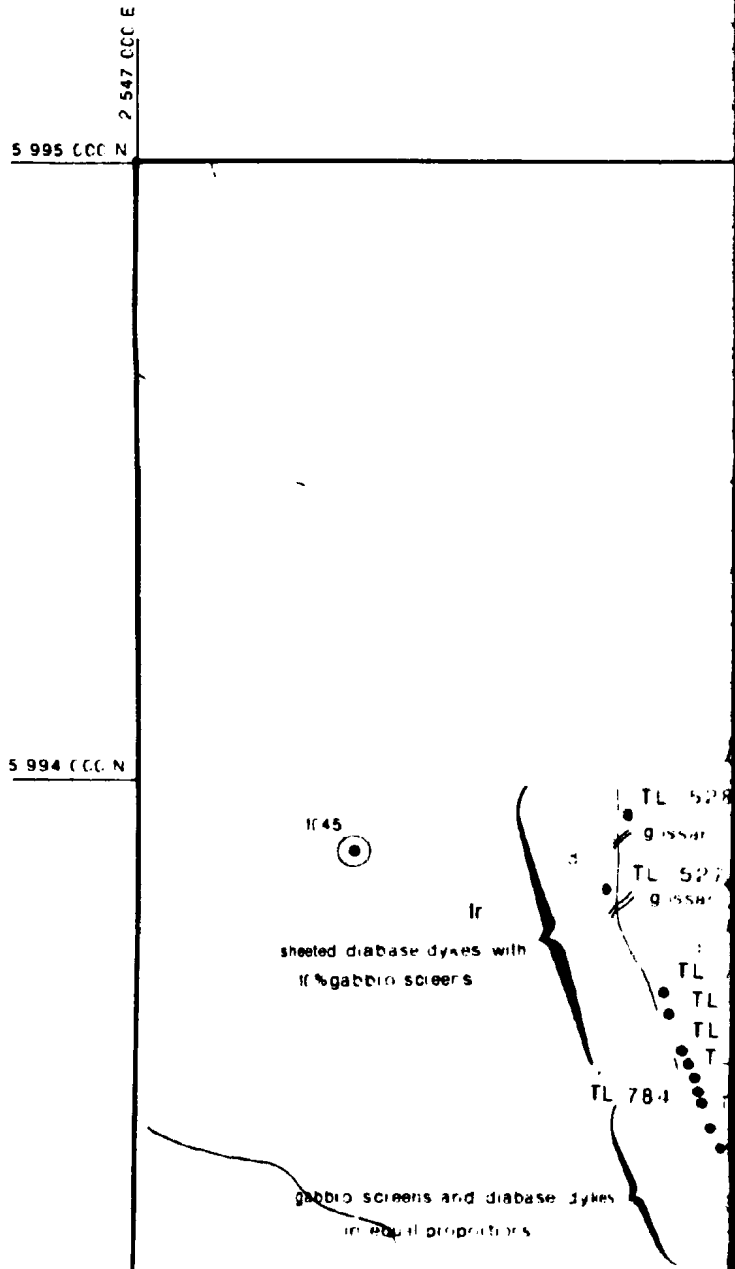
1. 2. 3. 4. 5. 6. 7. 8. 9. 10. 11. 12. 13. 14. 15. 16. 17. 18. 19. 20. 21. 22. 23. 24. 25. 26. 27. 28. 29. 30. 31. 32. 33. 34. 35. 36. 37. 38. 39. 40. 41. 42. 43. 44. 45. 46. 47. 48. 49. 50. 51. 52. 53. 54. 55. 56. 57. 58. 59. 60. 61. 62. 63. 64. 65. 66. 67. 68. 69. 70. 71. 72. 73. 74. 75. 76. 77. 78. 79. 80. 81. 82. 83. 84. 85. 86. 87. 88. 89. 90. 91. 92. 93. 94. 95. 96. 97. 98. 99. 100. 101. 102. 103. 104. 105. 106. 107. 108. 109. 110. 111. 112. 113. 114. 115. 116. 117. 118. 119. 120. 121. 122. 123. 124. 125. 126. 127. 128. 129. 130. 131. 132. 133. 134. 135. 136. 137. 138. 139. 140. 141. 142. 143. 144. 145. 146. 147. 148. 149. 150. 151. 152. 153. 154. 155. 156. 157. 158. 159. 160. 161. 162. 163. 164. 165. 166. 167. 168. 169. 170. 171. 172. 173. 174. 175. 176. 177. 178. 179. 180. 181. 182. 183. 184. 185. 186. 187. 188. 189. 190. 191. 192. 193. 194. 195. 196. 197. 198. 199. 200. 201. 202. 203. 204. 205. 206. 207. 208. 209. 210. 211. 212. 213. 214. 215. 216. 217. 218. 219. 220. 221. 222. 223. 224. 225. 226. 227. 228. 229. 230. 231. 232. 233. 234. 235. 236. 237. 238. 239. 240. 241. 242. 243. 244. 245. 246. 247. 248. 249. 250. 251. 252. 253. 254. 255. 256. 257. 258. 259. 260. 261. 262. 263. 264. 265. 266. 267. 268. 269. 270. 271. 272. 273. 274. 275. 276. 277. 278. 279. 280. 281. 282. 283. 284. 285. 286. 287. 288. 289. 290. 291. 292. 293. 294. 295. 296. 297. 298. 299. 300. 301. 302. 303. 304. 305. 306. 307. 308. 309. 310. 311. 312. 313. 314. 315. 316. 317. 318. 319. 320. 321. 322. 323. 324. 325. 326. 327. 328. 329. 330. 331. 332. 333. 334. 335. 336. 337. 338. 339. 340. 341. 342. 343. 344. 345. 346. 347. 348. 349. 350. 351. 352. 353. 354. 355. 356. 357. 358. 359. 360. 361. 362. 363. 364. 365. 366. 367. 368. 369. 370. 371. 372. 373. 374. 375. 376. 377. 378. 379. 380. 381. 382. 383. 384. 385. 386. 387. 388. 389. 390. 391. 392. 393. 394. 395. 396. 397. 398. 399. 400. 401. 402. 403. 404. 405. 406. 407. 408. 409. 410. 411. 412. 413. 414. 415. 416. 417. 418. 419. 420. 421. 422. 423. 424. 425. 426. 427. 428. 429. 430. 431. 432. 433. 434. 435. 436. 437. 438. 439. 440. 441. 442. 443. 444. 445. 446. 447. 448. 449. 450. 451. 452. 453. 454. 455. 456. 457. 458. 459. 460. 461. 462. 463. 464. 465. 466. 467. 468. 469. 470. 471. 472. 473. 474. 475. 476. 477. 478. 479. 480. 481. 482. 483. 484. 485. 486. 487. 488. 489. 490. 491. 492. 493. 494. 495. 496. 497. 498. 499. 500. 501. 502. 503. 504. 505. 506. 507. 508. 509. 510. 511. 512. 513. 514. 515. 516. 517. 518. 519. 520. 521. 522. 523. 524. 525. 526. 527. 528. 529. 530. 531. 532. 533. 534. 535. 536. 537. 538. 539. 540. 541. 542. 543. 544. 545. 546. 547. 548. 549. 550. 551. 552. 553. 554. 555. 556. 557. 558. 559. 560. 561. 562. 563. 564. 565. 566. 567. 568. 569. 570. 571. 572. 573. 574. 575. 576. 577. 578. 579. 580. 581. 582. 583. 584. 585. 586. 587. 588. 589. 590. 591. 592. 593. 594. 595. 596. 597. 598. 599. 600. 601. 602. 603. 604. 605. 606. 607. 608. 609. 610. 611. 612. 613. 614. 615. 616. 617. 618. 619. 620. 621. 622. 623. 624. 625. 626. 627. 628. 629. 630. 631. 632. 633. 634. 635. 636. 637. 638. 639. 640. 641. 642. 643. 644. 645. 646. 647. 648. 649. 650. 651. 652. 653. 654. 655. 656. 657. 658. 659. 660. 661. 662. 663. 664. 665. 666. 667. 668. 669. 670. 671. 672. 673. 674. 675. 676. 677. 678. 679. 680. 681. 682. 683. 684. 685. 686. 687. 688. 689. 690. 691. 692. 693. 694. 695. 696. 697. 698. 699. 700. 701. 702. 703. 704. 705. 706. 707. 708. 709. 710. 711. 712. 713. 714. 715. 716. 717. 718. 719. 720. 721. 722. 723. 724. 725. 726. 727. 728. 729. 730. 731. 732. 733. 734. 735. 736. 737. 738. 739. 740. 741. 742. 743. 744. 745. 746. 747. 748. 749. 750. 751. 752. 753. 754. 755. 756. 757. 758. 759. 760. 761. 762. 763. 764. 765. 766. 767. 768. 769. 770. 771. 772. 773. 774. 775. 776. 777. 778. 779. 780. 781. 782. 783. 784. 785. 786. 787. 788. 789. 790. 791. 792. 793. 794. 795. 796. 797. 798. 799. 800. 801. 802. 803. 804. 805. 806. 807. 808. 809. 810. 811. 812. 813. 814. 815. 816. 817. 818. 819. 820. 821. 822. 823. 824. 825. 826. 827. 828. 829. 830. 831. 832. 833. 834. 835. 836. 837. 838. 839. 840. 84

10

1

LOGICAL LEGEND

- > poorly bedded, green to grey sandstones, muds, and dark grey to purple mudstones;
- 1 (bedded to poorly bedded, grey fine grained with minor units of fine grained green)
- urple to grey conglomerates and breccias of mafic volcanic and plutonic clasts in a grey to purple sand and mud matrix;
- hematite-stained mud matrix)
- phyric to augite and/or plagioclase phyric).
- augite and/or plagioclase phyric)
- cally foliated and amphibolized;
- S
- nded plutonic sequence of gabbroic (the rocks)
- omite pods and lenses)
- ods and lenses)
- grey siltstones, sandstones and
- rey to purple sandstones, siltstones



2 547 CCC E

2 548 CCC E

2 549 CCC E

CCC N

1045

sheeted diabase dykes with  
10% gabbro screens

gabbro screens and diabase dykes  
in equal proportions

TL-528

gossan

TL-527

gossan

TL-782

TL-526

TL-783

TL-530a,b

TL-784

TL-531

TL-532

TL-785

TL-525a,b

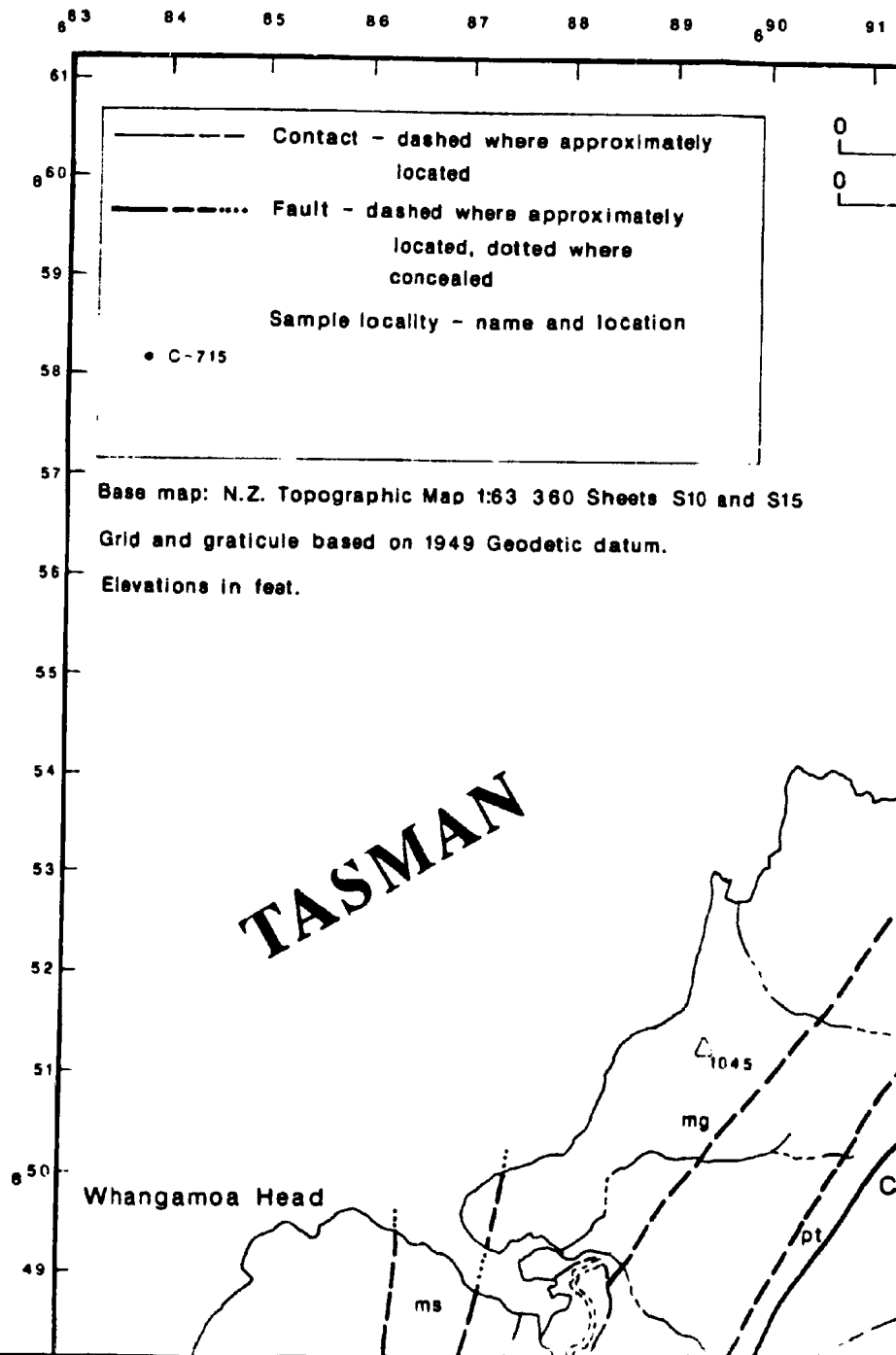
2 550 CCC E

5 995 CCC N

N

5 994 CCC N

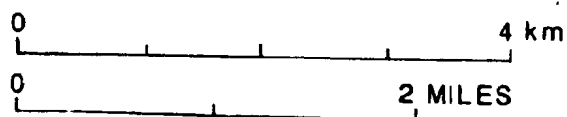




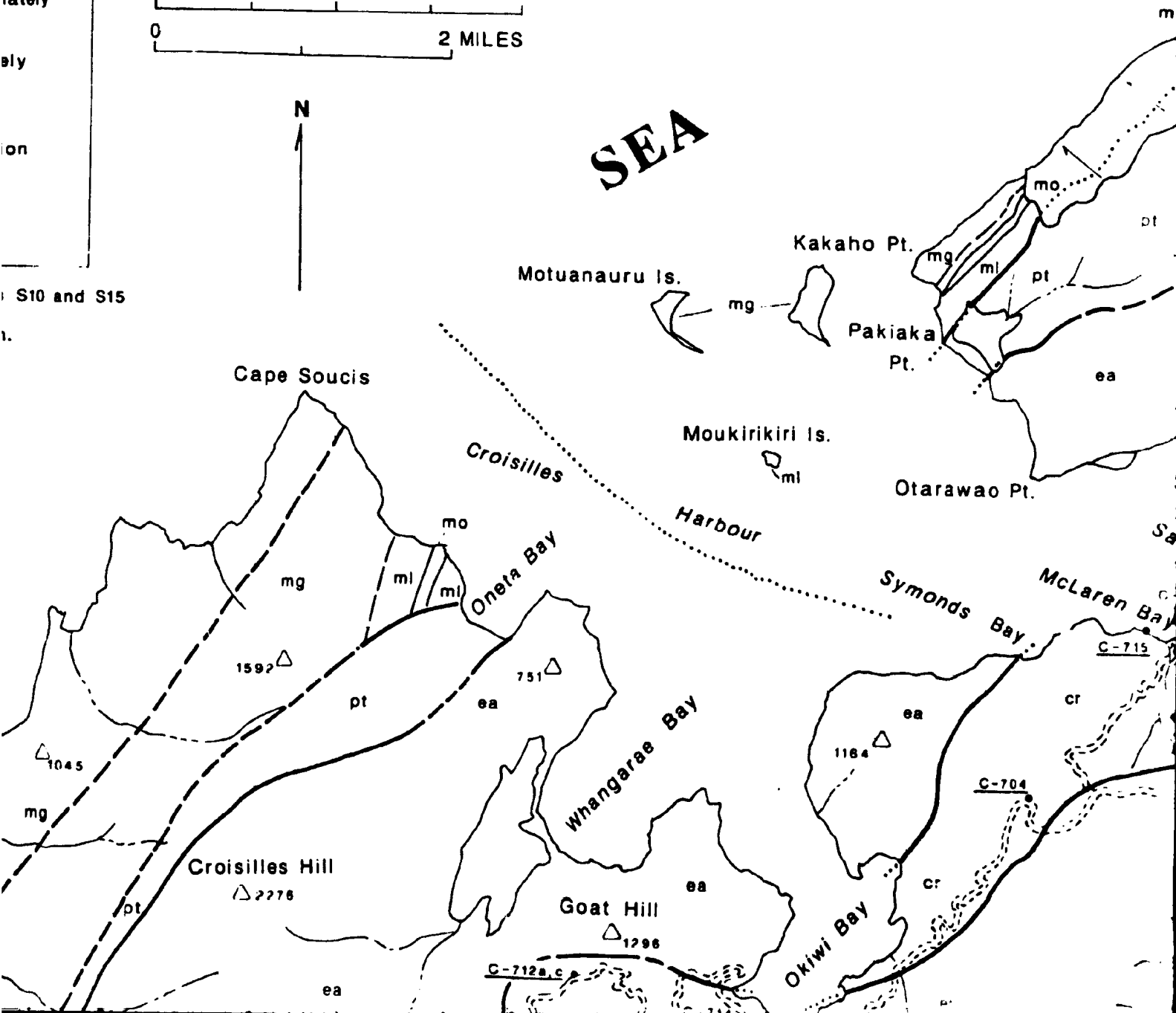
89 90 91 92 93 94 95 96 97 98 99 7 00 01 02

ately  
ely  
ion

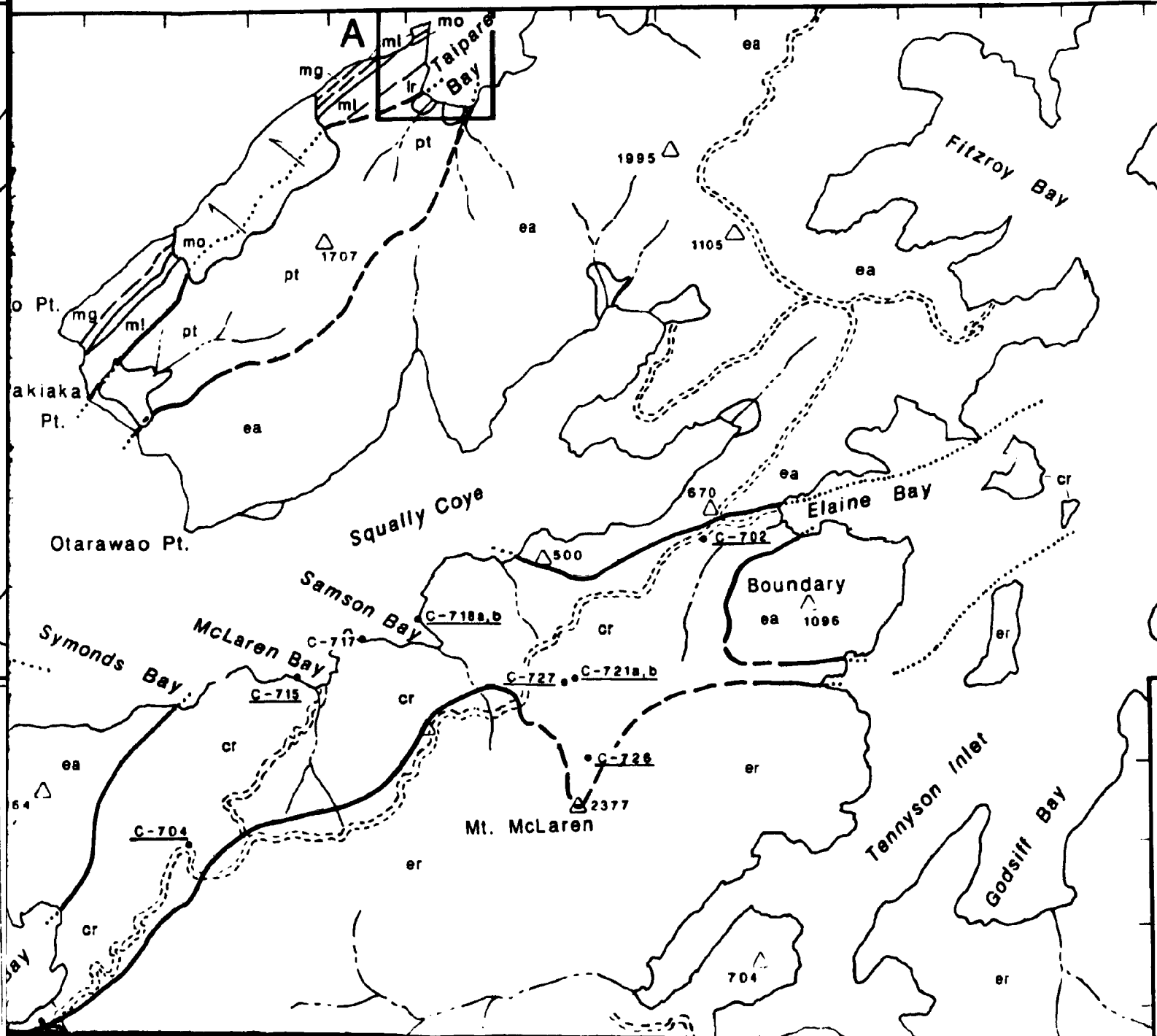
S10 and S15  
1.



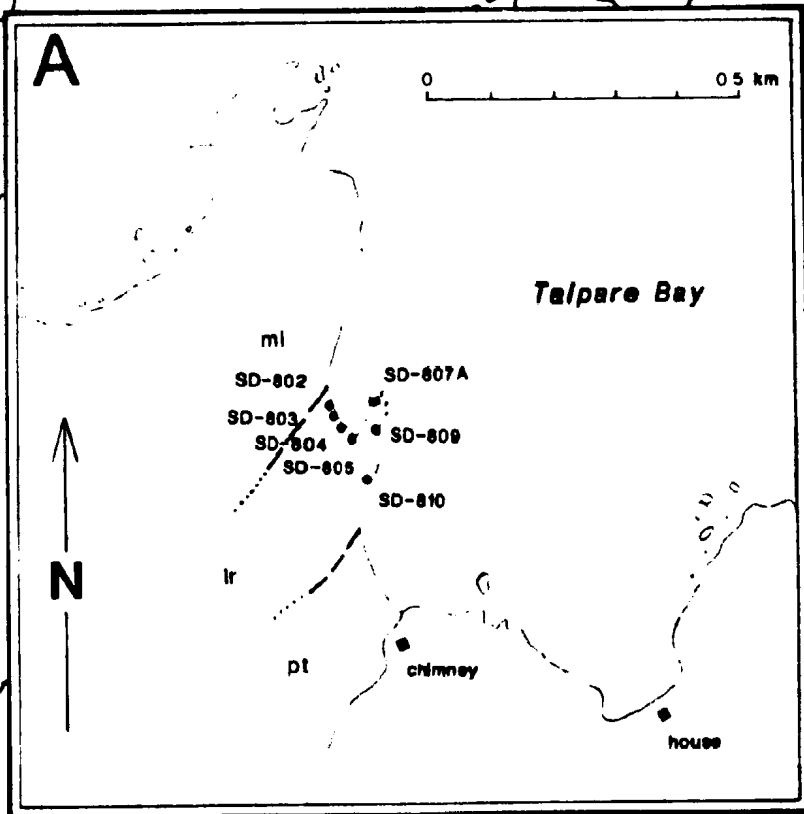
SEA



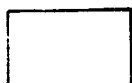
7 00 01 02 03 04 05 06 07 08 09 10 11 12 13



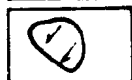
12 13 14 15 16 17 18 19 20 21 22



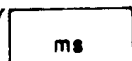
### LEGEND



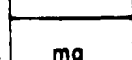
ALLUVIUM (Quaternary)



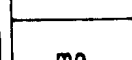
LANDSLIDE - Arrows show direction of movement (Quaternary)



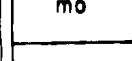
STEPHENS FORMATION  
(Upper Permian)



GREVILLE FORMATION  
(Upper Permian)



MAITAI OLISTOSTROMES  
(Upper Permian)



LITTLE BEN, TRAMAY, WOODED PEAK

ASSEMBLAGE

DUN  
MOUNTAIN  
MAITAI

MAITAI GROUP

### PATUKI MÉLANGE

|  |  |
|--|--|
|  | undifferentiated   |
|  | sediments (undifferentiated grey to purple sandstones and mudstones) |
|  | pillowed/massive basaltic flows (typically aphyric porphyritic)      |
|  | diabase dykes (aphyric)  |
|  | gabbro (typically isotropic locally amphibolized)                    |
|  | ultramafic rocks (undifferentiated)                                  |

### CROISILLES MÉLANGE

|  |  |
|--|--|
|  | undifferentiated   |
|  | sediments (undifferentiated grey to purple sandstones and mudstones) |
|  | pillowed/massive basaltic flows (typically aphyric porphyritic)      |
|  | diabase dykes (aphyric)  |
|  | gabbro (typically isotropic, often amphibolized)                     |
|  | ultramafic rocks (undifferentiated)                                  |

### MISCELLANEOUS

|  |                              |
|--|------------------------------|
|  | sheared serpentinite         |
|  | sediments (undifferentiated) |

## SYMBOL LEGEND

### GEOLOGICAL SYMBOLS

#### Geological Contact

|  |                        |
|--|------------------------|
|  | defined (dip 30°)      |
|  | approximate (vertical) |
|  | assumed                |

#### Fault

|  |             |
|--|-------------|
|  | defined     |
|  | approximate |
|  | assumed     |

#### Bedding

|  |                          |
|--|--------------------------|
|  | tops known               |
|  | horizontal               |
|  | vertical                 |
|  | dipping 40° southwest    |
|  | overturned 50° northwest |

|  |              |
|--|--------------|
|  | tops unknown |
|  | horizontal   |
|  | vertical     |
|  | dipping 40°  |

#### Fabrics

|  |                            |
|--|----------------------------|
|  | cleavage (strike and dip)  |
|  | foliation (strike and dip) |

break out map

TL 781

gabbro screens and diabase dykes  
in equal proportions

gabbro with 10% diabase dykes

5 993 000 N

5 992 000 N

5 991 000 N

2 547 000 E

ly to purple sandstones, siltstones  
es)  
lows typically aphyric to olivine

ly amphibolized)

ted)

r to purple sandstones siltstones  
s)

WS typically aphyric to olivine

amphibolized)

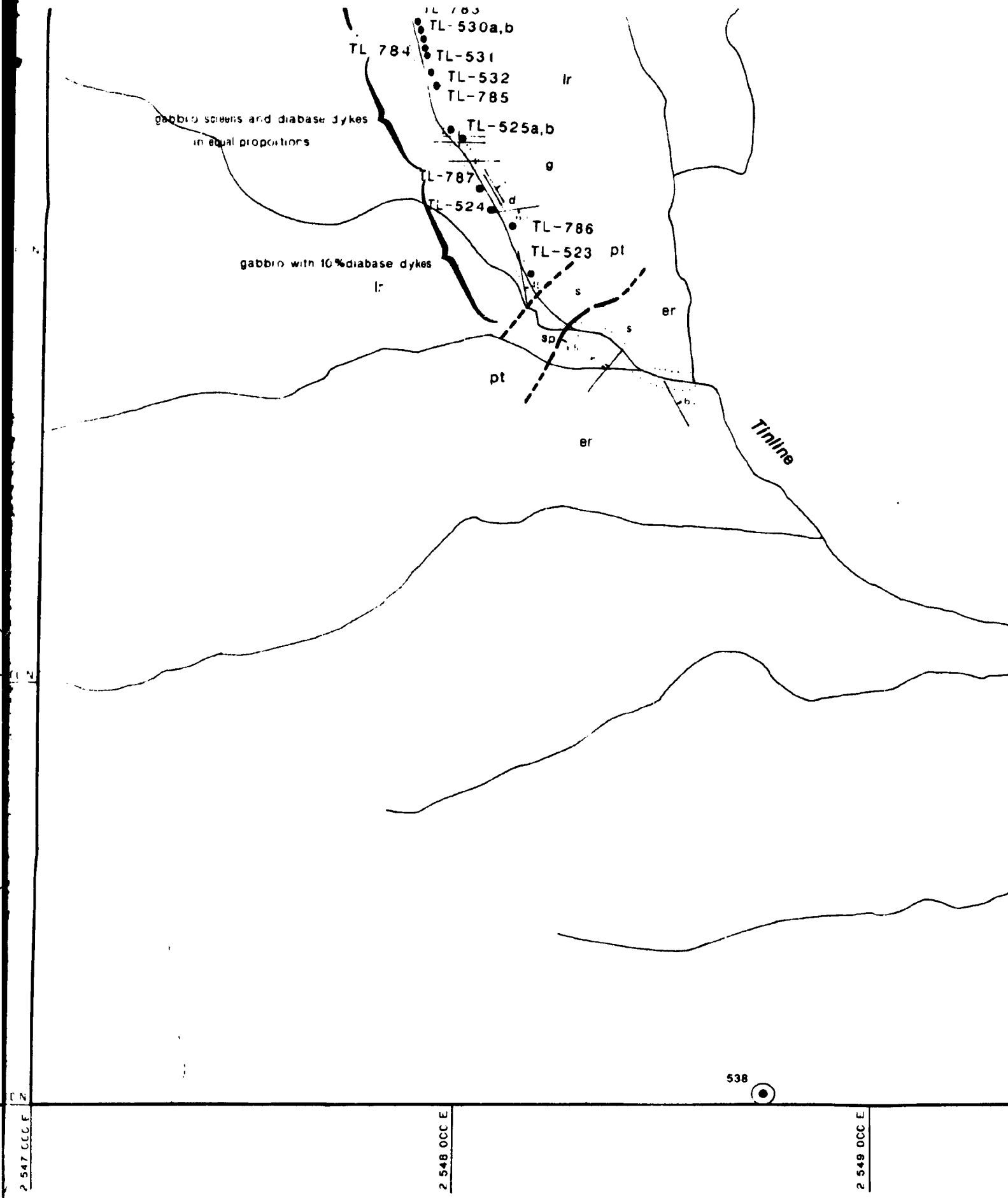
ed)

END

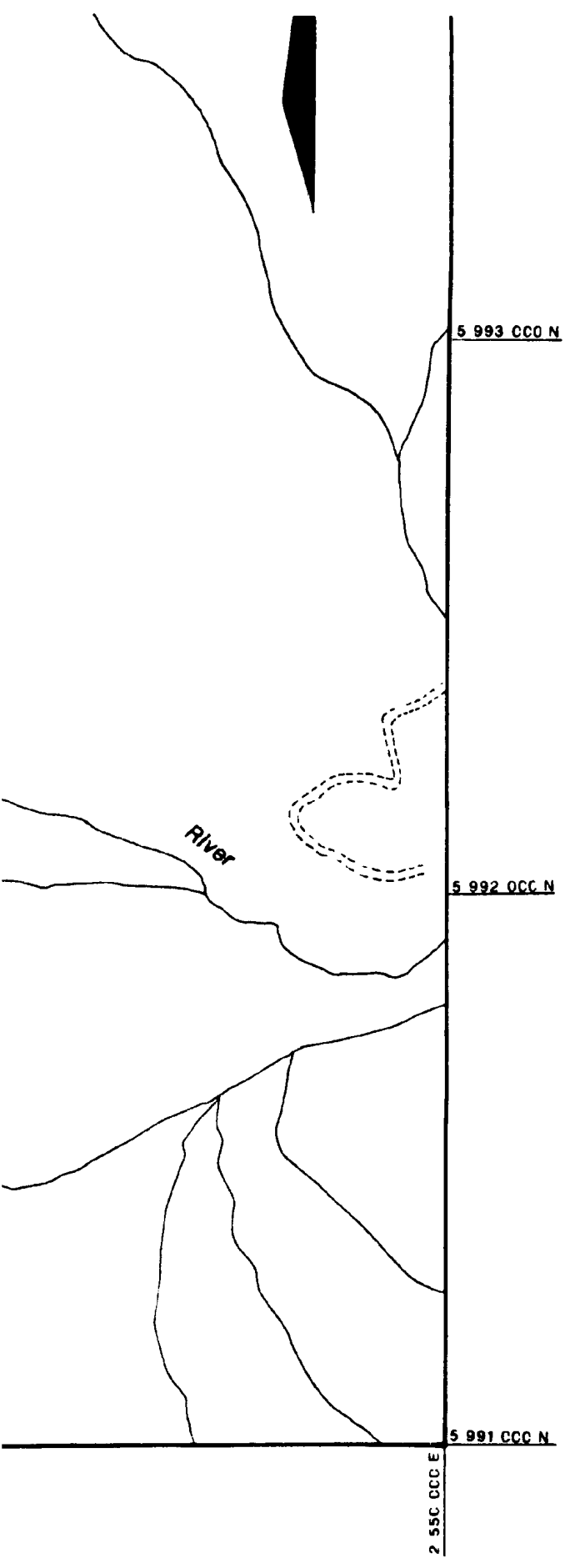
Fault

defined  
approximate  
assumed

tops unknown  
horizontal  
vertical  
dipping 40° southwest







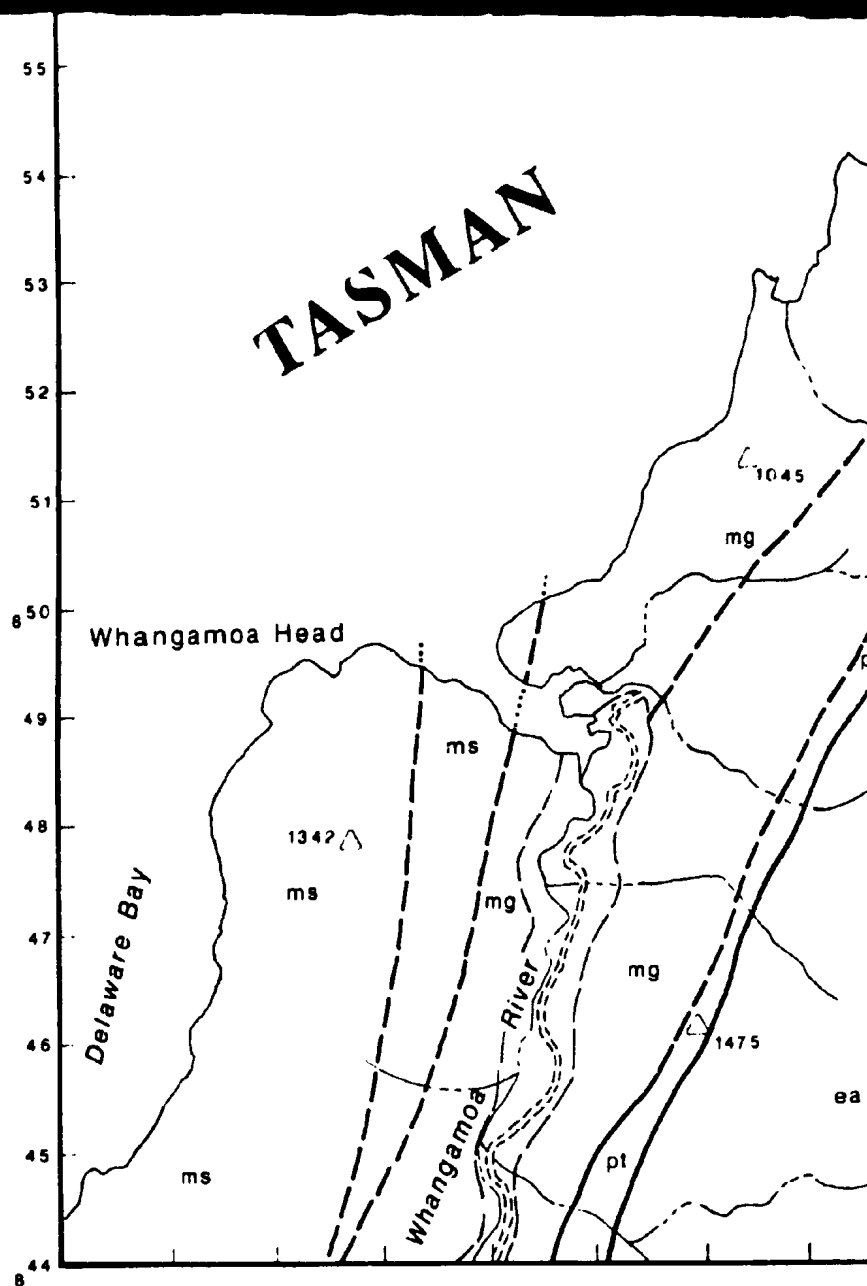
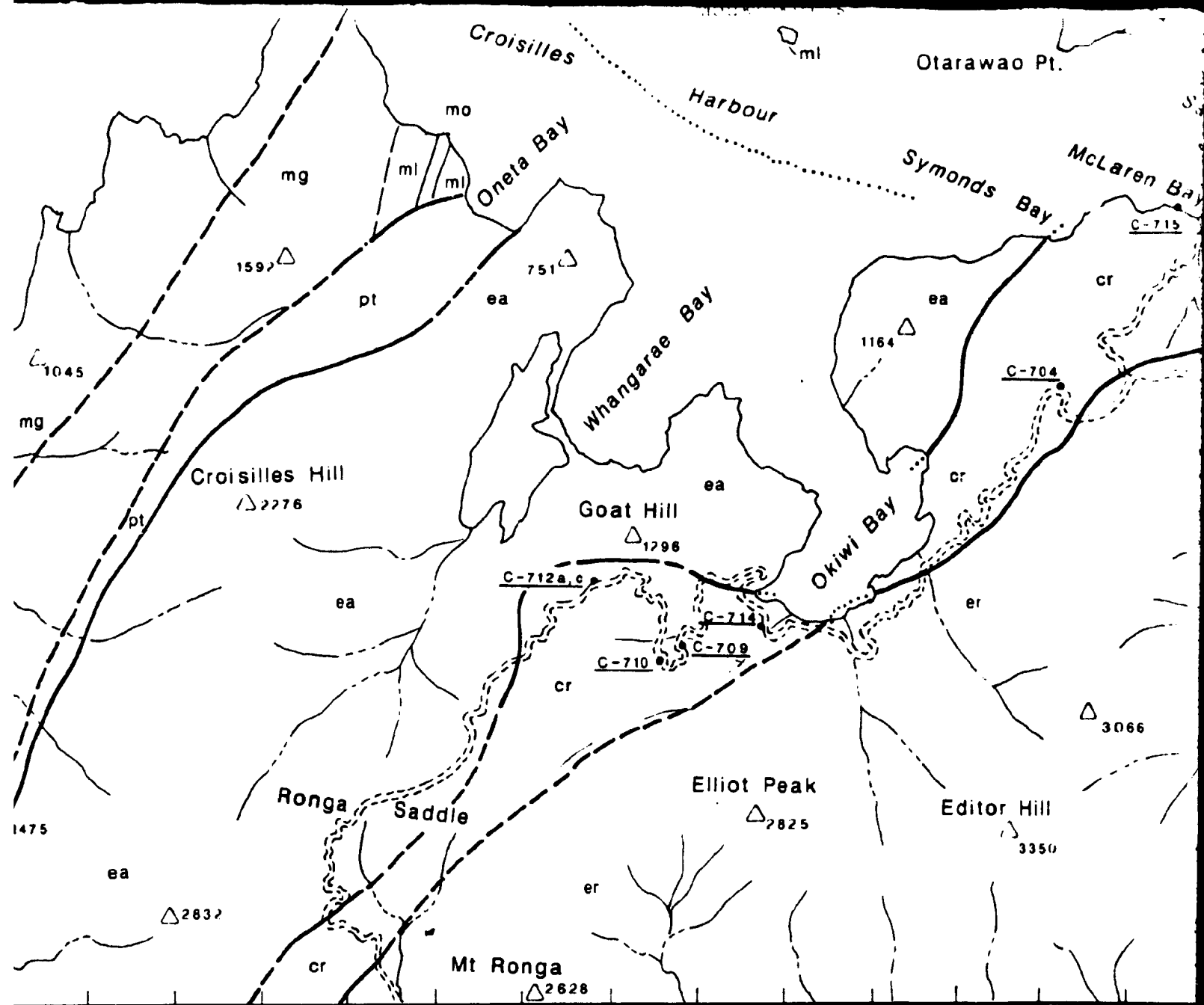
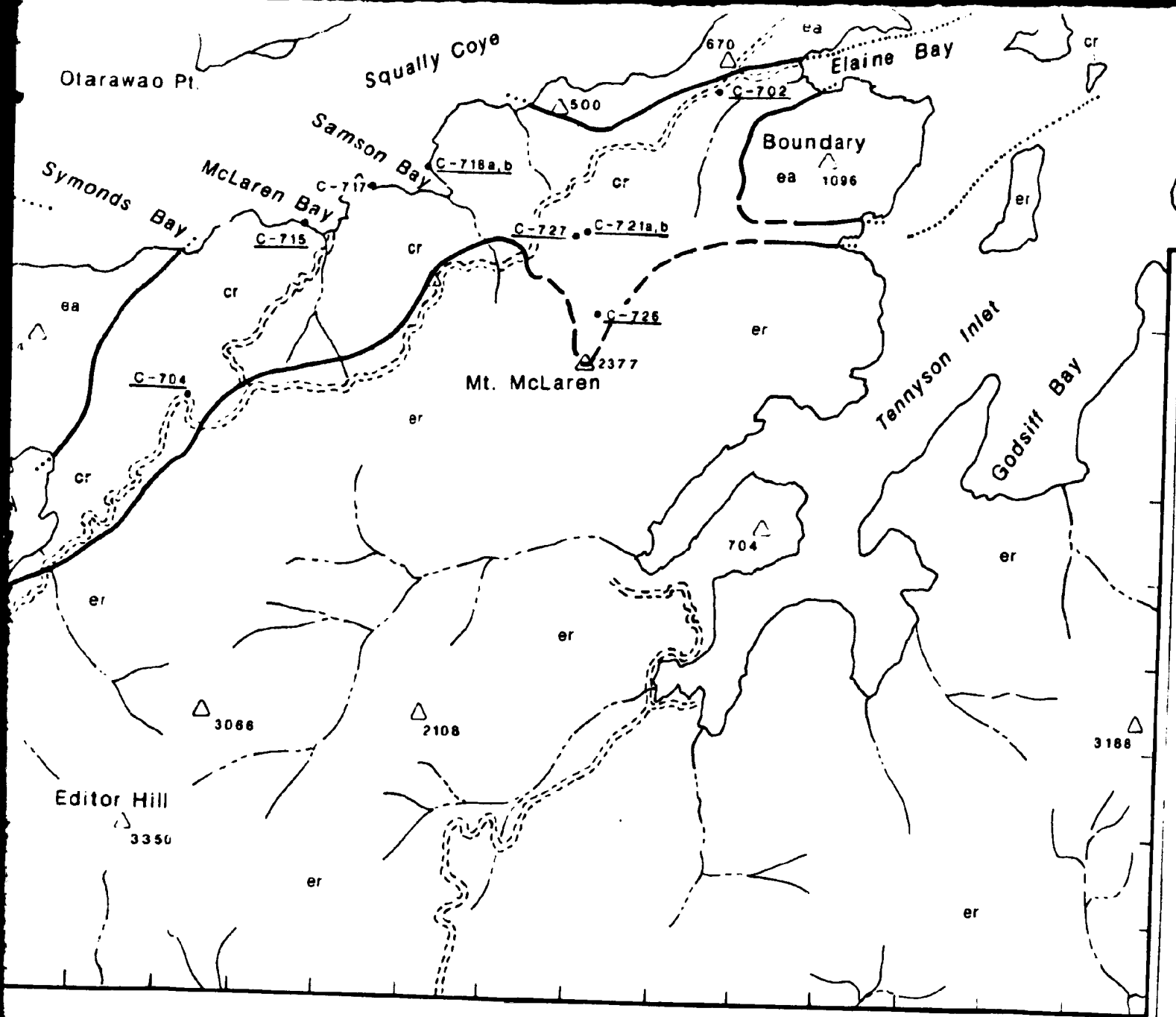


Figure 3.2.6 SAMPLE LOCATION MAP FOR THE CF



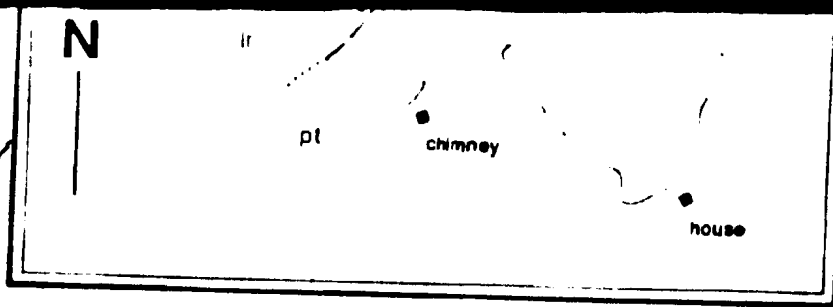
## THE CROISILLES HARBOUR AREA

Geologic map of Croisilles Harbour, Nelson Marborough S



Harbour, Nelson Marlborough Sounds after Landis et al. (1987).

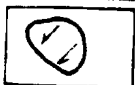
Inset A shows geology of the Taipare Bay area.



## LEGEND



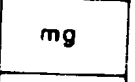
ALLUVIUM (Quaternary)



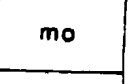
LANDSLIDE - Arrows show direction of movement (Quaternary)



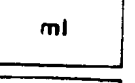
STEPHENS FORMATION  
(Upper Permian)



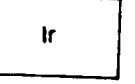
GREVILLE FORMATION  
(Upper Permian)



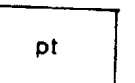
MAITAI OLISTOSTROMES  
(Upper Permian)



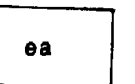
LITTLE BEN, TRAMAY, WOODED PEAK  
LIMESTONE FORMATIONS (U Permian)



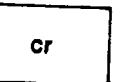
GLENNIE FORMATION  
(Permian)



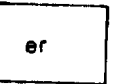
PATUKI  
MELANGE



RAI  
TERRANE



CROISILLES  
MELANGE



PELORUS  
TERRANE

HOKONUI ASSEMBLAGE

DUN  
MOUNTAIN  
MAITAI  
TERRANE

MAITAI GROUP  
LEE RIVER GROUP

TE ANAU  
ASSEMBLAGE

RAI  
TERRANE  
CROISILLES  
MELANGE  
PELORUS  
TERRANE

# Geological Contact

defined (dip 30°)  
approximate (vertical)  
assumed

fault

de  
af  
as

## Bedding

tops known

horizontal

vertical

dipping 40° southwest

overturned 50° northwest

top

ho

ve

a.p.

## Fabrics

cleavage (strike and dip)

foliation (strike and dip)

lineation (strike and plunge)

shearing (strike and dip)

## Sample location

● B-74 location and number

## Outcrop

area of outcrop

o/c ? questionable outcrop

△ △ boulders

## Miscellaneous

quarry

prospecting shaft or abandoned mine

Cr chromite

Cu copper

Serp serpentine

## TOPOGRAPHICAL REFERENCE

road

four wheel drive track




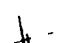
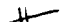


foot track

power lines

building

trig. station

spot elevation

-  defined
-  approximate
-  assumed
-  tops unknown
-  horizontal
-  vertical
-  dipping 40° south west

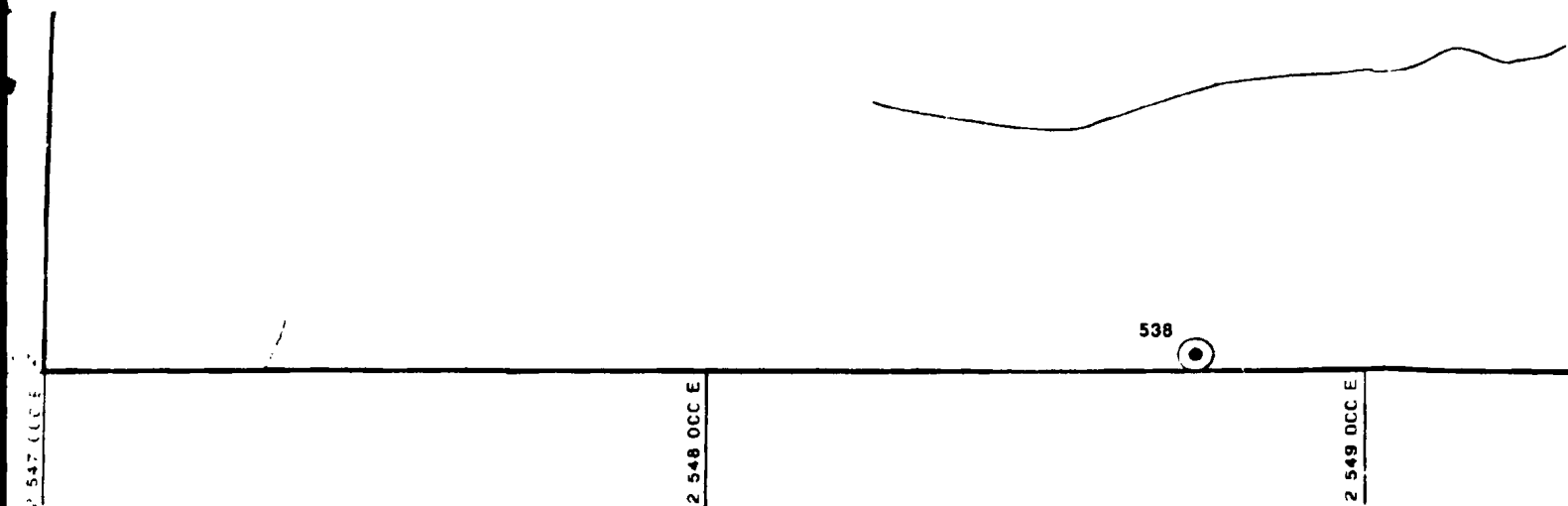
5 991 000 N  
2 547 000 E

Topographic data taken from map sheets N.Z.M.S. 270 027, N28, and N29 of the New Zealand Department of

Grid references are in reference to the New Zealand Map Grid.

Elevations in metres.





170 O27, N28, and N29 of the New Zealand Department of Lands and Survey.

d Map Grid.

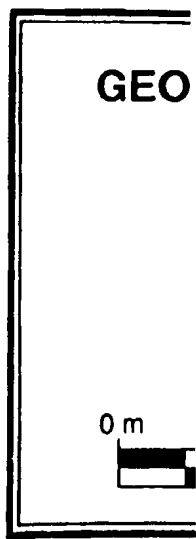
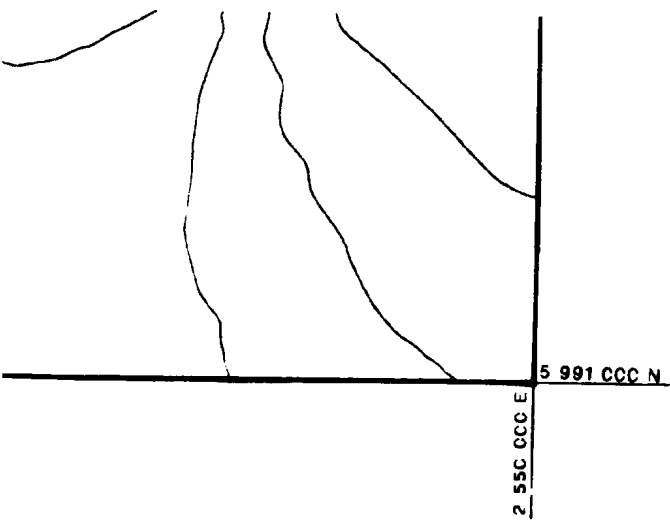


Figure 3.

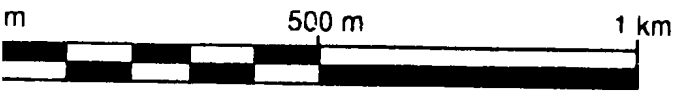


# GEOLOGY OF THE TINLINE RIVER


By Paul J. Moore

1988


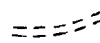

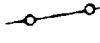



SCALE 1: 10 000

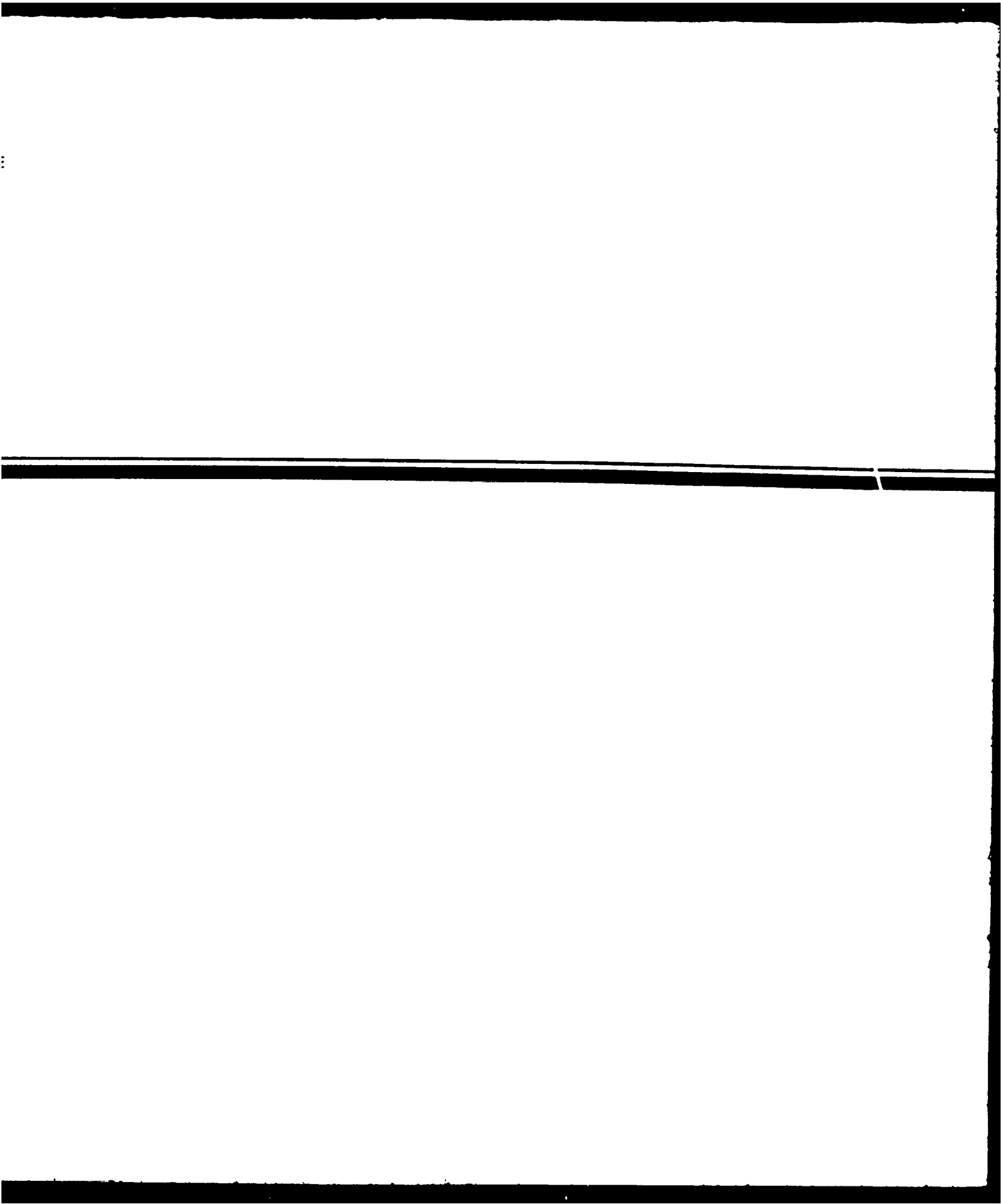


## 3.2.5 Geology of the Tinline River area.

 winding shift indicated line  
 Cr chromite  
 Cu copper  
 Serp serpentine

# TOPOGRAPHICAL REFERENCE

 road  
 four wheel drive track  
 foot track  
 power lines  
 building  
 trig. station  
 spot elevation



GEOI

0 m



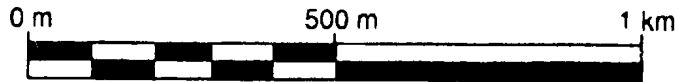
**Figure 3.**

# **GEOLOGY OF THE TINLINE RIVER**

**By Paul J. Moore**

**1988**

**SCALE 1: 10 000**



**Figure 3.2.5 Geology of the Tinline River area.**

## GEOLOGICAL LEGEND

### MAITAI GROUP

- |    |  |
|----|--|
| mt | undifferentiated (bedded to poorly bedded, green to grey siltstones, and dark grey to purple sandstones)                                   |
| wp | Wooded Peak Formation (bedded to poorly bedded limestone with minor units of fine grain sandstone)   |
| up | Upukerora Formation (purple to grey conglomerates consisting of mafic volcanic and plutonic rocks supported in a grey to purple sandstone) |

### LEE RIVER GROUP

- |       |   |
|-------|---|
| lr    | undifferentiated  |
| b     | basaltic breccia (often in a hematite-stained mud matrix)       |
| p / f | pillowed/massive flows (aphyric to augite and/or plagioclase)   |
| d     | diabase dykes (aphyric to augite and/or plagioclase)            |
| g     | gabbro (typically isotropic, locally foliated and amphibolized) |

### DUN MOUNTAIN ULTRAMAFICS

- |    |   |
|----|---|
| dm | undifferentiated  |
| sp | serpentinite  |
| t  | transition zone series (banded plutonic sequence of ultramafic and mafic rocks) |
| hz | harzburgite (with minor chromite pods and lenses)                               |
| du | dunite (with minor chromite pods and lenses)                                    |

### PELORUS GROUP

- |    |   |
|----|---|
| er | sediments (undifferentiated grey siltstones, sandstones, mudstones) |
|----|---|

### PATUKI MÉLANGE

- |    |   |
|----|---|
| pt | undifferentiated  |
| s  | sediments (undifferentiated grey to purple siltstones, sandstones, mudstones) |





